Stabilization of enzymes by chemical modifications

A thesis presented in partial fulfilment of the requirements for the degree of
Doctor of Philosophy in Biotechnology
at Massey University, New Zealand

PATTAMAWADEE TANANCHAI

2011

Abstract

This study focused on thermostabilization of enzymes in solution by intramolecular crosslinking of the specific functional groups within an enzyme molecule. Three model enzymes were used: α-amylase of *Aspergillus oryzae* (EC 3.2.1.1), β-galactosidase of *Aspergillus oryzae* (EC 3.2.1.23) and extracellular invertase (EC 3.2.1.26) of *Saccharomyces cerevisiae*. Crosslinking was examined using the following homobifunctional reagents: diisocyanates ($O=C=N(CH_2)_nN=C=O$, n = 4, 6, 8), diimidoesters ($CH_3O(=NH)C(CH_2)_nC(=NH)OCH_3$, n = 4, 5, 6) and diamines ($NH_2(CH_2)_nNH_2$, n = 0, 2, 4, 6, 8, 10, 12). The concentration of the enzymes was kept low at 0.9 μM in attempts to promote intramolecular crosslinking as opposed to intermolecular crosslinking. Only invertase could be stabilized relative to controls by crosslinking with diisocyanates.

Invertase (0.9 μM) crosslinked with 1,4-diisocyanatobutane (n = 4; or butamethylene diisocyanate, BMDC) and 1,6-diisocyanatohexane (n = 6) showed enhanced thermostability. Stability was improved dramatically by crosslinking invertase with 20-30 μM of the reagent. Molecular engineering of invertase by crosslinking reduced its first-order thermal denaturation constant at 60 °C from 1.232 min^{-1} for the native enzyme to 0.831 min^{-1} for the stabilized enzyme. Similarly, the best crosslinking treatment increased the activation energy for thermal denaturation from 372 $kJ \cdot mol^{-1}$ for the native invertase to 517 $kJ \cdot mol^{-1}$ for the stabilized enzyme. Values of the Michaelis-Menten parameters (K_m and v_{max}) showed a reduced efficiency of invertase after the crosslinking treatment.

The nature of the crosslinking was examined using size exclusion chromatography (SEC), sodium dodecyl sulfate polyacrylamide gel electrophoresis (SDS-PAGE), dynamic light scattering (DLS) and multiple angle laser light scattering (MALLS). Depending on the conditions used, both intermolecular and intramolecular crosslinking occurred. The estimated molecular weight of the intermolecularly crosslinked invertase appeared to be much higher compared to the intramolecularly crosslinked invertase and the native invertase. In attempts to simplify certain analyses, attempts were made to remove the carbohydrate moiety from crosslinked invertase (a glycoprotein) molecule.

Deglycosylation with PNGase F achieved a significant reduction of carbohydrate for the native invertase but not for the intra- and intermolecularly crosslinked invertase. Circular dichroism (CD) measurements showed that crosslinking with BMDC affected slightly the secondary structure of invertase.

The nature of the crosslinking that might be occurring in invertase molecule was further studied using small model oligopeptides, small nonglycosylated enzymes (hen egg white lysozyme and pepsin) and glycoprotein models (ovalbumin). Crosslinking of the model pentapeptide (0.9 μM) suggested that crosslinking with BMDC involved reaction between BMDC and the amino group of lysine or the carboxylate at C-terminal of the pentapeptide. Using a heptapeptide (1 mM) in crosslinking with BMDC showed a changed hydrophobicity of the crosslinked peptide. The crosslinking treatment of lysozyme (3.5 mM) with BMDC clearly produced an intermolecularly crosslinked lysozyme as evidenced by SEC and SDS-PAGE. A changed net charge of lysozyme after the crosslinking treatment was demonstrated using native PAGE. Mass spectrometry was used to then prove the intramolecular crosslinking of lysozyme with BMDC. CD spectra of the intramolecularly crosslinked lysozyme showed it be more resistant to thermal unfolding relative to native lysozyme.

Acknowledgements

I would like to thank many individuals for their support during my study. I greatly appreciate the support of my Thai friends, especially Piyamaz, Rattanawan, Tiyaporn, Tawan and Sureewan who made me feel like I was part of a large family. Thank you to my friends, Ziad, Azilah, Farhan, Xumei, Sadia, Ian, Thu and Carolina for sharing many thoughts during my study.

I would like to thank Michelle Tamehana for helping with the MALLS instrument; Janiene Gilliland for her help in using the zetasizer technique; Dr. Lara Matia-Merino for her knowledge of light scattering; Dr. Torsten Kleffmann, facility manager at Centre for Protein Research, Biochemistry Department, Otago University, Dunedin, New Zealand, for his help with MS analyses; and Dr. David Libich of Institute of Fundamental Sciences, Massey University, for his help with the interpretation and use of dynamic light scattering data.

I would like to thank Ann-Marie Jackson and all her laboratory staff in MicroSuit laboratory, as my experiments would not have been possible without their well organized management. My great appreciation to Trevor Loo, my biochemistry guru, who helped me in learning how to use many experimental techniques and made useful suggestions. I would like to thank my friends at Dr. Gill Norris' laboratory, including Komala for being a friend; Jana for kindly providing some of her enzymes; Judith and Matthew for saving me when I once nearly fainted.

I would like to thank Rajamangala University of Technology Lanna and Royal Thai Government for sponsoring my study. I greatly appreciate the financial support provided by Professor Yusuf Chisti and Massey University towards the end of my study. I would also like to thank Professor Ian Warington, Dr. Yoopayao Daroon and my colleagues at Rajamangala University of Technology Lanna, Lampang, Thailand for their encouragements.

I would like to gratefully thank my principal supervisor, Professor Yusuf Chisti, who was always supportive. I am especially thankful to Dr. Gill Norris, my co-supervisor, for her understanding and guidance.

Finally, I would like to express my gratitude to my parents (Khunpor Somboon and Khunmae Kammoon Tananchai), my brother (Mr. Thiti Tananchai), my sister (Mrs. Jutarat Payaklerd), my husband (Dr. Thamarath Pranamornkith), other family members in Thailand, my host parents (Mr. Brian and Mrs. Rosalie Kerr) for their unconditional love and support.

Table of Contents

List of Figures

List of Tables

Abbreviations

A	The Arrhenius parameter
Asn	Asparagine
Asp	Aspartic acid
BIC	Butyl isocyanate
BMDC	1,4-Diisocyanatobutane or butamethylene diisocyanate
BSA	Bovine serum albumin
CAPS	N-Cyclohexyl-3-aminopropanesulfonic acid
CD	Circular dichroism
CLECs	Crosslinked enzyme crystals
CPR	Centre for Protein Research, University of Otago, New Zealand
Cys	Cysteine
DA10	1,10-Diaminodecane
DAB	1,4-Diaminobutane
DAD	1,12-Diaminododecane
DAH	1,6-Diaminohexane
DAO	1,8-Diaminooctane
d_f	Dilution factor
DLS	Dynamic light scattering
dm	The surface-to-surface distance between enzyme molecules
DMA	Dimethyl adipimidate
DMP	Dimethyl pimelimidate
DMS	Dimethyl suberimidate
DNS	3,5-Dinitrosalycylic acid
dn/dc	A differential index of refraction
E	Enzyme concentration
E_0	Enzyme concentration at time zero
EA	Ethyl acetimidate
E_d	The deactivation energy
EDA	1,2-Diaminoethane
E_t	Enzyme concentration at time t

Glu	Glutamic acid
HMDC	1,6-Diisocyanatohexane or hexamethylene diisocyanate
k_{cat}	The rate constant
K_{av}	The gel phase distribution coefficient
k_d	The thermal denaturation rate constant
K_m	Michaelis-Menten constant
MALDI-MS	Matrix assisted laser desorption ionisation-mass spectrometry
MALLS	Multi angle laser light scattering
$[M+H]^+$	Molecular ion in positive ionisation mode
$[M–H]^–$	Molecular ion in negative ionisation mode
MW	Molecular weight
MWCO	Molecular weight cut-off
OMDC	1,8-Diisocyanatooctane or octamethylene diisocyanate
PDB	Protein Data Bank
PNGase F	Peptide-N-glycosidase F
R	Gas constant
RCSB	Research Collaboratory for Structural Bioinformatics
R_f	Relative mobility
RI	Refractive index
RP-HPLC	Reverse phase-high performance liquid chromatography
S	Substrate concentration
SDS-PAGE	Sodiumdodecylsulfate polyacrylamide gel electrophoresis
SEC	Size exclusion chromatography
TEMED	N,N,N′,N′-Tetramethylenediamine
v	Rate of enzymatic reaction
v_f	Fraction of initial activity at time t
v_i	Initial activity
v_{max}	Maximum rate of enzymatic reaction
V_c	Geometric column volume
V_e	Elution volume
V_o	Column void volume

CHAPTER 1

Introduction

Enzymes have been extensively used as industrial catalysts, medicinal products and constituents of household products for decades (Gavrilescu and Chisti, 2005; Gerhartz, 1990; Uhlig and Linsmaier-Bednar, 1998; Wiseman, 1975). Compared to conventional chemical catalysts, enzymes tend to be highly specific; consequently, enzymes are used to carry out molecular transformations that are often unachievable by chemical catalysis (Liese *et al.*, 2000). Industrial enzymes are used in production and processing of chemicals, foods, pharmaceuticals, pulp, paper, hides, textiles and other products (Gavrilescu and Chisti, 2005; Wiseman, 1975). In view of their utility, the market for industrial enzymes has been growing at an average annual rate of 3.3% in value since 2002 (Rajan, 2004). To date this market has been dominated by proteases and amylases. By the year 2012, the global sales of industrial enzymes are expected to be over US$2.9 billion, mostly in the areas of food, feed constituents, beverages, and pharmacy. The enzyme market is mainly influenced by biotechnology research (Jose, 2008).

The starch processing industry is a major user of enzymes, especially of alpha amylase. Amylase is used to produce glucose, maltose and maltodextrin for making syrups from starch. The production of ethanol for fuel and alcoholic beverages also uses this enzyme. In baking processes, alpha amylase is used to improve the quality of dough. Amylase is used in the textile industry as a starch desizing agent for coating threads during fabric weaving. It is added to detergents to enhance their ability to remove starchy stains (Wong and Robertson, 2003). Another widely used enzyme is invertase. It is typically used in candy processing, artificial honey production, wine making and bread bakery (Cantarella *et al.*, 2003). β-galactosidase is another enzyme used in food applications to remove lactose from dairy products intended for lactose intolerant individuals (Mahoney, 2003; Richmond *et al.*, 1981).

Enzymes have certain important limitations: typically, enzymes do not withstand temperatures much higher than 40 °C and they are susceptible to denaturation at extreme values of pH and pressure. Enzymes that can withstand relatively high temperatures are

desirable because the rate of a reaction typically doubles with every 10 °C increase in temperature (Cornish-Bowden, 2004). There are other advantages to carrying out reactions at higher temperatures; firstly, when reactions are carried out at temperature above 70 °C, the risk of microbial contamination is reduced. Secondly, substrate dissolve more easily when the temperature is increased (Klibanov, 1983). Many processes using enzymes also require elevated temperatures. Washing processes, starch hydrolysis and textile desizing are typically carried out at 60-70 °C, 100 °C and 80-90 °C, respectively (Iyer and Ananthanarayan, 2008). Thus the use of a thermally stable enzyme will greatly increase the productivity of the enzyme-catalyzed reaction, potentially reducing the unit cost of the product. Consequently, improvement of the ability of an enzyme to withstand a relatively high temperature is an important objective.

Although many methods have been successfully used to stabilize some enzymes, as discussed in the literature review (Chapter 2), many of these have their drawbacks. This work is focused on chemically modifying the structure of enzymes to improve their thermal stability without immobilization. Enzyme stabilization by immobilization is already used extensively and has many benefits (Cao, 2005); immobilization can, however, slow down reactions by imposing significant mass transfer limitations, particularly if the substrate of the enzyme is a slow-diffusing large molecule (Chisti, 1999; Goldstein, 1976), as is the case for enzymes such as proteases and amylases.

The ability to stabilize enzymes by chemically modifying their molecular structure is of potential commercial value to many of the processes that use enzyme catalysis. Stabilization can be achieved by crosslinking some of the functional groups on the surface of the enzyme with chemical reagents (Ó'Fágáin, 1995, 2003; Reiner *et al.*, 1977a, b; Torchilin *et al.*, 1978; Torchilin *et al.*, 1979; Torchilin and Martinek, 1979) so that the molecule is prevented from unfolding at temperatures that are moderately (e.g. ≥10 °C) elevated compared to the optimal reaction temperature of the native enzyme. Such crosslinking should occur without any change to either the active site of the enzyme or its substrate binding site.

The aim of this study is to achieve thermal stabilization of selected enzymes by using bifunctional crosslinking reagents. Three relatively well-known, commercially significant and easily denatured enzymes: α-amylase from *Aspergillus oryzae*; β-galactosidase from *Aspergillus oryzae*; and invertase from *Saccharomyces cerevisiae*, were investigated. The crosslinking between enzymes and crosslinking reagents used in

this study was investigated using both intramolecular and intermolecular crosslinking treatment. Because intermolecular crosslinking can create oligomeric enzymes, significantly increasing the molecular weight of the enzyme and adversely altering the mass transfer properties of a reaction system, it is not desirable. The aim is therefore to preferentially achieve intramolecular crosslinking. Several techniques were used to measure the size of enzyme molecules after the crosslinking treatment to identify the nature of the crosslinking. Peptides, small enzymes (e.g. lysozyme and pepsin) and a small glycoprotein (ovalbumin) were used as models in attempts to elucidate the nature of the crosslinking.

CHAPTER 2

Literature Review

This chapter reviews the methods for enzyme stabilization and some properties of the chemical crosslinkers used in this study. Unfolding of enzymes because of heat is discussed briefly and the structure of the enzymes selected, and the relevant experimental techniques are reviewed.

2.1 Stabilization methods

Because of its potential significance, stabilization of enzymes against thermal denaturation has been studied since at least the 1940s. Stabilization methods have included the following: 1) immobilization of enzymes on or within solid supports and matrices, including covalent binding of an enzyme to soluble matrices such as starch and other macromolecules; 2) use of stabilizing additives such as multivalent metal ions, substrates, salts, small organics such as sorbitol, and soluble polymers such as polyethylene glycol; 3) protein engineering; 4) chemical modification of the enzyme molecule (e.g. surface modifications, inter- and intramolecular crosslinking); and 5) crosslinked enzyme crystals (CLECs) technology. Heat stability of numerous enzymes has been improved by using these methods.

2.1.1 Immobilization on supports and matrices

Enzymes immobilized in various forms are widely used, and the methods used to immobilize them on/in solid matrices and soluble polymer supports have been extensively discussed (Cao, 2005). In most cases, the objective of immobilization is not stabilization *per se*, but to enable the reuse and recycling of enzymes (Cao, 2005). Improvement to thermostability conferred by immobilization is believed to be due to both the physical confinement and multipoint covalent binding of the enzyme molecule that restricts its freedom to unfold, and hence, denature. This method of stabilization is of no further direct interest to the present work although many of the reagents that are used to bind

enzymes to inert matrices can also be used in binding functional groups within an enzyme molecule to stabilize it.

2.1.2 Use of additives

Although of no direct relevance to this study, use of additives for stabilizing enzymes is briefly reviewed as it helps to understand the factors that contribute to enzyme stability in other situations. Additives used include multivalent metal ions, salts, sugars, surfactants and organic solvents (e.g. polyols), and soluble inert polymers such as polyethylene glycol (Whitaker and Tappel, 1962; Whitaker *et al.*, 1962). Metal ions such as Ca^{2+} (Khajeh *et al.*, 2001a; Ram *et al.*, 1954) have been used to stabilize trypsin, α-chymotrypsin and α-amylase. The Ca^{2+} ion is known to result in the formation of ionic bridging in enzyme molecules (Janecek and Baláž, 1992) and it is necessary for the activity of α-amylase. Addition of $CaCl_2$ during storage at room temperature has been shown to improve the stability of α-amylase by 63% relative to a control (Shah *et al.*, 1990). The addition of Co^{2+} or Mn^{2+} has been shown to improve the thermostability of cyclic phosphodiesterase (Shimada and Sugino, 1969). Furthermore, Mg^{2+} (Whitaker and Tapel, 1962), Sr^{2+} and Zn^{2+} have been shown to stabilize some enzymes (Torchilin *et al.*, 1979).

The effect of salts containing ions such as Li^+, Na^+, NH_4^+, Rb^+, Cs^+, K^+, I^-, F^-, NO_3^-, SO_4^{2-}, Br^-, Cl^- and PO_4^{2-} on enzyme stability has been extensively studied (Ohnishi and Hatano, 1970; Shah *et al.*, 1990; Shimizu *et al.*, 1969; Whitaker and Tapel, 1962) and, depending on the concentration used, can both negatively and positively influence enzyme activity. For example, alcohol dehydrogenase is activated by low concentrations of Na^+, K^+ and Li^+, but inhibited by high concentrations of the same cations. Furthermore, enzymes respond to salt additives differently. For example, the presence of Na^+, K^+, Li^+ and SO_4^{2-} improves the activity of peroxidase whereas hematin is inhibited by $K^+$and Li^+. SO_4^{2-} and PO_4^{2-} stabilize phosphotransacetylase against heat during its purification. Increasing the ionic strength of enzyme solutions by adding salts such as Na_2SO_4, NaCl, KCl, CCl_3COOK and $(CH_3)_4NBr$, stabilizes α-chymotrypsin (Torchilin *et al.*, 1979), and sodium chloride stabilizes α-amylase during storage.

Sugars, sugar alcohols and polyol are known to stabilize enzymes (Khajeh *et al.*, 2006; Samborska *et al.*, 2006; Sola-Penna and Meyer-Fernandes, 1998). The stabilizing

sugars include glucose, fructose, maltose, sucrose, trehalose, mannitol, sorbitol, lactitol and glycerol. The stabilizing action of these compounds is associated with hydrogen bonding, hydrophobic interaction, and ionic and Van der Waals forces between the sugar and the enzyme molecules. Furthermore, some of these compounds indirectly influence the solution properties of the system, improving stability. The effectiveness of a compound as a stabilizing agent has been shown to depend on the number of hydroxyl groups it contains, its hydrated volume, and the surface tension of the resulting solution. Stabilizing effects also depend on the concentration of the additive. For example, among the different sugars trehalose effectively stabilizes G-6-phosphate dehydrogenase because of its larger hydrated volume. This leads to the higher preferential solubility of trehalose in bulk water of enzyme. As a consequence, less amount of trehalose needs to be used to restrict the freedom of the enzyme molecule to flex. Sucrose is reported to most effectively stabilize α-amylases from *Bacillus amyloliquefaciens*, *B. licheniformis* and *Aspergillus oryzae* at 60–90 °C than other sugars and polyols.

Surfactants are other possible stabilizers. The Triton X-series of non-ionic or neutral detergents has been shown to reduce heat induced unfolding of enzymes. For example, the addition of Triton X-100 to solutions of β-amylase from sweet potato (Takeda and Hizukuri, 1972) and bovine carbonic anhydrase (Ota *et al.*, 1998) has been shown to improve their thermostability. Triton X-100 added at a concentration of 0.02% w/w to porcine pancreatic α-amylase improved its thermostability by 41% (Yoon and Robyt, 2005).

The effects of organic solvents on both enzyme activity and stability have also been reported (George *et al.*, 1969; Ono *et al.*, 1970; Whitaker *et al*, 1962; Yoon and Robyt, 2005). Glycerol has been shown to significantly stabilize both lactate and malate dehydrogenase during storage at 4° C. Ethanol, methanol, propanol, isopropanol, butanol, n-butanol, isobutanol and acetone, have also been shown to stabilize these enzymes, and the addition of polyvinyl alcohol at low concentration enhanced activity of *Aspergillus niger* glucoamylase by 48%. The stabilizing effects of solvents are associated with their ability to displace water molecules from the vicinity of the enzyme. Interactions between the solvent and the active site of the enzyme are also linked with improved stability.

Although some additives can improve stability, the converse is also true, in that some additives may actually inhibit an enzyme. For example, non-ionic detergents such as Tween-80 and some monocarboxylic acids can inhibit α-amylase. Similarly,

monosaccharides, disaccharides, and sugar alcohols are known to inhibit α-amylase. The effect of additives on enzyme stability is therefore difficult to predict and has to be examined on a case-by-case basis. For example, alcohols (ethanol, isopropanol, propylene glycol, glycerol, ethylene glycol, and methanol) have been reported to increase the activity of trypsin on several synthetic substrates, in contrast to the effect of ethanol on α-amylase which reduces its ability to hydrolyse starch (Whitaker *et al*., 1962). Similarly, urea, glycine or saccharin can also inhibit α-amylase. In view of the diverse effects of additives, it is essential to compare activity of any chemically modified preparation of the enzyme with the activity of the native enzyme under identical conditions.

2.1.3 Protein engineering

Protein engineering techniques have been used to improve thermostability and other physicochemical characteristics of enzymes since the early 1980s. Protein engineering has been used to increase resistance to unfolding by making specific changes in the amino acid sequence to: 1) introduce stabilizing disulfide bonds within or on the surface of the molecule; 2) eliminate internal spaces in the molecule and modify internal hydrophobic packing; 3) enhance internal hydrogen bonding; and 4) introduce surface ion pairs. Examples of many such modifications are cited by Gupta (1993), Janeček (1993), Ó Fágáin (2003) and Alberghina (2003). Protein engineered enzymes are usually produced in recombinant organisms (Berka and Cherry, 2006).

2.1.4 Chemical modification

Chemical modification of enzymes was first used to gain information on protein structure, conformation, and structure–function correlations. Subsequently, chemical modifications were used to stabilize enzymes against various kinds of severe treatments. Chemical modifications can be divided into two types: 1) modifications involving only the surface functional groups of a protein without causing crosslinks; and 2) modifications that involve intermolecular and intramolecular crosslinking of functional groups in protein molecule. The enzyme functional groups that are commonly modified, the modifying reagents/reactions, and examples of some of the enzymes that have been modified, are given in Table 2.1.

Table 2.1 Examples of chemical modification reactions (Gupta, 1993)

Functional group	Reaction/reagent	Enzyme modified
Free amino group (N terminal or lysine side chain)	Acylation	Biliverdin reductase, chymotrypsin
	Alkylation	Biliverdin reductase, chymotrypsin
	Carbamylation	Ribonuclease
Carboxyl group (aspartic acid and glutamic acid)	Carbodiimide	Beta-glucosidase
Guanidine group (arginine)	Glyoxal	Salicylate hydroxylase
Imidazole group (histidine)	Bromoacetic acid	Beta-glucosidase
Phenolic group (tyrosine)	Diisopropylphosphofluoridate	Chymotrypsin
Sulfhydryl group (cysteine)	N-ethylmaleimide	Biliverdin reductase
Indole group (tryptophan)	N-bromosuccinimide	Abrin A

2.1.4.1 Surface modification

Modification of amino acid residues on the surface of an enzyme molecule is used to alter the nature of the surface charge and hydrophobicity/hydrophilicity. These changes modify the conformation of the enzyme. Modification reactions include acetylation ($E–NH–C(O)CH_3$), succinylation ($E–NH–C(O)–(CH_2)_2COO^-$) and alkylation (e.g. $E–NH–CH(OH)CH=CH_2$) of free amino groups. These reactions have been widely used to alter pH stability and thermal stability. Other surface groups of the enzyme may be reacted in various ways to enhance the utility of this technique. Trypsin (Riordan and Bier, 1959; Terminiello *et al.*, 1958), horseradish peroxidase (Ugarova *et al.*, 1979), α-amylase (Khajeh *et al.*, 2001b) and α-chymotrypsin (Torchilin *et al.*, 1979) have been modified by reaction with anhydrides of mono- and dicarboxylic acids (succinic and itaconic), acetic acid, or monosulfonic acid (β-sulfopropionic).

Many enzymes have been modified by compounds that react with the primary amine (ε-amino group) of lysine, and the effects of such modification, such as an increase in thermostability, are directly related to the number of the enzyme's surface functional groups reacted. *p*-Nitrophenyl acetate (Urabe *et al.*, 1973), N-hydroxysuccinimide and 1-hydroxybenzotriazole (Hora, 1973) have been used to add acyl groups to specific side chains of α-amylase enhancing its resistance to heat-induced unfolding. The hydrophobicity of free amino groups in thermolysin molecule was altered by acylation with 4-oxatetradecanoic acid, 4,7-dioxatetradecanoic acid, 4,7,10-trioxatetradecanoic acid

and 4,7,10,13-tetraoxatetradecanoic acid (Urabe *et al.*, 1978), producing insoluble modified enzyme products. The most hydrophobic preparation was however, the most stable to temperature and maintained an activity profile similar to the native enzyme. Other nonpolar reagents such as dioxane, 2-propanol, ethanol, dimethyl sulfoxide and propylene glycol can also be used to strengthen hydrophobic interactions in an enzyme molecule (Sanwal *et al.*, 1966). Formation of additional hydrogen or ionic bonds can be achieved by introducing new polar or charged groups to the protein surface (Janecek and Baláž, 1992).

2.1.4.2 Chemical crosslinking

Crosslinking is the chemical reaction of joining two or more functional groups together by covalent bonding. Links within the same molecule are intramolecular crosslinks. Those between two molecules are known as intermolecular crosslinks. Crosslinking is useful for examining the relationship between neighbouring functional groups, and can give some idea of the three dimensional structure of a protein by indicating the distances between two specific surface residues. The use of intramolecular crosslinking of the enzyme to make it more resistant to heat denaturation is the main focus of this study (Figure 2.1).

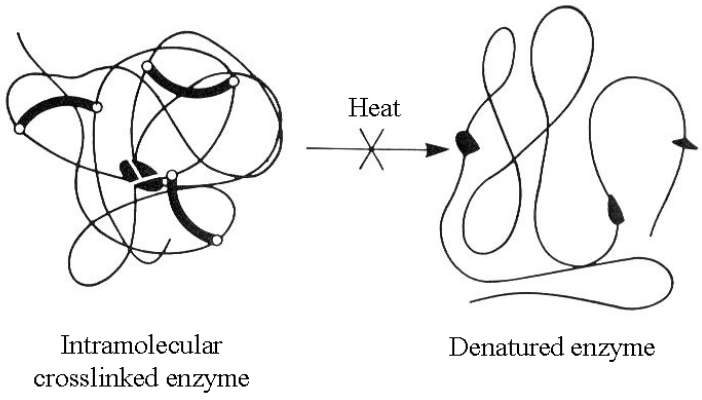

Figure 2.1 Preventing thermal unfolding by intramolecular crosslinking (Klibanov, 1983).

Bifunctional reagents (Wold, 1972) can be used to covalently crosslink two surface functional groups within an enzyme molecule or between two enzyme molecules. These reagents are the essential chemical modifying agents in crosslinking of two reactive groups. Bifunctional reagents interact specifically with the nucleophilic functional groups of the side chains of amino acid residues. These functional groups include the thiol group

of cysteine, the amino group of lysine, the N-terminal amine, the C-terminal carboxylate, the carboxylic acid groups of aspartic and glutamic acids, the imidazole group of histidine and the thioether group of methionine (Wong and Wong, 1992). Bifunctional reagents are classified as homobifunctional or heterobifunctional crosslinkers (Ó'Fágáin, 1995; Wold, 1972). The two reactive groups of a homobifunctional reagent are identical whereas the reactive groups of a heterobifunctional reagent are different. Bifunctional reagents may be further subdivided into those having noncleavable crosslinks and those having cleavable crosslinks (Han *et al.*, 1984). The various possible ways a homobifunctional reagent (Y—Y) can react with the enzyme with functional group —X are shown in Figure 2.2.

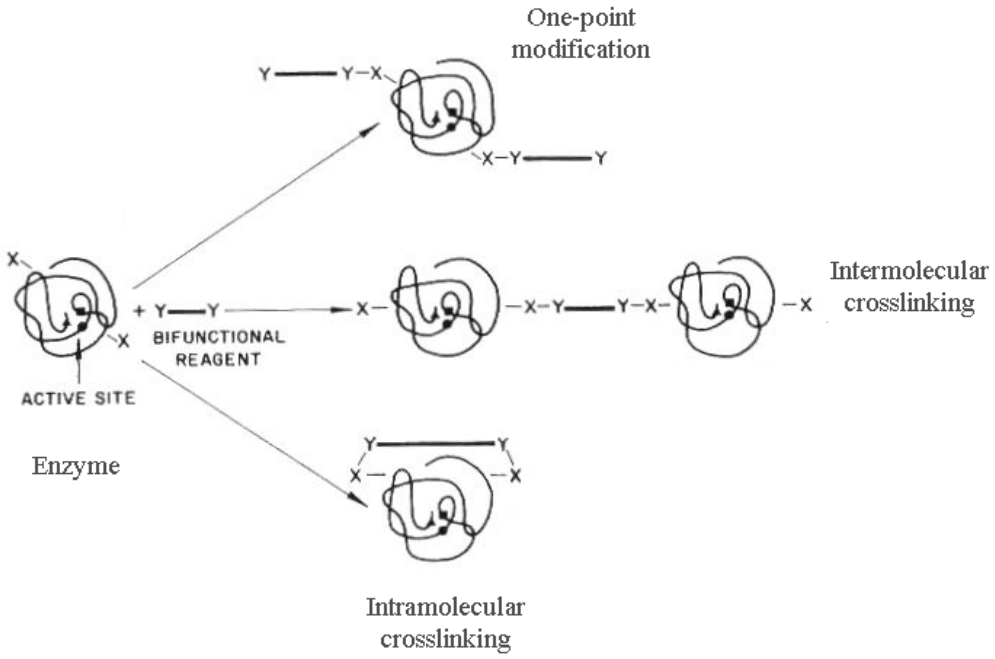

Figure 2.2 Reactions of a homobifunctional crosslinking reagent with an enzyme (Martinek and Torchilin, 1988).

The nature of the crosslinking obtained depends on the nature of the reactive groups of the reagent, the size of the reagent, the enzyme, and the ratio of the reagent-to-enzyme concentration used for crosslinking. Some of the bifunctional reagents that have been used to stabilize enzymes are listed in Table 2.2. Others have been reviewed in the literature (Fernandez-Lafuente *et al.*, 1995; Govardhan, 1999; Gupta, 1993; Han *et al.*, 1984; Ó'Fágáin, 2003; Torchilin *et al.*, 1979; Wong and Wong, 1992).

Table 2.2 Applications of bifunctional crosslinking reagents

Reagent type	Reagent name	Enzymes cross linked
Homofunctional	Glutaraldehyde	Glycogen phosphorylase b (Wang and Tu, 1969)
	Dimethyl suberimidate	Bovine heart creatine kinase (Sheehan *et al.*, 1990)
	Dimethyl adipimidate	Catalase (Shaked and Wolf, 1988)
Heterofunctional	Succinimidyl-4-(N-maleimidomethyl) cyclohexane-1-carboxylate	Horseradish peroxidase (Yoshitake *et al.*, 1982)
	M-maleimido benzoyl-N-hydroxysuccinimidoester	β-Galactosidase (Freytag *et al.*, 1984)
Cleavable	Dimethyl-3,3'-dithiobis-propionimidate	ATPase (Pont, 1979)
	Dithio-bis-succinimidyl-propionate	Bovine heart transhydrogenase (Anderson and Fisher, 1981)
Non-cleavable	Hexamethylene diisocyanate	Alpha galactosidase A (Snyder *et al.*, 1974)
	Dimethyl pimelimidate	Lactose synthetase and galactosyl transferase (Brew *et al.*, 1975)

Several examples of the use of crosslinking reagents to stabilize enzymes have been reported. Crystalline α-chymotrypsin was reacted with formaldehyde to protect it against heat and urea-induced unfolding (Marini and Martin, 1971; Saidel *et al.*, 1964), and the shelf life of α-chymotrypsin in solution could be extended by crosslinking with bis-iodoacetamide (Reiner *et al.*, 1977b). The effect of using diamine bifunctional reagents (i.e. $NH_2(CH_2)_nNH_2$; n = 0–12) of different lengths for crosslinking α-chymotrypsin has also been assessed (Reiner *et al.*, 1977b). Intramolecular crosslinking of α-chymotrypsin with dithiols of HS-$(CH_2)_n$-SH type with n = 4–6 resulted in the highest stability (Torchilin *et al.*, 1978). Treatment of glycogen phosphorylase b by covalent crosslinkage using glutaraldehyde made the enzyme more resistant to heat denaturation (50–51°C) than the native enzyme (Wang and Tu, 1969). Crosslinking the lysine residues with aliphatic aldehyde derivatives also improved the thermal stability of glycogen phosphorylase b (Shatsky *et al.*, 1973). Crosslinking pig heart lactate dehydrogenase using the dialdehyde pentanedial improved the heat stability of the enzyme (Foster and Thomson, 1973). An enhanced thermal stability was observed when lysine residues of α-amylase were intramolecularly crosslinked with ethylene glycol bis succinic acid *N*-hydroxyl succinimide ester (Habibi *et al.*, 2006). Treatment of α-

galactosidase A with hexamethylene diisocyanate stabilized the enzyme against heat inactivation (Snyder Jr *et al.*, 1974). Soluble bifunctional reagents such as imidoester have also been used to significantly improve enzyme stability. For example, when dimethyl adipimidate, dimethyl pimelimidate and dimethyl suberimidate were used to crosslink lactate dehydrogenase (Minotani *et al.*, 1979), horse radish peroxidase (Ryan *et al.*, 1994), elastase (Besson *et al.*, 1995) and bovine heart creatine kinase (Sheehan *et al.*, 1990), all enzymes showed increased heat tolerance. Intersubunit crosslinking of glyceraldehyde-3-phosphate dehydrogenase using diacids of the HOOC-$(CH_2)_n$-COOH type has also been shown to improve stability (Torchilin *et al.*, 1983).

For this study, the focus will be on the use of the homobifunctional reagents di-imidoesters ($CH_3O(=NH)C(CH_2)_nC(=NH)OCH_3$), diisocyanates $O=C=N(CH_2)_nN=C=O$) and diamines ($H_2N(CH_2)_nNH_2$) to stabilize enzymes. These homobifunctional reagents are readily soluble in water which simplifies reaction protocols. These reagents form non-cleavable crosslinks that are stable in the conditions used for catalysis by the stabilized enzyme. They are commercially available and require only mild conditions for the cross-linking reaction to occur, resulting in minimal damage to the enzyme during stabilization.

2.1.4.2.1 Imidoesters

Imidoesters have a high specific reactivity with ε- and α-amino groups on the enzyme molecule in alkaline solution (pH 7-10) (Lundblad, 2005) (Figure 2.3). At lower pH, the α- amino group reacts faster than the ε- amino group of lysine as the latter is protonated under physiological conditions (Hunter and Ludwig, 1962). Imidoesters are hydrolysed slowly to an amide and alcohol in aqueous solution. However, at pH 7-11 the hydrolysis rate is lower than their reaction rate with amine (Means and Feeney, 1971). The crosslinked product, either an amidine or an imidoamide, is quite stable in acid and neutral conditions, but slowly breaks down at high pH. Treating the crosslinked product with a solution of ammonia:acetic acid (30:2 v/v) can cleave the crosslink (Wold, 1972). Diimidoesters of different chain lengths have been synthesized and reported to be useful in crosslinking the lysine residues within a protein (Hunter and Ludwig, 1972). Crosslinking by diimidoesters does not affect the net charge of the protein molecule, thus treatment with monofunctional imidoesters is likely to have minimal effect on the conformation and biological function of enzymes treated with the reagent (Dutton *et al.*, 1966). In this study, dimethyl adipimidate (DMA) (Iyer and Ananthanarayan, 2008),

dimethyl pimelimidate (DMP), dimethyl suberimidate (DMS), with estimated chain lengths of 8.6, 9.2 and 11 angstroms (Å), respectively, were investigated (Nowak *et al.*, 2005). Ethyl acetimidate was used as a monofunctional crosslinker.

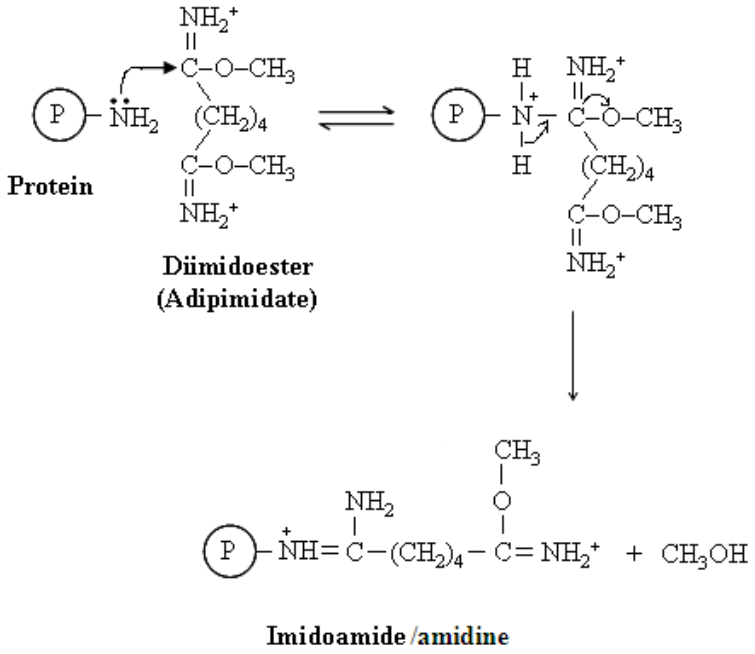

Figure 2.3 The reaction of diimidoester with amino side chain of an enzyme molecule (Han *et al.*, 1984; Means and Feeney, 1971).

Dimethyl adipimidate (DMA) has been used to crosslink several proteins for various purposes. Crosslinking of lysine and the exact location of crosslinks have been reported (Ohara and Takahashi, 1980). Intramolecularly and intermolecularly crosslinked bovine pancreatic ribonuclease has been produced by using adipimidate. The crosslinking can be used to estimate the distance between the surface residues of a protein molecule in a diluted solution (Hartman and Wold, 1967). Human red blood cells' surface crosslinked with DMA strengthened their resistance to hemolysis (Niehaus *et al.*, 1970). The crosslinking of trypsin with DMA made the enzyme resistant to autolysis (Rajput and Gupta, 1987). Crosslinking penicillin G acylase with DMA made the enzyme stable outside its optimal pH range (Kazan *et al.*, 1996). Crosslinking using dimethyl adipimidate to enhance thermal stability of enzymes has also been investigated. Crosslinked endonuclease *Bam*HI was found to have a significantly improved thermostability (Dubey *et al.*, 1989). Treatment of cellulase with DMA improved its thermal stability albeit only slightly (Bilen and Bakir, 1998).

Dimethyl pimelimidate (DMP) has been used to study both the conformational mobility and the structure of glutamate dehydrogenase (Smith and Bell, 1985). DMP has been used to improve the binding between antigens and antibodies (Schneider *et al.*, 1982). Stabilization of cytosol progesterone receptor by reacting with dimethyl pimelimidate has been investigated (Aránvi *et al.*, 1988). The reagent has also proved useful in the thermal stabilization of enzymes such as *Bacillus amyloliquefaciens* α-amylase (Habibi *et al.*, 2006) and *Aspergillus niger* amyloglucosidase (Tatsumoto *et al.*, 1989) which are widely used in industry. It was reported that DMP can react efficiently with α- and ε- amino groups at pH 7-8 and pH 9-10, respectively (Michielsen *et al.*, 2005).

Dimethyl suberimidate (DMS) has been used to both stabilize and study multimeric proteins and enzymes. For example, it was used to crosslink oligomeric proteins and nucleoprotein: aldolase, glyceraldehyde-3-phosphate dehydrogenase, tryptophan synthetase B protein, L-arabinose isomerise, and aspartate transcarbamylase (Davies and Stark, 1970; Dodson, 2000). The reaction of DMS with phycobilisomes stabilized phycobiliproteins (Papageorgiou and Lagoyanni, 1983). Crosslinking of invertase with dimethyl suberimidate has stabilized the enzyme against extreme pH (Kaplan and Bakir, 1998) and temperature (Kaplan *et al.*, 1997; Woodward and Wiseman, 1979). The quaternary structure of formyltetrahydrofolate synthetase could be stabilized by crosslinking with DMS (Renobales *et al.*, 1980).

2.1.4.2.2 Isocyanates

The cyanate functional group (–NCO) of isocyanates can react with protein molecules through amino, thiol, imidazole, tyrosyl and carboxyl groups, depending on the pH (Figure 2.4). The reaction with amino groups leads to a more stable product compared to reactions with other functional groups. Isocyanates can react with sulfhydryl groups faster than with amino groups, but the reaction is reversible (Means and Feeney, 1971) and have been used for modifying proteins for various purposes (Brown *et al.*, 1987; Torchilin *et al.*, 1979).

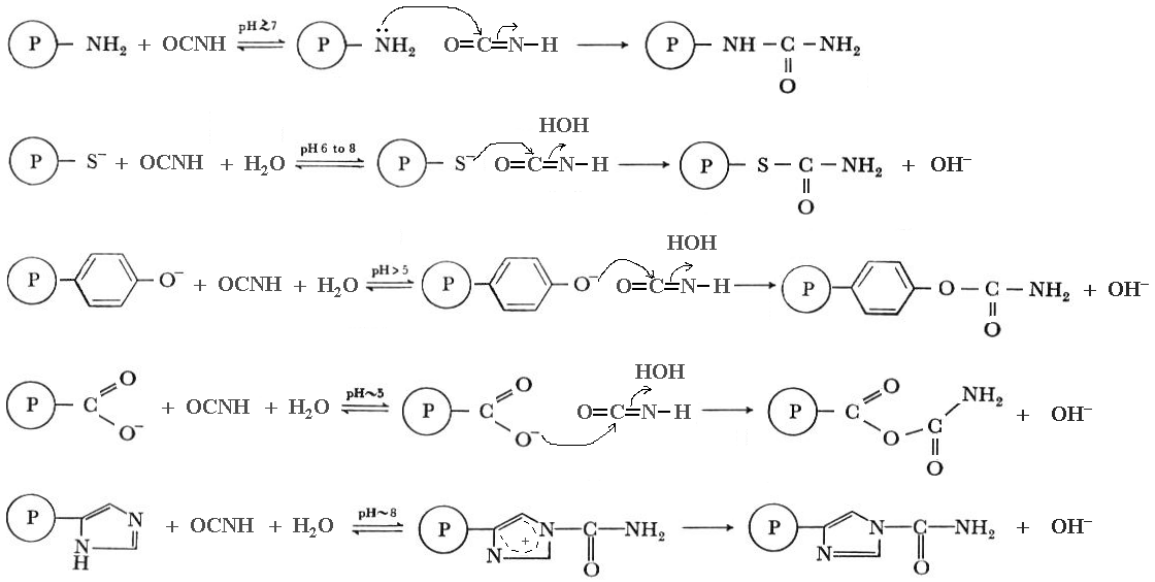

Figure 2.4 Isocyanate reactions at various pH values. Ⓟ **represents protein (Means and Feeney, 1971).**

Crosslinkers in the aliphatic diisocyanate family ($OCN(CH_2)_nNCO$) are available with various lengths of the hydrocarbon chain between the functional groups. Butylisocyanate (BIC), butamethylene diisocyanate (BMDC), hexamethylene diisocyanate (HMDC) and octamethylene diisocyanate (OMDC) with n = 0, 4, 6 and 8, respectively, were used in this study. The spacer lengths of BIC, BMDC and HMDC are 4.87, 5.17 and 6.92 Å, respectively (Baylor, 1996). Hexamethylene diisocyanate is the most commonly used bifunctional reagent among the aliphatic diisocyanate crosslinkers, and there are a number of studies on protein crosslinking using this reagent (Klemes and Citri, 1979; Ozawa, 1967).

2.1.4.2.3 Amines

Various aliphatic diamines were used to modify the target enzymes in this study because diamines react with carboxyl groups (Figure. 2.5) which are presented in a high percentage on some of the target enzymes. The reagents used in this study are commercially available and inexpensive. Diamines have been reported for crosslinking of activated alpha chymotrypsin. The enzyme attained the greatest thermal stability when treated with tetramethylenediamine (Torchilin *et al.*, 1978).

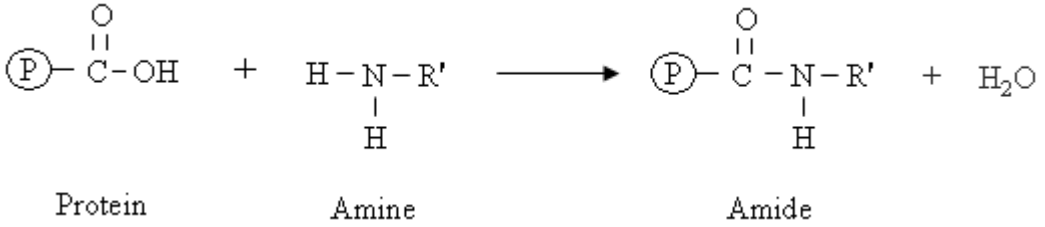

Figure 2.5 The reaction of amine with carboxyl group.

2.1.5 Crosslinked enzyme crystals (CLECs)

Crosslinked enzyme crystals (CLECs) are a relatively recent technology. Biologically active enzyme crystals (1–100 μm in size) are crosslinked using bifunctional reagents to produce larger porous agglomerates or CLECs. CLECs exhibit substantially improved storage and thermostability relative to native soluble enzymes and several enzymes such as lipases, esterases and proteases have been converted to CLECs. This technology is not of direct relevance here, as the CLECs are insoluble (Govardhan, 1999).

Stabilization methods such as protein engineering typically involve modification of the protein through genetic engineering. Stabilization methods involving immobilization can be expensive, laborious and, because of mass transfer and substrate binding limitations, are not well suited to reactions involving macromolecular substrates (Chisti, 1999; Goldstein, 1976). The use of additives for enzyme stabilization is generally applicable to specific cases, as the additive may become an unacceptable contaminant in the final product and not every additive works with every enzyme. Surface modification and intramolecular crosslinking can be rapid, inexpensive and provide a long-lasting stabilizing effect. Other more comprehensive reviews of specific methods exist (Govardhan, 1999; Gupta, 1993; Ó'Fágáin, 1995, 2003; Torchilin *et al.*, 1979; Wong and Wong, 1992).

2.2 Thermal denaturation of enzymes

The general structure of enzymes is well established and has been thoroughly reviewed in textbooks such as Lehninger *et al.* (1993) and Copeland (2000). A brief summary follows. Enzymes are globular proteins that contain up to 20 different primary amino acid

residues. The sequence of amino acids residues in single or multiple polypeptide chains of the enzyme constitutes its primary structure. The N- and C-termini of the polypeptide chains display free $-NH_2$ and –COOH functional groups, respectively. As a consequence of hydrogen bonding between main chain –NH and –C=O groups, the polypeptide chains fold into α-helices and β-pleated sheets which constitute the secondary structure of the enzyme. Coiled and pleated polypeptide chains further fold onto themselves in specific configurations to form the tertiary structure of the enzyme. Tertiary structure is held together by Van der Waals forces, hydrophobic interactions among side chain alkyl groups, hydrogen bonds between polar side chain groups and ionic bonds between charged side chain groups. In addition, disulfide bonds between cysteines within a single polypeptide chain, or on different chains, contribute in establishing and maintaining the tertiary structure (Figure 2.6). How multiple polypeptide chains are held together by these interactions determines the quaternary structure. Some enzymes have complexed metal ions and covalently linked carbohydrate or lipid groups that are important for their biological activity and stability.

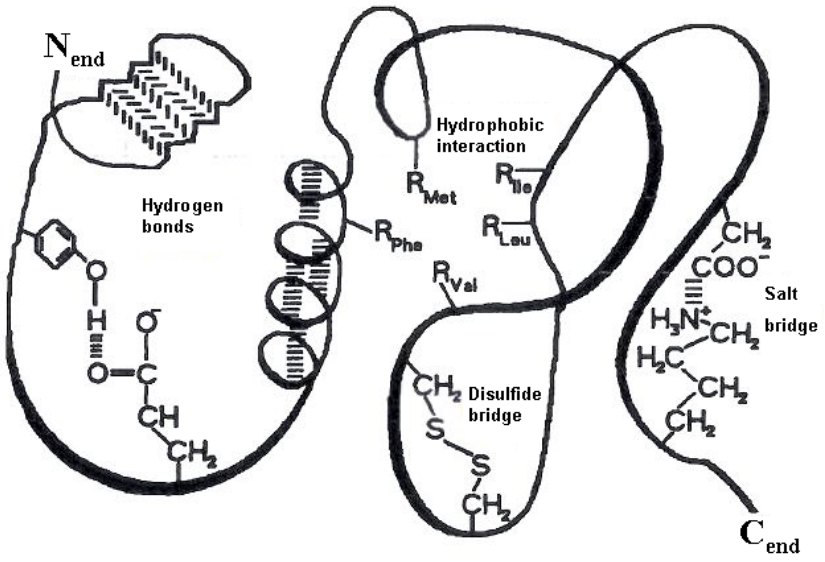

Figure 2.6 Bonds and interactions contributing to stability of enzyme structure (Janecek, 1993).

Loss of quaternary and tertiary structure as a consequence of heat-induced unfolding of the polypeptide chain, is responsible for loss of biological activity at elevated temperature. The unfolding of polypeptide chains disturbs the structure of the active site of the enzyme, altering or eliminating its ability to carry out a chemical transformation. Thermal denaturation commonly occurs at temperature of ≥55 °C

(Freeman, 1984). Temperature induced unfolding of the enzyme molecule results in the normally internal hydrophobic regions becoming exposed, which leads to aggregation of protein molecules. Unfolding by heat denaturation is generally an irreversible process and the denatured protein does not usually reform its native structure even when the temperature returns to normal.

In addition to temperature, other factors can denature, or inactivate, enzymes. These denaturing factors may include pH, ionic strength, displacement of essential metal ions by chelating reagents, displacement of one metal ion by a different metal and proteolytic cleavage of polypeptide chains through the action of proteases. Furthermore, loss of carbohydrates moieties of the enzyme can commonly modify enzyme stability and sometimes activity (Rouf *et al.*, 1996).

2.3 The structure and properties of proteins

In this work, examples of some important industrial enzymes, α-amylase, invertase and β-galactosidase were selected for study. These specific enzymes were selected for the following reasons: 1) they covered a broad range of molecular sizes to allow for the possible effects of size on stabilization by crosslinking to be examined; 2) they all process the same basic type of substrate (i.e. carbohydrates), but of a broad range of sizes (i.e. disaccharides for invertase and β-galactosidase; a larger polysaccharide (starch) for α-amylase); 3) they are sensitive to thermal denaturation; 4) they are readily available and relatively inexpensive; 5) their activities are easily measured; and 6) their molecular structures are known. In addition to the aforementioned enzymes, some experiments used small peptides, nonglycosylated model enzymes (lysozyme and pepsin), and ovalbumin as a small model glycoprotein for proving the reaction between specific functional groups and the crosslinking reagent.

2.3.1 Enzymes of interest

2.3.1.1 α-Amylase from Aspergillus oryzae

α-Amylases (EC 3.2.1.1) occur widely in nature, where they hydrolyze endo α-1,4-glycosidic bonds in starch and related compounds, to produce glucose, maltose and other oligosaccharides (Janecek and Baláž, 1992). The α-amylase family of enzymes has been

reviewed extensively in the literature (Kuriki and Imanaka, 1999; Maarel *et al.*, 2002; MacGregor, 1988, 1993; MacGregor *et al.*, 2001; Wong and Robertson, 2003), and depending on their source, differ greatly in thermostability. For example, some of the bacterial α-amylases are able to withstand temperatures in excess of 70 °C for long periods, whereas the fungal α-amylase of *Aspergillus oryzae* is denatured within 40-minutes at 50 °C at pH 6–7. *A. oryzae* α-amylase is of interest in this work because of its low thermostability and, therefore, offers a significant potential for improvement. The investigation of the thermal stability of *A. oryzae* α-amylase has been cited previously (Raviyan *et al.*, 2003).

A. oryzae alpha amylase is known commercially as Taka-Amylase A, TAA for short, and also as 1,4-alpha-D-glucan glucanohydrolase. It is a monomeric glycoprotein with a molecular weight that varies between 51 to 51.7 kDa (Isemura and Fujita, 1957a, b; Stein *et al.*, 1960). It is a metaloenzyme that has tightly bound calcium ion which is required for stability (Janecek and Baláž, 1992). Residues involved in calcium binding are Asn-121, Glu-162, Asp-175, Asp-206, His-210, and Glu-230. The pH and temperature optima are pH 5.0 and 50-60 °C, respectively. At these temperatures, however, the enzyme has a relatively short lifetime (Wiseman, 1975). Taka-amylase is used in baking processes where it is eventually denatured by heat (Wiseman, 1975). The molecular structure of Taka-amylase is known (Matsuura *et al.*, 1984) and its coordinates are deposited in the RCSB Protein Data Bank (www.rcsb.org). Its 478 amino acid residues (Table 2.3) are arranged in two globular domains containing both α-helix and β-sheet regions (Figure 2.7) (Swift *et al.*, 1991) The isoelectric point (pI) is 4.52.

The N-terminal domain consists of residues 1–376 while residues 385–478 form the C-terminal domain. The domains are connected by residues 377–384 (Amylase Research Society of Japan., 1988). Complete amino acid sequence has been reported (Toda *et al.*, 1982) (Table 2.3).

Table 2.3 The amino acid composition of alpha amylase from *Aspergillus oryzae*

Amino acid	Number of residues/molecule	Residues (%)/molecule
1. Ionizable side chains		
1.1 Cationic		
Arginine	10	2.1
Lysine	20	4.2
Histidine	7	1.5
1.2 Anionic		
Aspartic acid	42	8.8
Glutamic acid	12	2.5
2. Polar side chains		
Serine	36	7.5
Threonine	40	8.4
Tyrosine	34	7.1
Asparagine	26	5.4
Glutamine	19	4.0
3. Hydrophobic side chains		
Glycine	42	8.8
Alanine	37	7.7
Valine	29	6.1
Leucine	33	6.9
Isoleucine	28	5.9
Proline	21	4.4
Phenylalanine	14	2.9
Tryptophan	10	2.1
Methionine	9	1.9
Cysteine	9	1.9
Total amino acid residues	478	100

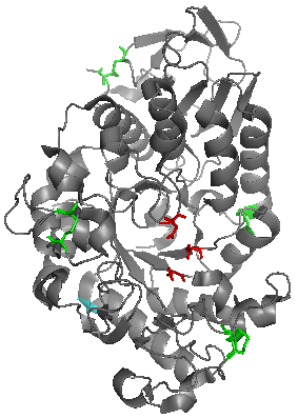

Figure 2.7 Structure of *Aspergillus oryzae* Taka-amylase [PDB 3KWX (positions 22-499)] drawn using PyMOL (Delano, 2002). Disulfide bridges are shown in green (Cys-30-38, Cys-150-164, Cys-240-283 and Cys-441-475), Active site residues are shown in red (Asp-206, 297 and Glu-230) and Asn carrying N-linked glycan is shown in light blue (N-197) (Matsuura *et al.*, 1984).

2.3.1.2 β-Galactosidase from *Aspergillus oryzae*

Beta-galactosidase (EC 3.2.1.23), or lactase, is used to hydrolyze β-1,4-glycosidic bond in lactose to produce glucose and galactose (Baret, 1987; Panesar *et al.*, 2006). β-galactosidase is produced by many microorganisms and by mammals. β-galactosidase of the bacterium *Escherichia coli* is perhaps the best known (Goldberg, 1969; Huber *et al.*, 1994; Kuby and Lardy, 1953; Matthews, 2005), but is not accepted for use in food processing (Gerhartz, 1990) in view of the intestinal origins of *E. coli*. The structures and properties of other β-galactosidases have been reported in the literature (Fowler and Zabin, 1983; Poltorak *et al.*, 2007), where the role of the quaternary structure of β-galactosidases in thermal inactivation process has been discussed (Shishkin *et al.*, 1990).

The β-galactosidase of interest in this study is that produced by the filamentous fungus *Aspergillus oryzae*, as this enzyme is widely used in the food industry. This extracellular glycoprotein contains approximately 10% (g residue/100 g protein) of glycan chains consisting of glucose, galactose, mannose and glucosamine residues (Fraguas *et al.*, 1999; Mega and Matsushima, 1979). The carbohydrate is attached to asparagine residues 159, 373, 402, 453, 478, 522, 622, 760, 777, 805 and 914. The enzyme has a molecular weight of 56-59 kDa by SDS-PAGE, 105 kDa by SEC and sucrose density gradient centrifugation, and 112 kDa by analytical centrifugation (Mega and Matsushima, 1979; Tanaka *et al.*, 1975). The active enzyme is a homodimer and has

an isoelectric pH of 4.4 (Mega and Matsushima, 1979; Tanaka *et al.*, 1975), with temperature and pH optima of 50–60 °C and pH 4–5, respectively (Mahoney, 2003; Uhlig and Linsmaier-Bednar, 1998). The denaturation kinetics of β-galactosidase have been studied previously (Yoshioka *et al.*, 1994). Its primary structure contains 1,005 amino acid residues (Table 2.4), and its structure is shown in Figure 2.8.

Table 2.4 The amino acid composition of β-galactosidase from *Aspergillus oryzae*

Amino acid	Number of residues/molecule	Residues (%)/molecule
1. Ionizable side chains		
1.1 Cationic		
Arginine	33	3.3
Lysine	50	5.0
Histidine	20	2.0
1.2 Anionic		
Aspartic acid	58	5.8
Glutamic acid	50	5.0
2. Polar side chains		
Serine	87	8.7
Threonine	66	6.6
Tyrosine	55	5.5
Asparagine	51	5.1
Glutamine	26	2.6
3. Hydrophobic side chains		
Glycine	103	10.2
Alanine	73	7.3
Valine	59	5.9
Leucine	91	9.1
Isoleucine	47	4.7
Proline	59	5.9
Phenylalanine	45	4.5
Tryptophan	20	2.0
Methionine	7	0.7
Cysteine	5	0.5
Total amino acid residues	1005	100

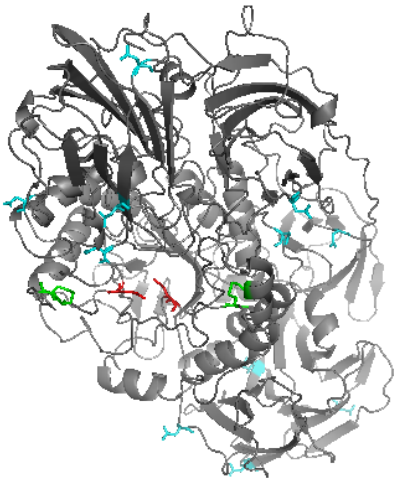

Figure 2.8 Structure of β-galactosidase from *Aspergillus oryzae* [PDB Q2UCU3 (positions 41-1,005)] drawn by PyMOL (Delano, 2002). Disulfide bridges are shown in green (Cys-205-206 and Cys-266-315), active site residues are shown in red (Glu-200 and Glu-298)] and Asns carrying N-linked glycans are shown in light blue (N-156, N-373, N-402, N-453, N-478, N-522, N-622, N-760, N-777, N-805 and N-914).

2.3.1.3 Invertase from Saccharomyces cerevisiae

Invertase (EC 3.2.1.26), sucrase, saccharase, or beta-fructofuranosidase, catalyzes the hydrolysis of terminal non reducing β-D-fructofuranosidase of sucrose to produce glucose and fructose. It occurs widely in microorganisms and was first isolated in 1860 by Berthelot using alcohol precipitation (Neumann and Lampen, 1967). Bakers' yeast *Saccharomyces cerevisiae* contains both intracellular and extracellular invertases with molecular weights of about 135 kDa and 270 kDa, respectively (Cantarella *et al.*, 2003; Gascón *et al.*, 1968). The enzyme used in this work was the extracellular invertase. This enzyme is a dimeric glycoprotein, composed of about 1,064 amino acid residues (Table 2.5). Invertase polymorphism in yeast has been associated with variable states of oligosaccharide chain phosphorylation (Frevert and Ballou, 1982). The extracellular enzyme molecule consists of 50% of phosphomanan and 3% of glucosamine (Moreno *et al.*, 1975; Wiseman and Woodward, 1975). Glycan chains composed of 18-20 units are attached to asparagine (N-linked polysaccharide) on one subunit of the protein (Lehle *et al.*, 1979; Moreno *et al.*, 1990). Removing the carbohydrate with endo-β-N-acetyl-glucosaminidase H from *Streptomyces plicatus* produces two identical 60 kDa subunits

on SDS-PAGE (Trimble and Maley, 1977). The structure of the extracellular invertase is shown in Figure 2.9.

Table 2.5 The amino acid composition of invertase from *Saccharomyces cerevisiae*

Amino acid	Number of residues/molecule	Residues (%)/molecule
1. Ionizable side chains		
1.1 Cationic		
Arginine	26	2.4
Lysine	52	4.9
Histidine	8	0.8
1.2 Anionic		
Aspartic acid	64	6.0
Glutamic acid	60	5.6
2. Polar side chains		
Serine	96	9.0
Threonine	78	7.3
Tyrosine	62	5.8
Asparagine	88	8.3
Glutamine	38	3.6
3. Hydrophobic side chains		
Glycine	62	5.8
Alanine	68	6.4
Valine	58	5.5
Leucine	78	7.3
Isoleucine	38	3.6
Proline	52	4.9
Phenylalanine	78	7.3
Tryptophan	32	3.0
Methionine	22	2.1
Cysteine	4	0.4
Total amino acid residues	1,064	100

Figure 2.9 Structure of a monomeric extracellular invertase (*Saccharomyces cerevisiae*) [PDB P00724 (positions 26-516)] drawn by PyMOL (Delano, 2002). Active site residue is shown in red (Asp-42) and Asns carrying N-linked glycans are shown in light blue (N-64, N-111, N-118, N-165, N-266, N-275, N-356, N-369, N-384 and N-398.

Glycosylation has been shown to have no effect on the thermal stability of invertase (Schülke and Schmid, 1988). Invertase has an isoelectric point of 4.61 and is active over a broad range of pH (3.5–5.5), with an optimal pH of 4.5. The enzyme is most active over the temperature range of 50–60 °C with an optimum temperature at 55 °C in dilute sucrose solution. In the absence of substrate, almost all activity is lost within 15 min at 65 °C. However, the enzyme is stable at up to 70 °C in concentrated solutions of sucrose. The thermal inactivation parameters (K_m and v_{max}) for native invertase have been studied previously (Kaplan *et al.*, 1997). The structure and properties of yeast invertase have been well studied (Chu *et al.*, 1983; Kern *et al.*, 1992; Moreno *et al.*, 1975; Myrbäck, 1957; Neumann and Lampen, 1969; Trimble and Maley, 1977).

2.3.2 Enzyme and protein models

2.3.2.1 Lysozyme from hen egg white

Lysozyme or mucopeptide N-acetyl-muramoylhydrolase from hen egg white (E.C. 3.2.1.17) is a small enzyme which has a molecular weight of 14.4 kDa by centrifugation and 14.3 kDa by amino acid analysis (Hash, 1974). The lysozyme molecule contains 129 amino acid residues and 4 disulfide bonds as shown in Figure 2.10 (Fokunang *et al.*, 2005). The amino acid composition of this single polypeptide is shown in Table 2.6. Its

catalytic activity is based on its ability to hydrolyse β-(1,4) glycosidic bonds between N-acetylglycosamine and N-acetylmuramic acid of the peptidoglycan polymer in the cell wall of bacteria. Hen egg white lysozyme is a basic protein with an isoelectric pH of 11.1. Lysozyme is active at neutral pH and is reasonably stable to high temperatures at acidic pH (Smolelis and Hartsell, 1952), a stability associated with the 4 disulfide bonds constraining the polypeptide chain.

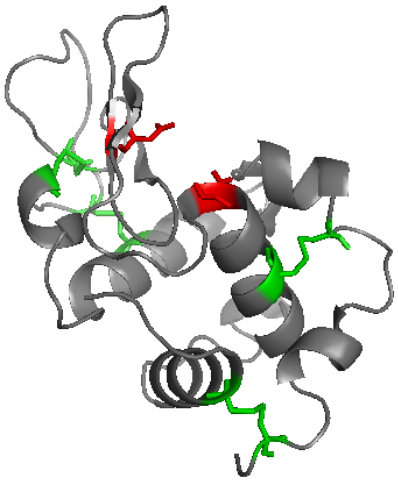

Figure 2.10 The structure of hen egg white lysozyme (PDB 3A8Z) drawn by PyMOL (Delano, 2002). Disulfide bridges are shown in green (Cys-6-127, Cys-30-115, Cys-64-80 and Cys-76-94) and Active site residues are shown in red (Glu-35 and Asp-52)] (Phillips, 1974).

Table 2.6 The amino acid composition of lysozyme from hen egg white (Lewis *et al.*, 1950; Thomson, 1955)

Amino acid	Number of residues/molecule	Residues (%)/molecule
1. Ionizable side chains		
1.1 Cationic		
Arginine	10	7.8
Lysine	8	6.2
Histidine	2	1.6
1.2 Anionic		
Aspartic acid	7	5.4
Glutamic acid	2	1.6
2. Polar side chains		
Serine	10	7.8
Threonine	7	5.4
Tyrosine	3	2.3
Asparagine	13	10.1
Glutamine	3	2.3
3. Hydrophobic side chains		
Glycine	12	9.3
Alanine	12	9.3
Valine	7	5.4
Leucine	7	5.4
Isoleucine	5	3.9
Proline	2	1.6
Phenylalanine	3	2.3
Tryptophan	6	4.7
Methionine	2	1.6
Cysteine	8	6.2
Total amino acid residues	129	100

2.3.2.2 Pepsin from porcine mucosa

Pepsin (E.C. 4.3.3.1) is a proteolytic enzyme found in the stomach of mammals. The enzyme is secreted as inactive pepsinogen by the stomach mucosa and it is activated through cleavage into the following polypeptides: a minor pepsins, B (parapepsin I); C (gastricsin); D and a major pepsin, A. Porcine pepsin A has a molecular weight of 34.6 kDa with 327 amino acid residues (Table 2.7). The enzyme has 2 domains, is monomeric, and is made up of mainly beta pleated sheet with many acidic residues (Figure 2.11) and

has a low pI. The enzyme has an optimal pH between 1 and 4 and is irreversibly denatured at pH ≥ 7. Its optimal activity temperature is 37-42 °C under acidic conditions.

Table 2.7 The amino acid composition of procine pepsin (Tang *et al.*, 1973)

Amino acid	Number of residues/molecule	Residues (%)/molecule
1. Ionizable side chains		
1.1 Cationic		
Arginine	2	0.6
Lysine	1	0.3
Histidine	1	0.3
1.2 Anionic		
Aspartic acid	30	9.2
Glutamic acid	13	4.0
2. Polar side chains		
Serine	43	13.1
Threonine	27	8.3
Tyrosine	15	4.6
Asparagine	12	3.7
Glutamine	13	4.0
3. Hydrophobic side chains		
Glycine	35	10.7
Alanine	16	4.9
Valine	22	6.7
Leucine	27	8.3
Isoleucine	25	7.6
Proline	15	4.6
Phenylalanine	14	4.3
Tryptophan	5	1.5
Methionine	4	1.2
Cysteine	6	1.8
Total amino acid residues	327	100

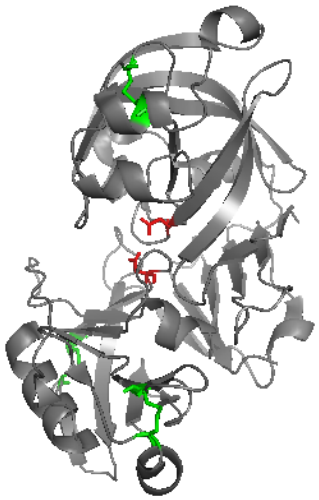

Figure 2.11 The structure of porcine pepsin (PDB 1YX9) drawn by PyMOL (Delano, 2002). Disulfide bridges are shown in green (Cys-45-50, Cys-206-210 and Cys-249-282) and active site residues are shown in red (Asp-32 and Asp-215)].

2.3.2.3 Ovalbumin from chicken egg white

Ovalbumin is a glycoprotein found mainly in chicken egg white. It is a monomer with a molecular weight between 45 and 46 kDa containing 385 amino acid residues (Nisbet *et al.*, 1981; Smith, 1966). The molecular structure and amino acids composition of ovalbumin are shown in Figure 2.12 and Table 2.8, respectively. The carbohydrate moieties are N linked and can be complex (Hughes, 1983). It has a pI of 4.7 (Moritz and Simpson, 2005; Poltorak *et al.*, 2007) and is heat stable to 80 °C at neutral pH (Tani *et al.*, 1997).

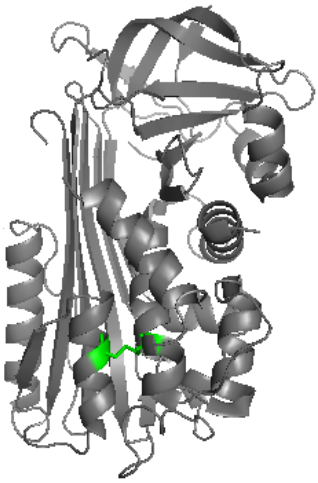

Figure 2.12 The structure of chicken egg white ovalbumin (PDB 1UGH) drawn by PyMOL (Delano, 2002). Disulfide bridge is shown in green (Cys-73-120) (Stein *et al.*, 1991; Tani *et al.*, 1997).

Table 2.8 The amino acid composition of chicken egg white ovalbumin (Nisbet *et al.*, 1981; Smith, 1966)

Amino acid	Number of residues/molecule	Residues (%)/molecule
1. Ionizable side chains		
1.1 Cationic		
Arginine	15	3.9
Lysine	20	5.2
Histidine	7	1.8
1.2 Anionic		
Aspartic acid	14	3.6
Glutamic acid	33	8.6
2. Polar side chains		
Serine	38	9.9
Threonine	15	3.9
Tyrosine	10	2.6
Asparagine	17	4.4
Glutamine	15	3.9
3. Hydrophobic side chains		
Glycine	19	4.9
Alanine	35	9.1
Valine	31	8.1
Leucine	32	8.3
Isoleucine	25	6.5
Proline	14	3.6
Phenylalanine	20	5.2
Tryptophan	3	0.8
Methionine	16	4.2
Cysteine	6	1.6
Total amino acid residues	385	100

2.4 Intramolecular crosslinking of an enzyme molecule

Many factors can influence whether intramolecular crosslinking occurs and its specific characteristics. For example, the size of the protein molecule and its concentration in solution determine the average spacing between molecules and this affects whether intramolecular crosslinking will occur in preference to intermolecular crosslinking. The nature of the protein (e.g. acid protein, basic protein) and its size determine the types of

functional groups that may be available on its surface for crosslinking. The size of the molecule may affect the average spacing between the adjacent crosslinkable functional groups on its surface. Also, the nature of the functional groups at the active site of the enzyme will influence whether reaction with a specific crosslinking reagent might inactivate the enzyme as a consequence of crosslinking. The nature of the functional group on the crosslinking reagent will affect which functional groups of the enzyme the crosslinker binds to. The length of the crosslinker relative to the average intermolecular spacing among the enzyme molecules in solution will affect whether crosslinking is predominantly intermolecular or intramolecular. In sufficiently dilute solution of the enzyme, the length of the crosslinker will determine which two functional groups on the surface of the enzyme are able to crosslink. These aspects are considered in the following sections.

2.4.1 Size of enzyme molecule (Erickson, 2004)

Most enzymes are globular and have the average partial specific volume of 0.73 cm^3/g. Therefore the volume of an enzyme molecule of molar mass M (Da) can be calculated as follows:

$$V\,(nm^3) = \frac{(0.73\ cm^3/g)\times(10^{21}\ nm^3/cm^3)}{(6.023\times10^{23}\ Da/g)}\times M\,(Da), \qquad (2.1)$$

where:

0.73 = the average partial specific volume (cm^3/g)

6.023×10^{23} = Avogadro's number (mol^{-1})

Thus, if the protein molecule is assumed to be spherical, its radius (R_{min}) would be:

$$R_{min}\,(nm) = (3V/4\pi)^{1/3} \qquad (2.2)$$

The protein shape is of course not an exact sphere and this generally leads to a larger apparent radius than the calculated R_{min} (Erickson, 2004).

Equation 2.1 and Equation 2.2 were used to estimate the minimum molecular radii of the enzymes and proteins of relevance in this work. The estimates are shown in Table 2.9.

Table 2.9 The estimated radii of the enzymes and protein molecules

Enzymes and protein	MW (Da)	R_{min} (nm)
Alpha amylase	51,000	2.45
Beta galactosidase	105,000	3.12
Invertase	270,000	4.27
Lysozyme	14,307	1.61
Pepsin	34,644	2.16
Ovalbumin	54,000	2.35

2.4.2 The distance between molecules in an enzyme solution (Erickson, 2004)

The average distance between molecules (center to center) in solution can be calculated. At a concentration of 1 M, one litre contains 6×10^{23} molecules. On the other hand, there are 1.66 nm^3 per molecule. Therefore, the total volume of solution available to one molecule is:

$$\frac{1 \times 10^{24}\ nm^3}{6 \times 10^{23}} = 1.66\ nm^3 \qquad (2.3)$$

The average separation (d) of molecules in a solution of molar concentration C is then calculated as follows:

$$d = 1.18C^{-1/3}, \qquad (2.4)$$

where:

d = average separation of molecules (nm)

C = concentration (M)

From Equation 2.4, the average separation of molecules was calculated at the various concentrations shown in Table 2.10. The surface-to-surface distance (dm) between enzyme molecules at molar concentration C could then be calculated:

dm = d – diameter of enzyme molecule (2.5)

Table 2.10 The relation between the concentration and the average distance between molecules

Concentration (M)	Average separation (nm)
1	1.18
10^{-3}	11.8
10^{-6}	118
10^{-9}	1,180

2.4.3 The length of the crosslinker molecules

The fully stretched backbone length of all the relevant crosslinkers was estimated on the basis of bond lengths (Silberberg, 2010). These were 1.54 Å for C–C, 1.43 Å for C–O, 1.47 Å for C–N, 1.23 Å for C=O, 1.27 Å for C=N and 1.46 Å for N–N. The estimates are shown in Table 2.11. The actual length of a crosslinker would be somewhat shorter than the estimates (Table 2.11) because the estimates disregarded the various bond angles.

Table 2.11 The theoretical fully stretched backbone length of the relevant crosslinkers

Crosslinker	Backbone length	
	nm	Å
Butyl isocyanate [$CH_3(CH_2)_3NCO$]	8.59×10^{-1}	8.59
1,4-Diisocyanatobutane [$OCN(CH_2)_4NCO$]	12.56×10^{-1}	12.56
1,6-Diisocyanatohexane [$OCN(CH_2)_6NCO$]	15.64×10^{-1}	15.64
1,8-diisocyanatooctane [$OCN(CH_2)_8NCO$]	18.72×10^{-1}	18.72
Ethyl acetimidate [$CH_3C(=NH)OC_2H_5$]	4.40×10^{-1}	4.40
Dimethyl adipimidate [$CH_3OC(=NH)(CH_2)_4C(=NH)OCH_3$]	13.42×10^{-1}	13.42
Dimethyl pimelimidate [$CH_3OC(=NH)(CH_2)_5C(=NH)OCH_3$]	14.96×10^{-1}	14.96
Dimethyl suberimidate [$CH_3OC(=NH)(CH_2)_6C(=NH)OCH_3$]	16.50×10^{-1}	16.50
Hydrazine monohydrate (NH_2NH_2)	1.46×10^{-1}	1.46
1,2-Diaminoethane [$NH_2(CH_2)_2NH_2$]	4.48×10^{-1}	4.48
1,4-Diaminobutane [$NH_2(CH_2)_4NH_2$]	7.56×10^{-1}	7.56
1,6-Diaminohexane [$NH_2(CH_2)_6NH_2$]	10.64×10^{-1}	10.64
1,8-Diaminooctane [$NH_2(CH_2)_8NH_2$]	13.72×10^{-1}	13.72
1,10-Decanediamine [$NH_2(CH_2)_{10}NH_2$]	16.80×10^{-1}	16.80
1,12-Diaminododecane [$NH_2(CH_2)_{12}NH_2$]	19.88×10^{-1}	19.88

2.4.4 Availability of surface functional groups for intramolecular crosslinking

Based on the known amino acid sequences (Section 2.3.1.1-2.3.1.3) of alpha amylase, beta galactosidase and invertase, this section discusses the availability of suitable functional groups for intramolecular crosslinking by the selected reagents of diimidoester, diisocyanate and diamine. The maximum distances between the specific functional groups on the enzyme molecules that the crosslinkers could reach were calculated by using the PyMOL Viewer software program and the enzyme structure data available at ExPASy Proteomics Server and RCSB Protein Data Bank. This analysis took into

account only the protein structure of the enzyme molecules and not the carbohydrate component. Therefore, not all the identified crosslinking scenarios could occur in practice because of the steric hindrance of the carbohydrate component.

2.4.4.1 Alpha amylase from *A. oryzae*

2.4.4.1.1 Crosslinking by diimidoesters

A fully stretched molecule of a diimidoester would have a length in the range of 4.40-16.50 Å (Table 2.11). This suggests the possibility of 10 crosslinks that could be formed on treatment of the enzyme by diimidoester series of crosslinkers. These crosslinks would be between the amino functional groups of the lysine residues of the enzyme. Specifically, crosslinks could occur between lysine residues at positions 180 and 184 with a distance of 13.10 Å; lysine residues at positions 184 and 213 with a distance of 14.51 Å; lysine residues at positions 209 and 213 with a distance of 12.12 Å; lysine residues at positions 184 and 221 with a distance of 12.64 Å; lysine residues at positions 280 and 383 with a distance of 9.26 Å; lysine residues at positions 383 and 398 with a distance of 8.36 Å; lysine residues at positions 312 and 360 with a distance of 7.32 Å; lysine residues at positions 389 and 412 with a distance of 12.62 Å; lysine residues at positions 375 and 468 with a distance of 9.25 Å; and lysine residues at positions 375 and 473 with a distance of 13.57 Å (Figure 2.13).

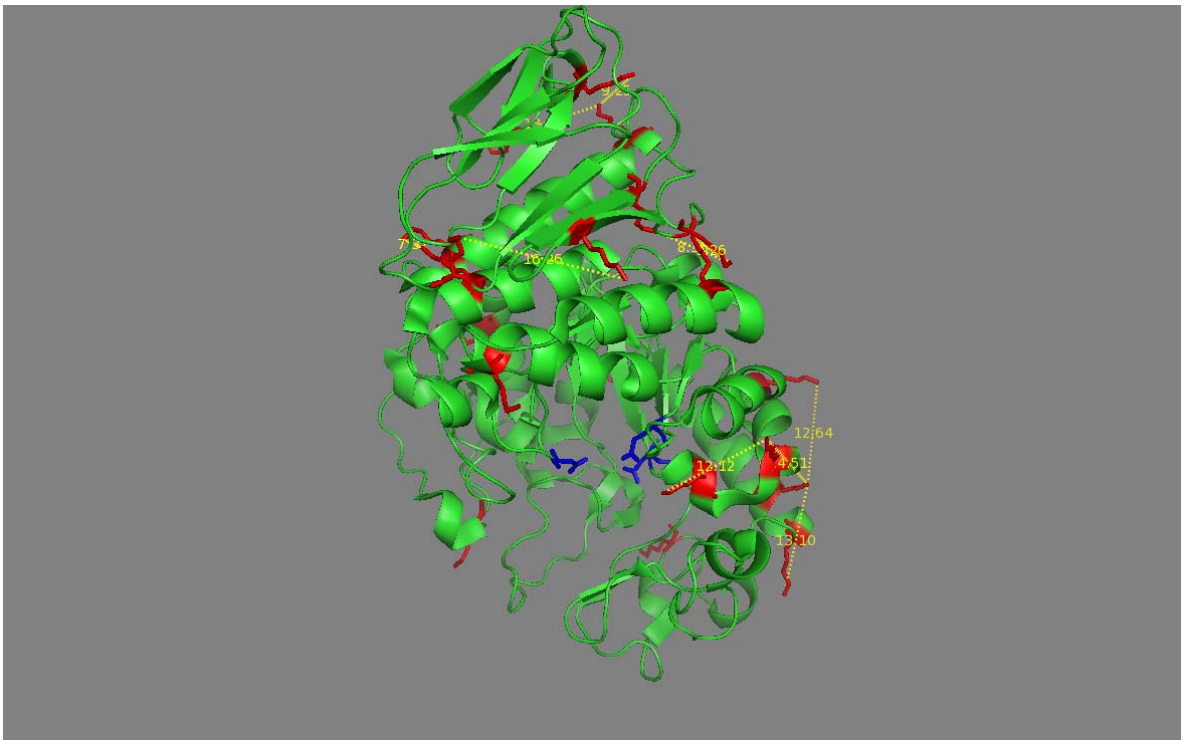

Figure 2.13 The possibilities of intramolecular crosslinking in an alpha amylase molecule treated with diimidoesters. The red colour represents lysine residues and the dark blue colour represents the active site residues (glutamic acid at position 230 and aspartic acids at positions 206 and 297).

2.4.4.1.2 Crosslinking by diisocyanates

Diisocyanates can react with several different functional groups in an enzyme molecule depending on the pH used, as explained in Section 2.1.4.2.2. The intramolecular crosslinking possibilities for amylase treated with diisocyanates at pH 5-8 are illustrated in Figures 2.14–2.17.

At pH 5, diisocyanates can react with the carboxylate side chain of aspartic acid and glutamic acid residues. This suggests a possible ~54 crosslinks in the amylase molecule (Figure 2.14).

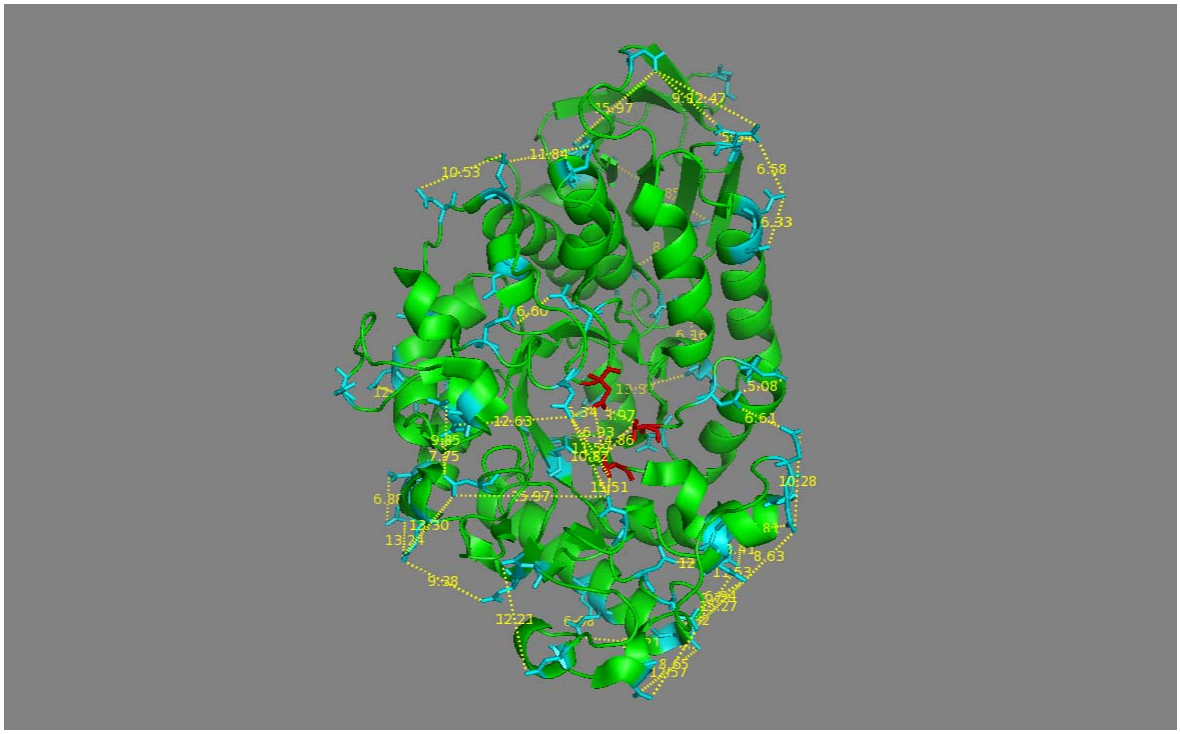

Figure 2.14 The possibilities of intramolecular crosslinking in an alpha amylase molecule treated with diimidoesters at pH 5. The light blue colour represents aspartic acid and glutamic acid residues and the red colour represents the active site residues (glutamic acid at position 230 and aspartic acids at positions 206 and 297).

At pH 6, diisocyanates can react with thiol group of cysteine residues and hydroxyl group of tyrosine residues. However, all the thiol groups in amylase molecule have already formed disulfide bonds. In this circumstance, only the hydroxyl groups of tyrosine are available to react with diisocyanates. This leads to a possible 23 crosslinks being formed in the amylase molecule (Figure 2.15).

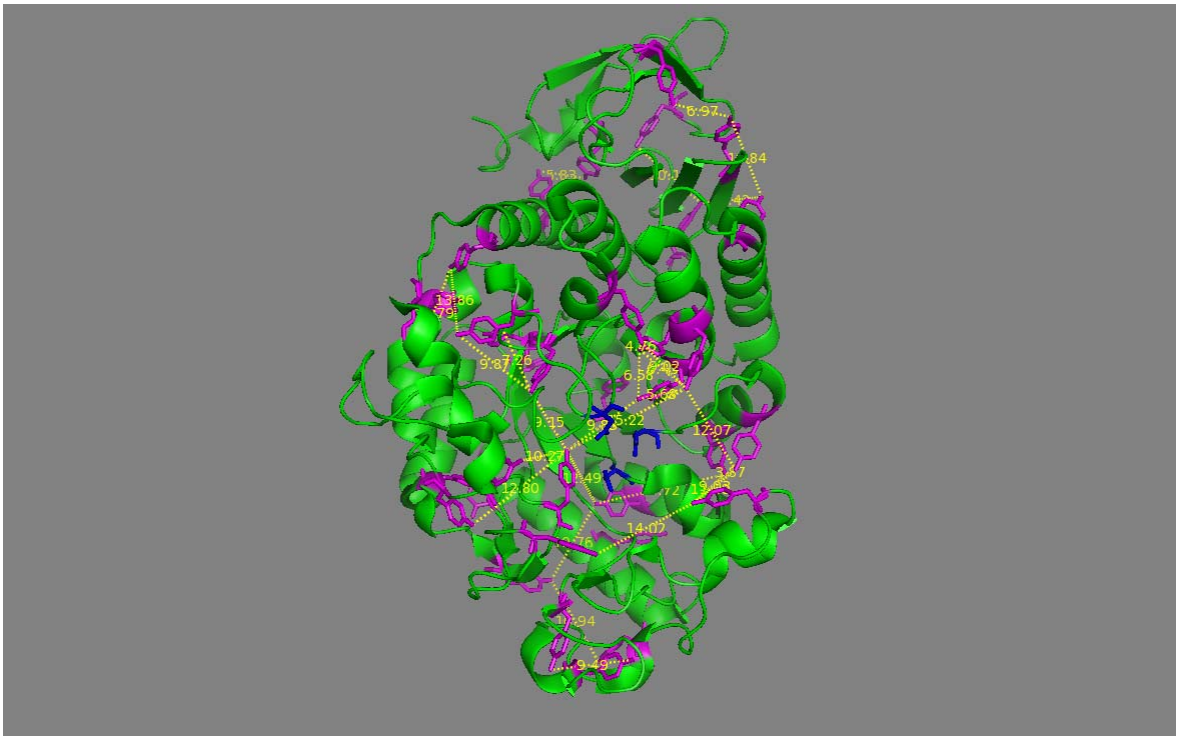

Figure 2.15 The possibilities of intramolecular crosslinking in an alpha amylase molecule treated with diimidoesters at pH 6. The purple colour represents tyrosine residues and the dark blue colour represents the active site residues (glutamic acid at position 230 and aspartic acids at positions 206 and 297).

At pH 7, the hydroxyl group of tyrosine, the amino group of lysine and the sulfhydril group of cysteine can be reacted with diisocyanates. As explained above, the sulfhydril groups are not available for crosslinking reaction. This leads to approximately 45 crosslinks in the amylase molecule (Figure 2.16).

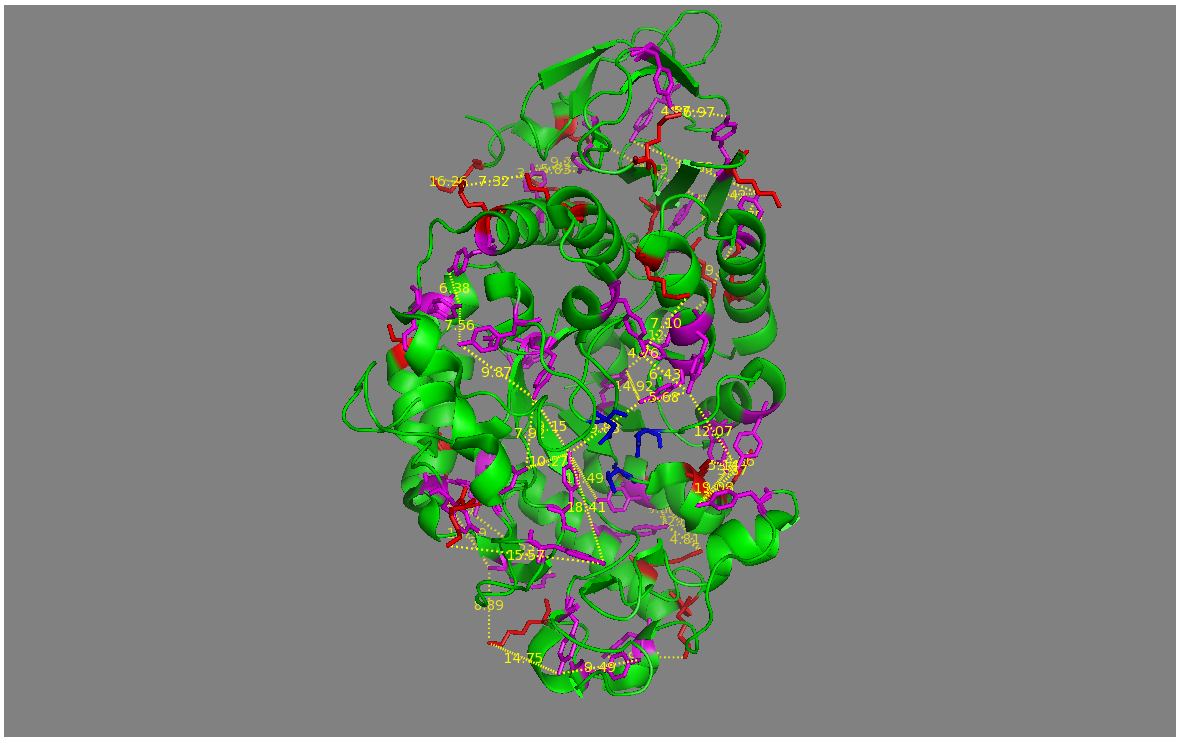

Figure 2.16 The possibilities of intramolecular crosslinking in an alpha amylase molecule treated with diimidoesters at pH 7. The purple colour represents tyrosine residues, the red colour represents lysine residues and the dark blue colour represents the active site residues (glutamic acid at position 230 and aspartic acids at positions 206 and 297).

At pH 8, diisocyanates can theoretically react with hydroxyl group of tyrosine, thiol group of cysteine, amino group of lysine and imidazole group of histidine. Excluding the already reacted thiol groups of cysteins, this leaves a possible 52 crosslinks (Figure 2.17).

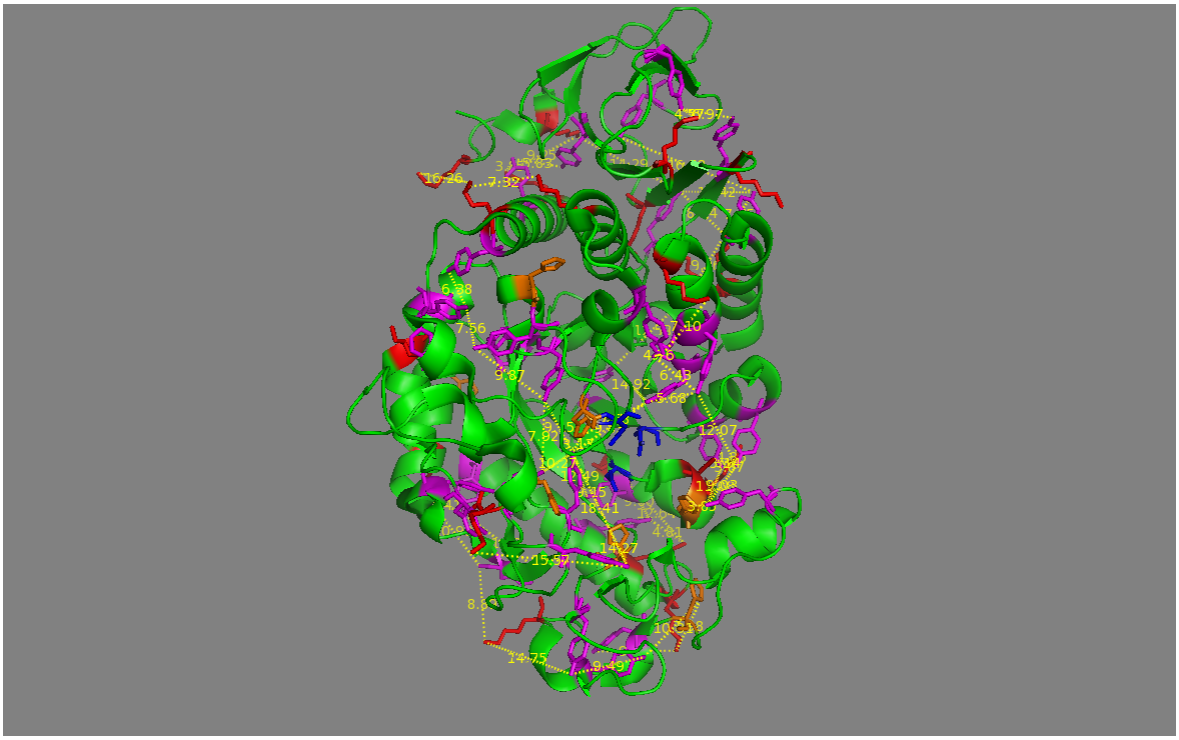

Figure 2.17 The possibilities of intramolecular crosslinking in an alpha amylase molecule treated with diimidoesters at pH 8. The purple colour represents tyrosine residues, the red colour represents lysine residues, the orange colour represents histidine residue and the dark blue colour represents the active site residues (glutamic acid at position 230 and aspartic acids at positions 206 and 297).

2.4.4.1.3 Crosslinking by diamines

Diamines can react with carboxylate groups in an enzyme molecule. For amylase this suggests a maximum of 59 possible crosslinking scenarios as shown in Figure 2.18.

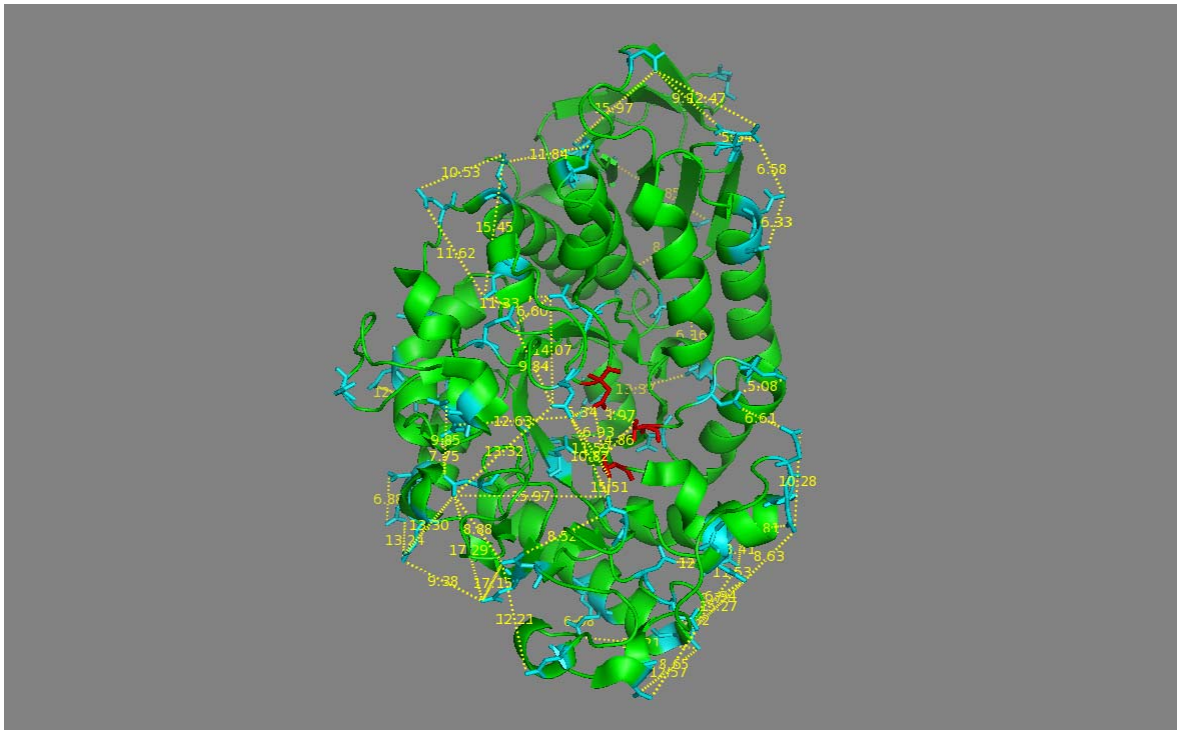

Figure 2.18 The possibilities of intramolecular crosslinking in an alpha amylase molecule treated with diamines. The purple light blue colour represents glutamic acid and aspartic acid residues and the red colour represents the active site residues (glutamic acid at position 230 and aspartic acids at positions 206 and 297).

2.4.4.2 Beta galactosidase from *A. oryzae*

2.4.4.2.1 Crosslinking by diimidoesters

Treatment of the amino functional groups of lysine residues in beta galactosidase by diimidoesters provides opportunities for 14 possible crosslinks (Figure 2.19). The possible crosslinks include the following: between lysine residues at positions 501 and 520 with a distance of 6.33 Å; lysine residues at positions 496 and 520 with a distance of 6.51 Å; lysine residues at positions 702 and 704 with a distance of 8.25 Å; lysine residues at positions 823 and 739 with a distance of 11.57 Å; lysine residues at positions 538 and 446 with a distance of 12.15 Å; lysine residues at positions 446 and 444 with a distance of 12.34 Å; lysine residues at positions 704 and 105 with a distance of 12.94 Å; lysine residues at positions 645 and 637 with a distance of 13 Å; lysine residues at positions 823 and 781 with a distance of 13.43 Å; lysine residues at positions 886 and 971 with a distance of 14.54 Å; lysine residues at positions 781 and 739 with a distance of 14.87 Å; lysine residues at positions 168 and 814 with a distance of 15.23 Å; lysine residues at

positions 902 and 668 with a distance of 15.64 Å and lysine residues at positions 814 and 902 with a distance of 15.64 Å.

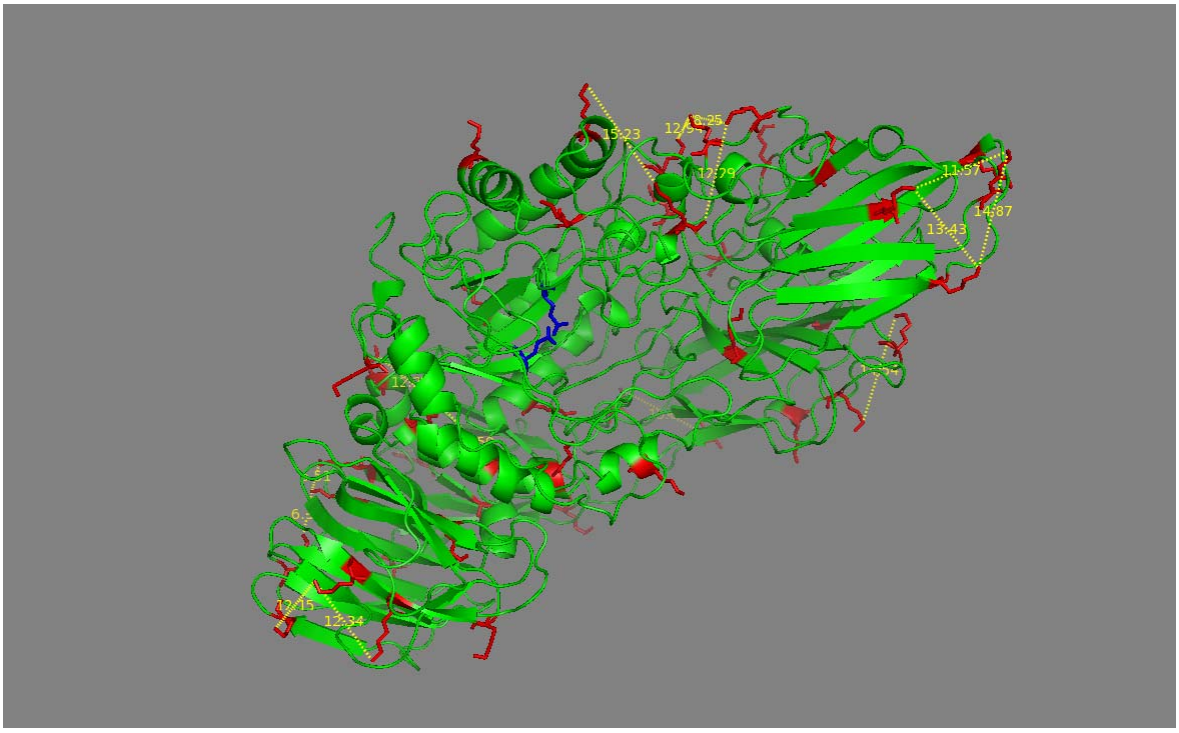

Figure 2.19 The intramolecular crosslinking possibilities for beta galactosidase treated with diimidoesters. The red colour represents lysine residues and the dark blue colour represents the active site residues (glutamic acids at positions 200 and 298).

2.4.4.2.2 Crosslinking by diisocyanates

For the crosslinking reaction carried out at pH 5, 68 possible crosslinks can be produced in a beta galactosidase molecule treated with diisocyanates (Figure 2.20). The reactive groups of the reagent molecule react with carboxylate groups of the enzyme to form the crosslinks.

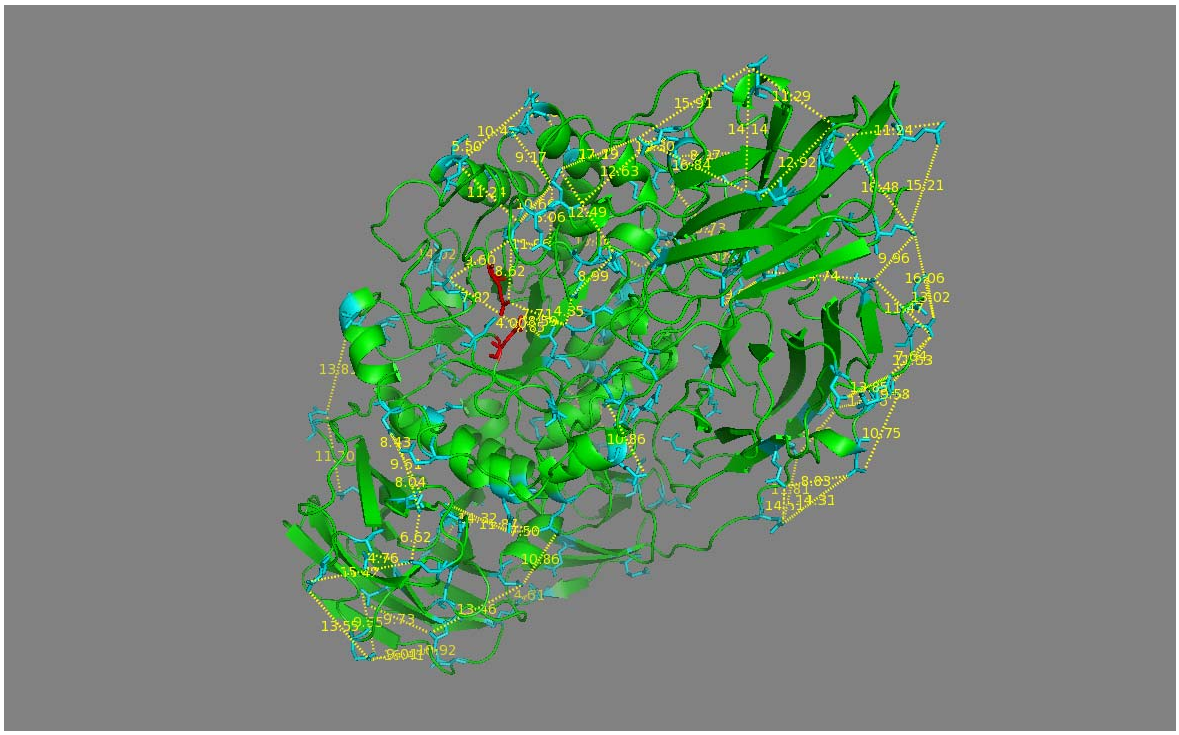

Figure 2.20 The intramolecular crosslinking possibilities for beta galactosidase treated with diisocyanates at pH 5. The light blue colour represents aspartic acid and glutamic acid residues and the red colour represents the active site residues (glutamic acids at positions 200 and 298).

If the crosslinking reaction is carried out at pH 6, the hydroxyl groups of tyrosine residues are likely to react with diisocyanates to form 34 possible crosslinks in the enzyme molecule (Figure 2.21).

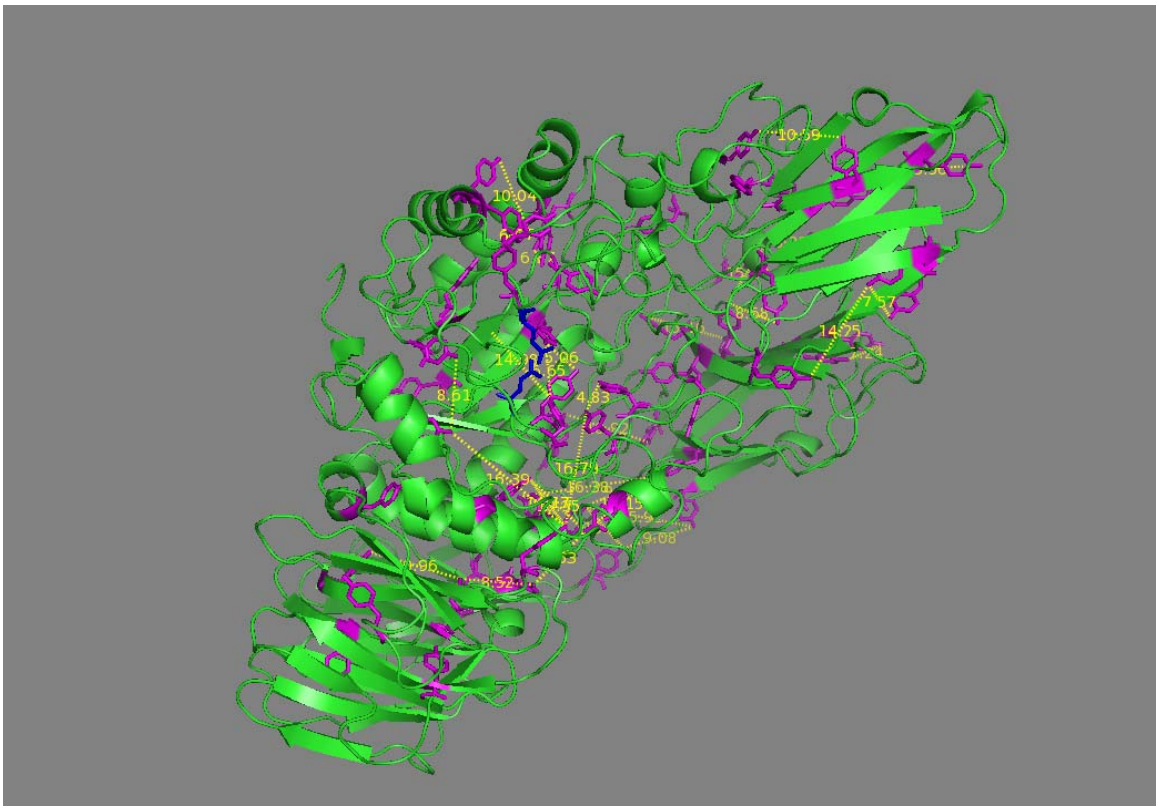

Figure 2.21 The intramolecular crosslinking possibilities for beta galactosidase treated with diisocyanates at pH 6. The purple colour represents tyrosine residues and the dark blue colour represents the active site residues (glutamic acids at positions 200 and 298).

At pH 7 of the crosslinking reaction, the reactive groups of diisocyanates can react with the amino groups of lysine residues and the phenolic hydroxyl groups of tyrosine residues. This can potentially result in 56 crosslinks being formed in beta galactosidase (Figure 2.22).

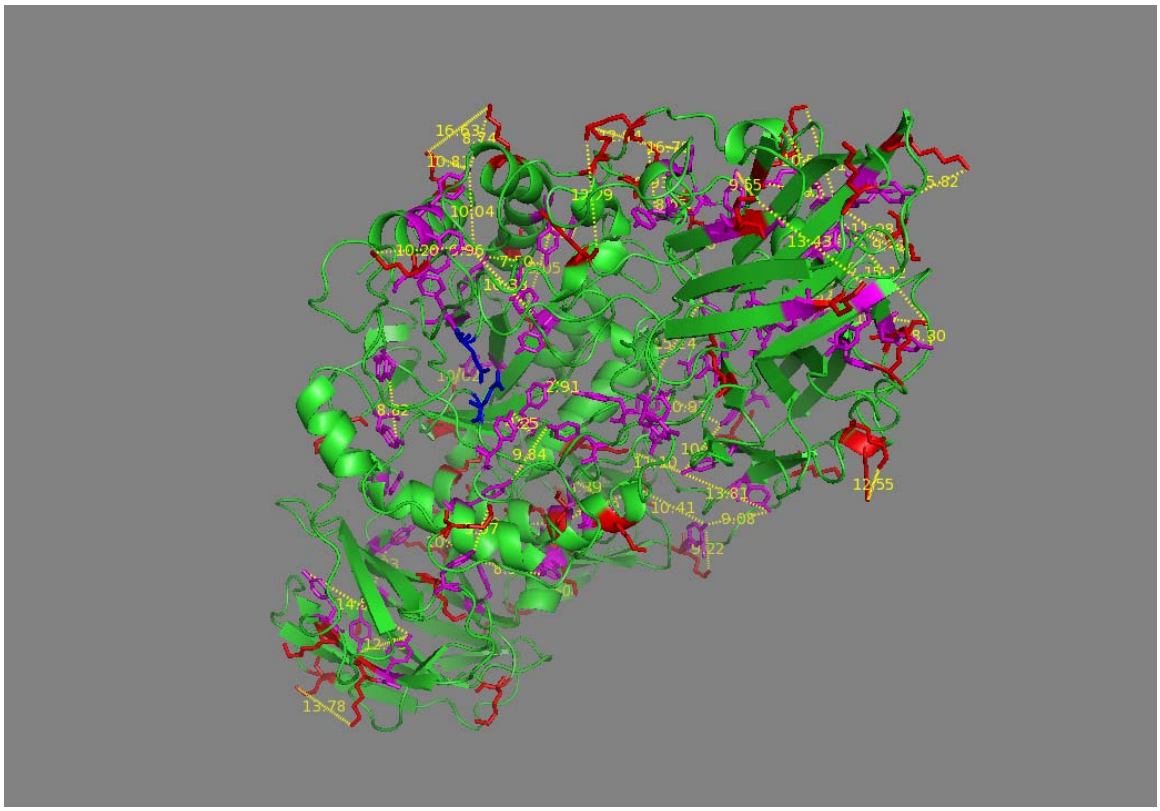

Figure 2.22 The intramolecular crosslinking possibilities for beta galactosidase treated with diisocyanates at pH 7. The purple colour represents tyrosine residues, the red colour represents lysine residues and the dark blue colour represents the active site residues (glutamic acids at positions 200 and 298).

In an alkaline reaction environment (pH 8), the number of possible crosslinks that can form in a beta galactosidase molecule treated with diisocyanates is 71 (Figure 2.23). At pH 8, the diisocyanates react with amino groups of lysine residues, the hydroxyl groups of tyrosine residues and the imidazole groups of histidine residues.

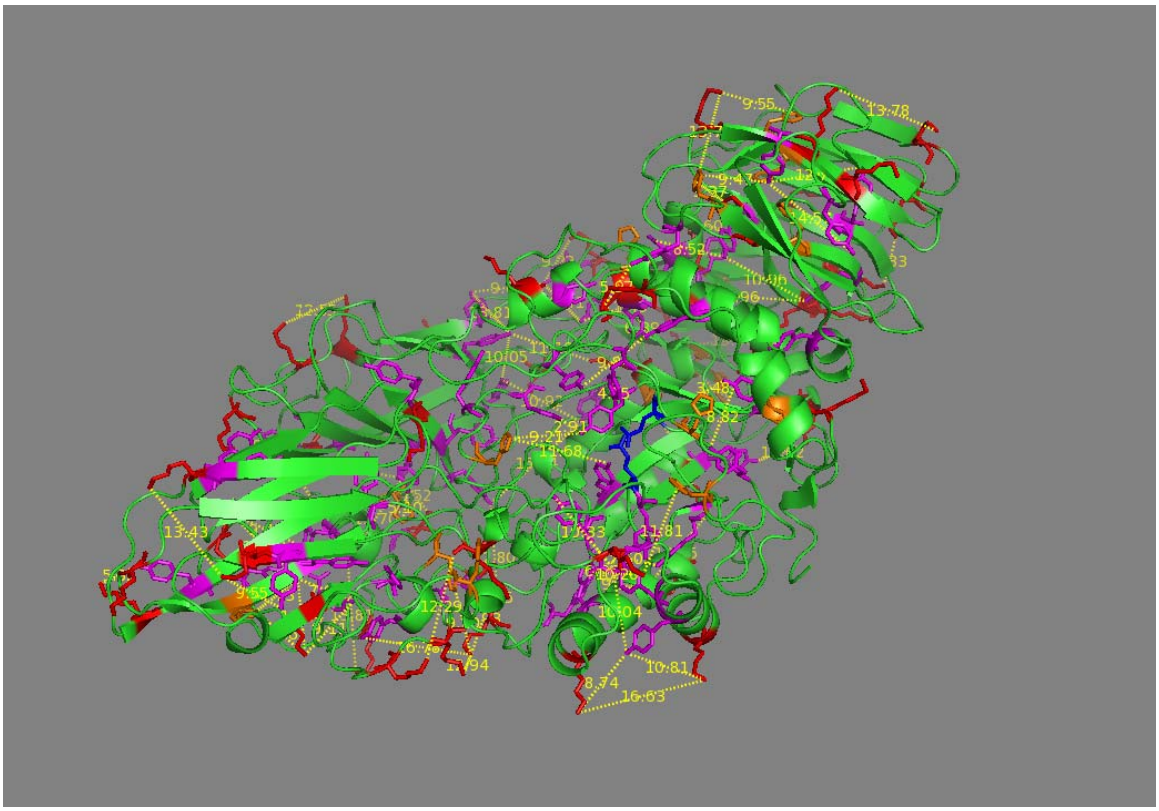

Figure 2.23 The intramolecular crosslinking possibilities for beta galactosidase treated with diisocyanates at pH 8. The purple colour represents tyrosine residues, the red colour represents lysine residues, the orange colour represents histidine residues and the dark blue colour represents the active site residues (glutamic acids at positions 200 and 298).

2.4.4.2.3 Crosslinking by diamines

Diamines react only with the carboxylate groups of aspartic acid and glutamic acid residues in an enzyme molecule. The treatment of beta galactosidase with diamine has the potential to produce 75 possible crosslinks as shown in Figure 2.24.

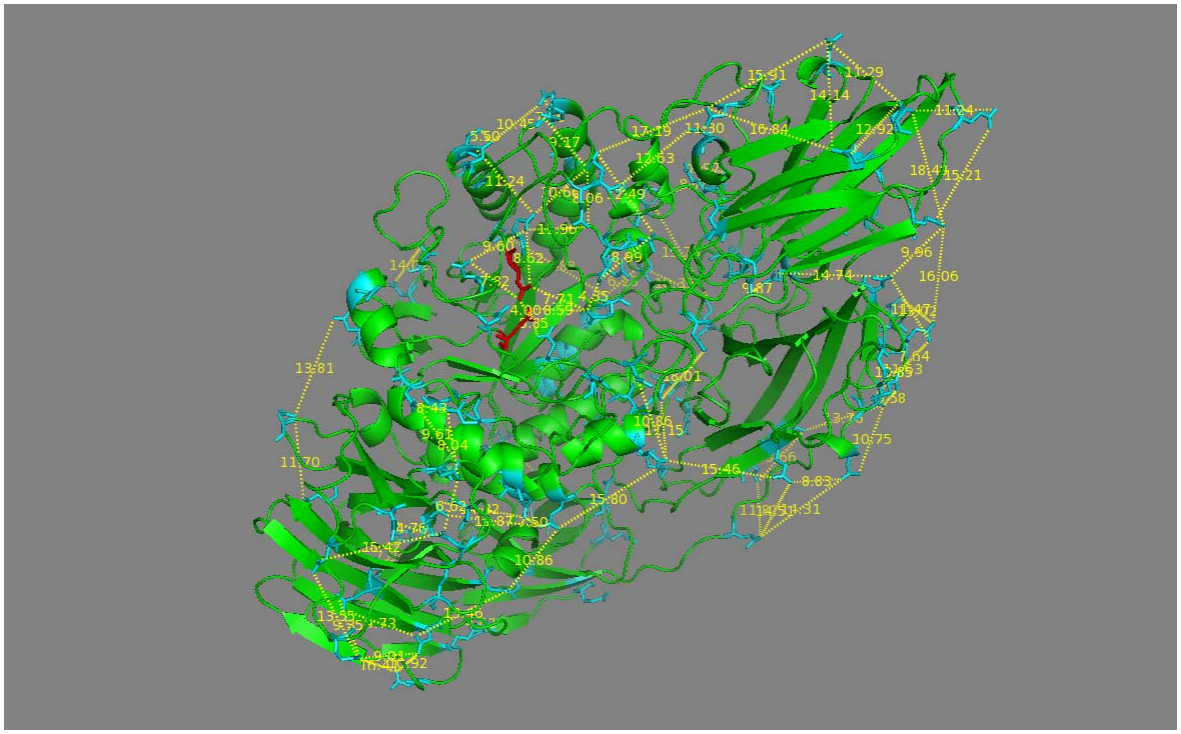

Figure 2.24 The intramolecular crosslinking possibilities for beta galactosidase treated with diamines. The light blue colour represents glutamic acid and aspartic acid residues and the red colour represents the active site residues (glutamic acids at positions 200 and 298).

2.4.4.3 Invertase from *S. cerevisiae*

2.4.4.3.1 Crosslinking by diimidoesters

Twelve possible crosslinks can be produced in a monomer of invertase on treatment with diimidoesters (Figure 2.25). Diimidoesters can react only with the amino groups of lysine residues. The possible crosslinks are: between the lysine residues at positions 284 and 446 with a distance of 4.88 Å; between the lysine residues at positions 182 and 207 with a distance of 8.70 Å; between the lysine residues at positions 51 and 54 with a distance of 9.51 Å; between the lysine residues at positions 204 and 158 with a distance of 10.01 Å; between the lysine residues at positions 331 and 350 with a distance of 11.30 Å; between the lysine residues at positions 194 and 189 with a distance of 11.48 Å; between the lysine residues at positions 350 and 475 with a distance of 11.58 Å; between the lysine residues at positions 284 and 449 with a distance of 11.99 Å; between the lysine residues at positions 466 and 350 with a distance of 13.14 Å; between the lysine residues at positions 331 and 475 with a distance of 14.09 Å; between the lysine residues at positions

284 and 444 with a distance of 13.36 Å; and between the lysine residues at positions 446 and 449 with a distance of 15.78 Å.

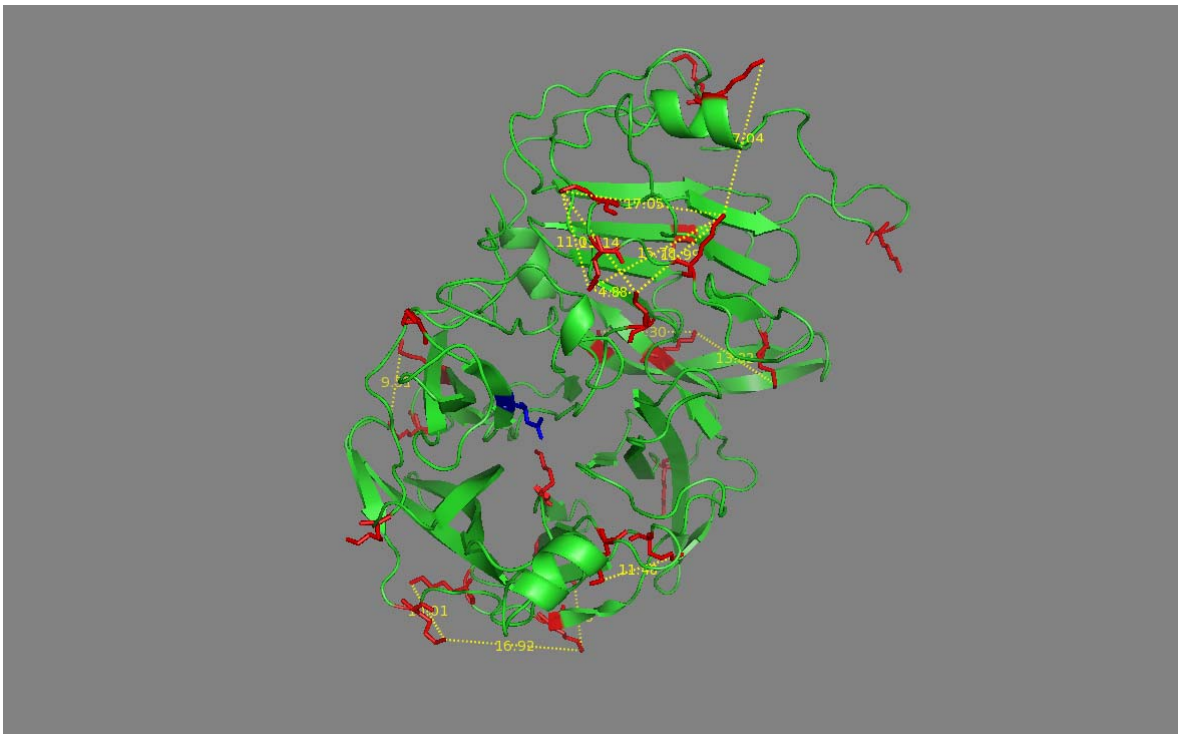

Figure 2.25 The intramolecular crosslinking possibilities in an invertase molecule treated with diimidoesters. The red colour represents lysine residues and the dark blue colour represents the active site residue (aspartic acid at position 42).

2.4.4.3.2 Crosslinking by diisocyanates

As discussed in Section 2.1.4.2.2, diisocyanates can react with different functional groups on an enzyme molecule depending on the pH of the crosslinking reaction.

Under acid conditions (pH 5), only the carboxylate groups of aspartic acid and glutamic acid residues in a monomeric invertase molecule can react with diisocyanates. This can lead to a possible 37 crosslinks being formed as shown in Figure 2.26.

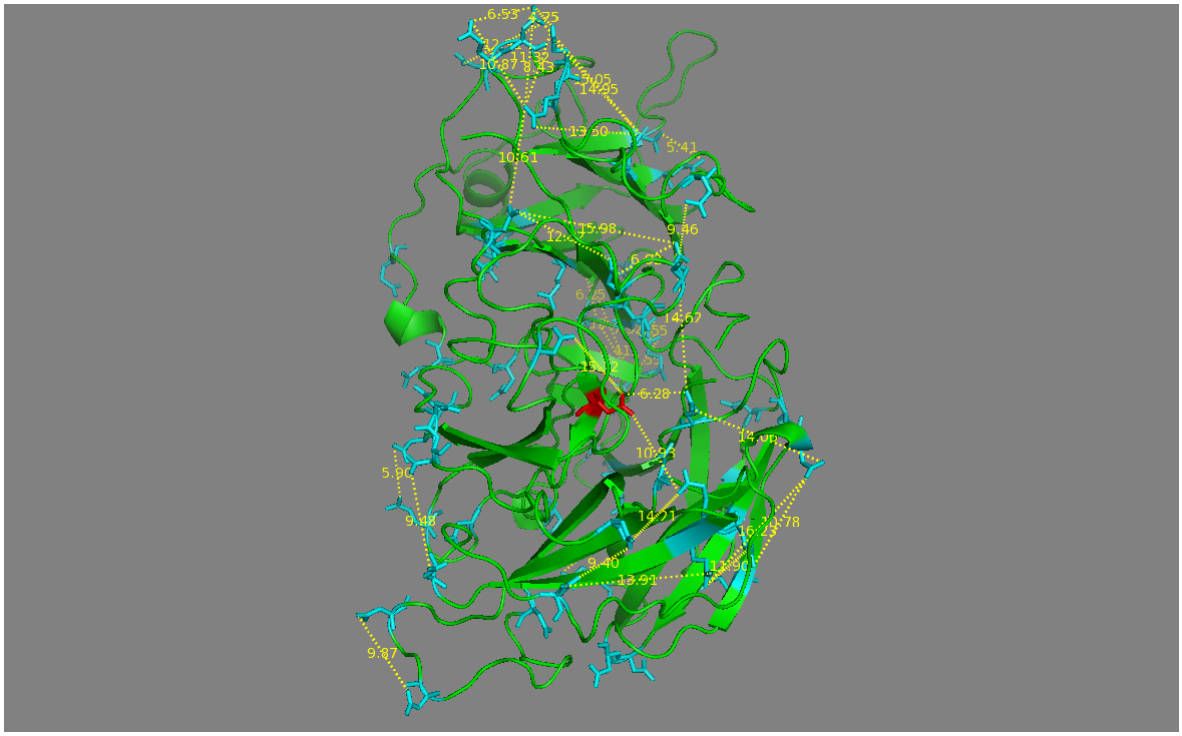

Figure 2.26 The intramolecular crosslinking possibilities in an invertase molecule treated with diisocyanates at pH 5. The light blue colour represents glutamic acid and aspartic acid residues and the red colour represents the active site residue (aspartic acid at position 42).

If the crosslinking reaction is carried out under weak acidic conditions at pH 6, 16 possible crosslinks may be generated in an invertase monomeric molecule (Figure 2.27). At pH 6, diisocyanates can react with the phenolic hydroxyl groups of tyrosine residues in the invertase molecule.

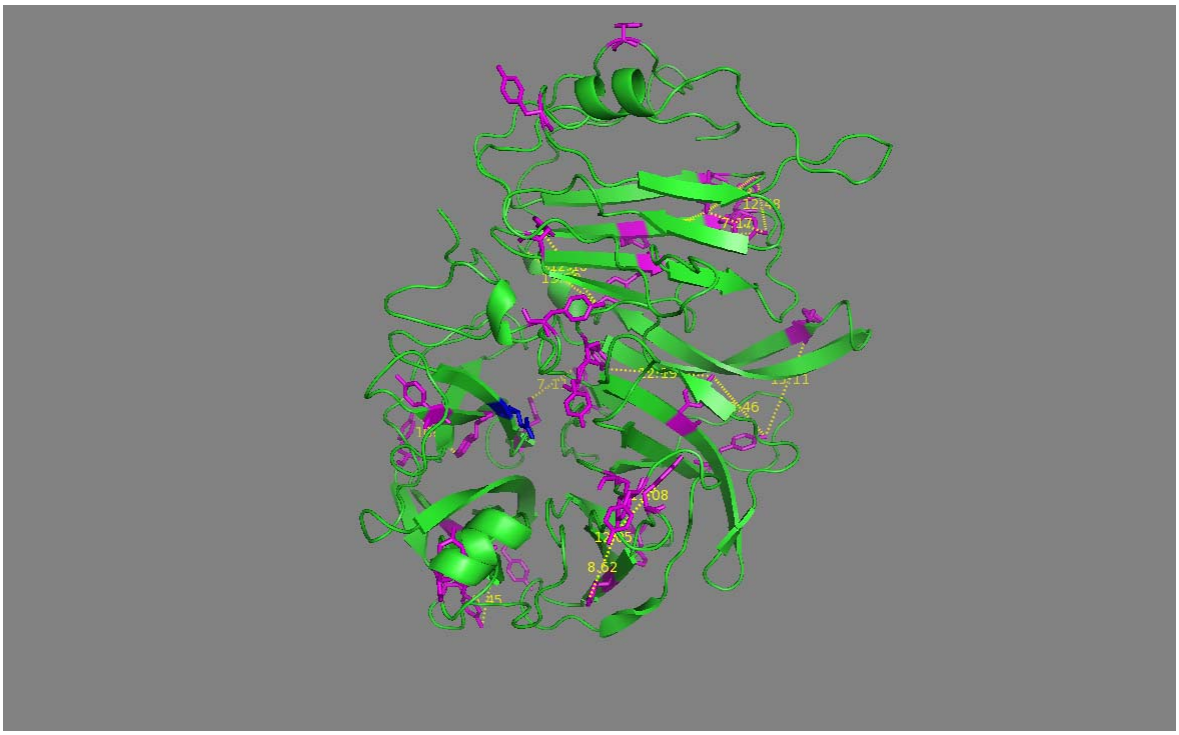

Figure 2.27 The intramolecular crosslinking possibilities in an invertase molecule treated with diisocyanates at pH 6. The purple colour represents tyrosine residues and the dark blue colour represents the active site residue (aspartic acid at position 42).

At pH 7 of the crosslinking reaction, diisocyanates react with the amino side chains of lysine residues and the hydroxyl side chains of tyrosine residues in an enzyme molecule. This can lead to a possible 38 crosslinks being formed in a monomer of invertase (Figure 2.28).

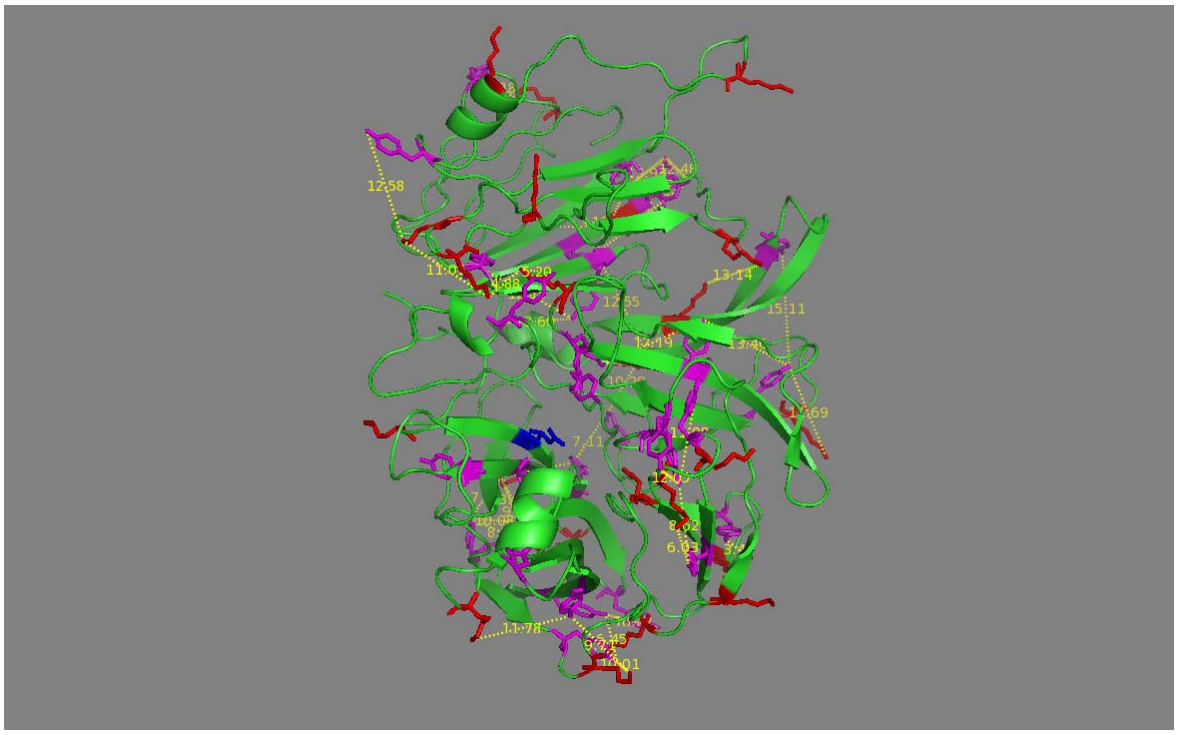

Figure 2.28 The intramolecular crosslinking possibilities in an invertase molecule treated with diisocyanates at pH 7. The purple colour represents tyrosine residues, red colour represents lysine residues and the dark blue colour represents the active site residue (aspartic acid at position 42).

A maximum of 42 possible crosslinks can be formed in a monomeric invertase molecule at pH 8 of the crosslinking reaction (Figure 2.29). Crosslinks can occur between the hydroxyl groups of tyrosine residues, the amino groups of lysine residues and the imidazole groups of histidine residues.

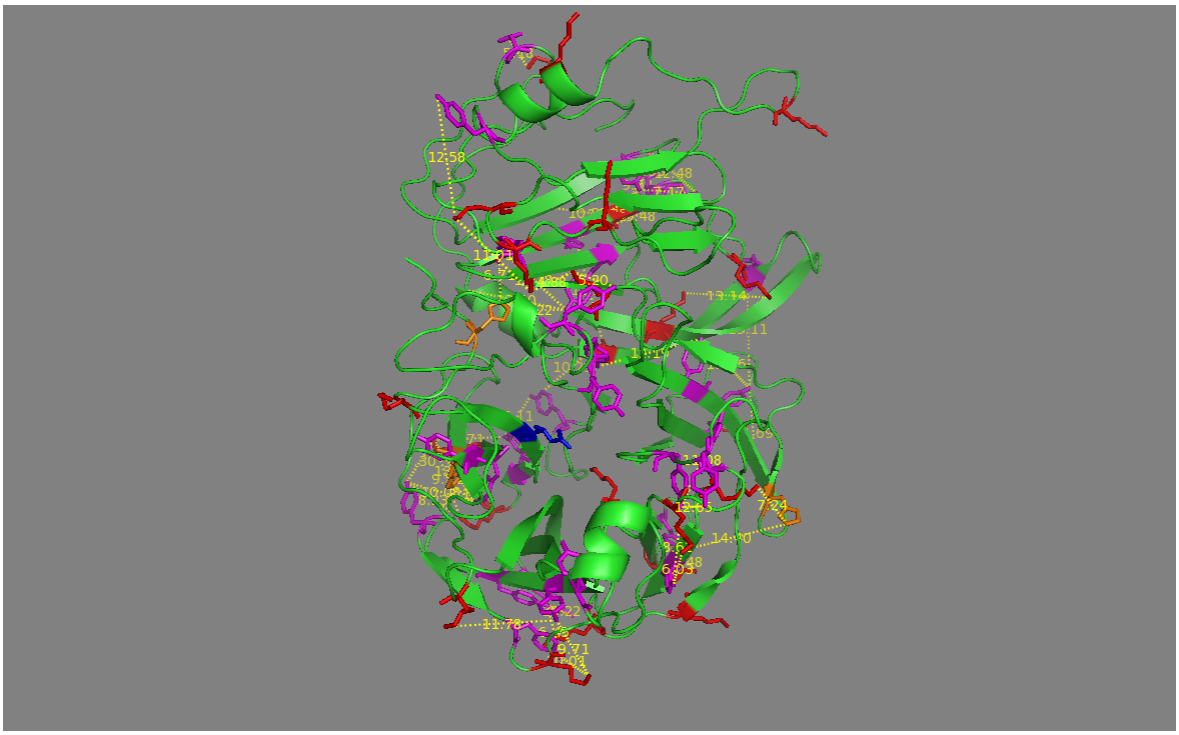

Figure 2.29 The intramolecular crosslinking possibilities in an invertase molecule treated with diisocyanates at pH 8. The purple colour represents tyrosine residues, red colour represents lysine residues, the orange colour represents histidine residues and the dark blue colour represents the active site residue (aspartic acid at position 42).

2.4.4.3.3 Crosslinking by diamines

Only the carboxylate groups of aspartic acid residues and glutamic acid residues can react with diamine so this can produce up to 48 possible crosslinks (Figure 2.30).

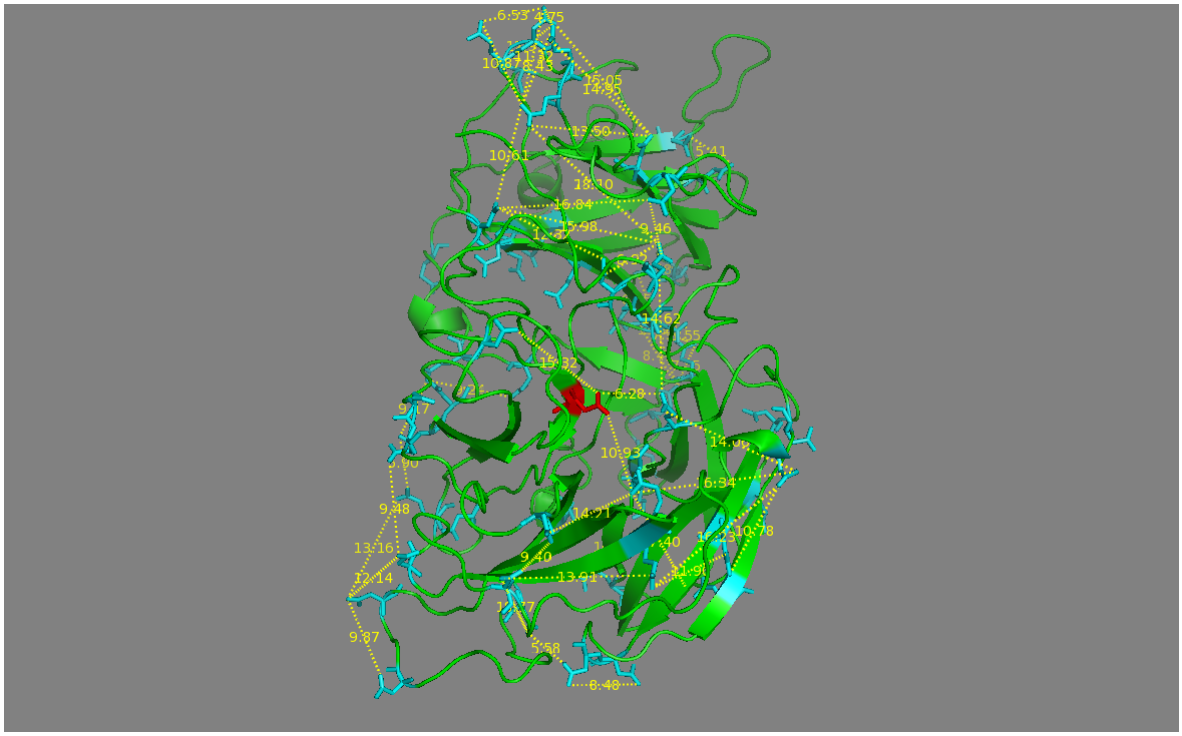

Figure 2.30 The possibilities of intramolecular crosslinking in an invertase molecule treated with diamines. The light blue colour represents glutamic acid and aspartic acid residues and the red colour represents the active site residue (aspartic acid at position 42).

2.5 Structure characterization methods for enzymes and proteins

Changes in the structures of enzymes and proteins as a consequence of various crosslinking treatments were characterized using a number of methods including polyacrylamide gel electrophoresis (Laemmli, 1970), size exclusion chromatography (SEC), dynamic light scattering (DLS), multiple angle laser light scattering (MALLS), circular dichroism (CD), high performance liquid chromatography (HPLC) and mass spectrometry (MS). These methods are briefly reviewed in Sections 2.5.1-2.5.6.

2.5.1 Size-exclusion chromatography (Striegel, 2009)

This liquid column chromatographic technique separates proteins on the basis of their size. A mixture of molecules of different sizes dissolved in a buffer solution flows through a column packed with porous gel beads. Molecules that are larger than the pore size of the beads do not enter the pores and consequently take a shorter path down the column, exiting the column earlier than the small molecules as the latter diffuse into gel

pores and take a longer meandering path down the column. Size exclusion chromatography is widely used in desalting protein solutions and for separating proteins that differ significantly in molecular weights (i.e. molecular size). Size exclusion chromatography has been further discussed by Striegel (2009).

2.5.2 Polyacrylamide gel electrophoresis PAGE (Shi and Jackowski, 1998)

At a given pH, molecules of different proteins carry a different net charge. Protein separation by polyacrylamide gel electrophoresis (Papageorgiou and Lagoyanni, 1983) is based on the migration of charged molecules on a polyacrylamide gel held in an electric field in a running buffer reservoir. Polyacrylamide gel electrophoresis can be used to characterize the size, the amount, the purity and the isoelectric point of a protein. Denaturing and non-denaturing one dimensional PAGE was used to characterize enzyme molecules before and after crosslinking. SDS-PAGE involves the use of SDS plus reducing agents dithiothreitol or mercaptoethanol followed by heating at 100 °C to completely unfold the protein prior to PAGE. In native PAGE (i.e. no prior treatment to break disulfides or unfold the protein), the protein moves on the gel in its native form. PAGE has been reviewed by Shi and Jackowski (1998).

2.5.3 Reversed-phase high performance liquid chromatography (Meyer, 2004)

High performance liquid chromatography (HPLC) is a highly efficient technique for separating proteins and peptides. A schematic of the HPLC instrument is shown in Figure 2.31. A protein sample injected at 4 (Figure 2.31) is eluted through the thermostated HPLC column 5 using the solvent system 1. The high pressure pump 3 forces the eluting solvent through the column 5 at a preset flow rate. The eluent flowing out of the column passes through a detector 7 that typically detects proteins based on UV-absorbance. The output of the detector is recorded on a chromatogram 8 (Figure 2.31).

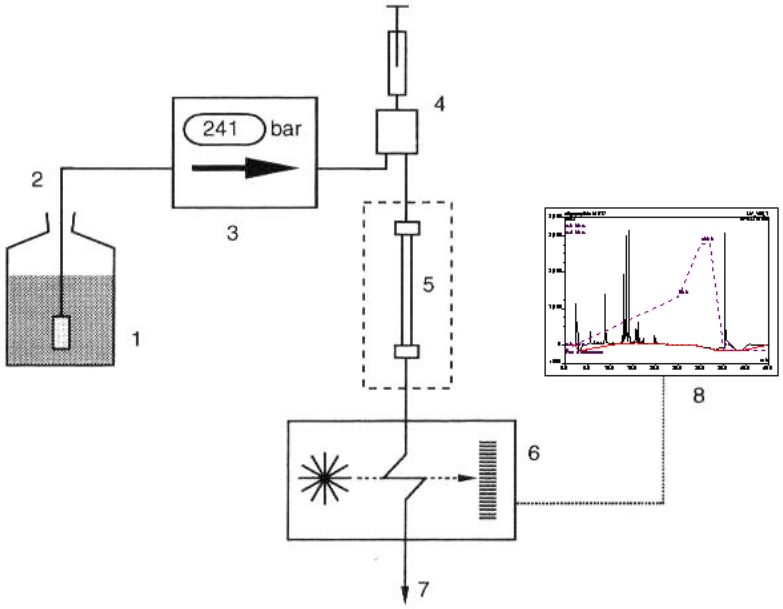

Figure 2.31 HPLC system: 1-solvent reservoir, 2-transfer line, 3-pump, 4-injection port, 5-column, 6-detector, 7-waste, 8-data interpreter (Meyer, 2004).

A reversed phase HPLC was used. In reverse phase HPLC, the hydrophobic stationary phase is typically silica modified with alkane chains typically between 4-18 carbons long. The mobile phase is polar, consisting of a mixture of water and a less polar solvent, containing modifying agents such as trifluoroacetic acid (TFA). Depending on their hydrophobicity, different peptides and proteins are partitioned between the mobile and stationary phases. The most hydrophobic proteins bind most strongly to the stationary phase and therefore elute last.

2.5.4 Light scattering

Various light scattering methods can be used to determine the native molecular mass or hydrodynamic volume of a protein and characterize changes in its structure. Light scattering methods are most suitable for large oligomeric proteins and glycoproteins with a molecular mass of >30 kDa. The intensity of the scattered light from a sample in solution is analysed at one or several angles in terms of a time-averaged intensity (static light scattering) or intensity fluctuations with time (dynamic light scattering). The output provides information about the oligomeric state of the solute. Light of different wavelengths and polarization is used in these studies. Light scattering methods for characterizing proteins have been reviewed by Harding and Jumel (1998).

2.5.4.1 Dynamic light scattering

Dynamic light scattering (DLS) or photon correlation spectroscopy (PCS) measures the size of a molecule based on its Brownian motion (Brownian motion is the irregular movement of molecules in a solution because of bombardment by molecules of the surrounding fluid.) Brownian motion affects the intensity of the scattered light. Because of their mass, large molecules move more slowly than small molecules. The intensity fluctuation of the scattered light occurs because molecular motion is related to the rate of diffusion and the size of the molecules. Small molecules cause light intensity to fluctuate more rapidly than large molecules. The molecular size and speed of motion are linked by the Stokes-Einstein equation which is based on the motion of a hard sphere. The equation is:

$$DH = \frac{kT}{f} = \frac{kT}{3\pi\eta D},$$

where:

DH	=	Hydrodynamic diameter of molecule;
k	=	Boltzman constant;
f		Particle frictional coefficient;
η	=	Solvent viscosity
T	=	Absolute temperature
D	=	Diffusion coefficient

DLS technique has been recently applied to study the interactions of BSA in aqueous sodium chloride solution (Li *et al.*, 2004), where it was found to be an effective technique for studying of protein interaction.

2.5.4.2 Multiple angle laser light scattering (Oliva *et al.*, 2004)

On-line multi angle laser light scattering (MALLS) is commonly combined with SEC to characterize the aggregation status of proteins. MALLS is based on Rayleigh scattering, where the quantity of light scattered by the molecules in solution is proportional to their molecular weight because size effects the angle of the scattered light. Large molecules scatter light at a small angle compare to the scattering resulting from small molecules. The molecular weight is determined by the amount of light scattered by a molecule at a given angle (Oliva *et al.*, 2004). MALLS can be used to determine the molecular weight

of only the polypeptide part of a glycoprotein if the extinction coefficient of the protein moiety is used in the measurement (Wen *et al.*, 1996). MALLS is very useful in establishing whether a protein is a monomer or oligomer. MALLS has been reviewed by Oliva et al. (2004).

2.5.5 Circular dichroism (CD) spectroscopy

Circular dichroism spectroscopy or spectropolarimetry is useful for detecting changes in both the secondary and tertiary structure of a protein molecule. CD measures the difference between the absorbance of the left and right circularly polarized light. Because protein molecules contain chiral bonds, this difference in absorbance is affected by the changes in the structure of the protein molecule. Far ultraviolet light at wavelength between 180-260 nm is used to monitor changes in the secondary structure of a protein including the amount of α-helixes and β-pleated sheets. Near ultraviolet light from 260-320 nm is used to determine changes in tertiary structure (i.e. the environment of the aromatic amino acid side chains) (Kelly *et al.*, 2005). Conformational changes resulting from denaturation or from substrate binding can be monitored using this technique.

2.5.6 Mass spectrometry (Sinz, 2007)

In mass spectrometry (MS) a protein or peptide is vaporized and ionized then accelerated in an electric field to compute its mass to charge ratio. Molecules can also be fragmented under controlled conditions to produce fragments with various mass to charge ratios. Differences in fragmentation patterns can be used to characterize and identify the parent molecule. Compounds can be ionised using a laser in matrix-assisted laser desorption ionization (MALDI) or in electrospray (ES) ionization (Chapman, 1996).

In this study, MALDI ionization technique was used, and involved the following steps: sample preparation and deposition on the matrix surface, laser ablation (vaporization) and desorption, electronic excitation, charged particle generation, separation and detection of ions according to mass to charge ratio. Identification of peptides and products of crosslinking by mass spectrometry is illustrated in Figure 2.32 and Figure 2.33, respectively.

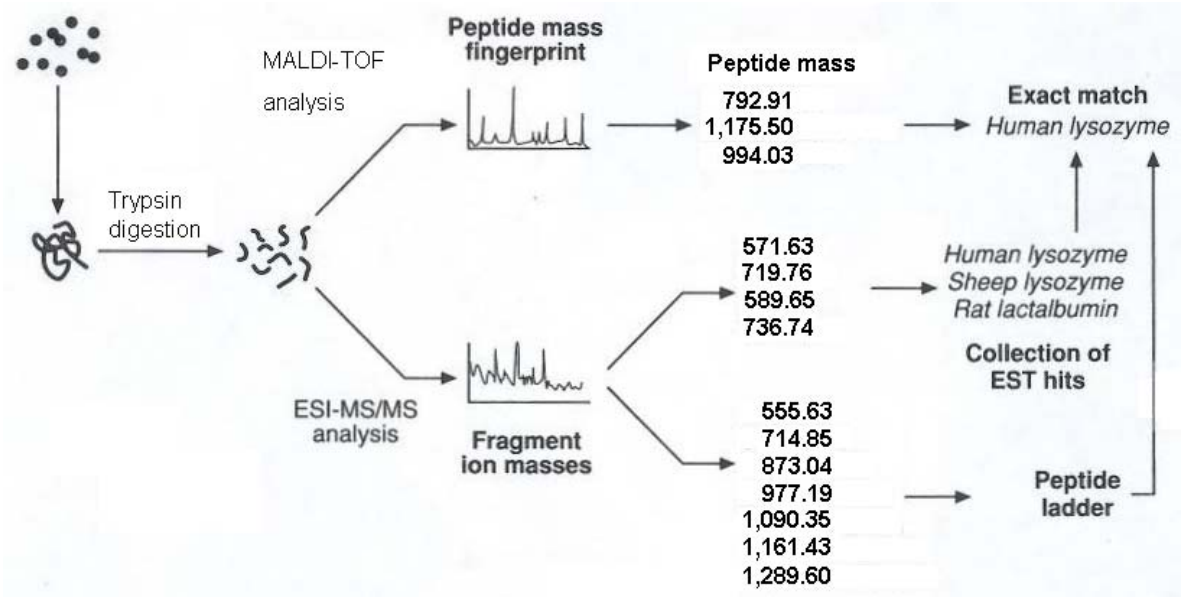

Figure 2.32 Protein identification by mass spectrometry (Twyman, 2004).

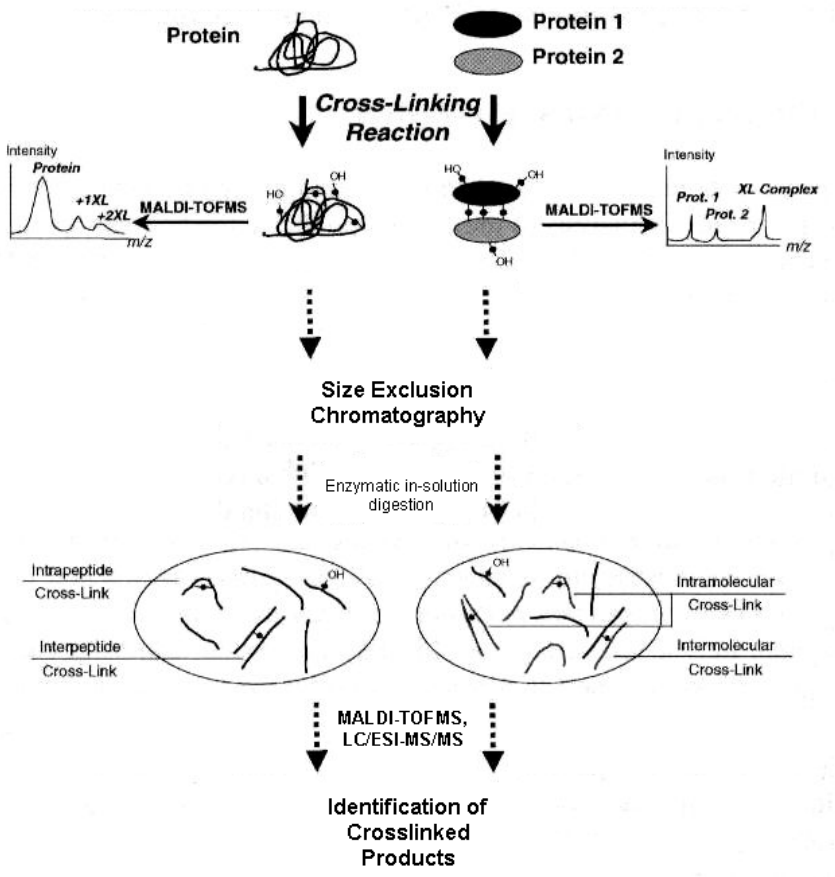

Figure 2.33 Crosslinking identification by mass spectrometry (Downard, 2007).

2.6 Objectives

The overall objective of this study was to attempt to stabilize target enzymes against thermal denaturation by chemically crosslinking parts of the molecules using the selected bifunctional crosslinking reagents. The specific aims were as follows;

1. Establish whether enzymes are chemically modified using selected bifunctional reagents, and whether such modifications stabilize target enzymes against thermal denaturation.
2. To optimise the strategies used to modify target enzymes, to achieve maximal thermal stabilization. Specifically, identify:
    - the optimal length of the crosslinking reagent molecule;
    - the optimal homobifunctional crosslinking reagent for crosslinking with target enzymes;
    - the optimal molar ratio of crosslinking reagents and enzymes necessary to achieve the desired extent of intramolecular crosslinking.
3. Characterize enhancements in thermal stability of target enzymes crosslinked with selected crosslinking reagents relative to native enzymes (and native enzymes that have been crosslinked by reacting with monofunctional crosslinking reagents) in terms of changes in thermal denaturation rate constants.
4. Evaluate the impact of stabilization on the reaction kinetics in comparison with the native enzymes.
5. Establish the exact nature of the crosslinking achieved as a consequence of the stabilizing treatment in comparison with the native enzymes using techniques such as PAGE, SEC, DLS, MALLS, HPLC and MS.
6. Establish the exact nature of the crosslinking reaction by using model proteins and peptides.
7. Investigate the unfolding behaviour and the melting curve following the intramolecular crosslinking treatment for stabilization of the enzymes.

CHAPTER 3

Materials and Methods

3.1 Materials

3.1.1 Enzymes, peptides and proteins

The following commercially available enzymes, synthetic peptides and glycoprotein were used in this study:

1. *Saccharomyces cervisiae* invertase (Sigma Chemical Co., product no. 57629, activity ~100 μM/min);
2. β-Galactosidase from *Aspergillus oryzae* (Sigma Chemical Co., product no. G5160, activity ~11.8 μM/min);
3. α-Amylase from *Aspergillus oryzae* (Sigma Chemical Co., product no. 10065, activity ~30 μM/min);
4. Lysozyme from hen egg white (Merk Chemical Co., product no.105281, activity 1.32 M/min);
5. Pepsin from porcine gastric mucosa (Sigma Chemical Co., product no. P6887, activity 62-88 mM/min);
6. Custom made peptide Ac-Gly-Ser-Lys-Gly-Thr-OH (molecular weight 491 Da, Auspep Pty. Ltd., batch no. U10281);

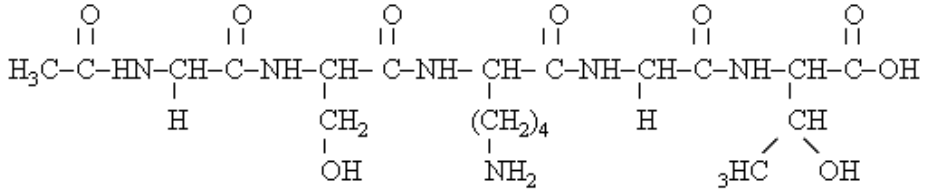

Theoretical monoisotopic mass = 490.23870 Da

$[M+H]^+$ = 491.24598 Da

$[M-H]^-$ = 489.23142 Da

Theoretical average mass = 490.51399 Da

[MolE-Molecular Mass Calculator v2.02 by Jeff Rozenski (1999)]

7. Custom made peptide Ac-Gly-Asp-Phe-Tyr-Arg-Ala-Asp-OH (molecular weight 885 Da, Auspep Pty. Ltd., batch no. Q20867);

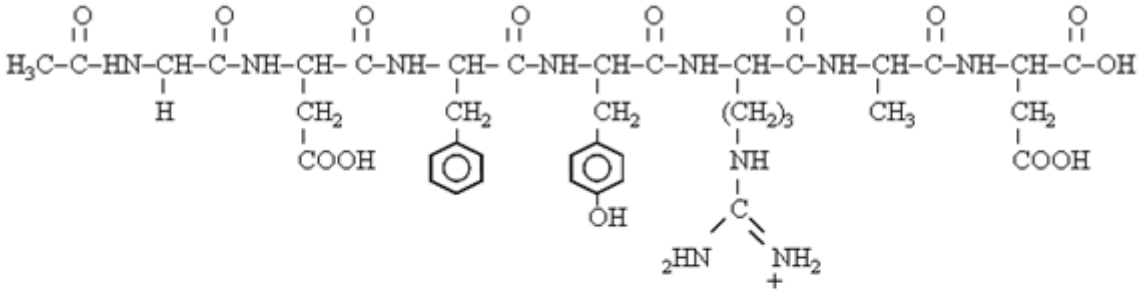

Theoretical monoisotopic mass = 884.36641 Da
$[M+H]^+$ = 885.37369 Da
$[M-H]^-$ = 883.35913 Da
Theoretical average mass = 884.90087 Da
[MolE-Molecular Mass Calculator v2.02 by Jeff Rozenski (1999)]

8. Ovalbumin from chicken egg white (Sigma Chemical Co., product no. A 5503, grade V, ≥98% pure, agarose gel electrophoresis).

3.1.2 Crosslinking reagents

The following monofunctional and bifunctional reagents were purchased from Sigma Chemical Company, St Louis, MO, USA:

1. Isocyanates

   1.1 Butyl isocyanate, $CH_3(CH_2)_3NCO$ (Sigma product no. B95736), BIC

   1.2 1,4-Diisocyanatobutane, $OCN(CH_2)_4NCO$ (Sigma product no. 371130), or butamethylene diisocyanate, BMDC

   1.3 1,6-Diisocyanatohexane, $OCN(CH_2)_6NCO$ (Sigma product no. D124702), or hexamethylene diisocyanate, HMDC

   1.4 1,8-Diisocyanatooctane, $OCN(CH_2)_8NCO$ (Sigma product no. 427373), or octamethylene diisocyanate, OMDC

2. Imidoesters

   2.1 Ethyl acetimidate, $CH_3C(=NH)OC_2H_5$ (Sigma product no. 188840), EA

2.2 Dimethyl adipimidate, $CH_3OC(=NH)(CH_2)_4C(=NH)OCH_3$ (Sigma product no. 285625), DMA

2.3 Dimethyl pimelimidate, $CH_3OC(=NH)(CH_2)_5C(=NH)OCH_3$ (Sigma product no. D8388), DMP

2.4 Dimethyl suberimidate, $CH_3OC(=NH)(CH_2)_6C(=NH)OCH_3$ (Sigma product no. 74835), DMS

3. Diamines

3.1 Hydrazine monohydrate, NH_2NH_2 (Sigma product no. 207942)

3.2 1,2-Diaminoethane, $NH_2(CH_2)_2NH_2$ (Sigma product no. E1521), or ethylene diamine, EDA

3.3 1,4-Diaminobutane, $NH_2(CH_2)_4NH_2$ (Sigma product no. D13208), DAB

3.4 1,6-Diaminohexane, $NH_2(CH_2)_6NH_2$ (Sigma product no. H11696), DAH

3.5 1,8-Diaminooctane, $NH_2(CH_2)_8NH_2$ (Sigma product no. D22401), DAO

3.6 1,10-Decanediamine, $NH_2(CH_2)_{10}NH_2$ (Sigma product no. D14204), or diaminodecane, DA10

3.7 1,12-Diaminododecane, $NH_2(CH_2)_{12}NH_2$ (Sigma product no. D16401), DAD

3.2 Methods

3.2.1 Chemical modification protocols

3.2.1.1 Isocyanates

The crosslinking protocol was adapted from Snyder *et al.* (1974). A specified amount (1–50 mM) of a bifunctional reagent was mixed with enzymes, peptides and protein (0.9 μM or 50 mg/mL) in the specified buffer solutions (pH 5-8) at room temperature. The reaction mixture was mixed vigorously (vortex mixer) and allowed to stand at room temperature for 15 minutes. The excess reagent was removed by a PD-10 (GE

Healthcare) desalting column following the instructions provided by the manufacturer (GE Healthcare). Enzyme activity was determined by the relevant enzymatic assays (Section 3.2.3). For the control experiments, a monofunctional isocyanate reagent (butyl isocyanate) was used in the reaction vial instead of the bifunctional reagent. The molar concentration of the monofunctional reagent was always double the molar concentration of the bifunctional reagent.

3.2.1.2 Imidoesters

Relevant protocols have been reported by Ryan *et al.* (1994) and Habibi *et al.* (2006). Chemical modification was achieved by mixing 0.9 μM of an enzyme dissolved in the specified buffer (pH 5-8), with the reagent. The stock solutions of the reagent (0.1, 1, 5, 10 mg/mL) were added to the enzyme solution to 2% of the final volume. After reaction at room temperature for 1 hour, the mixture was run through a PD-10 desalting column to remove excess reagent as previously specified (Section 3.2.1.1). Enzyme activity was determined by the relevant enzymatic assay (Section 3.2.3). As a control, the bifunctional reagent was replaced with doubled the molar amount of the monofunctional reagent (ethyl acetimidate, EA).

3.2.1.3 Diamines

Crosslinking was carried out at room temperature for 1 hour (Torchilin *et al.*, 1978). The reagent (0.1-10 mg/mL) was added to enzyme solution (0.9 μM in the specified buffer solutions, pH 5-8) to 2% of the final volume. The resulting solution was mixed by a vortex mixer and allowed to stand as specified above. The excess reagent was removed using a PD-10 desalting column (Section 3.2.1.1), and the desalted enzyme was collected for further analysis.

3.2.2 Enzyme stability measurements

Enzyme stability was measured by exposing both the native and modified enzymes dissolved in an appropriate buffer of the specified pH, to various temperatures (50–80 °C; water bath). Samples were taken at specified time intervals, cooled on ice, and the activity was measured using the methods specified in Section 3.2.3.

3.2.3 Activity assays

3.2.3.1 α-Amylase

Alpha amylase activity was measured according to the method of Bernfeld (Bernfeld, 1955) as adapted by the Sigma Chemical Co. (Sigma Chemical Co. Ltd., 1997) using starch as the substrate. In this method, DNS (dinitrosalicylic acid) reacts with the hydrolysis product (maltose) to produce a red-brown compound. A unit of enzyme activity was the quantity that liberated 1 mg of maltose from starch per minute at pH 6.9 (Na-phosphate buffer) and 20 °C. A blank and the reaction sample were prepared in separate test tubes, as specified in Table 3.1. The Absorbance was measured at 540 nm (UV-visible spectrophotometer; Hitachi, model 2000). The absorbance was converted to mg maltose using a standard curve (Figure 3.1). Enzyme activity was calculated using the following formula:

$$\text{Enzyme (units/mL)} = \frac{\text{Released maltose (mg/mL)} \times \text{Total volume of reaction mixture(mL)} \times df}{\text{Volume of enzyme solution (mL)} \times \text{Reaction time (min)}}$$

where *df* is a dilution factor.

The standard curve in Figure 3.1 was prepared from a standard solution of maltose (Sigma cat no. M-5885) as specified by Sigma Chemical Co. Six test tubes (including the blank) having known concentrations of maltose were prepared as specified in Table 3.2. Absorbance was measured at 540 nm. Data are shown in Figure 3.1.

Table 3.1 The activity assay of α-amylase

	Volume (mL)	
Reagents	Blank	Sample
1. 1% w/v (g/100 mL) starch	0.50	0.50
	20 °C	
2. enzyme solution	0	0.10
	Mix at 20 °C for 3 min exactly	
3. Coomassie reagent	0.50	0.50
4. enzyme solution	0.10	0
	Cap and boil in water bath for 15 min exactly Cool on ice	
5. deionized water	4.90	4.90

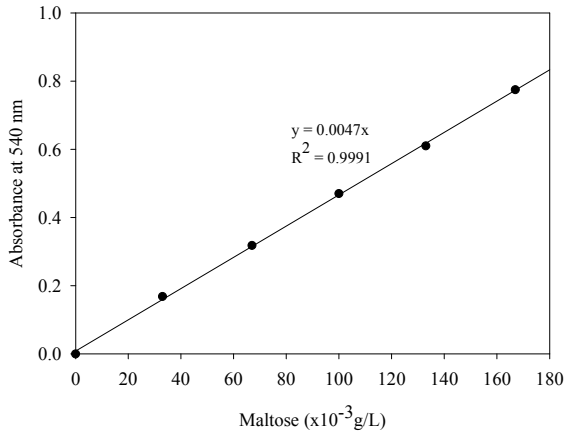

Figure 3.1 The calibration curve of standard maltose.

Table 3.2 The measurement of standard maltose

	Volume (mL)					
Reagents	Blank	1	2	3	4	5
1. 0.2% w/v (g/100 mL) maltose	0	0.10	0.20	0.30	0.40	0.50
2. deionized water	1.00	0.90	0.80	0.70	0.60	0.50
3. Coomassie reagent	0.50	0.50	0.50	0.50	0.50	0.50
	Cap and boil in water bath for 15 min exactly Cool on ice					
4. deionized water	4.50	4.50	4.50	4.50	4.50	4.50
	Mix and measure absorbance at 540 nm					

3.2.3.2 β-Galactosidase

β-Galactosidase activity was measured using *o*-nitrophenyl-β-galactopyranoside (Sigma Chemical Co., product no. N1127) as the substrate (Sigma Chemical Co. Ltd., 1994). Blank and sample test tubes were prepared as specified in Table 3.3. Absorbance was measured at 410 nm (UV-visible spectrophotometer; Hitachi, model 2000). One unit of enzyme activity was defined as the quantity that hydrolyzed 1 mmole of *o*-nitrophenyl-β-D-galactoside to *o*-nitrophenol and D-galactose per minute at pH 3.5 (Na-citrate buffer) and 25 °C. Enzyme activity was calculated using the following formula:

$$\text{Enzyme}\,(\text{units/mL}) = \frac{\text{A}_{410} \times 4 \times df}{10 \times 4.6 \times 0.1},$$

where:

A_{410} = Absorbance at 410 nm;

4.0 = total volume of assay (mL);

df = dilution factor;

10 = time of incubation (min);

4.6 = the molar extinction coefficient of *o*-nitrophenol at 410 nm ($mM^{-1}cm^{-1}$);

0.1 = volume (mL) of enzyme solution used.

Table 3.3 Activity assay of β-galactosidase

	Volume (mL)	
Reagents	Blank	Sample
1. 0.01 mM *o*-nitrophenyl-β-galactopyranoside	0.50	0.50
2. 0.4 M citrate buffer, pH 3.5	0.40	0.40
	Mix at 25°C	
3. enzyme solution	0	0.10
	Mix at 25°C for 10 min exactly	
4. 0.2 M borate buffer, pH 9.8	3.00	3.00
5. enzyme solution	0.10	0
	Mix and measure absorbance at 410 nm	

3.2.3.3 Invertase

Invertase activity was measured using the DNS (dinitrosalicylic acid) method (Boyer, 1993) with sucrose as the substrate. This method is based on the reaction of DNS reagent with the reducing sugars (glucose and fructose) produced from sucrose. The reaction produces a red-brown complex that can be measured spectrophotometrically at a wavelength of 540 nm. The DNS method used for this study had been validated against a commercially available enzymatic assay of amylase and invertase (Sigma Chemical Co. Ltd., 1997, 1999). One unit of invertase activity was defined as the quantity that liberated 1 μmol of reducing sugars per minute at pH 4.6 (Na-acetate buffer) and 20 °C.

A standard calibration curve was prepared as specified in Table 3.4. An equimolar solution containing 0.2% w/v (g/100 mL) glucose (Sigma cat. no. 284508W) and fructose (Sigma cat. no. 103672G) was used as the standard.

Table 3.4 The measurement of standard reducing sugars

Reagents	Volume (mL)						
	Blank	1	2	3	4	5	6
1. 0.2% w/v (g/100 mL) standard glucose and fructose solution	0	0.05	0.10	0.15	0.20	0.25	0.30
2. deionized water	1.00	0.95	0.90	0.85	0.80	0.75	0.70
3. colour reagent	0.50	0.50	0.50	0.50	0.50	0.50	0.50
	Cap and boil in water bath for 5 min exactly Cool on ice and place at room temp.						
4. deionized water	4.50	4.50	4.50	4.50	4.50	4.50	4.50
	Mix and measure absorbance at 540 nm						

Blank and reaction samples were prepared in separate test tubes, as specified in Table 3.5. The absorbances of the resulting solutions were measured at 540 nm (UV-visible spectrophotometer; Hitachi, model 2000) and invertase activity was calculated using a standard curve (Figure 3.2) and the following formula:

$$\text{Enzyme activity (unit/mL)} = \frac{\text{Produced reducing sugars (μg/mL)} \times \text{total reaction volume (mL)} \times df}{\text{Used enzyme solution (mL)} \times \text{MW of glucose or fructose} \times \text{reaction time (min)}}$$

where *df* is dilution factor.

Table 3.5 Enzymatic activity assay for invertase

Reagents	Volume (mL)	
	Blank	Sample
1. 10% w/v (g/100 mL) sucrose	0.50	0.50
	20°C	
2. enzyme solution	0	0.10
	Mix at 20°C for 5 min exactly	
3. colour reagent	0.50	0.50
4. enzyme solution	0.10	0
	Cap and boil in water bath for 5 min	
5. deionized water	4.90	4.90

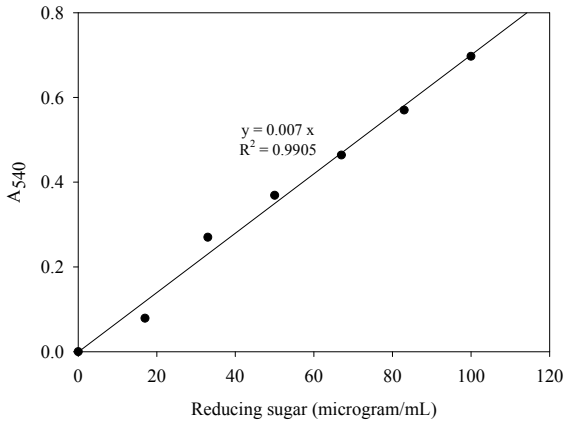

Figure 3.2 Standard curve of reducing sugars.

3.2.4 Determination of Michaelis-Menten kinetic parameters

Enzyme catalyzed reaction frequently obey Michaelis-Menten kinetics (Marangoni, 2003). Thus, the rate of reaction (v) depends on the substrate concentration (S) as follows:

$$v = \frac{v_{max}}{K_m + S}, \tag{3.1}$$

where v_{max} and K_m are constants at given temperature and pH. v_{max} is the maximum rate of the reaction at a given concentration of the enzyme and K_m is Michaelis-Menten constant. Numerically, K_m is the value of the substrate concentration S at which the rate of the reaction is $v_{max}/2$. For estimating the values of v_{max} and K_m from the measured rate (v) at various substrate concentrations S, Equation (3.1) must be linearized. This can be done in three different ways as discussed in detail by Shuler and Kargi (2002). A preferred linear transformation of Michaelis-Menten equation for estimating the value of v_{max} from experimental data (Cook and Cleland, 2007) is the Lineweaver-Burk equation:

$$\frac{1}{v} = \frac{K_m}{v_{max}} \cdot \frac{1}{S} + \frac{1}{v_{max}} \tag{3.2}$$

Thus, plot of $1/v$ against $1/S$ for a reaction obeying Michaelis-Menten kinetics is a straight line with the slope of K_m/v_{max} and the y-intercept of $1/v_{max}$.

Although both v_{max} and K_m can be estimated from Lineweaver-Burk plot, in practice, this plot should be used only to estimate v_{max} from the y-intercept (Cook and Cleland, 2007). This is because the slope of the plot (i.e. K_m/v_{max}) is susceptible to errors that are magnified by linear regression. (The data with low magnitudes (and high errors)

of v and S appear furthest from the origin in a Lineweaver-Burk plot. Such erroneous data have the strongest influence on the slope of a line plotted by linear regression.). The value of the y-intercept of Lineweaver-Burk plot is not highly susceptible to being influenced by the erroneous data that occur furthest from the origin. In practice, only v_{max} is estimated from Lineweaver-Burk plot. For estimating K_m, the data are plotted as v against S (Figure 3.3). A horizontal line corresponding to $v_{max}/2$ is plotted (v_{max} obtained from Lineweaver-Burk plot). Where this line intercepts the reaction rate curve, the value of S is read as being equal to K_m.

The Hanes-Woolf plot is another option for estimating the v_{max} and K_m values of enzymes. The Hanes-Woolf equation is a linearized form of Michaelis-Menten equation, as follows:

$$\frac{S}{v} = \frac{K_m}{v_{max}} + \frac{1}{v_{max}} \cdot S \qquad (3.3)$$

v_{max} is estimated using the slope of the Hanes-Woolf plot of S/v against S. The y-intercept provides the value of K_m/v_{max}.

The Michaelis-Menten parameters (K_m and v_{max}) for invertase were measured as a means of characterizing it before and after the crosslinking treatment. A solution of native or treated invertase was mixed with various concentrations of sucrose solution as per Table 3.6, at room temperature (Boyer, 1993; Plummer, 1987). After 5 min, the reaction was stopped by boiling and the concentration of reducing sugars was determined by the DNS (dinitrosalicylic acid) method (Boyer, 1993) (Section 3.2.3.3).

Thus v-values could be obtained at various initial concentrations of the substrate, sucrose. A plot of v versus sucrose concentration (S) is shown in Figure 3.3. The curve in Figure 3.3 has the shape expected for Michaelis-Menten kinetics.

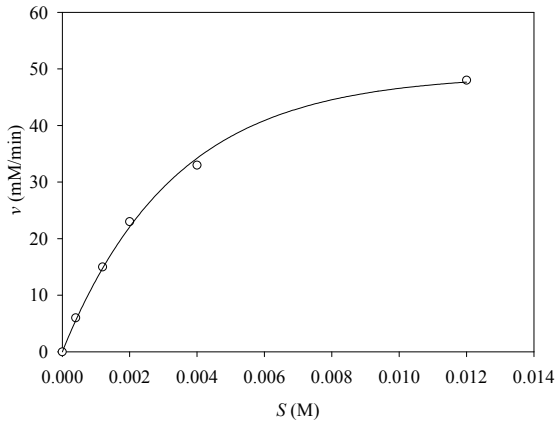

Figure 3.3 The measured rate of reaction (v) at sucrose concentration S.

Table 3.6 Test tube preparation for determination of the initial rate v

Reagents	Tubes					
	Blank	2	3	4	5	6
Invertase solution (μL)	325	325	325	325	325	325
Distilled water (μL)	300	50	50	50	50	50
Citrate buffer (μL)	125	125	125	125	125	125
0.3 M sucrose solution (μL)	-	250	-	-	-	-
0.1 M sucrose solution (μL)	-	-	250	-	-	-
0.05 M sucrose solution (μL)	-	-	-	250	-	-
0.03 M sucrose solution (μL)	-	-	-	-	250	-
0.01 M sucrose solution (μL)	-	-	-	-	-	250
Mixed and allowed to stand at room temperature for 5 mins						
DNS (μL)	500	500	500	500	500	500
Boiled for 5 mins and cooled to room temperature						
Distilled water (mL)	5	5	5	5	5	5
Absorbance measurement at 540 nm						

3.2.5 Quantification of enzyme stabilities

Enzyme stability was quantified in terms of a thermal denaturation rate constant k_d and the activation energy of denaturation, E_d.

For otherwise fixed conditions, the rate v of an enzymatic reaction generally depends on the concentration of active enzyme (Shuler and Kargi, 2002; Vrábel *et al.*, 1997), as follows:

$$v = k_{\text{cat}}[E_t] \tag{3.4}$$

where k_{cat} is a temperature-dependent rate constant and [E] is the molar concentration of the active enzyme. At any fixed temperature, the concentration of active enzyme declines with time because of thermal denaturation. Thermal denaturation rate is typically first-order in the concentration of the active enzyme (Shuler and Kargi, 2002; Vrábel *et al.*, 1997); thus,

$$-\frac{d[E]}{dt} = k_d[E] \tag{3.5}$$

where k_d is the denaturation rate constant and t is time.

At a constant temperature, Eq. (3.5) can be integrated between the limits t = 0, [E] = [E_o] and $t = t$, [E] = [E_t], or:

$$-\int_{[E_o]}^{[E_t]} \frac{d[E]}{[E]} = k_d \int_0^t dt \tag{3.6}$$

where [E_t] and [E_o] are the active enzyme concentrations at times t and zero, respectively. Concentration [E_t] and [E_o] in Eq. (3.6) can be replaced with the corresponding activities without any impact on the outcome. Solution of Eq. (3.6) is as follows:

$$\ln\frac{[E_t]}{[E_o]} = -k_d t\,, \tag{3.7}$$

or

$$[E_t] = [E_o]e^{-k_d t}\,. \tag{3.8}$$

Substitution of Eq. (3.8) in Eq. (3.4) leads to the following:

$$v = k_{\text{cat}}[E_o]e^{-k_d t}\,, \tag{3.9}$$

where both k_{cat} and k_d depend on temperature. From Eq. (3.9) the rate of reaction at t = 0, i.e. the initial activity v_i at a given temperature, is

$$v_i = k_{\text{cat}}[E_o] \tag{3.10}$$

From Eq. (3.9) and Eq. (3.10), the fraction of initial activity (i.e. v_f) at any time t, is:

$$v_f = \frac{v}{v_i} = e^{-k_d t}\,. \tag{3.11}$$

Therefore,

$$\ln v_f = -k_d t\,, \tag{3.12}$$

Thus, a plot of ln v_f versus t should be a straight line of slope $-k_d$. This allows calculation of the denaturation rate constant.

As for the rate constant of any chemical reaction, the rate constant for enzyme denaturation depends on absolute temperature T, as follows (Copeland, 2000):

$$k_d = Ae^{-E_d / RT} \tag{3.13}$$

where A is the Arrhenius parameter, E_d is the deactivation energy ($J \cdot mol^{-1}$), and R is the gas constant (= 8.314 $J \cdot mol^{-1}K^{-1}$). Activation energy for thermal denaturation of enzymes is typically in the range of 40 to 130 $kcal \cdot mol^{-1}$ or 167 to 544 kJ mol^{-1}. Arrhenius parameter is constant at a constant temperature.

Equation (3.13) can be linearized as follows:

$$\ln k_d = \ln A - \frac{E_d}{RT} \tag{3.14}$$

Denaturation energy for the enzyme can be determined by calculating k_d at various constant temperatures, plotting ln k_d versus $1/T$, and reading the slope of the resulting straight line as $-E_d/R$.

3.2.6 Determination of crosslinking

Several methods were used in attempts to determine whether crosslinking of an enzyme, peptide or protein occurred as a consequence of the reaction with a crosslinking reagent. The methods included native and sodium dodecyl sulfate polyacrylamide gel electrophoresis (SDS-PAGE), size exclusion chromatography, dynamic light scattering (DLS), multiple angle laser light scattering (MALLS), deglycosylation, trypsin digestion, high performance liquid chromatography (HPLC) and mass spectrometry (MS). These methods are outlined in the rest of this chapter.

3.2.6.1 Native PAGE (Davis, 1964; Laemmli, 1970; Ornstein, 1964; Simpson, 2003; Trudel and Asselin, 1989)

The system used for forming and running gels was a Mini-PROTEAN® 3 system (Bio-Rad Laboratories Inc., US; Catalog no. 165-3301 and 165-3302). Resolving gels of 6.5% and 14% acrylamide were prepared from a 40% w/v bis/acrylamide stock solution for the analysis of invertase and lysozyme, respectively. The separating gel was prepared with 0.375 M Tris buffer, pH 8.8. It had the composition shown in Table 3.7. The gel was initially polymerized by 10% ammonium persulfate followed by TEMED (N,N,N',N'-tetramethylethylenediamine).

To prepare the 4% w/v acrylamide stacking gel with 0.125 M Tris buffer pH, 6.8, and 0.1% TEMED, the same components as used in the running gel were mixed and polymerized (Table 3.8). The resolving buffer, pH 10.2, with 37 mM ammonia and 20 mM CAPS (N-cyclohexyl-3-aminopropanesulfonic acid), was used to complete the electrophoresis system. Sample buffer consisted of 0.0625 M Tris, pH 6.8, 10% glycerol and 0.001% bromophenol blue. Before loading of samples, the sample buffer (5 times concentrated) was mixed with protein samples. Gels were run at a constant voltage of 200 volts until the dye front reached the bottom of the gel (1½ hours approximately). They were then stained for 30 minutes with 0.1% Coomassie blue R-250 in 40% methanol and 10% acetic acid. The gels were later destained with a mixture of 40% methanol and 10% acetic acid. The normal time of destaining was approximately 1-2 hours.

The gels with protein bands were dried by using the conventional drying technique, as follows: Cellophane film and glass frame were used for gel drying. Two square sheets of cellophane film (15 cm × 15 cm) were cut and soaked in distilled water. The wet film was smoothed over the glass plate and the gel was placed in the center. A second sheet of the wet cellophane film was used to cover the gel which was then clamped in the frame and allowed to dry.

Table 3.7 Preparation of resolving gel (0.375 M Tris, pH 8.3) for native PAGE

Reagents	Volume	
	6.5%	14%
Distilled water	5.77 mL	3.9 mL
1.5 M Tris-HCl, pH 8.8	2.5 mL	2.5 mL
40% Stock acrylamide/bis solution	1.63 mL	3.5 mL
Degas at room temperature for 15 minute		
10% Ammonium persulfate (prepared fresh)	100 µL	100 µL
TEMED[a]	5 µL	5 µL
Total	10 mL	10 mL

[a]N,N,N',N'-Tetramethylethylenediamine

Table 3.8 Preparation of stacking gel (0.125 M Tris, pH 6.8) for native PAGE

Reagents	Volume
Distilled water	6.5 mL
0.5 M Tris-HCl pH, 6.8	2.5 mL
40% Stock acrylamide/bis solution	1 mL
Degas at room temperature for 15 minute	
10% Ammonium persulfate (prepared fresh)	100 μL
TEMED	10 μL
Total	10 mL

3.2.6.2 SDS-PAGE (Laemmli, 1970; Shi and Jackowski, 1998; Simpson, 2003; Weber and Osborn, 1969)

The protocol for running the SDS-PAGE was similar to that of the native-PAGE except that SDS detergent was added to various gels and buffers. SDS was used to fully denature the protein prior to the separation. The resolving gel, stacking gel and the resolving buffer contained 0.1% SDS while the sample buffer contained 2% SDS. A 6.5% acrylamide gel was prepared for invertase. A 10% acrylamide gel was used for pepsin and ovalbumin. For lysozyme, the separation was carried out on a 14% acrylamide gel (Table 3.9). The stacking gel was prepared using the composition in Table 3.10. The protein sample mixed with the sample buffer was heated at 95 °C for 4 min and cooled to room temperature before loading. The electrophoresis was carried out for 35 min approximately or until the bromophenol blue reached the bottom of the gel. The gel was fixed by soaking in staining solution (0.1% coomassie blue R-250 in fixative, 40% methanol and 10% acetic acid) for 30 minutes. The destaining and gel drying procedures were the same as described for native PAGE (Section 3.2.6.1).

Table 3.9 Preparation of resolving gel (0.375 M Tris, pH 8.3) for SDS-PAGE

Reagents	Volume		
	6.5%	10%	14%
Distilled water	5.67 mL	4.8 mL	3.8 mL
1.5 M Tris-HCl pH, 8.8	2.5 mL	2.5 mL	2.5 mL
10% (w/v) SDS	100 µL	100 µL	100 µL
40% Stock acrylamide/bis solution	1.63 mL	2.5 mL	3.5 mL
Degas at room temperature for 15 minute			
10% Ammonium persulfate (prepared fresh)	100 µL	100 µL	100 µL
TEMED	5 µL	5 µL	5 µL
Total	10 mL	10 mL	10 mL

Table 3.10 Preparation of stacking gel (0.125 M Tris, pH 6.8) for SDS-PAGE

Reagents	Volume
Distilled water	6.4 mL
0.5 M Tris-HCl pH, 6.8	2.5 mL
40% Stock acrylamide/bis solution	1 mL
10% (w/v) SDS	100 µL
Degas at room temperature for 15 minute	
10% Ammonium persulfate (prepared fresh)	100 µL
TEMED	10 µL
Total	10 mL

Low molecular weights (14-97 kDa, product code 17-0446-01) and high molecular weights (53-220 kDa, product code 17-0615-01) protein markers for SDS-PAGE were purchased from GE Healthcare.

3.2.6.3 Size-exclusion chromatography (SEC) (GE Healthcare, 2002)

For invertase, Sephacryl^{TM} S-300 High Resolution (HR) (code no. 17-0599-10; GE Healthcare) was used to separate the oligomers obtained after crosslinking. Sephacryl HR gel is composed of allyl dextran covalently crosslinked with N,N′-methylene bisacrylamide to form a hydrophilic resin. The average particle size of Sephacryl S-300 is 47 µm and the fractionation range of the resin is 10-1,500 kDa. The resin was packed in an econo-column (15×470 mm) with 83 mL bed volume. The eluent solution (pH 6)

contained 0.1 M Na-citrate buffer and 0.15 M NaCl. The column was calibrated using a molecular weight protein standards kit (code no. 28-4038-42, GE Healthcare).

Superdex™ 75 10/300 GL pre-packed column (10×300-310 mm, code no. 17-5174-01; GE Healthcare) connected to the ÄKTA™ Explorer FPLC system (GE Healthcare) was used to separate lysozyme oligomers after crosslinking. Superdex is a bead-formed gel prepared from agarose crosslinked with dextran, with a particle size of 13 μm. The bed volume of the pre-packed column is 24 mL. The column was suitable for separating globular proteins in the molecular weight range of 3-70 kDa. The column was equilibrated and eluted with 20 mM Na-phosphate buffer, pH 7, 0.15 M NaCl.

Before each run, the column was washed with distilled water. This was followed by at least one column volume of the buffer used for the separation being run through the column, or until the base line signal of the detector was stable. The flow rate for separation was 0.3-0.4 mL/min.

3.2.6.4 Dynamic light scattering (DLS) (Malvern Instruments Ltd., 2004)

The Zetasizer Nano ZS series (size range for molecular weights was $1\text{-}2\times10^4$ kDa; Malvern Instrument Ltd., UK) was used to measure the size of both monomers and oligomers of invertase. The estimated average particle diameter in terms of intensity, volume and number distributions was measured by the instrument. The measurement was performed at 25 °C. Sample solutions were filtered through a 0.2 μm (Millipore) filter before measuring, and the detector was set at 173° for backscatter detection. Sample solutions were then poured into a 1 mL disposable cuvette until a height of 15 mm. The cuvette was placed in the sample holder and the instrument was run automatically.

3.2.6.5 Multiple angle laser light scattering (MALLS) (Wyatt Technology Corporation, 1997)

The molecular weight of invertase was measured online with a MALLS DAWN® DSP laser photometer (Wyatt Technology Corporation) installed downstream from a size exclusion HPLC column (Superose™ 6 HR 10/30, GE Healthcare). Samples were filtered through a 0.22 μm filter (Millipore) before being subjected to HPLC (GBC®; LC 1440 system organiser, LC 1200 UV/Vis detector and LC 1120/1150 HPLC pump). The refractive index detector (RI 2000 Refractometer, Germany) was normalized using bovine

serum albumin (BSA) as a protein standard. A differential index of refraction (*dn*/*dc*) value of 0.190 for a general protein was used for the measurement and sodium chloride solutions of different concentrations were used to calibrate the detector. The buffer system used in the separation was imidazole pH 7 at a flow rate of 0.4 mL/min. The scattering data were analysed by the Wyatt ASTRA^{TM} software programme.

3.2.6.6 Deglycosylation (Lee and Park, 2002; Rehm, 2006; Tarentino *et al.*, 1985)

The N-linked carbohydrate moieties of glycoproteins can be enzymatically removed by treatment with the endoglycosidase, peptide-N-glycosidase F (PNGase F). PNGase F was added to the glycoprotein in the mass ratio of 1:300, in 0.2 μM Na-phosphate buffer pH 7. The hydrolysis was carried out at 37 °C overnight, and the efficacy of deglycosylation was analysed by SDS-PAGE.

3.2.6.7 Trypsin digestion (Simpson, 2003)

Lysozyme 2 mg/mL was dissolved in 0.1 M ammonium bicarbonate. A 1 mg/mL trypsin solution in 1 mM HCl and 20 mM $CaCl_2$ was added at a weight ratio of trypsin and lysozyme of between 1:50-1:200. Two controls, one without trypsin and the other without lysozyme, were prepared. Thesit, a nonionic detergent, was added to a final concentration of 0.002% to the protein solution to improve peptide recovery (Hubbard and McHugh, 1996). The reaction was stopped by the addition of 2% v/v of acetic acid followed by sonication for 5 minute before further analysis by HPLC (Section 3.2.6.8).

3.2.6.8 Reverse phase high performance liquid chromatography (RP-HPLC)

HPLC Ultimate 3000 series (Model WPS-3000 TSL, Analytical) controlled by Chromeleon software programme was used to separate and measure peptides and proteins. A Phenomenex® RP-HPLC (Jupiter 4U Proteo, 90 Angstrom pore size) column was used to analyse peptide models. RP-HPLC of proteins and the peptides produced by hydrolysis with trypsin were carried out on a Jupiter 5U C18 column with 300 Angstrom pore size matrix. Samples were eluted using a linear gradient of solvents A and B (A: 0.1% TFA (trifluoroacetic acid) in HPLC grade water; B: 0.08% TFA in acetronitrile) using a flow rate of 1 mL/min at a temperature of 45 °C. The pentapeptide, was eluted with a linear gradient of 70% solvent B for 35 min. The heptapeptide was eluted with a

linear gradient of 50% solvent B for 25 min. Lysozyme was eluted with linear gradient of 40% solvent B for 20 min. Peptides and protein were monitored at 214 nm (peptide bonds) and 280 nm (aromatic amino acids) wavelengths, respectively.

3.2.6.9 Mass spectrometry (MS)

Mass of peptides was determined at the Centre of Protein Research (CPR), Otago University, Dunedin, New Zealand. A MALDI-MS system was used. For sample preparation, freezed dried fractions from the RP-HPLC (Section 3.2.6.8) were dissolved in 30% v/v acetronitrile and 0.1% TFA in water. One μL of the sample was mixed with 1 μL of matrix (10 mg/mL of alpha cyano-4-hydroxycinnamic acid in 65% aqueous acetronitrile with 0.1% TFA). The mixture (0.8 μL) was spotted onto an opti-TOF 384 well plate and then dried. The prepared sample was analysed by mass spectrometry on a 4800 MALDI tandem Time of Flight Analyser.

3.2.7 Folding behaviour of enzyme by circular dichroism (Greenfield, 2007; Kelly *et al.*, 2005)

CD spectra were recorded with Chirascan™ Circular Dichroism spectrometer (Applied Photophysics, UK) in the detection range between 160-850 nm. A Julabo AWC 100 GB recirculating cooler (Julabo, Germany) was used to control the sample temperature. The TC 125™ Temperature Controller (Quantum Northwest, USA) was used for setting target temperatures and stirring speeds.

Before the CD measurements, samples were concentrated and the buffer was exchanged. These operations were performed on the protein fractions collected from the size exclusion chromatography column (Section 3.2.6.3), by ultrafiltration. Depending on the sample volume, either Vivaspin-500 (molecular weight cut-off (MWCO) of 10 kDa) or Vivaspin-2 (molecular weight cut-off (MWCO) of 10 kDa) centrifugal ultrafiltration devices were used for native and intramolecularly crosslinked lysozyme. For intermolecularly crosslinked lysozyme, either Vivascience (Nanosep^{TM} centrifugal device-500 μL with MWCO of 30 kDa, Pall Filtron) or Amicon® (Ultra-4 centrifugal filter device-4 mL with MWCO of 30 kDa, Millipore) were used. Before the measurements, the sample buffer was exchanged into 4 mM Na-phosphate buffer containing 30 mM NaCl to achieve a final protein concentration of 0.4-0.6 mg/mL. All

samples were filtered through a 0.1-0.2 μm filter to remove all particles and degassed under vacuum for 20 minutes to prevent gas bubbles from forming during the melting curve determination. A 0.01 cm quartz cell was used to measure the CD spectra in far UV range (180-260 nm). Thermal denaturation was done automatically by the equipment by raising the temperature from 20 to 90 °C in 10 °C intervals. The entire automated analysis was completed within 1.5 hours.

CHAPTER 4

Results and Discussion

4.1 Effect of chemical modifications on enzyme thermal stability

The aim in this section was to examine whether chemical modification by selected bifunctional crosslinking reagents could stabilize the target enzymes against heat denaturation. The crosslinkers used were isocyanates, imidoesters and amines (Section 3.1.2). The enzymes of interest were alpha amylase, beta galactosidase and invertase. The properties of native enzymes were characterized prior to the chemical modification treatments to obtain baseline data for comparison with the chemically modified enzymes. The stability of the modified enzymes was measured under conditions of optimal activity for the native enzyme. The stability of enzymes was characterized in terms of the fraction of the initial activity remaining after incubation at various constant temperatures. The kinetic parameters of the native and the modified enzymes were determined and compared. These included the Michaelis-Menten constant (K_m), the maximum reaction rate (v_{max}), the denaturation rate constant (k_d) and the activation energy for denaturation (E_d).

4.1.1 Alpha amylase

Alpha amylase from *Aspergillus oryzae* was used (Section 3.1.1). This enzyme is widely used in food processing, but has a very low thermal stability (Wiseman, 1975).

4.1.1.1 Properties of native alpha amylase

The activity of the enzyme was measured (Section 3.2.3.1) at 20 °C at the following pH values: 3 and 6 (Na-citrate buffer), 4 and 5 (Na-acetate buffer), 7 and 8 (Na-phosphate buffer), 9 (borate buffer) and 10 (glycine buffer). Maximum activity was observed at pH 4 (Figure 4.1 a). The effect of temperature on activity was characterized in 20 mM sodium phosphate buffer, pH 6.9, in presence of 6.7 mM NaCl (Sigma Chemical Co. Ltd.,

1997) at temperatures of 25 to 90 °C. Activity increased as the temperature increased to 60 °C (Figure 4.1 b). A further rise in temperature caused a rapid decline in activity (Figure 4.1 b). Similar results have been previously reported for *A. oryzae* alpha amylase (Uhlig and Linsmaier-Bednar, 1998).

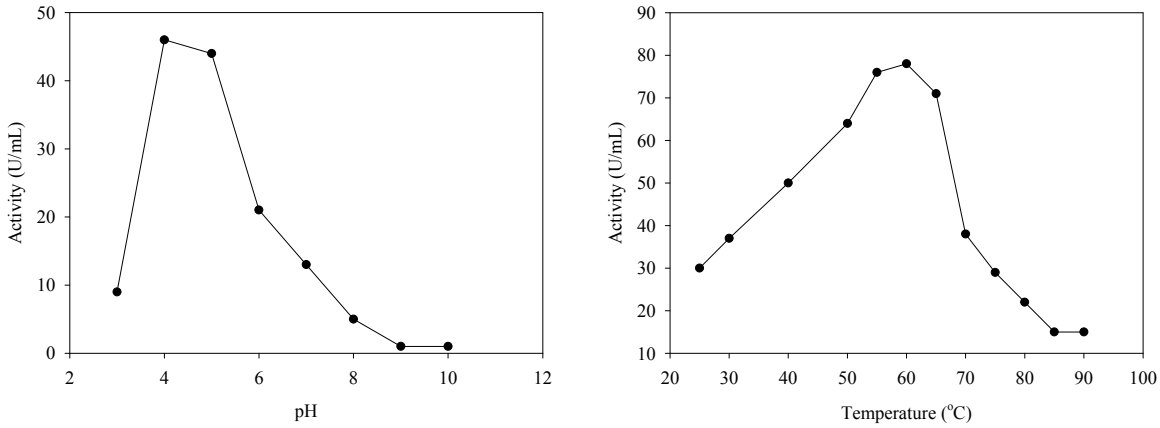

(a) (b)

Figure 4.1 (a) The optimal pH and (b) the optimal temperature for alpha amylase of *A. oryzae*.

The pH stability of alpha amylase in Na-acetate buffer (pH 4 and 5), Na-citrate buffer (pH 6), and Na-phosphate buffer (pH 7 and 8) was characterized at 25 and 55 °C. At 25 °C and pH 6.8, 100% of the initial activity remained for the entire duration (120 min) of the experiment (Figure 4.2 a) while at pH 4 and 5, 80-90% of the initial activity remained after the same time. In contrast, at 55 °C, the enzyme was unstable at every pH studied (Figure 4.2 b), being slightly more stable at pH 6 (Figure 4.2 b), and least stable at both the extreme alkaline and acidic pH.

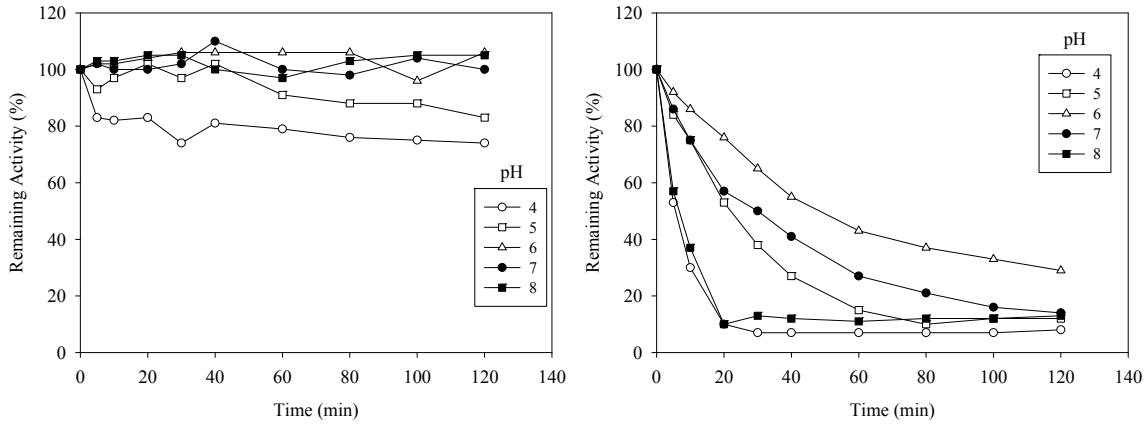

(a) (b)

Figure 4.2 pH stability of alpha amylase at (a) 25 °C and (b) 55 °C.

The thermal stability of the native alpha amylase at 25-60 °C was measured in 20 mM Na-phosphate buffer, pH 6.9 (Figure 4.3). The enzyme was quite stable at incubation temperatures of ≤40 °C over a period of 120 min, but progressively lost activity as the temperature increased above 40 °C (Figure 4.3). As previously reported, *A. oryzae* alpha amylase is not stable to heat and in the starch gelatinization process loses its activity when the temperature is raised to 68-70 °C (Uhlig and Linsmaier-Bednar, 1998).

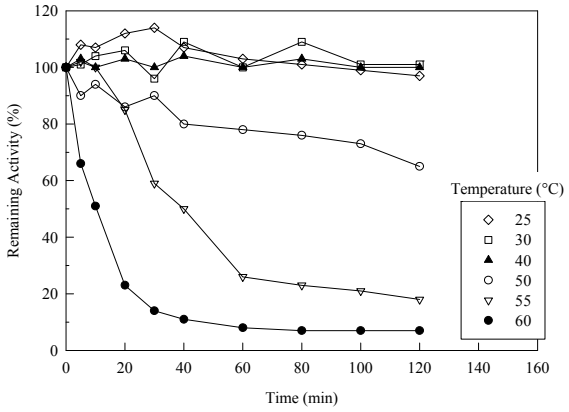

Figure 4.3 Thermal denaturation of native α-amylase as percent of initial activity remaining after incubation at various temperatures in 20 mM Na-phosphate buffer, pH 6.9.

The thermal denaturation rate constant (k_d) of alpha amylase at any given temperature was estimated as described in Section 3.2.5. Semilog plots of the fraction of the initial activity (ν_f) remaining at any time versus time were linear (Figure 4.4 a). Measurable denaturation was detectable only at temperatures of ≥50 °C. The k_d values at 50, 55, 60 and 65 °C were 0.0056, 0.0193, 0.1162 and 0.7313 min^{-1}, respectively. The activation energy of denaturation (E_d) was calculated (Section 3.2.5, Figure 4.4 b) to be 298 kJ/mol.

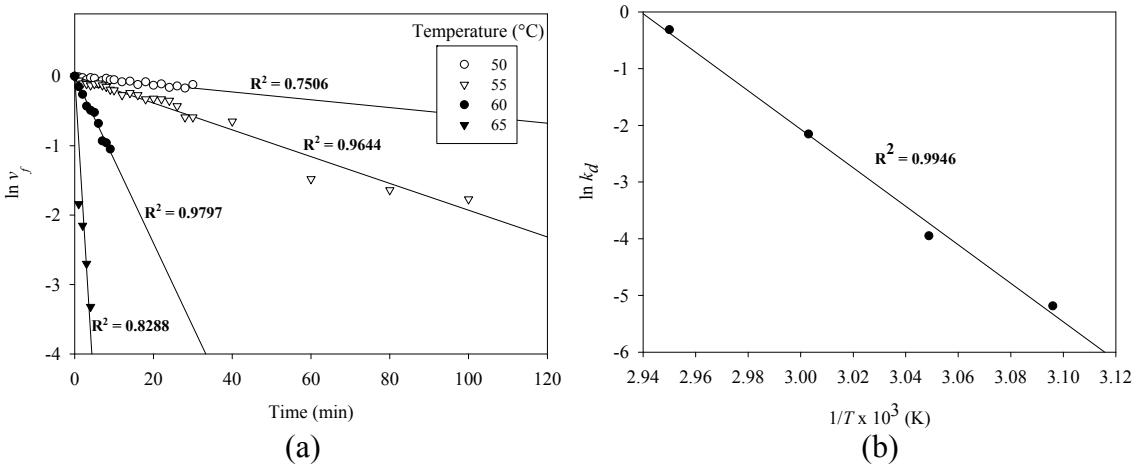

Figure 4.4 Estimation of (a) denaturation rate constant k_d and (b) activation energy of denaturation E_d for native alpha amylase in 0.1 M Na-citrate buffer, pH 6.

As expected, thermal denaturation was first-order with respect to enzyme concentration (Raviyan *et al.*, 2003). The denaturation constant increased with increasing temperature in conformance with Equation 3.13 (Section 3.2.5). The estimated value of the activation energy for denaturation was within the 167-544 kJ/mol range that is typical for enzymes (Shuler and Kargi, 2002).

4.1.1.2 Thermal stabilization by isocyanates

Alpha amylase (0.9 μM) was reacted with different concentrations (1-50 mM) of crosslinking reagents with various chain lengths. The crosslinkers were butyl isocyanate (BIC, C = 0) butamethylene diisocyanate (BMDC, C = 4), hexamethylene diisocyanate (HMDC, C = 6) and octamethylene diisocyanate (OMDC, C = 8). The specified concentration of crosslinking reagents was added to an aqueous solution of enzyme dissolved in 0.1 M Na-citrate buffer, pH 6, and left to shake vigorously at room temperature for 15 minutes. Excess crosslinking reagent was removed after the reaction using a PD 10 desalting column (Section 3.2.1.1). The thermal stability of the native (control) and modified enzymes was measured at 60 °C for 30 minutes. The results are shown in Figure 4.5.

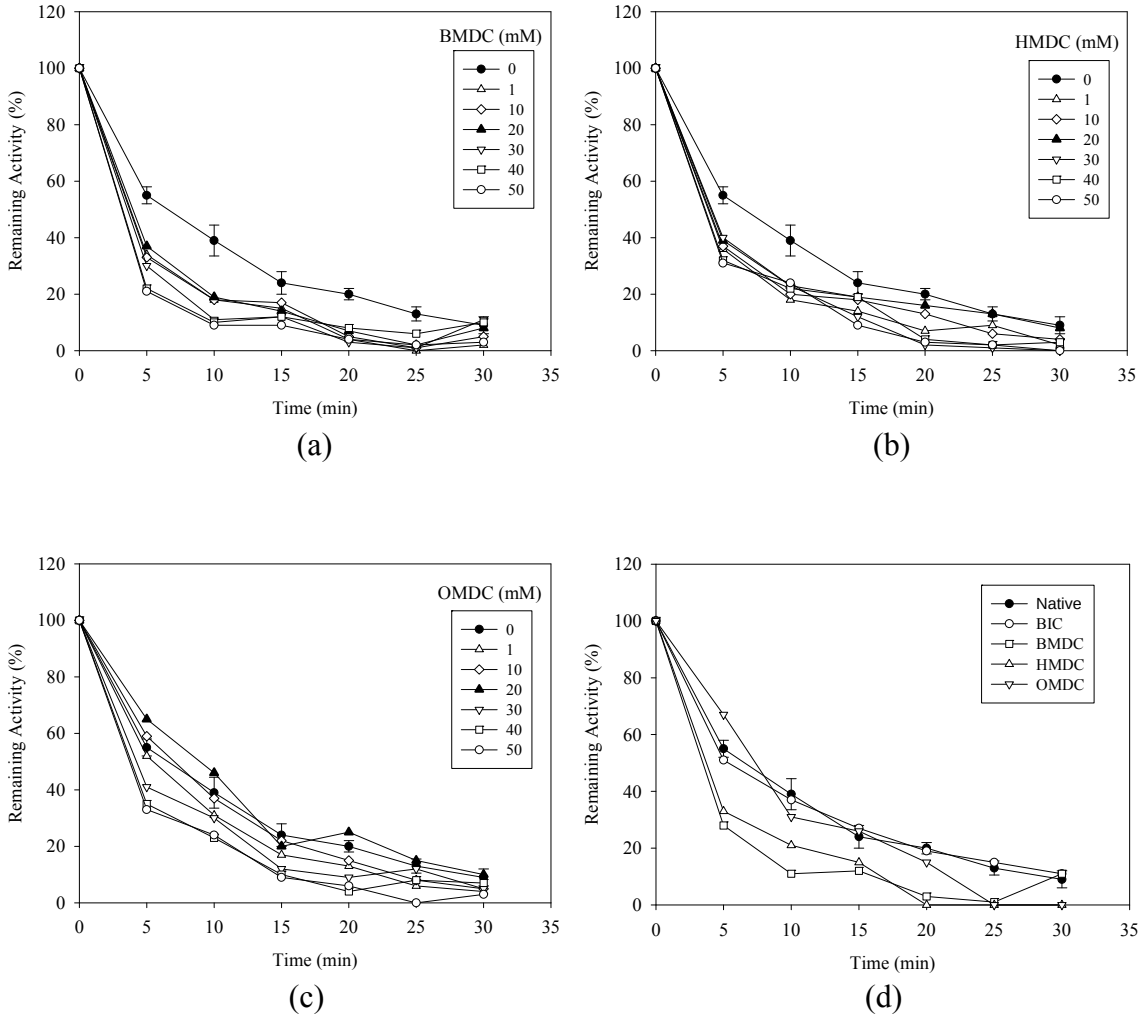

Figure 4.5 Thermal stability (60 °C) of alpha amylase (0.9 μM) modified with 1-50 mM diisocyanates: (a) BMDC; (b) HMDC; and (c) OMDC. (d) Thermal stability of the enzyme reacted with 20 mM diisocyanates (BMDC, HMDC, OMDC) and the monofunctional crosslinker, BIC.

Enzyme treatments with diisocyanates and the monofunctional butyl isocyanate did not improve thermal stability relative to the native enzyme (Figure 4.5). Crosslinking was carried out at pH 6 and room temperature. Under these conditions the native enzyme is fairly stable (Figure 4.2 a). Depending on pH of the crosslinking reaction, isocyanates can react with different functional groups present in an enzyme molecule (Means and Feeney, 1971). In view of the possibility that diisocyanate may crosslink a different set of the enzyme functional groups at different pH to produce a more stable enzyme, the enzyme was treated with one of the diisocyanates (octamethylene diisocyanate) at different pH. No stabilization was observed (Figure 4.6).

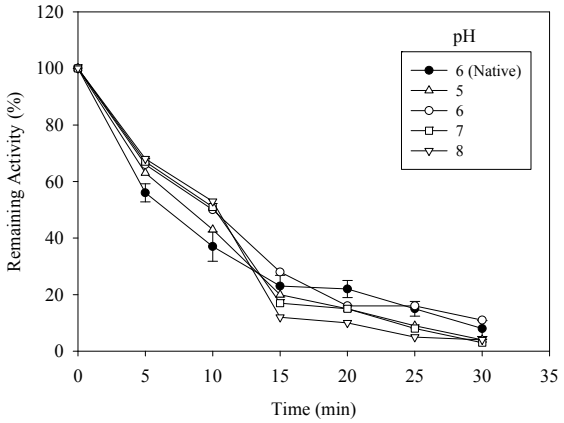

Figure 4.6 Thermal stability (60 °C) of alpha amylase (0.9 μM) modified with 20 mM of octamethylene diisocyanate. The modification reaction was carried out at the specified pH values (pH 5-8). The activity was measured at pH 6.

4.1.1.3 Thermal stabilization by imidoesters

Alpha amylase was modified using the imidoester reagents ethyl acetimidate (EA), dimethyl adipimidate (Iyer and Ananthanarayan, 2008), dimethyl pimelimidate (DMP) and dimethyl suberimidate (DMS), as described in Section 3.2.1.2. In all cases 0.9 μM enzyme was reacted with 0.1-10 mg/mL of the imidoester reagent. As shown in Figure 4.7, there appeared to be no effect from exposing the enzyme to different crosslinking reagents at a number of different concentrations. Similarly, no stabilization was observed when alpha amylase was treated with 10 mg/mL of imidoester crosslinkers with different chain lengths (Figure. 4.7, d).

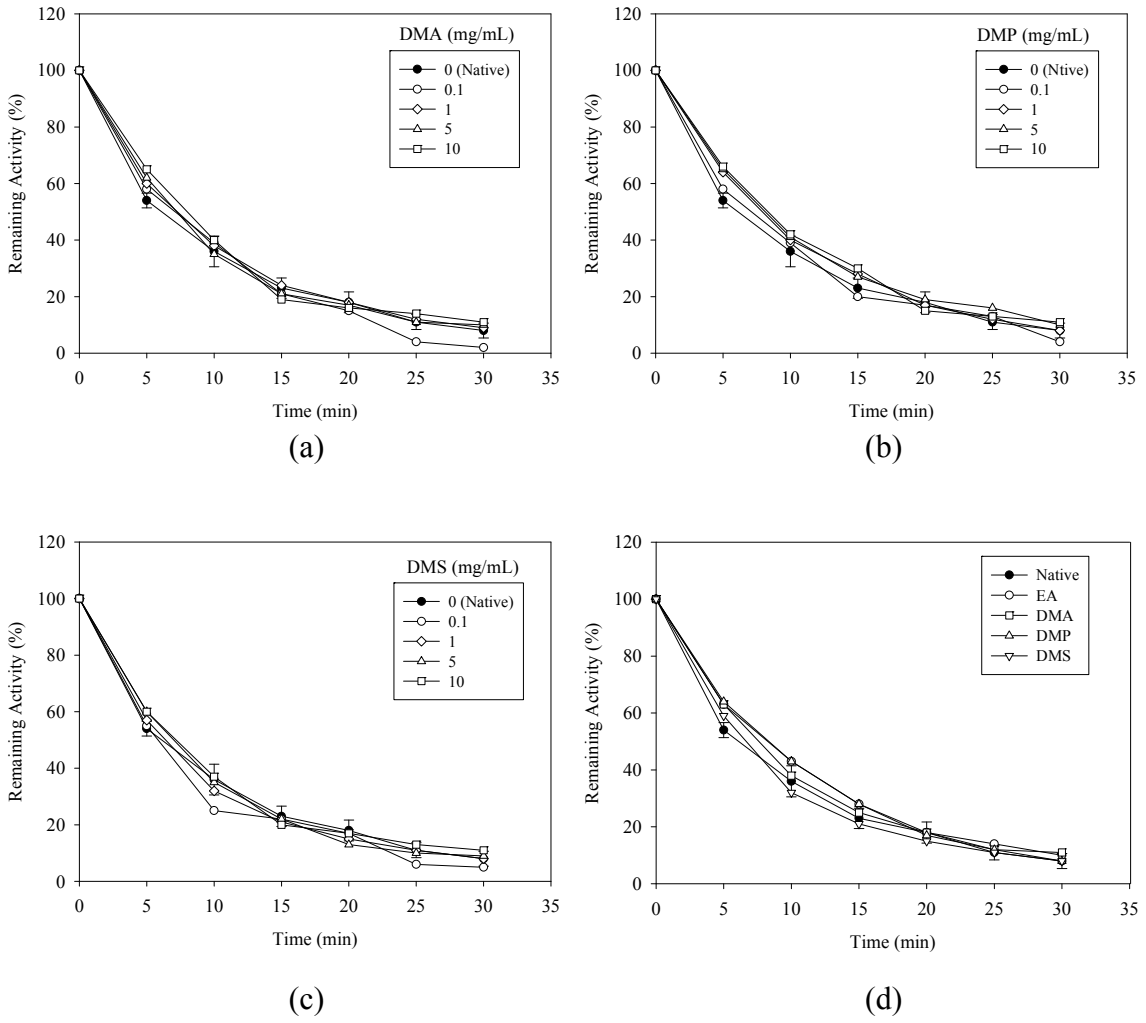

Figure 4.7 Thermal stability (60 °C) of alpha amylase (0.9 μM) modified with 0.1-10 mg/mL of diimidoesters: (a) DMA; (b) DMP; and (c) DMS. (d) Thermal stability of the enzyme modified with 10 mg/mL of diimidoesters and the corresponding monofunctional crosslinker, EA.

Crosslinking alpha amylase (0.9 μM) with dimethyl pimelimidate (10 mg/mL) was carried out in Na-acetate buffers (pH 4 and 5), Na-citrate buffer (pH 6) and Na-phosphate buffers (pH 7 and 8). The pH values of the crosslinking reaction had no significant effect on enzyme stability (Figure 4.8) relative to the control. All attempts to stabilize the enzyme using a number of different imidoesters over a range of pH, were therefore unsuccessful.

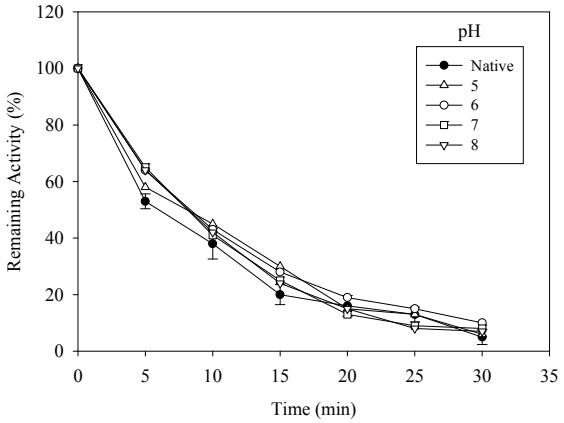

Figure 4.8 Thermal stability of alpha amylase (0.9 μM) crosslinked with 10 mg/mL of dimethyl pimelimidate (DMP) at pH 5-8.

4.1.1.4 Thermal stabilization by diamines

Alpha amylase (0.9 μM) was treated with a series of diamine crosslinkers (Section 3.1.2) with concentration ranging between 0.1-10 mg/mL as explained in Section 3.2.1.3. Again, none of the diamine series of crosslinkers improved the thermal stability of the enzyme (Figure 4.9). Use of the crosslinkers with different chain lengths and different reaction conditions (pH) did not affect the results (Figure 4.10).

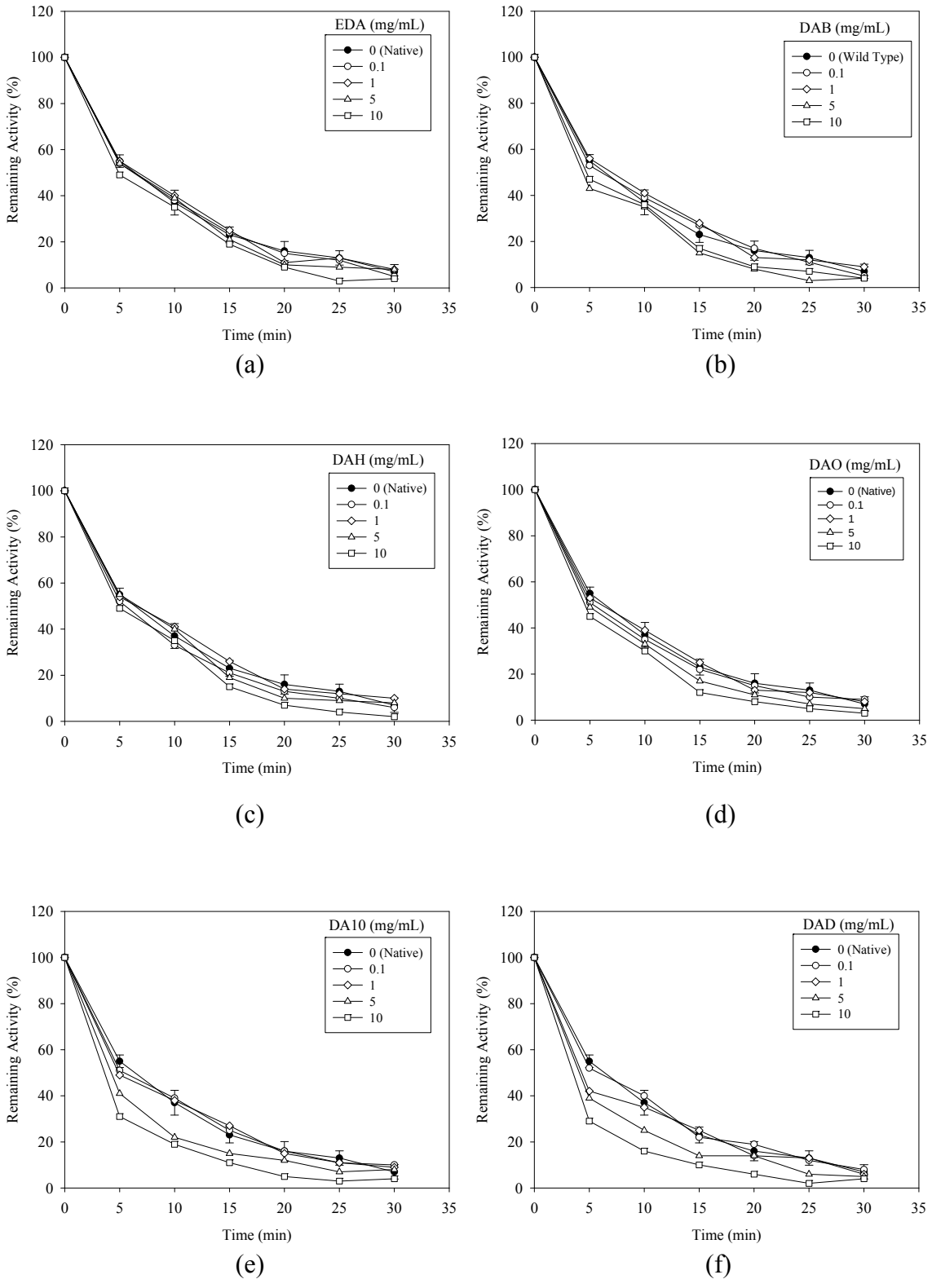

Figure 4.9 Thermal stability (60 °C) of alpha amylase (0.9 μM) modified with 0.1-10 mg/mL of diamines: (a) ethylene diamine, EDA; (b) diaminobutane, DAB; (c) diaminohexane, DAH; (d) diaminooctane, DAO; (e) diaminodecane, DA10; and (f) diaminododecane, DAD.

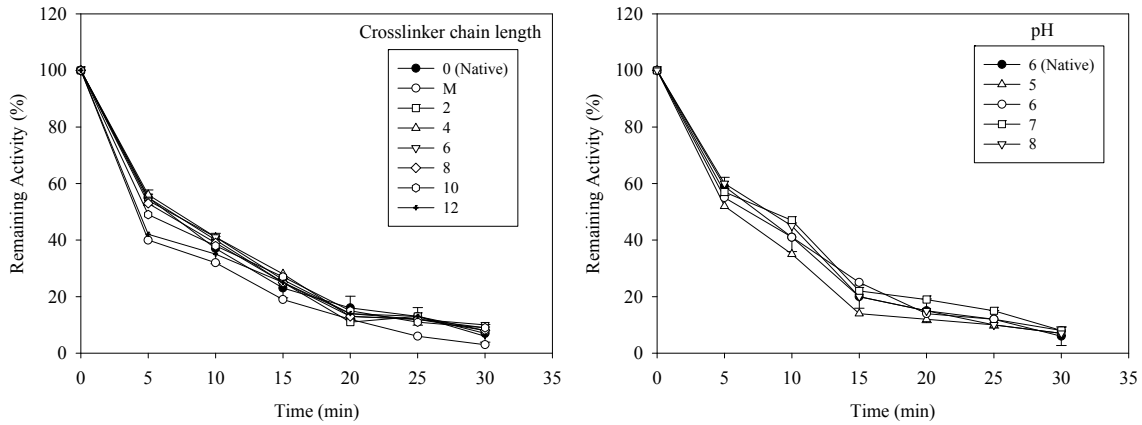

(a) (b)

Figure 4.10 (a) Thermal stability (60 °C) of alpha amylase (0.9 μM) modified with 1 mg/mL of diamine reagents of various chain lengths (C = 0-12). (b) Thermal stability (60 °C) of alpha amylase modified with 1 mg/mL of EDA (C = 2) at pH 5-8.

4.1.2 Beta galactosidase

4.1.2.1 Properties of native beta galactosidase

An activity (Section 3.2.3.2) versus pH profile for β-galactosidase (Section 3.1.1) at room temperature is shown in Figure 4.11 a. Maximum activity was observed under acidic conditions at pH 4-5, while the enzyme was barely active at pH values >6. The dependence of activity on temperature was determined at pH 3.5 (Section 3.2.3.2) at temperatures between 25 and 90 °C. The results are shown in Figure 4.11 b. The enzyme had a temperature optimum between 45 and 55 °C (Figure 4.11 b). In keeping with the general pattern for enzymes, the activity rose slowly with increasing temperature until it reached an optimum and then fell sharply as the temperature increased further, due to denaturation.

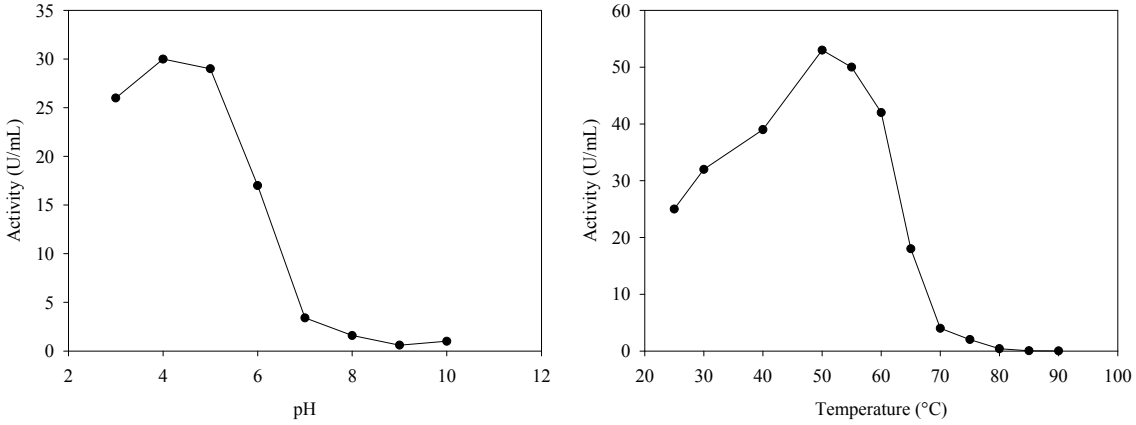

(a) (b)

Figure 4.11 (a) The optimal pH and (b) the optimal temperature of β-galactosidase from *A. oryzae.*

The stability of beta galactosidase between pH 4 and 8 was determined at 25 °C and 50 °C. As shown in Figure 4.12 a, the enzyme was quite stable at 25 °C particularly under acidic conditions (pH 4-6). At 50 °C, the stability of the enzyme was highly dependent on pH (Figure 4.12 b), being fairly stable for up to 90 min between pH 5 and 6, but less stable at pH 4 and pH >6.

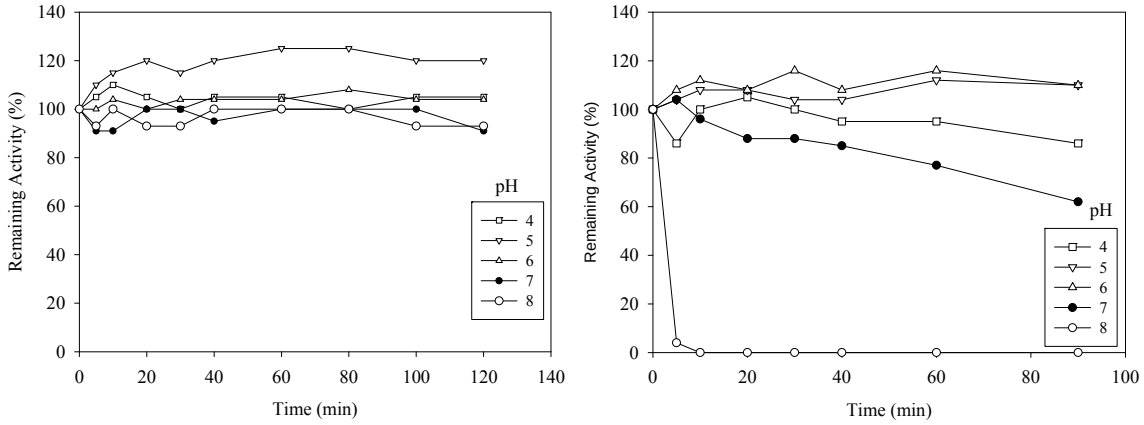

(a) (b)

Figure 4.12 The pH stability of β-galactosidase at (a) 25 °C and (b) 50 °C.

The stability of β-galactosidase in 0.1 M Na-phosphate buffer (pH 7) at temperatures between 25 and 65 °C was determined as described in Section 3.2.2 and Section 3.2.3.2. As shown in Figure 4.13, β-galactosidase was quite stable up to a

temperature of 55 °C, but the activity declined extremely rapidly at temperature ≥65 °C (Figure 4.13).

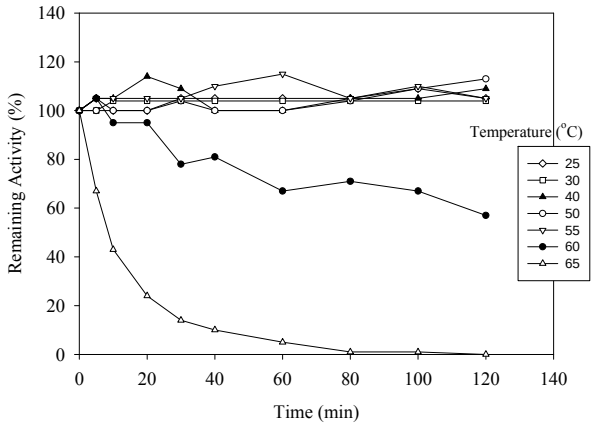

Figure 4.13 Thermal stability of native β-galactosidase as percent of initial activity remaining after incubation at various temperatures in 0.1 M Na-phosphate buffer, pH 7.

Data measured for the fraction of the initial enzyme activity (i.e. ν_f) remaining after incubation at a constant temperature were plotted (Figure 4.14 a) in accordance with Eq. (3.12). As expected, the plots were linear (Figure 4.14 a), allowing the thermal denaturation rate constant k_d to be calculated for each temperature (Section 3.2.5). For incubation temperatures ≤55 °C, β-galactosidase was quite stable and the denaturation rate constant was essentially zero, and the plot of log k_d versus $1/T$ was linear (Figure 4.14 b). This plot was used to calculate an activation energy (E_d) for thermal denaturation of 459 kJ/mol.

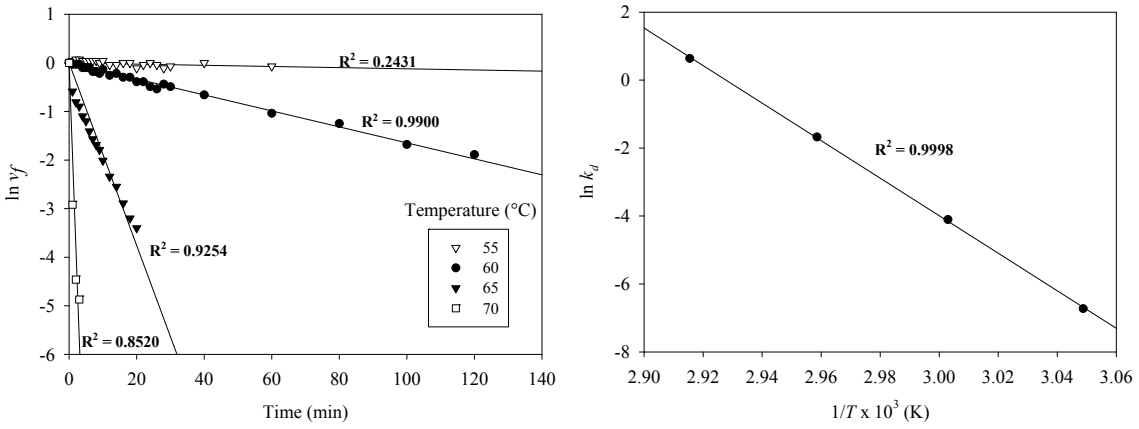

Figure 4.14 (a) The fraction of initial activity (ν_f) remaining versus incubation time for native β-galactosidase at various incubation temperatures. (b) Estimation of the activation energy for denaturation of the native enzyme.

4.1.2.2 Thermal stabilization by isocyanates

Beta galactosidase (0.9 μM in 0.1 M Na-citrate buffer, pH 6) was modified with 10-50 mM of a specified diisocyanate reagent at room temperature (Section 3.2.1.1). The thermal stability was measured as previously described (Section 3.2.2 and Section 3.2.3.2), and results are shown in Figure 4.15. At 60 °C, no significant improvement of enzyme stability was seen relative to the control (i.e. the native enzyme) for samples treated with any of the diisocyanate reagents at any of the concentrations used.

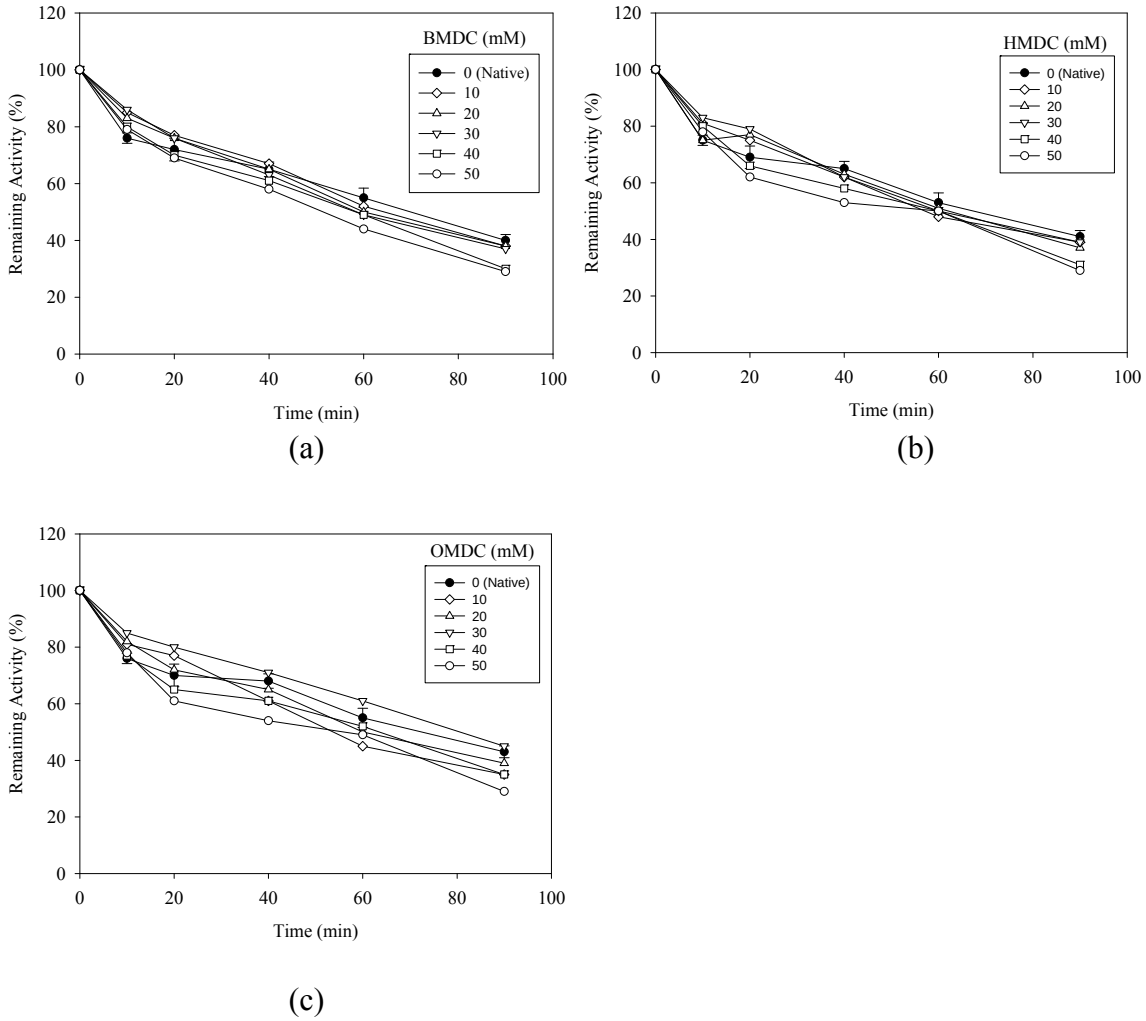

Figure 4.15 Thermal stability (60 °C) of β-galactosidase (0.9 μM) modified with 10-50 mM of (a) BMDC (butamethylene diisocyanate), (b) HMDC (hexamethylene diisocyanate) and (c) OMDC (octamethylene diisocyanate).

The thermal stability of β-galactosidase modified with diisocyanate crosslinkers of different chain lengths was then compared with the thermal stability of the enzyme modified with a monofunctional isocyanate crosslinker (Figure 4.16 a). Changes in chain

lengths (C = 4-8) of the crosslinker had no effect on stability. The use of the monofunctional reagent actually decreased enzyme stability compared to that observed with the bifunctional reagents (Figure 4.16 a; C = 0). The modification reactions shown in Figure 4.15 and Figure 4.16 a were carried out at pH 6. Isocyanates can react with different functional groups on the enzyme depending on pH (Means and Feeney, 1971). Therefore, reaction with one of the reagents (OMDC, octamethylene diisocyanate) was attempted at different pH values. No improvement in enzyme stability was observed at different pH (Figure 4.16 b).

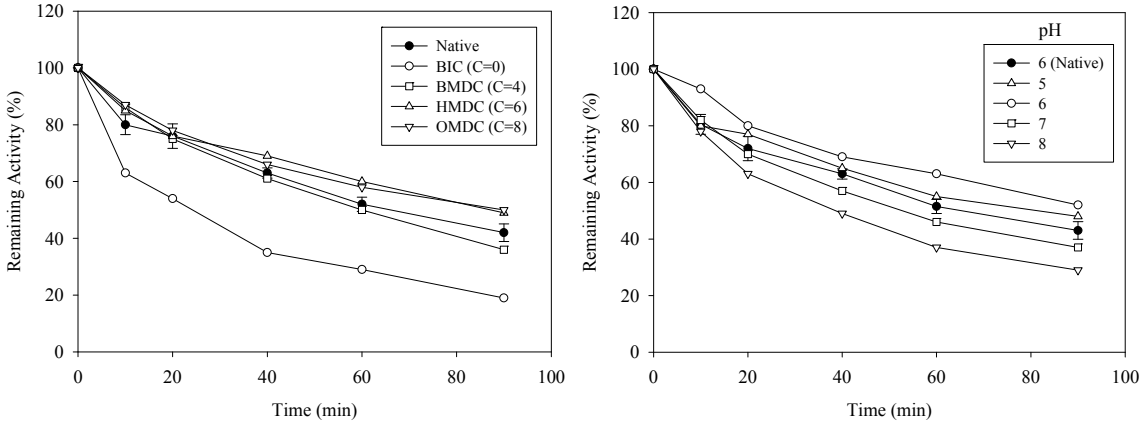

Figure 4.16 (a) Thermal stability (60 °C) of β-galactosidase (0.9 μM) modified with isocyanates (30 mM): BIC (butyl isocyanate), BMDC (butamethylene diisocyanate), HMDC (hexamethylene diisocyanate) and OMDC (octamethylene diisocyanate). (b) Thermal stability (60 °C) of β-galactosidase (0.9 μM) modified with 30 mM OMDC (octamethylene diisocyanate) at different pH values during crosslinking.

4.1.2.3 Thermal stabilization by imidoesters

Treatment of β-galactosidase (0.9 μM) with 1-10 mg/mL of diimidoester crosslinkers in Na-citrate buffer at pH 6 did not improve enzymes thermal stability as shown in Figure 4.17. Thermal stability was not affected by the chain length (C = 4-6) of the crosslinker or the use of the monofunctional reagent (Figure 4.18 a). Changes in pH (Na-acetate, Na-citrate and Na-phosphate buffer) of the crosslinking reaction did not affect the outcome (Figure 4.18 b).

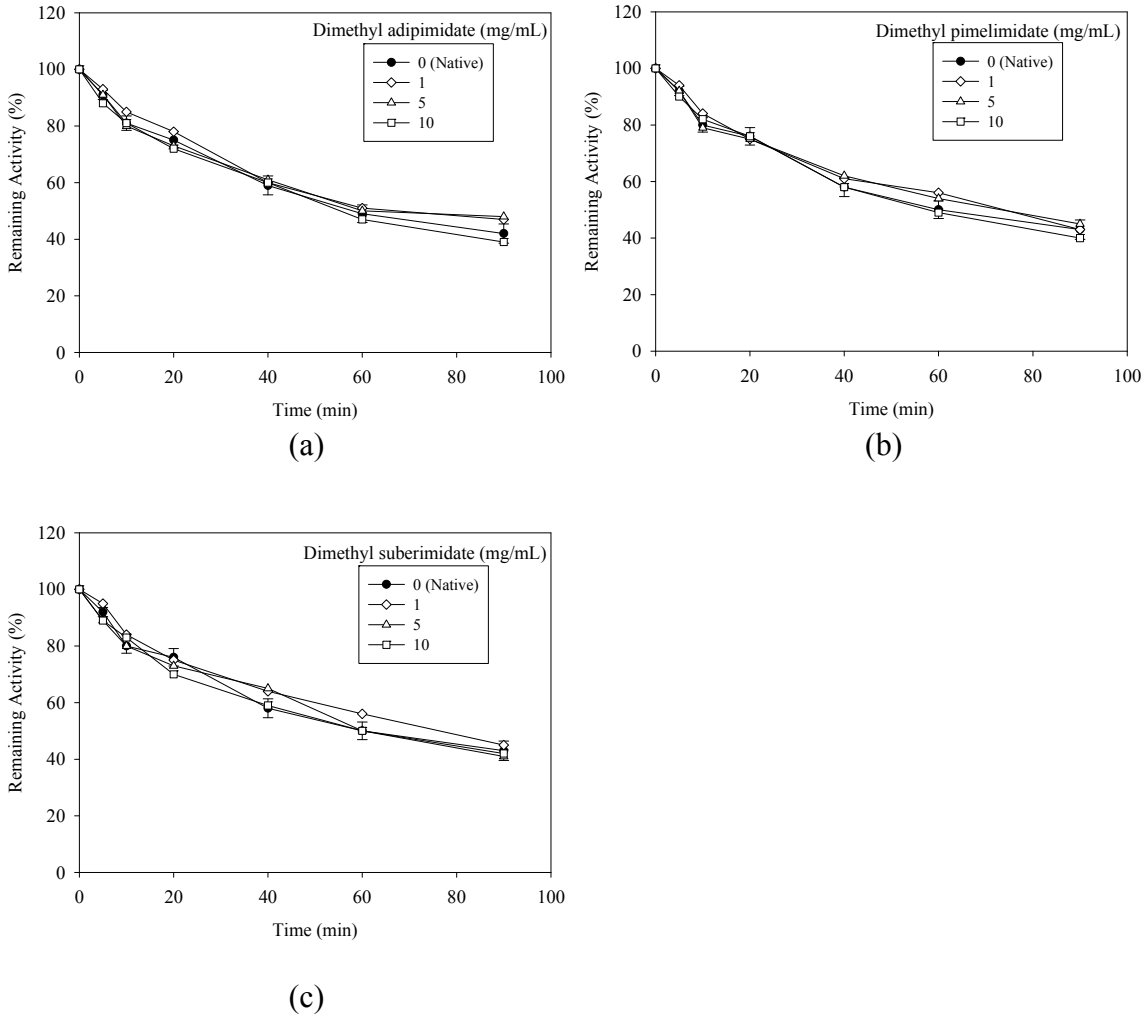

Figure 4.17 Thermal stability (60 °C) of β-galactosidase (0.9 μM) modified with 1-10 mg/mL of (a) dimethyl adipimidate, (b) dimethyl pimelimidate and (c) dimethyl suberimidate. The crosslinking reaction was carried out in Na-citrate buffer at pH 6.

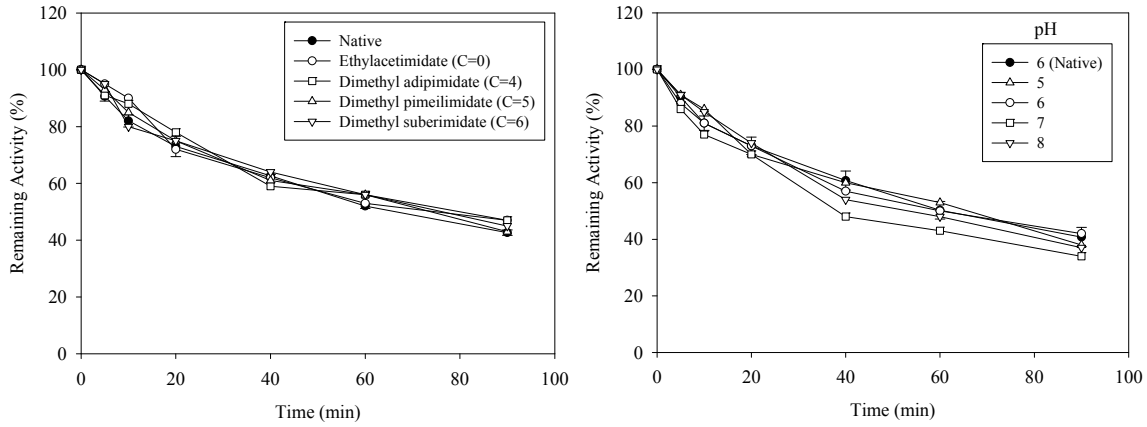

(a) (b)

Figure 4.18 Thermal stability (60 °C) of β-galactosidase (0.9 μM) modified with: (a) imidoesters (1 mg/mL) of different chain lengths (Na-citrate buffer, pH 6); and (b) dimethyl suberimidate (1 mg/mL) at different crosslinking pH values.

4.1.2.4 Thermal stabilization by diamines

Reaction of β-galactosidase with diamines of different chain lengths (Na-citrate buffer pH 6) (Section 3.2.1.3) resulted in no change in thermal stability compared to the native enzyme (Figure 4.19).

Crosslinking of β-galactosidase with diaminooctane produced a slight improvement in thermal stability compared to that achieved with diamines of both shorter and longer chain lengths than diaminooctane (Figure 4.20 a). However, no significant improvement in the thermal stability of the modified β-galactosidase was found relative to the control at any pH used for crosslinking (Figure 4.20 b).

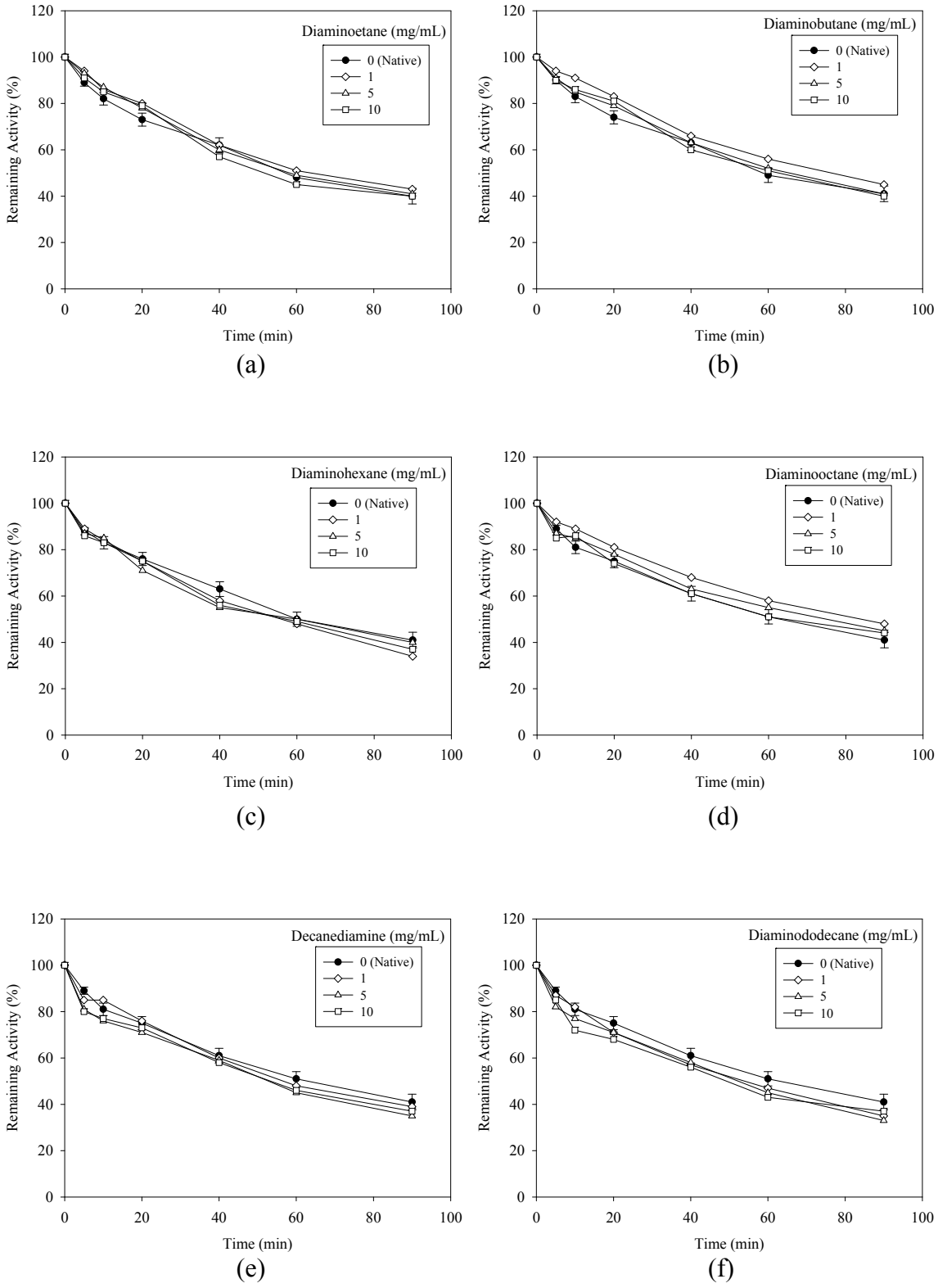

Figure 4.19 Thermal stability (60 °C) of β-galactosidase (0.9 μM) modified with 1-10 mg/mL of: (a) diaminoetane, EDA; (b) diaminobutane, DAB; (c) diaminohexane, DAH; (d) diaminooctane, DAO; (e) decanediamine, DA10; and (f) diaminododecane, DAD.

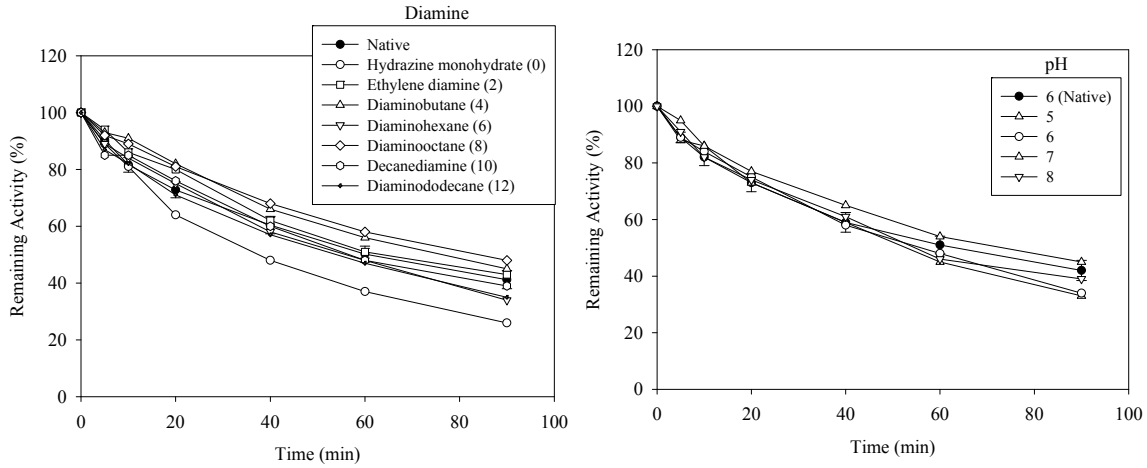

(a) (b)

Figure 4.20 (a) Thermal stability (60 °C) of β-galactosidase (0.9 μM) modified with 1 mg/mL diamines of various chain lengths (C = 0-12). (b) Thermal stability (60 °C) of β-galactosidase modified with 1,8-diaminooctane at various crosslinking pH values.

4.1.3 Invertase

4.1.3.1 Properties of native invertase

The optimal pH for *S. cerevisiae* invertase was determined by measurements of activity at room temperature (Section 3.2.3.3). The activity was measured in Na-citrate buffers (pH 3 and 6), Na-acetate buffers (pH 4 and 5), Na-phosphate buffers (pH 7 and 8), borate buffer (pH 9) and glycine buffer, pH 10. An activity maximum was seen at pH 5 (Figure 4.21 a).

The temperature for optimum activity was determined in 0.1 M Na-acetate buffer, pH 4.6. The highest activity was found at 50-65 °C (Figure 4.21 b). The activity declined at temperature ≥65 °C.

The pH stability was measured at 25 °C in Na-acetate buffer at pH 4 and 5, Na-citrate buffer at pH 6 and Na-phosphate buffers at pH 7 and 8. The results are shown in Figure 4.22 a. Native invertase was quite stable at 25 °C over the entire range of pH values tested. In contrast, at 50 °C, the stability at pH values of 4 and 5 (Na-acetate buffers) was acceptable, but was poor at pH >5 (Figure 4.22 b).

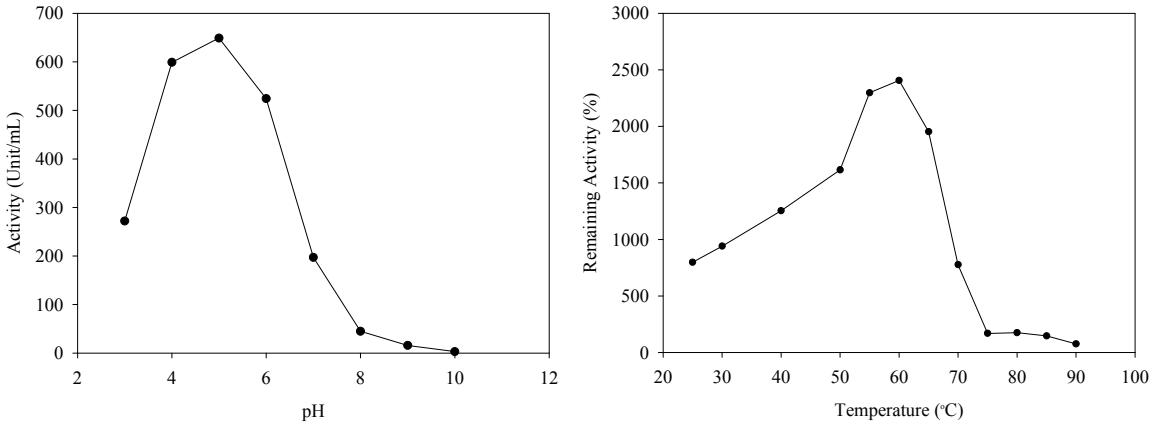

(a) (b)

Figure 4.21 (a) The optimal pH and (b) the optimal temperature of invertase.

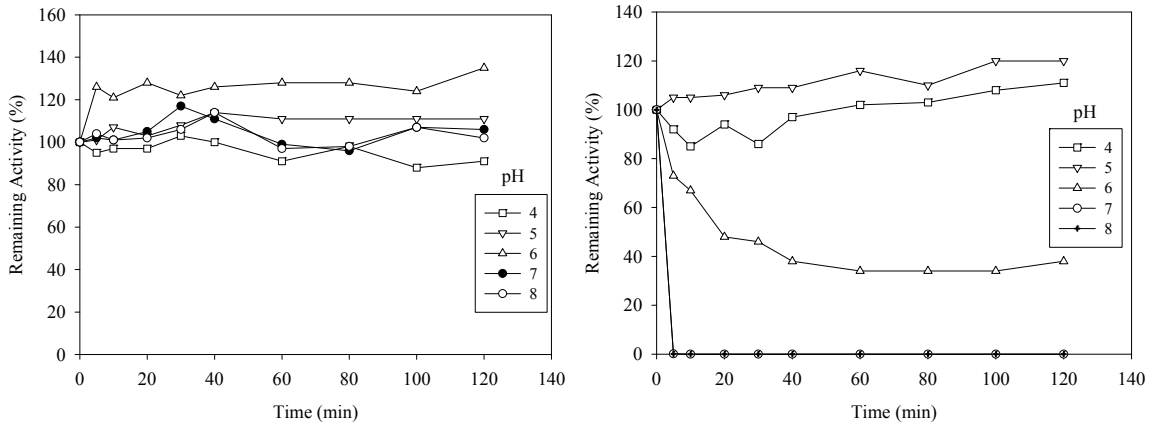

(a) (b)

Figure 4.22 The pH stability of invertase at (a) 25 °C and (b) 50°C.

At pH 5 (0.1 M Na-acetate buffer), the enzyme stability was measured at various incubation temperatures to obtain data for determining the activation energy of thermal denaturation. The data are shown in Figure 4.23. The enzyme was quite stable at up to 40 °C, but degraded increasingly rapidly as the incubation temperature increased.

The denaturation rate constant (k_d) at any given temperature was estimated as explained previously (Section 3.2.5). The semilog plots of the fraction of the initial activity (v_f) remaining at time t are shown in Figure 4.24 a. The k_d values obtained from the slopes (Figure 4.24 a) of these plots were plotted as in Figure 4.24 b to obtain a value of 368 kJ/mol for the activation energy of thermal denaturation.

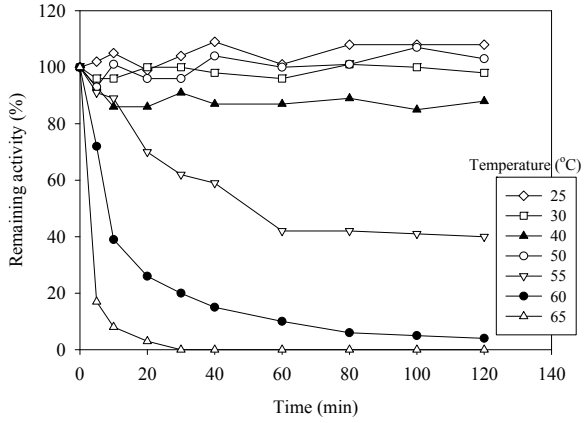

Figure 4.23 Thermal stability of native invertase as percent of the initial activity remaining after incubation at various temperatures in 0.1 M Na-acetate buffer, pH 5.

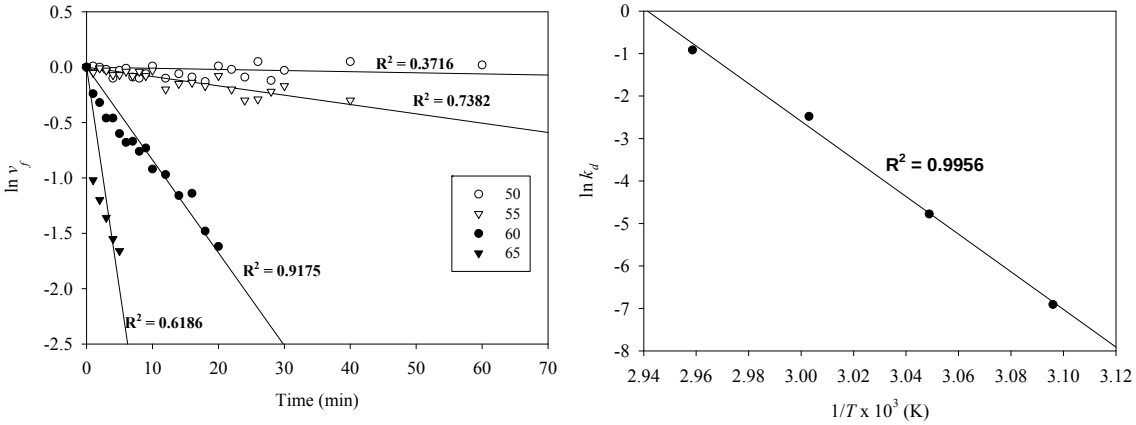

(a) (b)

Figure 4.24 (a) The fraction of initial activity (i.e. v_f) remaining versus incubation time, for native invertase at various incubation temperatures. (b) A plot of ln k_d versus 1/T.

4.1.3.2 Stabilization by isocyanates

Stability data for invertase (0.9 μM) modified with diisocyanate reagents (1-50 mM) are shown in Figure 4.25 along with that for the native enzyme (control). The highest level of thermal stabilization was observed for the enzyme treated with 20-30 mM of BMDC and HMDC (Figure 4.25 a, b). OMDC was also an effective stabilizer (Figure 4.25 c), but not as good as BMDC and HMDC.

The monofunctional reagent (BIC) was an ineffective stabilizer because it could not produce any crosslinks but instead reacted with the hydrophilic functional groups on

the surface of the enzyme, making the surface hydrophobic. BMDC and HMDC on the other hand could both form intramolecular crosslinks and were shown to act as the effective stabilizers. This was most likely because their lengths (BMDC, C = 4, nominal length 5.17 Å; HMDC, C = 6, nominal length 6.92 Å) were such that they could tightly crosslink surface functional groups that resulted in helping prevent the enzyme from unfolding. In contrast, OMDC (C = 8, nominal length >6.92 Å) proved to be less effective in stabilizing the enzyme because although it could form crosslinks, they were likely to be "loose" crosslinks (because of its longer length) that were not as stabilizing. As shown in Figure 4.26 a), all diisocyanates (C = 4, 6, 8) that could crosslink were effective in stabilizing the enzyme relative to the control. In contrast, the monofunctional reagent (BIC) had no stabilizing effect, but rather made the enzyme less stable relative to control.

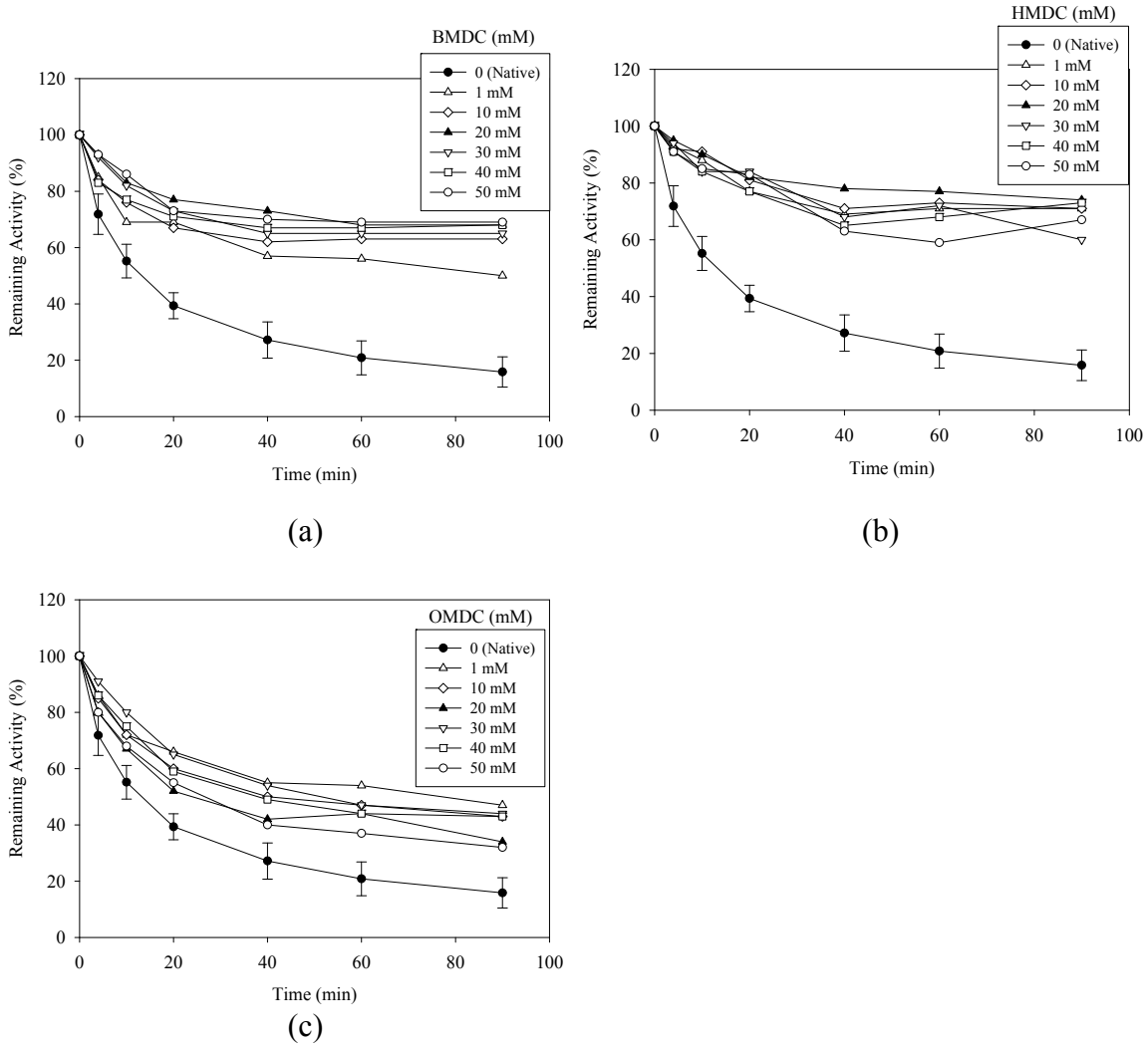

Figure 4.25 Thermal stability (60 °C, acetate buffer, pH 5) of invertase (0.9 μM) modified with: (a) BMDC (butamethylene diisocyanate), (b) HMDC (hexamethylene diisocyanate) and (c) OMDC (octamethylene diisocyanate).

As BMDC was the most effective stabilizer, its reaction with the enzyme was carried out at different pH (pH 5-8) to see if pH might improve stabilization of the enzyme. The results are shown in Figure 4.26 b. The most effective stabilization was obtained by conducting the crosslinking reaction at pH 6.

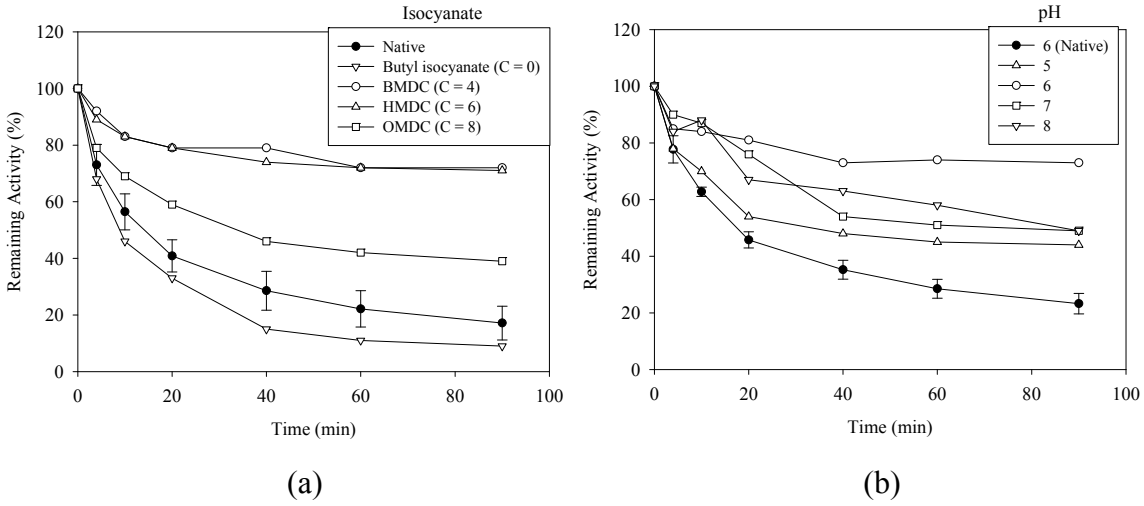

(a) (b)

Figure 4.26 (a) Thermal stability (60 °C, Na-acetate buffer, pH 5) of invertase (0.9 μM) modified with 30 mM isocyanate crosslinkers. (b) Thermal stability (60 °C, Na-acetate buffer, pH 5) of enzyme modified with BMDC at various pH values.

Although Figure 4.25 and Figure 4.26 clearly reveal the stabilizing effect of certain crosslinking treatments on invertase, they do not show how a treatment influences the absolute activity of the enzyme. The absolute activity versus time profiles for native and variously crosslinked invertase incubated at 60 °C, are shown in Figure 4.27. These data are for exactly the same experiments as in Figure 4.25. Figure 4.27 clearly shows that for invertase crosslinked with BMDC and HMDC, the activity exceeds that of the native invertase within 10-20 min of incubation eventhough the native enzyme had a higher initial activity than the crosslinked enzyme samples. The crosslinked preparations continue to perform at a higher activity than the native enzyme for the duration of experiment (time ≥20 min, Figure 4.27 a; time ≥10 min, Figure 4.27 b).

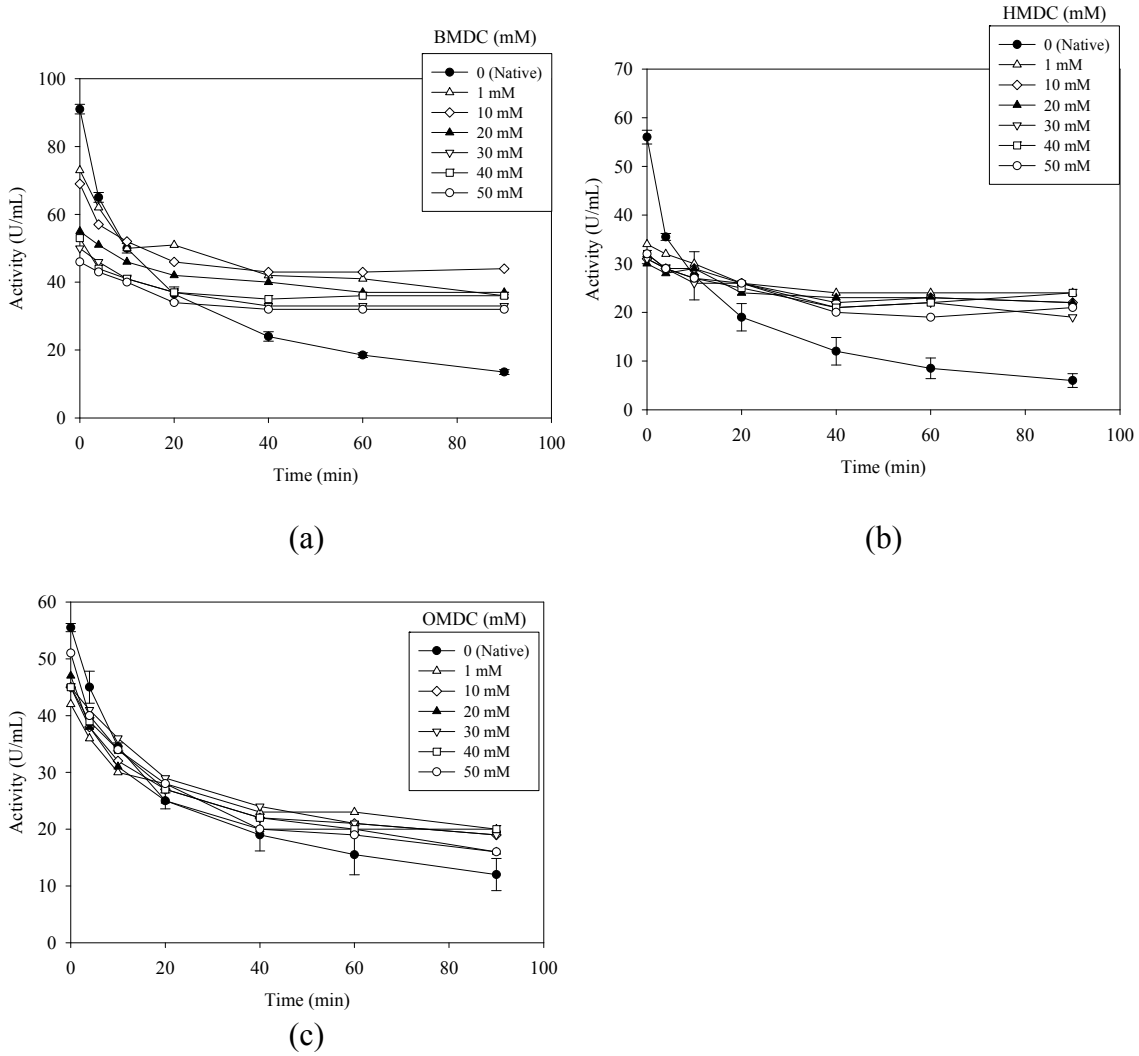

Figure 4.27 Activity change (60 °C, Na-acetate buffer, pH 5) versus time for invertase (0.9 μM) modified with: (a) BMDC (butamethylene diisocyanate), (b) HMDC (hexamethylene diisocyanate) and (c) OMDC (octamethylene diisocyanate).

As reaction with BMDC appeared to effectively stabilize the enzyme, a batch of the enzyme (0.9 μM) modified with 30 mM of this reagent at a reaction pH of 6 (Na-citrate buffer) was prepared to further investigate its thermostability. Aliquots of crosslinked enzyme in 0.1 M Na-acetate buffer, pH 5, were incubated at constant temperatures between 54 and 60 °C for various length of time. Semilog plots of the fraction of the initial activity (i.e. ν_f) remaining at various times (Figure 4.28 a) were used to estimate the denatuation rate constant (k_d, Table 4.1), and subsequently the activation energy of thermal denaturation was estimated (Figure 4.28 b).

Values estimated for the activation energy of denaturation were 372 and 517 kJ/mol for the native and the crosslinked enzyme, respectively. For the native enzyme, the

value of 372 kJ/mol was calculated (Figure 4.28 b) using data from an independent experiment was quite comparable to the value of 368 kJ/mol obtained earlier in this work (Figure 4.24 b), confirming the reproducibility experimental results.

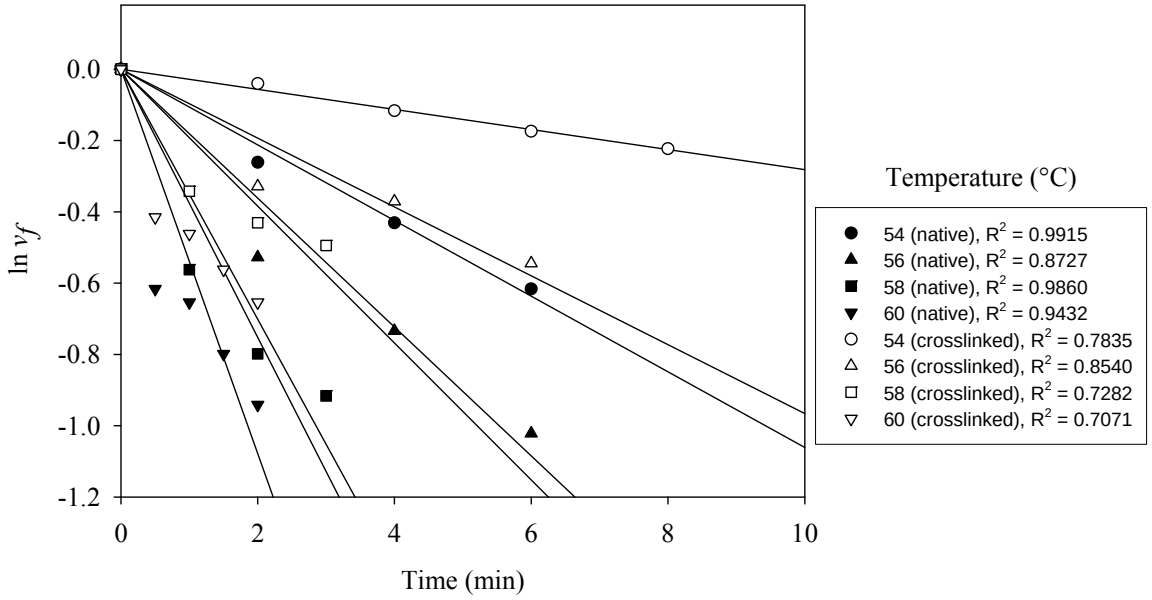

(a)

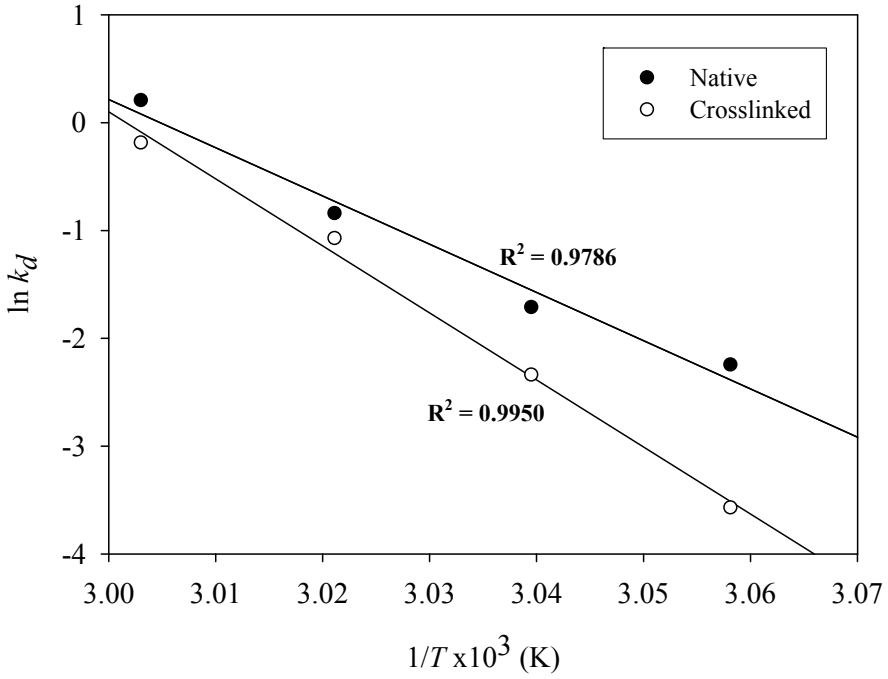

(b)

Figure 4.28 Estimation of (a) denaturation rate constant (k_d) and (b) activation energy of denaturation (E_d) for native and modified invertase at various temperatures in 0.1 M Na-acetate buffer, pH 5.

Table 4.1 Denaturation rate constants at various temperatures

Temperature (°C)	k_d (min^{-1})	
	Native invertase	Crosslinked invertase
54	10.61×10^{-2}	2.82×10^{-2}
56	18.07×10^{-2}	9.66×10^{-2}
58	43.18×10^{-2}	34.25×10^{-2}
60	123.24×10^{-2}	83.1×10^{-2}

As invertase could be effectively stabilized by BMDC, the substrate conversion kinetics of the stabilized enzyme were compared with that of the native enzyme. The invertase-catalysed conversion of sucrose to glucose and fructose is known to obey Michaelis-Menten kinetics (Voet and Voet, 2004). Therefore, the initial rate of reaction v was measured at various initial concentrations of the substrate (0.01-0.3 M) at room temperature, pH 6 (Na-citrate buffer), as specified in Section 3.2.4. The plots of v versus S are shown in Figure 4.29. The data were transformed using a Lineweaver-Burk plot (Equation 3.2) and a Hanes-Woolf plot (Equation 3.3). The plots were straight lines (Figure 4.30), as expected. The y-intercepts of the lines (Figure 4.30) were used to estimate the v_{max} values. The slopes of the lines were then used to calculate the K_m values. The values of these parameters for the native and modified enzyme (0.9 μM enzyme reacted with 30 mM BMDC at pH 6, Na-citrate buffer; Section 3.2.1.1) are shown in Table 4.2.

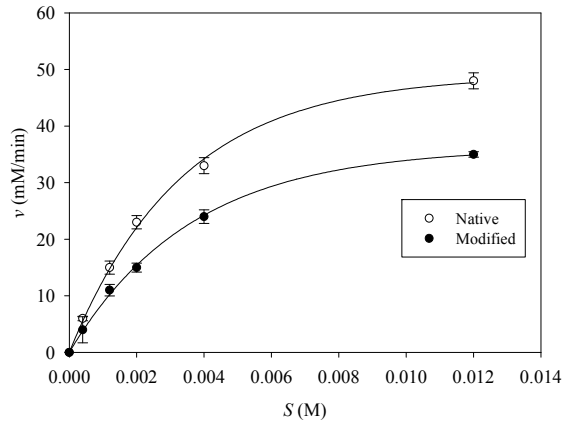

Figure 4.29 The rate of reaction at various sucrose concentrations *S*, for native and modified invertase.

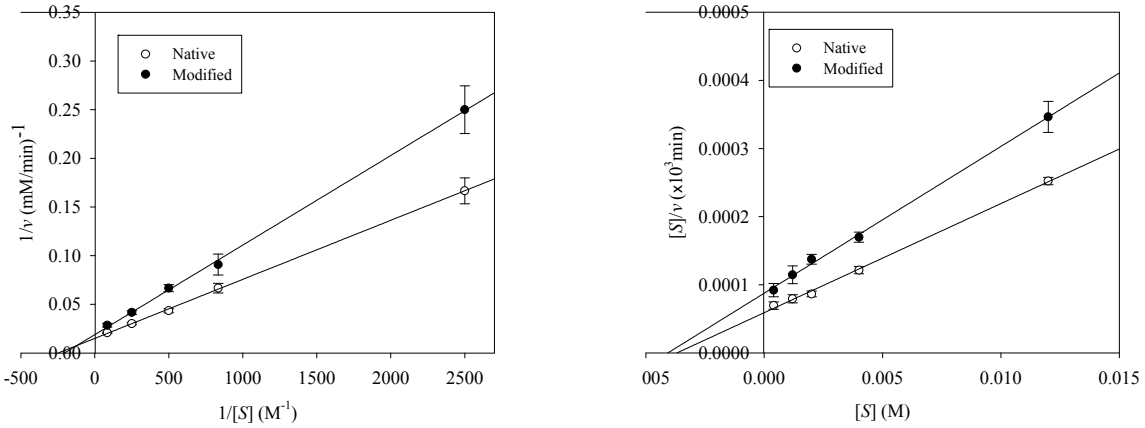

(a) (b)

Figure 4.30 (a) Lineweaver-Burk plot and (b) Hanes-Woolf plot for determination of Michaelis-Menten parameters.

Table 4.2 Michaelis-Menten parameters for the native and modified invertase using Lineweaver-Burk plot and Hanes-Woolf plot

Parameter	Lineweaver-Burk plot		Hanes-Woolf plot	
	Native invertase	Modified invertase	Native invertase	Modified invertase
K_m (mM)	4.0	4.8	3.8	4.2
v_{max} (mM/min)	67	53	63	47
k_{cat} (min^{-1})	74.4×10^3	58.9×10^3	70.0×10^3	52.2×10^3
k_{cat}/K_m $(mM\ min)^{-1}$	18.6×10^6	12.3×10^6	18.4×10^6	12.4×10^6

In view of Table 4.2, thermal stabilization with BMDC reduced the v_{max} value by approximately 21-25% relative to the native enzyme using both Lineweaver-Burk plot and Hanes-Woolf plot. K_m increased by 10-20% relative to the native enzyme, indicating reduction in enzyme affinity towards the substrate. A decrease in k_{cat}/K_m by crosslinking suggested a decrease in turn over number of the crosslinked enzyme. ($k_{cat} = v_{max}/e_0$, where e_0, the total concentration of invertase, was 0.9 μM.)

For intermolecular crosslinking, the ratio of the enzyme (50 mg/mL or 185 μM invertase) to the crosslinking reagent (1-50 mM BMDC, HMDC and OMDC) was varied in order to investigate the relationship between the type of crosslinking achieved and enzyme stability. The results are shown in Figure 4.31. All diisocyanate reagents (i.e. BMDC, HMDC and OMDC) stabilized the enzyme, and there was a direct correlation

between the ratio of the enzyme-reagent and enzyme stability. For BMDC which had the strongest stabilizing effect, an enzyme-to-reagent ratio of 185 μM to 30 mM had the strongest stabilizing effect. The presence of an excessive amount of reagent during crosslinking actually reduced stability relative to the best case.

One micromolar concentration of various diisocyanate reagents were used to stabilize 185 μM of the enzyme to investigate the effect of crosslinkers' chain length on enzyme thermal stability (Figure 4.31 d). An enzyme:BMDC ratio of 185 μM:30 mM produced the most stable enzyme (Figure 4.31 a) as previously pointed out. Reaction with twice the concentration of the monofunctional reagent, BIC, on the otherhand did not have a stabilizing effect (Figure 4.32). Thus, although the monofunctional reagent could presumably interact with some of the same functional groups in the protein as BMDC, it was not able to form the crosslinks responsible for the increased stability of the enzyme. The native enzyme had a stability profile that was virtually the same as for the "native control" (i.e. the native enzyme that underwent exactly the same protocol as involved in diisocyanate crosslinking treatment, but without the reagent, water was used instead of the reagent). Again BMDC at 30 mM proved extremely effective in stabilizing the enzyme (Figure 4.32) in an independent run (i.e. BMDC data in Figure 4.32 and Figure 4.31 a are from independent runs).

The denaturation rate constant (k_d) and denaturation energy (E_d) of 185 μM invertase modified with 30 mM BMDC were estimated in comparison with the native invertase (Figure 4.33). The relevant data are shown in Table 4.3. The calculated E_d values for the native and the modified invertase were 390 and 455 kJ/mol, respectively.

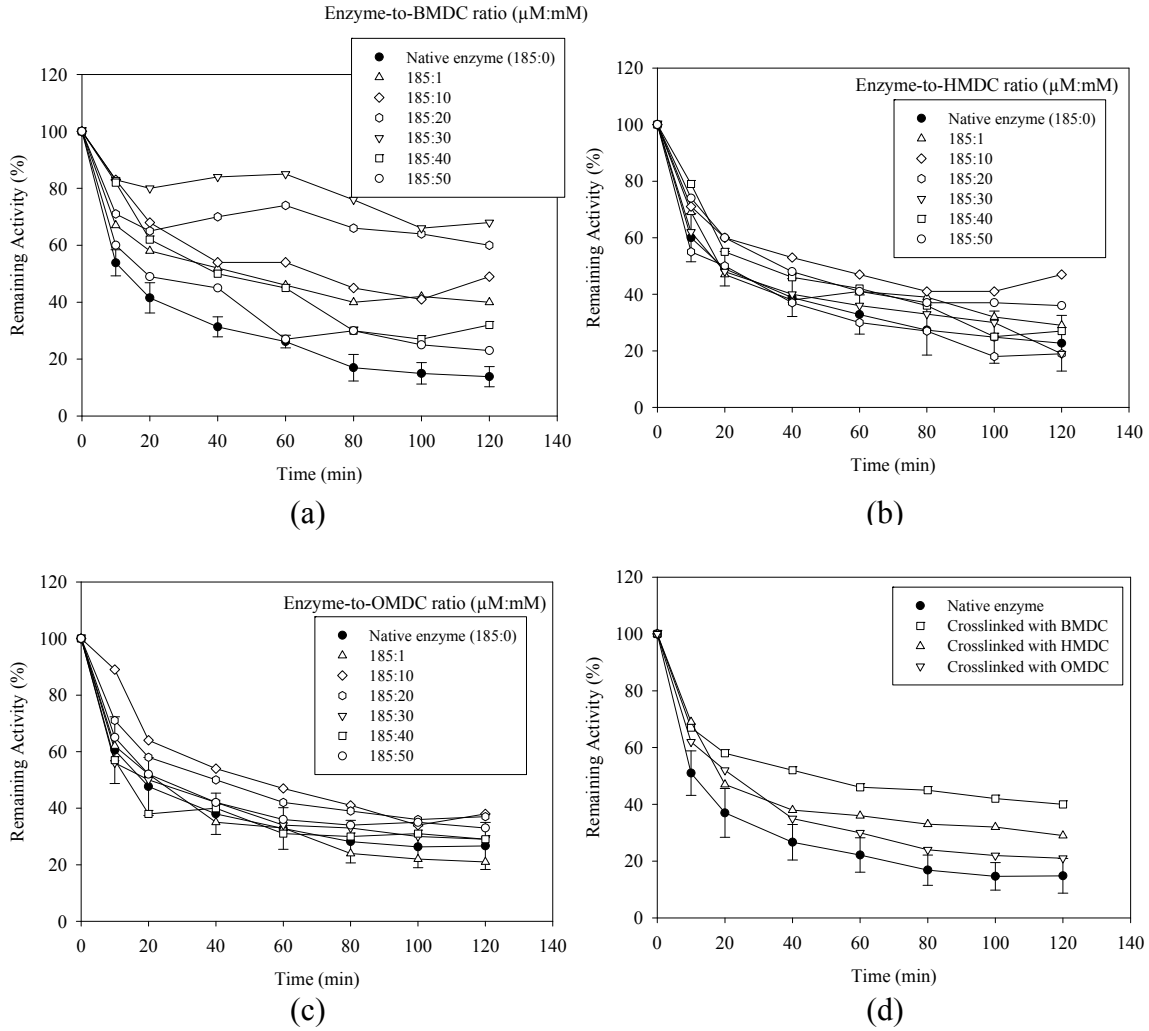

Figure 4.31 Thermal stability of 185 μM invertase (55 °C, Na-citrate buffer, pH 6) modified with 1-50 mM of (a) BMDC, (b) HMDC and (c) OMDC. (d) Thermal stability of 185 μM invertase (55 °C, Na-citrate buffer, pH 6) modified with 1 μM of various diisocyanate crosslinkers.

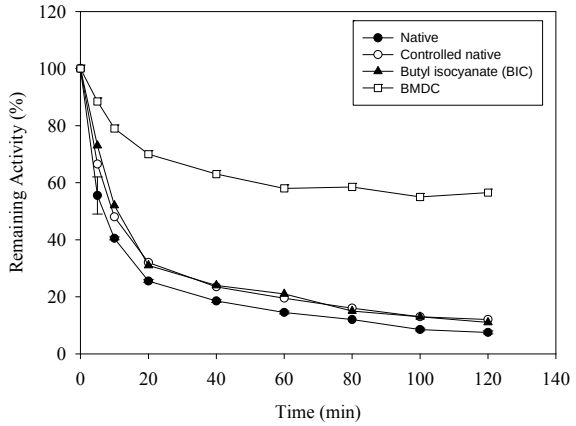

Figure 4.32 Thermal stability of invertase (55 °C, Na-citrate buffer, pH 6) modified with 30 μM of BMDC and the double concentration of the monofunctional reagent butylisocyanate (BIC).

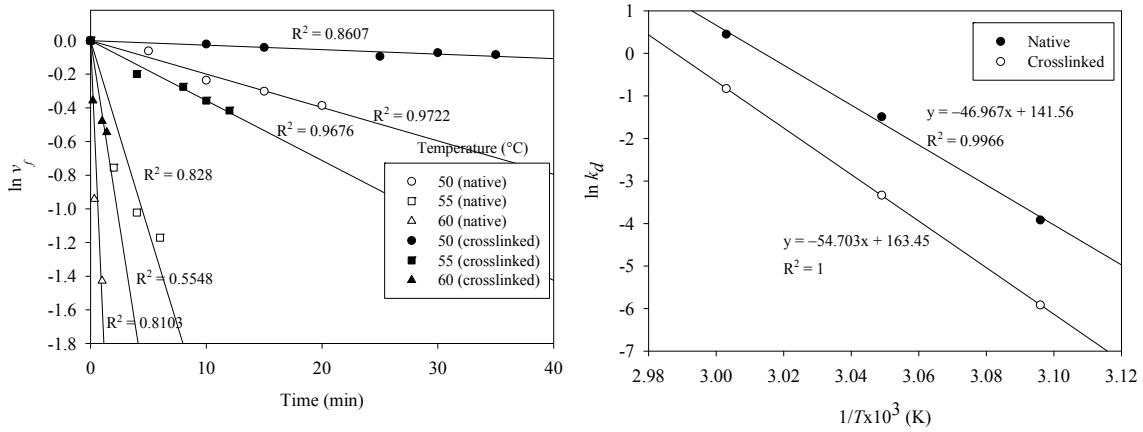

(a) (b)

Figure 4.33 (a) Estimation of denaturation rate constant (k_d) and (b) activation energy of denaturation (E_d) for native and crosslinked invertase. The enzyme (185 µM) was crosslinked with 30 µM BMDC in 0.1 M Na-citrate buffer, pH 6.

Table 4.3 Denaturation rate constants at various temperatures

Temperature (°C)	k_d (min^{-1})	
	Native invertase	Crosslinked invertase
50	1.99×10^{-2}	2.7×10^{-2}
55	22.54×10^{-2}	3.56×10^{-2}
60	156.72×10^{-2}	43.73×10^{-2}

4.1.3.3 Stabilization by imidoesters

Thermal stability of invertase modified with the various bifunctional imidoesters was investigated. As shown in Figure 4.34 a-c, none of imidoesters was effective in stabilizing the enzyme. Conducting the crosslinking reaction at different pH had no effect on altering the stability of the enzyme (Figure 4.34 d).

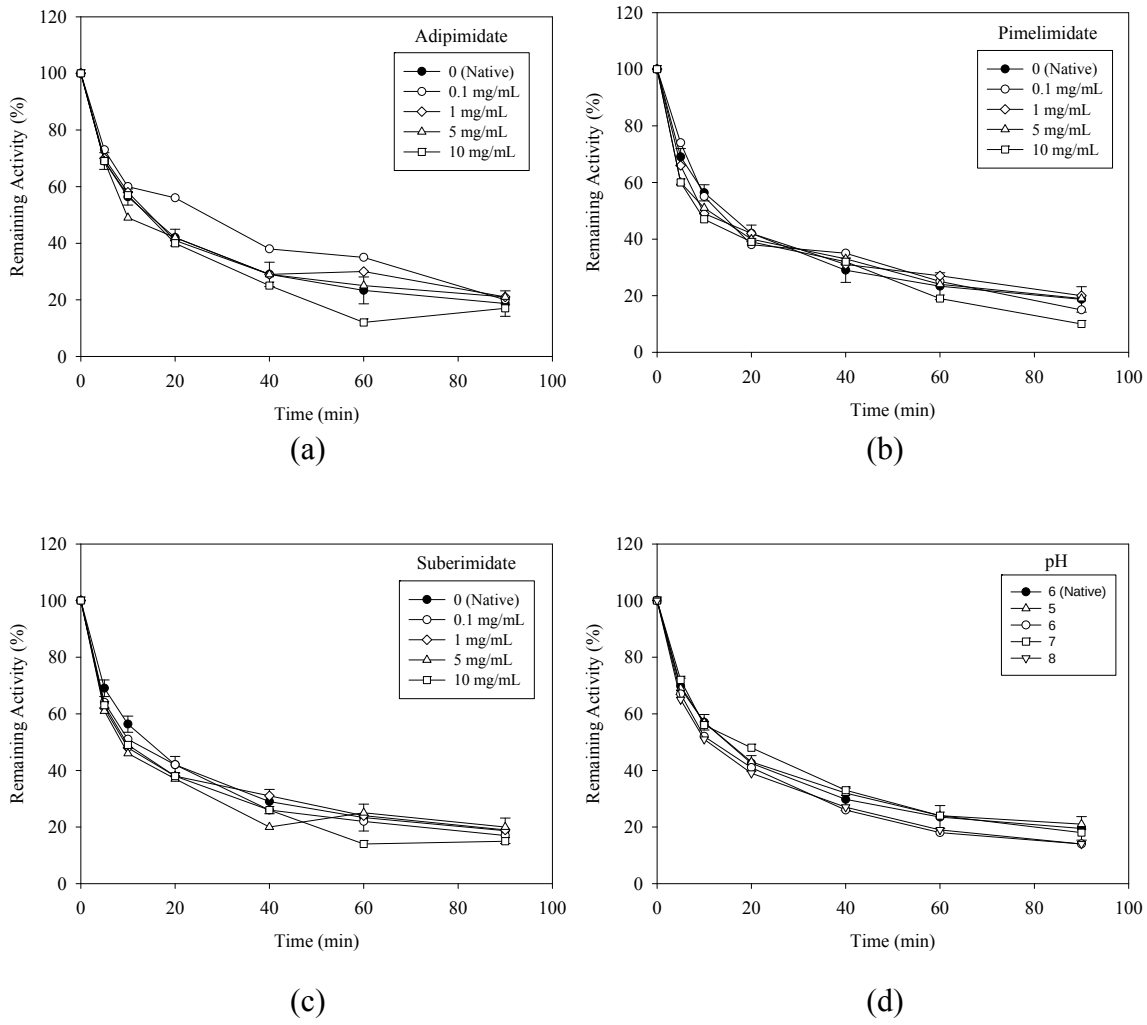

Figure 4.34 Thermal stability of invertase modified with (a) dimethyl adipimidate, (b) dimethyl pimelimidate and (c) dimethyl suberimidate at 60 °C (pH 5, Na-acetate buffer). (d) Thermal stability (65 °C, pH 5, Na-acetate buffer) of invertase modified with 1 mg/mL of dimethyl adipimidate at different pH.

4.1.3.4 Stabilization by diamines

Modification of invertase (0.9 μM) by any of the five diamine reagents tested (Section 3.1.2) did not enhance thermal stability as shown in Figure 4.35 and Figure 4.36. In many cases, the stability of the modified enzyme was actually reduced relative to the control.

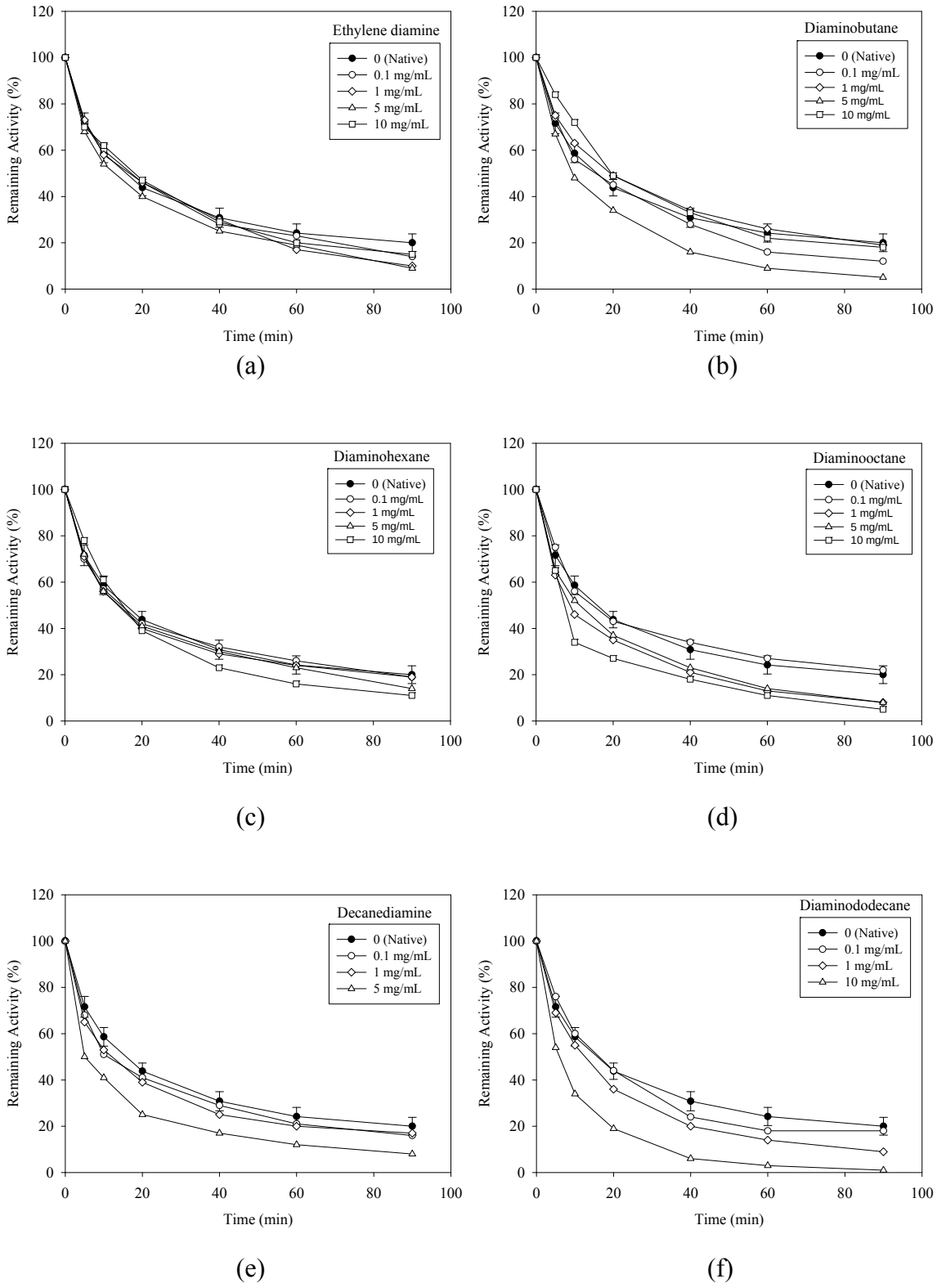

Figure 4.35 Thermal stability (60°C, pH 5, Na-acetate buffer) of invertase modified with (a) ethylene diamine, (b) diaminobutane, (c) diaminohexane, (d) diaminooctane, (e) decanediamine and (f) diaminododecane.

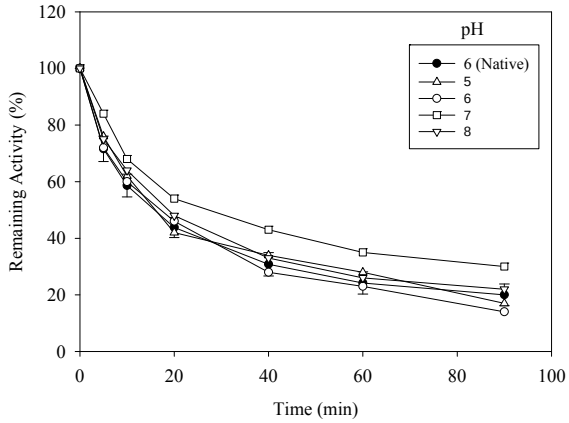

Figure 4.36 Thermal stability (60°C, pH 5, Na-acetate buffer) of invertase modified with 1,2-ehtylene diamine (1 mg/mL) at different pH.

Reacting a bifunctional crosslinkers with an enzyme can produce at least three distinct outcomes: 1) only one of the functional groups of the crosslinker may react with an enzyme functional group to chemically modify the enzyme without any crosslinking occurring; 2) both the functional groups of a crosslinker may react with enzyme functional groups within one enzyme molecule to produce intramolecular crosslinking; and 3) the functional groups on a given crosslinker molecule may react with enzyme functional groups located on two different enzyme molecules to produce bridging, or intermolecular crosslinking. Intermolecular crosslinking was not a desired outcome as it would have led to production of really large enzyme networks and aggregates with associated mass transfer limitations.

To favour intramolecular crosslinking over intermolecular crosslinking, a low concentration (≤1 μM) of the enzymes was used during the crosslinking reaction. Use of a dilute solution of the enzyme can reduce the likelihood of intermolecular crosslinks forming if the dilution is such that the average distance between adjacent enzyme molecules in a uniform dispersion is greater than the fully expanded length of the crosslinker molecule. However, even in a sufficiently dilute solution, the molar ratio of the enzyme to the crosslinker, can influence the nature of the modified enzyme. For example, if too much of a crosslinker is presented, the probability of only one end of a crosslinker reacting with the enzyme functional group increases. This therefore reduces the likelihood of the crosslinker being able to reduce the thermal unfolding of the enzyme and thereby stabilize it.

Treatment with diimidoester reagents, produced no significant improvement of thermal stability for modified enzymes (Figures 4.7, 4.17, 4.18, and 4.34). The amount and chain length of diimidoesters had no impact on increasing thermal stability. Furthermore, the same results were found even if the crosslinking reaction was carried out at different pH values (pH of 5-8). Although crosslinking at pH ≥7 has been reported to favour reaction of diimidoester with the amino groups of enzymes, particularly with the amino groups of lysine residues (Lundblad, 2005), none of pH values (pH 5-8) tested for the reaction had any effect on stability of the enzyme. This may be because the three enzymes used were acidic in nature, and contained a relatively small amount of lysine residues in their amino acid sequence. Thus the amino groups may have been too far apart in the tertiary structure for the crosslinking molecules to react. Diimidoester reagents may be suitable for enhancing the thermal stability of basic enzymes which are rich in lysine residues. Interestingly, two reports suggest that dimethyl suberimidate slightly enhanced the stability of cellulase under basic conditions (Bilen and Bakir, 1998; Schmid, 1979).

Because the enzymes selected for this study happened to be acidic in nature, the use of a diamine series of crosslinkers (Section 3.1.2) was evaluated for improving their thermal stabilities. According to the literature, diamine reagents react with carboxylate groups and have been used previously to crosslink carboxylates in α-chymotrypsin (Torchilin *et al.*, 1978). However, no remarkable increase in the thermal stability of α-amylase, β-galactosidase and invertase was observed even though a wide range of reagent chain lengths and concentrations were tested. Crosslinking at different pH did not significantly improve the outcome. This may be due to enzyme inactivation as the active sites of many of these enzymes contain acidic catalytic residues. Reaction of these residues with the reagent would decrease the enzyme activity markedly.

The active site of alpha amylase contains two aspartic residues (Asp 206 and Asp 297) and one glutamic residue, Glu 230. Under acidic conditions (pH 5-6), the –COOH groups associated with the active site as well as the surface –COOH groups could react with a diamine reagent. As the active site is exposed to the solvent (Delano, 2002), there is no impediment to reaction with diamines. At pH ≥7, the amino groups of lysine residues can react with diisocynates, but acidic enzymes have relatively few lysine residues to be crosslinked. The carbohydrate moiety constitutes 2% of the molar mass of amylase. Each mole of this carbohydrate contain 2 moles of glucosamine and 6 moles of mannose in a single oligosaccharide chain (McKelvy and Lee, 1969). The oligosaccharide

is linked to the amylase molecule through N-asparagine (Asn 197). The amount of carbohydrate appears to be too small to hinder the attachment of diisocyanate reagents to the active –COOH groups of the peptide chain. Beta galactosidase is also an acidic enzyme and contains ~10% of carbohydrate in its molecule (Nakao *et al.*, 1987). The carbohydrate portion may not be large enough to interfere with the attachment of the reagent. The active site Glu 200 and 298 are easy for the reagent to react with. This resulted in enzyme inactivation rather than an improved thermal stability.

Although invertase could be stabilized using diisocyanate, the thermal stability of α-amylase and β-galactosidase could not be increased using the same crosslinking reagent. This was probably because of the differences in the carbohydrate contents in these enzyme molecules. α-Amylase and β-galactosidase contain 2% and 10% of their molecular weights as carbohydrate, respectively. This is much less carbohydrate than the 53% level in invertase. Thus, a much larger surface of the polypeptide part of the α-amylase and β-galactosidase is likely accessible to the crosslinking reagent than the surface accessible in invertase under otherwise equivalent reaction conditions. Thus excessive surface crosslinking can potentially occur in α-amylase and β-galactosidase to make them too rigid to remain biologically active. Also, under the crosslinking treatment conditions at pH 5 and pH 6, the number of functional groups which can react with the crosslinker near the active sites of α-amylase (Figure 2.14 and Figure 2.15) and β-galactosidase (Figure 2.20 and Figure 2.21) are more than the number of the functional groups in the vicinity of the active site of the invertase molecule (Figure 2.26 and Figure 2.27). Thus excessive crosslinking can occur in the vicinity of the active sites of α-amylase and β-galactosidase to cause steric interference with the access of the substrates to the active sites.

The crosslinking reaction between invertase and diisocyanate at pH 6 had the greatest effect on thermal stability of the enzyme (Figure 4.26 b). At this pH the reagent is claimed to react mostly with the hydroxyl group of tyrosine, the carboxylate group of aspartic acid and glutamic acid residues (Means and Feeney, 1971). Also invertase molecule has many carboxylate groups at the weak acid condition (pH 6) of the reaction. In addition, invertase displays good biological activity at pH 6.

The use of a high concentration of enzyme during the crosslinking reaction can cause intermolecular crosslinking to occur. This possibility was investigated as a control on studies that focused on preferentially attaining intramolecular crosslinking rather than

intermolecular crosslinking. Thus, the crosslinking reaction of invertase with diisocyanates was carried out also at a high concentration of invertase (185 μM). Only the enzyme treated with BMDC had a clearly improved thermal stability (Figure 4.31 and Figure 4.32). BMDC is a relatively short (C = 4) crosslinker. At a high concentration of the enzyme, it is more likely to link together two different enzyme molecules especially if one end of the crosslinker has bound to an enzyme surface functional group that does not have a second reactable functional group within a distance of a single molecular length of the crosslinker (BMDC has an estimated fully extended molecular length of 12.56 Å).

Use of diisocyanate to crosslink invertase produced a modified enzyme with a substantially improved thermal stability. No stabilization occurred when the monofunctional reagent butyl isocyanate (BIC) was used. This lent credence to intramolecular crosslinking being the cause of stabilization. Using retention of activity to test the stability of a modified enzyme is widely used. However, it is also possible that active site residues or substrate binding sites of the enzyme will have also been modified by a crosslinking treatment. Such modifications will result in reduced activity. It is possible that such a reduction in activity might mask an increase in protein stability caused by the same reagents. Therefore, the use of activity as a measure of stability can be misleading. Use of techniques such as circular dichroism protein melting spectra which does not rely on activity, can be more informative. (This is discussed later in this thesis.)

4.2 Crosslinking of invertase

Crosslinking of a low concentration of invertase (0.9 μM) with the bifunctional crosslinker butamethylene diisocyanate (BMDC) was found to enhance the thermal stability of the enzyme. The molecular basis of this improved stability was thought to be intramolecular crosslinking between different functional groups in the polypeptide chain.

In order to establish that this was indeed the cause of the improved stability, further experiments were carried out. Firstly, the crosslinking was carried out using higher concentrations of the enzyme (185 μM) in order to produce intermolecular crosslinking for use as a control for intramolecular crosslinking. In this discussion, the crosslinking achieved using low and high concentrations of invertase are referred to as the intramolecular crosslinking and the intermolecular crosslinking, respectively. The crosslinked products produced by both intra- and intermolecular crosslinking were

characterized by size exclusion chromatography (SEC), dynamic light scattering (DLS), SEC-multiple angle laser light scattering (SEC-MALLS), polyacrylamide gel electrophoresis (SDS-PAGE), and circular dichroism (CD) spectroscopy.

4.2.1 Size exclusion chromatography (SEC)

The products produced after the crosslinking reaction were subjected to the size exclusion chromatography (Sephacryl^{TM} S-300, 2.6 × 100 cm, XK column (GE Healthcare)). Molecular species were separated and their molecular weights were estimated from a standard curve produced using the same column and molecular weight standards (Appendix I).

Sample (0.2 mL in 0.1 M Na-citrate buffer, pH 6, containing 0.15 M NaCl) was applied to the top of the column and eluted in the same buffer at a flow rate of 0.5 mL/min. Samples included native invertase, crosslinked invertase after intra- and intermolecular crosslinking reactions, and the modified invertase that had been treated with a double concentration of the monofunctional crosslinker, butylisocyanate. The elution profiles of all the samples are shown in Figure 4.37.

The elution profile of the product from the intramolecular crosslinking (Figure 4.37 c) showed a major peak with a similar elution volume to that of the native protein (Figure 4.37 g) and the protein produced in the control reaction (Figure 4.37 a). This showed that the molecular size of the treated invertase molecule using these reaction conditions was similar to that of the native invertase. A little higher molecular weight of invertase after the intramolecular crosslinking may be because of the additional mass of the crosslinking reagent being attached to the molecule of invertase either by one end or by both ends. These two products are named here as the one-end modified invertase and the intramolecularly crosslinked invertase. Some BMDC molecules may form intramolecular crosslinks but others may not. This however depends on the distance between the amino acid residues located on the enzyme molecule. Some amino acid residues may be located sufficiently close to be crosslinked with the two ends of a BMDC molecule. Furthermore, the additional mass of the crosslinked products produced under this condition may also depend on the number of intramolecular crosslinks which may have formed during the crosslinking.

Invertase (0.9 μM) treated with 60 mM monofunctional crosslinker produced two broad peaks (Figure 4.37 b). The main peak occurred at a similar elution volume to that of the native and the native control whereas a minor peak eluted at an elution volume of less than the main peak. The SEC profile of invertase treated with double the concentration of the monofunctional crosslinker (butylisocyanate, BIC), had peaks corresponding to a larger molecule as well as a molecule with a size similar to that of the native invertase. Under this treatment, no crosslinks could have been produced as BIC has only one reactive end. The reaction of the hydrophilic functional groups of the enzyme with BIC does make the enzyme surface more hydrophobic. This can easily lead to aggregation of the modified invertase molecules and may explain the occurance of the higher molecular weight peak of the profile (Figure 4.37 b).

Compared to the profiles for the intramolecular crosslinking treatment, the size exclusion chromatogram for the intermolecular crosslinking treatments showed a different behavior (Figure 4.37 f). The main peak with a similar elution volume to the native invertase was also found under this condition. As for intramolecular crosslinking, this peak may be due to molecules of invertase with only one end of the crosslinker attached and the intramolecularly crosslinked invertase. The shoulder of the main peak may be the result of two or more molecules of invertase being intermolecularly crosslinked. For the elution profile of invertase (185 μM) crosslinked with a double concentration of the monofunctional crosslinker BIC (Figure 4.37 e), the main peak eluted from the column earlier than in the other profiles and no peak was found at the elution volume corresponding to native invertase. The crosslinking treatment with BIC seems to produce protein aggregation as a consequence of the changed surface hydrophobicity and the high concentration of invertase.

The results suggest that intramolecular crosslinking treatment could produce both the one-end modified invertase and intramolecularly crosslinked invertase. Apparently up to three species could be produced by intermolecular crosslinking treatment. These were the one-end modified invertase, the intramolecularly crosslinked invertase and also the intermolecularly crosslinked invertase.

The molecular weights of invertase species after intra- and intermolecular crosslinking treatments were estimated using the SEC standard curve (Appendix I). These results are shown in Table 4.4. The apparent molecular weight for the native invertase obtained using the size exclusion technique (302 kDa) was somewhat higher than

reported in the literature (270 kDa). This anomalous behaviour has been reported for other glycoproteins where the hydrodynamic volume is increased due to water absorption by the carbohydrate compared to that of the pure protein (Andrews, 1965). A molecule of dimeric invertase contains around 18 neutral oligosaccharide chains of 26-54 manosyl residues (Chu et al., 1978) of approximate molecular weight of 143 kDa.

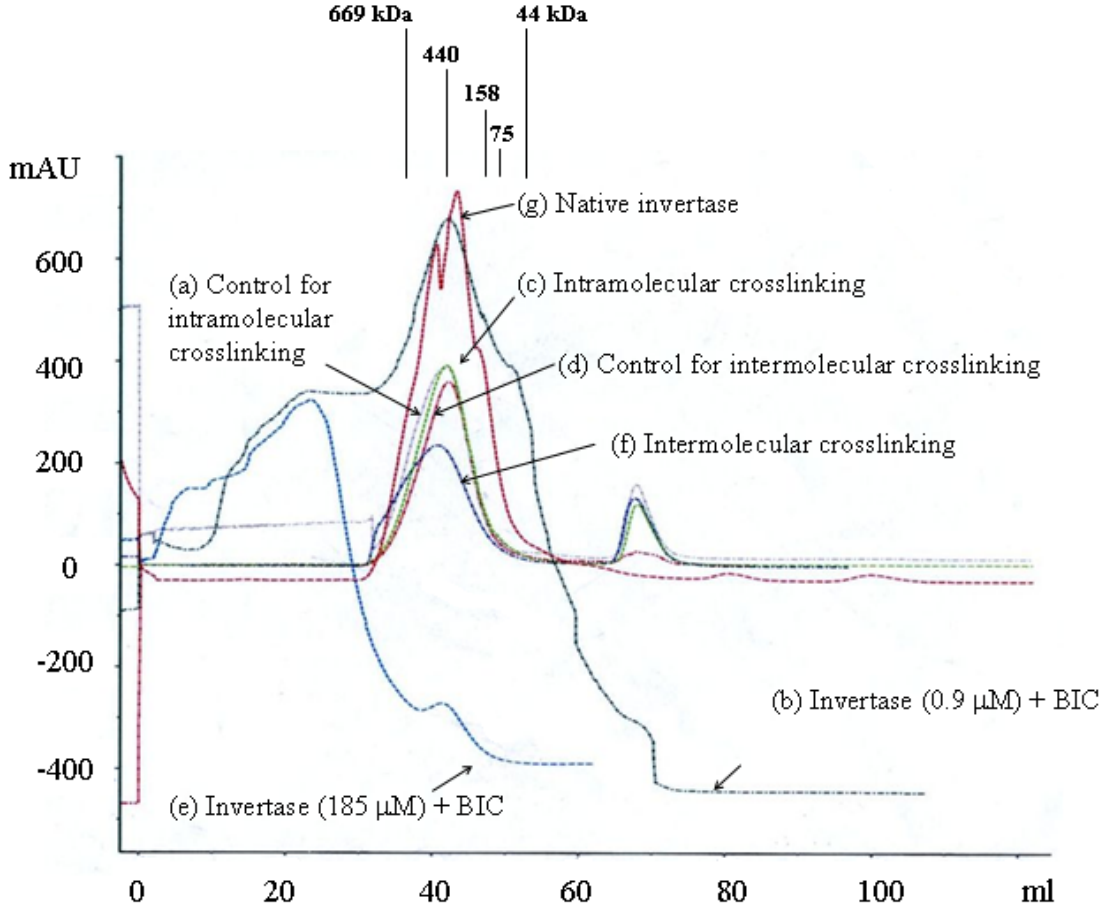

Figure 4.37 The chromatographic profiles of: (a) control for intramolecular crosslinking (grey line); (b) invertase (0.9 μM) treated with 60 mM of butylisocyanate (BIC) (dark green line); (c) intramolecular crosslinking (light green line); (d) control for intermolecular crosslinking (the small red main peak); (e) invertase (185 μM) treated with 60 mM butylisocyanate (light blue line); (f) intermolecular crosslinking (dark blue line); (g) native invertase (the large red peak) on Sephacryl S-300 size exclusion chromatography column with flow rate of 0.5 mL/min.

Table 4.4 Size measurement (size exclusion chromatography) of native invertase and invertase after the crosslinking reaction

Invertase	Elution volume (mL)	Molecular weight (kDa)
Native	43.268	302
Control for intramolecular crosslinking	41.636	409
Intramolecularly crosslinked invertase	41.804	396
Control for intermolecular crosslinking	42.269	363
Intramolecularly crosslinked invertase (the highest of the main peak for intermolecular crosslinking)	40.629	495
Intermolecularly crosslinked invertase (the shoulder of the main peak for intermolecular crosslinking)	32.866	2,376
Native	42.615	341
Deglycosylated invertase	42.758-44.805	229-332
Control for deglycosylated invertase after intramolecular crosslinking	42.616	341
Deglycosylated invertase after intramolecular crosslinking	44.411	245
Control for deglycosylated invertase after intermolecular crosslinking	40.657	492
Deglycosylated invertase after intermolecular crosslinking (the highest of the main peak)	43.430	293
Deglycosylated invertase after intermolecular crosslinking (the shoulder of the main peak)	34.682	1,620

As expected, all the SEC peaks after the deglycosylation treatment were shifted to the higher elution volume compared to the samples without the PNGase F treatment. This was a result of the loss of carbohydrate as a consequence of deglycosylation. The estimated molecular weight of native invertase was 341 kDa but this decreased to 229-332 kDa (Figure 4.38) after the deglycosylation treatment. This implied that 3-33% of carbohydrate was removed by deglycosylation. The estimated molecular weight of intramolecularly crosslinked invertase was 396 kDa but it decreased to 245 kDa after deglycosylation. The estimated molecular weight of intermolecularly crosslinked invertase was 2,376 kDa and reduced to 1,620 kDa after deglycosylation. Extended incubation with deglycosylating enzyme at room temperature (25 °C, 2 days) resulted in the removal of more carbohydrate from invertase (Figure 4.39, Figure 4.40 and Table 4.4). However, the molecular weight at the highest peak of the control for deglycosylated invertase after intra- and intermolecular crosslinking should be roughly the same as the controls are the invertase after intra and intermolecular crosslinking but without PNGase

treatment. The deglycosylated intramolecularly crosslinked invertase obtained after intra- and intermolecular crosslinking treatment were expected to show no significant difference in their molecular weight. The results showed the removal of carbohydrate as the difference in the molecular weight of invertase before and after the deglycosylation.

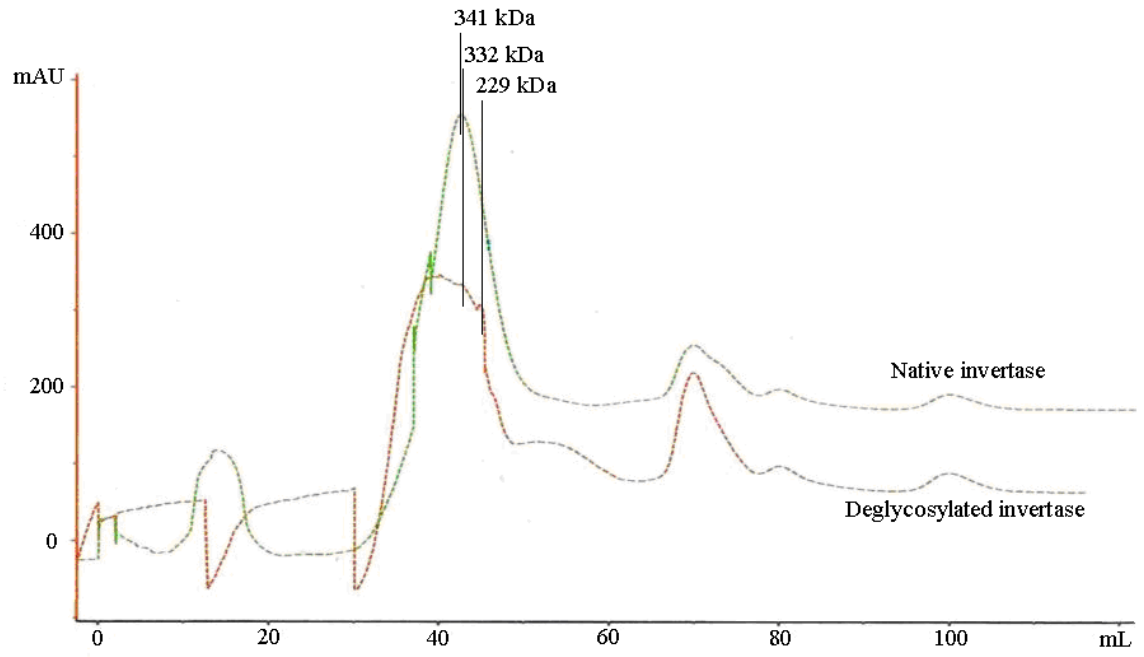

Figure 4.38 The chromatographic profiles of native invertase before and after deglycosylation (at 37 °C overnight) on Sephacryl S-300 size exclusion chromatography column with a flow rate of 0.5 mL/min.

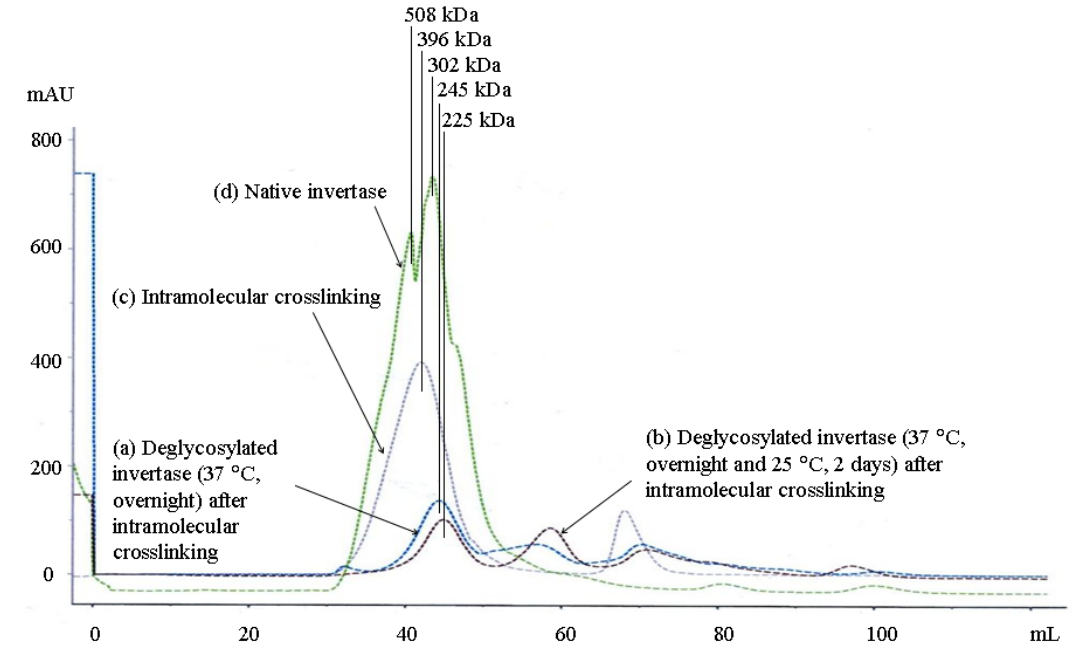

Figure 4.39 The chromatographic profiles of: (a) deglycosylated invertase (37 °C, overnight) after intramolecular crosslinking (blue line); (b) deglycosylated invertase (37 °C, overnight and then 25 °C, over 2 days) after intramolecular crosslinking (brown line) compared to (c) invertase after intramolecular crosslinking (grey line) and (d) native invertase (green line) on Sephacryl S-300 size exclusion chromatography column with a flow rate of 0.5 mL/min.

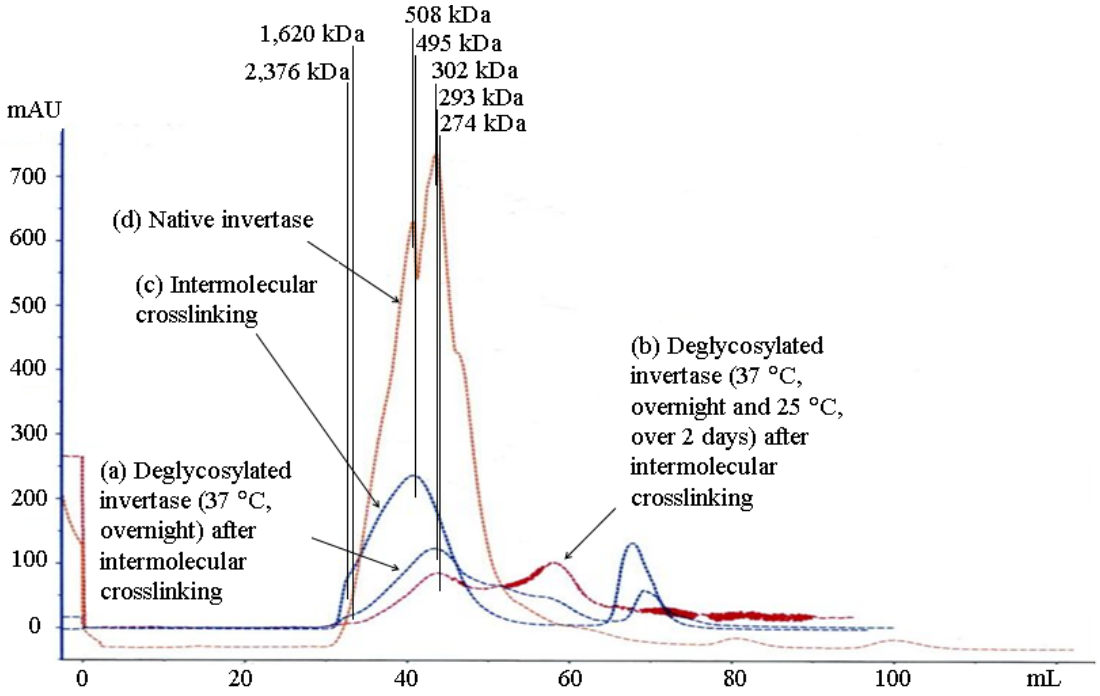

Figure 4.40 The chromatographic profiles of: (a) deglycosylated invertase (37 °C, overnight) after intermolecular crosslinking (blue small main peak); (b) deglycosylated invertase (37 °C, overnight and then 25 °C, over 2 days) after intermolecular crosslinking (red line) compared to (c) invertase after intermolecular crosslinking (blue large main peak) and (d) native invertase (orange line) on Sephacryl S-300 size exclusion chromatography column with a flow rate of 0.5 mL/min.

4.2.2 Dynamic light scattering (DLS)

To measure the molecular size of invertase before and after crosslinking, the relevant fractions were collected from the size exclusion chromatography column (Section 4.2.1) and analysed by DLS. The hydrodynamic diameter estimated using this technique is characterised by the Z-average value. Before measuring the invertase samples, the instrument was standardised by measuring the Z-average values of the standard proteins that had been used to calibrate the size exclusion column (Table 4.5). Most of the standard proteins (except ferritin) had a DLS estimated size close to that of the literature value (Table 4.5). The fractions of crosslinked invertase before and after deglycosylation were also analysed by DLS. The estimated Z-average values and the molecular weights of all the samples are shown in Table 4.6. An example of a DLS protein characterization report in terms of the size distribution according to the measured signal intensity for native invertase is shown in Figure 4.41.

Table 4.5 Size measurement of standard proteins by DLS

Standard proteins	Estimated sizes		Literature sizes	
	Diameter (nm)	MW (kDa)	Diameter (nm) (Fasman, 1989)	MW (kDa)
Ovalbumin	6.55	54	6.10	44
Conalbumin	8.34	95	NA	75
Aldolase	10.24	154	9.62	158
Ferritin	17.77	558	12.20	440
Thyroglobulin	19.56	699	17.00	669

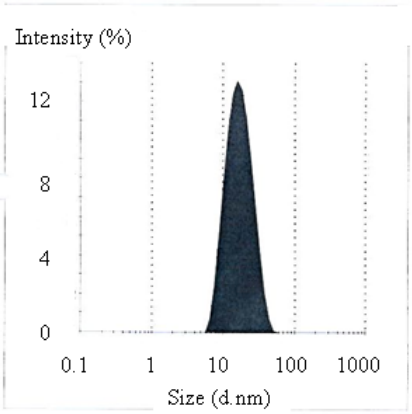

Size Distribution by Intensity

Figure 4.41 Results from DLS for native invertase. Ten or more measurements, performed at a count rate (kcps) of 292.8 with the polydispersity index of 0.223, were averaged.

The size of crosslinked products was bigger compared to the native invertase whereas the size was reduced by deglycosylation (Table 4.6). Roughly 7% of the carbohydrate moiety of the native invertase was removed by deglycosylation as estimated using DLS measurement. Invertase with a DLS molecular weight of 252-295 kDa was obtained by deglycosylation. The Z-average of native invertase and the controls for intra- and intermolecular crosslinking, should be the same. The Z-averages of the intramolecularly crosslinked invertase samples obtained after both the intra- and intermolecular crosslinking treatments were also expected to have similar values. These values were higher than that of the native invertase (Table 4.6) and this implied that the invertase molecule likely had a significant number of intramolecular crosslinks, i.e. the molecular size was larger than the native but not twice as large. The intermolecularly crosslinked invertase shown at the shoulder of the peak for intermolecular crosslinking (Figure 4.37) had a much higher estimated Z-average than the control and the native enzyme as expected (Table 4.6).

Table 4.6 Size measurements of invertase and crosslinked invertase by Dynamic Light Scattering

Invertase	**Z-average (nm)**	**Molecular weight (kDa)**
Native	13.05	271
Control for intramolecular crosslinking	13.96	317
Intramolecularly crosslinked invertase	17.30	524
Control for intermolecular crosslinking	12.60	250
Intramolecularly crosslinked invertase (the highest of the main peak for intermolecular crosslinking)	15.50	406
Intermolecularly crosslinked invertase (the shoulder of the main peak for intermolecular crosslinking)	27.74	1,580
Deglycosylated invertase	12.64-13.52	252-295
Control for deglycosylated invertase after intramolecular crosslinking	11.16	188
Deglycosylated invertase after intramolecular crosslinking	12.14	229
Control for deglycosylated invertase after intermolecular crosslinking	15.07	380
Deglycosylated invertase after intermolecular crosslinking (the highest of the main peak)	14.53	349
Deglycosylated invertase after intermolecular crosslinking (the shoulder of the main peak)	18.04	578

Both size exclusion chromatography and DLS failed to estimate the molecular weight of the invertase molecule correctly. Nevertheless, both SEC and DLS methods gave molecular weight results that were roughly comparable. It was therefore concluded that the SEC-DLS method was not useful for detecting the formation of oligomeric species. The DLS measurements may not be suitable for determining the hydrodynamic diameters of certain crosslinked products. This is because after the crosslinking reaction, some molecules of the crosslinker have only one end attached to the surface of the enzyme and the other free end may interfere with the motion of the molecule in a fluid to introduce error in the DLS analysis (Yang *et al.*, 1994). (The DLS measurements of hydrodynamic diameter depend on the movement of the molecule in the suspending fluid. See Section 2.5.4.1.)

4.2.3 SEC-multiple angle laser light scattering (SEC-MALLS)

Size exclusion chromatography with online light scattering is another tool available for measuring the molecular weights of proteins and glycoproteins (Jumel *et al.*, 1996). SEC-MALLS measures only the polypeptide component in a glycoprotein molecule when the extinction coefficient for the protein is used in the relevant calculations (Wen *et al.*, 1996). The molecular weights of the invertase samples treated by inter- and intramolecular crosslinking protocols were analysed by SEC-MALLS. To calibrate the SEC-MALLS system, bovine serum albumin (BSA) was used as the protein standard. The estimated molecular weight of BSA by MALLS was 67.8 kDa (Figure 4.42) which was similar to the literature value of 66.6 kDa. A prepacked Superose 6 column (Superose^{TM} 6, 10 × 300-310 cm, HR column (GE Healthcare), imidazole buffer pH 7, flow rate of 0.4 mL/min) connected in series to MALLS and UV detectors was used to measure the crosslinked products.

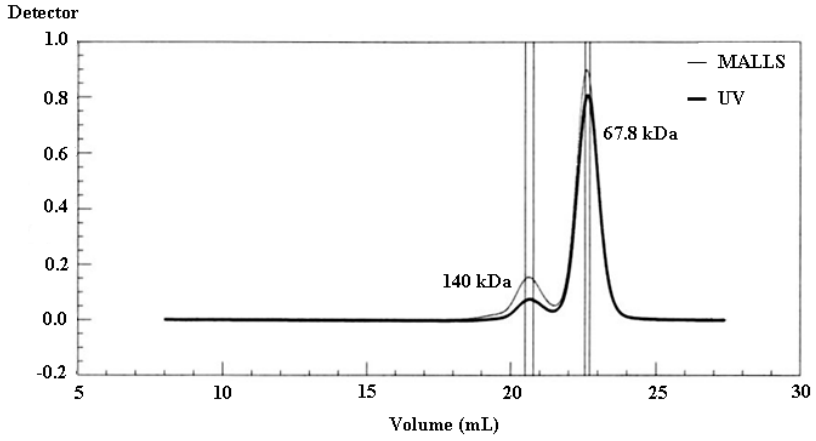

Figure 4.42 The molecular weight measurements of standard bovine serum albumin (BSA) by SEC-MALLS on Superose 6 size exclusion column. (The light and dark black lines show the intensity of the light scattering signal (MALLS) and the UV absorbance signal, respectively.)

The chromatograms of native invertase, and invertase after intra- and intermolecular crosslinking treatments were identical (Figures 4.43-4.45). The estimated molecular weights of these invertase species using MALLS are shown in Table 4.7. The estimated molecular weight of native invertase was 122 kDa whereas the literature value for only the polypeptide moiety of invertase is 127 kDa. The molecular weight of native and intramolecularly crosslinked invertase species produced by intra- and intermolecular crosslinking treatments were similar (Table 4.7) as expected.

The molecular weight of intermolecularly crosslinked invertase could not be obtained using the Superose 6 size exclusion column because the shoulder of the peak did not elute and therefore a MALLS measurement was not obtained. This was possibly because the prepacked Superose 6 column that preceded MALLS had too broad a fractionation range (5-5,000 kDa) to clearly separate the crosslinked products that differed only a little in the molecular weights (i.e. 270 kDa, 540 kDa and 810 kDa). (The column used in SEC (Section 4.2.1), i.e. Sephacryl S-300 with a fractionation range of 10-1,500 kDa, could do this separation somewhat more distinctly.) Using SEC-MALLS generaly gave good results and accurate molecular weights. To further improve the SEC-MALLS data, additional measurements were made with the Superose 6 column of SEC-MALLS replaced with the Sephacryl S-300 column (Figures 4.46-4.48). The estimated molecular weights using SEC-MALLS with the Sephacryl S-300 size exclusion column are also shown in Table 4.7. As expected, the shoulder of the intermolecularly crosslinked

invertase reappeared and it corresponded to a molecular weight of 379 kDa. Intermolecularly crosslinked invertase is of course larger than the native invertase and the intramolecularly crosslinked invertase produced by intra- and intermolecular crosslinking treatments. The molecular weight of the protein moiety of native invertase was 115 kDa using Sephacryl S-300 column and this was similar to the value obtained using Superose 6 column (Table 4.7).

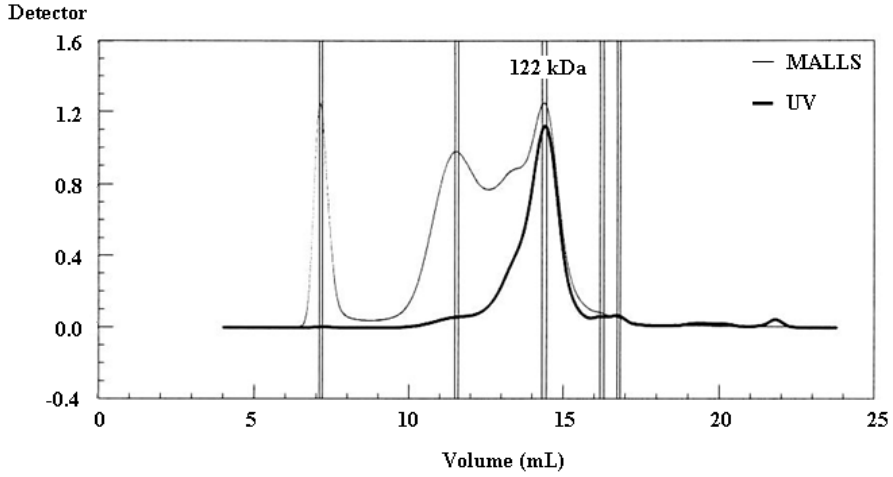

Figure 4.43 The molecular weight measurements of native invertase by SEC-MALLS on Superose 6 size exclusion column. (The light and dark black lines show the intensity of the light scattering signal (MALLS) and the UV absorbance signal, respectively.)

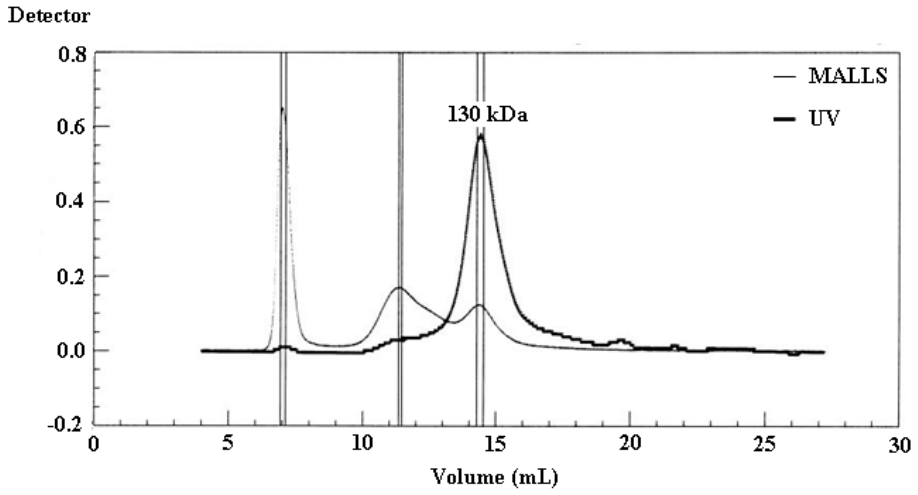

Figure 4.44 The molecular weight measurements of invertase after intramolecular crosslinking treatment (0.9 μM invertase) by SEC-MALLS on Superose 6 size exclusion column. (The light and dark black lines show the intensity of the light scattering signal (MALLS) and the UV absorbance signal, respectively.)

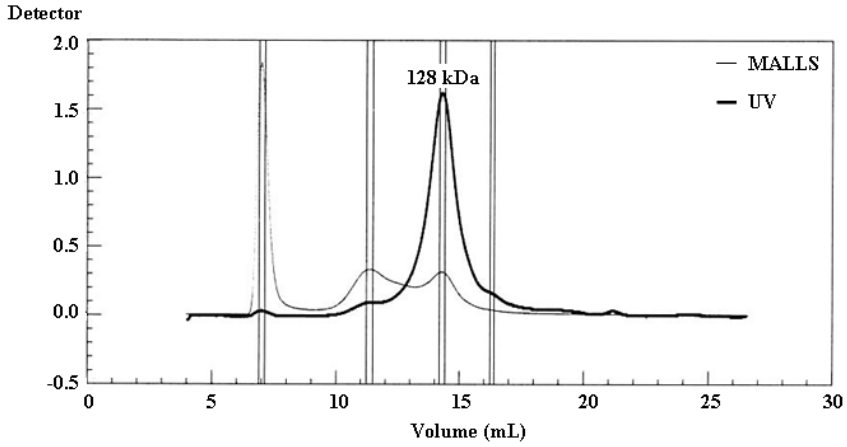

Figure 4.45 The molecular weight measurements of invertase after intermolecular crosslinking treatment (185 μM invertase) by SEC-MALLS on Superose 6 size exclusion column. (The light and dark black lines show the intensity of the light scattering signal (MALLS) and the UV absorbance signal, respectively.)

Table 4.7 Size measurements of invertase and its crosslinked products by SEC-MALLS

Invertase	**Molecular weight (kDa) by Superose 6**	**Molecular weight (kDa) by Sephacryl S-300**
Native invertase	122	115
Intramolecularly crosslinked invertase	130	126
Intramolecularly crosslinked invertase (the highest of the main peak for intermolecular crosslinking treatment)	128	173
Intermolecularly crosslinked invertase (shoulder of the main peak for intermolecular crosslinking treatment)	-	379

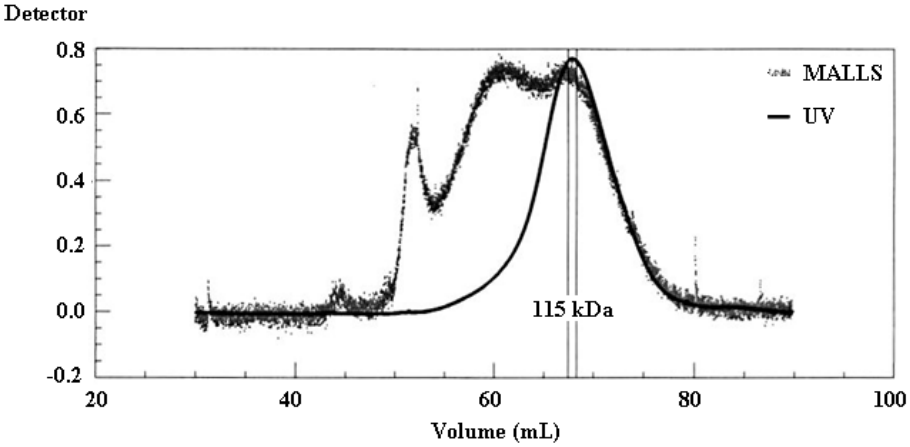

Figure 4.46 The molecular weight measurements of native invertase by SEC-MALLS on Sephacryl S-300 size exclusion column. (The light and dark black lines show the intensity of the light scattering signal (MALLS) and the UV absorbance signal, respectively.)

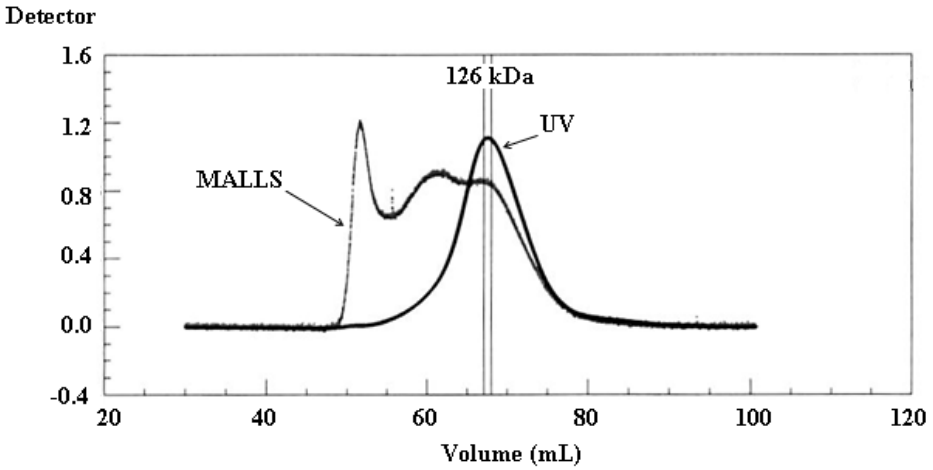

Figure 4.47 The molecular weight measurements of invertase after intramolecular crosslinking treatment (0.9 μM invertase), by SEC-MALLS on Sephacryl S-300 size exclusion column. (The light and dark black line show the intensity of the light scattering signal (MALLS) and the UV absorbance signal, respectively.)

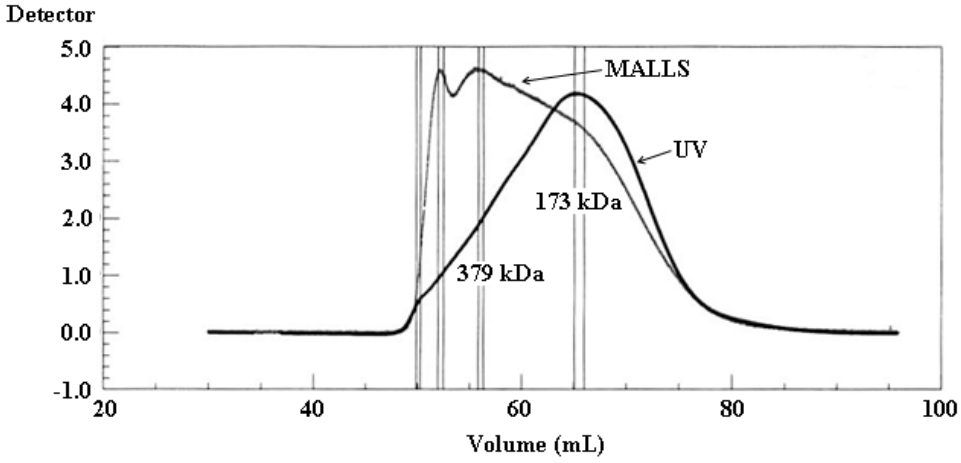

Figure 4.48 The molecular weight measurements of invertase after intramolecular crosslinking treatment (0.9 μM invertase), by SEC-MALLS on Sephacryl S-300 size exclusion column. (The light and dark black lines show the intensity of the light scattering signal (MALLS) and the UV absorbance signal, respectively.)

The determination of molecular weight by SEC-MALLS has been reported to have many advantages over the SEC technique alone and the other techniques such as electrophoresis, ultracentrifugation, and even mass spectrometry (Ye, 2006). In addition, SEC-MALLS is inexpensive, efficient, accurate and simple to operate. SEC-MALLS technique is also usable over a broad range of molecular weights with a proper selection of the column (Ye, 2006).

4.2.4 Polyacrylamide gel electrophoresis (Laemmli, 1970; Papageorgiou and Lagoyanni, 1983)

The molecular weight of native and crosslinked invertase was further studied by PAGE. SDS-PAGE using 6.5% acrylamide gels was used to prove that crosslinking occurred after the crosslinking treatment. Intermolecular crosslinking of invertase was firstly investigated as a control for intramolecular crosslinking. Intermolecularly crosslinked invertase was predicted to be produced by reacting 185 μM concentration of invertase with 30 mM BMDC. This treatment was expected to produce a molecule that was double the size of native invertase or even larger. The molecular weights of all species were estimated by comparison with the standard curve shown in Figure 4.49. The relative mobility (R_f) and log MW values of the standard protein are shown in Table 4.8.

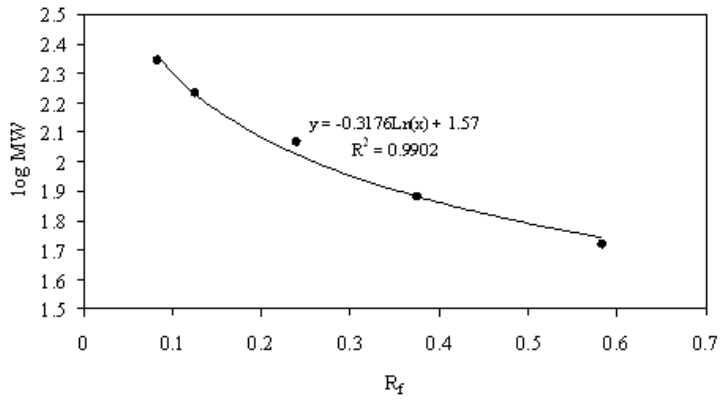

Figure 4.49 Standard curve for molecular weight estimation of invertase and its crosslinked products separated by SDS-PAGE.

Table 4.8 Relative mobility (R_f) and log MW of standard proteins for SDS-PAGE gel (Figure 4.50)

Standard protein	MW (kDa)	Log MW	R_f
Myosin	220	2.34	0.083
α_2-Macroglobulin	170	2.23	0.125
β-Galactosidase	116	2.06	0.240
Transferrin	76	1.88	0.375
Glutamic dehydrogenase	53	1.72	0.583

Results showed the presence of only a single band for the native invertase at a molecular weight of 91.2 kDa (Figure 4.50). The protein ran anomalously in SDS-PAGE because of its high proportion of carbohydrate (Beeley, 1985). Invertase reacted with

double concentration of the monofunctional reagent butylisocyanate, BIC, also showed a single band at the same position as the native enzyme (Figure 4.50). Intermolecularly crosslinked invertase, however, showed two bands at a MW of 91.20 kDa and ~282 kDa (Figure 4.50). A protein band of the molecular weight greater than 282 kDa was also obtained. Protein bands with molecular weights ≤53 kDa were also found and revealed impurities in the commercial invertase.

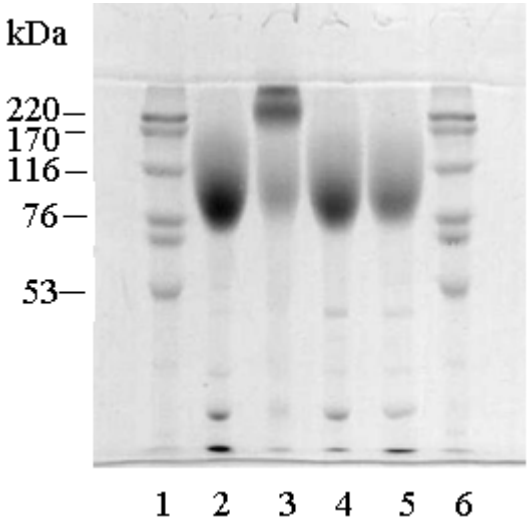

Figure 4.50 SDS-PAGE pattern of invertase. Lanes 1 and 6: molecular weight markers; lanes 2 and 5: invertase control for crosslinking reaction and native invertase as purchased, respectively; lane 3: invertase after intermolecular crosslinking; lane 4: 185 μM invertase linked by 60 mM monofunctional reagent, butyl isocyanate (BIC).

The literature value of the molecular weight of invertase is ~270 kDa (Cantarella *et al.*, 2003; Gascón *et al.*, 1968). Of this about 143 kDa is carbohydrate and ~127 kDa is the two polypeptide chains (Moreno *et al.*, 1975; Wiseman and Woodward, 1975). The invertase monomer molecular weight should therefore be ~135 kDa. The monomeric invertase runs however at a much lower molecular weight ~91.20 kDa (lane 2 and lane 5, Figure 4.50) due to the large amount of covalently linked carbohydrate which decrease the hydrophobic interactions between SDS and protein and the high amount of negatively charged acidic amino acid residues which repel the negative charge of SDS (Shi and Jackowski, 1998).

Treatment of invertase with the monofunctional butylisocyanate produced a species that ran at exactly the same position as the native protein (lane 4, Figure 4.50) indicating a lack of higher molecular weight species. When treated with BMDC at a high

concentration, most of the monomer disappeared and was replaced with bands with an apparent molecular weight ~282 kDa (lane 3, Figure 4.50). Furthermore, the molecular weight values of greater than 282 kDa confirmed that intermolecular crosslinking was indeed occurring. What these crosslinked species are exactly is not known. They are more than double the molecular weight of the monomer and are likely due to the crosslinking of 4 or more monomers.

Sample of invertase that had been subjected to the intermolecular crosslinking treatment was then subjected to size exclusion chromatography (Sephacryl S-300, GE Healthcare, 0.1 M Na-citrate buffer (pH 6) containing 0.15 M NaCl, flow rate of 0.5 mL/min). Fractions of 0.5 mL were collected and analysed by SDS-PAGE (6.5% acrylamide) (Figure 4.51). The molecular weights of all protein bands were estimated using the standard curve (Figure 4.52) based on the relative mobility data shown in Table 4.9. Two protein bands with the molecular weights ranging between 79-117 kDa and ≥170 kDa (Figure 4.51) appeared in most of the fractions. The fractions A11-A15 contained mainly the very high molecular weight species. Fractions B3-B10 each contained two bands; the lower band was a smear that ranged between ~79-117 kDa, the smear being due to different glycoforms. The higher band ranged between 170-≥220 kDa the range again being due to the large number of glycoforms.

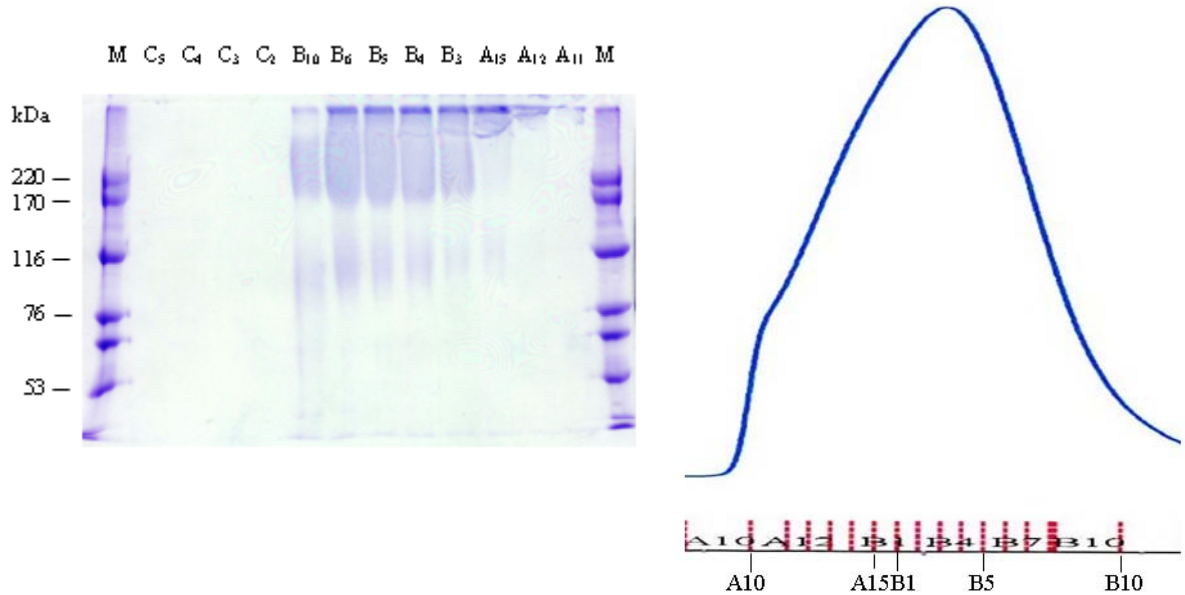

Figure 4.51 Elution profile and SDS-PAGE pattern of invertase after intermolecular crosslinking treatment. From right to left, A11-C5 represent the fractions across the main peak from size exclusion chromatography on Sephacryl S-300 column.

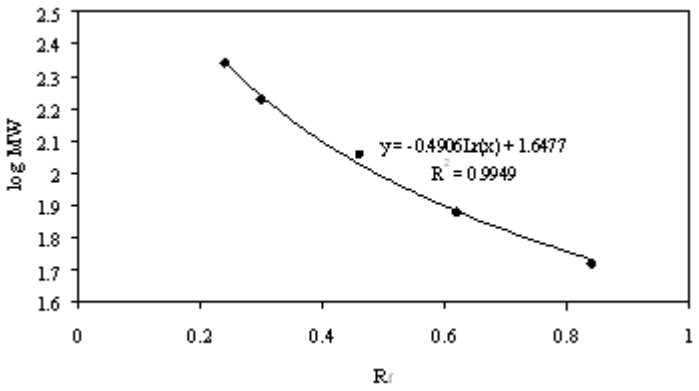

Figure 4.52 Relative mobility (R_f) and log MW of standard proteins for SDS-PAGE gel (Figure 4.51)

Table 4.9 Relative mobility (R_f) and log MW of standard proteins for SDS-PAGE gel (Figure 4.51)

Standard protein	MW (kDa)	Log MW	R_f
Myosin	220	2.34	0.083
α_2-Macroglobulin	170	2.23	0.125
β-Galactosidase	116	2.06	0.240
Transferrin	76	1.88	0.375
Glutamic dehydrogenase	53	1.72	0.583

Native invertase was also subjected to size exclusion chromatography using the same conditions as for the crosslinked species. The molecular weights of protein bands were estimated using a standard curve (Figure 4.53) based on the data shown in Table 4.10. Analysis of these fractions by SDS-PAGE showed a single species to be migrating between 81-170 kDa (Figure 4.54).

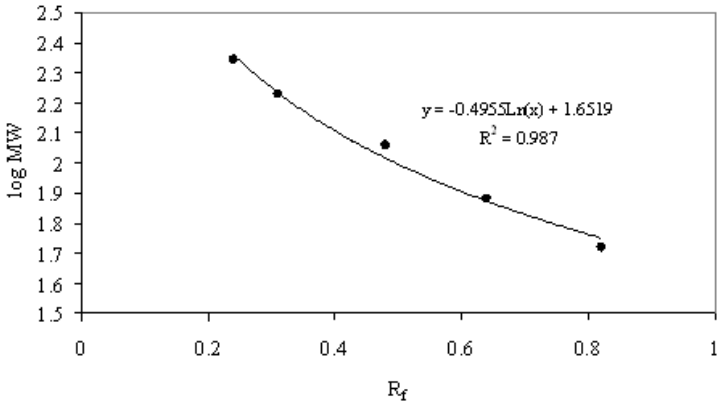

Figure 4.53 Relative mobility (R_f) and log MW of standard proteins for SDS-PAGE gel (Figure 4.54)

Table 4.10 Relative mobility (R_f) and log MW of standard proteins for SDS-PAGE gel (Figure 4.54)

Standard protein	MW (kDa)	Log MW	R_f
Myosin	220	2.34	0.24
α_2-Macroglobulin	170	2.23	0.31
β-Galactosidase	116	2.06	0.48
Transferrin	76	1.88	0.64
Glutamic dehydrogenase	53	1.72	0.82

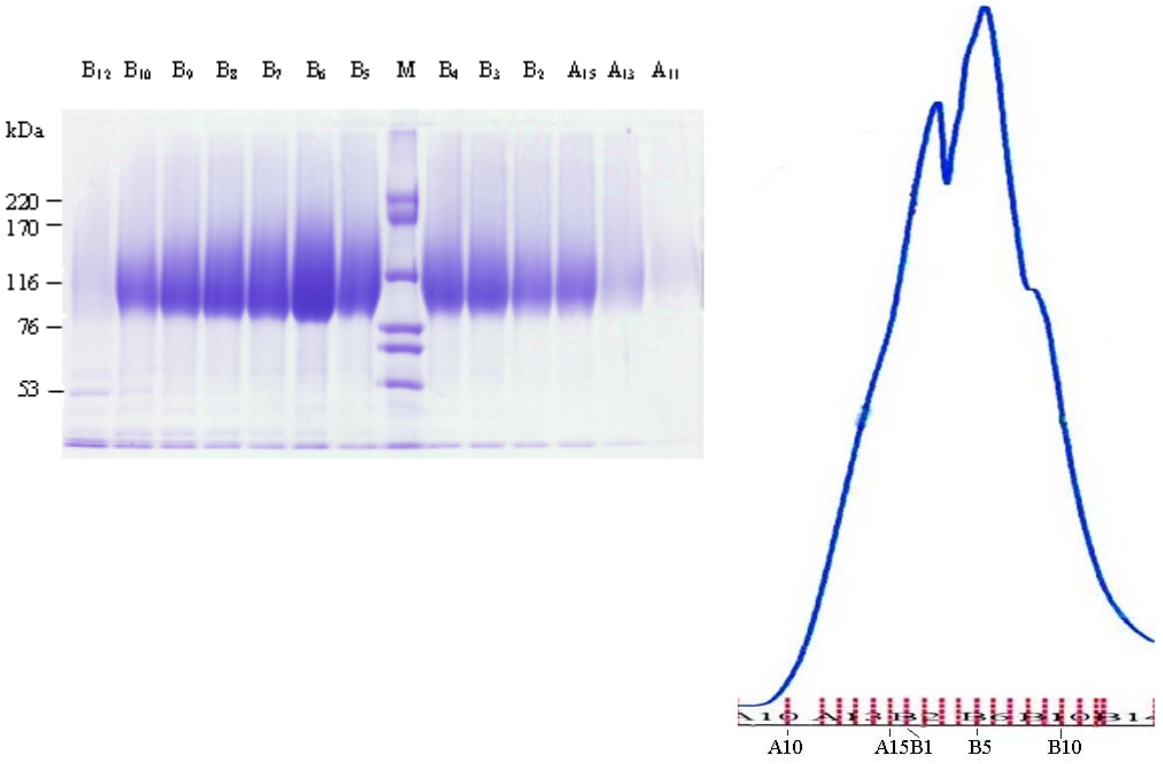

Figure 4.54 Elution profile and SDS-PAGE pattern of native invertase. From right to left, A11-B12 represent the fractions across the main peak from size exclusion chromatography on Sephacryl S-300 column.

Sample produced by intramolecular crosslinking treatment was analysed in exactly the same way as shown in Figure 4.54. The molecular weights of obtained protein bands were estimated using the standard curve of relative mobility versus log MW (Table 4.11and Figure 4.55). The molecular weights of the fractions A13-B9 across the peak of intramolecular crosslinked invertase ranged between 89-141 kDa (Figure 4.56). The results appeared to be no different for the intramolecularly crosslinked invertase and the native invertase. Protein bands with an apparent molecular weight ≥170 kDa were only present in the sample produced by intermolecular crosslinking treatment. In contrast, no

large molecules of intermolecularly crosslinked invertase were found after the intramolecular crosslinking treatment.

Table 4.11 Relative mobility (R_f) and log MW of standard proteins for SDS-PAGE gel (Figure 4.56)

Standard protein	MW (kDa)	Log MW	Rf
Myosin	220	2.34	0.30
α_2-Macroglobulin	170	2.23	0.34
β-Galactosidase	116	2.06	0.51
Transferrin	76	1.88	0.66
Glutamic dehydrogenase	53	1.72	0.88

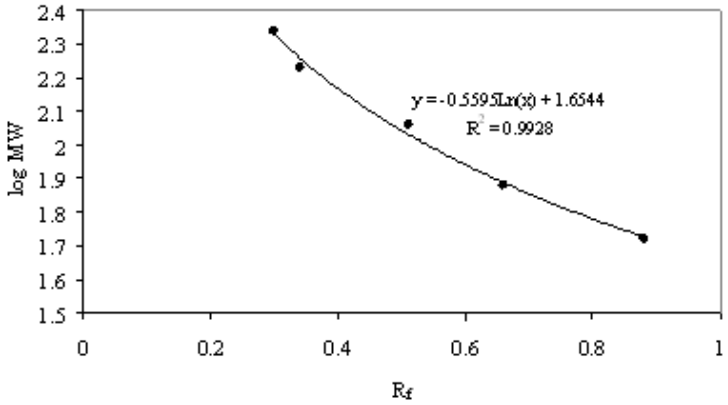

Figure 4.55 Relative mobility and log MW of standard proteins for SDS-PAGE gel (Figure 4.56)

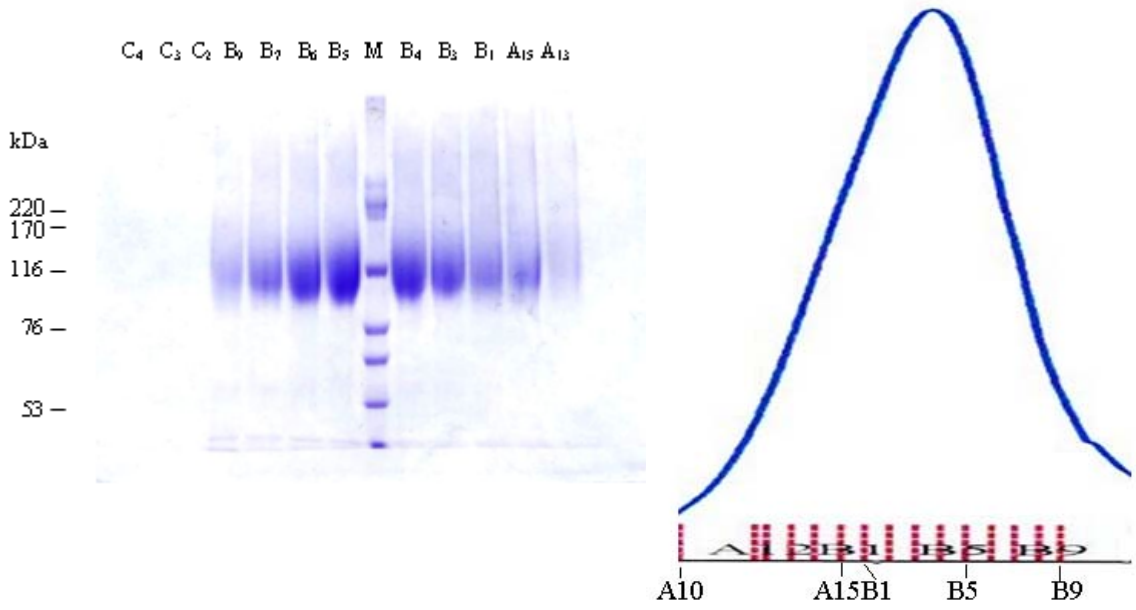

Figure 4.56 Elution profile and SDS-PAGE pattern of invertase after intramolecular crosslinking. From right to left, A13-C4 represent the fractions across the main peak from size exclusion chromatography on Sephacryl S-300 column.

SDS-PAGE was also used to analyse deglycosylated invertase after the crosslinking treatments. Two deglycosylation treatments by PNGase F were tested: 1) overnight deglycosylation at 37 °C; 2) deglycosylation at 37 °C overnight and then at 25 °C for 2 days. SDS-PAGE gels (6.5% acrylamide) shown in Figure 4.57 (overnight deglycosylation at 37 °C) and Figure 4.58 (deglycosylation at 37 °C overnight and then at 25 °C for 2 days).

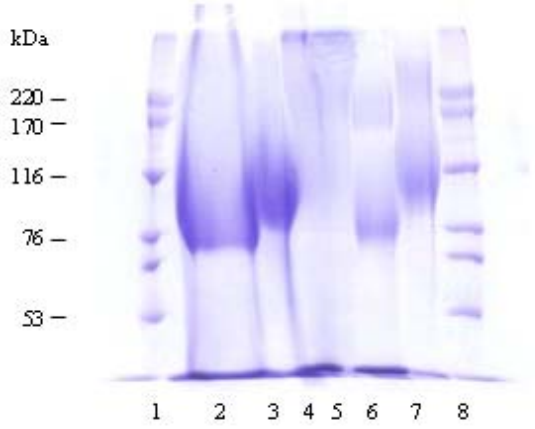

Figure 4.57 SDS-PAGE (6.5% acrylamide) of invertase and its crosslinked products after deglycosylation by PNGase F (37 °C, overnight). Lanes 1 and 8: molecular weight markers; lane 2 partially deglycosylated native invertase; lane 3: native invertase; lane 4: partially deglycosylated invertase after intermolecular crosslinking; lane 5: invertase after intermolecular crosslinking; lane 6: partially deglycosylated invertase after intramolecular crosslinking; lane 7: invertase after intramolecular crosslinking.

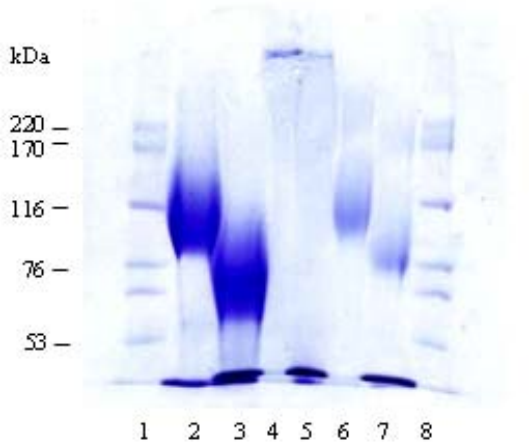

Figure 4.58 SDS-PAGE (6.5% acrylamide) of invertase and its crosslinked products after deglycosylation by PNGase F (37 °C, overnight and then for 2 days at 25 °C). Lanes 1 and 8: molecular weight markers; lane 2 native invertase; lane 3: partially deglycosylated native invertase; lane 4: invertase after intermolecular crosslinking; lane 5: partially deglycosylated invertase after intermolecular crosslinking; lane 6: invertase after intramolecular crosslinking; lane 7: partially deglycosylated invertase after intramolecular crosslinking.

The molecular weights of the protein bands were estimated using the relationship between MW and R_f as provided in Table 4.12 and Figure 4.59. A comparison of Figure 4.57 and Figure 4.58 raises some interesting points. Firstly, native invertase appeared to run higher in lane 2, Figure 4.58, than in lane 3, Figure 4.57, with a molecular weight of ~102 kDa in Figure 4.58, but 93 kDa in Figure 4.57. This difference is most probably due to differences in the quality of the gels. Secondly, all samples that had been digested with PNGase F showed a significant loss in molecular mass. The lower bands (near dye front in Figure 4.57 and Figure 4.58) visible in the deglycosylated samples were due to PNGase F (MW 38 kDa). It was clear that the longer incubation treatment of the invertase sample particularly the native sample with PNGase F was more effective in removing the carbohydrate. The molecular weight of 93 kDa for native invertase (lane 3, Figure 4.57) was decreased to 81 kDa (lane 2, Figure 4.57) after the deglycosylated incubation for overnight at 37 °C whereas removal of the N-linked glycan chains decreased the molecular mass from 102 kDa (lane 2, Figure 4.58) to 76 kDa (lane 3, Figure 4.58) after the deglycosylated incubation at 37 °C, overnight and then at 25 °C for two days. Therefore 13% and 25% of carbohydrate were removed on incubating the native invertase at 37 °C overnight and at longer incubation, respectively. There was no significant difference in the SDS-PAGE behaviour of the glycosylated native invertase (lane 2, Figure 4.58, and lane 3, Figure 4.57) and invertase after intramolecular crosslinking treatment (lane 7, Figure 4.57, and lane 6, Figure 4.58). There may have been a decreased efficiency of deglycosylation of the latter. This was not so for the invertase after intermolecular crosslinking (Figure 4.57 and Figure 4.58) where there appeared to be no difference between the sample that had been exposed to PNGase F and the sample without PNGase F treatment. It is plausible that intra- and intermolecular crosslinking hinders the access of PNGase F to the sites of glycosylation and thereby reduces the deglycosylation efficacy.

Table 4.12 Relative mobility (R_f) and log MW of standard proteins on SDS-PAGE gels (Figure 4.57 and Figure 4.58)

Standard protein	MW (kDa)	Log MW	R_f	
			Figure 4.57	Figure 4.58
Myosin	220	2.34	0.18	0.21
α_2-Macroglobulin	170	2.23	0.24	0.28
β-Galactosidase	116	2.06	0.39	0.44
Transferrin	76	1.88	0.57	0.64
Glutamic dehydrogenase	53	1.72	0.80	0.86

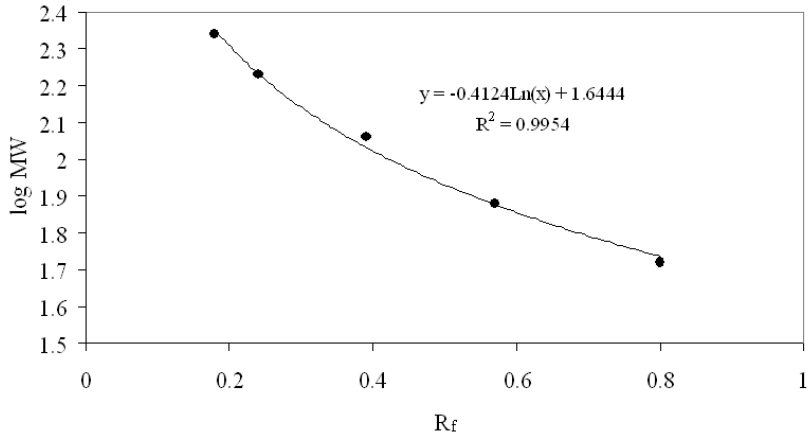

(a)

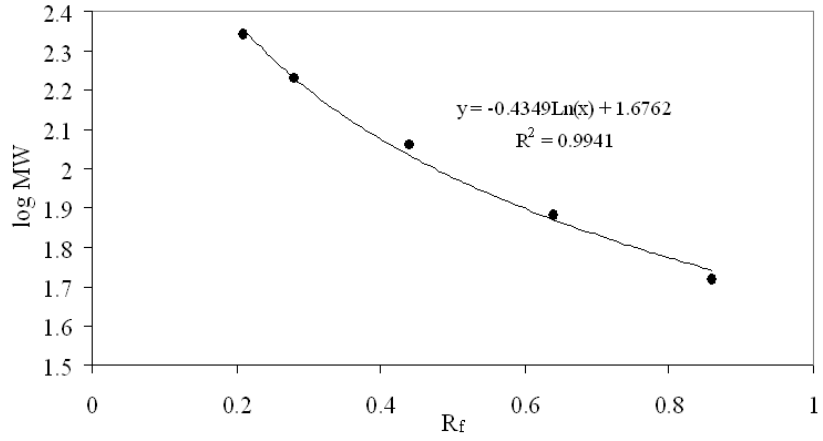

(b)

Figure 4.59 Relative mobility (R_f) and log MW of standard proteins for SDS-PAGE gels in (a) Figure 4.57 and (b) Figure 4.58.

The percentage of the carbohydrate remaining was not directly measured. It has been previously reported that 85% of the carbohydrate could be removed from the native

invertase after exposing it to 0.5 units of PNGase F at 37 °C for 18 hours (Patel *et al.*, 1997). Partial denaturation of the crosslinked protein may be required prior to the addition of PNGase F as this protocol has been shown to increase the rate of deglycosylation substantially (Chu, 1986). Another N glycanase, the endo-β-N-acetylglucosaminidase H, has been reported to be able to remove all of the polymannosyl chains from denatured invertase (Williams *et al.*, 1985). The carbohydrate moiety of invertase may affect its stability. For example, in one study the removal of manose residues by α-mannosidase (30 °C, 15 hours) reduced the stability of invertase (Takegawa *et al.*, 1990). The mannose depleted invertase was much more succeptible to proteolysis and was less stable in the presence of low concentrations of SDS (Takegawa *et al.*, 1990). In general, the carbohydrate moietiy of a glycoprotein does not influence either the protein conformation or catalytic activity (Schülke and Schmid, 1988).

As noted above, size exclusion chromatography with a separation range of 10-1,500 kDa proved to be insufficiently capable of separation of the native and the crosslinked invertase especially if the samples had been either fully or partially deglycosylated. The larger molecule of oligomeric invertase (estimated molecular weight of ≥540 kDa) expected as a consequence of intermolecular crosslinking only appeared as a shoulder of the main peak. Furthermore, the native invertase of 270 kDa and the intramolecularly crosslinked invertase species with the estimated molecular weight range of 270-540 kDa (depending on the number of intramolecular crosslinks that could occur in one molecule of invertase) produced overlapping peaks. Using ion exchange chromatography instead of SEC probably offers a better separation option as the crosslinked products differ in the net molecular charge after the crosslinking reaction.

4.2.5 Circular dichroism (CD)

The effect of covalent crosslinking on the secondary structure of invertase was investigated using circular dichroism spectrometry (Applied Photophysics, UK, Chirascan^{TM} Circular Dichroism Spectrometer). The far UV spectrum of native invertase showed a maximum ellipticity at around 210-220 nm in agreement with a previous report (Chu *et al.*, 1978). The spectra of native invertase, invertase that had undergone the intermolecular crosslinking treatment and invertase after intramolecular crosslinking were identical (Figure 4.60), implying no change in secondary structure as a consequence of the crosslinking treatment.

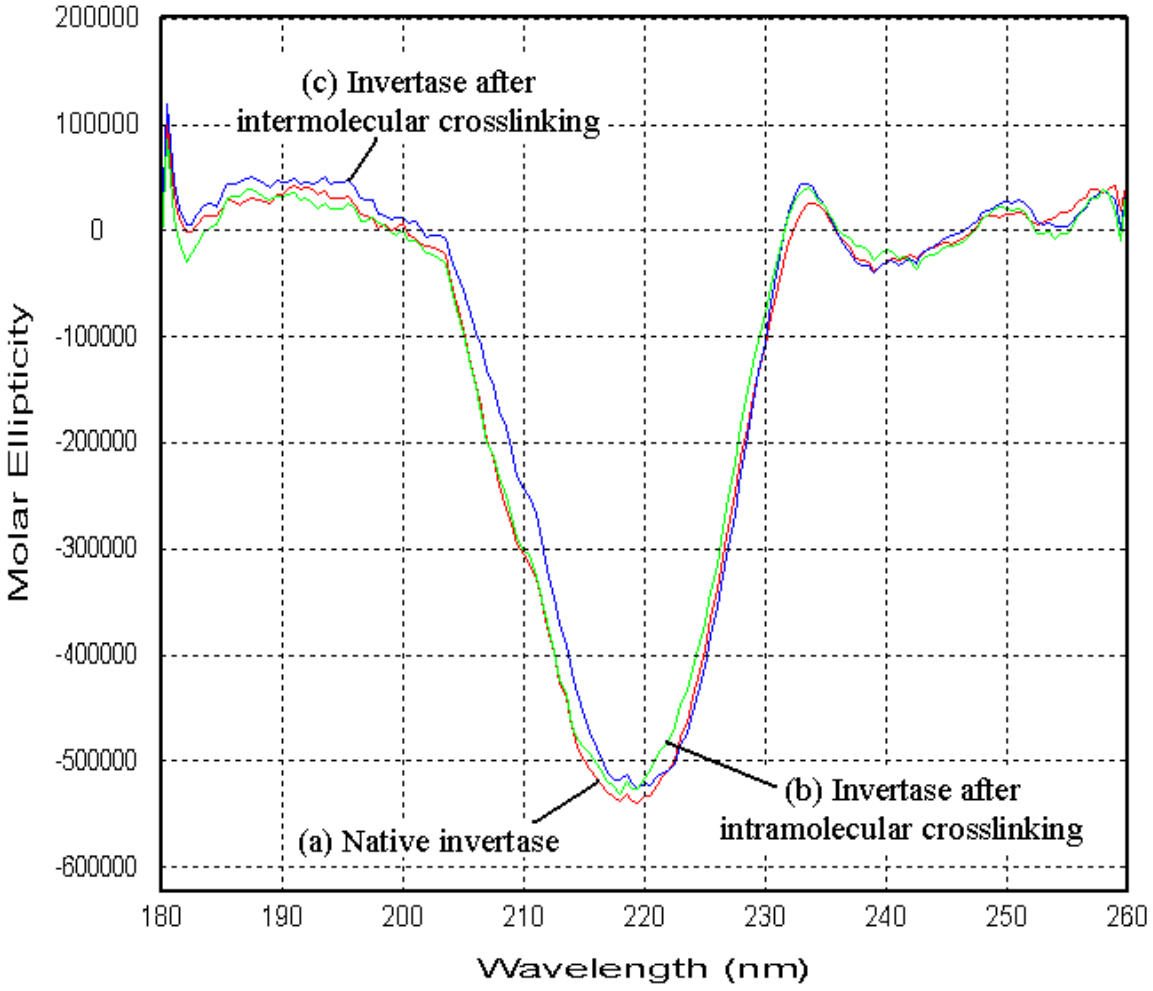

Figure 4.60 CD spectra of (a) native invertase (red line), (b) invertase (0.9 μM) crosslinked with BMDC (green line) and (c) invertase (185 μM) crosslinked with BMDC (blue line) in 4 mM sodium phosphate buffer with 30 mM NaCl. Enzyme solutions were measured at 0.4-0.6 mg/mL and the cell path length was 0.1 cm.

Reaction of invertase with BMDC produced an enzyme with increased stability. Whether this was due to the formation of intermolecular or intramolecular crosslinks has been the focus of this chapter. Several methods were used to estimate the sizes of the enzyme molecules that had been treated with the crosslinker to produce intermolecular crosslinks and intramolecular crosslinks. These methods were SEC, SEC with MALLS detection, DLS and SDS-PAGE. The results obtained from SEC and DLS were unclear and inconclusive, probably because a high proportion of the covalently bound carbohydrate caused the sample to behave anomalously with respect to structural globular proteins.

The clearest results were obtained using SDS-PAGE. This showed that the product formed by crosslinking treatment at a high enzyme concentration was indeed multimeric with more than one invertase molecule being part of a covalently linked complex. The molecular weight of the product formed by crosslinking at a lower invertase concentration however was not significantly different to that of the native protein.

In attempts to establish whether intramolecular crosslinks were being made under the treatment conditions, a model system was developed using peptides with a controlled number of functional groups. This and the relevant studies are discussed in Section 4.3.

4.3 Investigations into molecular basis of BMDC crosslinking

As discussed in the previous sections, treatment of a low concentration of invertase with BMDC resulted in a dramatic increase in its thermal stability. It was hyphothesised that this was due to intramolecular crosslinking which could "clamp" the enzyme molecule in an active state and reduce its tendency to be denatured by heat. Because invertase is highly glycosylated, a mass spectroscopic analysis of the molecule that had been subjected to the crosslinking treatment was difficult. Therefore simple synthetic model oligopeptides and nonglycosylated model enzymes subjected to the crosslinking treatment were used to prove by mass spectroscopy and other methods, the nature of the crosslink formation. Model peptides and proteins were subjected to crosslinking using the exact same conditions as were used for invertase. The presence of crosslinks was confirmed using SDS-PAGE, protein/peptide proteolysis and RP-HPLC, CD and mass spectrometry.

4.3.1 Oligopeptides

Two small synthetic oligopeptides were used in this study. One was a pentapeptide and the other was a heptapeptide. Both contained amino acid residues which had been shown to specifically react with BMDC. After exposure to the crosslinking reagent the reaction mixture was examined using a number of different techniques to establish the presence of crosslinks, and the amino acid residues involved in their formation. The synthetic oligopeptides used are explained in Section 3.1.1. These oligopeptides were custom made by Auspep Pty Ltd., Parkville, Australia.

4.3.1.1 Synthetic pentapeptide

Pentapeptide (0.9 μM) was reacted with 30 mM of BMDC in buffers ranging in pH from pH 5-8 (the same buffers as those used for crosslinking invertase) at room temperature for 15 minutes with vigorous shaking. The contents of the reaction vial were then analysed by RP-HPLC (Ultimate 3000 Dionex) using a Jupiter Proteo 250×4.6 mm column. Eluted protein was detected using a UV detector set at wavelengths of 214 and 280 nm. The HPLC chromatograms of the native pentapeptide and its crosslinked products after reaction at various pH values are shown in Figure 4.61. The main peak of the native oligopeptide eluted with a retention time of 6.43 minutes. Crosslinking at different pH provided a peak of similar size to the main peak of the native peptide but at an increased retention time of approximately 8 minutes (Figure 4.61). At pH 5 and 7, a small peak with the same retention time as that of the native peptide was observed. This disappeared in the samples crosslinked at pH 6 and 8 (Figure 4.61).

The synthetic pentapeptide with a sequence of Ac-Gly-Ser-Lys-Gly-Thr-OH (GSKGT, Figure 4.62) was designed to investigate the reaction of the amino side chain of lysine with BMDC. Depending on pH, BMDC was later found to be able to react with other functional groups in this peptide such as the carboxylate group. According to the literature, there are seven different possible ways that BMDC can interact with the pentapeptide used. These are shown in Figure 4.62. Of the configuration illustrated in Figure 4.62 c can not occur because the length of BMDC (5.17 Å) is too short to reach the amino group of lysine residue in the peptide chain. The backbone length between R group of lysine residue and C-terminal of peptide chain is ~8.81 Å calculated using bond length, bond angles and Handy math software (www.handymath.com)

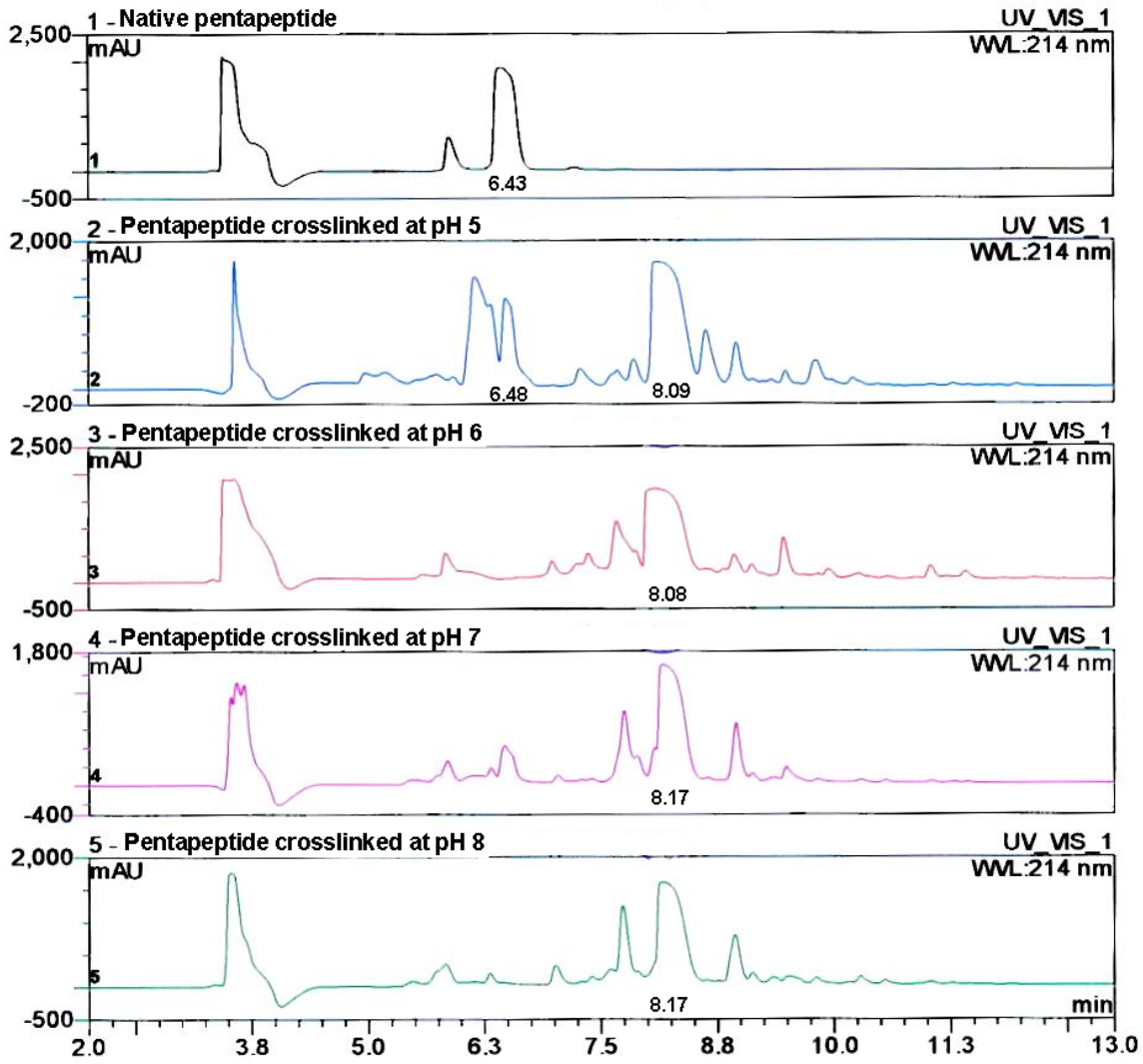

Figure 4.61 RP-HPLC chromatograms of the native pentapeptide and pentapeptide after intramolecular crosslinking with BMDC at pH 5-8 (Jupiter Proteo column with flow rate of 1 mL/min).

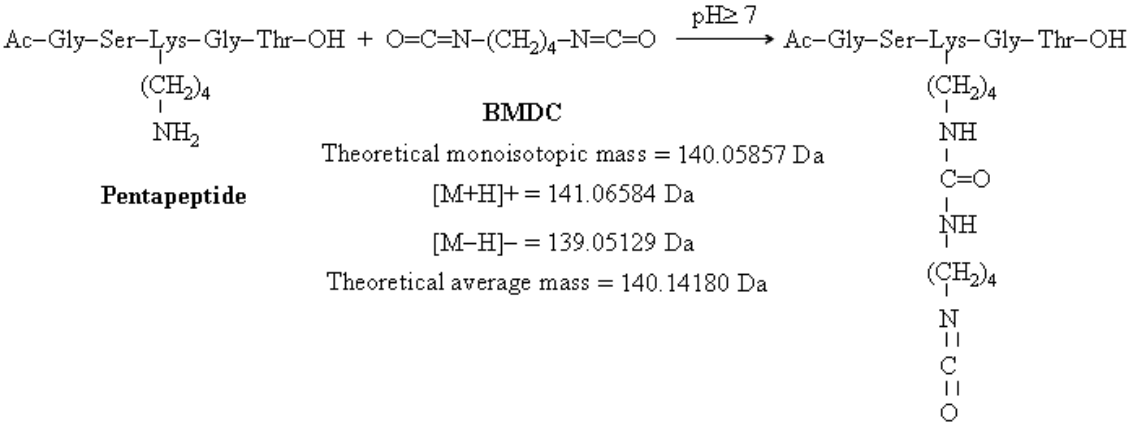

Pentapeptide

BMDC

Theoretical monoisotopic mass = 140.05857 Da

[M+H]+ = 141.06584 Da

[M–H]– = 139.05129 Da

Theoretical average mass = 140.14180 Da

One-end modified pentapeptide

Theoretical monoisotopic mass = 630.29727 Da

$[M+H]^+$ = 631.30455 Da

$[M-H]^-$ = 629.29000 Da

Theoretical average mass = 630.65580 Da

[MolE-Molecular Mass Calculator v2.02 by Jeff Rozenski (1999)]

(a)

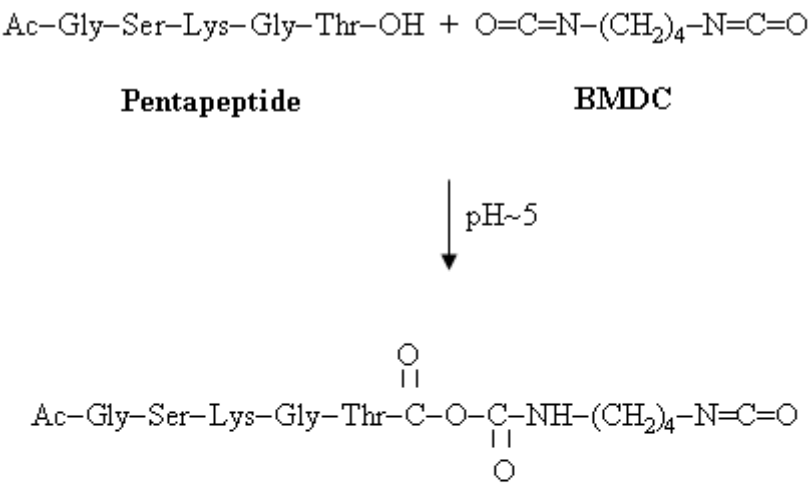

Pentapeptide **BMDC**

One-end modified pentapeptide

Theoretical monoisotopic mass = 630.29727 Da

$[M+H]^+$ = 631.30455 Da

$[M-H]^-$ = 629.29000 Da

Theoretical average mass = 630.65580 Da

[MolE-Molecular Mass Calculator v2.02 by Jeff Rozenski (1999)]

(b)

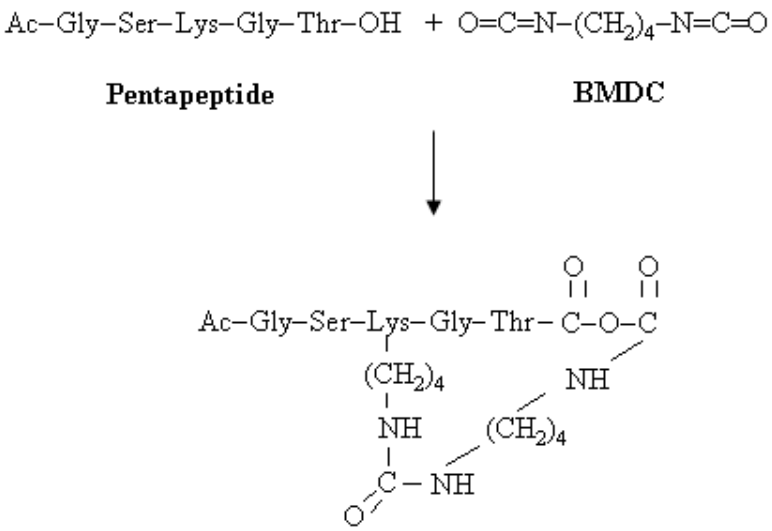

Intramolecularly crosslinked pentapeptide

Theoretical monoisotopic mass = 630.29727 Da

$[M+H]^+$ = 631.30455 Da

$[M-H]^-$ = 629.29000 Da

Theoretical average mass = 630.65580 Da

[MolE-Molecular Mass Calculator v2.02 by Jeff Rozenski (1999)]

(c)

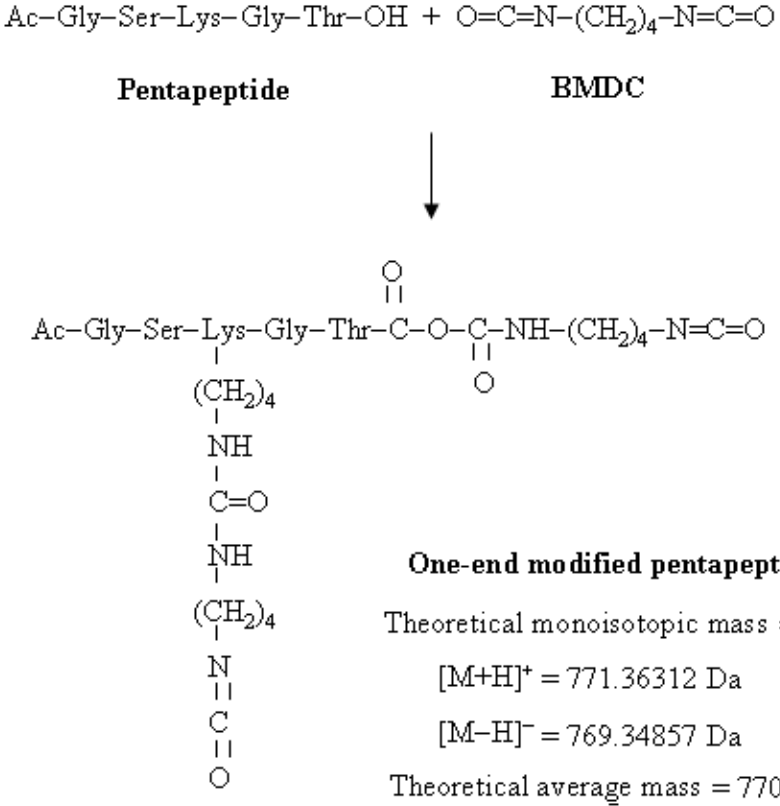

One-end modified pentapeptide

Theoretical monoisotopic mass = 770.35585 Da

$[M+H]^+$ = 771.36312 Da

$[M-H]^-$ = 769.34857 Da

Theoretical average mass = 770.79760 Da

[MolE-Molecular Mass Calculator v2.02 by Jeff Rozenski (1999)]

(d)

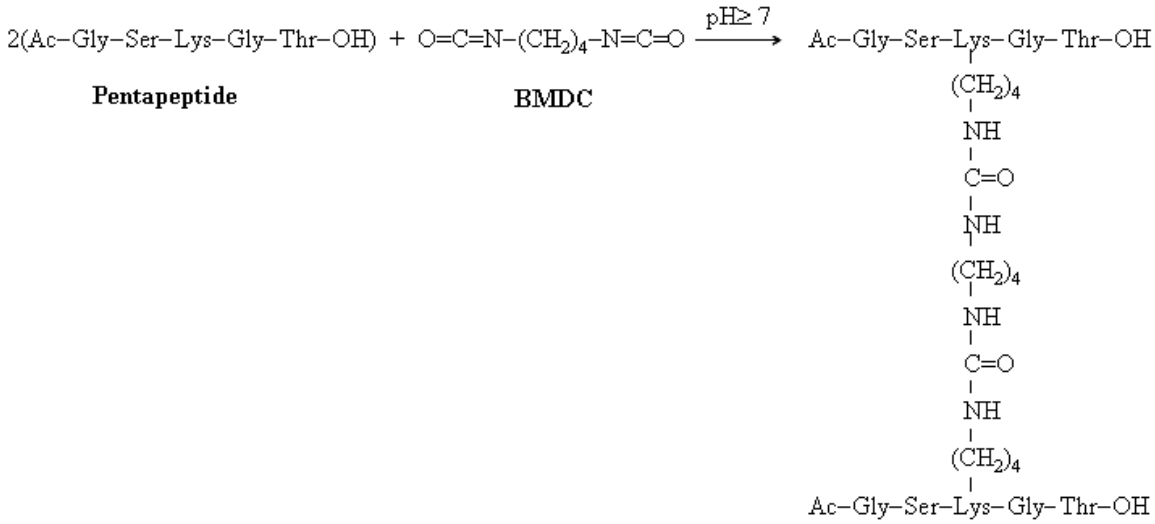

Pentapeptide **BMDC**

Intermolecularly crosslinked pentapeptide

Theoretical monoisotopic mass = 908.59192 Da

$[M+H]^+$ = 909.59920 Da

$[M-H]^-$ = 907.58465 Da

Theoretical average mass = 909.14339 Da

[MolE-Molecular Mass Calculator v2.02 by Jeff Rozenski (1999)]

(e)

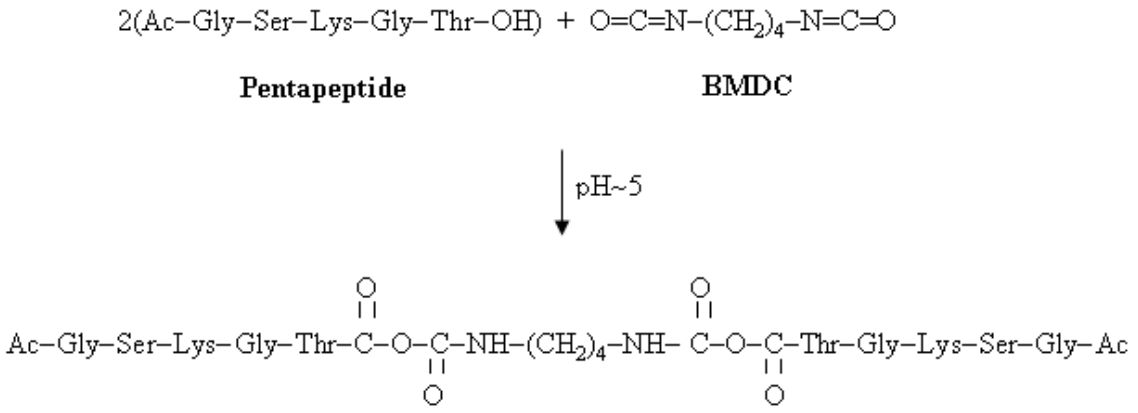

Pentapeptide **BMDC**

Intermolecularly crosslinked pentapeptide

Theoretical monoisotopic mass = 908.59192 Da

$[M+H]^+$ = 909.59920 Da

$[M-H]^-$ = 907.58465 Da

Theoretical average mass = 909.14339 Da

[MolE-Molecular Mass Calculator v2.02 by Jeff Rozenski (1999)]

(f)

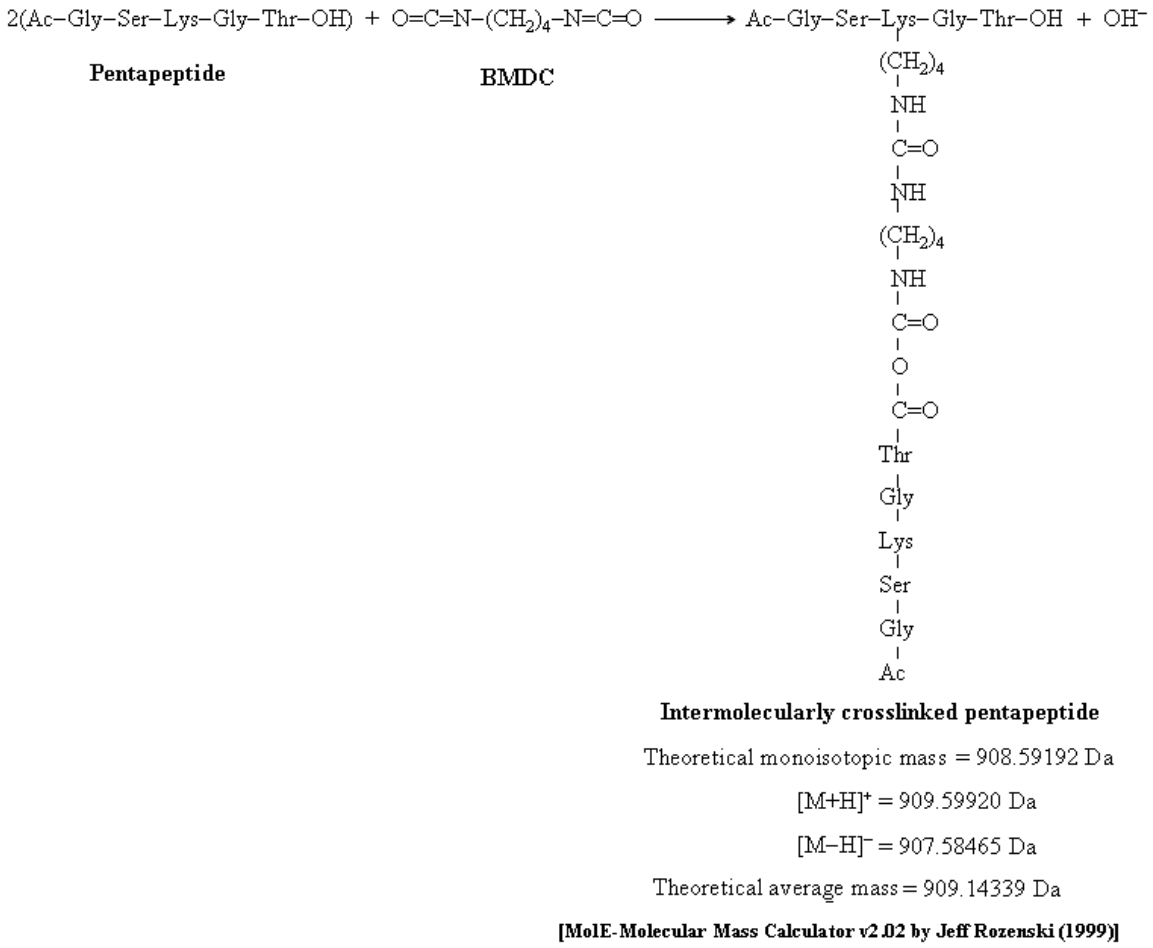

(g)

Figure 4.62 The possibilities (a-g) of products of crosslinking the pentapeptide with BMDC.

Samples corresponding to various chromatographic peaks were collected and analysed by mass spectrometry in positive and negative modes of operation. The mass spectrum of native pentapeptide showed peaks ($[M–H]^-$) and ($[M+H]^+$) with respective masses of 489.73 Da and 491.81 Da (Figure 4.63). These agreed with the average mass of 490.5 Da provided by Auspep Pty Ltd for the native pentapeptide. After the crosslinking treatment, the main peak resulting from the reaction at pH 8 (retention time 8.28 minutes) was analysed by the Otago University in an ABI TOF/TOF instrument which was capable of higher mass accuracy than the instrument available at Massey University. An average mass of 630.65580 Da which is expected to be due to entities illustrated in Figure 4.62 a and b, appeared as a peak ($[M–H]^-$) with a mass of 629.3473 Da (Figure 4.64) in the negative mode and a little peak of 631.2775 Da in the positive mode measurement (Figure 4.65). There was no peak with a mass of 908.59192 Da, the mass expected for an

intermolecularly crosslinked peptide made up of two pentapeptides linked by a single molecule of BMDC.

BMDC can react with functional groups other than the amino side chain. Invertase is an acidic protein that has only a few lysine residues in its polypeptide chain. For this reason another model peptide containing two carboxylate side chains (see Section 4.3.1.2) was used to carry out similar studies.

4.3.1.2 Synthetic heptapeptide

In this study, a synthetic heptapeptide with two carboxylate functional groups, one aromatic hydroxyl functional group and a guanidinium side chain, was reacted with BMDC and the reaction product was analysed. The amino acid sequence of the synthetic heptapeptide was Ac-Gly-Asp-Phe-Tyr-Arg-Ala-Asp-OH (Ac-GDFYRAD-OH) (Section 3.1.1).

The heptapeptide 1 mg/mL (1 mM) was treated with 30 mM BMDC at various pH values between pH 5 and 8 using the same conditions as used for invertase. The products of the reaction were analysed by RP-HPLC (Jupiter Proteo, 2.5 × 4.6, 90 Å, Phenomenex) and mass spectrometry. The elution profiles from HPLC detected at 214 nm are shown in Figure 4.66.

The native heptapeptide eluted after 13.94 minute whereas BMDC eluted at 8.15 minute of the separation. Product peaks appeared at a retention time of 14.07 minutes for the reactions carried out at pH 5, 7 and 8 (Figure 4.66). No reaction appears to have occurred at pH 6. A main peak appeared at a higher retention time of 14.13 minute in the reaction carried out at pH 8 (Figure 4.66). Possible products and their theoretical masses are shown in Figure 4.67.

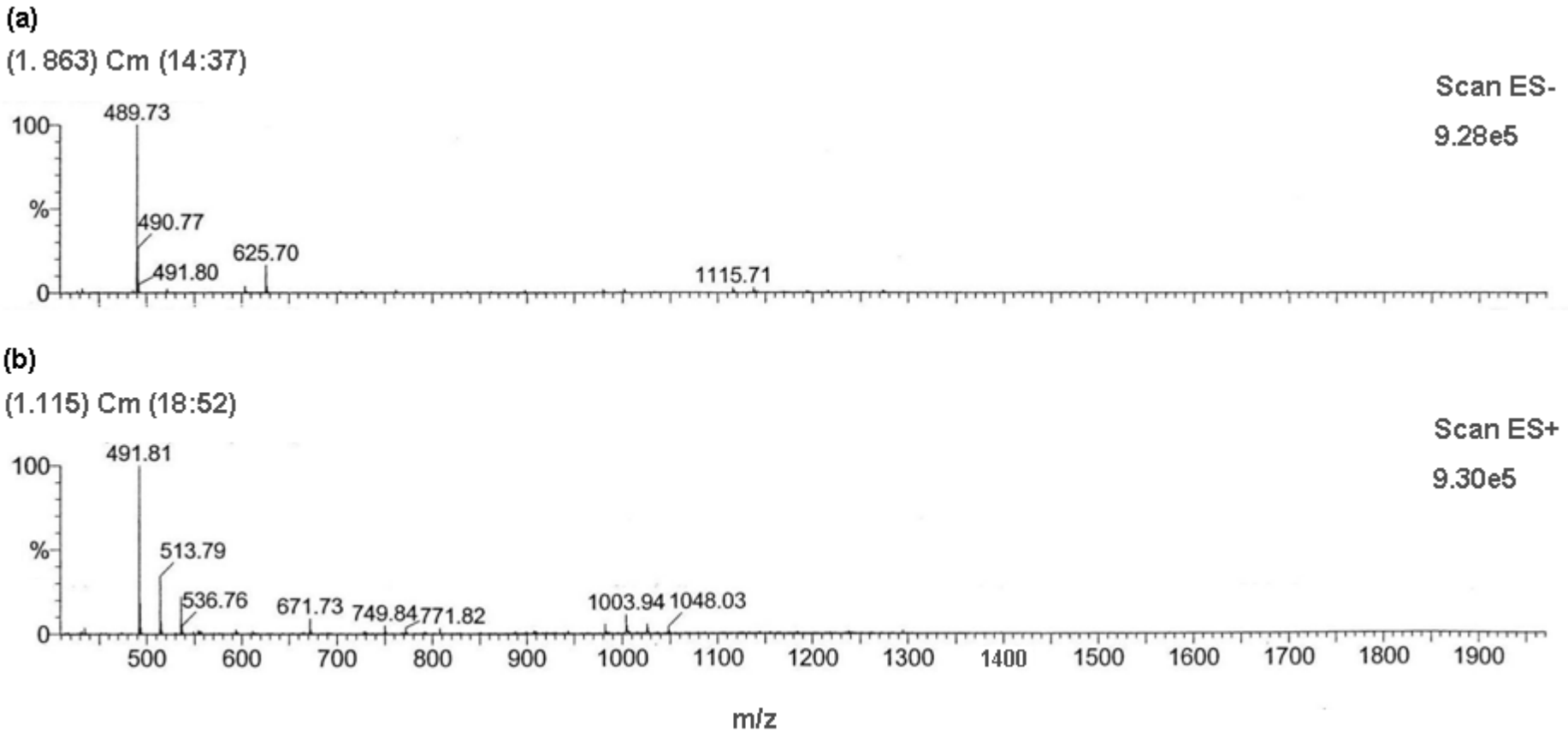

Figure 4.63 Mass spectrum (MALDI-TOF MS) of native pentapeptide in Na-citrate buffer pH 7 in (a) negative ion mode and (b) positive ion mode.

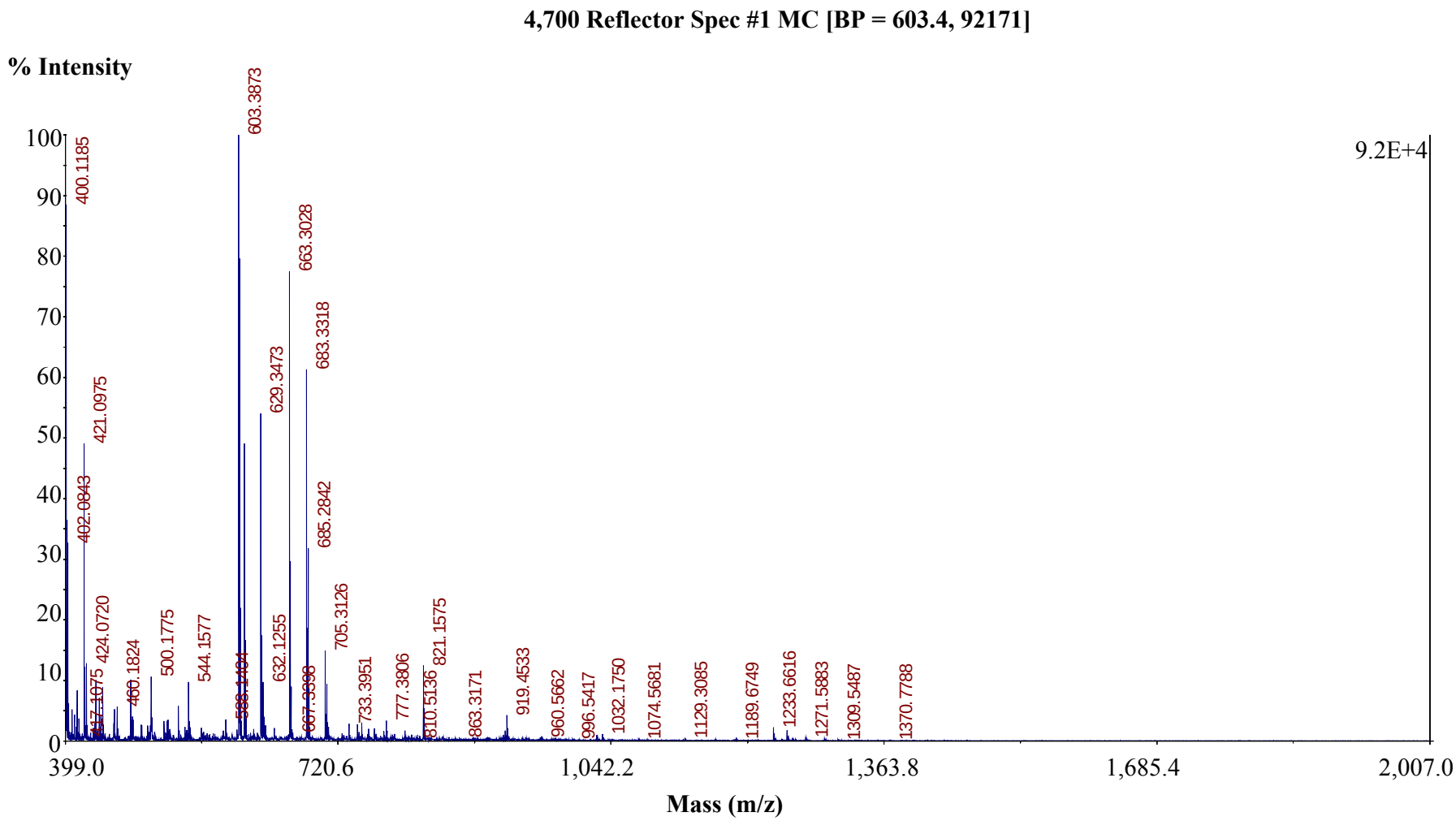

Figure 4.64 Mass spectrum (ABI TOF/TOF analyzer in negative ion mode, mass range m/z 400-2000 from CPR, Otago University) of the pentapeptide crosslinked at pH 8.

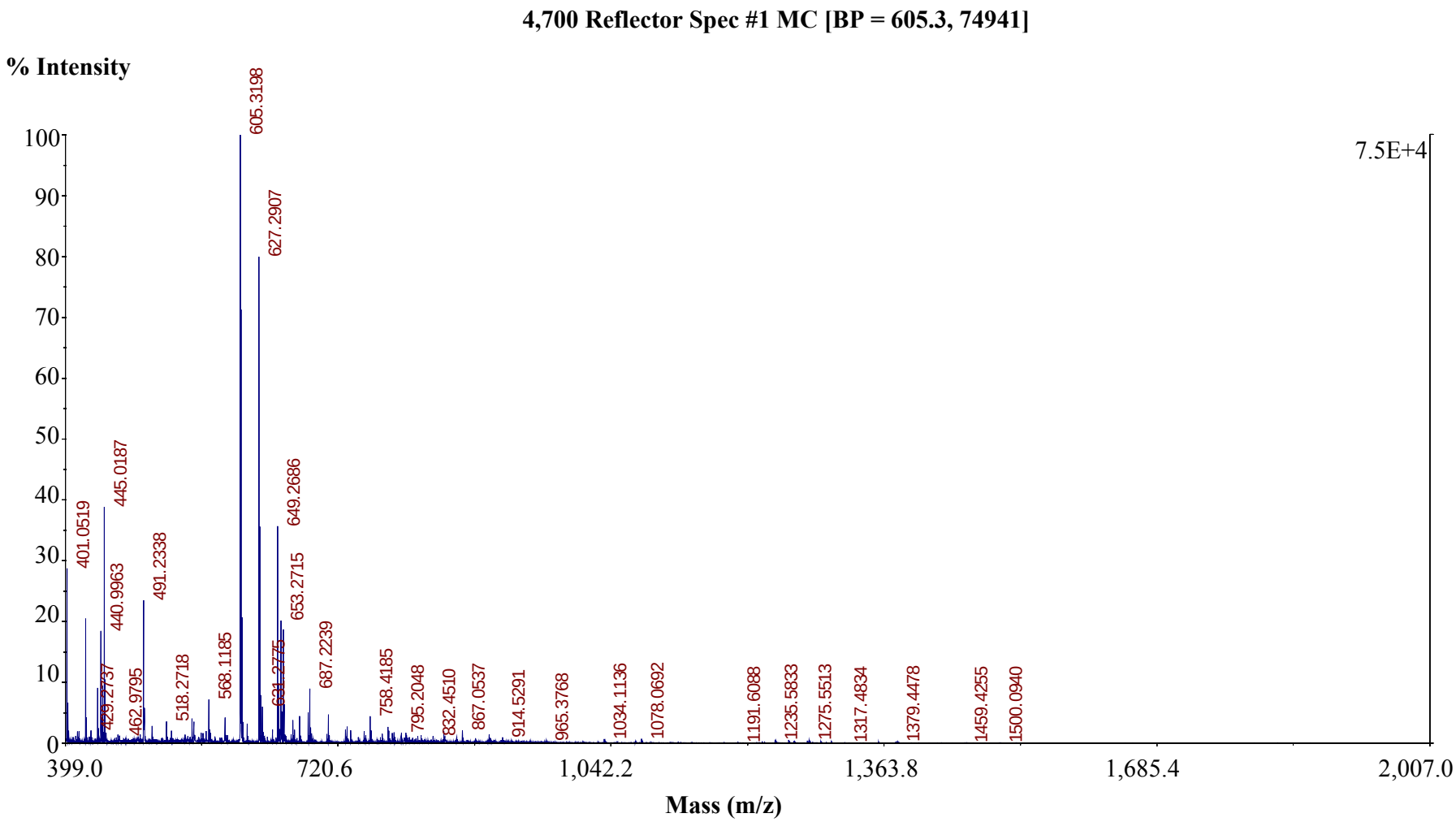

Figure 4.65 Mass spectrum (ABI TOF/TOF analyzer in positive ion mode, mass range m/z 400-2000 from CPR, Otago University) of the pentapeptide crosslinked at pH 8.

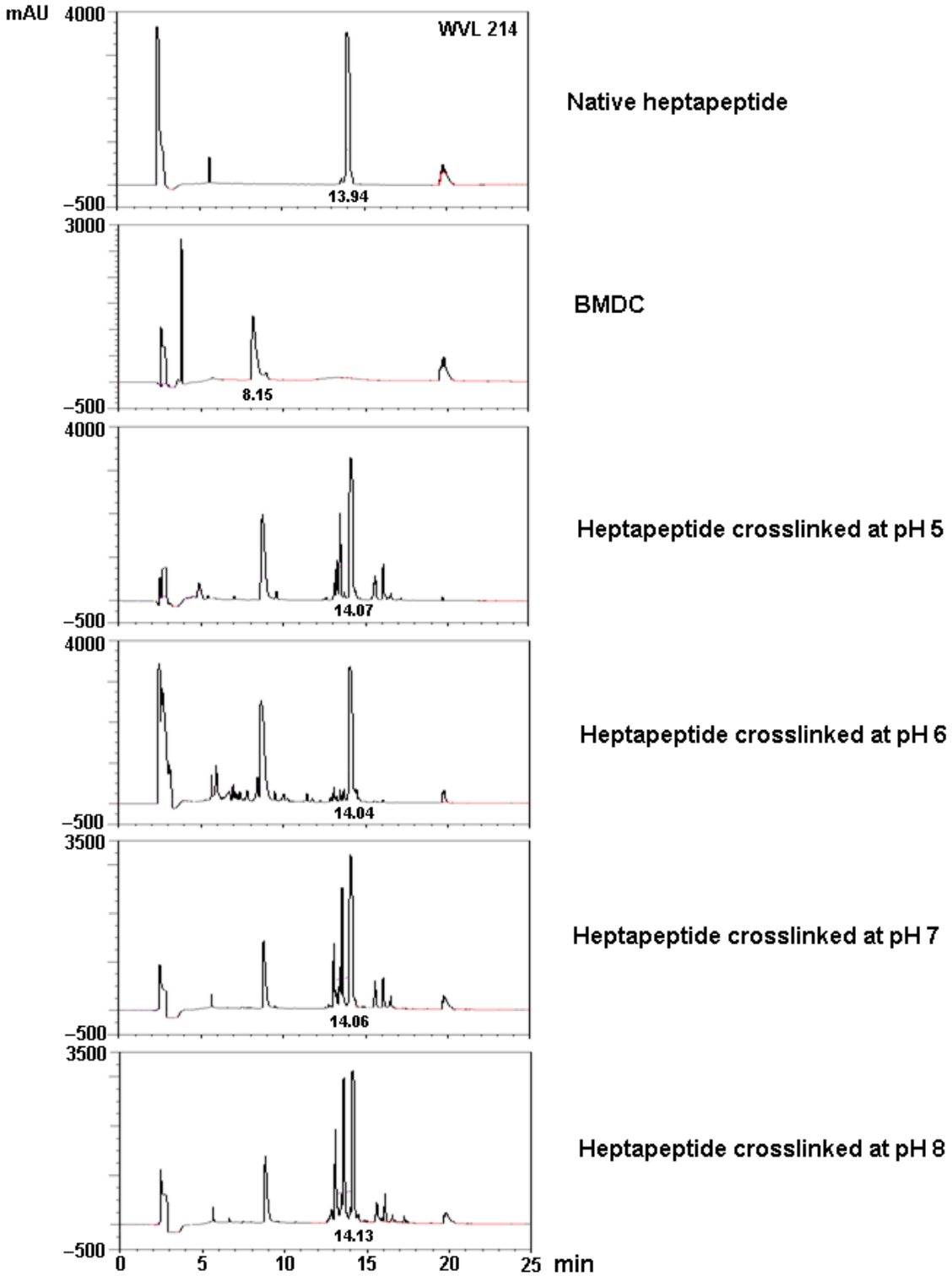

Figure 4.66 RP-HPLC chromatograms of native heptapeptide, BMDC and the heptapeptide crosslinked with BMDC at pH 5-8 on Jupiter Proteo column with flow rate of 1 mL/min.

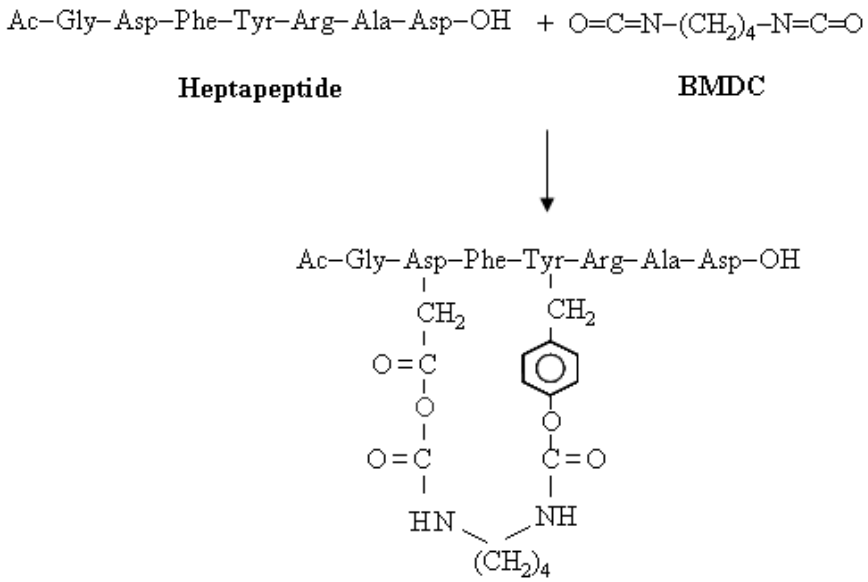

Intramolecularly crosslinked heptapeptide

Theoretical monoisotopic mass = 1,024.42498 Da

$[M+H]^+$ = 1,025.43226 Da

$[M-H]^-$ = 1,023.41771 Da

Theoretical average mass = 1,025.04268 Da

[MolE-Molecular Mass Calculator v2.02 by Jeff Rozenski (1999)]

(a)

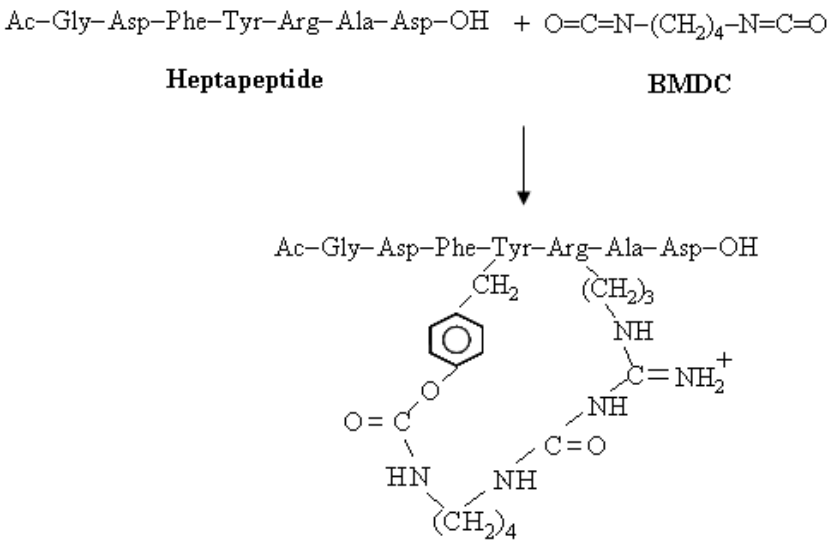

Intramolecularly crosslinked heptapeptide

Theoretical monoisotopic mass = 1,024.42498 Da

$[M+H]^+$ = 1,025.43226 Da

$[M-H]^-$ = 1,023.41771 Da

Theoretical average mass = 1,025.04268 Da

[MolE-Molecular Mass Calculator v2.02 by Jeff Rozenski (1999)]

(b)

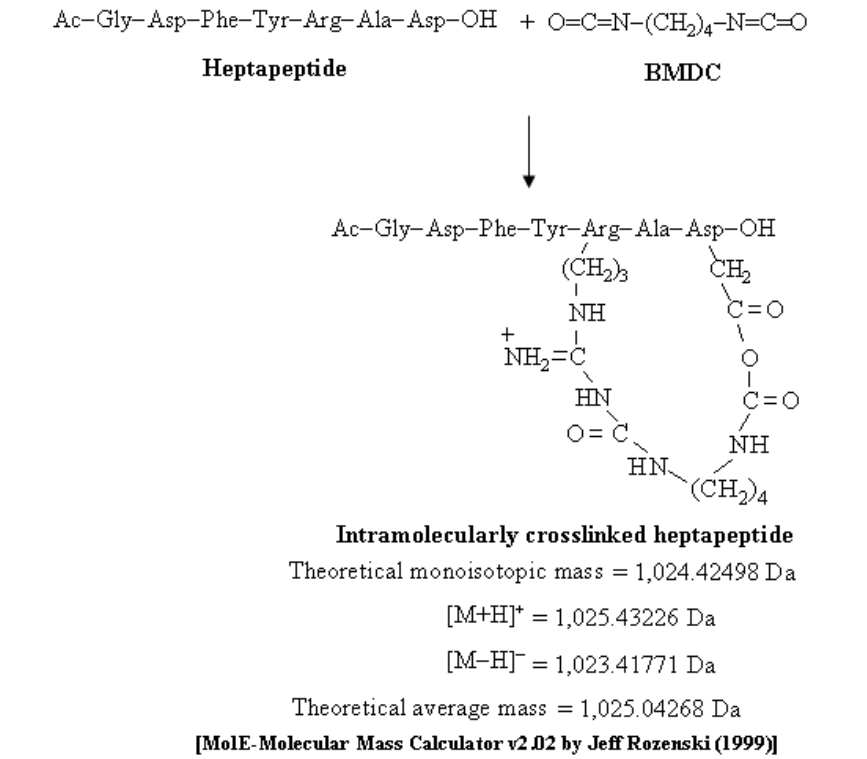

(c)

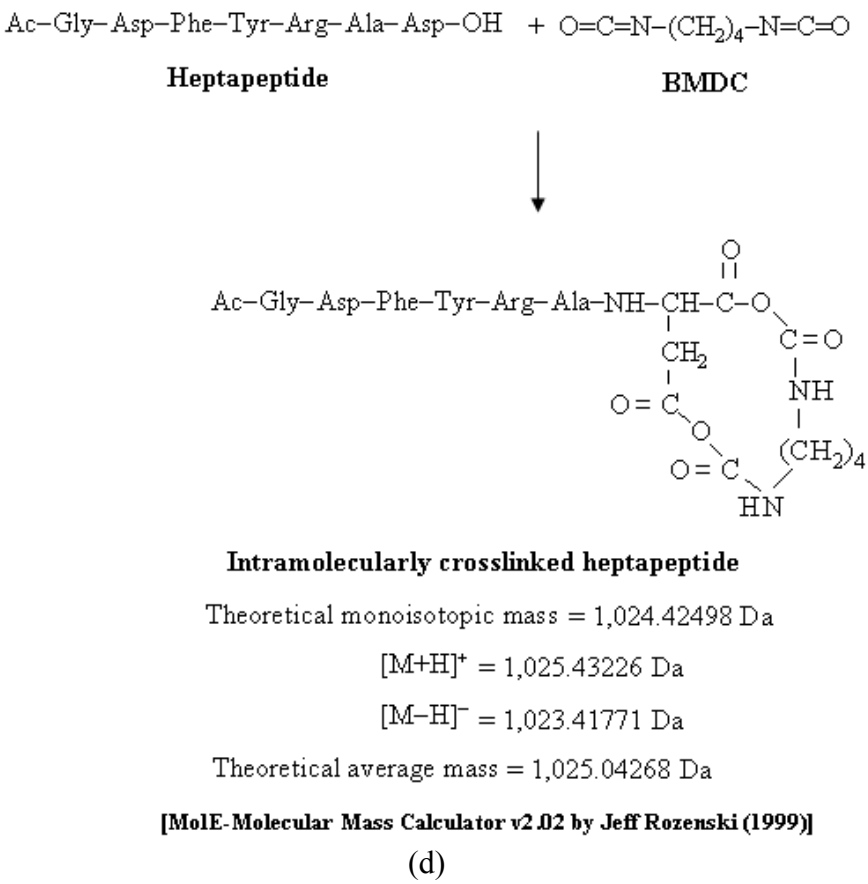

(d)

Figure 4.67 (a-d) The possible products of the crosslinking reaction between BMDC and the heptapeptide.

The possible products of intramolecular crosslinking of the peptide are as follows:

1. The reaction between carboxylate group of Asp2 and hydroxyl group of Tyr4 (Figure 4.67 a);
2. The binding of hydroxyl group of Tyr4 and primary amine of the guanidinium group of Arg5 (Figure 4.67 b);
3. The crosslink between primary amine of the guanidinium group of Arg5 and the carboxylate side chain of Asp7 (Figure 4.67 c);
4. The linkage between the carboxylate side chain of Asp7 and the C-terminal carboxylate (Figure 4.67 d).

However, some of the above products may not occur in practice in view of the distance between the relevant functional groups in the peptide chain and the length of BMDC molecule (5.17 Å). For example, the configurations in Figure 4.67 a and c may not be produced because of the distance between R groups of the three amino acid residues is ~7.57 Å which is too far for BMDC to reach. The configurations in Figure 4.67 b and d can possibly occur because the distance between R groups of the two relevant amino acid residues (~5.03 Å) is sufficiently short.

Inaddition, the crosslinking could occur between the above mentioned heptapeptide functional groups on two different molecules of the heptapeptide via a molecule of BMDC in a scenario involving a high concentration of the peptide. Because of a lack of funds, the peaks (Figure 4.66) could not be subjected to mass spectrometry.

4.3.2 Lysozyme

Hen egg white lysozyme is a small enzyme (14.4 kDa) that is very basic (isoelectric pH = 11) whose structure and function are well characterized. Lysozyme (3.5 mM) was reacted with BMDC (30 mM, 60 mM and 0.8 M) at pH 6 (0.1 M Na-citrate, pH 6) and 8 (0.1 M Na-phosphate, pH 8) at room temperature for 15 minute (Section 3.2.1.1). Under these conditions, BMDC is expected to react with the free amino groups of the protein. However, depending on pH, BMDC can react with other functional groups such as thiol, hydroxyl, imidazole and carboxylate (Means and Feeney, 1971) and produce both intra- and intermolecularly crosslinked products. At the end of crosslinking reaction, the samples were filtered through a 0.22 μm filter (Amicon) and analysed by SDS-PAGE (14% acrylamide). The results are shown in Figure 4.68. For this gel, the relationship

between R_f and log MW values of various standard proteins is provided in Table 4.13 and Figure 4.69.

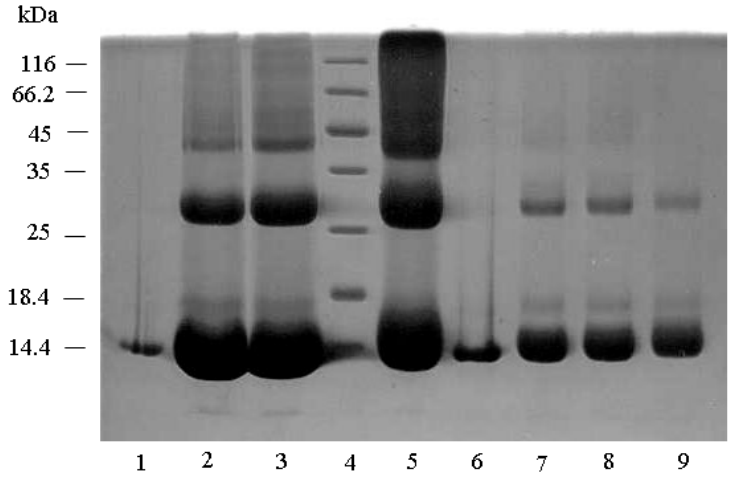

Figure 4.68 SDS-PAGE of (lanes 1-3 and 5) lysozyme crosslinked at pH 6 and (lanes 6-9) pH 8. Lanes 1 and 6: native lysozyme; lanes 2 and 7: lysozyme crosslinked with 30 mM BMDC; lanes 3 and 8: lysozyme crosslinked with 60 mM BMDC; lane 4: protein marker; lanes 5 and 9: lysozyme crosslinked with 0.8 M BMDC.

Table 4.13 Relative mobility (R_f) and log MW of standard proteins for SDS-PAGE gel (Figure 4.68)

Standard protein	MW (kDa)	Log MW	R_f
β-Galactosidase	116	2.06	0.07
Bovine serum albumin	66.2	1.82	0.15
Ovalbumin	45	1.65	0.26
Lactate dehydrogenase	35	1.54	0.36
Restriction endonuclease Bsp 981	25	1.40	0.51
β-Lactoglobulin	18.4	1.26	0.68
Lysozyme	14.4	1.16	0.82

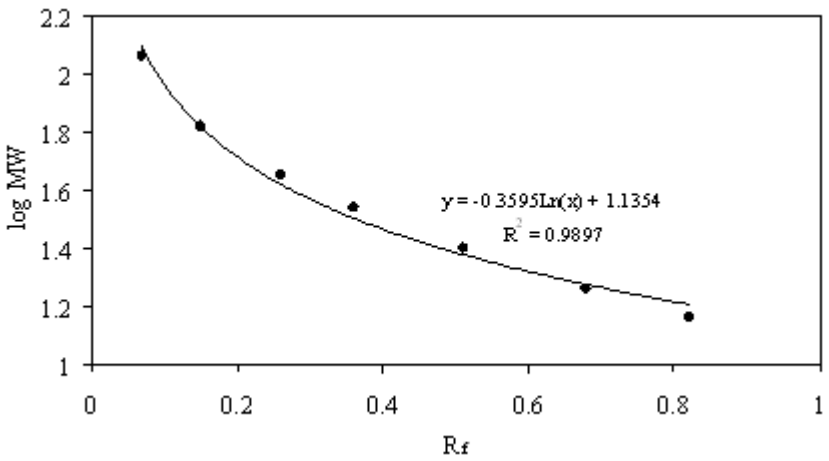

Figure 4.69 Standard curve for molecular weight estimation of lysozyme and its crosslinked products separated by SDS-PAGE.

The electrophoretic patterns of native and crosslinked lysozyme confirmed the formation of crosslinks particularly intermolecular crosslink at all concentrations of BMDC. The products produced by the reaction corresponded to a band (~16.6 kDa, Figure 4.68) with a similar size to that of the native protein (14.4 kDa), bands with approximately double (~26.3 kDa) and triple (~37.2 kDa) the molecular weight of the native lysozyme (Figure 4.68). There were also bands at higher molecular weights that were most likely the larger intermolecularly crosslinked oligomers of lysozyme.

To examine whether the structural features of lysozyme were disrupted as a consequence of the crosslinking treatment, native-PAGE was used to analyse the sample. Thus, 10% polyacrylamide gels were made with no SDS in the gel buffer. Samples were loaded without reduction and the detergent. The developed gel is shown in Figure 4.70. The results (Figure 4.70) show a change in the net charge of the protein molecule after the crosslinking treatment. This can only be due to the covalent attachment of the ionisable BMDC (–NCO) to carboxylate side chains of the enzyme. The characterization of native and modified lysozyme using native PAGE has been previously reported for acetylation and phosphopyridoxylation (Masuda *et al.*, 2005).

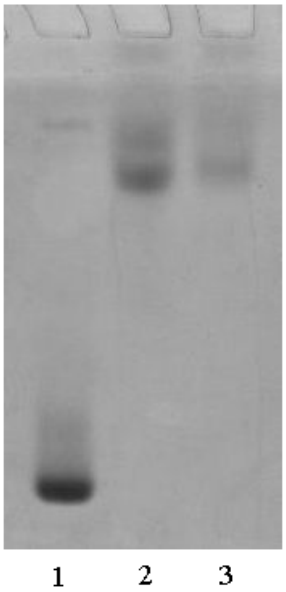

Figure 4.70 Native-PAGE of lysozyme crosslinked at pH 6. Lane 1: native lysozyme; lane 2: lysozyme crosslinked with 30 mM BMDC; lane 3: lysozyme crosslinked with 60 mM BMDC.

All the crosslinked products were analysed by size exclusion chromatography (Superdex G 75 10/300 GL, GE Healthcare) using a flow rate of 0.3 mL/min. The elution profiles were monitored at 280 nm. For native lysozyme, the profile (Figure 4.71) showed one main peak at elution volume of 16.28 mL and a shoulder eluting at 17.82 mL. The elution profile of the crosslinked lysozyme showed three overlaping peaks of 107 kDa, 39 kDa and 18 kDa at elution volumes of 8.92, 11.08 and 12.70 mL, respectively (Figure 4.72). This implied that the crosslinked product was of a higher molecular weight than the native protein. (The calibration of the size exclusion column for lysozyme is shown in Appendix I.)

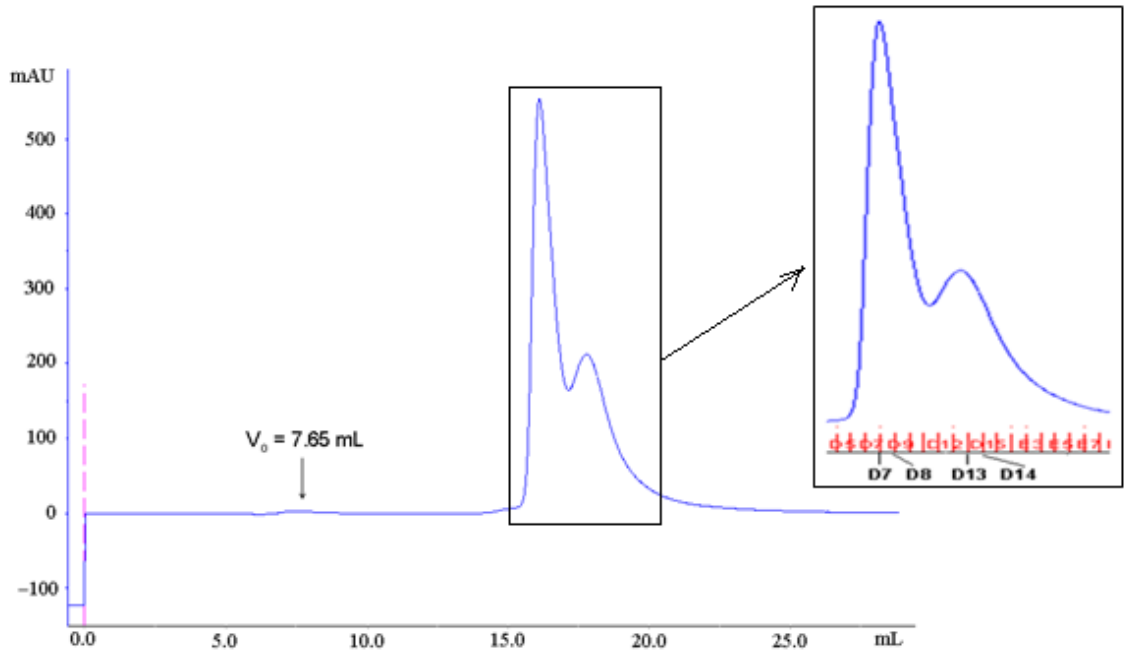

Figure 4.71 Elution profile of native lysozyme in 20 mM phosphate buffer containing 0.15 M NaCl, pH 7, on Superdex G-75 size exclusion column with flow rate of 0.3 mL/min.

The fractions from SEC were then analysed by SDS-PAGE. The gels showed the presence of covalently linked lysozyme molecules in the crosslinked sample (Figure 4.73). The molecular weight of protein bands were estimated using the calibration data shown in Table 4.14, Figure 4.74 and Figure 4.75. For the native protein (Fractions D7 and D8, Figure 4.71), the size of the molecular species (14.4 kDa) in the main peak corresponded to a monomeric lysozyme. The small shoulder also contained a monomer (apparent mass ~14.4 kDa). The SDS gel of the crosslinked lysozyme showed the first peak (Figure 4.73) to be made up of a very high molecular weight species towards the end of the elution. These were the monomeric species of ~16.22-17.38 kDa (Fractions C10-D1), the dimeric species of ~27.5 kDa, the trimer with 44.7 kDa and a higher molecular weight species of ≥ 44.7 kDa.

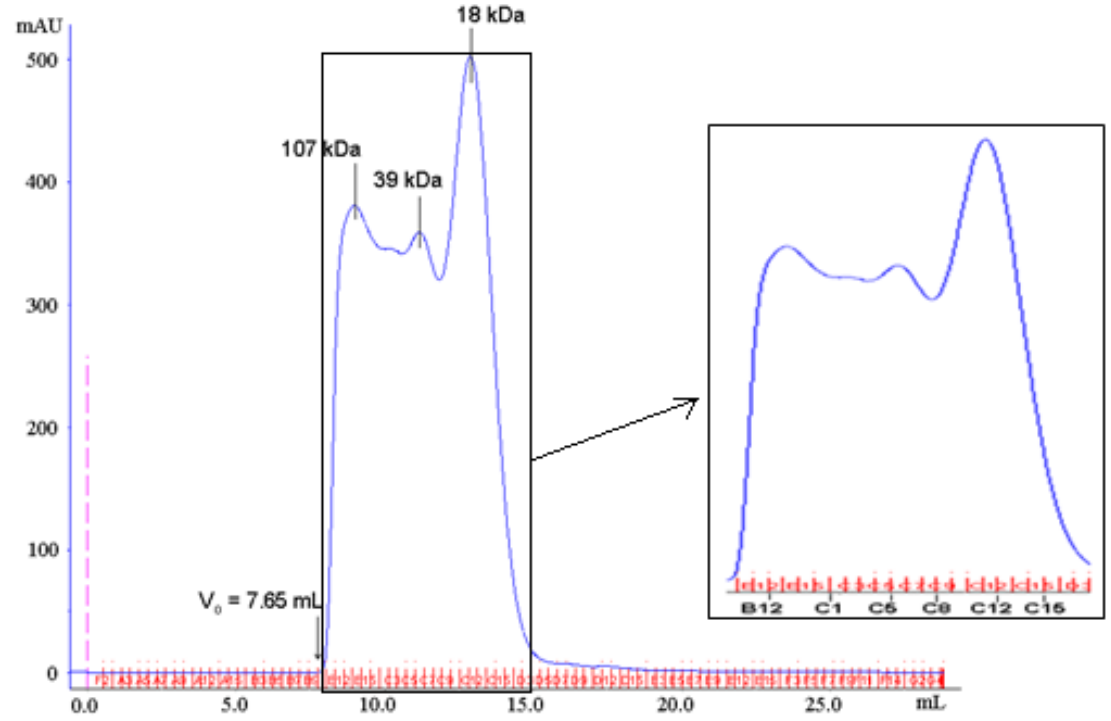

Figure 4.72 Chromatographic separation (Superdex G-75 size exclusion column with flow rate of 0.3 mL/min) of lysozyme (3.5 mM) after crosslinking at pH 6.

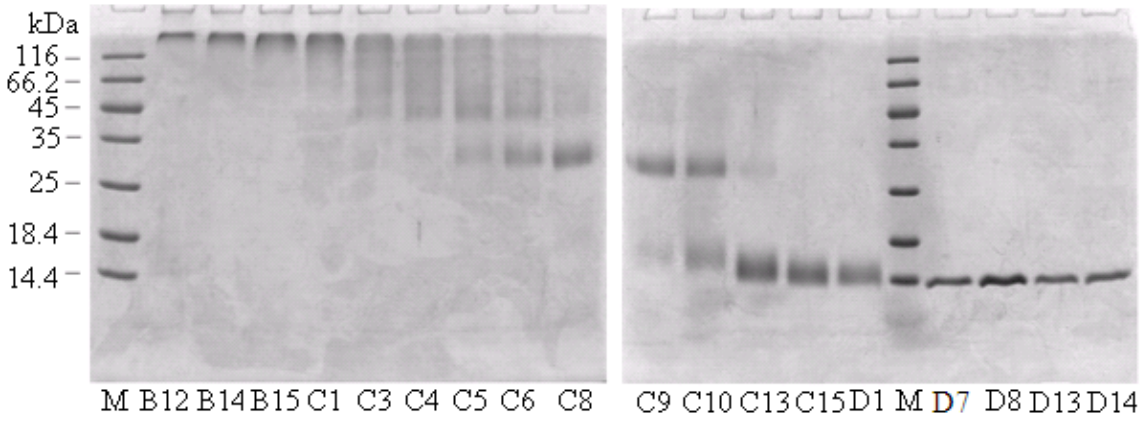

Figure 4.73 SDS-PAGE pattern of crosslinked lysozyme from the selected fractions across the main peak on size exclusion column. Lane M: protein markers; lanes B12-D1: fractions from the elution profile of BMDC crosslinked lysozyme as shown in Figure 4.72; lanes D7-D14 fractions from the elution profile of native lysozyme as shown in Figure 4.71.

Table 4.14 Relative mobility (R_f) and log MW of standard proteins for SDS-PAGE gels (Figure 4.73)

Standard protein	MW (kDa)	Log MW	R_f	
			Gel for M-C8, Figure 4.73	Gel for C9-D14, Figure 4.73
β-Galactosidase	116	2.06	0.08	0.09
Bovine serum albumin	66.2	1.82	0.16	0.17
Ovalbumin	45	1.65	0.26	0.27
Lactate dehydrogenase	35	1.54	0.37	0.37
Restriction endonuclease Bsp 981	25	1.40	0.53	0.54
β-Lactoglobulin	18.4	1.26	0.71	0.71
Lysozyme	14.4	1.16	0.83	0.84

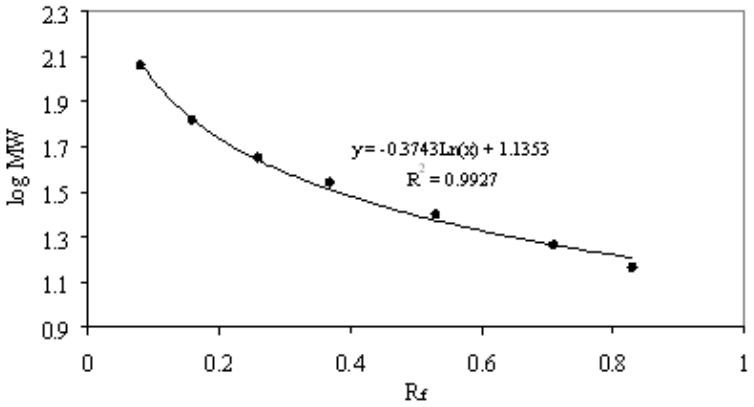

Figure 4.74 Standard curve for molecular weight estimation of crosslinked products of lysozyme analysed by SDS-PAGE (gel for M-C8).

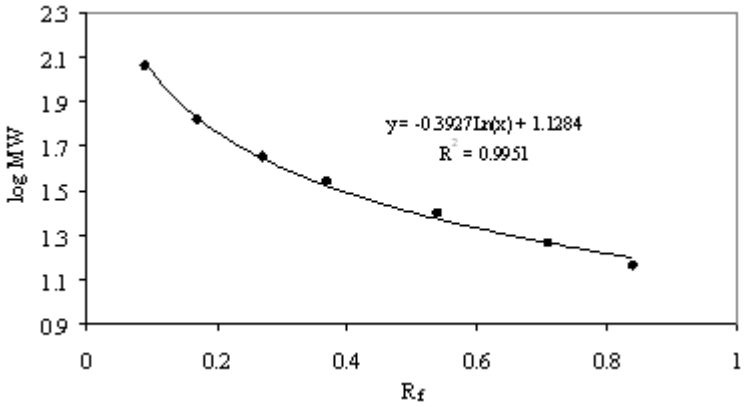

Figure 4.75 Standard curve for molecular weight estimation of lysozyme and its crosslinked products analysed by SDS-PAGE (gel for C9-D14).

Fractions that contained at least one crosslinked lysozyme species were further analysed by RP-HPLC using a Jupiter 5U C18 300 Å column (eluent A: 0.1% TFA;

eluent B; 0.08% TFA in acetonitrile with a flow rate of 1 mL/min). For native lysozyme, the Fraction D8 (Figure 4.71) was also collected for further analysis by RP-HPLC. The RP-HPLC chromatogram is shown in Figure 4.76.

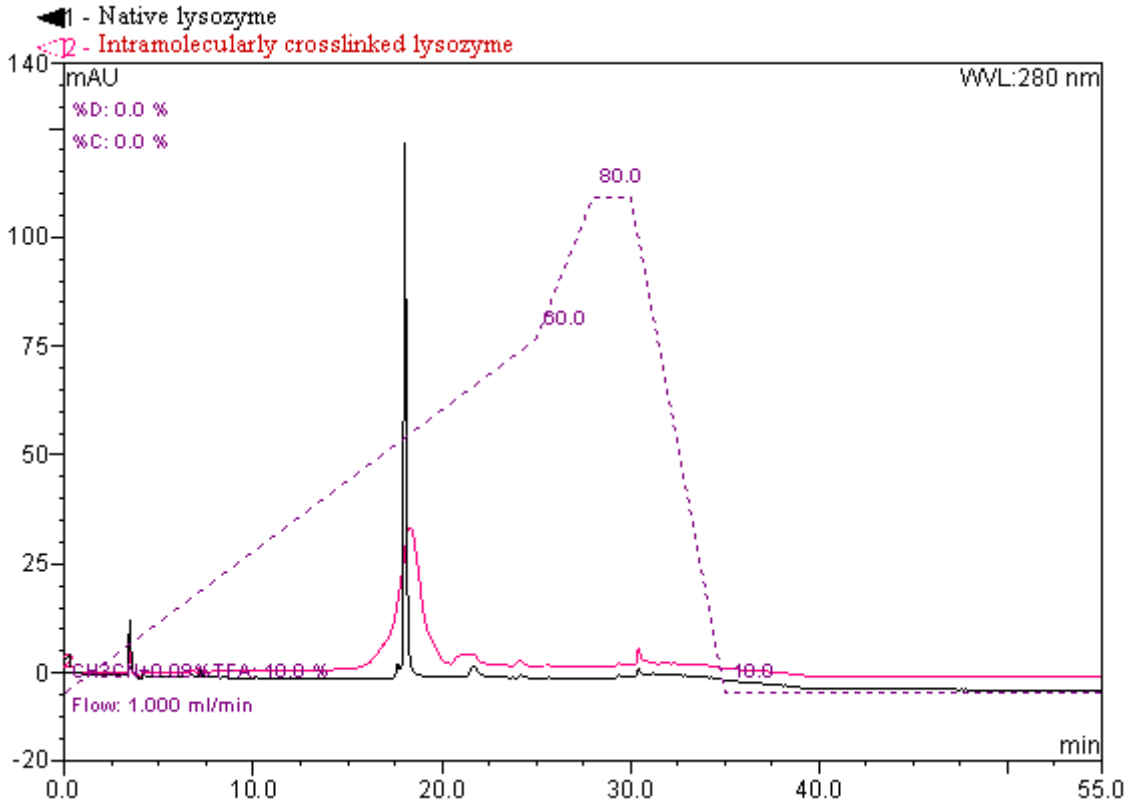

Figure 4.76 RP-HPLC chromatogram of native enzyme and the crosslinked lysozyme (intramolecularly crosslinked lysozyme) on Jupiter 5U C18 300A column with a flow rate of 1 mg/mL.

The HPLC chromatograms of the native and intramolecularly crosslinked lysozyme showed little difference in retention times for the native and the crosslinked enzyme (Figure 4.76). This was unexpected for the large intermolecularly crosslinked species. Possibly the very large molecule got trapped on the column either because of its size, or altered hydrophobicity of the surface. Nevertheless, presence of some intramolecularly crosslinked species was proved. Some difference between the hydrophobicities of the native and crosslinked species would not be surprising in light of the results from the native gel (Figure 4.70).

The fractions corresponding to the main peaks (Figure 4.76) of native and the crosslinked lysozyme from RP-HPLC were collected and freeze dried prior to further analysis by MALDI-TOF MS at the Centre for Protein Research (CPR), Department of

Biochemistry, Otago University, New Zealand. A comparison of the mass spectra of native lysozyme (Figure 4.77) and intramolecularly crosslinked lysozyme (Figure 4.78) showed a difference in their masses. The mass of the intramolecularly crosslinked lysozyme was 16,035.27 Da compared to a mass of 14,310.77 for the native lysozyme. The average mass difference between the two enzyme species was 1,725 Da. This was due to formation of intramolecular crosslinks by BMDC. The average mass of BMDC itself is 140.14180 Da and crosslinking reaction itself causes no change in mass as a proton is lost in the protein but gained by the crosslinker. Therefore, the calculated number of expected crosslinks was 12.31. According to the literature (Section 2.1.4.2.2), the protein functional group which can react with BMDC are the hydroxyl of tyrosine, the carboxylates of glutamic acid and aspartic acid, the amino group of lysine and the imidazole of histidine. In lysozyme (Section 2.3.2.1), there are 48 such groups. The native gel (Figure 4.70) suggested the involvement of mainly the carboxylate groups in crosslinking. Lysozyme contains one aspartic acid residue and two glutamic acid residues as well as the C-terminal carboxylate group. It is not unreasonable to suggest that these may be involved in crosslinking. It is likely that other residues were also involved in the intramolecular crosslinking as the main peak (Figure 4.78) was quite broad suggesting a lot of heterogeneity. A clearer result may have been achieved by using an OrbiTrap analyzer which has a higher resolution (above m/z 100,000) and accuracy than the TOF system that was recommended by the Centre for Protein Research, University of Otago (Downard, 2007).

It is possible in principle to determine the specific sites involved in crosslinking by digesting the crosslinked lysozyme with trypsin, separating the peptides produced by RP-HPLC and then analyzing the fragments by fragmentation mass spectrometry. Native lysozyme, lysozyme that had been intramolecularly crosslinked with BMDC and lysozyme that had been treated with the monofunctional BIC were digested by trypsin at a weight ratio (lysozyme:trypsin) of 100:1 at 37 °C for 4 days. The tryptic digests were subjected to RP-HPLC (Jupiter 5U C18 300 Å Phenomenex). The relevant chromatograms are shown in Figure 4.79. The chromatograms in Figure 4.79 were recorded using detectors set at wavelengths of 214 nm and 280 nm.

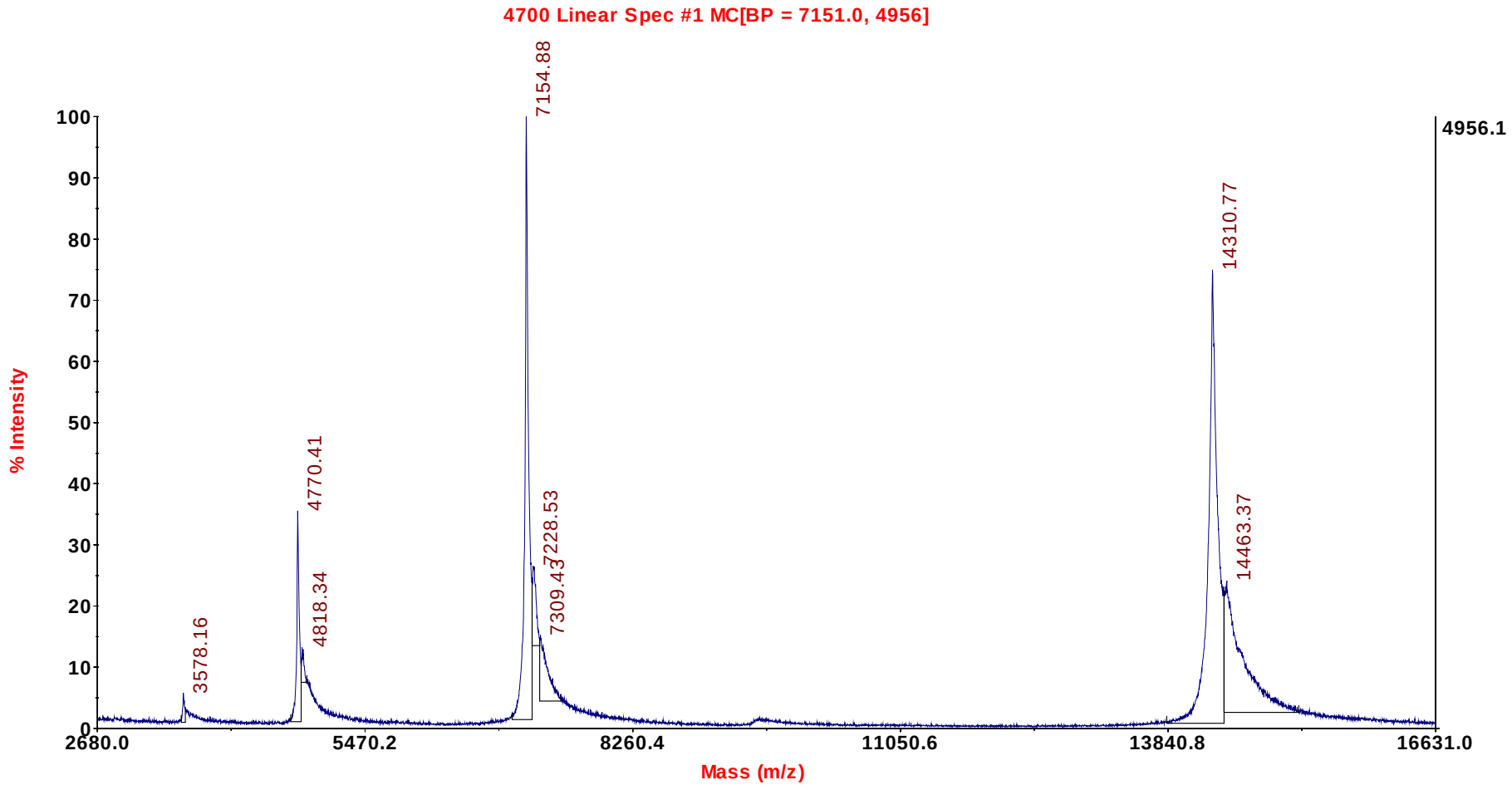

Figure 4.77 Mass spectrum of native lysozyme (MALDI-MS).

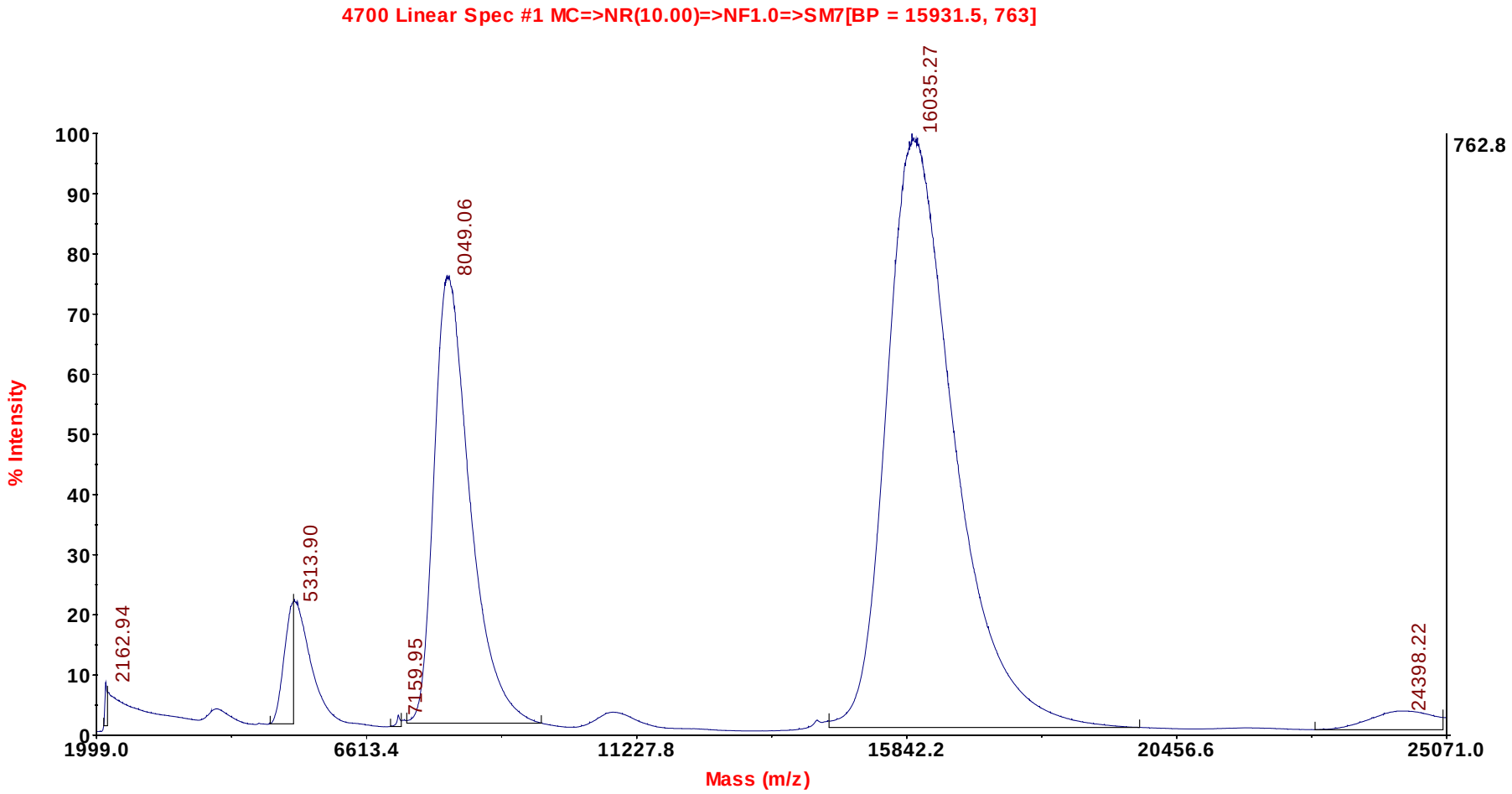

Figure 4.78 Mass spectrum of presumably intramolecularly crosslinked lysozyme by MALDI-MS.

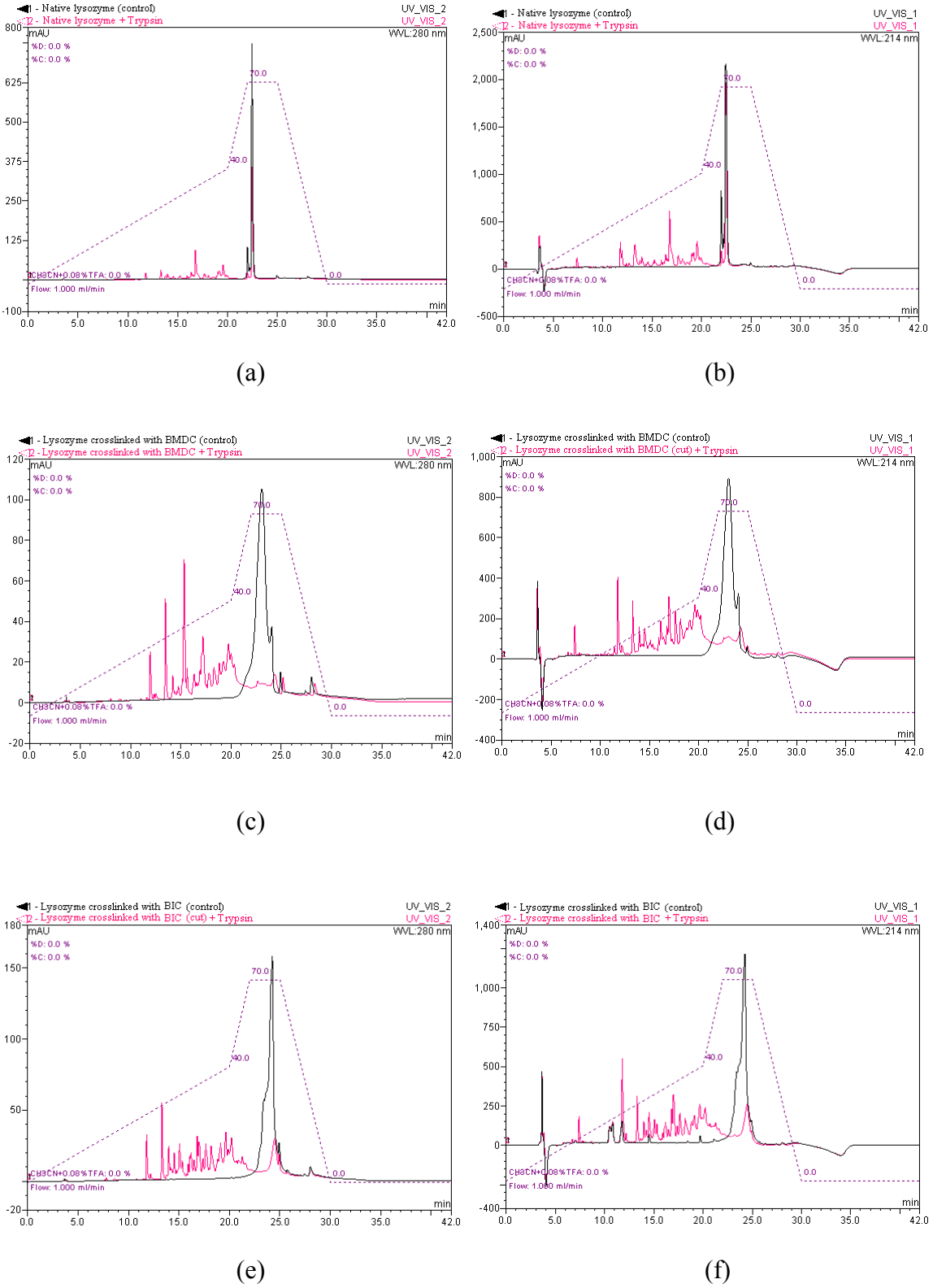

Figure 4.79 RP-HPLC chromatograms (Jupiter 5U C18 300 Å column with a flow rate of 1 mg/mL) of (a, b) native lysozyme, (c, d) lysozyme intramolecularly crosslinked with BMDC and (e, f) lysozyme treated with BIC before and after digestion by trypsin.

RP-HPLC chromatograms of the tryptic digests of native lysozyme, intramolecularly crosslinked lysozyme and lysozyme treated with BIC are compared in Figure 4.80 and Figure 4.81. The data shown were recorded at wavelengths of 214 (Figure 4.80) and 280 nm (Figure 4.81). The peptide pattern from intramolecularly crosslinked lysozyme showed a few more peaks than that from native lysozyme. However the number of observable peaks from the tryptic digestion of intramolecularly crosslinked lysozyme was less than those of lysozyme treated with BIC. This suggested that lysozyme treated with BIC is more susceptible to trypsin than both intramolecularly crosslinked lysozyme and native lysozyme.

Native lysozyme did not seem to be as susceptible to trypsin as intramolecularly crosslinked lysozyme, suggesting that the crosslinking treatment had partially denatured the protein. As reported previously, lysozyme needs to be in its reduced form before it can be efficiently digested with trypsin (Canfield, 1963; Madin *et al.*, 2007). In addition, the evidence proved that no crosslinks were formed through the amino groups of lysine as trypsin would not digest unless a free lysine was available (Metzler *et al.*, 2001). If intramolecular crosslinks had formed through other specific functional groups such as carboxylate groups as illustrated in Figure 4.82, there would have been fewer fragments in the digest of the intramolecularly crosslinked sample compared to the digest of the native protein.

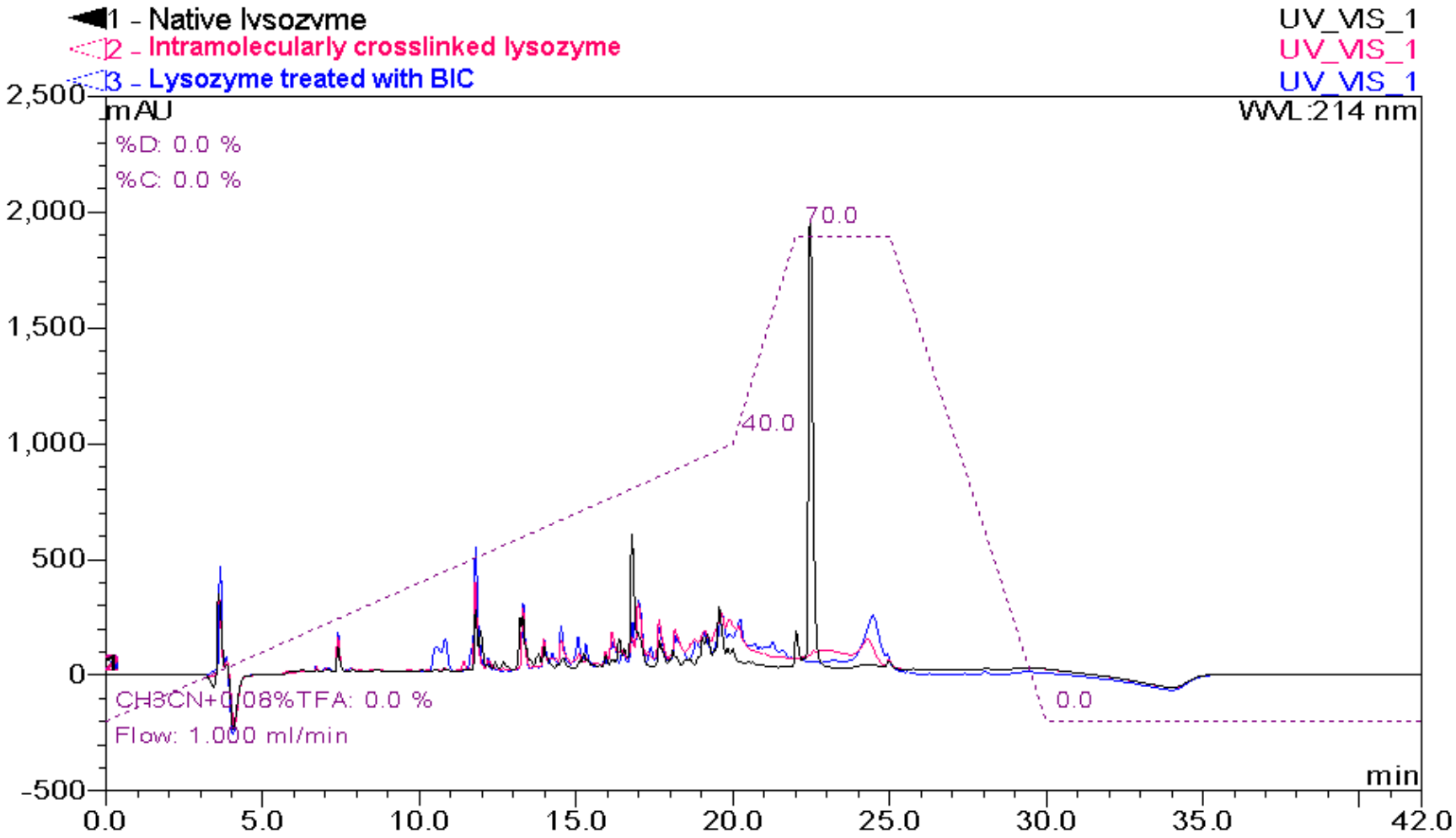

Figure 4.80 RP-HPLC chromatograms of tryptic digests of native lysozyme, intramolecularly crosslinked lysozyme and lysozyme treated with BIC recorded at 214 nm.

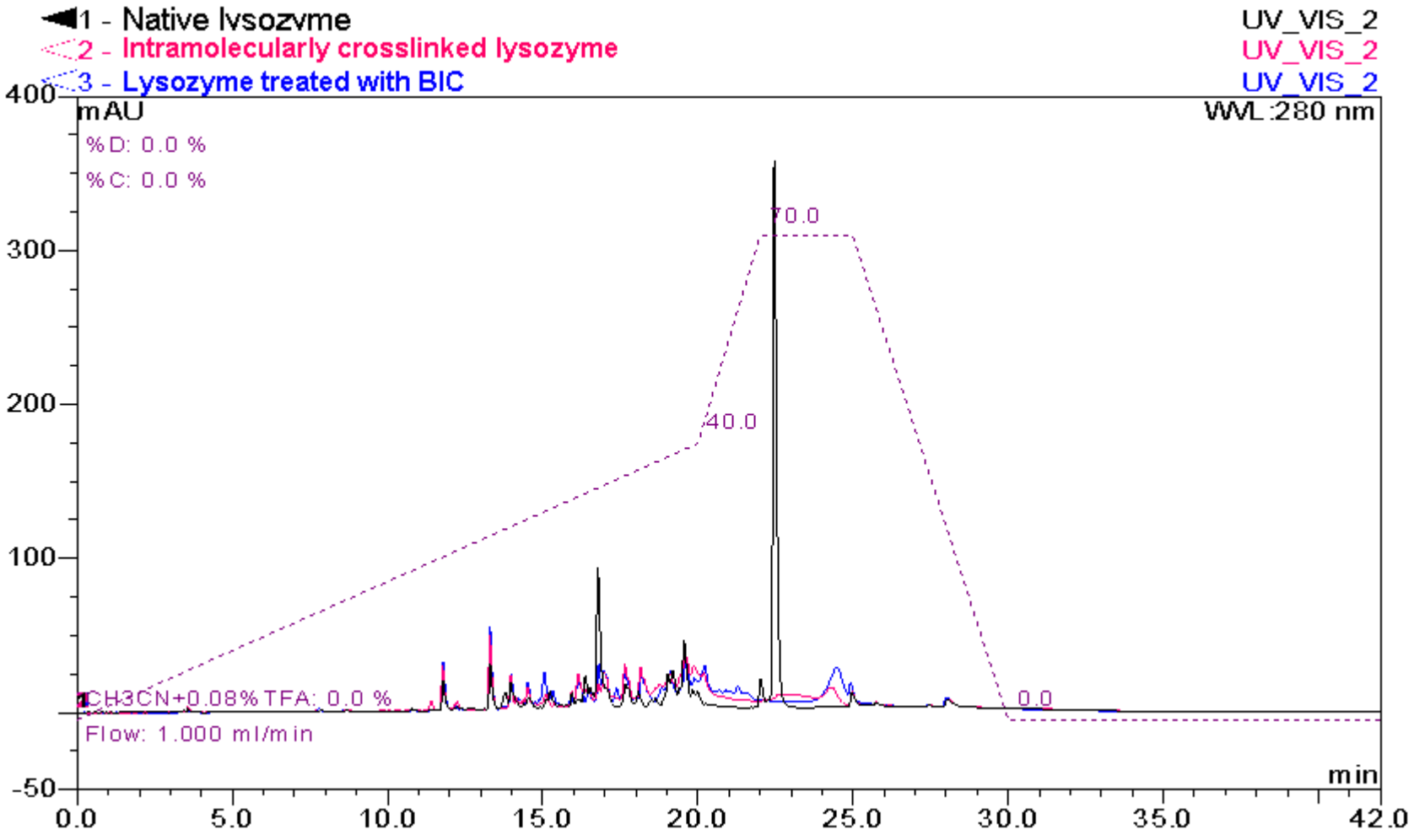

(b)

Figure 4.81 RP-HPLC chromatograms of tryptic digests of native lysozyme, intramolecularly crosslinked lysozyme and lysozyme treated with BIC recorded at 280 nm.

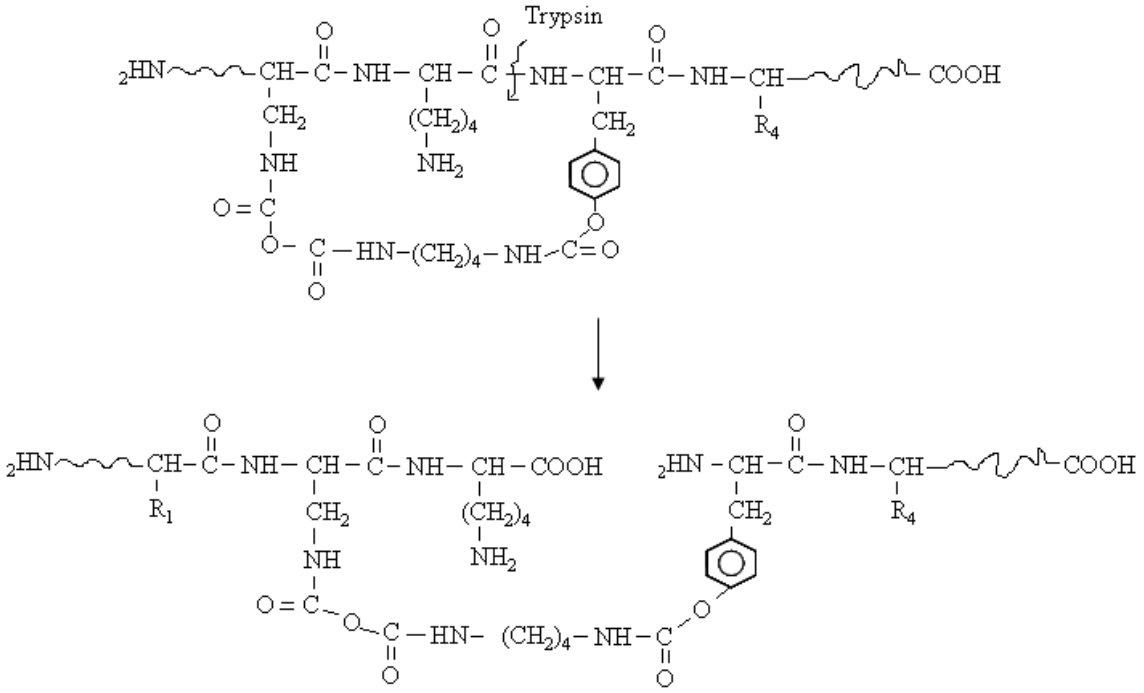

Figure 4.82 The expected product of tryptic digestion scheme for lysozyme intramolecularly crosslinked through carboxylate group and hydroxyl group.

The thermostability of native and intramolecularly crosslinked lysozyme was investigated using circular dichroism spectrometry. Possible changes in secondary structure for both the species were characterized in the far UV region. The spectra of both native and intramolecularly crosslinked lysozyme recorded at a fixed temperature of 25 °C showed a similar pattern (Figure 4.83) that is typical of lysozyme (Greenfield, 2007). The CD spectrometric changes brought about by the chemical modification of lysozyme by N-bromosuccinimide compared to the native lysozyme have been previously reported (Tanaka *et al.*, 1975). In addition, the structural properties of lysozyme determined by CD in water and glycerol solutions have been reported (Knubovets *et al.*, 1999).

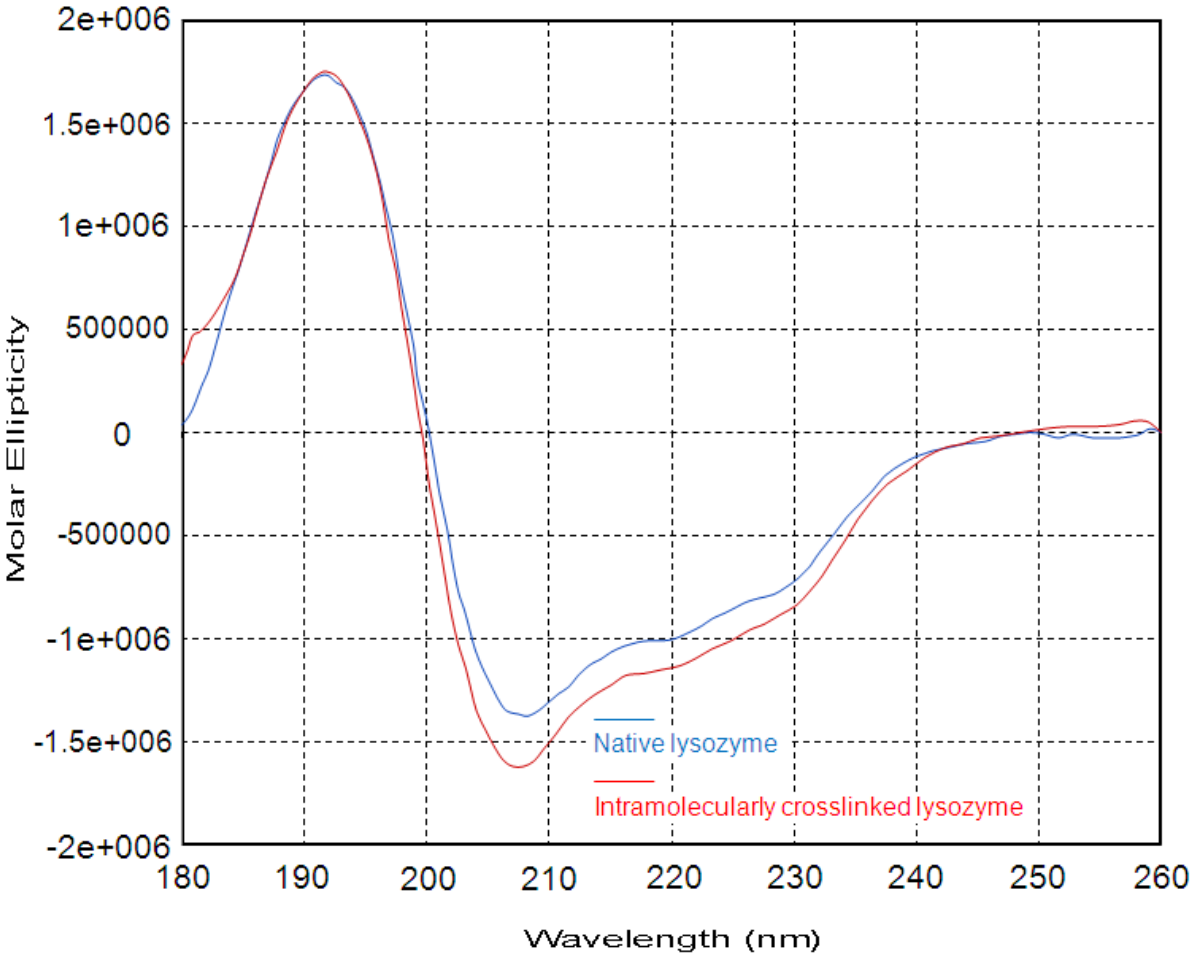

Figure 4.83 CD spectra of native and intramolecularly crosslinked lysozyme in 4 mM sodium phosphate buffer pH 7, 30 mM NaCl. Enzyme solutions were presented at 0.4-0.6 mg/mL and the cell path length was 0.01 cm. Recorded at 25 °C constant temperature.

In this study, circular dichroism was used to follow the thermal stability of native and intramolecularly crosslinked lysozyme. Melting curves of both proteins were followed in the far UV region of the spectrum (Figure 4.84) and suggested that the crosslinked molecule was more stable than the native. The basis of this conclusion was a shift in the maxima from ~207 nm (reported previously for lysozyme by Jasco Inc.) to 202 nm (Figure 4.84 a). Similar use of CD spectra to explore the structural flexibility of intramolecularly crosslinked the extrinsic 33-kDa protein of photosystem II (PSII) has been reported (Enami *et al.*, 1998).

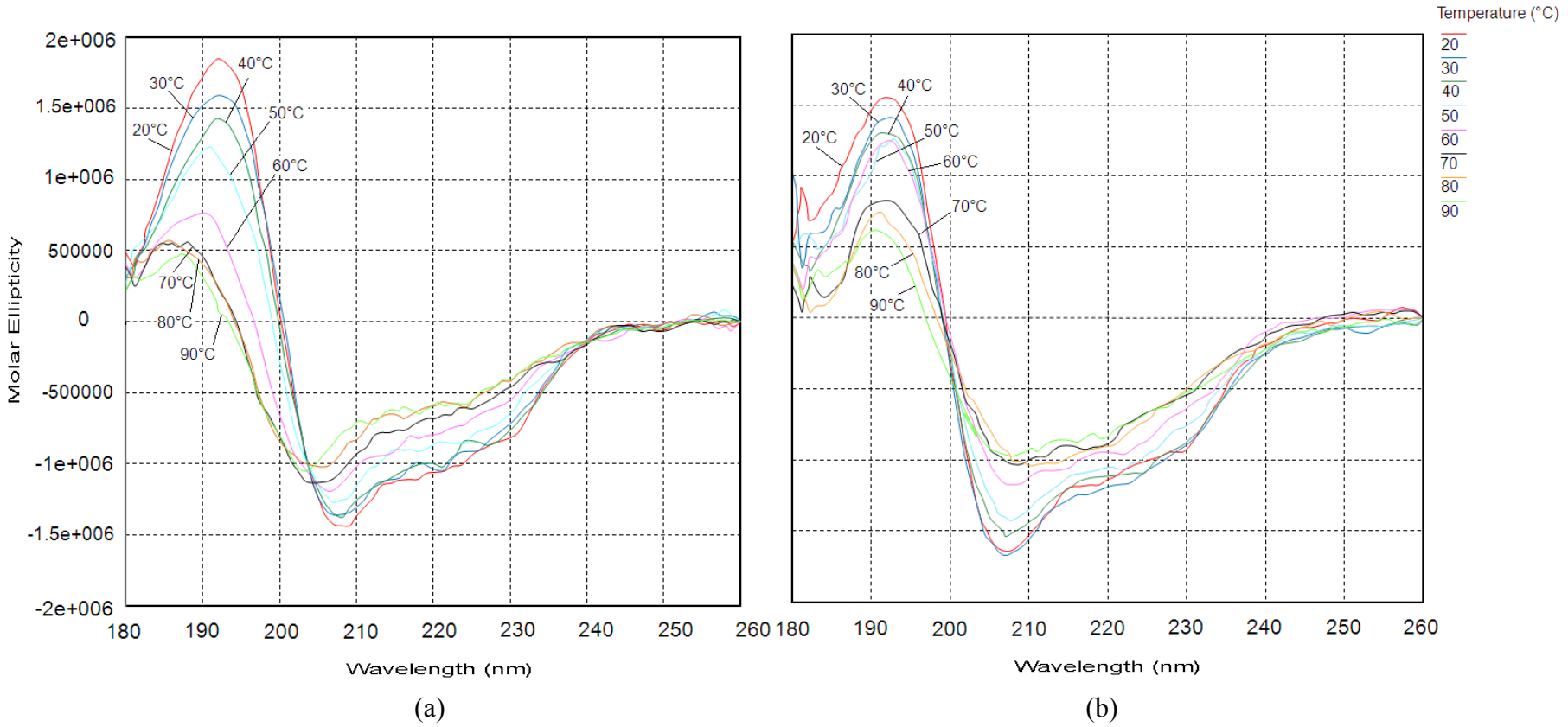

Figure 4.84 Melting curves of (a) native lysozyme and (b) intramolecularly crosslinked lysozyme in 4 mM sodium phosphate buffer, pH 8, with 30 mM NaCl at 20-90 °C. Enzyme solutions were presented at 0.4-0.6 mg/mL and the cell path length was 0.01 cm.

4.3.3 Pepsin

Pepsin, a small acidic enzyme was selected as a simple model for further study of possible crosslinking between mainly the carboxylate groups and BMDC. The crosslinking of pepsin at a high concentration (1.4 mM) with BMDC was carried out (Section 3.2.1.1) and characterized by SDS-PAGE (Figure 4.85). SDS-PAGE (10% acrylamide) of pepsin after crosslinking with various concentration of BMDC at pH 5 was obtained. The developed gel showed protein bands at around ~40.7 kDa for native pepsin (molecular weight estimation using Table 4.15 and Figure 4.86). The intermolecularly cosslinked molecules of ~79.4 kDa and ~112 kDa which are larger than native pepsin were clearly found (Figure 4.85).

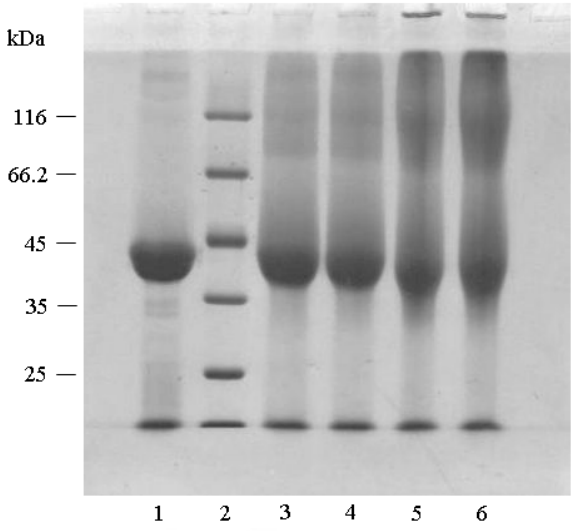

Figure 4.85 SDS-PAGE of pepsin crosslinked with various amount of BMDC at pH 5. Lane 1: native pepsin; lane 2: protein markers; lane 3: pepsin crosslinked with 30 mM BMDC; lane 4: pepsin crosslinked with 60 mM BMDC; lanes 5 and 6: pepsin crosslinked with 0.8 M BMDC.

Table 4.15 Relative mobility (R_f) and log MW of standard proteins for SDS-PAGE gel (Figure 4.85)

Standard protein	MW (kDa)	Log MW	R_f
β-Galactosidase	116	2.06	0.17
Bovine serum albumin	66.2	1.82	0.33
Ovalbumin	45	1.65	0.51
Lactate dehydrogenase	35	1.54	0.66
Restriction endonuclease Bsp 981	25	1.40	0.86

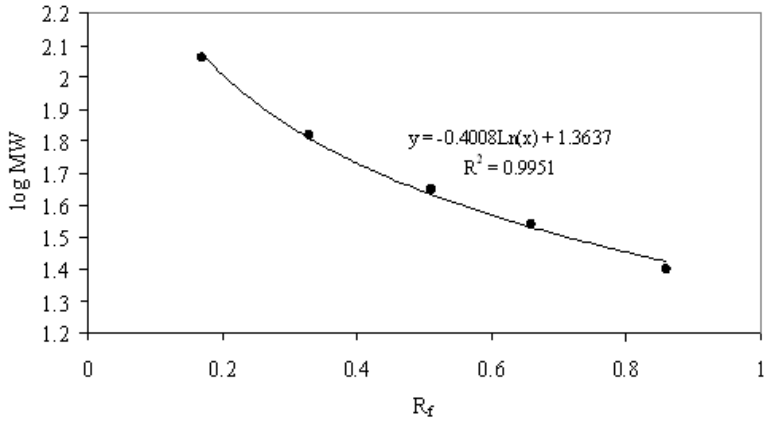

Figure 4.86 Standard curve for molecular weight estimation of pepsin and its crosslinked products separated by SDS-PAGE.

4.3.4 Ovalbumin

Positive evidence for intermolecular crosslinking was seen when ovalbumin was used as a simple glycoprotein model in the crosslinking treatment. The treatment used 1 mM ovalbumin and various concentrations of BMDC (30 mM, 60 mM and 0.8 mM) at pH 7. Ten percent of acrylamide gel was again used in SDS gel electrophoresis to observe native ovalbumin and its crosslinked products. The protein band of native ovalbumin appeared at ~36.3-40.7 kDa (Figure 4.87, molecular weight estimation using Table 4.16 and Figure 4.88). After crosslinking, the ovalbumin protein band occurred at a higher value of molecular weight (~79.4 kDa). This showed that crosslinking, particularly intermolecular crosslinking, likely occurred with this glycoprotein. However, intramolecularly crosslinked species need to be further investigated possibly in a future separate study.

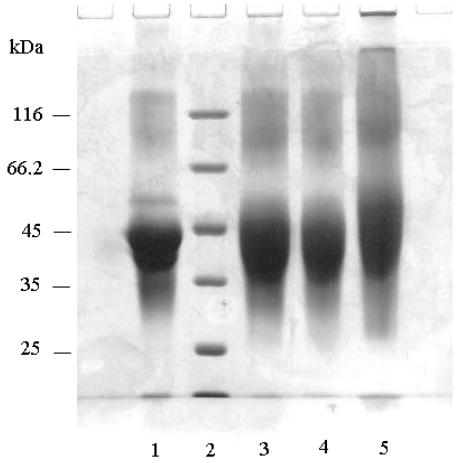

Figure 4.87 SDS-PAGE of ovalbumin crosslinked at pH 7. Lane 1: native ovalbumin; lane 2: protein markers; lane 3: ovalbumin crosslinked with 30 mM BMDC; lane 4: ovalbumin crosslinked with 60 mM BMDC; lane 5: ovalbumin crosslinked with 0.8 M BMDC.

Table 4.16 Relative mobility (R_f) and log MW of standard proteins for SDS-PAGE gel (Figure 4.87)

Standard protein	MW (kDa)	Log MW	R_f
β-Galactosidase	116	2.06	0.17
Bovine serum albumin	66.2	1.82	0.33
Ovalbumin	45	1.65	0.51
Lactate dehydrogenase	35	1.54	0.66
Restriction endonuclease Bsp 981	25	1.40	0.86

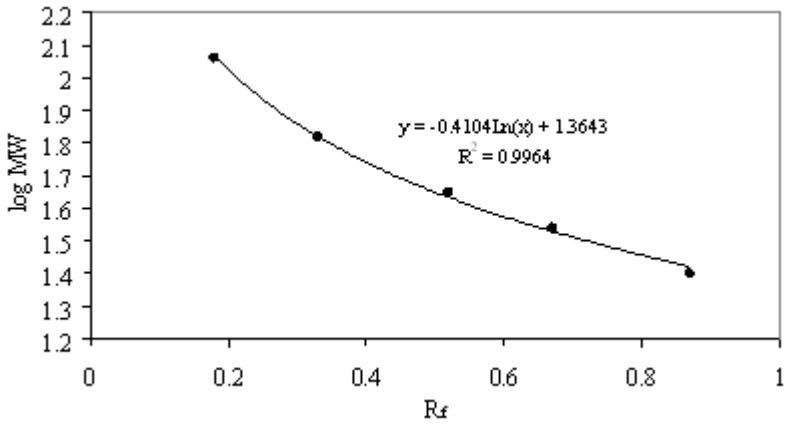

Figure 4.88 Standard curve for molecular weight estimation of pepsin and its crosslinked products separated by SDS-PAGE.

CHAPTER 5

Overall Discussion and Conclusions

5.1 Overall discussion

This study focused on intramolecular crosslinking as a method of improving the thermal stability of enzymes. The enzymes selected for the study were: 1. α-amylase of *Aspergillus oryzae*; 2. β-galactosidase of *Aspergillus oryzae*; and 3. invertase from *Saccharomyces cerevisiae*. The rationale for using these enzymes was previously mentioned (Section 2.3). A variety of homobifunctional crosslinking reagents were used, as identified in Section 3.1.2.

The control enzyme for intramolecular crosslinking and the intramolecularly crosslinked invertase had nearly the same molecular weights by SEC (Figure 4.37). This is expected as intramolecular crosslinking of the enzyme with BMDC is not expected to increase the molecular weight sufficiently for it to be distinguished from the control by SEC. However, as expected, the molecular weight (or elution volume) of native invertase by SEC was similar to the molecular weights for the control enzyme for intramolecular crosslinking and the intramolecularly crosslinked invertase (Figure 4.37). For invertase reacted with the monofunctional crosslinker BIC under both intramolecular crosslinking condition (i.e. an enzyme concentration of 0.9 μM), and the intermolecular crosslinking condition, there was evidence for BIC altering the surface hydrophobicity of invertase, as discussed in Section 4.2.1, and therefore the elution profiles (b) and (e) in Figure 4.37 cannot be reasonably compared with the other profiles in the same figure. Other than the above, no other conclusive inference could be drawn for the SEC measurements.

Dynamic light scattering (DLS) provides a direct measure of the hydrodynamic diameter of a protein molecule, but translating the measured hydrodynamic diameter to a molecular weight is inexact, particularly for the case of some of the protein used in this work. For example, crosslinker molecules linked by a single end to the surface of a protein can potentially significantly affect the hydrodynamic diameter without actually affecting the molecular weight, or the true diameter, very much. Thus, the results of DLS

analysis (Table 4.6) made sense, but there were anomalies. For example, consistent with expectations, the z-average values for native invertase, the control for intramolecular crosslinking and the control for intermolecular crosslinking, were comparable (Table 4.6). Similarly, and consistent with expectaions, the intermolecularly crosslinked invertase had a substantially higher z-average than the intramolecularly crosslinked enzyme (Table 4.6). As example of an explicable anomaly, the intramolecularly crosslinked invertase had a significantly higher hydrodynamic diameter than the native invertase (Table 4.6), possibly because of loose unreacted ends of the crosslinker.

Just as SEC cannot distinguish between small changes in protein molecular weight, for example the difference between the native enzyme and the same enzyme with multiple small crosslinker molecules bound to it, SEC-MALLS cannot make such distinctions either. Therefore, the SEC-MALLS molecular weights (Table 4.7) for the native enzyme and the intramolecularly crosslinked enzyme are essentially the same and consistent with expectations. However, the SEC-MALLS molecular weight for intermolecular crosslinked enzyme is distinctly greater than for the native protein (Table 4.7), as expected.

Compared to SEC, SEC-MALLS and DLS, SDS-PAGE is perhaps a much more sensitive and less ambiguous technique for detecting molecular weights. SDS-PAGE provided clear evidence that intermolecular crosslinking of invertase did occur (Section 4.2.4), but no conclusive evidence for intramolecular crosslinking.

CD spectra (Figure 4.60) confirmed that none of the crosslinking treatments affected the secondary structure of invertase. This was of course a required attribute of the crosslinking reaction, as damage to the secondary structure of the protein would have inactivated it.

5.2 Conclusions

The principal conclusions are as follows:

1. The three native enzymes were confirmed to have the pH optimum in the 4-5 pH range, showing them to be acidic enzymes. The temperature for optimal activity of these enzymes was confirmed to be in the 50-60 °C range. All the enzymes were stable at between pH 5 and 6 and at temperatures of <50-55 °C. The inactivation energy for the thermal denaturation of these enzymes was in the range of 167-544

kJ/mol, as is typical for enzymes. These characteristics provided a baseline for the evaluation of the effects of various crosslinking treatments on enzyme stability.

2. Crosslinking treatments were carried out at room temperature and pH 5-8. The treatment time was either 15 minutes, or 1 hour, depending on the crosslinking reagents investigated. Enzyme concentrations were selected to favour either the intermolecular crosslinking, or both the inter- and intramolecular crosslinking. Intermolecularly crosslinked enzyme was used as a control for comparison with the products of intramolecular crosslinking treatments. The effects of the type of the crosslinking reagent and its chain length on possible enzyme stabilization were examined. Diisocyanates, diimidoesters and diamines were the three classes of the crosslinking reagents used. (A total of 15 reagents as noted in Section 3.1.2.) None of the stabilizing treatments improved the thermal stability of α-amylase and β-galactosidase. Only invertase could be stabilized by crosslinking treatments.
3. Optimal stabilization of invertase occurred at an enzyme concentration of 0.9 μM treated with 20-30 mM of diisocyanate reagent at pH 6, 15 minutes, and room temperature. Efficacy of thermostabilization depended on the chain length of the reagent used for the crosslinking. Among diisocyanate crosslinker series (1,4-diisocyanatobutane (BMDC); 1,6-diisocyanotohexane (HMDC); 1,8-diisocyanatooctane (OMDC)), BMDC and HMDC proved to be the most effective stabilizing crosslinkers compared to controls. Crosslinking using BMDC and HMDC provided a mild, rapid and highly effective method of stabilizing invertase against thermal inactivation. Stabilized invertase retained more than 60% of its initial activity after 90 min of incubation at 60 °C in sodium citrate buffer, pH 6, whereas over the same period the native enzyme lost more than 80% of its initial activity. The activation energy of denaturation of the crosslinked invertase was higher at 517 kJ/mol compared to 372 kJ/mol for native invertase. Stabilization by crosslinking did affect the enzyme's Michaelis-Menten kinetic parameters K_m and v_{max}, to reduce activity relative to the control.
4. Invertase stabilized by crosslinking treatments (item 3) was examined in various ways in attempts to elucidate the nature of the crosslinking, whether intermolecular or intramolecular. Characterization of the stabilized enzyme was carried out relative to controls, using SEC, SDS-PAGE, DLS, SEC-MALLS and CD. Depending on the crosslinking treatment used, evidence was found for both

inter- and intramolecular crosslinking. A clear interpretation of results was impeded by the large carbohydrate moiety of invertase, a glycoprotein. Thus, SEC and SDS-PAGE analyses were repeated after the crosslinked invertase had been deglycosylated with PNGase F. Native invertase was also deglycosylated as a control. Data showed that crosslinking treatments affected the efficacy of deglycosylation, implying that the carbohydrate moiety was being affected by crosslinking treatments. It is possible that crosslinking may reduce the accessibility of PNGase F to point of attachment of glycan chains, thus reducing the efficiency of deglycosylation. Various crosslinking treatments were shown to affect the molecular weight of the treated invertase in ways that were consistant with expectations.

5. Crosslinking treatments with BMDC appeared to alter at least slightly the tertiary structure of invertase, as suggested directly by CD data and indirectly by the kinetic observations (item 3).
6. Studies with two small model peptides revealed that under intramolecular crosslinking conditions BMDC could react with either C-terminal carboxylate groups or with the amino groups of lysine residue. Reaction with BMDC was shown to affect the protein/peptide hydrophobicity and net charge.
7. Using a different model enzyme (lysozyme) at a relatively high concentration (3.5 mM), BMDC was shown to react with the enzyme both intra- and intermolecularly. Once again, crosslinking with BMDC affected the net charge and hydrophobicity of the treated enzyme.
8. The tryptic digestion patterns suggested that BMDC may not be crosslinked via the amino groups of lysine residues in lysozyme. Crosslinking treatment with BMDC appeared to somehow partially denature lysozyme as this treatment made the enzyme more susceptible to trypsin digestion relative to control.
9. BMDC crosslinking treatments of lysozyme reduced its susceptibility to thermally induced unfolding, as revealed by melting curves measured at 20-90 °C.

Overall, under appropriate treatment protocols, an enhanced thermal stabilization of invertase by crosslinking with diisocyanates, particularly 1,4-diisocyanatobutane (BMDC) was clearly demonstrated. Cause of stabilization was demonstrated to be the intramolecular crosslinking of enzyme by the bifunctional reagent. Using model enzymes,

BMDC crosslinking treatments were shown to improve the resistance to thermally induced unfolding of the polypeptide chain.

CHAPTER 6

Recommendations

The intramolecular crosslinking strategy demonstrated here for stabilizing enzymes, proved successful for invertase but not for the other enzymes. Further work is therefore required to attempt to make the intramolecular crosslinking strategy broadly applicable. Any further work should address some of the following aspects:

1. A detailed molecular investigation of why exactly some of the other enzymes could not be stabilized by certain intramolecular crosslinking treatments: did such treatments somehow block the active site, or did the crosslinking reagents used react with certain enzyme functional groups at the active site. Such knowledge would be useful in any future selection of appropriate crosslinking reagents for achieving the stabilization objective.
2. The reactive groups on some of the bifunctional crosslinking reagents have the potential to react with several different functional groups (e.g. hydroxyl, carboxylate, thiol, amino) on the amino acid residue of an enzyme. Using synthetic peptides with only a specific type of reactive group available, crosslinking reagents with different functional groups need to be evaluated for crosslinking ability and for identifying the specific pH at which reaction with a certain type of enzyme functional groups is favored compared to reaction with the other potential reactive groups.
3. With suitable crosslinking reagents that do not react with functional groups at the active site of the enzyme, there is a need to identify the maximum enzyme concentration in the reaction mixture to predominantly obtain the intramolecularly crosslinked enzyme and not intermolecular crosslinking.
4. The optimal extent of crosslinking needs to be clarified. A certain amount of flexibility within an enzyme molecule is known to be required for facilitating binding of the substrate(s) at the active site and the unbinding of the products. Thus the extent of crosslinking (e.g. the number of crosslinks per molecule and the tautness of those links (determined by chain length of the crosslinker) need to

be such as to prevent thermally induced unfolding of the enzyme while not restricting the intramolecular movement that is necessary for activity.

5. It would be useful to examine the crosslinking treatments with the active site of the enzyme temporarily blocked (e.g. by using a high concentration of substrate) so that the active site functional groups have a reduced opportunity to react with a crosslinker. This should be possible if for example the substrate (or substrate analog) does not have reactive groups that could bind to the crosslinker.
6. For glycosylated enzymes, a deglycosylation treatment may be useful prior to crosslinking treatments for thermal stabilization. This of course would be feasible only if the carbohydrate moiety has no effect on biological function, as is the case for many enzymes.

Studies with simple synthetic model peptides can be useful, but they are expensive to do because of the cost of suitable synthetic peptides. Moreover, studies with model peptides can prove conclusively whether a certain crosslinking reaction occurs, they cannot prove the effect of the crosslinking treatment on the secondary (and higher level) structures of an enzyme, or the impact of crosslinking on stability and biological activity. Therefore, studies with enzymes themselves would always be necessary.

References

Albergina, L. (2003) Protein Engineering in Industrial Biotechnology, Taylor & Francis, London.

Amersham Biosciences (2002) Gel Filtration: Principles and Methods, Uppsala.

Amylase Research Society of Japan. (1988) Handbook of Amylases and Related Enzymes: their Sources, Isolation Methods, Properties and Applications. Pergamon Press, Oxford.

Anderson, W. M. and Fisher, R. R. (1981) The Subunit Structure of Bovine Heart Mitochondrial Transhydrogenase. Biochim. Biophys. Acta, Bioenerg., 635, 194-199.

Andrews, P. (1965) The Gel-Filtration Behaviour of Proteins Related to their Molecular Weights over a Wide Range. Biochem. J., 96, 595-606.

Aranyi, P., Radanyi, C., Renoir, M., Devin, J. and Baulieu, E. E. (1988) Covalent Stabilization of the Nontransformed Chick Oviduct Cytosol Progesterone Receptor by Chemical Crosslinking. Biochemistry, 27, 1330-1336.

Baret, J. L. (1987) Large-Scale Production and Application of Immobilized Lactase. Methods Enzymol., 136, 411-423.

Baylor, K. J. (1996) Biochemical Studies on the Toxicity of Isocyanates. Ph.D. Thesis, University College Cork, Ireland.

Beeley, J. G. (1985) Glycoprotein and Proteoglycan Techniques. Elsevier, Amsterdam.

Berka, R. M. and Cherry, J. R. (2006) Enzyme Biotechnology. In Ratledge, C. and Kristiansen, B. (eds), Basic Biotechnology, Cambridge University Press, Cambridge.

Bernfeld, P. (1955) Amylases, α and β. Methods Enzymol., 1, 149-158.

Besson, C., Favre-Bonvin, G., O'Fagain, C. and Wallach, J. (1995) Chemical Derivatives of *Pseudomonas aeruginosa* Elastase Showing Increased Stability. Enzyme Microb. Technol., 17, 877-881.

Bilen, J. and Bakir, U. (1998) The Effect of Crosslinking in Thermal Inactivation of Cellulases. Progress Biotechnol. 15, 151-156.

Boyer, R. F. (1993) Modern Experimental Biochemistry. Benjamin/Cummings Pub. Co., Redwood City, California.

Brew, K., Shaper, J. H., Olsen, K. W., Trayer, I. P. and Hill, R. L. (1975) Cross-Linking of the Components of Lactose Synthetase with Dimethylpimelimidate. J. Biol. Chem., 250, 1434-1444.

Brown, W. E., Green, A. H., Cedel, T. E. and Cairns, J. (1987) Biochemistry of Protein-Isocyanate Interactions: A Comparison of the Effects of Aryl vs. Alkyl Isocyanates. Environ. Health Perspect., 72, 5-11.

Canfield, R. E. (1963) Peptides Derived from Tryptic Digestion of Egg White Lysozyme. J. Biol. Chem., 238, 2691-2697.

Cantarella, L., Alfani, F. and Cantarella, M. (2003) β-D-Fructofuranoside Fructohydrolase. In Whitaker, J.R., Voragen, A.G.J., et al. (eds), Handbook of Food Enzymology, Marcel Dekker, Basel.

Cao, L. (2005) Carrier-Bound Immobilized Enzymes: Principles, Applications and Design. Wiley-VCH, Weinheim.

Chapman, J. R. (1996) Mass Spectrometry: Ionization Methods and Instrumentation. In Chapman, J.R. (ed), Protein and Peptide Analysis by Mass Spectrometry. Methods in Molecular Biology, 61. Humana Press, Totowa, N.J.

Chisti, Y. (1999) Mass Transfer. In Flickinger, M.C. and Drew, S.W. (eds), Encyclopedia of Bioprocess Technology: Fermentation, Biocatalysis, and Bioseparation, Wiley, New York.

Chu, F. K. (1986) Requirements of Cleavage of High Mannose Oligosaccharides in Glycoproteins by Peptide N-Glycosidase F. J. Biol. Chem., 261, 172-177.

Chu, F. K., Trimble, R. B. and Maley, F. (1978) The Effect of Carbohydrate Depletion on the Properties of Yeast External Invertase. J. Biol. Chem., 253, 8691-8693.

Chu, F. K., Watorek, W. and Maley, F. (1983) Factors Affecting the Oligomeric Structure of Yeast External Invertase. Arch. Biochem. Biophys., 223, 543-555.

Cook, P. F. and Cleland, W. W. (2007) Enzyme Kinetics and Mechanism. Garland Science, New York.

Cornish-Bowden, A. (2004) Fundamentals of Enzyme Kinetics. Portland Press, London.

Copeland, R. A. (2000) Enzymes: A Practical Introduction to Structure, Mechanism, and Data Analysis. Wiley, Chichester.

Davies, G. E. and Stark, G. R. (1970) Use of Dimethyl Suberimidate, a Cross-Linking Reagent, in Studying the Subunit Structure of Oligomeric Proteins. Proc. Nat. Acad. Sci. U.S.A., 66, 651-656.

Davis, B. J. (1964) Disc Electrophoresis II Method and Application to Human Serum Proteins. Ann. N. Y. Acad. Sci., 121, 404-427.

Delano, W. L. (2002) The PyMOL Molecular Graphics System, Delano Scientific, San Carlos, USA, http://www.pymol.org.

Dodson, M. S. (2000) Dimethyl Suberimidate Cross-Linking of Oligo(dT) to DNA-Binding Proteins. Bioconjugate Chem., 11, 876-879.

Dubey, A. K., Bisaria, V. S., Mukhopadhyay, S. N. and Ghose, T. K. (1989) Stabilization of Restriction Endonuclease *Bam* HI by Cross-Linking Reagents. Biotechnol. Bioeng., 33, 1311-1316.

Dutton, A., Adams, M. and Singer, S. J. (1966) Bifunctional Imidoesters as Cross-Linking Reagents. Biochem. Biophys. Res. Commun., 23, 730-739.

Enami, I., Kamo, M., Ohta, H., Takahashi, S., Miura, T., Kusayanagi, M., Tanabe, S., Kamei, A., Motoki, A., Hirano, M., Tomo, T. and Satoh, K. (1998) Intramolecular Cross-linking of the Extrinsic 33-kDa Protein Leads to Loss of Oxygen Evolution but Not Its Ability of Binding to Photosystem II and Stabilization of the Manganese Cluster. J. Biol. Chem., 273, 4629-4634.

Erickson, H. P. (2004) Protein-Protein Interactions: Chapter 1. Protein Structure-Size and Shape at the nm Level. Revised Jan, 2004, from: http://www.cellbio.duke.edu/faculty/Erickson/pdf's/Prot-p%20biophys%20Ch1.pdf.

Fasman, G. D. (1989) Practical Handbook of Biochemistry and Molecular Biology. CRC Press, Boca Raton, Fla.

Fernandez-Lafuente, R., Rosell, C. M., Rodriguez, V. and Guisan, J. M. (1995) Strategies for Enzyme Stabilization by Intramolecular Crosslinking with Bifunctional Reagents. Enzyme Microb. Technol., 17, 517-523.

Fokunang, C. N., Watson, K. A., Purvis, A. and Tembe-Fokunang, E. A. (2005) Crystallization and Structural Studies of Lysozyme from Hen Egg White, using Vapour Diffusion Technique. Biotechnol., 4 (4), 341-346.

Foster, R. L. and Thomson, A. R. (1973) Modification of Pig Heart Lactate Dehydrogenase: A Derivative Possessing Enhanced Thermal Stability. Biochim. Biophys. Acta, Enzymol., 321, 409-412.

Fowler, A. V. and Zabin, I. (1983) Purification, Structure, and Properties of Hybrid Beta-Galactosidase Proteins. J. Biol. Chem., 258, 14354-14358.

Fraguas, L. F., Bolón, V. and Viera, F. B. (1999). Affinity Immobilisation of β-Galactosidase from *Aspergillus oryzae* on Lectin-Based Adsorbents [Electronic Version] from http://plab.ku.dk/tcbh/Lectins13/Fraguas/paper.htm.

Freeman, A. (1984) Biotech Workshop: Understanding Enzyme Stabilization. Trends Biotechnol., 2, 147-148.

Frevert, J. and Ballou, C. E. (1982) Yeast Invertase Polymorphism is Correlated with Variable States of Oligosaccharide Chain Phosphorylation. Proc. Nat. Acad. Sci. U.S.A., 79, 6147-6150.

Freytag, J. W., Dickinson, J. C. and Tseng, S. Y. (1984) A Highly Sensitive Affinity-Column-Mediated Immunometric Assay, as Exemplified by Dioxin. Clin. Chem., 30, 417-420.

Gascón, S., Neumann, N. P. and Lampen, J. O. (1968) Comparative Study of the Properties of the Purified Internal and External Invertases from Yeast. J. Biol. Chem., 243, 1573-1577.

Gavrilescu, M. and Chisti, Y. (2005) Biotechnology--a Sustainable Alternative for Chemical Industry. Biotechnol. Adv., 23, 471-499.

George, H., McMahan, J., Bowler, K. and Elliott, M. (1969) Stabilization of Lactate and Malate Dehydrogenase by Organic Solvents. Biochim. Biophys. Acta, Enzymol., 191, 466-468.

Gerhartz, W. (1990) Enzymes in Industry: Production and Applications. VCH, Weinheim.

Gianfreda, L. and Scarfi, M. R. (1991) Enzyme Stabilization: State of the Art. Mol. Cell. Biochem., 100, 97-128.

Goldberg, M. E. (1969) Tertiary Structure of *Escherichia coli* [Beta]--Galactosidase. J. Mol. Biol., 46, 441-446.

Goldstein, L. (1976) Kinetic Behavior of Immobilized Enzyme Systems. Methods Enzymol., 44, 397-443.

Govardhan, C. P. (1999) Crosslinking of Enzymes for Improved Stability and Performance. Curr. Opin. Biotechnol., 10, 331-335.

Greenfield, N. J. (2007) Using Circular Dichroism Spectra to Estimate Protein Secondary Structure. Nat. Protoc., 1, 2876-2890.

Gupta, M. N. (1993) Thermostability of Enzymes. Springer, Berlin.

Habibi, A. E., Khajeh, K., Naderi-Manesh, H., Ranjbar, B. and Nemat-Gorgani, M. (2006) Thermostabilization of *Bacillus amyloliquefaciens* [Alpha]-Amylase by Chemical Cross-Linking. J. Biotechnol., 123, 434-442.

Han, K.-K., Richard, C. and Delacourte, A. (1984) Chemical Cross-Links of Proteins by Using Bifunctional Reagents. Int. J. Biochem., 16, 129-145.

Hartman, F. C. and Wold, F. (1967) Cross-Linking of Bovine Pancreatic Ribonuclease A with Dimethyl Adipimidate. Biochemistry, 6, 2439-2448.

Hash, J. H. (1974) Crystallographic Studies of Lysozyme and its Interactions with Inhibitors and Substrates. In Osserman, E.F., Canfield, R.E., et al. (eds), Lysozyme, Academic Press, New York.

Hora, J. (1973) Stabilization of *Bacillus subtilis* [Alpha]-Amylase by Amino Group Acylation. Biochim. Biophys. Acta, Protein Struct., 310, 264-267.

Hubbard, M. J. and McHugh, N. J. (1996) Mitochondrial ATP Synthase F1-[Beta]-Subunit is a Calcium-Binding Protein. FEBS Lett., 391, 323-329.

Huber, R. E., Gupta, M. N. and Khare, S. K. (1994) The Active Site and Mechanism of the [Beta]-Galactosidase from *Escherichia coli*. Int. J. Biochem., 26, 309-318.

Hughes, C. R. (1983) Glycoproteins. Chapman and Hall, London.

Hunter, M. J. and Ludwig, M. L. (1962) The Reaction of Imidoesters with Proteins and Related Small Molecules. J. Am. Chem. Soc., 84, 3491-3504.

Hunter, M. J. and Ludwig, M. L. (1972) Amidination. Methods Enzymol., 25, 585-596.

Isemura, T. and Fujita, S. (1957a) Physico-Chemical Studies on Taka-Amylase a: II. On the Compactness and the Hydration of the Molecule. J. Biochem., 44, 797-805.

Isemura, T. and Fujita, S. (1957b) Physicochemical Studies on Taka-Amylase a: I. Size and Shape Determination by the Measurement of Sedimentation Constant, Diffusion Coefficient, and Viscosity. J. Biochem., 44, 443-451.

Iyer, P. V. and Ananthanarayan, L. (2008) Enzyme Stability and Stabilization--Aqueous and Non-aqueous Environment. Process Biochem., 43, 1019-1032.

Janecek, Š. (1993) Strategies for Obtaining Stable Enzymes. Process Biochem., 28, 435-445.

Janecek, Š. and Baláz, Š. (1992) [Alpha]-Amylases and Approaches Leading to their Enhanced Stability. FEBS Lett., 304, 1-3.

Jasco Inc. (2009) Thermal Denaturation of Hen-Egg Lysozyme with Concurrent CD and Fluorescence Detection. CD Application Note 01-03, Jasco, Inc., 2009, from://www.jascoinc.com/Libraries/Product_Spec_Sheets/CD_01_03.sflb.ashx.

Jose, S. (2008) World Market for Industrial Enzymes to Exceed $2.9 Billon by 2012, According to a New Report by Global Industry Analysts, Inc. California (PRWEB), Revised November 11, 2008, from: http://www.prweb.com/releases/industrial_enzymes/carbohydrases_proteases/prweb1569084.htm.

Jumel, K., Fiebrig, I. and Harding, S. E. (1996) Rapid Size Distribution and Purity Analysis of Gastric Mucus Glycoproteins by Size Exclusion Chromatography/Multi Angle Laser Light Scattering. Int. J. Biol. Macromol., 18, 133-139.

Kaplan, Ö. and Bakir, U. (1998) The Effect of Chemical Crosslinking of Invertase with Dimethyl Suberimidate on its pH Stability. World J. Microbiol. Biotechnol., 14, 277-280.

Kaplan, Ö., Bakir, U. and Erarslan, A. (1997) Thermal Inactivation of Native and Crosslinked Invertases. Biotechnology Tech., 11, 621-623.

Kazan, D., Ertan, H. and Erarslan, A. (1996) Stabilization of Penicillin G Acylase against pH by Chemical Cross-linking. Process Biochem., 31, 135-140.

Kelly, S. M., Jess, T. J. and Price, N. C. (2005) How to Study Proteins by Circular Dichroism. Biochim. Biophys. Acta, Proteins Proteomics, 1751, 119-139.

Kern, G., Schulke, N., Schmid, F. X. and Jaenicke, R. (1992) Stability, Quaternary Structure, and Folding of Internal, External, and Core-Glycosylated Invertase from Yeast. Protein Sci., 1, 120-131.

Khajeh, K., Ranjbar, B., Naderi-Manesh, H., Ebrahim Habibi, A. and Nemat-Gorgani, M. (2001a) Chemical Modification of Bacterial [Alpha]-Amylases: Changes in Tertiary Structures and the Effect of Additional Calcium. Biochim. Biophys. Acta, Protein Struct. Mol. Enzymol., 1548, 229-237.

Khajeh, K., Naderi-Manesh, H., Ranjbar, B., Moosavi-Movahedi, A. A. and Nemat-Gorgani, M. (2001b) Chemical Modification of Lysine Residues in Bacillus [Alpha]-amylases: Effect on Activity and Stability. Enzyme Microb. Technol., 28, 543-549.

Khajeh, K., Shokri, M. M., Asghari, S. M., Moradian, F., Ghasemi, A., Sadeghi, M., Ranjbar, B., Hosseinkhani, S., Gharavi, S. and Naderi-Manesh, H. (2006) Acidic and Proteolytic Digestion of [Alpha]-Amylases from *Bacillus licheniformis* and *Bacillus amyloliquefaciens*: Stability and Flexibility Analysis. Enzyme Microb. Technol., 38, 422-428.

Klemes, Y. and Citri, N. (1979) Catalytic and Conformational Properties of Cross-Linked Derivatives of Penicillinase. Biochim. Biophys. Acta, Enzymol., 567, 401-409.

Klibanov, A. M. (1983) Stabilization of Enzymes against Thermal Inactivation. In Laskin, A.I. (ed), Adv. Appl. Microbiol. Academic Press, New York.

Knubovets, T., Osterhout, J. J., Connolly, P. J. and Klibanov, A. M. (1999) Structure, Thermostability, and Conformational Flexibility of Hen Egg-White Lysozyme Dissolved in Glycerol. Proc. Nat. Acad. Sci. U.S.A., 96, 1262-1267.

Kuby, S. A. and Lardy, H. A. (1953) Purification and Kinetics of β-D-Galactosidase from *Escherichia coli*, Strain K-12[1,2]. J. Am. Chem. Soc., 75, 890-896.

Kuriki, T. and Imanaka, T. (1999) The Concept of the [Alpha]-Amylase Family: Structural Similarity and Common Catalytic Mechanism. J. Biosci. Bioeng., 87, 557-565.

Laemmli, U. K. (1970) Cleavage of Structural Proteins during the Assembly of the Head of Bacteriophage T4. Nature, 227, 680-685.

Lee, J. Y. and Park, T. H. (2002) Enzymatic *in vitro* Glycosylation Using Peptide-N-Glycosidase F. Enzyme Microb. Technol., 30, 716-720.

Lehle, L., Cohen, R. E. and Ballou, C. E. (1979) Carbohydrate Structure of Yeast Invertase. Demonstration of a Form with only Core Oligosaccharides and a Form with Completed Polysaccharide Chains. J. Biol. Chem., 254, 12209-12218.

Lehninger, A. L., Nelson, D. L. and Cox, M. M. (1993) Principles of Biochemistry. Worth Publishers, New York.

Lewis, J. C., Snell, N. S., Hirschmann, D. J. and Fraenkel-Conrat, H. (1950) Amino Acid Composition of Egg Proteins. J. Biol. Chem., 186, 23-35.

Li, S., Xing, D. and Li, J. (2004) Dynamic Light Scattering Application to Study Protein Interactions in Electrolyte Solutions. J. Biol. Phys., 30, 313-324.

Liese, A., Seelbach, K. and Wandrey, C. (2000) Industrial Biotransformations. Wiley-VCH, Weinheim.

Lundblad, R. L. (2005) Chemical Reagents for Protein Modification. CRC Press, Boca Raton, FL.

Maarel, M. J. E. C. v. d., Veen, B. v. d., Uitdehaag, J. C. M., Leemhuis, H. and Dijkhuizen, L. (2002) Properties and Applications of Starch-Converting Enzymes of the [Alpha]-Amylase Family. J. Biotechnol., 94, 137-155.

MacGregor, E. A. (1988) Alpha-Amylase Structure and Activity. J. Protein Chem., 7 (4), 399-415.

MacGregor, E. A. (1993) Relationships between Structure and Activity in the Alpha-Amylase Family of Starch-Metabolizing Enzymes. Starch-Starke, 45 (7), 232-237.

MacGregor, E. A., Janecek, Š. and Svensson, B. (2001) Relationship of Sequence and Structure to Specificity in the [Alpha]-Amylase Family of Enzymes. Biochim. Biophys. Acta, Protein Struct. Mol. Enzymol., 1546, 1-20.

Madin, K., Hermann, S., Kirr, C., Schmitt, D. and Koch, T. (2007) Enzymatic Protein Digest for Mass-spectrometric Analysis. Biochemica, 3, 23-25.

Mahoney, R. R. (2003) β-Galactosidase. In Whitaker, J.R., Voragen, A.G.J., et al. (eds), Handbook of Food Enzymology, Marcel Dekker, Basel.

Malvern Instruments Ltd. (2004) Zetasizer Nano Series: User Manual, Worcestershire.

Marangoni, A. G. (2003) Enzyme Kinetics: A Modern Approach. Wiley, New Jersey.

Marini, M. A. and Martin, C. J. (1971) Chymotrypsin Catalysis in the Presence of Formaldehyde. Eur. J. Biochem., 19, 153-161.

Martinek, K. and Torchilin, V. P. (1988) Stabilization of Enzymes by Intramolecular Cross-Linking Using Bifunctional Reagents. Methods Enzymol., 137, 615-626.

Masuda, T., Ide, N. and Kitabatake, N. (2005) Effects of Chemical Modification of Lysine Residues on the Sweetness of Lysozyme. Chem. Senses, 30, 253-264.

Matsuura, Y., Kusunoki, M., Harada, W. and Kakudo, M. (1984) Structure and Possible Catalytic Residues of Taka-Amylase A. J. Biol. Chem., 95, 697-702.

Matthews, B. W. (2005) The Structure of *E. coli* Beta-Galactosidase. C. R. Biol., 328, 549-556.

McKelvy, J. F. and Lee, Y. C. (1969) Microheterogeneity of the Carbohydrate Group of *Aspergillus oryzae* [alpha]-Amylase. Arch. Biochem. Biophys., 132, 99-110.

Means, G. E. and Feeney, R. E. (1971) Chemical Modification of Proteins. Holden-Day, San Francisco.

Mega, T. and Matsushima, Y. (1979) Comparative Studies of Three Exo-[beta]-Glycosidases of *Aspergillus oryzae*. J. Biochem., 85, 335-341.

Metzler, D. E., Metzler, C. M. and Sauke, D. J. (2001) Biochemistry: the Chemical Reactions of Living Cells. Harcourt Academic Press, San Diego.

Meyer, V. (2004) Practical High-Performance Liquid Chromatography. Wiley, Chichester.

Michielsen, E. C. H. J., Diris, J. H. C., Hackeng, C. M., Wodzig, W. K. W. H. and Dieijen-Visser, M. P. V. (2005) Highly Sensitive Immunoprecipitation Method for Extracting and Concentrating Low-Abundance Proteins from Human Serum. Clin. Chem., 51, 222-224.

Minotani, N., Sekiguchi, T., Bautista, J. G. and Nosoh, Y. (1979) Basis of Thermostability on Pig Heart Lactate Dehydrogenase Treated with O-Methylisourea. Biochim. Biophys. Acta, Protein Struct., 581, 334-341.

Moreno, F., Ochoa, A. G., Gascón, S. and Villanueva, J. R. (1975) Molecular Forms of Yeast Invertase. Eur. J. Biochem., 50, 571-579.

Moreno, S., Sanchez, Y. and Rodriguez, L. (1990) Purification and Characterization of the Invertase from *Schizosaccharomyces pombe*. Biochem. J., 267, 697-702.

Moritz, R. L. and Simpson, R. J. (2005) Liquid-Based Free-Flow Electrophoresis-Reversed-Phase HPLC: a Proteomic Tool. Nat. Methods, 2, 863-873.

Myrbäck, K. (1957) Studies on Yeast Invertase. Soluble and Insoluble Invertase (Saccharase) of Baker's Yeast. Arch. Biochem. Biophys., 69, 138-148.

Nakao, Y., Kozutsumi, Y., Funakoshi, I., Kawasaki, T., Yamashina, I., Mutsaers, J. H. G. M., Van Halbeek, H. and Vliegenthart, J. F. G. (1987) Structures of Oligosaccharides on [beta]-Galactosidase from *Aspergillus oryzae*. J. Biochem., 102, 171-179.

Neumann, N. P. and Lampen, J. O. (1967) Purification and Properties of Yeast Invertase. Biochemistry, 6, 468-475.

Neumann, N. P. and Lampen, J. O. (1969) Glycoprotein Structure of Yeast Invertase. Biochemistry, 8, 3552-3556.

Niehaus, W. G., Jr. and Wold, F. (1970) Cross-Linking of Erythrocyte Membranes with Dimethyl Adipimidate. Biochim. Biophys Acta, Biomembr., 196, 170-175.

Nisbet, A. D., Saundry, R. H., Moir, A. J. G., Fothergill, L. A. and Fothergill, J. E. (1981) The Complete Amino-Acid Sequence of Hen Ovalbumin. Eur. J. Biochem., 115, 335-345.

Nowak, D. E., Tian, B. and Brasier, A. R. (2005) Two-step Cross-linking Method for Identification of NF-kappaB Gene Network by Chromatin Immunoprecipitation. Biotechniques, 39, 715-725.

Ó'Fágáin, C. (1995) Understanding and Increasing Protein Stability. Biochim. Biophys. Acta, Protein Struct. Mol. Enzymol., 1252, 1-14.

Ó'Fágáin, C. (2003) Enzyme Stabilization--Recent Experimental Progress. Enzyme Microb. Technol., 33, 137-149.

Ohara, O. and Takahashi, S. (1980) Analysis of Adipimidate-Crosslinked Lysine. Anal. Biochem., 107, 314-317.

Ohnishi, M. and Hatano, H. (1970) Chemical Modification of Bacterial [Alpha]-Amylase by Monoiodoacetate. Biochim. Biophys. Acta, Enzymol., 220, 350-353.

Oliva, A., Llabrés, M. and Fariña, J. B. (2004) Applications of Multi-Angle Laser Light-Scattering Detection in the Analysis of Peptides and Proteins. Current Drug Discovery Technologies, 1 (3), 229-242.

Ono, K., Nozaki, M. and Hayaishi, O. (1970) Purification and Some Properties of Protocatechuate 4,5-dioxygenase. Biochim. Biophys. Acta, Enzymol., 220, 224-238.

Ornstein, L. (1964) Disc Electrophoresis, 1, Background and Theory. Ann. N. Y. Acad. Sci., 121, 321-349.

Ota, H., Yamahara, K. and Kuboi, R. (1998) Stabilization of Enzyme by Using Hydrophobic Ligands. J. Chem. Eng. Jpn., 31, 118-122.

Ozawa, H. (1967) Bridging Reagent for Protein: I. The Reaction of Diisocyanates with Lysine and Enzyme Proteins. J. Biochem., 62, 419-423.

Panesar, P. S., Panesar, R., Ram, S. S., Kennedy, J. F. and Kumar, H. (2006) Microbial Production, Immobilization and Applications of Beta-D-galactosidase. J. Chem. Technol. Biotechnol., 81, 530-543.

Papageorgiou, G. C. and Lagoyanni, T. (1983) Effects of Chaotropic Electrolytes on the Structure and Electronic Excitation Coupling of Glutaraldehyde- and Diimido Ester-Cross-Linked Phycobilisomes. Biochim. Biophys. Acta, Bioenerg., 724, 323-332.

Patel, V., Saunders, G. and Bucke, C. (1997) N-Deglycosylation of Fructosyltransferase and Invertase from *Fusarium oxysporum* decreases Stability but has Little Effect on Kinetics and Synthetic Specificity. Biotechnol. Lett., 19, 75-77.

Phillips, D. C. (1974) Crystallographic Studies of Lysozyme and its Interactions with Inhibitors and Substrates. In Osserman, E.F., Canfield, R.E., et al. (eds), Lysozyme. Academic Press, New York.

Plummer, D. T. (1987) An Introduction to Practical Biochemistry. McGraw-Hill, New York.

Poltorak, O. M., Chukhrai, E. S., Pilipenko, O. S., Atyaksheva, L. F. and Beregalov, A. E. (2007) A Comparative Study of the Structure and Properties of Beta-Galactosidases. Russ. J. Phys. Chem., 81, 808-812.

Pont, J. J. H. H. M. D. (1979) Reversible Inactivation of (Na^+ + K^+)-ATPase by use of a Cleavable Bifunctional Reagent. Biochim. Biophys. Acta, Enzymol., 567, 247-256.

Rajan, M. (2004) Enzymes for Industrial Applications. Business Communications Co., Inc.

Rajput, Y. S. and Gupta, M. N. (1987) Reaction of Trypsin with some Crosslinking Reagents. Enzyme Microb. Technol., 9, 161-163.

Ram, J. S., Terminiello, L., Bier, M. and Nord, F. F. (1954) On the Mechanism of Enzyme Action. LVIII. Acetyltrypsin, a Stable Trypsin Derivative. Arch. Biochem. Biophys., 52, 464-477.

Raviyan, P., Tang, J. and Rasco, B. A. (2003) Thermal Stability of α-Amylase from *Aspergillus oryzae* Entrapped in Polyacrylamide Gel. J. Agric. Food Chem., 51, 5462-5466.

Rehm, H. (2006) Protein Biochemistry and Proteomics. Elsevier/Academic Press, Amsterdam.

Reiner, R., Siebeneick, H. U., Christensen, I. and Döring, H. (1977a) Chemical Modification of Enzymes II. Conformational Stability of Cross-Linked Bovine Pancreatic Ribonuclease. J. Mol. Catal., 2, 119-128.

Reiner, R., Siebeneick, H. U., Christensen, I. and Döring, H. (1977b) Chemical Modification of Enzymes III. Cross-Linked [Alpha]-Chymotrypsin. J. Mol. Catal., 2, 335-349.

Renobales, M. d., Welch, W. and Jr. (1980) Chemical Cross-Linking Stabilizes the Enzymic Activity and Quaternary Structure of Formyltetrahydrofolate Synthetase. J. Biol. Chem., 255, 10460-10463.

Richmond, M. L., Gray, J. I. and Stine, C. M. (1981) Beta-Galactosidase: Review of Recent Research Related to Technological Application, Nutritional Concerns, and Immobilization. J. Dairy Sci., 64, 1759-1771.

Riordan, J. F. and Bier, M. (1959) On the Mechanism of Enzyme Action. No. LXIX. The Influence of Chemical Modification on the Trypsin-Formaldehyde Reaction. Arch. Biochem. Biophys., 83, 327-336.

Rouf, S. A., Moo-Young, M. and Chisti, Y. (1996) Tissue-Type Plasminogen Activator: Characteristics, Applications and Production Technology. Biotechnol. Adv., 14, 239-266.

Ryan, O., Smyth, M. R. and Fágáin, C. Ó. (1994) Thermostabilized Chemical Derivatives of Horseradish Peroxidase. Enzyme Microb. Technol., 16, 501-505.

Saidel, L. J., Leitzes, S., Elfring, W. H. and Jr. (1964) The Stability of Chymotrypsin Cross-Linked with Formaldehyde. Biochem. Biophys. Res. Commun., 15, 409-413.

Samborska, K., Guiavarc'h, Y., Van, L., A and Hendrickx, M. (2006) The Thermal Stability of *Aspergillus oryzae* Alpha-amylase in Presence of Sugars and Polyols. J. Food Process Eng., 29, 287-303.

Sanwal, B. D., Maeba, P. and Cook, R. A. (1966) Interaction of Macroions and Dioxane with the Allosteric Phosphoenolpyruvate Carboxylase. J. Biol. Chem., 241, 5177-5182.

Schmid, R. D. (1979) Stabilized Soluble Enzymes. Adv. Biochem. Eng./Biotechnol., 12, 41-118.

Schneider, C., Newman, R. A., Sutherland, D. R., Asser, U. and Greaves, M. F. (1982) A One-Step Purification of Membrane Proteins using a High Efficiency Immunomatrix. J. Biol. Chem., 257, 10766-10769.

Schülke, N. and Schmid, F. X. (1988) The Stability of Yeast Invertase is not Significantly Influenced by Glycosylation. J. Biol. Chem., 263, 8827-8831.

Shah, N. K., Upadhyay, C. M., Nehete, P. N., Kothari, R. M. and Hegde, M. V. (1990) An Economical, Upgraded, Stabilized and Efficient Preparation of [Alpha]-Amylase. J. Biotechnol., 16, 97-108.

Shaked, Z. and Wolf, S. (1988) Stabilization of Pyranose 2-Oxidase and Catalase by Chemical Modification. Methods Enzymol., 137, 599-615.

Shatsky, M. A., Ho, H. C. and Wang, J. H.-C. (1973) Stabilization of Glycogen Phosphorylase b by Reductive Alkylation with Aliphatic Aldehydes. Biochim. Biophys. Acta, Protein Struct., 303, 298-307.

Sheehan, H., O'Kennedy, R. and Kilty, C. (1990) Investigation of the Properties of Bovine Heart Creatine Kinase Cross-Linked with Dimethyl Suberimidate. Biochim. Biophys. Acta, Protein Struct. Mol. Enzymol., 1041, 141-145.

Shi, Q. and Jackowski, G. (1998) One-Dimensional Polyacrylamide gel electrophoresis. In Hames, B.D. (ed), Gel Electrophoresis of Proteins: a Practical Approach. Oxford University Press, Oxford.

Shimada, K. and Sugino, Y. (1969) Cyclic Phosphodiesterase having 3'-Nucleotidase Activity from *Bacillus subtilis*: Purification and some Properties of the Enzyme. Biochim. Biophys. Acta, Enzymol., 185, 367-380.

Shimizu, M., Suzuki, T., Kameda, K.-Y. and Abiko, Y. (1969) Phosphotransacetylase of *Escherichia coli* B, Purification and Properties. Biochim. Biophys. Acta, Enzymol., 191, 550-558.

Shishkin, A. A., Poltorak, O. M., Chukhrai, E. S., Nakhapetyan, L. A. and Suprun, V. L. (1990) Quaternary Structure of Beta-Galactosidase and its role in Thermoinactivation Processes. Zhurnal Fizicheskoi Khimii, 64, 2169-2174.

Shuler, M. L. and Kargi, F. (2002) Bioprocess Engineering: Basic Concepts. Prentice Hall, Upper Saddle River, NJ.

Sigma Chemical Co. Ltd. (1994) Enzymatic Assay of β-Galactosidase (EC 3.2.1.23). Revised March 16, 1994, from: http://www.sigmaaldrich.com/sigma/enzyme %20 assay/bgalactosidas eonp.pdf.

Sigma Chemical Co. Ltd. (1997) Enzymatic Assay of a-Amylase (EC 3.2.1.1). Document No. SSSTAR01, Revised June 13, 1997, from: http://www.SigmaAldrich.Com/ img/assets/18160 /a-Amylase.pdf.

Sigma Chemical Co. Ltd. (1999) Enzymatic Assay of Invertase (EC 3.2.1.26). Document No. SSSUCR06, Revised April 16, 1999, from: http://www.sigmaaldrich.com/ img/assets/18160/ Invertase_temp_25.pdf.

Silberberg, M. S. (2010) Principles of General Chemistry. McGraw-Hill, Dubuque.

Simpson, R. J. (2003) Proteins and Proteomics: a Laboratory Manual. Cold Spring Harbor Laboratory Press, Cold Spring Harbor, New York.

Sinz, A. (2007) Chemical Cross-Linking and Mass Spectrometry for Investigation of Protein-Protein Interactions. In Downard, K. (ed), Mass Spectrometry of Protein Interactions. Wiley-Interscience, Hoboken, N.J.

Smith, M. H. (1966) The Amino Acid Composition of Proteins. J. Theor. Biol., 13, 261-282.

Smith, T. J. and Bell, J. E. (1985) Investigation of the effects of crosslinking glutamate dehydrogenase with dimethyl pimelimidate. Arch. Biochem. Biophys., 239, 63-73.

Smolelis, A. N. and Hartsell, S. E. (1952) Factors Affecting the Lytic Activity of Lysozyme. J. Bacteriol., 63, 665-674.

Snyder, P. D., Jr., Wold, F., Bernlohr, R. W., Dullum, C., Desnick, R. J., Krivit, W. and Condie, R. M. (1974) Enzyme Therapy II Purified Human [Alpha]-Galactosidase A: Stabilization to Heat and Protease Degradation by Complexing with Antibody and by Chemical Modification. Biochim. Biophys. Acta, Enzymol., 350, 432-436.

Snyder, S. L. and Sobocinski, P. Z. (1975) An Improved 2,4,6-Trinitrobenzenesulfonic Acid Method for the Determination of Amines. Anal. Biochem., 64, 284-288.

Sola-Penna, M. and Meyer-Fernandes, J. R. (1998) Stabilization against Thermal Inactivation Promoted by Sugars on Enzyme Structure and Function: Why is Trehalose More Effective than Other Sugars? Arch. Biochem. Biophys., 360, 10-14.

Stein, E. A., Junge, J. M. and Fischer, E. H. (1960) The Amino Acid Composition of α-Amylase from *Aspergillus oryzae*. J. Biol. Chem., 235, 371-378.

Stein, P. E., Leslie, A. G. W., Finch, J. T. and Carrell, R. W. (1991) Crystal Structure of Uncleaved Ovalbumin at 1·95 Å Resolution. J. Mol. Biol., 221, 941-959.

Striegel, A. M. (2009) Modern Size-Exclusion Liquid Chromatography: Practice of Gel Permeation and Gel Filtration Chromatography. Wiley, Hoboken, N.J.

Swift, H. J., Brady, L., Derewenda, Z. S., Dodson, E. J., Dodson, G. G., P.Turkenburg, J. and Wilkinson, A. J. (1991) Structure and Molecular Model Refinement of *Aspergillus oryzae* (TAKA) [Alpha]-Amylase: An Application of the Simulated-annealing Method. Acta Cryst., B47, 535-544.

Takeda, Y. and Hizukuri, S. (1972) Effect of Triton X-100 on Sweet Potato [Beta]-Amylase. Biochim. Biophys. Acta, Enzymol., 268, 175-183.

Takegawa, K., Miki, S. and Iwahara, S. (1990) Effect of Deglycosylation of Polymannose chains on the Properties of Yeast External Invertase. J. Ferment. Bioeng., 70, 131-133.

Tanaka, Y., Kagamiishi, A., Kiuchi, A. and Horiuchi, T. (1975) Purification and Properties of Beta-Galactosidase from *Aspergillus oryzae*, 77, 241-247.

Tang, J., Sepulveda, P., Marciniszyn, J., Jr., Chen, K. C. S., Huang, W. Y., Tao, N., Liu, D. and Lanier, J. P. (1973) Amino-Acid Sequence of Porcine Pepsin. Proc. Nat. Acad. Sci. U.S.A., 70, 3437-3439.

Tani, F., Shirai, N., Onishi, T., Venelle, F., Yasumoto, K. and Doi, E. (1997) Temperature Control for Kinetic Refolding of Heat-Denetured Ovalbumin. Protein Sci., 6, 1491-1502.

Tarentino, A. L., Gomez, C. M. and Plummer, T. H. (1985) Deglycosylation of Asparagine-Linked Glycans by Peptide:N-Glycosidase F. Biochemistry, 24, 4665-4671.

Tatsumoto, K., Oh, K. K., Baker, J. O. and Himmel, M. E. (1989) Enhanced Stability of Glucoamylase through Chemical Crosslinking. Appl. Biochem. Biotechnol., 20-21, 293-308.

Terminiello, L., Bier, M. and Nord, F. F. (1958) On the Mechanism of Enzyme Action. LXIV. Succinyltrypsin and the Reversibility of its Denaturation. Arch. Biochem. Biophys., 73, 171-179.

Thomson, A. R. (1955) Amino Acid Sequence in Lysozyme 1. Displacement Chromatography of Peptides from a Partial Hydrolysate on Ion-Exchange Resins. Biochemistry, 60, 507-515.

Toda, H., Kondo, K. and Narita, K. (1982) The Complete Amino Acid Sequence of Taka-amylase A. Proceedings of the Japan Academy. Ser. B: Physical and Biological Sciences, 58 (B), 208-212.

Torchilin, V. P., Maksimenko, A. V., Smirknov, V. N., Berezin, I. V., Klibanov, A. M. and Martinek, K. (1978) The Principles of Enzyme Stabilization. III. The Effect of the Length of Intra-Molecular Cross-Linkages on Thermostability of Enzymes. Biochim. Biophys. Acta, Enzymol., 522, 277-283.

Torchilin, V. P., Maksimenko, A. V., Smirnov, V. N., Berezin, I. V., Klibanov, A. M. and Martinek, K. (1979) The Principles of Enzyme Stabilization IV. Modification of 'Key' Functional Groups in the Tertiary Structure of Proteins. Biochim. Biophys. Acta, Enzymol., 567, 1-11.

Torchilin, V. P. and Martinek, K. (1979) Enzyme Stabilization without Carriers. Enzyme Microb. Technol., 1, 74-82.

Torchilin, V. P., Trubetskoy, V. S., Omel'Yanenko, V. G. and Mratinek, K. (1983) Stabilization of Subunit Enzyme by Intersubunit Crosslinking with Bifunctional Reagents: Studies with Glyceraldehyde-3-Phosphate Dehydrogenase. J. Mol. Catal., 19, 291-301.

Trimble, R. B. and Maley, F. (1977) Subunit Structure of External Invertase from *Saccharomyces cerevisiae*. J. Biol. Chem., 252, 4409-4412.

Trudel, J. and Asselin, A. (1989) Detection of Chitinase Activity after Polyacrylamide Gel Electrophoresis. Anal. Biochem., 178, 362-366.

Twyman, R. M. (2004) Principles of Proteomics. BIOS Scientific, Abingdon.

Ugarova, N. N., Rozhkova, G. D. and Berezin, I. V. (1979) Chemical Modification of the [Epsilon]-amino Groups of Lysine Residues in Horseradish Peroxidase and its Effect on the Catalytic Properties and Thermostability of the Enzyme. Biochim. Biophys. Acta, Enzymol., 570, 31-42.

Uhlig, H. and Linsmaier-Bednar, E. M. (1998) Industrial Enzymes and their Applications. Wiley, Chichester.

Urabe, I., Nanjo, H. and Okada, H. (1973) Effect of Acetylation of *Bacillus subtilis* [Alpha]-Amylase on the Kinetics of Heat Inactivation. Biochim. Biophys. Acta, Enzymol., 302, 73-79.

Urabe, I., Yamamoto, M., Yamada, Y. and Okada, H. (1978) Effect of Hydrophobicity of Acyl Groups on the Activity and Stability of Acylated Thermolysin. Biochim. Biophys. Acta, Enzymol., 524, 435-441.

Voet, D. and Voet, J. G. (2004) Biochemistry. Wiley, New York.

Vrábel, P., Polakovic, M., Stefuca, V. and Báles, V. (1997) Analysis of Mechanism and Kinetics of Thermal Inactivation of Enzymes: Evaluation of Multitemperature Data Applied to Inactivation of Yeast Invertase. Enzyme Microb. Technol., 20, 348-354.

Wang, J. H.-C. and Tu, J.-I. (1969) Modification of Glycogen Phosphorylase b by Glutaraldehyde. Preparation and Isolation of Enzyme Derivatives with Enhanced Stability. Biochemistry, 8, 4403-4410.

Weber, K. and Osborn, M. (1969) The Reliability of Molecular Weight Determinations by Dodecyl Sulfate-Polyacrylamide Gel Electrophoresis. J. Biol. Chem., 244, 4406-4412.

Wen, J., Arakawa, T. and Philo, J. S. (1996) Size-Exclusion Chromatography with On-Line Light-Scattering, Absorbance, and Refractive Index Detectors for Studying Proteins and their Interactions. Anal. Biochem., 240, 155-166.

Whitaker, J. R. and Tappel, A. L. (1962) Modification of Enzymic Activity II. Effect of Salts on [Alpha]-Amylase, Alcohol Dehydrogenase, Peroxidase and Hematin Catalysis. Biochim. Biophys. Acta, 62, 310-317.

Whitaker, J. R., Tappel, A. L. and Wormser, E. (1962) Modification of Enzymic Activity I. Effect of Organic Additives on [Alpha]-Amylase Activity. Biochim. Biophys. Acta, 62, 300-309.

Williams, R. S., Trumbly, R. J., MacColl, R., Trimble, R. B. and Maley, F. (1985) Comparative Properties of Amplified External and Internal Invertase from the Yeast SUC2 Gene. J. Biol. Chem., 260, 13334-13341.

Wiseman, A. (1975) Handbook of Enzyme Biotechnology, Wiley, New York.

Wiseman, A. and Woodward, J. (1975) Industrial Yeast Invertase Stabilization. Process Biochem., 24-30.

Wold, F. (1972) Bifunctional Reagents. Methods Enzymol., 25, 623-651.

Wong, D. W. S. and Robertson, G. H. (2003) α-Amylases. In Whitaker, J.R., Voragen, A.G.J., et al. (eds), Handbook of Food Enzymology. Marcel Dekker, New York.

Wong, S. S. and Wong, L.-J. C. (1992) Chemical Crosslinking and the Stabilization of Proteins and Enzymes. Enzyme Microb. Technol., 14, 866-874.

Woodward, J. and Wiseman, A. (1979) Stabilisation of Invertases by Treatment with Cross-Linking Reagents. J. Chem. Technol. Biotechnol., 29, 122-126.

Wyatt Technology Corporation (1997) Astra for Windows User's Guide, Santa Barbara.

Yang, S.-T., Marchio, J. L. and Yen, J.-W. (1994) A Dynamic Light Scattering Study of Beta-Galactosidase: Environmental Effects on Protein Conformation and Enzyme Activity. Biotechnol. Progr., 10, 525-531.

Ye, H. (2006) Simultaneous Determination of Protein Aggregation, Degradation, and Absolute Molecular Weight by Size Exclusion Chromatography-Multiangle Laser Light Scattering. Anal. Biochem., 356, 76-85.

Yoon, S.-H. and Robyt, J. F. (2005) Activation and Stabilization of 10 Starch-Degrading Enzymes by Triton X-100, Polyethylene Glycols, and Polyvinyl Alcohols. Enzyme Microb. Technol., 37, 556-562.

Yoshioka, S., Aso, Y., Izutsu, K.-i. and Kojima, S. (1994) Is Stability Prediction Possible for Protein Drugs? Denaturation Kinetics of β-Galactosidase in Solution. Pharm. Res., 11, 1721-1725.

Yoshitake, S., Imagawa, M. and Ishikawa, E. (1982) Efficient Preparation of Rabbit Fab'-Horseardish Peroxidase Conjugates Using Maleimide Compounds and its Use for Enzme Immunoassay. Anal. Lett., 15, 147-160.

Appendix I

The standard curve for size exclusion chromatography (SEC)

Sephacryl S-300 column

The standard proteins with a molecular weight range of 44-669 kDa (ovalbumin, conalbumin, aldolase, ferritin and thyroglobulin) purchased from GE Healthcare were used for calibration of the SEC column. The K_{av} value for each of the standard proteins was calculated using the equation:

$$K_{av} = \frac{V_e - V_o}{V_c - V_o},$$

Where: V_c = geometric column volume (mL);
V_o = column void volume (mL);
V_e = elution volume (mL).

The geometric column volume was calculated as $\pi \times r^2 \times l$ where r is the internal radius of the column and l is the column length. The column volume used for the separation of oligomeric invertase was 83.41 mL. The column void volume V_o was determined by running Blue Dextran 2000 alone through the column with a flow rate of 0.5 mL/min in 0.1 M Na-citrate buffer, pH 6, with 0.15 M NaCl, as an eluent. The elution volume profile of Blue Dextran provided a V_o of 32.191 mL.

Molecules of Blue Dextran 2000 are larger than the pores of the resin and therefore are eluted from the column without entering the pores. This provides the void volume and the signal to start the sample collection. The void volume depends on the packing density of the column.

Standard protein samples were prepared as described in Gel Filtration Calibration Kit booklet (GE Healthcare, Code: 28-4038-42 High Molecular Weight) and injected into the column. The elution volume (V_e) of each sample was obtained from the profiles shown in Figures A1-A3. The V_e and K_{av} values are shown in Table A1. A calibration curve of K_{av} versus the logarithm of the molecular weight (MW) was plotted (Figure A4).

The standard curve was then used to estimate the molecular weights of the unknown proteins subsequently separated using the same column.

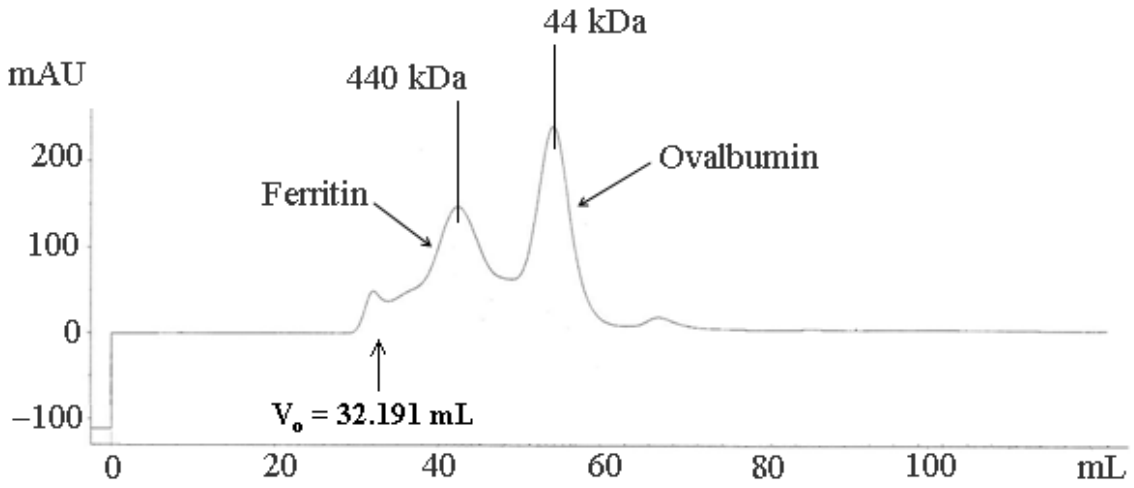

Figure A1 Chromatographic separation of ferritin and ovalbumin standards in 0.1 M Na-citrate buffer pH 6 on Sephacryl S-300 size exclusion column with a flow rate of 0.5 mL/min. V_o was determined using Blue Dextran 2000.

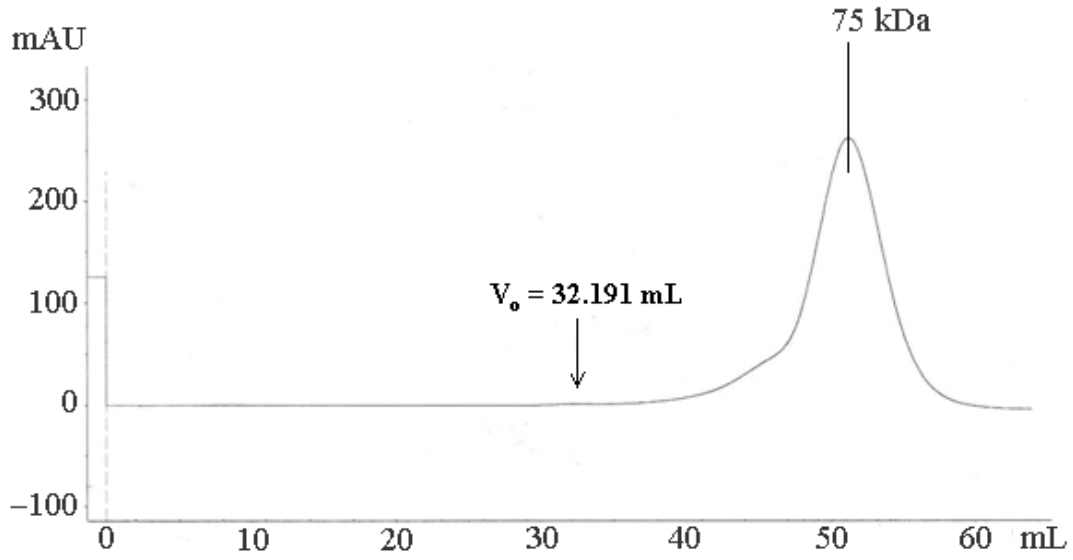

Figure A2 Chromatographic separation of conalbumin standard in 0.1 M Na-citrate buffer pH 6 on Sephacryl S-300 size exclusion column with a flow rate of 0.5 mL/min. V_o was determined using Blue Dextran 2000.

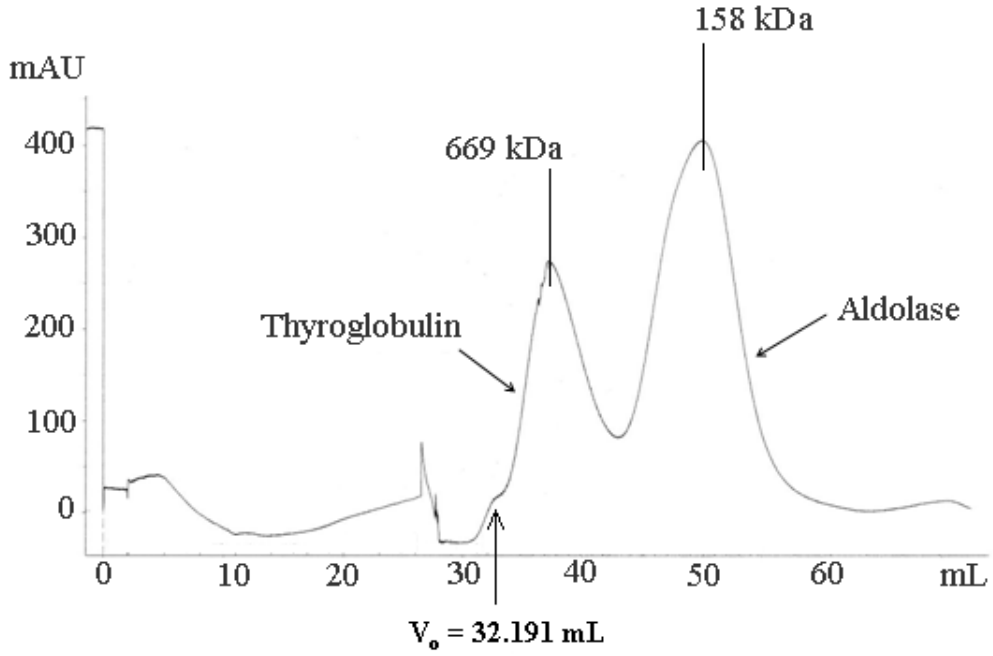

Figure A3 Chromatographic separation of thyroglobulin and aldolase standards in 0.1 M Na-citrate buffer pH 6 on Sephacryl S-300 size exclusion column with a flow rate of 0.5 mL/min. V_o was determined using Blue Dextran 2000.

Table A1 The V_e and K_{av} values for the standard proteins on Sephacryl S-300 size exclusion column

Standard protein	MW (Da)	Log MW	V_e (mL)	K_{av}
Ovalbumin	44,000	4.64	54.083	0.427
Conalbumin	75,000	4.88	51.190	0.371
Aldolase	158,000	5.20	47.863	0.306
Ferritin	440,000	5.64	42.542	0.202
Thyroglobulin	669,000	5.83	37.466	0.103

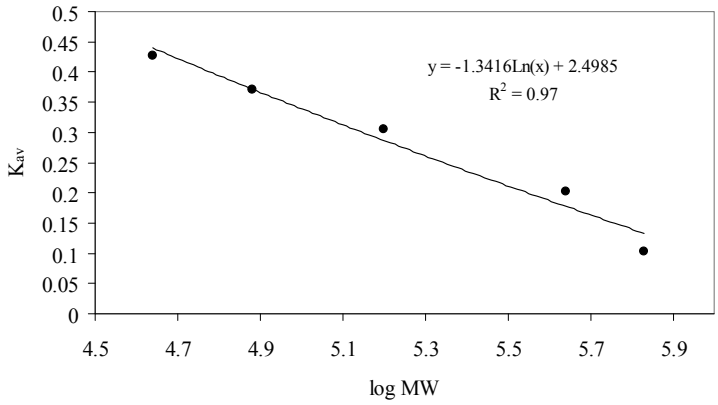

Figure A4 Calibration curve of standard proteins on Sephacryl S-300 size exclusion column (MW= protein molecular weight).

Superdex G-75 column

The standard proteins with a molecular weight range of 12.4-66 kDa (cytochrome C, carbonic anhydrase and bovine serum albumin) purchased from GE Healthcare were used for calibration of the Superdex G-75 size exclusion column. The K_{av} value for each of the standard proteins was calculated using the equation mentioned above. The column volume for this column was 24 mL. The column void volume V_o was determined by running Blue Dextran 2000 alone through the column with a flow rate of 0.3 mL/min in 20 mM Na-phosphate buffer, pH 7, with 0.15 M NaCl, as an eluent. The elution volume profile of Blue Dextran provided a V_o of 7.65 mL.

Standard protein samples (4 mg/mL, 50 µL) were injected into the column. The elution volume (V_e) of protein samples were obtained from the profiles shown in Figure A5. All The V_e and K_{av} values are shown in Table A2. A calibration curve of K_{av} versus the logarithm of the molecular weight (MW) was plotted (Figure A6).

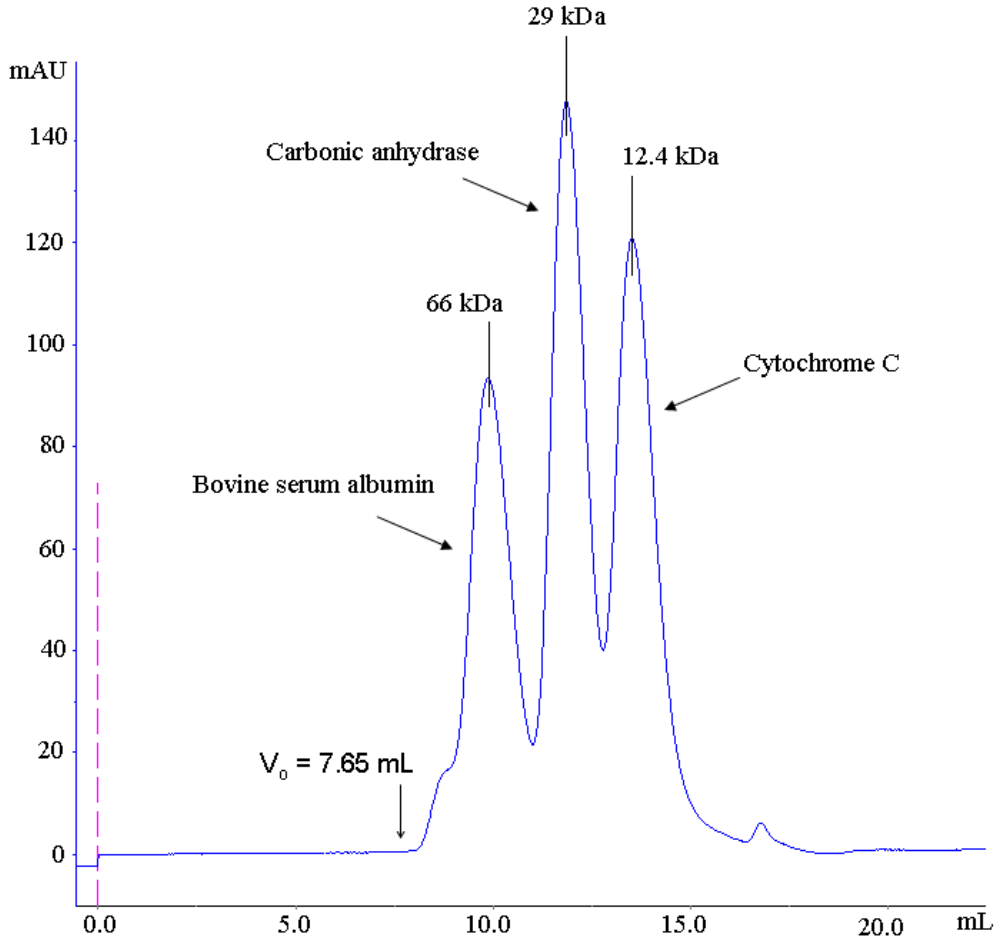

Figure A5 Chromatographic separation of bovine serum albumin, carbonic anhydrase and cytochrome C in 20 mM Na-phosphate buffer pH 6 on Superdex G-75 size exclusion column with a flow rate of 0.3 mL/min.

Table A2 The V_e and K_{av} values for the standard proteins on Superdex G-75 size exclusion column

Standard protein	MW (Da)	Log MW	V_e (mL)	K_{av}
Bovine serum albumin	66,000	4.82	9.92	0.14
Carbonic anhydrase	29,000	4.46	11.81	0.25
Cytochrome C	12,400	4.09	13.48	0.36

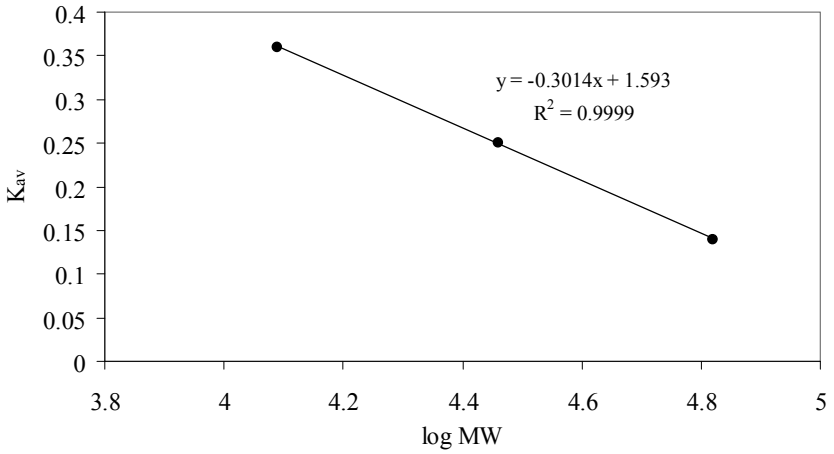

Figure A6 Calibration curve of standard proteins on Superdex G-75 size exclusion column (MW= protein molecular weight).

Appendix II

The certificate of analysis of synthetic pentapeptide provided by Auspep

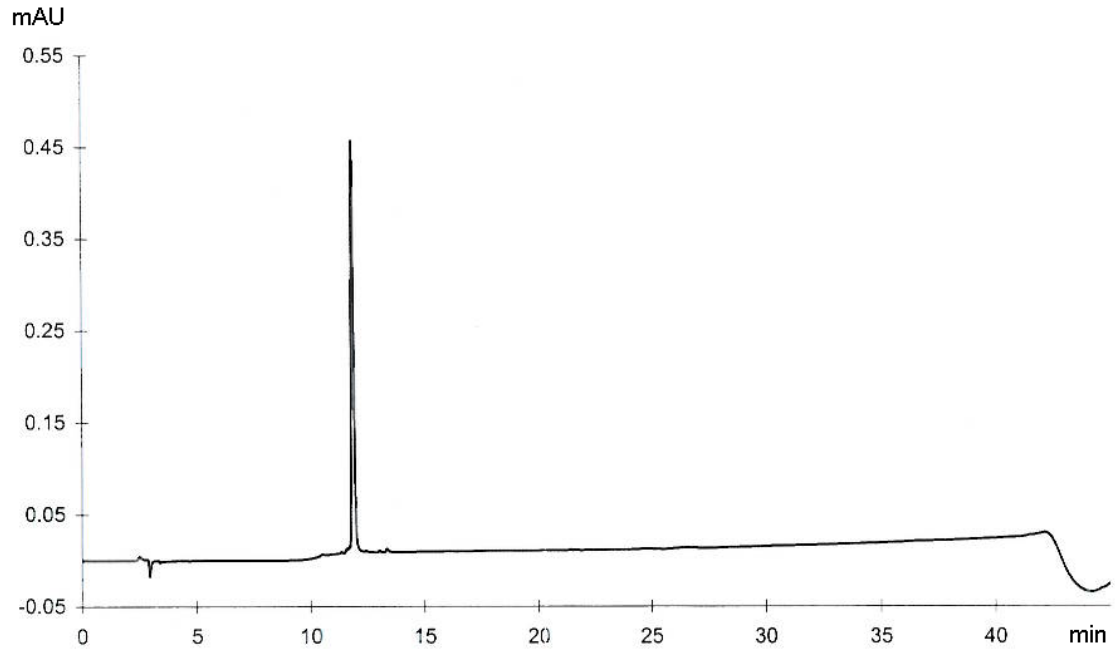

Figure A7 HPLC chromatogram of the synthetic pentapeptide.

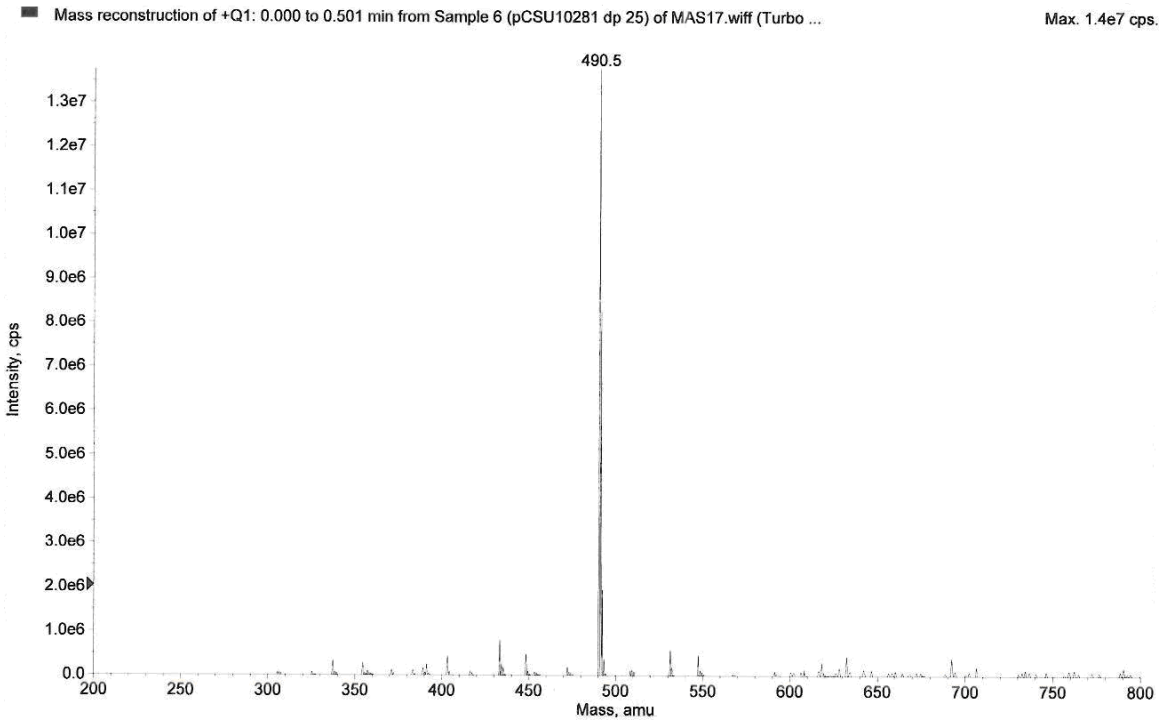

Figure A8 Mass spectrum of the synthetic pentapeptide.

Stabilization of enzymes by chemical modifications

Experimental Data

Pattamawadee Tananchai

1 Effect of chemical modifications on enzyme thermal stability

1.1 α-Amylase

1.1.1 Properties of native α-amylase

Table 1Optimum pH of α-amylase (5 mg/mL) at 20 °C

pH	Dilution (×)	A_{540}			Activity (Unit/mL)
		1	2	Average	
3	2	0.998	0.936	0.981	9
4	10	1.041	1.080	1.061	46
5	10	1.022	1.007	1.015	44
6	10	0.498	0.470	0.484	21
7	10	0.306	0.284	0.295	13
8	10	0.126	0.124	0.125	5
9	2	0.169	0.167	0.168	1
10	2	0.144	0.140	0.142	1

Activity calculations followed the methods in Section 3.2.3.1

Table 2 Optimum temperature of α-amylase at pH 6.9

Temperature (°C)	Dilution (×)	A_{540}			Activity (Unit/mL)
		1	2	Average	
25	100	0.347	0.350	0.349	30
30	100	0.419	0.439	0.429	37
40	100	0.559	0.593	0.576	50
50	100	0.775	0.687	0.731	64
55	100	0.859	0.894	0.877	76
60	100	0.902	0.896	0.899	78
65	100	0.812	0.820	0.816	71
70	100	0.442	0.433	0.438	38
75	100	0.329	0.333	0.331	29
80	100	0.249	0.260	0.255	22
85	100	0.153	0.188	0.171	15
90	100	0.161	0.177	0.169	15

Table 3 The absorbance at 540 nm of α-amylase (5 mg/mL, dilution = ×6) for pH stability at 25 °C

Time (min)	A_{540}														
	pH 4			pH 5			pH 6			pH 7			pH 8		
	1	2	Average	1	2	Average	1	2	Average	1	2	Average	1	2	Average
0	0.770	0.753	0.762	0.602	0.624	0.613	0.531	0.538	0.535	0.519	0.512	0.516	0.395	0.397	0.396
5	0.627	0.644	0.636	0.570	0.590	0.580	0.538	0.554	0.546	0.517	0.528	0.523	0.400	0.409	0.405
10	0.630	0.630	0.630	0.581	0.602	0.592	0.533	0.563	0.548	0.513	0.507	0.510	0.409	0.390	0.400
20	0.630	0.654	0.642	0.630	0.616	0.623	0.557	0.55	0.554	0.521	0.507	0.514	0.418	0.408	0.413
30	0.528	0.598	0.563	0.588	0.596	0.592	0.549	0.568	0.559	0.525	0.516	0.521	0.419	0.410	0.415
40	0.622	0.619	0.621	0.624	0.626	0.625	0.557	0.564	0.561	0.539	0.590	0.565	0.385	0.401	0.393
60	0.612	0.603	0.608	0.528	0.609	0.569	0.570	0.559	0.565	0.520	0.509	0.515	0.416	0.358	0.387
80	0.590	0.581	0.586	0.525	0.556	0.541	0.567	0.553	0.560	0.486	0.514	0.500	0.418	0.396	0.407
100	0.574	0.585	0.580	0.570	0.522	0.546	0.561	0.458	0.510	0.526	0.535	0.531	0.402	0.417	0.410
120	0.569	0.565	0.567	0.498	0.534	0.516	0.573	0.556	0.565	0.517	0.499	0.508	0.422	0.407	0.415

Table 4 pH stability of α-amylase at 25 °C

Time (min)	Activity (Unit/mL)					Relative activity (%)				
	pH 4	pH 5	pH 6	pH 7	pH 8	pH 4	pH 5	pH 6	pH 7	pH 8
0	24	19	17	16	12	100	100	100	100	100
5	20	18	17	16	13	83	93	102	102	103
10	20	19	17	16	13	82	97	102	100	103
20	20	20	17	16	13	83	102	104	100	105
30	18	19	18	16	13	74	97	106	102	105
40	19	20	18	18	12	81	102	106	110	100
60	19	18	18	16	12	79	91	106	100	97
80	18	17	18	16	13	76	88	106	98	103
100	18	17	16	17	13	75	88	96	104	105
120	18	16	18	16	13	74	83	106	100	105

Table 5 pH stability of α-amylase at 55 °C

Time (min)	Activity (Unit/mL)					Relative activity (%)				
	pH 4	pH 5	pH 6	pH 7	pH 8	pH 4	pH 5	pH 6	pH 7	pH 8
0	18	18	17	14	11	100	100	100	100	100
5	10	16	15	12	5	56	87	88	81	44
10	5	13	14	10	3	25	73	80	70	26
20	1.4	10	13	7	1.6	8	55	71	51	14
30	1.2	7	11	6	1.3	7	40	63	44	12
40	1.2	6	9	5	1.2	7	31	55	37	11
60	1.2	3	7	4	1.2	7	18	43	26	10
80	1.1	2	6	3	1.3	6	13	35	19	11
100	1.4	2	5	2	1.4	8	10	29	16	13
120	1.5	2	4	2	1.4	8	10	24	15	12

Table 6 The absorbance at 540 nm of α-amylase (5 mg/mL, dilution = ×5) for pH stability at 55 °C

Time (min)	A_{540}														
	pH 4			pH 5			pH 6			pH 7			pH 8		
	1	2	Average	1	2	Average	1	2	Average	1	2	Average	1	2	Average
0	0.837	0.835	0.836	0.901	0.844	0.873	0.774	0.773	0.774	0.654	0.659	0.657	0.526	0.521	0.524
5	0.475	0.475	0.475	0.739	0.736	0.738	0.691	0.673	0.682	0.545	0.530	0.538	0.232	0.235	0.234
10	0.211	0.211	0.211	0.618	0.616	0.617	0.625	0.644	0.635	0.476	0.456	0.466	0.132	0.146	0.138
20	0.064	0.068	0.066	0.444	0.468	0.456	0.559	0.538	0.549	0.337	0.341	0.339	0.077	0.072	0.075
30	0.053	0.061	0.057	0.346	0.332	0.339	0.482	0.486	0.484	0.293	0.278	0.286	0.065	0.056	0.061
40	0.058	0.051	0.055	0.260	0.251	0.256	0.420	0.438	0.429	0.251	0.240	0.246	0.059	0.051	0.055
60	0.056	0.055	0.056	0.158	0.156	0.157	0.333	0.338	0.336	0.171	0.155	0.163	0.053	0.055	0.054
80	0.05	0.049	0.050	0.107	0.103	0.105	0.277	0.287	0.282	0.126	0.125	0.126	0.064	0.054	0.059
100	0.066	0.06	0.063	0.084	0.092	0.088	0.225	0.230	0.228	0.105	0.110	0.108	0.068	0.064	0.066
120	0.068	0.071	0.070	0.082	0.078	0.08	0.187	0.194	0.191	0.098	0.093	0.096	0.067	0.063	0.065

Table 7 The absorbance at 540 nm of α-amylase (5 mg/mL, dilution = ×100) for its thermal stability at 25-60 °C, pH 6.9

Time (min)	25 °C			30 °C			40 °C			50 °C			55 °C			60 °C		
	1	2	Average	1	2	Average	1	2	Average	1	2	Average	1	2	Average	1	2	Average
0	0.292	0.294	0.293	0.302	0.288	0.295	0.309	0.289	0.299	0.301	0.302	0.302	0.251	0.250	0.251	0.281	0.278	0.280
5	0.331	0.296	0.314	0.285	0.315	0.300	0.308	0.305	0.307	0.258	0.287	0.273	0.246	0.263	0.255	0.186	0.182	0.184
10	0.296	0.328	0.312	0.305	0.310	0.308	0.303	0.295	0.299	0.284	0.281	0.283	0.257	0.249	0.253	0.144	0.140	0.142
20	0.325	0.324	0.325	0.284	0.343	0.314	0.299	0.315	0.307	0.260	0.258	0.259	0.217	0.208	0.213	0.068	0.059	0.064
30	0.337	0.326	0.332	0.279	0.286	0.283	0.298	0.301	0.300	0.277	0.266	0.272	0.142	0.156	0.149	0.391	0.379	0.385*
40	0.311	0.309	0.310	0.323	0.321	0.322	0.321	0.303	0.312	0.244	0.241	0.243	0.137	0.119	0.128	0.300	0.300	0.300*
60	0.308	0.285	0.297	0.293	0.298	0.296	0.294	0.300	0.297	0.232	0.240	0.236	0.663	0.672	0.668*	0.224	0.212	0.218*
80	0.282	0.308	0.295	0.312	0.332	0.322	0.311	0.305	0.308	0.230	0.230	0.230	0.583	0.585	0.584*	0.205	0.199	0.202*
100	0.293	0.285	0.289	0.295	0.298	0.297	0.298	0.295	0.297	0.229	0.218	0.224	0.520	0.530	0.525*	0.196	0.201	0.199*
120	0.301	0.265	0.283	0.297	0.298	0.298	0.296	0.303	0.300	0.204	0.186	0.195	0.449	0.443	0.446*	0.210	0.209	0.210*

* dilution = ×10

Table 8 Thermal denaturation of α-amylase at 25-60 °C, pH 6.9

Time (min)	Activity (Unit/mL)						Remaining activity (%)					
	25°C	30°C	40°C	50°C	55°C	60°C	25°C	30°C	40°C	50°C	55°C	60°C
0	25	26	26	26	22	24	100	100	100	100	100	100
5	27	26	27	24	22	16	108	101	103	90	102	66
10	27	27	26	25	22	12	107	104	100	94	100	51
20	28	27	27	23	19	6	112	106	103	86	85	23
30	29	25	26	24	13	3	114	96	100	90	59	14
40	27	28	27	21	11	3	107	109	104	80	50	11
60	26	26	26	21	6	2	103	100	100	78	26	8
80	26	28	27	20	5	2	101	109	103	76	23	7
100	25	26	26	19	5	2	99	101	100	73	21	7
120	25	26	26	17	4	2	97	101	100	65	18	7

Table 9 Absorbance at 540 nm of α-amylase (5 mg/mL, dilution = ×100) for the estimation of E_d and k_d (pH = 6)

Time (min)	A_{540}											
	50 °C			55 °C			60 °C			65 °C		
	1	2	Average	1	2	Average	1	2	Average	1	2	Average
0	0.335	0.344	0.340	0.330	0.342	0.336	0.343	.0351	0.347	0.318	0.327	0.323
1	0.338	0.333	0.336	0.321	0.317	0.319	0.310	0.290	0.300	0.207	0.214	0.211*
2	0.335	0.328	0.332	0.311	0.305	0.308	0.267	0.271	0.269	0.165	0.164	0.165*
3	0.326	0.326	0.326	0.302	0.306	0.304	0.230	0.221	0.226	0.160	0.166	0.163*
4	0.332	0.332	0.332	0.290	0.302	0.296	0.209	0.223	0.216	0.166	0.160	0.163*
5	0.323	0.332	0.328	0.306	0.301	0.303	0.213	0.200	0.207	0.176	0.155	0.166*
6	0.305	0.306	0.306	0.309	0.303	0.306	0.178	0.173	0.176	0.156	0.155	0.156*
7	0.321	0.318	0.320	0.301	0.289	0.295	0.139	0.138	0.139	0.158	0.161	0.160*
8	0.327	0.330	0.329	0.294	0.292	0.293	0.135	0.134	0.135	0.161	0.174	0.168*
9	0.327	0.327	0.327	0.280	0.282	0.281	0.127	0.114	0.121	0.164	0.164	0.1648
10	0.319	0.332	0.326	0.273	0.279	0.276	0.119	0.126	0.123	0.156	0.162	0.159*
12	0.313	0.315	0.314	0.256	0.254	0.255	0.099	0.104	0.102	0.160	0.162	0.161*
14	0.325	0.311	0.318	0.270	0.262	0.266	0.475	0.467	0.471*	0.154	0.153	0.154*
16	0.308	0.299	0.304	0.258	0.256	0.257	0.473	0.430	0.452*	0.162	0.155	0.159*
18	0.312	0.314	0.313	0.262	0.218	0.240	0.398	0.383	0.391*	0.158	0.187	0.173*
20	0.302	0.295	0.299	0.256	0.234	0.245	0.369	0.369	0.369*	0.180	0.194	0.187*
22	0.310	0.304	0.307	0.239	0.241	0.240	0.346	0.348	0.347*	0.159	0.169	0.164*
24	0.289	0.295	0.292	0.238	0.237	0.238	0.316	0.333	0.325*	0.168	0.175	0.172*

Time (min)	A_{540}											
	50 °C			55 °C			60 °C			65 °C		
	1	2	Average	1	2	Average	1	2	Average	1	2	Average
26	0.296	0.291	0.294	0.217	0.221	0.219	0.337	0.342	0.340*	0.164	0.160	0.162*
28	0.280	0.297	0.289	0.190	0.185	0.188	0.329	0.319	0.324*	0.167	0.186	0.177*
30	0.302	0.303	0.303	0.183	0.189	0.186	0.314	0.319	0.317*	0.166	0.168	0.167*
40	0.297	0.297	0.297	0.169	0.183	0.176	0.255	0.258	0.257*	0.188	0.205	0.197*
60	0.288	0.286	0.287	0.776	0.786	0.781*	0.222	0.222	0.222*	0.191	0.195	0.193*
80	0.289	0.284	0.287	0.662	0.644	0.653*	0.230	0.225	0.228*	0.227	0.211	0.219*
100	0.301	0.290	0.296	0.586	0.585	0.586*	0.228	0.245	0.237*	0.247	0.295	0.271*
120	0.317	0.321	0.319	0.529	0.550	0.540*	0.242	0.245	0.244*	0.305	0.301	0.303*

* dilution = ×10

Table 10 the estimation of E_d and k_d for α-amylase (pH = 6)

Time (min)	Activity (Unit/mL)				Relative activity (%)				ν_f				ln ν_f			
	50 °C	55°C	60 °C	65 °C	50 °C	55°C	60 °C	65 °C	50 °C	55°C	60 °C	65 °C	50 °C	55°C	60 °C	65 °C
0	30	29	30	28	100	100	100	100	1	1	1	1	0	0	0	0
1	29	28	26	1.8	99	94	86	6.5	0.99	0.94	0.86	0.07	-0.01	-0.06	-0.15	-2.73
2	29	27	23	1.4	98	91	77	5.1	0.98	0.91	0.77	0.05	-0.02	-0.10	-0.26	-2.97
3	28	26	20	1.4	96	90	65	5.1	0.96	0.90	0.65	0.05	-0.05	-0.11	-0.43	-2.97
4	29	26	19	1.4	98	88	62	5.1	0.98	0.88	0.62	0.05	-0.02	-0.13	-0.49	-2.97
5	29	26	18	1.4	97	90	59	5.1	0.97	0.90	0.59	0.05	-0.03	-0.11	-0.52	-2.97
6	27	27	15	1.4	90	91	51	4.9	0.9	0.91	0.51	0.05	-0.11	-0.10	-0.68	-3.02
7	28	26	12	1.4	94	88	40	5.0	0.94	0.88	0.40	0.05	-0.06	-0.13	-0.93	-3.00
8	29	25	12	1.5	97	86	38	5.2	0.97	0.86	0.38	0.05	-0.03	-0.15	-0.96	-2.95
9	28	24	11	1.4	96	83	35	5.1	0.96	0.83	0.35	0.05	-0.05	-0.19	-1.05	-2.97
10	28	24	11	1.4	96	82	35	4.9	0.96	0.82	0.35	0.05	-0.05	-0.20	-1.05	-3.02
12	27	22	9	1.4	92	76	30	5.0	0.92	0.76	0.30	0.05	-0.08	-0.27	-1.22	-3.00
14	28	23	4	1.3	93	78	13	4.8	0.93	0.78	0.13	0.05	-0.07	-0.24	-2.03	-3.04
16	26	22	4	1.4	89	76	13	4.9	0.89	0.76	0.13	0.05	-0.12	-0.27	-2.03	-3.02
18	27	21	3.3	1.5	92	72	11	5.4	0.92	0.72	0.11	0.05	-0.08	-0.33	-2.21	-2.93
20	26	21	3.2	1.6	88	73	11	5.8	0.88	0.73	0.11	0.06	-0.13	-0.32	-2.25	-2.84
22	27	21	3	1.4	90	72	10	5.1	0.90	0.72	0.10	0.05	-0.11	-0.33	-2.30	-2.97
24	25	21	2.8	1.3	85	70	9	5.4	0.85	0.70	0.09	0.05	-0.16	-0.35	-2.37	-2.93
26	26	19	3	1.4	87	65	10	5.0	0.87	0.65	0.10	0.05	-0.14	-0.43	-2.32	-3.00
28	25	16	2.8	1.5	84	56	9	5.5	0.84	0.56	0.09	0.06	-0.17	-0.59	-2.37	-2.90

Time (min)	Activity (Unit/mL)				Relative activity (%)				v_f				ln v_f			
	50 °C	**55°C**	**60 °C**	**65 °C**	**50 °C**	**55°C**	**60 °C**	**65 °C**	**50 °C**	**55°C**	**60 °C**	**65 °C**	**50 °C**	**55°C**	**60 °C**	**65 °C**
30	26	16	2.8	1.5	89	56	9	5.2	0.89	0.56	0.09	0.05	-0.12	-0.59	-2.39	-2.95
40	26	15	2.2	1.7	88	52	7	6.1	0.88	0.52	0.07	0.06	-0.13	-0.65	-2.61	-2.80
60	25	7	1.9	1.7	84	23	6	6.0	0.84	0.23	0.06	0.06	-0.17	-1.48	-2.75	-2.82
80	25	6	2	1.9	84	19	7	6.8	0.84	0.19	0.07	0.07	-0.17	-1.64	-2.72	-2.69
100	26	5	2.1	2.4	87	17	7	8.5	0.87	0.17	0.07	0.08	-0.14	-1.77	-2.69	-2.47
120	28	5	2.1	2.6	93	16	7	9.4	0.93	0.16	0.07	0.10	-0.07	-1.84	-2.65	-2.36

1.1.2 Thermal stabilization by isocyanates

Table 11 Thermal stability of native α-amylase at 60 °C, pH 6

Time (min)	Measurement 1					Measurement 2					Measurement 3					Relative activity (average,%)	SD
	A_{540}			Activity (U/mL)	Relative activity (%)	A_{540}			Activity (U/mL)	Relative activity (%)	A_{540}			Activity (U/mL)	Relative activity (%)		
	1	2	Average			1	2	Average			1	2	Average				
0	0.871	0.859	0.865	0.75	100	0.795	0.802	0.799	0.70	100	0.877	0.871	0.874	0.76	100	100	0
5	0.505	0.495	0.500	0.44	59	0.412	0.416	0.414	0.36	51	0.462	0.458	0.460	0.40	53	54	4.16
10	0.381	0.382	0.382	0.33	44	0.270	0.258	0.264	0.23	33	0.353	0.199	0.276	0.24	32	36	6.65
15	0.240	0.236	0.238	0.21	28	0.164	0.158	0.161	0.14	20	0.184	0.184	0.184	0.16	21	23	4.36
20	0.185	0.201	0.193	0.17	23	0.149	0.148	0.149	0.13	19	0.115	0.113	0.114	0.10	13	18	5.03
25	0.133	0.135	0.134	0.12	16	0.075	0.085	0.080	0.07	10	0.080	0.078	0.079	0.07	9	12	3.79
30	0.112	0.092	0.102	0.09	12	0.054	0.038	0.046	0.04	6	0.056	0.066	0.061	0.05	7	8	3.21

Table 12 Thermal stability at 60 °C, pH 6, of α-amylase crosslinked with BMDC (1-20 mM)

Time (min)	1 mM BMDC					10 mM BMDC					20 mM BMDC				
	A_{540}			Activity (U/mL)	Relative activity (%)	A_{540}			Activity (U/mL)	Relative activity (%)	A_{540}			Activity (U/mL)	Relative activity (%)
	1	2	Average			1	2	Average			1	2	Average		
0	0.240	0.242	0.241	0.21	100	0.320	0.278	0.299	0.26	100	0.177	0.191	0.184	0.16	100
5	0.076	0.088	0.082	0.07	33	0.084	0.114	0.099	0.09	35	0.067	0.069	0.068	0.06	38
10	0.041	0.045	0.043	0.04	19	0.050	0.058	0.054	0.05	19	0.033	0.037	0.035	0.03	19
15	0.036	0.035	0.036	0.03	14	0.046	0.056	0.051	0.04	15	0.021	0.031	0.026	0.02	13
20	0.004	0.016	0.010	0.01	5	0.014	0.016	0.015	0.01	4	0.012	0.013	0.013	0.01	6
25	0	0	0	0	0	0	0.006	0.003	0.003	1	0.003	0.005	0.004	0.003	2
30	0.009	0.001	0.005	0.004	2	0.012	0.020	0.016	0.01	4	0.012	0.018	0.015	0.01	6

Table 13 Thermal stability at 60 °C, pH 6, of α-amylase crosslinked with BMDC (30-50 mM)

Time (min)	30 mM BMDC					40 mM BMDC					50 mM BMDC				
	A_{540}			Activity (U/mL)	Relative activity (%)	A_{540}			Activity (U/mL)	Relative activity (%)	A_{540}			Activity (U/mL)	Relative activity (%)
	1	2	Average			1	2	Average			1	2	Average		
0	0.194	0.219	0.207	0.18	100	0.274	0.277	0.276	0.24	100	0.215	0.221	0.218	0.19	100
5	0.056	0.06	0.058	0.05	28	0.056	0.065	0.061	0.05	21	0.048	0.044	0.046	0.04	21
10	0.025	0.019	0.022	0.02	11	0.027	0.025	0.028	0.02	8	0.024	0.016	0.020	0.02	11
15	0.036	0.014	0.025	0.02	11	0.027	0.039	0.033	0.03	13	0.020	0.026	0.023	0.02	11
20	0.009	0.005	0.007	0.01	6	0.013	0.031	0.022	0.02	8	0.004	0.005	0.009	0.01	5
25	0	0.004	0.002	0.003	2	0.017	0.016	0.017	0.01	4	0.004	0.003	0.004	0.004	2
30	0.018	0.026	0.022	0.03	17	0.025	0.031	0.028	0.02	8	0.001	0.013	0.007	0.006	3

Table 14 Thermal stability at 60 °C, pH 6, of α-amylase crosslinked with HMDC (1-20 mM)

Time (min)	1 mM HMDC					10 mM HMDC					20 mM HMDC				
	A_{540}			Activity (U/mL)	Relative activity (%)	A_{540}			Activity (U/mL)	Relative activity (%)	A_{540}			Activity (U/mL)	Relative activity (%)
	1	2	Average			1	2	Average			1	2	Average		
0	0.153	0.169	0.161	0.14	100	0.141	0.135	0.138	0.12	100	0.082	0.102	0.092	0.08	100
5	0.062	0.054	0.058	0.05	36	0.047	0.055	0.051	0.04	33	0.036	0.035	0.036	0.03	38
10	0.027	0.031	0.029	0.03	21	0.033	0.023	0.028	0.02	17	0.023	0.019	0.021	0.02	25
15	0.022	0.024	0.023	0.02	14	0.027	0.023	0.025	0.02	17	0.022	0.012	0.017	0.02	25
20	0.016	0.006	0.011	0.01	7	0.026	0.010	0.018	0.02	17	0.011	0.019	0.015	0.01	13
25	0.017	0.011	0.014	0.01	7	0.008	0.007	0.008	0.007	6	0.015	0.009	0.012	0.01	13
30	0.003	0.002	0.003	0.003	2	0.007	0.005	0.006	0.005	4	0.009	0.005	0.007	0.01	13

Table 15 Thermal stability at 60 °C, pH 6, of α-amylase crosslinked with HMDC (30-50 mM)

Time (min)	30 mM HMDC					40 mM HMDC					50 mM HMDC				
	A_{540}			Activity (U/mL)	Relative activity (%)	A_{540}			Activity (U/mL)	Relative activity (%)	A_{540}			Activity (U/mL)	Relative activity (%)
	1	2	Average			1	2	Average			1	2	Average		
0	0.085	0.086	0.086	0.07	100	0.096	0.110	0.103	0.09	100	0.126	0.125	0.126	0.11	100
5	0.028	0.036	0.032	0.03	43	0.032	0.031	0.033	0.03	33	0.036	0.042	0.039	0.03	27
10	0.019	0.018	0.019	0.02	29	0.020	0.026	0.023	0.02	22	0.028	0.032	0.030	0.03	27
15	0.011	0.009	0.010	0.01	14	0.024	0.016	0.020	0.02	22	0.009	0.012	0.011	0.01	9
20	0.002	0.002	0.002	0.001	1	0.004	0.003	0.004	0.004	4	0.003	0.005	0.004	0.003	3
25	0.001	0.001	0.001	0.001	1	0.002	0.001	0.002	0.002	2	0.003	0.003	0.003	0.002	2
30	0	0	0	0	0	0.002	0.004	0.003	0.003	3	0	0	0	0	0

Table 16 Thermal stability at 60 °C, pH 6, of α-amylase crosslinked with OMDC (1-20 mM)

Time (min)	1 mM OMDC					10 mM OMDC					20 mM OMDC				
	A_{540}			Activity (U/mL)	Relative activity (%)	A_{540}			Activity (U/mL)	Relative activity (%)	A_{540}			Activity (U/mL)	Relative activity (%)
	1	2	Average			1	2	Average			1	2	Average		
0	0.315	0.329	0.322	0.28	100	0.224	0.212	0.218	0.19	100	0.247	0.259	0.253	0.22	100
5	0.169	0.165	0.167	0.15	54	0.133	0.125	0.129	0.11	58	0.161	0.167	0.164	0.14	64
10	0.101	0.099	0.100	0.09	32	0.086	0.076	0.081	0.07	37	0.116	0.115	0.116	0.10	45
15	0.055	0.054	0.055	0.05	18	0.048	0.048	0.048	0.04	21	0.054	0.048	0.051	0.04	18
20	0.036	0.048	0.042	0.04	14	0.031	0.035	0.033	0.03	16	0.059	0.067	0.063	0.06	27
25	0.019	0.018	0.019	0.02	7	0.019	0.015	0.017	0.02	11	0.037	0.039	0.038	0.03	14
30	0.015	0.011	0.013	0.01	4	0.011	0.010	0.011	0.01	5	0.021	0.029	0.025	0.02	9

Table 17 Thermal stability at 60 °C, pH 6, of α-amylase crosslinked with OMDC (30-50 mM)

Time (min)	30 mM OMDC					40 mM OMDC					50 mM OMDC				
	A_{540}			Activity (U/mL)	Relative activity (%)	A_{540}			Activity (U/mL)	Relative activity (%)	A_{540}			Activity (U/mL)	Relative activity (%)
	1	2	Average			1	2	Average			1	2	Average		
0	0.270	0.258	0.264	0.23	100	0.229	0.231	0.230	0.20	100	0.295	0.279	0.287	0.25	100
5	0.107	0.109	0.108	0.09	39	0.085	0.075	0.080	0.07	35	0.092	0.098	0.095	0.08	32
10	0.092	0.066	0.079	0.07	30	0.052	0.054	0.053	0.05	25	0.071	0.067	0.069	0.06	24
15	0.032	0.032	0.032	0.03	13	0.027	0.019	0.023	0.02	10	0.025	0.027	0.026	0.02	8
20	0.022	0.026	0.024	0.02	9	0.009	0.008	0.009	0.01	5	0.015	0.019	0.017	0.02	8
25	0.028	0.038	0.032	0.03	13	0.021	0.015	0.018	0.02	10	0	0	0	0	0
30	0.013	0.012	0.013	0.01	4	0.017	0.015	0.016	0.01	5	0.009	0.009	0.009	0.01	4

Table 18 Thermal stability at 60 °C, pH 6, of α-amylase crosslinked with 20 mM isocyanates

Time (min)	BIC					BMDC					HMDC					OMDC				
	A_{540}			Act (U/mL)	RA (%)	A_{540}			Act (U/mL)	RA (%)	A_{540}			Act (U/mL)	RA (%)	A_{540}			Act (U/mL)	RA (%)
	1	2	Av			1	2	Av			1	2	Av			1	2	Av		
0	0.191	0.199	0.195	0.17	100	0.194	0.219	0.207	0.18	100	0.085	0.086	0.086	0.07	100	0.285	0.234	0.260	0.23	100
5	0.102	0.098	0.100	0.09	53	0.056	0.060	0.058	0.05	28	0.025	0.030	0.028	0.02	29	0.142	0.206	0.174	0.15	67
10	0.080	0.064	0.072	0.06	35	0.025	0.019	0.022	0.02	11	0.019	0.016	0.018	0.02	29	0.088	0.072	0.08	0.07	31
15	0.053	0.053	0.053	0.05	29	0.036	0.014	0.025	0.02	11	0.018	0.008	0.013	0.01	14	0.055	0.078	0.067	0.06	26
20	0.033	0.041	0.037	0.03	18	0.009	0.005	0.007	0.01	6	0	0	0	0	0	0.049	0.031	0.040	0.03	15
25	0.036	0.022	0.029	0.03	18	0	0.004	0.002	0.003	2	0	0	0	0	0	0	0	0	0	0
30	0.020	0.022	0.021	0.02	12	0.018	0.026	0.022	0.02	11	0	0	0	0	0	0	0	0	0	0

RA Relative Activity

Table 19 Thermal stability at 60 °C, pH 6, of α-amylase crosslinked with 20 mM OMDC at pH 5, 6, 7 and 8

Time (min)	pH 5					pH 6					pH 7					pH 8				
	A_{540}			Act (U/mL)	RA (%)	A_{540}			Act (U/mL)	RA (%)	A_{540}			Act (U/mL)	RA (%)	A_{540}			Act (U/mL)	RA (%)
	1	2	Av			1	2	Av			1	2	Av			1	2	Av		
0	0.304	0.294	0.299	0.26	100	0.307	0.313	0.310	0.27	100	0.295	0.279	0.287	0.25	100	0.228	0.254	0.241	0.21	100
5	0.187	0.189	0.188	0.16	62	0.199	0.211	0.205	0.18	67	0.199	0.187	0.193	0.17	68	0.162	0.166	0.164	0.14	67
10	0.140	0.118	0.129	0.11	42	0.146	0.164	0.155	0.14	52	0.159	0.135	0.147	0.13	52	0.125	0.131	0.128	0.11	52
15	0.061	0.059	0.060	0.05	19	0.079	0.095	0.087	0.08	30	0.050	0.048	0.049	0.04	16	0.029	0.029	0.029	0.03	14
20	0.039	0.051	0.045	0.04	15	0.049	0.051	0.050	0.04	15	0.040	0.046	0.043	0.04	16	0.017	0.031	0.024	0.02	10
25	0.023	0.031	0.027	0.02	8	0.049	0.049	0.049	0.04	15	0.034	0.012	0.023	0.02	8	0	0.024	0.012	0.01	5
30	0.003	0.021	0.012	0.01	4	0.047	0.021	0.034	0.03	11	0.001	0.017	0.009	0.01	4	0.015	0.005	0.010	0.01	5

RA Relative Activity

1.1.3 Thermal stabilization by imidoesters

Table 20 Thermal stability of native α-amylase at 60 °C, pH 6

Time (min)	Measurement 1					Measurement 2					Measurement 3					Relative activity (average,%)	SD
	A_{540}			Activity (U/mL)	Relative activity (%)	A_{540}			Activity (U/mL)	Relative activity (%)	A_{540}			Activity (U/mL)	Relative activity (%)		
	1	2	Average			1	2	Average			1	2	Average				
0	0.935	0.927	0.931	0.81	100	0.851	0.850	0.851	0.74	100	0.906	0.888	0.897	0.78	100	100	0
5	0.475	0.474	0.475	0.41	51	0.498	0.488	0.493	0.43	58	0.475	0.457	0.466	0.41	53	54	3.61
10	0.255	0.247	0.251	0.22	27	0.059	0.355	0.357	0.31	42	0.341	0.340	0.341	0.30	38	36	7.77
15	0.152	0.164	0.158	0.14	17	0.229	0.231	0.230	0.20	27	0.216	0.214	0.215	0.19	24	23	5.13
20	0.117	0.125	0.121	0.11	14	0.188	0.156	0.170	0.15	20	0.195	0.199	0.197	0.17	22	19	4.16
25	0.063	0.067	0.065	0.06	7	0.117	0.121	0.119	0.10	14	0.106	0.110	0.108	0.09	12	11	3.61
30	0.016	0.058	0.037	0.03	4	0.101	0.086	0.094	0.08	11	0.093	0.087	0.090	0.08	10	8	3.79

Table 21 Thermal stability at 60 °C, pH 6, of α-amylase crosslinked with DMA (0.1-1 mg/mL)

Time (min)	0.1 mg/mL DMA					1 mg/mL DMA				
	A_{540}			Activity (U/mL)	Relative Activity (%)	A_{540}			Activity (U/mL)	Relative Activity (%)
	1	2	Average			1	2	Average		
0	0.619	0.645	0.632	0.55	100	0.650	0.638	0.644	0.56	100
5	0.370	0.364	0.367	0.32	58	0.389	0.383	0.386	0.34	61
10	0.243	0.251	0.247	0.21	38	0.232	0.258	0.245	0.21	38
15	0.137	0.129	0.133	0.12	22	0.142	0.166	0.154	0.13	23
20	0.102	0.088	0.095	0.08	15	0.118	0.114	0.116	0.10	18
25	0.029	0.021	0.025	0.02	4	0.085	0.069	0.077	0.07	13
30	0.015	0.011	0.013	0.01	2	0.058	0.057	0.058	0.05	9

Table 22 Thermal stability at 60 °C, pH 6, of α-amylase crosslinked with DMA (5-10 mg/mL)

Time (min)	5 mg/mL DMA					10 mg/mL DMA				
	A_{540}			Activity (U/mL)	Relative Activity (%)	A_{540}			Activity (U/mL)	Relative Activity (%)
	1	2	Average			1	2	Average		
0	0.689	0.667	0.678	0.59	100	0.618	0.624	0.621	0.54	100
5	0.414	0.426	0.420	0.37	63	0.404	0.402	0.403	0.35	65
10	0.237	0.236	0.237	0.21	36	0.237	0.259	0.248	0.22	41
15	0.128	0.156	0.142	0.12	20	0.117	0.119	0.118	0.10	19
20	0.117	0.113	0.115	0.10	17	0093	0.105	0.099	0.09	17
25	0.072	0.078	0.075	0.06	10	0.087	0.087	0.087	0.08	15
30	0.072	0.064	0.068	0.06	10	0.067	0.068	0.068	0.06	11

Table 23 Thermal stability at 60 °C, pH 6, of α-amylase crosslinked with DMP (0.1-1 mg/mL)

Time (min)	0.1 mg/mL DMP					1 mg/mL DMP				
	A_{540}			Activity (U/mL)	Relative Activity (%)	A_{540}			Activity (U/mL)	Relative Activity (%)
	1	2	Average			1	2	Average		
0	0.676	0.658	0.667	0.58	100	0.636	0.652	0.644	0.56	100
5	0.395	0.379	0.387	0.34	59	0.410	0.414	0.412	0.36	64
10	0.261	0.259	0.260	0.23	40	0.245	0.269	0.257	0.22	39
15	0.137	0.129	0.133	0.12	21	0.185	0.175	0.180	0.16	29
20	0.105	0.121	0.113	0.10	17	0.109	0.109	0.109	0.10	18
25	0.083	0.091	0.087	0.08	14	0.087	0.067	0.077	0.07	13
30	0.019	0.035	0.027	0.02	3	0.029	0.073	0.051	0.04	7

Table 24 Thermal stability at 60 °C, pH 6, of α-amylase crosslinked with DMP (5-10 mg/mL)

Time (min)	5 mg/mL DMP					10 mg/mL DMP				
	A_{540}			Activity (U/mL)	Relative Activity (%)	A_{540}			Activity (U/mL)	Relative Activity (%)
	1	2	Average			1	2	Average		
0	0.647	0.549	0.598	0.52	100	0.702	0.654	0.678	0.59	100
5	0.383	0.395	0.389	0.34	65	0.451	0.445	0.448	0.39	66
10	0.237	0.253	0.245	0.21	40	0.291	0.279	0.285	0.25	42
15	0.160	0.161	0.161	0.14	27	0.202	0.205	0.203	0.18	31
20	0.107	0.121	0.114	0.10	19	0.098	0.106	0.102	0.09	15
25	0.085	0.107	0.096	0.08	15	0.085	0091	0.088	0.08	14
30	0.063	0.057	0.060	0.05	10	0.078	0.072	0.075	0.06	10

Table 25 Thermal stability at 60 °C, pH 6, of α-amylase crosslinked with DMS (0.1-1 mg/mL)

Time (min)	0.1 mg/mL DMS					1 mg/mL DMS				
	A_{540}			Activity (U/mL)	Relative Activity (%)	A_{540}			Activity (U/mL)	Relative Activity (%)
	1	2	Average			1	2	Average		
0	0.605	0.591	0.598	0.52	100	0.628	0.636	0.632	0.55	100
5	0.337	0.321	0.329	0.29	56	0.358	0.362	0.360	0.31	56
10	0.147	0.151	0.149	0.13	25	0.202	0.202	0.202	0.18	33
15	0.124	0.138	0.131	0.11	21	0.137	0.129	0.133	0.12	22
20	0.101	0.103	0.102	0.09	17	0.101	0.089	0.095	0.08	15
25	0.031	0.041	0.036	0.03	6	0069	0.071	0.070	0.06	11
30	0.019	0.041	0.030	0.03	6	0.060	0.042	0.051	0.04	7

Table 26 Thermal stability at 60 °C, pH 6, of α-amylase crosslinked with DMS (5-10 mg/mL)

Time (min)	5 mg/mL DMS					10 mg/mL DMS				
	A_{540}			Activity (U/mL)	Relative Activity (%)	A_{540}			Activity (U/mL)	Relative Activity (%)
	1	2	Average			1	2	Average		
0	0.588	0.584	0.586	0.51	100	0.623	0.641	0.632	0.55	100
5	0.355	0.349	0.352	0.31	61	0.387	0.371	0.379	0.33	60
10	0.198	0.212	0.205	0.18	35	0.236	0.232	0.234	0.20	36
15	0.131	0.127	0.129	0.11	22	0.126	0.125	0.126	0.11	20
20	0.076	0.075	0.076	0.07	14	0.109	0.105	0.107	0.09	16
25	0.064	0.054	0.059	0.05	10	0.088	0.076	0.082	0.07	13
30	0.053	0.052	0.053	0.05	10	0.055	0.071	0.063	0.06	11

Table 27 Thermal stability at 60 °C, pH 6, of α-amylase crosslinked with 10 mg/mL imidoesters

Time (min)	EA					DMA					DMP					DMS				
	A_{540}			Act	RA	A_{540}			Act	RA	A_{540}			Act	RA	A_{540}			Act	RA
	1	2	Av	(U/mL)	(%)	1	2	Av	(U/mL)	(%)	1	2	Av	(U/mL)	(%)	1	2	Av	(U/mL)	(%)
0	0.618	0.636	0.627	0.55	100	0.644	0648	0.646	0.56	100	0.636	0.644	0.640	0.56	100	0.626	0.632	0.629	0.55	100
5	0.400	0.396	0.398	0.35	63	0.409	0.405	0.407	0.35	63	0.409	0.411	0.410	0.36	64	0.364	0.374	0.369	0.32	59
10	0.269	0.271	0.270	0.23	43	0.243	0.247	0.245	0.21	38	0.278	0.274	0.276	0.24	43	0.201	0.205	0.203	0.18	32
15	0.175	0.174	0.175	0.15	28	0.162	0.162	0.162	0.14	25	0.167	0.185	0.176	0.15	28	0.129	0.141	0.135	0.12	21
20	0.110	0.116	0.113	0.10	18	0.111	0.121	0.116	0.10	18	0.109	0.105	0.107	0.09	17	0.092	0.094	0.093	0.08	15
25	0.082	0.094	0.088	0.08	14	0.083	0.071	0.077	0.07	12	0.075	0.074	0.075	0.07	12	0.069	0.069	0.069	0.06	11
30	0.063	0.064	0.064	0.06	10	0.071	0.072	0.072	0.06	11	0.044	0.054	0.049	0.04	8	0.051	0.047	0.049	0.04	8

RA Relative Activity

Table 28 Thermal stability at 60 °C, pH 6, of α-amylase crosslinked with 10 mg/mL DMP at pH 5, 6, 7 and 8

Time (min)	pH 5					pH 6					pH 7					pH 8				
	A_{540}			Act (U/mL)	RA (%)	A_{540}			Act (U/mL)	RA (%)	A_{540}			Act (U/mL)	RA (%)	A_{540}			Act (U/mL)	RA (%)
	1	2	Av			1	2	Av			1	2	Av			1	2	Av		
0	0.662	0.648	0.655	0.57	100	0.770	0.663	0.667	0.58	100	0.632	0.631	0.632	0.55	100	0.687	0.669	0.678	0.59	100
5	0.385	0.375	0.380	0.33	58	0.433	0.421	0.427	0.37	64	0.409	0.411	0.410	0.36	65	0.432	0.436	0.434	0.38	64
10	0.294	0.295	0.295	0.26	46	0.290	0.284	0.287	0.25	43	0.254	0.264	0.259	0.23	41	0.089	0.281	0.285	0.25	42
15	0.203	0.191	0.197	0.17	30	0.192	0.182	0.187	0.16	28	0.164	0.152	0.158	0.14	25	0.163	0.162	0.163	0.14	24
20	0.102	0.094	0.098	0.09	16	0.129	0.125	0.127	0.11	19	0.078	0.086	0.082	0.07	13	0.100	0.104	0.102	0.09	15
25	0086	0084	0.085	0.07	12	0.090	0.110	0.100	0.09	16	0.056	0.058	0.057	0.05	9	0.055	0.053	0.054	0.05	8
30	0.041	0.037	0.039	0.03	5	0.061	0.073	0.067	0.06	10	0.045	0.057	0.051	0.04	7	0.045	0.049	0.047	0.04	7

RA Relative Activity

1.1.4 Thermal stabilization by diamines

Table 29 Thermal stability of native α-amylase at 60 °C, pH 6, (Measurements 1-3)

Time (min)	Measurement 1					Measurement 2					Measurement 3				
	A_{540}			Activity (U/mL)	Relative activity (%)	A_{540}			Activity (U/mL)	Relative activity (%)	A_{540}			Activity (U/mL)	Relative activity (%)
	1	2	Average			1	2	Average			1	2	Average		
0	0.797	0.789	0.793	0.69	100	0.865	0.859	0.862	0.75	100	0.938	0.924	0.931	0.81	100
5	0.448	0.456	0.452	0.39	57	0.457	0.475	0.466	0.41	55	0.515	0.509	0.512	0.45	56
10	0.095	0.291	0.293	0.26	38	0.371	0.371	0.371	0.32	43	0.375	0.369	0.372	0.32	40
15	0.201	0.195	0.198	0.17	25	0.235	0.247	0.241	0.21	28	0.181	0.191	0.186	0.16	20
20	0.139	0.131	0.135	0.12	17	0.080	0.076	0.078	0.07	9	0.158	0.157	0.158	0.14	17
25	0.115	0.123	0.119	0.10	14	0.060	0.059	0.060	0.05	7	0.144	0.136	0.140	0.12	14
30	0.077	0.081	0.079	0.07	10	0.029	0.039	0.034	0.03	4	0056	0.038	0.047	0.04	5

Table 30 Thermal stability of native α-amylase at 60 °C, pH 6, (Measurements 4-6)

Time (min)	Measurement 4					Measurement 5					Measurement 6					Relative activity (average,%)	SD
	A_{540}			Activity (U/mL)	Relative activity (%)	A_{540}			Activity (U/mL)	Relative activity (%)	A_{540}			Activity (U/mL)	Relative activity (%)		
	1	2	Average			1	2	Average			1	2	Average				
0	0.949	0.959	0.954	0.83	100	0.838	0.818	0.828	0.72	100	0.881	0.867	0.874	0.76	100	100	0
5	0.559	0.567	0.563	0.49	59	0.418	0.442	0.430	0.37	51	0.443	0.449	0.446	0.39	51	55	3.25
10	0.291	0.281	0.286	0.25	30	0.343	0.335	0.339	0.30	42	0.251	0.255	0.253	0.22	29	37	6.07
15	0.186	0.176	0.181	0.16	19	0.185	0.179	0.182	0.16	22	0.229	0.225	0.227	0.20	26	23	3.56
20	0.133	0.135	0.134	0.12	14	0.124	0.123	0.124	0.11	15	0.218	0.184	0.201	0.17	22	16	4.27
25	0.100	0.110	0.105	0.09	11	0.082	0.100	0.091	0.08	11	0.143	0.137	0.140	0.12	16	12	3.19
30	0.038	0.037	0.038	0.03	4	0.039	0.061	0.050	0.04	6	0.096	0.096	0.096	0.08	11	7	3.08

Table 31 Thermal stability at 60 °C, pH 6, of α-amylase crosslinked with EDA (0.1-1 mg/mL)

Time (min)	0.1 mg/mL EDA					1 mg/mL EDA				
	A_{540}			Activity (U/mL)	Relative Activity (%)	A_{540}			Activity (U/mL)	Relative Activity (%)
	1	2	Average			1	2	Average		
0	0.560	0.566	0.563	0.49	100	0.533	0.547	0.540	0.47	100
5	0.297	0.311	0.304	0.26	53	0.296	0.287	0.297	0.26	55
10	0.210	0.218	0.214	0.19	39	0.223	0.209	0.216	0.19	40
15	0.135	0.134	0.135	0.12	24	0.139	0.131	0.135	0.12	26
20	0.086	0.082	0.084	0.07	14	0.065	0.053	0.059	0.05	11
25	0.072	0.064	0.068	0.06	12	0.072	0.068	0.070	0.06	13
30	0.035	0.021	0.028	0.02	4	0.041	0.045	0.043	0.04	9

Table 32 Thermal stability at 60 °C, pH 6, of α-amylase crosslinked with EDA (5-10 mg/mL)

Time (min)	5 mg/mL EDA					10 mg/mL EDA				
	A_{540}			Activity (U/mL)	Relative Activity (%)	A_{540}			Activity (U/mL)	Relative Activity (%)
	1	2	Average			1	2	Average		
0	0.582	0.568	0.575	0.50	100	0.536	0.522	0.529	0.46	100
5	0.309	0.311	0.310	0.27	54	0.255	0.263	0.259	0.23	50
10	0.231	0.217	0.224	0.20	40	0.183	0.187	0.185	0.16	35
15	0.117	0.125	0.121	0.11	22	0.100	0.099	0.100	0.09	20
20	0.055	0.059	0.057	0.05	10	0.055	0.041	0.048	0.04	9
25	0.052	0.051	0.052	0.05	10	0.016	0.015	0.016	0.01	2
30	0.048	0.044	0.046	0.04	8	0.014	0.028	0.021	0.02	4

Table 33 Thermal stability at 60 °C, pH 6, of α-amylase crosslinked with DAB (0.1-1 mg/mL)

Time (min)	0.1 mg/mL DAB					1 mg/mL DAB				
	A_{540}			Activity (U/mL)	Relative Activity (%)	A_{540}			Activity (U/mL)	Relative Activity (%)
	1	2	Average			1	2	Average		
0	0.450	0.446	0.448	0.39	100	0.550	0.554	0.552	0.48	100
5	0.245	0.231	0.238	0.21	54	0.311	0.307	0.309	0.27	56
10	0.174	0.176	0.175	0.15	38	0.231	0.221	0.226	0.20	42
15	0.108	0.134	0.121	0.11	28	0.154	0.153	0.154	0.13	27
20	0.076	0.076	0.076	0.07	18	0.067	0.077	0.072	0.06	13
25	0.043	0.055	0.049	0.04	10	0063	0.069	0.066	0.06	13
30	0031	0.013	0.022	0.02	5	0.054	0.046	0.050	0.04	8

Table 34 Thermal stability at 60 °C, pH 6, of α-amylase crosslinked with DAB (5-10 mg/mL)

Time (min)	5 mg/mL DAB					10 mg/mL DAB				
	A_{540}			Activity (U/mL)	Relative Activity (%)	A_{540}			Activity (U/mL)	Relative Activity (%)
	1	2	Average			1	2	Average		
0	0.483	0.459	0.471	0.41	100	0.492	0.474	0.483	0.42	100
5	0.201	0.205	0.203	0.18	44	0.229	0.225	0.227	0.20	48
10	0.164	0.166	0.165	0.14	34	0.167	0.181	0.174	0.15	36
15	0.058	0.084	0.071	0.06	15	0.088	0.076	0.082	0.07	17
20	0.047	0.029	0.038	0.03	7	0.042	0.043	0.043	0.04	10
25	0.013	0.015	0.014	0.01	2	0.031	0.037	0.034	0.03	7
30	0.019	0.019	0.019	0.02	5	0.022	0.016	0.019	0.02	5

Table 35 Thermal stability at 60 °C, pH 6, of α-amylase crosslinked with DAH (0.1-1 mg/mL)

Time (min)	0.1 mg/mL DAH					1 mg/mL DAH				
	A_{540}			Activity (U/mL)	Relative Activity (%)	A_{540}			Activity (U/mL)	Relative Activity (%)
	1	2	Average			1	2	Average		
0	0.594	0.578	0.586	0.51	100	0.666	0.598	0.632	0.55	100
5	0.299	0.311	0.305	0.27	53	0.340	0.342	0.341	0.30	55
10	0.201	0.185	0.193	0.17	33	0.271	0.247	0.259	0.23	42
15	0.122	0.124	0.123	0.11	22	0.161	0.167	0.164	0.14	25
20	0.081	0.071	0.076	0.07	14	0.076	0.102	0.089	0.08	15
25	0.064	0054	0.059	0.05	10	0.071	0.081	0.076	0.07	13
30	0037	0.032	0.035	0.03	6	0.066	0.060	0.063	0.06	11

Table 36 Thermal stability at 60 °C, pH 6, of α-amylase crosslinked with DAH (5-10 mg/mL)

Time (min)	5 mg/mL DAH					10 mg/mL DAH				
	A_{540}			Activity (U/mL)	Relative Activity (%)	A_{540}			Activity (U/mL)	Relative Activity (%)
	1	2	Average			1	2	Average		
0	0.540	0.564	0.552	0.48	100	0.540	0.518	0.529	0.46	100
5	0.301	0.305	0.303	0.26	54	0.251	0.267	0.259	0.23	50
10	0.220	0.221	0.221	0.19	40	0.181	0.189	0.185	0.17	37
15	0.096	0.114	0.105	0.09	19	0097	0.061	0.079	0.07	15
20	0.056	0.054	0.055	0.05	10	0.042	0.034	0.038	0.03	7
25	0.050	0.050	0.050	0.04	8	0.018	0.024	0.021	0.02	4
30	0.047	0.041	0.044	0.04	8	0.016	0.006	0.011	0.01	2

Table 37 Thermal stability at 60 °C of, pH 6, α-amylase crosslinked with DAO (0.1-1 mg/mL)

Time (min)	0.1 mg/mL DAO					1 mg/mL DAO				
	A_{540}			Activity (U/mL)	Relative Activity (%)	A_{540}			Activity (U/mL)	Relative Activity (%)
	1	2	Average			1	2	Average		
0	0.555	0.571	0.563	0.49	100	0.465	0.431	0.448	0.39	100
5	0.290	0.284	0.287	0.25	51	0.247	0.229	0.238	0.21	54
10	0.209	0.185	0.197	0.17	35	0.174	0.176	0.175	0.15	38
15	0.121	0.127	0.124	0.11	22	0.108	0.116	0.112	0.10	26
20	0.074	0.094	0.084	0.07	14	0.057	0.058	0.058	0.05	13
25	0.060	0.052	0.056	0.05	10	0.044	0.049	0.054	0.05	13
30	0.047	0.055	0.051	0.04	8	0.036	0.036	0.036	0.03	8

Table 38 Thermal stability at 60 °C, pH 6, of α-amylase crosslinked with DAO (5-10 mg/mL)

Time (min)	5 mg/mL DAO					10 mg/mL DAO				
	A_{540}			Activity (U/mL)	Relative Activity (%)	A_{540}			Activity (U/mL)	Relative Activity (%)
	1	2	Average			1	2	Average		
0	0.043	0.051	0.047	0.41	100	0.487	0.479	0.483	0.42	100
5	0.228	0.234	0.231	0.20	49	0.222	0.212	0.217	0.19	45
10	0.156	0.155	0.156	0.14	34	0.139	0.151	0.145	0.13	31
15	0.083	0.077	0.080	0.07	17	0.059	0.057	0.058	0.05	12
20	0.049	0.055	0.052	0.05	12	0.051	0.027	0.039	0.03	7
25	0.035	0.031	0.033	0.03	7	0.027	0.021	0.024	0.02	5
30	0.023	0.024	0.024	0.02	5	0.012	0.016	0.014	0.01	2

Table 39 Thermal stability at 60 °C, pH 6, of α-amylase crosslinked with DA10 (0.1-1 mg/mL)

Time (min)	0.1 mg/mL DA10					1 mg/mL DA10				
	A_{540}			Activity (U/mL)	Relative Activity (%)	A_{540}			Activity (U/mL)	Relative Activity (%)
	1	2	Average			1	2	Average		
0	0.539	0.541	0.540	0.47	100	0.514	0.498	0.506	0.44	100
5	0.272	0.280	0.276	0.24	51	0.252	0.244	0.248	0.22	50
10	0.205	0.217	0.211	0.18	38	0.198	0.186	0.192	0.17	39
15	0.135	0.135	0.135	0.12	26	0.140	0.134	0.137	0.12	27
20	0.081	0.091	0.086	0.08	17	0.075	0.077	0.076	0.07	16
25	0.055	0.063	0.059	0.05	11	0.056	0.055	0.056	0.05	11
30	0.056	0.052	0.054	0.05	11	0.038	0.054	0.046	0.04	9

Table 40 Thermal stability at 60 °C, pH 6, of α-amylase crosslinked with DA10 (5-10 mg/mL)

Time (min)	5 mg/mL DA10					10 mg/mL DA10				
	A_{540}			Activity (U/mL)	Relative Activity (%)	A_{540}			Activity (U/mL)	Relative Activity (%)
	1	2	Average			1	2	Average		
0	0.503	0.485	0.494	0.43	100	0.473	0.469	0.471	0.41	100
5	0.192	0.214	0.203	0.18	42	0.148	0.144	0.146	0.13	32
10	0.109	0.108	0.109	0.09	21	0096	0.084	0.090	0.08	20
15	0.081	0.067	0.074	0.06	14	0.055	0.049	0.052	0.05	12
20	0.057	0.061	0.059	0.05	12	0.021	0.027	0.024	0.02	5
25	0.032	0.038	0.035	0.03	7	0.014	0.014	0.014	0.01	2
30	0.036	0.044	0.040	0.03	7	0.029	0.009	0.019	0.02	5

Table 41 Thermal stability at 60 °C, pH 6, of α-amylase crosslinked with DAD (0.1-1 mg/mL)

Time (min)	0.1 mg/mL DAD					1 mg/mL DAD				
	A_{540}			Activity (U/mL)	Relative Activity (%)	A_{540}			Activity (U/mL)	Relative Activity (%)
	1	2	Average			1	2	Average		
0	0.540	0.564	0.552	0.48	100	0.579	0.571	0.575	0.50	100
5	0.298	0.276	0.287	0.25	52	0.240	0.241	0.241	0.21	42
10	0.216	0.226	0.221	0.19	40	0.203	0.199	0.201	0.18	36
15	0.119	0.123	0.121	0.11	23	0.141	0.147	0.144	0.13	26
20	0.104	0.105	0.105	0.09	19	0.081	0.079	0.080	0.07	14
25	0.075	0.057	0.066	0.06	13	0.071	0.079	0.075	0.07	14
30	0.053	0.035	0.044	0.04	8	0.027	0.041	0.034	0.03	6

Table 42 Thermal stability at 60 °C, pH 6, of α-amylase crosslinked with DAD (5-10 mg/mL)

Time (min)	5 mg/mL DAD					10 mg/mL DAD				
	A_{540}			Activity (U/mL)	Relative Activity (%)	A_{540}			Activity (U/mL)	Relative Activity (%)
	1	2	Average			1	2	Average		
0	0.522	0.512	0.517	0.45	100	0.534	0.546	0.540	0.47	100
5	0.202	0.201	0.202	0.18	40	0.160	0.154	0.157	0.14	30
10	0.137	0.121	0.129	0.11	24	0.081	0.091	0.086	0.08	17
15	0.072	0.071	0.072	0.06	13	0.051	0.057	0.054	0.05	11
20	0.064	0.078	0.071	0.06	13	0.032	0.032	0.032	0.03	7
25	0.029	0.033	0.031	0.03	7	0.017	0.005	0.011	0.01	2
30	0.026	0.025	0.026	0.02	4	0.020	0.024	0.022	0.02	4

Table 43 Thermal stability at 60 °C, pH 6, of α-amylase crosslinked with 1 mg/mL diamines

Time (min)	hydrazine					EDA					DAB				
	A_{540}			Activity (U/mL)	Relative activity (%)	A_{540}			Activity (U/mL)	Relative activity (%)	A_{540}			Activity (U/mL)	Relative activity (%)
	1	2	Average			1	2	Average			1	2	Average		
0	0.518	0.516	0.517	0.45	100	0.545	0.559	0.552	0.48	100	0.556	0.570	0.563	0.49	100
5	0.200	0.214	0.207	0.18	40	0.289	0.317	0.303	0.26	54	0.319	0.311	0.315	0.27	55
10	0.159	0.173	0.166	0.14	31	0.211	0.231	0.221	0.19	40	0.230	0.231	0.231	0.20	41
15	0.097	0.099	0.098	0.09	20	0.142	0.134	0.138	0.12	25	0.149	0.167	0.158	0.14	29
20	0.058	0.066	0.062	0.05	11	0.055	0.067	0.061	0.05	10	0.072	0.074	0.073	0.06	12
25	0.035	0.027	0.031	0.03	6	0.070	0.074	0.072	0.06	13	0.074	0.062	0.068	0.06	12
30	0.018	0.014	0.016	0.01	2	0.056	0.032	0.044	0.04	8	0.056	0.046	0.051	0.04	8

RA Relative Activity

Table 44 Thermal stability at 60 °C, pH 6, of α-amylase crosslinked with 1 mg/mL diamines

Time (min)	DAH					DAO					DA10					DAD				
	A_{540}			Act (U/mL)	RA (%)	A_{540}			Act (U/mL)	RA (%)	A_{540}			Act (U/mL)	RA (%)	A_{540}			Act (U/mL)	RA (%)
	1	2	Av			1	2	Av			1	2	Av			1	2	Av		
0	0.624	0.594	0.609	0.53	100	0.063	0.457	0.460	0.40	100	0.519	0.534	0.529	0.46	100	0.591	0.581	0.586	0.51	100
5	0.323	0.335	0.329	0.29	55	0.254	0.234	0.244	0.21	53	0.257	0.261	0.259	0.23	50	0.241	0.251	0.246	0.21	41
10	0.249	0.251	0.250	0.22	42	0.183	0.175	0.179	0.16	40	0.199	0.203	0.201	0.17	37	0.199	0.211	0.205	0.18	35
15	0.163	0.153	0.158	0.14	26	0.117	0.113	0.115	0.10	25	0.149	0.137	0.143	0.12	26	0.150	0.144	0.147	0.13	25
20	0.078	0.092	0.085	0.07	13	0.059	0.061	0.060	0.05	13	0.084	0.074	0.079	0.07	15	0.082	0.082	0.082	0.07	14
25	0.073	0.073	0.073	0.06	11	0.059	0.051	0.055	0.05	13	0.058	0.057	0.058	0.05	11	0.074	0.077	0.076	0.07	14
30	0.063	0.059	0.061	0.05	9	0.036	0.038	0.037	0.03	8	0.057	0.039	0.048	0.04	9	0.047	0.023	0.035	0.03	6

RA Relative Activity

Table 45 Thermal stability at 60 °C, pH 6, of α-amylase crosslinked with 1 mg/mL ethylenediamine at pH 5, 6, 7 and 8

Time (min)	pH 5					pH 6					pH 7					pH 8				
	A_{540}			Act (U/mL)	RA (%)	A_{540}			Act (U/mL)	RA (%)	A_{540}			Act (U/mL)	RA (%)	A_{540}			Act (U/mL)	RA (%)
	1	2	Av			1	2	Av			1	2	Av			1	2	Av		
0	0.555	0.571	0.563	0.49	100	0.593	0.579	0.586	0.51	100	0.539	0.541	0.540	0.47	100	0.501	0.511	0.506	0.44	100
5	0.305	0.281	0.293	0.26	53	0.323	0.321	0.322	0.28	55	0.305	0.311	0.308	0.27	57	0.292	0.314	0.303	0.26	59
10	0.208	0.186	0.197	0.17	35	0.235	0.245	0.240	0.21	41	0.247	0.261	0.254	0.22	47	0.222	0.234	0.228	0.20	45
15	0.084	0.074	0.079	0.07	14	0.146	0.148	0.147	0.13	25	0.127	0.111	0.119	0.10	21	0.101	0.100	0.101	0.09	20
20	0.078	0.058	0.068	0.06	12	0.079	0.085	0.082	0.07	14	0.094	0.112	0.103	0.09	19	0071	0.081	0.076	0.07	16
25	0.056	0.055	0.056	0.05	10	0.072	0.068	0.070	0.06	12	0.085	0.077	0.081	0.07	15	0.043	0.059	0.051	0.04	9
30	0.047	0.31	0.039	003	6	0.055	0.039	0.047	0.04	8	0.042	0.044	0.043	0.04	9	0.033	0.037	0.035	0.03	7

RA Relative Activity

1.2 β-Galactosidase

1.2.1 Properties of native β-Galactosidase

Table 46 Optimum pH of β-galactosidase (5 mg/mL) at room temperature

pH	Dilution (×)	A_{410}			Activity (Unit/mL)
		1	2	Average	
3	100	0.296	0.302	0.299	26
4	100	0.344	0.340	0.342	30
5	100	0.329	0.338	0.334	29
6	100	0.187	0.195	0.191	17
7	10	0.389	0.397	0.393	3.4
8	10	0.182	0.184	0.183	1.6
9	5	0.144	0.141	0.143	0.6
10	-	0.041	0.040	0.141	0.1

Activity calculations followed the methods in Section 3.2.3.2

Table 47 Optimum temperature of β-galactosidase, pH 3.5

Temperature (°C)	Dilution (×)	A_{410}			Activity (Unit/mL)
		1	2	Average	
25	100	0.282	0.289	0.286	25
30	100	0.394	0.343	0.369	32
40	100	0.450	0.438	0.444	39
50	100	0.613	0.609	0.611	53
55	100	0.574	0.585	0.580	50
60	10	0.492	0.463	0.478	42
65	10	0.222	0.201	0.212	18
70	-	0.521	0.512	0.517	4
75	-	0.218	0.184	0.201	2
80	-	0.477	0.520	0.499	0.4
85	-	0.056	0.044	0.050	0.04
90	-	0.016	0.021	0.019	0.02

Table 48 The absorbance at 410 nm of β-galactosidase (5 mg/mL, dilution = ×10) for pH stability at 25 °C

Time (min)	A_{410}														
	pH 4			pH 5			pH 6			pH 7			pH 8		
	1	2	Average	1	2	Average	1	2	Average	1	2	Average	1	2	Average
0	0.412	0.410	0.411	0.430	0.323	0.377	0.466	0.452	0.459	0.177	0.177	0.177	0.261	0.271	0.266
5	0.420	0.410	0.415	0.399	0.440	0.420	0.452	0.456	0.454	0.210	0.180	0.195	0.252	0.264	0.258
10	0.438	0.435	0.437	0.450	0.431	0.441	0.475	0.464	0.470	0.181	0.216	0.199	0.267	0.259	0.263
20	0.421	0.431	0.426	0.457	0.456	0.457	0.466	0.440	0.453	0.217	0.205	0.211	0.265	0.245	0.255
30	0.397	0.385	0.391	0.425	0.464	0.445	0.492	0.473	0.483	0.204	0.203	0.203	0.245	0.259	0.252
40	0.433	0.410	0.422	0.460	0.462	0.461	0.477	0.483	0.480	0.204	0.152	0.178	0.269	0.254	0.261
60	0.443	0.380	0.414	0.468	0.474	0.471	0.499	0.464	0.482	0.219	0.209	0.214	0.270	0.254	0.262
80	0.414	0.406	0.410	0.480	0.472	0.476	0.487	0.492	0.490	0.222	0.180	0.201	0.268	0.268	0.268
100	0.414	0.417	0.416	0.420	0.470	0.445	0.490	0.454	0.472	0.196	0.225	0.211	0.276	0.241	0.259
120	0.431	0.427	0.429	0.468	0.433	0.451	0.485	0.482	0.484	0.228	0.165	0.197	0.259	0.249	0.254

Table 49 pH stability of β-galactosidase at 25 °C

Time (min)	Activity (Unit/mL)					Relative activity (%)				
	pH 4	pH 5	pH 6	pH 7	pH 8	pH 4	pH 5	pH 6	pH 7	pH 8
0	21	20	24	11	14	100	100	100	100	100
5	22	22	24	10	13	105	110	100	91	93
10	23	23	25	10	14	110	115	104	91	100
20	22	24	24	11	13	105	120	100	100	93
30	20	23	25	11	13	95	115	104	100	93
40	22	24	25	9	14	105	120	104	82	100
60	22	25	25	11	14	105	125	104	100	100
80	21	25	26	11	14	100	125	108	100	100
100	22	24	25	11	13	105	120	104	100	93
120	22	24	25	10	13	105	120	104	91	93

Table 50 pH stability of β-galactosidase at 50 °C

Time (min)	Activity (Unit/mL)					Relative activity (%)				
	pH 4	pH 5	pH 6	pH 7	pH 8	pH 4	pH 5	pH 6	pH 7	pH 8
0	22	25	25	26	27	100	100	100	100	100
5	19	26	27	27	1.2	86	104	108	104	4
10	22	27	28	25	0	100	108	112	96	0
20	23	27	27	23	0	105	108	108	88	0
30	22	26	29	23	0	100	104	116	88	0
40	21	26	27	22	0	95	104	108	85	0
60	21	28	29	20	0	95	112	116	77	0
80	18	29	27	15	0	82	116	108	58	0
100	20	30	30	17	0	91	120	120	65	0
120	18	31	33	18	0	82	124	132	69	0

Table 51 The absorbance at 410 nm of β-galactosidase (5 mg/mL, dilution = ×10) for pH stability at 50 °C

Time (min)	A_{410}														
	pH 4			pH 5			pH 6			pH 7			pH 8		
	1	2	Average	1	2	Average	1	2	Average	1	2	Average	1	2	Average
0	0.520	0.505	0.513	0.577	0.562	0.570	0.566	0.572	0.569	0.603	0.598	0.601	0.608	0.641	0.625
5	0.428	0.440	0.434	0.586	0.592	0.589	0.618	0.633	0.626	0.606	0.620	0.613	0.042	0.011	0.027
10	0.475	0.520	0.498	0.624	0.623	0.624	0.642	0.626	0.634	0.591	0.563	0.577	0	0	0
20	0.537	0.518	0.528	0.641	0.593	0.617	0.580	0.657	0.619	0.548	0.527	0.538	0	0	0
30	0.547	0.455	0.501	0.580	0.615	0.598	0.665	0.649	0.657	0.536	0.524	0.530	0	0	0
40	0.516	0.472	0.494	0.623	0.584	0.604	0.627	0.597	0.612	0.505	0.488	0.497	0	0	0
60	0.483	0.464	0.474	0.652	0.650	0.651	0.669	0.651	0.660	0.460	0.462	0.461	0	0	0
80	0.412	0.396	0.404	0.646	0.691	0.669	0.554	0.677	0.616	0.344	0.448	0.346	0	0	0
100	0.461	0.443	0.452	0.693	0.709	0.701	0.673	0.706	0.690	0.361	0.434	0.398	0	0	0
120	0.451	0.372	0.417	0.726	0.713	0.720	0.794	0.742	0.768	0.384	0.451	0.418	0	0	0

Table 52 The absorbance at 540 nm of β-galactosidase (5 mg/mL, dilution = ×50) for its thermal stability at 25-65 °C, pH 7

Time (min)	25 °C			30 °C			40 °C			50 °C			55 °C			60 °C			65 °C		
	1	2	Av	1	2	Av	1	2	Av	1	2	Av	1	2	Av	1	2	Av	1	2	Av
0	0.527	0.502	0.515	0.524	0.532	0.528	0.507	0.523	0.515	0.550	0.519	0.535	0.461	0.457	0.459	0.484	0.463	0.474	0.485	0.468	0.477
5	0.520	0.532	0.526	0510	0.553	0.532	0.520	0.552	0.536	0.530	0.526	0.528	0.481	0.485	0.483	0.501	0.501	0.501	0.320	0.322	0.321
10	0.509	0.518	0.514	0.545	0.549	0.547	0.514	0.550	0.532	0.524	0.518	0.521	0.502	0.451	0.477	0.458	0.459	0.459	0.213	0.215	0.214
20	0.523	0.504	0.514	0.558	0.548	0.553	0.563	0.574	0.569	0.531	0.549	0.540	0.509	0.438	0.474	0.442	0.458	0.450	0.111	0.113	0.112
30	0.535	0.533	0.534	0.551	0.535	0.543	0.567	0.545	0.556	0.550	0.536	0.543	0.516	0.472	0.494	0.357	0.353	0.355	0.292	0.292	0.292*
40	0.517	0.537	0.527	0.562	0.552	0.557	0.521	0.500	0.511	0.543	0.525	0.534	0.526	0.486	0.506	0.389	0.380	0.385	0.200	0.202	0.201*
60	0.526	0.535	0.531	0.556	0.552	0.554	0.495	0.509	0.502	0.503	0.535	0.519	0.534	0.519	0.527	0.318	0.335	0.327	0.090	0.084	0.087*
80	0.534	0.540	0.537	0.552	0.555	0.554	0.544	0.533	0.539	0.552	0.539	0.546	0.470	0.475	0.473	0.356	0.354	0.355	0.040	0.040	0.040*
100	0.539	0.560	0.550	0.561	0.552	0.557	0.566	0.493	0.530	0.579	0.585	0.582	0.544	0.552	0.548	0.333	0.326	0.330	0.022	0.023	0.023*
120	0.540	0.532	0.536	0.562	0.551	0.557	0.566	0.534	0.550	0.587	0.592	0.590	0.458	0.515	0.487	0.271	0.289	0.280	0.013	0.014	0.014*

* dilution = ×10

Table 53 Thermal denaturation of β-galactosidase at 25-65 °C, pH 6

Time (min)	Activity (Unit/mL)						
	25 °C	30 °C	40 °C	50 °C	55 °C	60 °C	65 °C
0	22	23	22	23	20	21	21
5	23	23	23	23	21	22	14
10	22	24	23	23	21	20	9
20	22	24	25	23	21	20	5
30	23	24	24	24	21	15	3
40	23	24	22	23	22	17	2
60	23	24	22	23	23	14	1
80	23	24	23	24	21	15	0.3
100	24	24	23	25	24	14	0.2
120	23	24	24	26	21	12	0.1

Table 54 Absorbance at 540 nm of β-galactosidase (5 mg/mL, dilution = ×50) for the estimation of E_d and k_d at pH 6

Time (min)	A_{410}											
	55 °C			60 °C			65 °C			70 °C		
	1	2	Average	1	2	Average	1	2	Average	1	2	Average
0	0.663	0.603	0.633	0.713	0.699	0.706	0.632	0.623	0.628	0.555	0.625	0.590
1	0.678	0.660	0.669	0.694	0.693	0.694	0.344	0.350	0.347	0039	0.026	0.033
2	0.688	0.670	0.679	0.693	0.690	0.692	0.283	0.273	0.278	0.037	0.036	0.037*
3	0.697	0.663	0.680	0.680	0.682	0.681	0.248	0.243	0.246	0.214	0.223	0.219**
4	0.684	0.667	0.676	0.667	0.643	0.655	0.205	0.211	0.208	0.097	0.097	0.097
5	0.674	0.651	0.663	0.660	0.625	0.643	0.187	0.186	0.187	-	-	-
6	0.671	0.668	0.670	0.658	0.620	0.639	0.153	0.148	0.151	-	-	-
7	0.662	0.665	0.664	0.605	0.599	0.602	0.135	0.123	0.129	-	-	-
8	0.665	0.676	0.671	0.640	0.572	0.606	0.116	0.112	0.114	-	-	-
9	0.654	0.646	0.650	0.588	0.575	0.582	0.104	0.102	0.103	-	-	-
10	0.666	0.671	0.669	0.632	0.587	0.610	0.082	0.084	0.083	-	-	-
12	0.620	0.637	0.629	0.557	0.547	0.552	0.062	0.058	0.060	-	-	-
14	0.625	0.636	0.631	0.586	0.542	0.564	0.047	0.048	0.048	-	-	-
16	0.634	0.642	0.638	0.572	0.493	0.533	0.035	0.035	0.035	-	-	-
18	0.655	0.643	0.649	0.526	0.517	0.522	0.132	0.120	0.126*	-	-	-
20	0.589	0.582	0.586	0.511	0.460	0.486	0.113	0.101	0.107*	-	-	-
22	0.627	0.599	0.613	0.488	0.488	0.488	0.097	0.090	0.094*	-	-	-
24	0.643	0.653	0.648	0.457	0.396	0.427	0.080	0.071	0.076*	-	-	-

Time (min)	A_{410}											
	55 °C			60 °C			65 °C			70 °C		
	1	2	Average	1	2	Average	1	2	Average	1	2	Average
26	0.622	0.614	0.618	0.424	0.420	0.422	0.051	0.055	0.053*	-	-	-
28	0.570	0.574	0.572	0.464	0.461	0.463	0.050	0.046	0.048*	-	-	-
30	0.590	0.592	0.591	0.444	0.445	0.445	0.052	0.042	0.047*	-	-	-
40	0.638	0.635	0.637	0.366	0.347	0.357	0.225	0.216	0.221**	-	-	-
60	0.600	0.606	0.603	0.276	0.241	0.259	0.052	0.049	0.051**	-	-	-
80	0.656	0.643	0.650	0.207	0.203	0.205	0.027	0.022	0.025**	-	-	-
100	0.686	0.705	0.696	0.133	0.133	0.133	0.026	0..026	0.026**	-	-	-
120	0.710	0.617	0.664	0.102	0.111	0.107	-	-	-	-	-	-

* dilution = ×10

** no dilution

Table 55 The estimation of E_d and k_d for β-galactosidase, pH 6

Time (min)	Activity (Unit/mL)				Relative activity (%)				v_f				ln v_f			
	55 °C	60°C	65 °C	70 °C	55 °C	60°C	65 °C	70 °C	55 °C	60°C	65 °C	70 °C	55 °C	60°C	65 °C	70 °C
0	28	31	27	26	100	100	100	100	1	1	1	1	0	0	0	0
1	29	30	15	1.4	104	97	56	5.4	1.04	0.97	0.56	0.05	0.04	-0.03	-0.59	-2.92
2	30	30	12	0.3	107	97	44	1.2	1.07	0.97	0.44	0.01	0.07	-0.03	-0.81	-4.46
3	30	30	11	0.2	107	97	41	0.8	1.07	0.97	0.41	0.01	0.07	-0.03	-0.90	-4.87
4	29	28	9	0.1	104	90	33	0.4	1.04	0.90	0.33	0	0.04	-0.10	-1.10	-5.56
5	29	28	8.1	-	104	90	30	-	1.04	0.90	0.30	-	0.04	-0.10	-1.20	-
6	29	28	6.6	-	104	90	24	-	1.04	0.90	0.24	-	0.04	-0.10	-1.41	-
7	29	26	5.6	-	104	84	21	-	1.04	0.84	0.21	-	0.04	-0.18	-1.57	-
8	29	26	5.0	-	104	84	19	-	1.04	0.84	0.19	-	0.04	-0.18	-1.69	-
9	28	25	4.5	-	100	81	17	-	1	0.81	0.17	-	0	-0.22	-1.79	-
10	29	27	3.6	-	104	87	13	-	1.04	0.87	0.13	-	0.04	-0.14	-2.01	-
12	27	24	2.6	-	96	77	9.6	-	0.96	0.77	0.10	-	-0.04	-0.26	-2.34	-
14	27	25	2.1	-	96	81	7.8	-	0.96	0.81	0.08	-	-0.04	-0.22	-2.55	-
16	28	23	1.5	-	100	74	5.6	-	1	0.74	0.06	-	0	-0.30	-2.89	-
18	28	23	1.1	-	100	74	4.1	-	1	0.74	0.04	-	0	-0.30	-3.20	-
20	25	21	0.9	-	89	68	3.3	-	0.89	0.68	0.03	-	-0.11	-0.39	-3.40	-
22	27	21	0.8	-	96	68	3.0	-	0.96	0.68	0.03	-	-0.04	-0.39	-3.52	-
24	28	19	0.7	-	100	61	2.6	-	1	0.61	0.03	-	0	-0.49	-3.65	-
26	27	18	0.5	-	96	58	1.9	-	0.96	0.58	0.02	-	-0.04	-0.54	-3.99	-
28	25	20	0.4	-	89	65	1.5	-	0.89	0.65	0.01	-	-0.11	-0.44	-4.21	-

Time (min)	Activity (Unit/0.4mL)				Relative activity (%)				v_f				ln v_f			
	55 °C	**60°C**	**65 °C**	**70 °C**	**55 °C**	**60°C**	**65 °C**	**70 °C**	**55 °C**	**60°C**	**65 °C**	**70 °C**	**55 °C**	**60°C**	**65 °C**	**70 °C**
30	26	19	0.4	-	93	61	1.5	-	0.93	0.61	0.01	-	-0.07	-0.49	-4.21	-
40	28	16	0.19	-	100	52	0.7	-	1	0.52	0.01	-	0	-0.66	-4.96	-
60	26	11	0.04	-	93	35	0	-	0.93	0.35	0	-	-0.07	-1.04	-6.51	-
80	28	8.9	0.02	-	100	29	0	-	1	0.29	0	-	0	-1.25	-7.21	-
100	30	5.8	0.02	-	107	19	0	-	1.07	0.19	0	-	0.07	-1.68	-7.21	-
120	29	4.7	-	-	104	15	-	-	1.04	0.15	-	-	0.04	-1.89	-	-

1.2.2 Thermal stabilization by isocyanates

Table 56 Thermal stability of native β-galactosidase at 60 °C, pH 6

Time (min)	Measurement 1					Measurement 2					Measurement 3					Relative activity (average,%)	SD
	A_{410}			Activity (U/mL)	Relative activity (%)	A_{410}			Activity (U/mL)	Relative activity (%)	A_{410}			Activity (U/mL)	Relative activity (%)		
	1	2	Average			1	2	Average			1	2	Average				
0	0.0167	0.166	0.167*	2.9	100	0.142	0.146	0.144*	2.5	100	0.146	0.164	0.155*	2.7	100	100	0
10	0.131	0.119	0.125*	2.2	76	0.106	0.118	0.112*	2.0	80	0.119	0.117	0.118*	2.1	78	78	2
20	0.228	0.218	0.223**	1.9	66	0.213	0.219	0.216**	1.9	76	0.238	0.216	0.227**	2.0	74	72	5.29
40	0.198	0.216	0.207**	1.8	62	0.197	0.189	0.193**	1.7	68	0.199	0.211	0.205**	1.8	67	66	3.21
60	0.169	0.177	0.173**	1.5	52	0.169	0.147	0.158**	1.4	56	0.182	0.184	0.183**	1.6	59	56	3.51
90	0.135	0.125	0.130**	1.1	38	0.108	0.134	0.121**	1.1	44	0.127	0.109	0.118**	1.0	37	40	3.79

*dilution = ×20

**dilution = ×10

Table 57 Thermal stability at 60 °C, pH 6, of β-galactosidase crosslinked with BMDC (10-20 mM)

Time (min)	10 mM BMDC					20 mM BMDC				
	A_{410}			Activity (U/mL)	Relative activity (%)	A_{410}			Activity (U/mL)	Relative activity (%)
	1	2	Average			1	2	Average		
0	0.123	0.119	0.121*	2.1	100	0.124	0.106	0.115*	2.0	100
10	0.092	0.114	0.103*	1.8	86	0.091	0.099	0.095*	1.7	85
20	0.186	0.185	0.186**	1.6	76	0.173	0.177	0.175**	1.5	75
40	0.159	0.165	0.162**	1.4	67	0.156	0.142	0.149**	1.3	65
60	0.133	0.119	0.126**	1.1	52	0.134	0.124	0.129**	1.1	55
90	0.086	0.098	0.092**	0.8	38	0.083	0.091	0.087**	0.8	40

Table 58 Thermal stability at 60 °C, pH 6, of β-galactosidase crosslinked with BMDC (30-50 mM)

Time (min)	30 mM BMDC					40 mM BMDC					50 mM BMDC				
	A_{410}			Activity (U/mL)	Relative activity (%)	A_{410}			Activity (U/mL)	Relative activity (%)	A_{410}			Activity (U/mL)	Relative activity (%)
	1	2	Average			1	2	Average			1	2	Average		
0	0.102	0.104	0.103*	1.8	100	0.125	0.127	0.126*	2.2	100	0.120	0.122	0.121*	2.1	100
10	0.088	0.090	0.089*	1.5	83	0.096	0.106	0.101*	1.8	82	0.103	0.087	0.095*	1.7	81
20	0.159	0.155	0.157**	1.4	78	0.176	0.177	0.177**	1.5	68	0.068	0.166	0.167**	1.4	67
40	0.132	0.128	0.130**	1.1	61	0.147	0.161	0.154**	1.3	59	0.139	0.141	0.140**	1.2	57
60	0.088	0.114	0.101**	0.9	50	0.124	0.124	0.124**	1.1	50	0.105	0.106	0.106**	0.9	43
90	0.089	0.065	0.077**	0.7	39	0.074	0.078	0.076**	0.7	32	0.065	0.075	0.070**	0.6	29

*dilution = ×20

**dilution = ×10

Table 59 Thermal stability at 60 °C, pH 6, of β-galactosidase crosslinked with HMDC (10-20 mM)

Time (min)	10 mM HMDC					20 mM HMDC				
	A_{410}			Activity (U/mL)	Relative activity (%)	A_{410}			Activity (U/mL)	Relative activity (%)
	1	2	Average			1	2	Average		
0	0.132	0.131	0.132*	2.3	100	0.131	0.121	0.126*	2.2	100
10	0.096	0.118	0.107*	1.9	83	0.093	0.097	0.095*	1.7	77
20	0.194	0.196	0.198**	1.7	74	0.202	0.188	0.195**	1.7	77
40	0.160	0.168	0.164**	1.4	61	0.163	0.155	0.159**	1.4	64
60	0.123	0.131	0.127**	1.1	48	0.134	0.124	0.129**	1.1	50
90	0.103	0.102	0.103**	0.9	39	0.086	0.102	0.094**	0.8	36

Table 60 Thermal stability at 60 °C, pH 6, of β-galactosidase crosslinked with HMDC (30-50 mM)

Time (min)	30 mM HMDC					40 mM HMDC					50 mM HMDC				
	A_{410}			Activity (U/mL)	Relative activity (%)	A_{410}			Activity (U/mL)	Relative activity (%)	A_{410}			Activity (U/mL)	Relative activity (%)
	1	2	average			1	2	average			1	2	average		
0	0.143	0.145	0.144*	2.5	100	0.145	0.131	0.138*	2.4	100	0.129	0.123	0.126*	2.2	100
10	0.129	0.109	0.119*	2.1	84	0.108	0.112	0.110*	1.9	79	0.097	0.101	0.099*	1.7	77
20	0.231	0.223	0.227**	2.0	80	0.182	0.181	0.182**	1.6	67	0.157	0.156	0.157**	1.4	64
40	0.189	0.167	0.178**	1.6	64	0.166	0.154	0.160**	1.4	58	0.139	0.129	0.134**	1.2	54
60	0.149	0.139	0.144**	1.3	52	0.143	0.133	0.138**	1.2	50	0.130	0.122	0.126**	1.1	50
90	0.112	0.112	0.112**	1.0	40	0.108	0.107	0.108**	0.9	38	0.071	0.075	0.073**	0.6	27

*dilution = ×20

**dilution = ×10

Table 61 Thermal stability at 60 °C, pH 6, of β-galactosidase crosslinked with OMDC (10-20 mM)

Time (min)	10 mM OMDC					20 mM OMDC				
	A_{410}			Activity (U/mL)	Relative activity (%)	A_{410}			Activity (U/mL)	Relative activity (%)
	1	2	Average			1	2	Average		
0	0.126	0.138	0.132*	2.3	100	0.137	0.151	0.144*	2.5	100
10	0.109	0.105	0.107*	1.9	83	0.120	0.116	0.118*	2.1	84
20	0.201	0.207	0.204**	1.8	78	0.203	0.211	0.207**	1.8	72
40	0.160	0.161	0.161**	1.4	61	0.186	0.188	0.187**	1.6	64
60	0.127	0.111	0.119**	1.0	43	0.153	0.135	0.144**	1.3	52
90	0.090	0.096	0.093**	0.8	35	0.126	0.098	0.112**	1.0	40

Table 62 Thermal stability at 60 °C, pH 6, of β-galactosidase crosslinked with OMDC (30-50 mM)

Time (min)	30 mM OMDC					40 mM OMDC					50 mM OMDC				
	A_{410}			Activity (U/mL)	Relative activity (%)	A_{410}			Activity (U/mL)	Relative activity (%)	A_{410}			Activity (U/mL)	Relative activity (%)
	1	2	Average			1	2	Average			1	2	Average		
0	0.140	0.132	0.138*	2.4	100	0.126	0.116	0.121*	2.1	100	0.135	0.141	0.138*	2.4	100
10	0.112	0.122	0.117*	2.0	83	0.091	0.095	0.093*	1.6	76	0.103	0.113	0.108*	1.9	79
20	0.220	0.222	0.221**	1.9	79	0.152	0.162	0.157**	1.4	67	0.173	0.163	0.168**	1.5	63
40	0.204	0.184	0.196**	1.7	71	0.150	0.144	0.147**	1.3	62	0.157	0.141	0.149**	1.3	54
60	0.181	0.155	0.168**	1.4	58	0.121	0.131	0.126**	1.1	52	0.141	0.129	0.135**	1.2	50
90	0.124	0.123	0.124**	1.1	46	0.089	0.079	0.084**	0.7	33	0.087	0.073	0.080**	0.7	29

*dilution = ×20

**dilution = ×10

Table 63 Thermal stability at 60 °C, pH 6, of β-galactosidase crosslinked with 30 mM isocyanates

Time (min)	BIC					BMDC					HMDC					OMDC				
	A_{410}			Act (U/mL)	RA (%)	A_{410}			Act (U/mL)	RA (%)	A_{410}			Act (U/mL)	RA (%)	A_{410}			Act (U/mL)	RA (%)
	1	2	Av			1	2	Av			1	2	Av			1	2	Av		
0	0.130	0.125	0.128*	2.2	100	0.116	0.117	0.117*	2.0	100	0.137	0.138	0.138*	2.4	100	0.141	0.137	0.139*	2.4	100
10	0.080	0.080	0.080*	1.4	63	0.202	0.200	0.201*	1.7	86	0.234	0.236	0.235*	2.0	85	0.244	0.238	0.241*	2.1	87
20	0.143	0.130	0.137**	1.2	54	0.173	0.176	0.175**	1.5	75	0.199	0.220	0.210**	1.8	76	0.216	0.217	0.217**	1.9	78
40	0.087	0.089	0.088**	0.8	35	0.145	0.140	0.143**	1.2	61	0.190	0.187	0.189**	1.6	69	0.186	0.181	0.184**	1.6	66
60	0.075	0.072	0.074**	0.6	29	0.116	0.117	0.117**	1.0	50	0.165	0.165	0.165**	1.4	60	0.160	0.163	0.162**	1.4	58
90	0.051	0.047	0.049**	0.4	19	0.083	0.084	0.084**	0.7	36	0.137	0.135	0.136**	1.2	49	0.140	0.138	0.139**	1.2	50

RA Relative Activity

*dilution = ×20

**dilution = ×10

Table 64 Thermal stability at 60 °C, pH 6, of β-galactosidase crosslinked with 30 mM OMDC at pH 5, 6, 7 and 8

Time (min)	pH 5					pH 6					pH 7					pH 8				
	A_{410}			Act (U/mL)	RA (%)	A_{410}			Act (U/mL)	RA (%)	A_{410}			Act (U/mL)	RA (%)	A_{410}			Act (U/mL)	RA (%)
	1	2	Av			1	2	Av			1	2	Av			1	2	Av		
0	0.249	0.146	0.428*	2.2	100	0.253	0.250	0.252*	2.2	100	0.263	0.261	0.262*	2.3	100	0.164	0.162	0.163	1.4	100
10	0.180	0.217	0.199*	1.7	80	0.230	0.238	0.234*	2.0	93	0.214	0.215	0.215*	1.9	82	0.127	0.127	0.127	1.1	78
20	0.192	0.188	0.190*	1.7	77	0.195	0.208	0.202*	1.8	80	0.184	0.182	0.183*	1.6	70	0.100	0.100	0.100	0.89	63
40	0.160	0.164	0.162*	1.4	65	0.173	0.172	0.173*	1.5	69	0.150	0.150	0.150*	1.3	57	0.080	0.080	0.080	0.70	49
60	0.268	0.274	0.271**	1.2	55	0.312	0.321	0.317**	1.4	63	0.241	0.241	0.241**	1.0	46	0.123	0.118	0.118	0.52	37
90	0.240	0.238	0.239**	1.0	48	0.262	0.266	0.264**	1.1	52	0.194	0.198	0.196**	0.9	37	0.094	0.094	0.094	0.41	29

RA Relative Activity

*dilution = ×10

**dilution = ×5

1.2.3 Thermal stabilization by imidoesters

Table 65 Thermal stability of native β-galactosidase at 60 °C, pH 6

Time (min)	Measurement 1					Measurement 2					Measurement 3					Relative activity (average,%)	SD
	A_{410}			Activity (U/mL)	Relative activity (%)	A_{410}			Activity (U/mL)	Relative activity (%)	A_{410}			Activity (U/mL)	Relative activity (%)		
	1	2	Average			1	2	Average			1	2	Average				
0	0.309	0.311	0.310*	2.7	100	0.295	0.303	0.299*	2.6	100	0.325	0.321	0.323*	2.8	100	100	0
5	0.277	0.275	0.276*	2.4	89	0.278	0.277	0.278*	2.4	92	0.296	0.290	0.293*	2.5	89	90	1.73
10	0.255	0.261	0.258*	2.2	81	0.238	0.246	0.242*	2.1	81	0.247	0.255	0.251*	2.2	79	80	1.15
20	0.235	0.249	0.242*	2.1	78	0.216	0.214	0.215*	1.9	73	0.243	0.247	0.245*	2.1	75	75	2.52
40	0.179	0.181	0.180*	1.6	59	0.193	0.183	0.188*	1.6	62	0.178	0.188	0.183*	1.6	57	59	2.52
60	0.308	0.288	0.298**	1.3	48	0.322	0.312	0.317**	1.4	54	0.302	0.303	0.303**	1.3	46	49	4.16
90	0.255	0.241	0.248**	1.1	41	0.275	0.274	0.275**	1.2	46	0.248	0.254	0.251**	1.1	39	42	3.61

*dilution = ×10

**dilution = ×5

Table 66 Thermal stability at 60 °C, pH 6, of β-galactosidase crosslinked with DMA (1-10 mg/mL)

Time (min)	1 mg/mL DMA					5 mg/mL DMA					10 mg/mL DMA				
	A_{410}			Activity (U/mL)	Relative activity (%)	A_{410}			Activity (U/mL)	Relative activity (%)	A_{410}			Activity (U/mL)	Relative activity (%)
	1	2	Average			1	2	Average			1	2	Average		
0	0.308	0.312	0.310*	2.7	100	0.289	0.285	0.287*	2.5	100	0.324	0.320	0.322*	2.8	100
5	0.299	0.298	0.299*	2.5	93	0.261	0.261	0.261*	2.3	92	0.285	0.281	0.283*	2.5	89
10	0.259	0.267	0.263*	2.3	85	0.232	0.228	0.230*	2.0	80	0.268	0.254	0.261*	2.3	82
20	0.245	0.239	0.242*	2.1	78	0.194	0.216	0.210*	1.8	72	0.232	0.231	0.232*	2.0	71
40	0.188	0.184	0.186*	1.6	59	0.178	0.172	0.175*	1.5	60	0.195	0.191	0.193*	1.7	61
60	0.325	0.309	0.317**	1.4	52	0.287	0.288	0.287**	1.3	52	0.301	0.305	0.303**	1.3	46
90	0.293	0.291	0.292**	1.3	48	0.281	0.271	0.276**	1.2	48	0.248	0.254	0.251**	1.1	39

*dilution = ×10

**dilution = ×5

Table 67 Thermal stability at 60 °C, pH 6, of β-galactosidase crosslinked with DMP (1-10 mg/mL)

Time (min)	1 mg/mL DMP					5 mg/mL DMP					10 mg/mL DMP				
	A_{410}			Activity (U/mL)	Relative activity (%)	A_{410}			Activity (U/mL)	Relative activity (%)	A_{410}			Activity (U/mL)	Relative activity (%)
	1	2	Average			1	2	Average			1	2	Average		
0	0.303	0.295	0.299*	2.6	100	0.324	0.320	0.322*	2.8	100	0.309	0.311	0.310*	2.7	100
5	0.280	0.281	0.281*	2.4	92	0.227	0.221	0.224*	2.6	93	0.281	0.277	0.279*	2.4	89
10	0.254	0.248	0.251*	2.2	85	0.258	0.250	0.254*	2.2	79	0.253	0.255	0.254*	2.2	81
20	0.227	0.221	0.224*	2.0	77	0.239	0.243	0.241*	2.1	75	0.231	0.241	0.236*	2.1	78
40	0.174	0.188	0.182*	1.6	62	0.199	0.201	0.200*	1.7	61	0.176	0.184	0.180*	1.6	59
60	0.332	0.338	0.335**	1.5	58	0.349	0.347	0.348**	1.5	54	0.306	0.302	0.304**	1.3	48
90	0.255	0.259	0.257**	1.1	42	0.292	0.288	0.290**	1.3	46	0.253	0.243	0.248**	1.1	41

*dilution = ×10

**dilution = ×5

Table 68 Thermal stability at 60 °C, pH 6, of β-galactosidase crosslinked with DMS (1-10 mg/mL)

Time (min)	1 mg/mL DMS					5 mg/mL DMS					10 mg/mL DMS				
	A_{410}			Activity (U/mL)	Relative activity (%)	A_{410}			Activity (U/mL)	Relative activity (%)	A_{410}			Activity (U/mL)	Relative activity (%)
	1	2	Average			1	2	Average			1	2	Average		
0	0.347	0.343	0.345*	3.0	100	0.361	0.351	0.356*	3.1	100	0.337	0.329	0.333*	2.9	100
5	0.334	0.322	0.328*	2.9	97	0.322	0.312	0.317*	2.8	90	0.303	0.291	0.297*	2.6	90
10	0.289	0.291	0.290*	2.5	83	0.284	0286	0.285*	2.5	81	0.277	0.276	0.277*	2.4	83
20	0.260	0.298	0.259*	2.3	77	0.257	0.263	0.260*	2.3	74	0.231	0.235	0.233*	2.0	69
40	0.218	0.224	0.221*	1.9	63	0.229	0.235	0.232*	2.0	65	0.200	0.194	0.197*	1.7	59
60	0.384	0.388	0.386**	1.7	57	0.355	0.357	0.356**	1.6	52	0.335	0.331	0.333**	1.5	52
90	0.209	0.311	0.310**	1.4	47	0.290	0.294	0.292**	1.3	42	0.281	0.279	0.280**	1.2	41

*dilution = ×10

**dilution = ×5

Table 69 Thermal stability at 60 °C, pH 6, of β-galactosidase crosslinked with 1 mg/mL imidoesters

Time (min)	EA					DMA					DMP					DMS				
	A_{410}			Act (U/mL)	RA (%)	A_{410}			Act (U/mL)	RA (%)	A_{410}			Act (U/mL)	RA (%)	A_{410}			Act (U/mL)	RA (%)
	1	2	Av			1	2	Av			1	2	Av			1	2	Av		
0	0.316	0.327	0.322*	2.8	100	0.325	0.325	0.325*	2.8	100	0.318	0.321	0.320*	2.8	100	0.350	0.351	0.351*	3.0	100
5	0.303	0.308	0.306*	2.7	95	0.297	0.297	0.297*	2.6	91	0.298	0.297	0.298*	2.6	93	0.340	0.328	0.334*	2.9	95
10	0.295	0.284	0.290*	2.5	90	0.283	0.288	0.286*	2.5	88	0.274	0.271	0.273*	2.4	85	0.283	0.278	0.281*	2.4	80
20	0.229	0.237	0.233*	2.0	72	0.252	0.252	0.252*	2.2	78	0.246	0.234	0.240*	2.1	75	0.268	0.260	0.264*	2.3	75
40	0.193	0.204	0.199*	1.7	62	0.198	0.188	0.193*	1.7	59	0.194	0.195	0.195*	1.7	61	0.227	0.224	0.226*	2.0	64
60	0.330	0.354	0.342**	1.5	53	0.356	0.374	0.365**	1.6	56	0.361	0.351	0.356**	1.5	56	0.374	0.412	0.393**	1.7	56
90	0.301	0.298	0.300**	1.3	47	0.303	0.309	0.306**	1.3	47	0.288	0.260	0.274**	1.2	43	0.319	0.315	0.317**	1.4	45

RA Relative Activity

*dilution = ×10

**dilution = ×5

Table 70 Thermal stability at 60 °C, pH 6, of β-galactosidase crosslinked with 1 mg/mL DMS at pH 5, 6, 7 and 8

Time (min)	pH 5					pH 6					pH 7					pH 8				
	A_{410}			Act (U/mL)	RA (%)	A_{410}			Act (U/mL)	RA (%)	A_{410}			Act (U/mL)	RA (%)	A_{410}			Act (U/mL)	RA (%)
	1	2	Av			1	2	Av			1	2	Av			1	2	Av		
0	0.317	0.328	0.323*	2.8	1000	0.339	0.338	0.339*	2.9	100	0.272	0.309	0.291*	2.5	100	0.277	0.286	0.282*	2.4	100
5	0.284	0.300	0.292*	2.5	91	0.297	0.297	0.297*	2.6	88	0.248	0.251	0.250*	2.2	86	0.255	0.257	0.256*	2.2	91
10	0.280	0.272	0.276*	2.4	86	0.277	0.273	0.275*	2.4	81	0.227	0.223	0.225*	2.0	77	0.238	0.238	0.238*	2.1	85
20	0.230	0.220	0.225*	2.0	70	0.247	0.248	0.248*	2.2	73	0.202	0.202	0.202*	1.8	70	0.208	0.208	0.208*	1.8	74
40	0.192	0.196	0.194*	1.7	60	0.198	0.189	0.194*	1.7	57	0.138	0.140	0.139*	1.2	48	0.152	0.150	0.151*	1.3	54
60	0.338	0.340	0.339**	1.5	53	0.330	0.343	0.337**	1.5	50	0.262	0.234	0.248**	1.1	43	0.274	0.262	0.268**	1.2	48
90	0.246	0.248	0.247**	1.1	38	0.280	0.282	0.281**	1.2	42	0.196	0.197	0.197**	0.9	34	0.209	0.205	0.207**	0.9	37

RA Relative Activity

*dilution = ×10

**dilution = ×5

1.2.4 Thermal stabilization by diamines

Table 71 Thermal stability of native β-galactosidase at 60 °C, pH 6, (Measurements 1-3)

Time (min)	Measurement 1					Measurement 2					Measurement 3				
	A_{410}			Activity (U/mL)	Relative activity (%)	A_{410}			Activity (U/mL)	Relative activity (%)	A_{410}			Activity (U/mL)	Relative activity (%)
	1	2	Average			1	2	Average			1	2	Average		
0	0.299	0.311	0.310*	2.7	100	0.322	0.322	0.322*	2.8	100	0.371	0.376	0.374*	3.2	100
5	0.273	0.272	0.273*	2.4	89	0.293	0.287	0.290*	2.5	89	0.333	0.329	0.331*	2.9	91
10	0.249	0.241	0.245*	2.1	78	0.264	0.269	0.274*	2.4	86	0.312	0.306	0.309*	2.7	84
20	0.220	0.220	0.220*	1.9	70	0.231	0.233	0.232*	2.0	71	0.282	0.270	0.276*	2.4	75
40	0.190	0.214	0.202*	1.8	67	0.186	0.188	0.187*	1.6	57	0.244	0.230	0.237*	2.1	63
60	0.307	0.301	0.304**	1.3	48	0.307	0.295	0.301**	1.3	46	0.352	0.354	0.353**	1.5	47
90	0.225	0.221	0.223**	1.0	37	0.245	0.244	0.245**	1.1	39	0.311	0.307	0.309**	1.3	41

*dilution = ×10

**dilution = ×5

Table 72 Thermal stability of native β-galactosidase at 60 °C, pH 6, (Measurements 4-6)

Time (min)	Measurement 4					Measurement 5					Measurement 6					Relative activity (average,%)	SD
	A_{410}			Activity (U/mL)	Relative activity (%)	A_{410}			Activity (U/mL)	Relative activity (%)	A_{410}			Activity (U/mL)	Relative activity (%)		
	1	2	Average			1	2	Average			1	2	Average				
0	0.354	0.344	0.349*	3.0	100	0.336	0.323	0.330*	2.9	100	0.359	0.358	0.359*	3.1	100	100	0
5	0.318	0.319	0.319*	2.8	93	0.293	0.293	0.293*	2.5	86	0.313	0.315	0.314*	2.7	87	89	2.56
10	0.281	0.277	0.279*	2.4	80	0.264	0.262	0.263*	2.3	79	0.289	0.289	0.289*	2.5	81	81	3.08
20	0.252	0.252	0.252*	2.2	73	0.233	0.233	0.233*	2.0	69	0.267	0.261	0.264*	2.3	74	72	2.37
40	0.221	0.220	0.221*	1.9	63	0.192	0.218	0.210*	1.8	62	0.222	0.212	0.217*	1.9	61	62	3.25
60	0.320	0.314	0.317**	1.4	47	0.345	0.346	0.346**	1.5	52	0.334	0.322	0.328**	1.4	45	48	2.43
90	0.303	0.303	0.303**	1.3	43	0.275	0.271	0.273**	1.2	41	0.278	0.277	0.278**	1.2	39	40	2.10

*dilution = ×10

**dilution = ×5

Table 73 Thermal stability at 60 °C, pH 6, of β-galactosidase crosslinked with EDA (1-10 mg/mL)

Time (min)	1 mg/mL EDA					5 mg/mL EDA					10 mg/mL EDA				
	A_{410}			Activity (U/mL)	Relative activity (%)	A_{410}			Activity (U/mL)	Relative activity (%)	A_{410}			Activity (U/mL)	Relative activity (%)
	1	2	Average			1	2	Average			1	2	Average		
0	0.241	0.240	0.241*	2.1	100	0.232	0.231	0.230*	2.0	100	0.262	0.266	0.264*	2.3	100
5	0.228	0.226	0.227*	2.0	95	0.218	0.210	0.214*	1.9	95	0.240	0.242	0.241*	2.1	91
10	0.206	0.300	0.208*	1.8	86	0.200	0.200	0.200*	1.7	85	0.229	0.221	0.225*	2.0	85
20	0.189	0.197	0.193*	1.7	81	0.183	0.175	0.179*	1.6	80	0.209	0.209	0.209*	1.8	79
40	0.151	0.149	0.150*	1.3	62	0.137	0.139	0.138*	1.2	60	0.153	0.149	0.151*	1.3	57
60	0.251	0.241	0.246**	1.1	52	0.225	0.224	0.225**	1.0	50	0.236	0.240	0.238**	1.0	45
90	0.207	0.208	0.208**	0.9	43	0.189	0.189	0.189**	0.8	40	0.211	0.210	0.211**	0.9	40

*dilution = ×10

**dilution = ×5

Table 74 Thermal stability at 60 °C, pH 6, of β-galactosidase crosslinked with DAB (1-10 mg/mL)

Time (min)	1 mg/mL DAB					5 mg/mL DAB					10 mg/mL DAB				
	A_{410}			Activity (U/mL)	Relative activity (%)	A_{410}			Activity (U/mL)	Relative activity (%)	A_{410}			Activity (U/mL)	Relative activity (%)
	1	2	Average			1	2	Average			1	2	Average		
0	0.115	0.114	0.115*	1.0	100	0.142	0.134	0.138*	1.2	100	0.126	0.125	0.126*	1.1	100
5	0.108	0.108	0.108*	0.9	94	0.128	0.124	0.126*	1.1	91	0.114	0.114	0.114*	0.1	90
10	0.103	0.107	0.105*	0.9	91	0.115	0.119	0.117*	1.0	85	0.109	0.108	0.109*	0.9	86
20	0.099	0.091	0.095*	0.8	83	0.115	0.103	0.109*	0.9	79	0.101	0.103	0.102*	0.9	81
40	0.076	0.075	0.076*	0.7	66	0.89	0.085	0.087*	0.8	63	0.762	0.756	0.759*	0.7	60
60	0.133	0.125	0.129**	0.6	56	0.145	0.141	0.143**	0.6	52	0.129	0.129	0.129**	0.6	51
90	0.099	0.107	0.103**	0.5	45	0.115	0.111	0.113**	0.5	41	0.101	0.100	0.101**	0.4	40

*dilution = ×10

**dilution = ×5

Table 75 Thermal stability at 60 °C, pH 6, of β-galactosidase crosslinked with DAH (1-10 mg/mL)

Time (min)	1 mg/mL DAH					5 mg/mL DAH					10 mg/mL DAH				
	A_{410}			Activity (U/mL)	Relative activity (%)	A_{410}			Activity (U/mL)	Relative activity (%)	A_{410}			Activity (U/mL)	Relative activity (%)
	1	2	Average			1	2	Average			1	2	Average		
0	0.210	0.204	0.207*	1.8	100	0.221	0.215	0.218*	1.9	100	0.201	0.189	0.195*	1.7	100
5	0.180	0.188	0.184*	1.6	89	0.190	0.189	0.190*	1.7	87	0.167	0.169	0.168*	1.5	86
10	0.175	0.173	0.174*	1.5	84	0.186	0.186	0.186*	1.6	85	0.162	0.162	0.162*	1.4	83
20	0.155	0.154	0.155*	1.4	75	0.156	0.154	0.155*	1.3	71	0.149	0.145	0.147*	1.3	75
40	0.119	0.121	0.120*	1.0	58	0.116	0.126	0.120*	1.0	55	0.111	0.107	0.109*	1.0	56
60	0.201	0.197	0.199**	0.9	48	0.226	0.210	0.218**	1.0	50	0.191	0.190	0.191**	0.8	49
90	0.140	0.142	0.141**	0.6	34	0.173	0.177	0.175**	0.8	40	0.146	0.144	0.145**	0.6	37

*dilution = ×10

**dilution = ×5

Table 76 Thermal stability at 60 °C, pH 6, of β-galactosidase crosslinked with DAO (1-10 mg/mL)

Time (min)	1 mg/mL DAO					5 mg/mL DAO					10 mg/mL DAO				
	A_{410}			Activity (U/mL)	Relative activity (%)	A_{410}			Activity (U/mL)	Relative activity (%)	A_{410}			Activity (U/mL)	Relative activity (%)
	1	2	Average			1	2	Average			1	2	Average		
0	0.207	0.206	0.207*	1.8	100	0.218	0.217	0.218*	1.9	100	0.196	0.194	0.195*	1.7	100
5	0.192	0.188	0.190*	1.7	92	0.190	0.190	0.190*	1.7	87	0.163	0.169	0.166*	1.4	85
10	0.184	0.184	0.184*	1.6	89	0.189	0.183	0.186*	1.6	85	0.168	0.167	0.168*	1.5	86
20	0.172	0.164	0.168*	1.5	81	0.169	0.171	0.170*	1.5	78	0.143	0.147	0.145*	1.3	74
40	0.136	0.146	0.141*	1.2	68	0.145	0.131	0.138*	1.2	63	0.122	0.116	0.119*	1.0	61
60	0.239	0.241	0.240**	1.0	58	0.240	0.240	0.240**	1.0	55	0.201	0.197	0.199**	0.9	51
90	0.207	0.191	0.199**	0.9	48	0.196	0.197	0.197**	0.9	45	0.171	0.173	0.172**	0.7	44

*dilution = ×10

**dilution = ×5

Table 77 Thermal stability at 60 °C, pH 6, of β-galactosidase crosslinked with DA10 (1-10 mg/mL)

Time (min)	1 mg/mL DA10					5 mg/mL DA10					10 mg/mL DA10				
	A_{410}			Activity (U/mL)	Relative activity (%)	A_{410}			Activity (U/mL)	Relative activity (%)	A_{410}			Activity (U/mL)	Relative activity (%)
	1	2	Average			1	2	Average			1	2	Average		
0	0.154	0.144	0.149*	1.3	100	0.124	0.128	0.126*	1.1	100	0.145	0.131	0.138*	1.2	100
5	0.127	0.126	0.127*	1.1	85	0.102	0.102	0.102*	0.9	81	0.110	0.109	0.110*	1.0	80
10	0.123	0.122	0.123*	1.1	85	0.098	0.094	0.096*	0.8	76	0.108	0.104	0.106*	0.9	77
20	0.113	0.115	0.114*	1.0	76	0.085	0.095	0.090*	0.8	71	0.101	0.101	0.101*	0.9	73
40	0.089	0.091	0.090*	0.8	60	0.075	0.075	0.075*	0.6	59	0.079	0.081	0.080*	0.7	58
60	0.143	0.143	0.143**	0.6	48	0.113	0.115	0.114**	0.5	45	0.130	0.124	0.127**	0.6	46
90	0.125	0.109	0.117**	0.5	39	0.092	0.086	0.089**	0.4	35	0.093	0.111	0.102**	0.4	37

*dilution = ×10

**dilution = ×5

Table 78 Thermal stability at 60 °C, pH 6, of β-galactosidase crosslinked with DAD (1-10 mg/mL)

Time (min)	1 mg/mL DAD					5 mg/mL DAD					10 mg/mL DAD				
	A_{410}			Activity (U/mL)	Relative activity (%)	A_{410}			Activity (U/mL)	Relative activity (%)	A_{410}			Activity (U/mL)	Relative activity (%)
	1	2	Average			1	2	Average			1	2	Average		
0	0.160	0.162	0.161*	1.4	100	0.167	0.177	0.172*	1.5	100	0.139	0.137	0.138*	1.2	100
5	0.140	0.140	0.140*	1.2	87	0.138	0.144	0.141*	1.2	82	0.117	0.116	0.117*	1.0	85
10	0.129	0.135	0.132*	1.1	82	0.133	0.133	0.133*	1.2	77	0.099	0.099	0.099*	0.9	72
20	0.113	0.114	0.114*	1.0	71	0.122	0.121	0.122*	1.1	71	0.095	0.93	0.094*	0.8	68
40	0.091	0.093	0.092*	0.8	57	0.094	0.106	0.100*	0.9	58	0.077	0.076	0.077*	0.7	56
60	0.147	0.155	0.151**	0.7	47	0.155	0.155	0.155**	0.7	45	0.119	0.118	0.119**	0.5	43
90	0.113	0.112	0.113**	0.5	35	0.111	0.117	0.114**	0.5	33	0.100	0.104	0.102**	0.4	37

*dilution = ×10

**dilution = ×5

Table 79 Thermal stability at 60 °C, pH 6, of β-galactosidase crosslinked with 1 mg/mL diamines

Time (min)	Hydrazine					EDA					DAB				
	A_{410}			Activity (U/mL)	Relative activity (%)	A_{410}			Activity (U/mL)	Relative activity (%)	A_{410}			Activity (U/mL)	Relative activity (%)
	1	2	Average			1	2	Average			1	2	Average		
0	0.264	0.265	0.265*	2.3	100	0.228	0.230	0.229*	2.0	100	0.093	0.093	0.093*	0.9	100
5	0.234	0.236	0.235*	2.0	89	0.214	0.216	0.215*	1.9	94	0.086	0.087	0.087*	0.8	93
10	0.216	0.215	0.216*	1.9	81	0.198	0.195	0.197*	1.7	86	0.084	0.085	0.085*	0.7	91
20	0.167	0.169	0.168*	1.5	64	0.184	0.182	0.183*	1.6	80	0.076	0.076	0.076*	0.7	82
40	0.124	0.128	0.126*	1.1	48	0.141	0.141	0.141*	1.2	62	0.062	0.061	0.062*	0.5	66
60	0.192	0.195	0.194**	0.8	37	0.225	0.239	0.232**	1.0	51	0.103	0.104	0.104**	0.5	56
90	0.136	0.135	0.136**	0.6	26	0.197	0.198	0.198**	0.9	43	0.083	0.085	0.084**	0.4	45

RA Relative Activity

*dilution = ×10

**dilution = ×5

Table 80 Thermal stability at 60 °C, pH 6, of β-galactosidase crosslinked with 1 mg/mL diamines

Time (min)	DAH					DAO					DA10					DAD				
	A_{410}			Act (U/mL)	RA (%)	A_{410}			Act (U/mL)	RA (%)	A_{410}			Act (U/mL)	RA (%)	A_{410}			Act (U/mL)	RA (%)
	1	2	Av			1	2	Av			1	2	Av			1	2	Av		
0	0.200	0.200	0.200*	1.7	100	0.221	0.219	0.220*	1.9	100	0.137	0.138	0.138*	1.2	100	0.146	0.143	0.145*	1.3	100
5	0.177	0.177	0.177*	1.5	89	0.201	0.205	0.203*	1.8	92	0.117	0.118	0.118*	1.0	85	0.127	0.125	0.126*	1.1	87
10	0.170	0.167	0.169*	1.5	84	0.192	0.198	0.195*	1.7	89	0.116	0.117	0.117*	1.0	85	0.118	0.118	0.118*	1.0	82
20	0.150	0.151	0.151*	1.3	75	0.180	0.176	0.178*	1.5	81	0.105	0.105	0.105*	0.9	76	0.103	0.103	0.103*	0.9	71
40	0.113	0.112	0.113*	1.0	58	0.148	0.150	0.149*	1.3	68	0.082	0.083	0.083*	0.7	60	0.082	0.082	0.082*	0.7	57
60	0.191	0.185	0.188**	0.8	48	0.260	0.250	0.255**	1.1	58	0.130	0.135	0.133**	0.6	48	0.137	0.132	0.135**	0.6	47
90	0.136	0.139	0.138**	0.6	34	0.216	0.208	0.212**	0.9	48	0.110	0.104	0.107**	0.5	39	0.105	0.100	0.103**	0.4	35

RA Relative Activity

*dilution = ×10

**dilution = ×5

Table 81 Thermal stability at 60 °C, pH 6, of β-galactosidase crosslinked with 1 mg/mL DAO at pH 5, 6, 7 and 8

Time (min)	pH 5					pH 6					pH 7					pH 8				
	A_{410}			Act (U/mL)	RA (%)	A_{410}			Act (U/mL)	RA (%)	A_{410}			Act (U/mL)	RA (%)	A_{410}			Act (U/mL)	RA (%)
	1	2	Av			1	2	Av			1	2	Av			1	2	Av		
0	0.221	0.215	0.218*	1.9	100	0.236	0.246	0.241*	2.1	100	0.286	0.288	0.287*	2.5	100	0.298	0.299	0.299*	2.6	100
5	0.191	0.192	0.192*	1.7	88	0.216	0.214	0.215*	1.9	89	0.269	0.277	0.273*	2.4	95	0.273	0.271	0.272*	2.4	91
10	0.189	0.187	0.188*	1.6	86	0.199	0.207	0.203*	1.8	84	0.247	0.247	0.247*	2.2	86	0.243	0.247	0.245*	2.1	82
20	0.161	0.157	0.159*	1.4	73	0.177	0.185	0.181*	1.6	75	0.221	0.220	0.221*	1.9	77	0.216	0.226	0.221*	1.9	74
40	0.134	0.124	0.129*	1.1	59	0.138	0.142	0.140*	1.2	58	0.189	0.185	0.187*	1.6	65	0.180	0.184	0.182*	1.6	61
60	0.197	0.196	0.197**	0.9	45	0.231	0.233	0.232**	1.0	48	0.309	0.311	0.310**	1.4	54	0.275	0.275	0.275**	1.2	46
90	0.144	0.144	0.144**	0.6	33	0.223	0.211	0.217**	0.9	45	0.263	0.255	0.259**	1.1	45	0.231	0.235	0.233**	1.0	39

RA Relative Activity

*dilution = ×10

**dilution = ×5

1.3 Invertase

1.3.1 Properties of native invertase

Table 82 Optimum pH of invertase (2 mg/mL) at room temperature

pH	Dilution (×)	A_{540}			Activity (Unit/mL)
		1	2	Average	
3	100	0.275	0.304	0.290	272
4	100	0.621	0.654	0.638	599
5	100	0.657	0.724	0.691	649
6	100	0.545	0.570	0.558	524
7	100	0.228	0.195	0.212	197
8	10	0.477	0.473	0.475	45
9	10	0.166	0.180	0.173	16
10	10	0.036	0.033	0.035	3

Activity calculations followed the methods in Section 3.2.3.3

Table 83 Optimum temperature of invertase at pH 4.6

Temperature (°C)	Dilution (×)	A_{540}			Activity (Unit/mL)
		1	2	Average	
25	500	0.843	0.855	0.849	798
30	500	1.028	0.971	1.000	940
40	1,000	0.660	0.674	0.667	1,254
50	1,000	0.850	0.868	0.859	1,615
55	2,000	0.613	0.599	0.611	2,297
60	2,000	0.640	0.641	0.640	2,406
65	1,000	1.064	1.013	1.039	1,953
70	500	0.840	0.811	0.826	776
75	500	0.172	0.188	0.180	169
80	500	0.195	0.179	0.187	176
85	500	0.155	0.157	0.156	147
90	100	0.365	0.458	0.412	77

Table 84 The absorbance at 540 nm of invertase (2 mg/mL, dilution = ×500 for sample at pH 4 and ×100 for sample at pH 5, 6, 7 and 8) for pH stability at 25 °C

Time (min)	A_{540}														
	pH 4			pH 5			pH 6			pH 7			pH 8		
	1	2	Average	1	2	Average	1	2	Average	1	2	Average	1	2	Average
0	0.126	0.107	0.117	0.670	0.550	0.610	0.442	0.401	0.422	0.484	0.483	0.484	0.418	0.427	0.423
5	0.090	0.096	0.093	0.670	0.564	0.615	0.528	0.534	0.531	0.492	0.498	0.495	0.443	0.435	0.439
10	0.112	0.115	0.114	0.666	0.657	0.654	0.504	0.519	0.512	0.473	0.505	0.489	0.432	0.420	0.426
20	0.117	0.111	0.114	0.651	0.601	0.626	0.513	0.570	0.542	0.526	0.489	0.508	0.426	0.438	0.432
30	0.130	0.110	0.120	0.650	0.623	0.661	0.516	0.516	0.516	0.518	0.555	0.568	0.435	0.462	0.449
40	0.116	0.117	0.117	0.698	0.685	0.692	0.543	0.524	0.534	0.549	0.527	0.538	0.480	0.481	0.481
60	0.106	0.107	0.107	0.699	0.678	0.676	0.543	0.536	0.540	0.483	0.471	0.477	0.394	0.428	0.411
80	0.114	0.115	0.115	0.673	0.672	0.677	0.531	0.547	0.539	0.457	0.474	0.466	0.424	0.403	0.414
100	0.099	0.107	0.103	0.682	0.712	0.676	0.518	0.530	0.524	0.525	0.510	0.518	0.435	0.470	0.453
120	0.108	0.106	0.107	0.670	0.690	0.680	0.573	0.562	0.568	0.513	0.512	0.510	0.436	0.430	0.433

Table 85 pH stability of invertase at 25 °C

Time (min)	Activity (Unit/mL)					Relative activity (%)				
	pH 4	pH 5	pH 6	pH 7	pH 8	pH 4	pH 5	pH 6	pH 7	pH 8
0	660	688	476	546	477	100	100	100	100	100
5	525	694	599	558	495	80	101	126	102	104
10	643	738	578	552	481	97	107	121	101	101
20	643	706	611	573	487	97	103	128	105	102
30	677	746	582	641	506	103	108	122	117	106
40	660	781	602	607	543	100	114	126	111	114
60	603	763	609	538	464	91	111	128	99	97
80	649	764	608	526	467	98	111	128	96	98
100	581	763	591	584	511	88	111	124	107	107
120	603	767	641	578	488	91	111	135	106	102

Table 86 pH stability of invertase at 50 °C

Time (min)	Activity (Unit/mL)					Relative activity (%)				
	pH 4	pH 5	pH 6	pH 7	pH 8	pH 4	pH 5	pH 6	pH 7	pH 8
0	758	663	596	638	554	100	100	100	100	100
5	678	700	433	74	51	89	105	73	0.1	0.1
10	616	701	409	26	27	81	105	69	0	0
20	713	666	271	0	0	94	106	45	0	0
30	625	726	274	0	0	82	109	46	0	0
40	740	727	227	0	0	97	109	38	0	0
60	775	771	198	0	0	102	116	34	0	0
80	779	575	199	0	0	103	110	34	0	0
100	820	800	198	0	0	108	120	34	0	0
120	839	796	224	0	0	111	120	38	0	0

Table 87 The absorbance at 540 nm of invertase (2 mg/mL, dilution = ×100) for pH stability at 50 °C

Time (min)	A_{540}														
	pH 4			pH 5			pH 6			pH 7			pH 8		
	1	2	Average	1	2	Average	1	2	Average	1	2	Average	1	2	Average
0	0.778	0.833	0.806	0.733	0.677	0.705	0.676	0.591	0.634	0.673	0.685	0.679	0.594	0.586	0.589
5	0.699	0.743	0.721	0.791	0.698	0.745	0.481	0.441	0.461	0.084	0.073	0.079	0.050	0.057	0.054
10	0.682	0.627	0.655	0.738	0.753	0.746	0.423	0.446	0.435	0.029	0.026	0.028	0.028	0.030	0.029
20	0.753	0.764	0.759	0.665	0.750	0.708	0.269	0.306	0.288	0	0	0	0	0	0
30	0.697	0.632	0.665	0.809	0.735	0.772	0.292	0.292	0.292	0	0	0	0	0	0
40	0.799	0.775	0.787	0.666	0.880	0.773	0.236	0.245	0.241	0	0	0	0	0	0
60	0.875	0.773	0.824	0.904	0.735	0.820	0.210	0.211	0.211	0	0	0	0	0	0
80	0.827	0.830	0.829	0.613	0.610	0.612	0.205	0.218	0.212	0	0	0	0	0	0
100	0.885	0.858	0.872	0.877	0.824	0.851	0.200	0.221	0.211	0	0	0	0	0	0
120	0.889	0.897	0.893	0.801	0.893	0.847	0.235	0.240	0.238	0	0	0	0	0	0

Table 88 The absorbance at 540 nm of invertase (2 mg/mL, dilution = ×500) for its thermal stability at 25-65 °C, pH 5

Time (min)	25 °C			30 °C			40 °C			50 °C			55 °C			60 °C			65 °C		
	1	2	Av	1	2	Av	1	2	Av	1	2	Av	1	2	Av	1	2	Av	1	2	Av
0	0.358	0.356	0.357	0.365	0.360	0.363	0.420	0.450	0.435	0.390	0.380	0.385	0.386	0.361	0.374	0.483	0.467	0.475	0.398	0.410	0.404
5	0.356	0.369	0.363	0.357	0.342	0.350	0.404	0.407	0.406	0.360	0.353	0.357	0.348	0.330	0.339	0.339	0.344	0.342	0.175	0.167	0.171*
10	0.373	0.379	0.376	0.345	0.348	0.347	0.364	0.385	0.375	0.398	0.378	0.388	0.328	0.340	0.334	0.465	0.467	0.466*	0.083	0.081	0.082*
20	0.352	0.357	0.355	0.361	0.365	0.363	0.378	0.371	0.375	0.400	0.341	0.371	0.258	0.264	0.261	0.313	0.302	0.306*	0.035	0.025	0.030*
30	0.371	0.369	0.370	0.363	0.362	0.363	0.400	0.392	0.396	0.365	0.372	0.369	0.238	0.227	0.233	0.233	0.241	0.237*	0	0	0
40	0.392	0.387	0.390	0.358	0.356	0.357	0.387	0.372	0.380	0.400	0.401	0.401	0.233	0.205	0.219	0.173	0.185	0.179*	0	0	0
60	0.351	0.368	0.360	0.345	0.353	0.349	0.379	0.374	0.377	0.388	0.381	0.385	0.151	0.159	0.155	0.122	0.116	0.119*	0	0	0
80	0.385	0.389	0.387	0.368	0.365	0.367	0.385	0.387	0.386	0.395	0.380	0.388	0.179	0.137	0.158	0.068	0.072	0.070*	0	0	0
100	0.386	0.383	0.385	0.364	0.359	0.362	0.377	0.364	0.371	0.427	0.397	0.412	0.160	0.143	0.152	0.056	0.059	0.057*	0	0	0
120	0.387	0.385	0.386	0.352	0.361	0.357	0.391	0.377	0.384	0.394	0.400	0.397	0.140	0.161	0.151	0.046	0.046	0.046*	0	0	0

* dilution = ×200

Av = average

Table 89 Thermal denaturation of invertase at 25-65 °C

Time (min)	Activity (Unit/mL)						
	25 °C	30 °C	40 °C	50 °C	55 °C	60 °C	65 °C
0	559	568	681	603	585	743	632
5	568	548	635	559	531	535	107
10	588	543	587	607	523	292	51
20	556	568	587	581	408	192	19
30	579	568	620	577	365	148	0
40	610	559	595	628	343	112	0
60	563	546	590	603	243	74	0
80	606	574	604	607	247	44	0
100	603	567	581	645	238	36	0
120	604	559	601	621	236	29	0

Table 90 Absorbance at 540 nm of invertase (2 mg/mL, dilution = ×500) for the estimation of E_d and k_d at pH 5

Time (min)	A_{540}											
	50 °C			55 °C			60 °C			65 °C		
	1	2	Average	1	2	Average	1	2	Average	1	2	Average
0	0.595	0.587	0.591	0.628	0.630	0.629	0.570	0.567	0.569	0.670	0.646	0.658
1	0.583	0.611	0.597	0.594	0.602	0.598	0.459	0.439	0.449	0.236	0.240	0.238
2	0.592	0.588	0.590	0.604	0.638	0.621	0.405	0.419	0.412	0.969	1.013	0.991[b]
3	0.599	0.559	0.579	0.624	0.595	0.610	0.340	0.377	0.359	0.865	0.824	0.845[b]
4	0.529	0.540	0.535	0.567	0.603	0.585	0.365	0.356	0.361	0.698	0.709	0.704[b]
5	0.563	0.579	0.571	0.594	0.582	0.588	0.313	0.312	0.313	0.626	0.630	0.628[b]
6	0.593	0.579	0.586	0.612	0.594	0.603	0.281	0.292	0.287	0.476	0.479	0.478[b]
7	0.541	0.541	0.541	0.584	0.578	0.581	0.285	0.300	0.293	0.460	0.457	0.459[b]
8	0.554	0.514	0.534	0.573	0.637	0.605	0.645	0.679	0.662[a]	0.478	0.460	0.469[b]
9	0.562	0.550	0.556	0.568	0.588	0.578	0.685	0.690	0688[a]	0.364	0.368	0.366[b]
10	0.613	0.576	0.595	0.598	0.621	0.610	0.569	0.562	0.566[a]	0.348	0.336	0.342[b]
12	0.537	0.533	0.535	0.532	0.496	0.514	0.543	0.539	0.541[a]	0.291	0.275	0.283[b]
14	0.563	0.549	0.556	0.562	0.525	0.544	0.454	0.437	0.446[a]	0.240	0.243	0.242[b]
16	0.543	0.542	0.543	0.563	0.535	0.549	0.350	0.339	0.345[a]	0.207	0.198	0.204[b]
18	0.498	0.537	0.518	0.518	0.541	0.530	0.313	0.335	0.324[a]	0.187	0.179	0.183[b]
20	0.612	0.588	0.600	0.575	0.576	0.576	0.285	0.281	0.283[a]	0.151	0.154	0.153[b]
22	0.579	0.579	0.579	0.520	0.510	0.515	0.251	0.262	0.257[a]	0.133	0.121	0.127[b]
24	0.533	0.543	0.538	0.477	0.452	0.465	0.251	0.255	0.253[a]	1.363	1.367	1.365[c]

Time (min)	A_{540}											
	50 °C			55 °C			60 °C			65 °C		
	1	2	Average	1	2	Average	1	2	Average	1	2	Average
26	0.612	0.629	0.621	0.460	0.480	0.470	0.237	0.242	0.240[a]	1.180	1.206	1.193[c]
28	0.531	0.523	0.527	0.502	0.508	0.505	0.206	0.205	0.206[a]	0.974	1.002	0.988[c]
30	0.588	0.563	0.576	0.544	0.518	0.531	0.213	0.197	0.205[a]	0.860	0.876	0.868[c]
40	0.635	0.608	0.622	0.461	0.470	0.466	0.265	0.252	0.259[b]	0.375	0.381	0.378[c]
60	0.602	0.608	0.605	0.485	0.481	0.483	0.142	0.138	0.140[b]	0.067	0.068	0.068[c]
80	0.621	0.641	0.631	0.449	0.450	0.450	0.953	0.969	0.961[c]	0.197	0.198	0.198[d]
100	0.662	0.649	0.656	0.440	0.417	0.429	0.440	0.452	0.446[c]	0.093	0.087	0.090[d]
120	0.659	0.674	0.667	0.484	0.501	0.493	0.234	0.228	0.231[c]	-	-	-

[a] dilution = ×200

[b] dilution = ×100

[c] dilution = ×10

[d] no dilution

Table 91 The estimation of E_d and k_d for invertase at pH 5

Time (min)	Activity (Unit/mL)				Relative activity (%)				ν_f				ln ν_f			
	50 °C	55°C	60 °C	65 °C	50 °C	55°C	60 °C	65 °C	50 °C	55°C	60 °C	65 °C	50 °C	55°C	60 °C	65 °C
0	556	591	535	619	100	100	100	100	1	1	1	1	0	0	0	0
1	561	562	422	224	101	95	79	36	1.01	0.95	0.79	0.36	0.01	-0.05	-0.24	-1.02
2	555	584	387	186	100	99	72	30	1	0.99	0.72	0.30	0	-0.01	-0.32	-1.20
3	544	573	337	159	98	97	63	26	0.98	0.97	0.63	0.26	-0.02	-0.03	-0.46	-1.36
4	503	550	339	132	90	93	63	21	0.90	0.93	0.63	0.21	-0.10	-0.07	-0.46	-1.55
5	537	553	294	118	97	94	55	19	0.97	0.94	0.55	0.19	-0.03	-0.07	-0.60	-1.66
6	551	567	270	90	99	96	50	15	0.99	0.96	0.50	0.15	-0.01	-0.04	-0.68	-1.93
7	509	546	275	86	92	92	51	14	0.92	0.92	0.51	0.14	-0.09	-0.08	-0.67	-1.97
8	502	569	249	88	90	96	47	14	0.90	0.96	0.47	0.14	-0.10	-0.04	-0.76	-1.95
9	523	543	259	69	94	92	48	11	0.94	0.92	0.48	0.11	-0.06	-0.08	-0.73	-2.19
10	559	573	213	64	101	97	40	10	1.01	0.97	0.40	0.10	0.01	-0.03	-0.92	-2.27
12	503	483	203	53	90	82	38	8.6	0.90	0.82	0.38	0.09	-0.10	-0.20	-0.97	-2.46
14	523	511	168	45	94	86	31	7.3	0.94	0.86	0.31	0.07	-0.06	-0.15	-1.16	-2.62
16	510	516	130	38	92	87	24	6.1	0.92	0.87	0.24	0.06	-0.09	-0.14	-1.41	-2.79
18	487	498	122	34	88	84	23	5.5	0.88	0.84	0.23	0.05	-0.13	-0.17	-1.48	-2.90
20	564	541	106	29	101	92	20	4.7	1.01	0.92	0.20	0.05	0.01	-0.08	-1.62	-3.06
22	544	484	97	24	98	82	18	3.9	0.98	0.82	0.18	0.04	-0.02	-0.20	-1.71	-3.25
24	506	437	95	26	91	74	18	4.2	0.91	0.74	0.18	0.04	-0.09	-0.30	-1.73	-3.17
26	584	442	90	22	105	75	17	3.6	1.05	0.75	0.17	0.04	0.05	-0.29	-1.78	-3.34
28	495	475	77	19	89	80	14	3.1	0.89	0.80	0.14	0.03	-0.12	-0.22	-1.94	-3.48

Time (min)	Activity (Unit/mL)				Relative activity (%)				v_f				ln v_f			
	50 °C	**55°C**	**60 °C**	**65 °C**	**50 °C**	**55°C**	**60 °C**	**65 °C**	**50 °C**	**55°C**	**60 °C**	**65 °C**	**50 °C**	**55°C**	**60 °C**	**65 °C**
30	541	499	77	16	97	84	14	2.6	0.97	0.84	0.14	0.03	-0.03	-0.17	-1.94	-3.66
40	585	438	49	7.1	105	74	9.2	1.1	1.05	0.74	0.09	0.01	0.05	-0.30	-2.39	-4.47
60	569	454	26	1.3	102	77	4.8	0.2	1.02	0.77	0.05	0	0.02	-0.26	-3.02	-6.17
80	593	423	18	0.4	107	72	3.4	0.06	1.07	0.72	0.03	0	0.06	-0.33	-3.39	-7.34
100	617	403	8.4	0.2	111	68	1.6	0.03	1.11	0.68	0.02	0	0.10	-0.38	-4.15	-8.04
120	627	463	4.3	-	113	78	0.8	-	1.13	0.78	0.01	-	0.12	-0.24	-4.82	-

1.3.2 Thermal stabilization by isocyanates

Table 92 Thermal stability of native invertase at 60 °C, pH 5, (Measurements 1-3)

Time (min)	Measurement 1					Measurement 2					Measurement 3				
	A_{540}			Activity (U/mL)	Relative activity (%)	A_{540}			Activity (U/mL)	Relative activity (%)	A_{540}			Activity (U/mL)	Relative activity (%)
	1	2	Average			1	2	Average			1	2	Average		
0	0.491	0.487	0.489[a]	92	100	0.478	0.482	0.480[a]	90	100	0.317	0.289	0.303[a]	57	100
4	0.670	0.690	0.680[b]	64	70	0.704	0.700	0.702[b]	66	73	0.387	0.383	0.385[b]	36	64
10	1.305	1.301	1.303[c]	49	53	0.536	0.540	0.538[b]	51	56	0.337	0.332	0.335[b]	31	55
20	0.991	1.025	1.008[c]	38	41	0.377	0.365	0.371[b]	35	39	0.224	0.221	0.223[b]	21	37
40	1.320	1.321	1.321[d]	25	27	0.598	0.612	0.605[c]	23	25	0.354	0.368	0.361[c]	14	24
60	0.971	1.004	0.988[d]	19	20	0.487	0.484	0.486[c]	18	20	0.273	0.280	0.277[c]	10	18
90	0.376	0.388	0.382[c]	14	16	0.345	0.351	0.348[c]	13	15	0.190	0.193	0.192[c]	7	13

[a] dilution = ×100

[b] dilution = ×50

[c] dilution = ×20

[d] dilution = ×20

Table 93 Thermal stability of native invertase at 60 °C, pH 5, (Measurements 4-6)

Time (min)	Measurement 4					Measurement 5					Measurement 6					Relative activity (average,%)	SD
	A_{540}			Activity (U/mL)	Relative activity (%)	A_{540}			Activity (U/mL)	Relative activity (%)	A_{540}			Activity (U/mL)	Relative activity (%)		
	1	2	Average			1	2	Average			1	2	Average				
0	0.294	0.289	0.292[a]	55	100	0.284	0.300	0.292[a]	55	100	0.298	0.302	0.300[a]	56	100	100	0
4	0.374	0.363	0.369[b]	35	63	0.456	0.451	0.454[b]	43	78	0.483	0.508	0.496[b]	47	83	72	7.83
10	0.238	0.270	0.254[b]	24	44	0.354	0.384	0.369[b]	35	63	0.364	0.357	0.361[b]	34	60	55	6.55
20	0.179	0.184	0.182[b]	17	31	0.269	0.274	0.272[b]	26	46	0.256	0.246	0.251[b]	24	42	39	5.09
40	0.264	0.267	0.266[c]	10	18	0.549	0.581	0.565[c]	21	39	0.446	0.442	0.444[c]	17	30	27	7.03
60	0.182	0.177	0.180[c]	7	12	0.469	0.468	0.469[c]	18	32	0.334	0.352	0.343[c]	13	23	21	6.59
90	0.126	0.120	0.123[c]	5	8	0.370	0.376	0.373[c]	14	26	0.255	0.260	0.258[c]	10	17	16	5.91

[a] dilution = ×100

[b] dilution = ×50

[c] dilution = ×20

Table 94 Thermal stability at 60 °C, pH 5, of invertase (0.9 μM) crosslinked with BMDC (1-20 mM)

Time (min)	1 mM BMDC					10 mM BMDC					20 mM BMDC				
	A_{540}			Activity (U/mL)	Relative activity (%)	A_{540}			Activity (U/mL)	Relative activity (%)	A_{540}			Activity (U/mL)	Relative activity (%)
	1	2	Aaverage			1	2	Average			1	2	Average		
0	0.394	0.386	0.390[a]	73	100	0.367	0.362	0.365[a]	69	100	0.297	0.286	0.292[a]	55	100
4	0.666	0.663	0.665[b]	62	85	0.606	0.614	0.610[b]	57	84	0.544	0.539	0.542[b]	51	93
10	0.545	0.550	0.537[b]	50	69	0.566	0.546	0.556[b]	52	76	0.483	0.486	0.485[b]	46	83
20	0.554	0.528	0.541[b]	51	69	0.487	0.485	0.486[b]	46	67	0.447	0.447	0.447[b]	42	77
40	1.111	1.097	1.104[c]	42	57	1.147	0.124	0.136[c]	43	62	1.058	1.071	1.065[c]	40	73
60	1.078	1.089	1.084[c]	41	56	1.128	1.155	1.142[c]	43	63	0.994	0.993	0.994[c]	37	68
90	1.936	1.925	1.931[d]	36	50	1.162	1.152	1.157[c]	44	63	0.995	0.993	0.994[c]	37	68

[a] dilution = ×100

[b] dilution = ×50

[c] dilution = ×20

Table 95 Thermal stability at 60 °C, pH 5, of invertase (0.9 μM) crosslinked with BMDC (30-50 mM)

Time (min)	30 mM BMDC					40 mM BMDC					50 mM BMDC				
	A_{540}			Activity (U/mL)	Relative activity (%)	A_{540}			Activity (U/mL)	Relative activity (%)	A_{540}			Activity (U/mL)	Relative activity (%)
	1	2	Average			1	2	Average			1	2	Average		
0	0.270	0.267	0.269[a]	50	100	0.273	0.290	0.282[a]	53	100	0.255	0.234	0.245[a]	46	100
4	0.497	0.492	0.495[b]	46	92	0.467	0.472	0.470[b]	44	83	0.455	0.451	0.453[b]	43	93
10	0.429	0.450	0.440[b]	41	82	0.439	0.426	0.433[b]	41	77	0.426	0.416	0.421[b]	40	86
20	0.398	0.382	0.390[b]	37	73	0.392	0.401	0.398[b]	37	71	0.361	0.353	0.357[b]	34	73
40	0.344	0.352	0.348[b]	33	65	0.368	0.381	0.375[b]	35	67	0.335	0.347	0.341[b]	32	70
60	0.362	0.336	0.349[b]	33	65	0.381	0.379	0.380[b]	36	67	0.339	0.334	0.337[b]	32	69
90	0.864	0.873	0.869[c]	33	65	0.940	0.966	0.953[c]	36	68	0.847	0.845	0.846[c]	32	69

[a] dilution = ×100

[b] dilution = ×50

[c] dilution = ×20

Table 96 Thermal stability at 60 °C, pH 5, of invertase (0.9 μM) crosslinked with HMDC (1-20 mM)

Time (min)	1 mM HMDC					10 mM HMDC					20 mM HMDC				
	A_{540}			Activity (U/mL)	Relative activity (%)	A_{540}			Activity (U/mL)	Relative activity (%)	A_{540}			Activity (U/mL)	Relative activity (%)
	1	2	Average			1	2	Average			1	2	Average		
0	0.191	0.175	0.183*	34	100	0.164	0.171	0.168*	31	100	0.160	0.157	0.159*	30	100
4	0.350	0.330	0.340**	32	93	0.310	0.308	0.309**	29	92	0.303	0.300	0.302**	28	95
10	0.319	0.325	0.322**	30	88	0.304	0.307	0.306**	29	91	0.307	0.300	0.304**	29	96
20	0.289	0.274	0.282**	26	77	0.272	0.274	0.273**	26	81	0.263	0.254	0.259**	24	82
40	0.252	0.253	0.253**	24	69	0.224	0.251	0.238**	22	71	0.249	0.244	0.247**	23	78
60	0.262	0.259	0.261**	24	71	0.239	0.252	0.246**	23	73	0.249	0.241	0.245**	23	77
90	0.267	0.251	0.259**	24	71	0.241	0.233	0.237**	22	71	0.235	0.235	0.235**	22	74

*dilution = ×100

**dilution = ×50

Table 97 Thermal stability at 60 °C, pH 5, of invertase (0.9 μM) crosslinked with HMDC (30-50 mM)

Time (min)	30 mM HMDC					40 mM HMDC					50 mM HMDC				
	A_{540}			Activity (U/mL)	Relative activity (%)	A_{540}			Activity (U/mL)	Relative activity (%)	A_{540}			Activity (U/mL)	Relative activity (%)
	1	2	Average			1	2	Average			1	2	Average		
0	0.164	0.168	0.166*	31	100	0.165	0.178	0.172*	32	100	0.176	0.160	0.168*	32	100
4	0.311	0.310	0.311**	29	94	0.310	0.311	0.311**	29	91	0.311	0.302	0.307**	29	91
10	0.287	0.272	0.280**	26	84	0.306	0.273	0.290**	27	84	0.279	0.294	0.287**	27	85
20	0.260	0.296	0.278**	26	84	0.253	0.278	0.266**	25	77	0.275	0.286	0.281**	26	83
40	0.217	0.233	0.225**	21	68	0.225	0.222	0.224**	21	65	0.206	0.214	0.210**	20	63
60	0.234	0.243	0.239**	22	72	0.241	0.223	0.232**	22	68	0.192	0.203	0.198**	19	59
90	0.193	0.208	0.201**	19	60	0.257	0.246	0.252**	24	73	0.220	0.228	0.224**	21	67

*dilution = ×100

**dilution = ×50

Table 98 Thermal stability at 60 °C, pH 5, of invertase (0.9 μM) crosslinked with OMDC (1-20 mM)

Time (min)	1 mM OMDC					10 mM OMDC					20 mM OMDC				
	A_{540}			Activity (U/mL)	Relative activity (%)	A_{540}			Activity (U/mL)	Relative activity (%)	A_{540}			Activity (U/mL)	Relative activity (%)
	1	2	Average			1	2	Average			1	2	Average		
0	0.220	0.227	0.224*	42	100	0.245	0.229	0.237*	45	100	0.255	0.246	0.251*	47	100
4	0.390	0.382	0.386**	36	86	0.414	0.393	0.404**	38	85	0.382	0.416	0.399**	38	80
10	0.316	0.332	0.324**	30	72	0.357	0.322	0.340**	32	72	0.340	0.330	0.335**	31	67
20	0.286	0.304	0.295**	28	66	0.287	0.284	0.286**	27	60	0.256	0.270	0.263**	25	52
40	0.250	0.246	0.248**	23	55	0.244	0.231	0.238**	22	50	0.190	0.226	0.208**	20	42
60	0.244	0.240	0.242**	23	54	0.220	0.228	0.224**	21	47	0.218	0.218	0.218**	20	44
90	0.217	0.202	0.210**	20	47	0.201	0.206	0.204**	19	43	0.177	0.167	0.172**	16	34

*dilution = ×100

**dilution = ×50

Table 99 Thermal stability at 60 °C, pH 5, of invertase (0.9 μM) crosslinked with OMDC (30-50 mM)

Time (min)	30 mM OMDC					40 mM OMDC					50 mM OMDC				
	A_{540}			Activity (U/mL)	Relative activity (%)	A_{540}			Activity (U/mL)	Relative activity (%)	A_{540}			Activity (U/mL)	Relative activity (%)
	1	2	Average			1	2	Average			1	2	Average		
0	0.241	0.233	0.237*	45	100	0.239	0.241	0.240*	45	100	0.274	0.264	0.269*	51	100
4	0.427	0.436	0.432**	41	91	0.422	0.401	0.412**	39	86	0.434	0.422	0.428**	40	80
10	0.381	0.377	0.379**	36	80	0.358	0.366	0.362**	34	75	0.360	0.373	0.367**	34	68
20	0.306	0.308	0.307**	29	65	0.280	0.289	0.285**	27	59	0.305	0.288	0.297**	28	55
40	0.257	0.252	0.255**	24	54	0.234	0.235	0.235**	22	49	0.207	0.225	0.216**	20	40
60	0.226	0.223	0.225**	21	47	0.214	0.208	0.211**	20	44	0.204	0.196	0.200**	19	37
90	0.212	0.201	0.207**	19	44	0.201	0.216	0.209**	20	43	0.172	0.177	0.175**	16	32

*dilution = ×100

**dilution = ×50

Table 100 Thermal stability at 60 °C, pH 5, of invertase (0.9 μM) crosslinked with 30 mM isocyanates

Time (min)	BIC					BMDC					HMDC					OMDC				
	A_{540}			Act (U/mL)	RA (%)	A_{540}			Act (U/mL)	RA (%)	A_{540}			Act (U/mL)	RA (%)	A_{540}			Act (U/mL)	RA (%)
	1	2	Av			1	2	Av			1	2	Av			1	2	Av		
0	0.360	0.352	0.356[a]	67	100	0.355	0.363	0.359[a]	67	100	0.418	0.416	0.417[a]	78	100	0.476	0.492	0.484[a]	91	100
4	0.481	0.481	0.481[b]	45	68	0.690	0.681	0.686[b]	64	95	0.759	0.733	0.746[b]	70	89	0.755	0.775	0.765[b]	72	79
10	0.331	0.330	0.331[b]	31	46	0.603	0.612	0.608[b]	57	85	0.695	0.687	0.691[b]	65	83	0.675	0.663	0.669[b]	63	69
20	0.230	0.240	0.235[b]	22	33	0.566	0.568	0.567[b]	53	79	0.658	0.665	0.662[b]	62	79	0.567	0.577	0.572[b]	54	59
40	0.385	0.373	0.379[c]	14	15	0.531	0.510	0.521[b]	49	72	0.611	0.620	0.616[b]	58	74	0.448	0.440	0.444[b]	42	46
60	0.290	0.296	0.293[c]	11	11	0.524	0.506	0.515[b]	48	72	0.602	0.604	0.603[b]	57	72	0.403	0.405	0.404[b]	38	42
90	0.223	0.212	0.218[c]	8	9	0.569	0.565	0.567[b]	53	79	0.588	0.601	0.595[b]	56	71	0.376	0.378	0.377[b]	35	39

RA Relative Activity

[a] dilution = ×100

[b] dilution = ×50

[c] dilution = ×20

Table 101 Thermal stability at 60 °C, pH 5, of α-amylase (0.9 μM) crosslinked with 20 mM OMDC at pH 5, 6, 7 and 8

Time (min)	pH 5					pH 6					pH 7					pH 8				
	A_{540}			Act (U/mL)	RA (%)	A_{540}			Act (U/mL)	RA (%)	A_{540}			Act (U/mL)	RA (%)	A_{540}			Act (U/mL)	RA (%)
	1	2	Av			1	2	Av			1	2	Av			1	2	Av		
0	0.195	0.198	0.197[a]	37	100	0.144	0.154	0.149[a]	28	100	0.118	0.118	0.118[a]	22	100	0.079	0.072	0.076[a]	14	100
4	0.311	0.305	0.308[b]	29	78	0.250	0.257	0.254[b]	24	85	0.234	0.227	0.231[b]	22	98	0.130	0.125	0.128[b]	12	84
10	0.275	0.274	0.275[b]	26	70	0.260	0.242	0.251[b]	24	84	0.202	0.210	0.206[b]	19	87	0.140	0.125	0.133[b]	12	88
20	0.217	0.209	0.213[b]	20	54	0.233	0.247	0.240[b]	23	81	0.176	0.181	0.180[b]	17	76	0.104	0.099	0.102[b]	10	67
40	0.465	0.470	0.468[c]	18	48	0.225	0.212	0.219[b]	21	73	0.124	0.132	0.128[b]	12	54	0.227	0.245	0.236[b]	9	63
60	0.440	0.436	0.438[c]	16	45	0.211	0.232	0.222[b]	21	74	0.127	0.116	0.122[b]	11	51	0.218	0.219	0.219[b]	8	58
90	0.439	0.433	0.436[c]	16	44	0.221	0.214	0.218[b]	20	73	0.114	0.118	0.116[b]	11	49	0.180	0.191	0.186[b]	7	49

RA Relative Activity

[a] dilution = ×100

[b] dilution = ×50

[c] dilution = ×20

Table 102 Absorbance at 540 nm of native invertase for the estimation of E_d and k_d at pH5

Time (min)	A_{540}											
	54 °C			56 °C			58 °C			60 °C		
	1	2	Average	1	2	Average	1	2	Average	1	2	Average
0	0.346	0.344	0.345[a]	0.297	0.286	0.292[a]	0.336	0.338	0.337[a]	0.356	0.355	0.356[a]
0.5	-	-	-	-	-	-	-	-	-	0.370	0.387	0.379[b]
1	-	-	-	-	-	-	0.357	0.379	0.368[b]	0.918	0.896	0.907[c]
1.5	-	-	-	-	-	-	-	-	-	0.808	0.789	0.799[c]
2	0.532	0.502	0.517[b]	0.347	0.346	0.347[b]	0.301	0.319	0.310[b]	0.719	0.688	0.704[c]
2.5	-	-	-	-	-	-	-	-	-	1.221	1.208	1.215[d]
3	-	-	-	-	-	-	0.279	0.269	0.274[b]	1.203	1.124	1.164[d]
3.5	-	-	-	-	-	-	-	-	-	1.060	1.074	1.067[d]
4	0.432	0.451	0.442[b]	0.282	0.276	0.279[b]	0.627	0.617	0.622[c]	0.953	0.920	0.962[d]
5	-	-	-	-	-	-	0.562	0.540	0.551[c]	0.814	0.859	0.837[d]
6	0.373	0.374	0.374[b]	0.229	0.211	0.220[b]	0.521	0.501	0.511[c]	-	-	-
7	-	-	-	-	-	-	0.460	0.447	0.454[c]	-	-	-
8	0.355	0.343	0.349[b]	0.515	0.522	0.519[c]	0.811	0.797	0.760[d]	-	-	-
9	-	-	-	-	-	-	0.724	0.708	0.716[d]	-	-	-
10	0.826	0.828	0.827[c]	0.497	0.477	0.478[c]	0.634	0.639	0.637[d]	-	-	-
12	0.764	0.753	0.759[c]	0.416	0.430	0.423[c]	-	-	-	-	-	-
14	0.698	0.708	0.703[c]	0.380	0.379	0.380[c]	-	-	-	-	-	-
16	0.686	0.677	0.682[c]	0.364	0.363	0.364[c]	-	-	-	-	-	-
18	0.653	0.629	0.641[c]	0.336	0.327	0.332[c]	-	-	-	-	-	-
20	0.604	0.590	0.597[c]	0.309	0.303	0.306[c]	-	-	-	-	-	-

[a] dilution = ×100

[b] dilution = ×50

[c] dilution = ×20

Table 103 The estimation of E_d and k_d for native invertase at pH 5

Time (min)	Activity (Unit/mL)				Relative activity (%)				v_f				ln v_f			
	54 °C	56°C	58 °C	60 °C	54 °C	56°C	58 °C	60 °C	54 °C	56°C	58 °C	60 °C	54 °C	56°C	58 °C	60 °C
0	65	55	63	67	100	100	100	100	1	1	1	1	0	0	0	0
0.5	-	-	-	36	-	-	-	54	-	-	-	0.54	-	-	-	-0.62
1	-	-	35	34	-	-	57	52	-	-	0.57	0.52	-	-	-0.56	-0.65
1.5	-	-	-	30	-	-	-	44	-	-	-	0.44	-	-	-	-0.80
2	49	33	29	26	77	59	45	39	0.77	0.59	0.45	0.39	-0.26	-0.53	-0.80	-0.94
2.5	-	-	-	23	-	-	-	34	-	-	-	0.34	-	-	-	-1.08
3	-	-	26	22	-	-	40	32	-	-	0.40	0.32	-	-	-0.92	-1.14
3.5	-	-	-	20	-	-	-	30	-	-	-	0.30	-	-	-	-1.20
4	42	26	23	18	65	48	37	27	0.65	0.37	0.37	0.27	-0.43	-0.73	-0.99	-1.31
5	-	-	21	16	-	-	33	23	-	-	0.33	0.23	-	-	-1.11	-1.47
6	35	21	19	-	54	36	30	-	0.54	0.36	0.30	-	-0.62	-1.02	-1.20	-
7	-	-	17	-	-	-	27	-	-	-	0.27	-	-	-	-1.31	-
8	33	19	14	-	50	35	23	-	0.50	0.35	0.23	-	-0.69	-1.05	-1.47	-
9	-	-	13	-	-	-	21	-	-	-	0.21	-	-	-	-1.56	-
10	31	18	12	-	48	33	19	-	0.48	0.33	0.19	-	-073	-1.11	-1.66	-
12	29	16	-	-	44	29	-	-	0.44	0.29	-	-	-0.82	-1.24	-	-
14	26	14	-	-	41	26	-	-	0.41	0.26	-	-	-0.89	-1.35	-	-
16	26	14	-	-	39	25	-	-	0.39	0.25	-	-	-0.94	-1.39	-	-
18	24	12	-	-	37	23	-	-	0.37	0.23	-	-	-0.99	-1.47	-	-
20	22	12	-	-	35	21	-	-	0.35	0.21	-	-	-1.05	-1.56	-	-

Table 104 Absorbance at 540 nm of crosslinked invertase (0.9 µM) for the estimation of E_d and k_d at pH 5

Time (min)	A_{540}											
	54 °C			56 °C			58 °C			60 °C		
	1	2	Average	1	2	Average	1	2	Average	1	2	Average
0	0.181	0.178	0.178[a]	0.193	0.195	0.194[a]	0.212	0.210	0.211[a]	0.209	0.213	0.211[a]
0.5	-	-	-	-	-	-	-	-	-	0.279	0.272	0.276[b]
1	-	-	-	-	-	-	0.305	0.301	0.303[b]	0.633	0.670	0.652[c]
1.5	-	-	-	-	-	-	-	-	-	0.603	0.602	0.603[c]
2	0.349	0.356	0.353[b]	0.277	0.274	0.276[b]	0.275	0.277	0.276[b]	0.558	0.587	0.573[c]
2.5	-	-	-	-	-	-	-	-	-	0.974	0.976	0.975[d]
3	-	-	-	-	-	-	0.252	0.260	0.256[b]	0.915	0.889	0.902[d]
3.5	-	-	-	-	-	-	-	-	-	0.887	0.873	0.880[d]
4	0.332	0.323	0.328[b]	0.270	0.261	0.266[b]	0.608	0.619	0.614[c]	0.818	0.792	0.805[d]
5	-	-	-	-	-	-	0.588	0.613	0.601[c]	0.748	0.744	0.746[d]
6	0.302	0.303	0.303[b]	0.242	0.221	0.232[b]	0.589	0.656	0.577[c]	-	-	-
7	-	-	-	-	-	-	0.527	0.573	0.550[c]	-	-	-
8	0.292	0.285	0.289[b]	0.591	0.574	0.583[c]	0.967	0.987	0.977[d]	-	-	-
9	-	-	-	-	-	-	0.947	0.947	0.947[d]	-	-	-
10	0.749	0.757	0.753[c]	0.568	0.588	0.578[c]	0.924	0.922	0.923[d]	-	-	-
12	0.749	0.716	0.733[c]	0.573	0.567	0.570[c]	-	-	-	-	-	-
14	0.723	0.733	0.728[c]	0.542	0.539	0.541[c]	-	-	-	-	-	-
16	0.752	0.728	0.740[c]	0.538	0.555	0.547[c]	-	-	-	-	-	-
18	0.696	0.709	0.703[c]	0.527	0.520	0.524[c]	-	-	-	-	-	-
20	0.719	0.709	0.714[c]	0.512	0.533	0.523[c]	-	-	-	-	-	-

[a] dilution = ×100

[b] dilution = ×50

[c] dilution = ×20

Table 105 The estimation of E_d and k_d for crosslinked invertase (0.9 µM) at pH 5

Time (min)	Activity (Unit/mL)				Relative activity (%)				ν_f				ln ν_f			
	54 °C	56°C	58 °C	60 °C	54 °C	56°C	58 °C	60 °C	54 °C	56°C	58 °C	60 °C	54 °C	56°C	58 °C	60 °C
0	34	36	40	40	100	100	100	100	1	1	1	1	0	0	0	0
0.5	-	-	-	26	-	-	-	66	-	-	-	0.66	-	-	-	-0.42
1	-	-	28	24	-	-	71	63	-	-	0.71	0.63	-	-	-0.34	-0.46
1.5	-	-	-	23	-	-	-	57	-	-	-	0.57	-	-	-	-0.56
2	33	26	26	22	96	72	65	52	0.96	0.72	0.65	0.52	-0.04	-0.33	-0.43	-0.65
2.5	-	-	-	18	-	-	-	46	-	-	-	0.46	-	-	-	-0.78
3	-	-	24	17	-	-	61	42	-	-	0.61	0.42	-	-	-0.49	-0.87
3.5	-	-	-	17	-	-	-	41	-	-	-	0.41	-	-	-	-0.89
4	31	25	23	15	89	69	57	38	0.89	0.69	0.57	0.38	-0.12	-0.37	-0.56	-0.97
5	-	-	23	14	-	-	56	35	-	-	0.56	0.35	-	-	-0.58	-1.05
6	28	22	22	-	84	58	54	-	0.84	0.58	0.54	-	-0.17	-0.54	-0.62	-
7	-	-	21	-	-	-	52	-	-	-	0.52	-	-	-	-0.65	-
8	27	22	18	-	80	61	46	-	0.80	0.61	0.46	-	-0.22	-0.49	-0.78	-
9	-	-	18	-	-	-	45	-	-	-	0.45	-	-	-	-0.80	-
10	28	22	17	-	84	60	43	-	0.84	0.60	0.43	-	-0.17	-0.51	-0.84	-
12	28	21	-	-	83	59	-	-	0.83	0.59	-	-	-0.19	-0.53	-	-
14	27	20	-	-	81	56	-	-	0.81	0.56	-	-	-0.21	-0.58	-	-
16	28	21	-	-	81	57	-	-	0.81	0.57	-	-	-0.21	-0.56	-	-
18	26	20	-	-	77	55	-	-	0.77	0.55	-	-	-0.26	-0.60	-	-
20	27	20	-	-	78	55	-	-	0.78	0.55	-	-	-0.25	-0.60	-	-

Table 106 The estimation of K_m and v_{max} of native invertase at pH 6 and room temperature (Measurements 1-3)

Sucrose (M)	Measurement 1				Measurement 2				Measurement 3			
	A_{540}			Activity (U/mL)	A_{540}			Activity (U/mL)	A_{540}			Activity (U/mL)
	1	2	Average		1	2	Average		1	2	Average	
0	0	0	0	0	0	0	0	0	0	0	0	0
0.004	0.358	0.360	0.362*	6	0.378	0.372	0.375*	6	0.366	0.362	0.364*	6
0.0012	0.184	0.202	0.193**	15	0.217	0.209	0.213**	17	0.199	0.200	0.200**	16
0.002	0.274	0.276	0.275**	22	0.280	0.288	0.288**	23	0.315	0.311	0.313**	25
0.004	0.219	0.219	0.219***	35	0.193	0.207	0.200***	32	0.206	0.220	0.213***	34
0.012	0.313	0.288	0.301***	48	0.292	0.296	0.294***	47	0.306	0.294	0.300***	48

*dilution ×10

**dilution ×50

**dilution ×100

Table 107 The estimation of K_m and v_{max} of native invertase at pH 6 and room temperature (Measurements 4-5)

Sucrose (M)	Measurement 4				Measurement 5				Average activity (U/mL)	SD
	A_{540}			Activity (U/mL)	A_{540}			Activity (U/mL)		
	1	2	Average		1	2	Average			
0	0	0	0	0	0	0	0	0	0	0
0.004	0.312	0.313	0.313*	5	0.373	0.361	0.367*	6	6	0.4
0.0012	0.183	0.177	0.180**	14	0.169	0.181	0.175**	14	15	1.17
0.002	0.295	0.305	0.300**	24	0.272	0.268	0.270**	22	23	1.17
0.004	0.208	0.209	0.209***	33	0.197	0.191	0.194***	31	33	1.41
0.012	0.305	0.306	0.306***	49	0.287	0.289	0.288***	46	48	1.02

*dilution ×10

**dilution ×50

**dilution ×100

Table 108 The estimation of K_m and v_{max} of crosslinked invertase at pH 6 and room temperature (Measurements 1-3)

Sucrose (M)	Measurement 1				Measurement 3				Measurement 4			
	A_{540}			Activity (U/mL)	A_{540}			Activity (U/mL)	A_{540}			Activity (U/mL)
	1	2	Average		1	2	Average		1	2	Average	
0	0	0	0	0	0	0	0	0	0	0	0	0
0.004	0.328	0.334	0.331*	4	0.453	0.439	0.446*	5	0.432	0.431	0.432*	5
0.0012	0.536	0.535	0.536**	12	0.458	0.428	0.443**	10	0.443	0.435	0.439**	10
0.002	0.627	0.623	0.625**	14	0.672	0.739	0.706**	15	0.613	0.613	0.613**	14
0.004	0.228	0.218	0.223***	25	0.203	0.207	0.205***	23	0.217	0.209	0.213***	24
0.012	0.302	0.306	0.304***	34	0.302	0.288	0.295***	33	0.331	0.335	0.339***	38

*dilution ×7

**dilution ×14

**dilution ×70

Table 109 The estimation of K_m and v_{max} of crosslinked invertase at pH 6 and room temperature (Measurements 4-5)

Sucrose (M)	Measurement 4				Measurement 5				Average activity (U/mL)	SD
	A_{540}			Activity (U/mL)	A_{540}			Activity (U/mL)		
	1	2	Average		1	2	Average			
0	0	0	0	0	0	0	0	0	0	0
0.004	0.324	0.346	0.335*	4	0.344	0.329	0.337*	4	4	0.49
0.0012	0.395	0.409	0.402**	9	0.525	0.533	0.529**	12	11	1.20
0.002	0.601	0.617	0.609**	14	0.712	0.716	0.714**	16	15	0.80
0.004	0.195	0.196	0.196***	22	0.206	0.211	0.209***	24	24	1.02
0.012	0.286	0.285	0.286***	32	0.333	0.327	0.330***	37	35	2.32

*dilution ×7

**dilution ×14

**dilution ×70

Table 110 Thermal stability of native invertase at 55 °C, pH 6, (Measurements 1-3)

Time (min)	Measurement 1					Measurement 2					Measurement 3				
	A_{540}			Activity (U/mL)	Relative activity (%)	A_{540}			Activity (U/mL)	Relative activity (%)	A_{540}			Activity (U/mL)	Relative activity (%)
	1	2	Average			1	2	Average			1	2	Average		
0	0.469	0.428	0.449*	141	100	0.502	0.493	0.498*	156	100	0.382	0.351	0.367*	115	100
10	0.250	0.265	0.258*	81	57	0.304	0.313	0.309*	97	62	0.175	0.183	0.179*	56	49
20	0.204	0.199	0.202*	63	45	0.214	0.219	0.217*	68	44	0.132	0.138	0.135*	42	37
40	0.137	0.141	0.139*	44	31	0.128	0.133	0.131*	41	26	0.098	0.106	0.102*	32	28
60	0.118	0.102	0.110*	34	24	0.126	0.128	0.127*	40	26	0.089	0.095	0.092*	29	25
80	0.507	0.508	0.508**	16	11	0.102	0.101	0.102*	32	21	0.512	0.528	0.520**	16	14
100	0.684	0.669	0.677**	21	15	0.069	0.088	0.079*	25	16	0.500	0.425	0.463**	14	12
120	0.671	0.630	0.651**	20	14	0.090	0.089	0.090*	28	18	0.412	0.440	0.426**	13	11

*dilution = ×100

**dilution = ×10

Table 111 Thermal stability of native invertase at 55 °C, pH 6, (Measurements 4-6)

Time (min)	Measurement 4					Measurement 5					Measurement 6					Relative activity (average,%)	SD
	A_{540}			Activity (U/mL)	Relative activity (%)	A_{540}			Activity (U/mL)	Relative activity (%)	A_{540}			Activity (U/mL)	Relative activity (%)		
	1	2	Average			1	2	Average			1	2	Average				
0	0.339	0.349	0.344*	108	100	0.535	0.505	0.520*	163	100	0.466	0.471	0.469*	147	100	100	0
10	0.176	0.175	0.176*	55	51	0.287	0.303	0.295*	92	56	0.227	0.222	0.225*	70	48	54	4.95
20	0.144	0.153	0.149*	47	44	0.241	0.254	0.248*	78	48	0.145	0.150	0.148*	46	31	42	5.74
40	0.122	0.118	0.120*	38	35	0.199	0.193	0.196*	61	37	0.150	0.141	0.146*	46	31	31	3.77
60	0.084	0.083	0.084*	26	24	0.156	0.169	0.163*	51	31	0.124	0.134	0.129*	40	27	26	2.41
80	0.518	0.549	0.534**	17	16	0.136	0.139	0.138*	43	26	0.064	0.061	0.063*	20	14	17	5.03
100	0.457	0.487	0.472**	15	14	0.112	0.127	0.120*	38	23	0.460	0.447	0.454**	14	10	15	4.17
120	0.446	0.441	0.444**	14	13	0.098	0.098	0.098*	31	19	0.371	0.368	0.370**	12	9	14	3.75

*dilution = ×100

**dilution = ×10

Table 112 Thermal stability at 55 °C, pH 6, of invertase (185 μM) crosslinked with BMDC (1-20 mM)

Time (min)	1 mM BMDC					10 mM BMDC					20 mM BMDC				
	A_{540}			Activity (U/mL)	Relative activity (%)	A_{540}			Activity (U/mL)	Relative activity (%)	A_{540}			Activity (U/mL)	Relative activity (%)
	1	2	Average			1	2	Average			1	2	Average		
0	0.366	0.358	0.362*	113	100	0.260	0.264	0.262*	82	100	0.275	0.295	0.285*	89	100
10	0.249	0.239	0.244*	76	67	0.216	0.215	0.216*	68	83	0.201	0.201	0.201*	63	71
20	0.209	0.209	0.209*	65	58	0.177	0.182	0.180*	56	68	0.187	0.184	0.186*	58	65
40	0.195	0.183	0.189*	59	52	0.140	0.140	0.140*	44	54	0.200	0.194	0.197*	62	70
60	0.167	0.163	0.165*	52	46	0.144	0.139	0.142*	44	54	0.225	0.197	0.211*	66	74
80	0.140	0.146	0.143*	45	40	0.116	0.122	0.119*	37	45	0.186	0.187	0.187*	59	66
100	0.162	0.145	0.154*	48	42	0.109	0.106	0.108*	34	41	0.173	0.191	0.182*	57	64
120	0.145	0.140	0.143*	45	40	0.130	0.128	0.129*	40	49	0.166	0.169	0.168*	53	60

*dilution = ×100

Table 113 Thermal stability at 55 °C, pH 6, of invertase (185 μM) crosslinked with BMDC (30-50 mM)

Time (min)	30 mM BMDC					40 mM BMDC					50 mM BMDC				
	A_{540}			Activity (U/mL)	Relative activity (%)	A_{540}			Activity (U/mL)	Relative activity (%)	A_{540}			Activity (U/mL)	Relative activity (%)
	1	2	Average			1	2	Average			1	2	Average		
0	0.256	0.256	0.256*	80	100	0.213	0.211	0.212*	66	100	0.246	0.247	0.247*	77	100
10	0.221	0.199	0.210*	66	83	0.181	0.163	0.172*	54	82	0.153	0.156	0.155*	46	60
20	0.207	0.205	0.206*	64	80	0.134	0.129	0.132*	41	62	0.118	0.123	0.121*	38	49
40	0.220	0.205	0.213*	67	84	0.112	0.100	0.106*	33	50	0.118	0.123	0.121*	38	49
60	0.214	0.218	0.216*	68	85	0.097	0.097	0.097*	30	45	0.688	0.659	0.674**	21	27
80	0.189	0.201	0.195*	61	76	0.638	0.139	0.138**	20	30	0.716	0.708	0.712**	22	30
100	0.158	0.168	0.163*	51	64	0.583	0.594	0.589**	18	27	0.642	0.596	0.619**	19	25
120	0.169	0.176	0.173*	54	68	0.677	0.662	0.670**	21	32	0.569	0.570	0.570**	18	23

*dilution = ×100

**dilution = ×10

Table 114 Thermal stability at 55 °C, pH 6, of invertase (185 μM) crosslinked with HMDC (1-20 mM)

Time (min)	1 mM HMDC					10 mM HMDC					20 mM HMDC				
	A_{540}			Activity (U/mL)	Relative activity (%)	A_{540}			Activity (U/mL)	Relative activity (%)	A_{540}			Activity (U/mL)	Relative activity (%)
	1	2	Average			1	2	Average			1	2	Average		
0	0.489	0.515	0.502*	157	100	0.339	0.342	0.341*	107	100	0.386	0.397	0.392*	123	100
10	0.349	0.345	0.347*	109	69	0.238	0.246	0.242*	76	71	0.210	0.221	0.216*	68	55
20	0.234	0.237	0.236*	74	47	0.205	0.204	0.205*	64	60	0.195	0.193	0.194*	61	50
40	0.181	0.195	0.188*	59	38	0.185	0.176	0.181*	57	53	0.144	0.144	0.144*	45	37
60	0.206	0.200	0.203*	64	41	0.154	0.168	0.161*	50	47	0.118	0.119	0.119*	37	30
80	0.200	0.198	0.199*	62	39	0.141	0.139	0.140*	44	41	0.104	0.109	0.107*	33	27
100	0.163	0.164	0.164*	51	32	0.140	0.138	0.139*	44	41	0.700	0.730	0.715**	22	18
120	0.148	0.144	0.146*	46	29	0.150	0.168	0.159*	50	47	0.731	0.740	0.736**	23	19

*dilution = ×100

**dilution = ×10

Table 115 Thermal stability at 55 °C, pH 6, of invertase (185 μM) crosslinked with HMDC (30-50 mM)

Time (min)	30 mM HMDC					40 mM HMDC					50 mM HMDC				
	A_{540}			Activity (U/mL)	Relative activity (%)	A_{540}			Activity (U/mL)	Relative activity (%)	A_{540}			Activity (U/mL)	Relative activity (%)
	1	2	Average			1	2	Average			1	2	Average		
0	0.347	0.336	0.342*	107	100	0.372	0.375	0.374*	117	100	0.371	0.399	0.385*	121	100
10	0.212	0.207	0.210*	66	62	0.323	0.262	0.293*	92	79	0.294	0.279	0.287*	90	74
20	0.163	0.163	0.163*	51	48	0.210	0.197	0.204*	64	55	0.222	0.238	0.230*	72	60
40	0.143	0.133	0.138*	43	40	0.182	0.166	0.174*	54	46	0.181	0.189	0.185*	58	48
60	0.121	0.123	0.122*	38	36	0.146	0.163	0.155*	49	42	0.159	0.159	0.159*	50	41
80	0.114	0.108	0.111*	35	33	0.133	0.136	0.135*	42	36	0.142	0.144	0.143*	45	37
100	0.103	0.101	0.102*	32	30	0.091	0.096	0.094*	29	25	0.144	0.146	0.145*	45	37
120	0.667	0.640	0.654**	20	19	0.105	0.097	0.101*	32	27	0.134	0.137	0.136*	43	36

*dilution = ×100

**dilution = ×10

Table 116 Thermal stability at 55 °C, pH 6, of invertase (185 μM) crosslinked with OMDC (1-20 mM)

Time (min)	1 mM OMDC					10 mM OMDC					20 mM OMDC				
	A_{540}			Activity (U/mL)	Relative activity (%)	A_{540}			Activity (U/mL)	Relative activity (%)	A_{540}			Activity (U/mL)	Relative activity (%)
	1	2	Average			1	2	Average			1	2	Average		
0	0.489	0.463	0.476*	149	100	0.581	0.595	0.588*	184	100	0.662	0.649	0.656*	205	100
10	0.300	0.289	0.295*	92	62	0.490	0.551	0.521*	163	89	0.469	0.464	0.467*	146	71
20	0.256	0.244	0.250*	78	52	0.367	0.383	0.375*	117	64	0.357	0.398	0.378*	118	58
40	0.158	0.171	0.165*	52	35	0.316	0.322	0.319*	100	54	0.330	0.328	0.329*	103	50
60	0.154	0.162	0.158*	49	33	0.281	0.268	0.275*	86	47	0.272	0.286	0.279*	87	42
80	1.168	1.152	1.160**	36	24	0.235	0.243	0.239*	75	41	0.260	0.253	0.257*	80	39
100	1.060	1.044	1.052**	33	22	0.197	0.200	0.199*	62	34	0.243	0.222	0.233*	73	36
120	0.991	1.000	0.996**	31	21	0.221	0.226	0.224*	70	38	0.245	0.237	0.241*	75	37

*dilution = ×100

**dilution = ×10

Table 117 Thermal stability at 55 °C, pH 6, of invertase (185 μM) crosslinked with OMDC (30-50 mM)

Time (min)	30 mM OMDC					40 mM OMDC					50 mM OMDC				
	A_{540}			Activity (U/mL)	Relative activity (%)	A_{540}			Activity (U/mL)	Relative activity (%)	A_{540}			Activity (U/mL)	Relative activity (%)
	1	2	Average			1	2	Average			1	2	Average		
0	0.530	0.526	0.528*	165	100	0.506	0.453	0.480*	150	100	0.533	0.516	0.525*	164	100
10	0.301	0.293	0.297*	93	56	0.269	0.278	0.274*	86	57	0.351	0.335	0.343*	107	65
20	0.265	0.258	0.262*	82	50	0.172	0.194	0.183*	57	38	0.276	0.267	0.272*	85	52
40	0.218	0.221	0.220*	69	42	0.197	0.186	0.192*	60	40	0.217	0.226	0.222*	69	42
60	0.186	0.174	0.180*	56	34	0.145	0.153	0.149*	47	31	0.188	0.192	0.190*	59	36
80	0.171	0.172	0.172*	54	33	0.150	0.139	0.145*	45	30	0.174	0.182	0.178*	56	34
100	0.155	0.164	0.160*	50	30	0.150	0.141	0.146*	46	31	0.179	0.191	0.185*	58	35
120	0.153	0.154	0.154*	48	29	0.137	0.141	0.139*	44	29	0.168	0.176	0.172*	54	33

*dilution = ×100

Table 118 Thermal stability of native invertase, controlled native invertase, invertase (185 μM) after treatment with BMDC and BIC

Time (min)	Native					Controlled native					Bifunctional crosslinker (BMDC)					Monofunctional crosslinker (BIC)				
	A_{410}			Act (U/mL)	RA (%)	A_{410}			Act (U/mL)	RA (%)	A_{410}			Act (U/mL)	RA (%)	A_{410}			Act (U/mL)	RA (%)
	1	2	Av			1	2	Av			1	2	Av			1	2	Av		
0	0.567	0.555	0.566[a]	1,064	100	0.493	0.481	0.487[a]	916	100	0.438	0.414	0.426[a]	801	100	0.504	0.537	0.521[a]	979	100
5	0.703	0.696	0.700[a]	658	62	0.600	0.626	0.613[b]	0.576	63	0.768	0.726	0.747[b]	702	88	0.755	0.758	0.757[b]	712	73
10	0.475	0.435	0.455[b]	428	40	0.438	0.436	0.437[b]	411	45	0.629	0.691	0.660[b]	620	77	0.539	0.546	0.543[b]	510	52
20	0.712	0.715	0.714[c]	268	25	0.277	0.281	0.279[b]	262	29	0.620	0.531	0.576[b]	541	68	0.326	0.314	0.320[b]	301	31
40	0.532	0.530	0.531[c]	200	19	0.582	0.555	0.569[c]	214	23	0.500	0.549	0.525[b]	494	62	0.627	0.640	0.634[c]	238	24
60	0.808	0.835	0.822[d]	155	15	0.461	0.473	0.467[c]	176	19	0.489	0.506	0.498[b]	460	57	0.522	0.555	0.539[c]	203	21
80	0.656	0.656	0.656[d]	123	12	0.371	0.370	0.371[c]	139	15	0.499	0.483	0.491[b]	454	57	0.368	0.385	0.377[c]	142	15
100	0.495	0.459	0.477[d]	90	8	0.591	0.596	0.594[d]	112	12	0.399	0.437	0.418[b]	411	51	0.702	0.701	0.702[d]	132	13
120	0.423	0.402	0.413[d]	78	7	0.512	0.516	0.514[d]	97	11	0.472	0.462	0.467[b]	434	54	0.591	0.602	0.597[d]	112	11

RA Relative Activity

[a] dilution ×1,000

[b] dilution ×500

[c] dilution ×200

[d] dilution ×100

Table 119 Absorbance at 540 nm of native invertase for the estimation of E_d and $k_d$at pH 6

Time (min)	A_{540}								
	50 °C			55 °C			60 °C		
	1	2	Average	1	2	Average	1	2	Average
0	0.722	0.777	0.750*	0.664	0.644	0.654*	0.695	0.667	0.681*
0.33	-	-	-	-	-	-	0.530	0.535	0.533**
1	-	-	-	-	-	-	0.298	0.332	0.315**
2	-	-	-	0.299	0.306	0.303*	-	-	-
4	-	-	-	0.231	0.237	0.234*	-	-	-
5	0.700	0.701	0.701*	0.208	0.202	0.205*	-	-	-
6	-	-	-	-	-	-	-	-	-
10	0.595	0.577	0.586*	-	-	-	-	-	-
15	0.558	0.541	0.550*	-	-	-	-	-	-
20	0.513	0.505	0.509*	-	-	-	-	-	-

*dilution = ×1000

**dilution = ×500

Table 120 The estimation of E_d and k_d for native invertase at pH 6

Time (min)	Activity (Unit/mL)			Relative activity (%)			ν_f			ln ν_f		
	50 °C	55 °C	60 °C	50 °C	55 °C	60 °C	50 °C	55 °C	60 °C	50 °C	55 °C	60 °C
0	1,409	1,230	1,280	100	100	100	1	1	1	0	0	0
0.33	-	-	501	-	-	39	-	-	0.39	-	-	-0.94
1	-	-	312	-	-	24	-	-	0.24	-	-	-1.43
2	-	575	-	-	47	-	-	0.47	-	-	-0.76	-
4	-	440	-	-	36	-	-	0.36	-	-	-1.02	-
5	1,318	-	-	94	-	-	0.94	-	-	-0.06	-	-
6	-	380	-	-	31	-	-	0.31	-	-	-1.17	-
10	1,119	-	-	79	-	-	0.79	-	-	-0.24	-	-
15	1,049	-	-	74	-	-	0.74	-	-	-0.30	-	-
20	964	-	-	68	-	-	0.68	-	-	-0.39	-	-

Table 121 Absorbance at 540 nm of crosslinked invertase (185 μM) for the estimation of E_d and k_d at pH 6

Time (min)	A_{540}								
	50 °C			55 °C			60 °C		
	1	2	Average	1	2	Average	1	2	Average
0	0.550	0.555	0.553*	0.533	0.532	0.533*	0.529	0.552	0.541*
0.2	-	-	-	-	-	-	0.738	0.753	0.746**
1	-	-	-	-	-	-	0.669	0.665	0.667**
1.4	-	-	-	-	-	-	0.627	0.635	0.631**
2	-	-	-	0.421	0.438	0.430*	-	-	-
4	-	-	-	0.436	0.427	0.432*	-	-	-
5	0.402	0.413	0.408*	-	-	-	-	-	-
6	-	-	-	0.381	0.370	0.376*	-	-	-
8	-	-	-	0.427	0.402	0.415*	-	-	-
10	0.522	0.542	0.532*	0.748	0.756	0.752**	-	-	-
15	0.530	0.487	0.509*	0.722	0.706	0.714**	-	-	-
20	0.487	0.494	0.491*	-	-	-	-	-	-
25	0.469	0.504	0.487*	-	-	-	-	-	-
30	0.531	0.514	0.523*	-	-	-	-	-	-
35	0.502	0.507	0.505*	-	-	-	-	-	-
40	0.546	0.479	0.513*	-	-	-	-	-	-

*dilution = ×1000

**dilution = ×500

Table 122 the estimation of E_d and k_d for crosslinked invertase (185 μM) at pH 6

Time (min)	Activity (Unit/mL)			Relative activity (%)			ν_f			ln ν_f		
	50 °C	55 °C	60 °C	50 °C	55 °C	60 °C	50 °C	55 °C	60 °C	50 °C	55 °C	60 °C
0	1,039	1,001	1,016	100	100	100	1	1	1	0	0	0
0.2	-	-	708	-	-	70	-	-	0.70	-	-	-0.36
1	-	-	627	-	-	62	-	-	0.62	-	-	-0.48
1.4	-	-	593	-	-	58	-	-	0.58	-	-	-0.54
2	-	823	-	-	82	-	-	0.82	-	-	-0.20	-
4	-	820	-	-	82	-	-	0.82	-	-	-0.20	-
5	776	-	-	75	-	-	0.75	-	-	-0.29	-	-
6	-	716	-	-	72	-	-	0.72	-	-	-0.33	-
8	-	756	-	-	76	-	-	0.76	-	-	-0.27	-
10	1,019	711	-	98	70	-	0.98	0.70	-	-0.02	-0.36	-
15	996	679	-	96	68	-	0.96	0.68	-	-0.04	-0.42	-
20	929	-	-	89	-	-	0.89	-	-	-0.12	-	-
25	948	-	-	91	-	-	0.91	-	-	-0.09	-	-
30	966	-	-	93	-	-	0.93	-	-	-0.07	-	-
35	953	-	-	92	-	-	0.92	-	-	-0.08	-	-
40	1,026	-	-	99	-	-	0.99	-	-	-0.01	-	-

1.3.3 Thermal stabilization by imidoesters

Table 123 Thermal stability of native invertase at 60 °C and pH 5

Time (min)	Measurement 1					Measurement 2					Measurement 3					Relative activity (average,%)	SD
	A_{540}			Activity (U/mL)	Relative activity (%)	A_{540}			Activity (U/mL)	Relative activity (%)	A_{540}			Activity (U/mL)	Relative activity (%)		
	1	2	Average			1	2	Average			1	2	Average				
0	0.253	0.252	0.253*	47	100	0.279	0.275	0.277*	52	100	0.243	0.235	0.239*	45	100	100	0
5	0.365	0.361	0.363**	34	72	0.354	0.366	0.360**	34	65	0.334	0.335	0.335**	32	70	69	2.94
10	0.300	0.309	0.305**	29	60	0.296	0.290	0.293**	28	53	0.272	0.264	0.268**	25	56	56	2.87
20	0.240	0.227	0.234**	22	46	0.233	0.221	0.227**	21	41	0.194	0.180	0.187**	18	39	42	2.94
40	0.179	0.173	0.176**	17	35	0.152	0.146	0.149**	14	27	0.119	0.121	0.120**	11	25	29	4.32
60	0.153	0.152	0.153**	14	30	0.111	0.110	0.111**	10	20	0.096	0.095	0.096**	9	20	23	4.71
90	0.126	0.127	0.127**	12	25	0.087	0.091	0.089**	8	16	0.086	0.074	0.080**	7	15	19	4.50

*dilution ×100

**dilution ×50

Table 124 Thermal stability at 60 °C, pH 5, of invertase crosslinked with DMA (0.1-1 mg/mL)

Time (min)	0.1 mg/mL DMA					1 mg/mL DMA				
	A_{540}			Activity (U/mL)	Relative Activity (%)	A_{540}			Activity (U/mL)	Relative Activity (%)
	1	2	Average			1	2	Average		
0	0.258	0.259	0.259*	49	100	0.242	0.245	0.244*	46	100
5	0.370	0.386	0.378**	36	73	0.344	0.340	0.342**	32	70
10	0.310	0.315	0.313**	29	60	0.281	0.283	0.282**	27	58
20	0.292	0.286	0.289**	27	56	0.201	0.198	0.200**	19	41
40	0.198	0.190	0.194**	18	38	0.158	0.155	0.157**	15	32
60	0.188	0.189	0.189**	18	36	0.131	0.126	0.129**	12	26
90	0.095	0.091	0.093**	9	18	0.101	0.103	0.102**	10	21

*dilution ×100

**dilution ×50

Table 125 Thermal stability at 60 °C, pH 5, of α-amylase crosslinked with DMA (5-10 mg/mL)

Time (min)	5 mg/mL DMA					10 mg/mL DMA				
	A_{540}			Activity (U/mL)	Relative Activity (%)	A_{540}			Activity (U/mL)	Relative Activity (%)
	1	2	Average			1	2	Average		
0	0.248	0.252	0.250*	47	100	0.226	0.222	0.224*	42	100
5	0.344	0.350	0.347**	33	69	0.308	0.311	0.310**	29	69
10	0.284	0.209	0.247**	23	49	0.257	0.253	0.255**	24	57
20	0.209	0.210	0.210**	20	42	0.179	0.175	0.179**	17	40
40	0.141	0.144	0.143**	13	29	0.113	0.108	0.111**	10	25
60	0.126	0.124	0.125**	12	25	0.076	0.075	0.076**	7	17
90	0.104	0.101	0.103**	10	21	0.054	0.050	0.052**	5	12

*dilution ×100

**dilution ×50

Table 126 Thermal stability at 60 °C, pH 5, of invertase crosslinked with DMP (0.1-1 mg/mL)

Time (min)	0.1 mg/mL DMP					1 mg/mL DMP				
	A_{540}			Activity (U/mL)	Relative Activity (%)	A_{540}			Activity (U/mL)	Relative Activity (%)
	1	2	Average			1	2	Average		
0	0.251	0.259	0.255*	48	100	0.248	0.242	0.245*	46	100
5	0.378	0.377	0.378**	36	74	0.320	0.326	0.323**	30	66
10	0.279	0.283	0.281**	26	55	0.239	0.241	0.240**	23	49
20	0.192	0.196	0.194**	18	38	0.201	0.211	0.206**	19	42
40	0.185	0.173	0.179**	17	35	0.149	0.155	0.152**	14	31
60	0.125	0.131	0.128**	12	25	0.125	0.139	0.132**	12	27
90	0.070	0.084	0.077**	7	15	0.098	0.098	0.098**	9	20

*dilution ×100

**dilution ×50

Table 127 Thermal stability at 60 °C, pH 5, of invertase crosslinked with DMP (5-10 mg/mL)

Time (min)	5 mg/mL DMP					10 mg/mL DMP				
	A_{540}			Activity (U/mL)	Relative Activity (%)	A_{540}			Activity (U/mL)	Relative Activity (%)
	1	2	Average			1	2	Average		
0	0.234	0.244	0.239*	45	100	0.225	0.221	0.223*	42	100
5	0.289	0.285	0.287**	27	60	0.268	0.267	0.268**	25	60
10	0.249	0.239	0.244**	23	51	0.207	0.213	0.210**	20	47
20	0.198	0.184	0.191**	18	40	0.182	0.166	0.174**	16	39
40	0.156	0.155	0.156**	15	33	0.139	0.147	0.143**	13	32
60	0.120	0.110	0.115**	11	24	0.085	0.084	0.085**	8	19
90	0.099	0.083	0.091**	9	19	0.049	0.041	0.045**	4	10

*dilution ×100

**dilution ×50

Table 128 Thermal stability at 60 °C, pH 5, of invertase crosslinked with DMS (0.1-1 mg/mL)

Time (min)	0.1 mg/mL DMS					1 mg/mL DMS				
	A_{540}			Activity (U/mL)	Relative Activity (%)	A_{540}			Activity (U/mL)	Relative Activity (%)
	1	2	Average			1	2	Average		
0	0.237	0.221	0.229*	43	100	0.234	0.256	0.245*	46	100
5	0.295	0.291	0.293**	28	64	0.303	0.303	0.303**	29	62
10	0.232	0.233	0.233**	22	51	0.231	0.239	0.235**	22	48
20	0.190	0.194	0.192**	18	42	0.193	0.179	0.186**	17	38
40	0.115	0.123	0.119**	11	26	0.164	0.165	0.165**	14	31
60	0.090	0.112	0.101**	9	22	0.125	0.111	0.118**	11	24
90	0.075	0.081	0.078**	7	17	0.090	0.096	0.093**	9	19

*dilution ×100

**dilution ×50

Table 129 Thermal stability at 60 °C, pH 5, of invertase crosslinked with DMS (5-10 mg/mL)

Time (min)	5 mg/mL DMS					10 mg/mL DMS				
	A_{540}			Activity (U/mL)	Relative Activity (%)	A_{540}			Activity (U/mL)	Relative Activity (%)
	1	2	Average			1	2	Average		
0	0.246	0.222	0.234*	44	100	0.216	0.217	0.217*	41	100
5	0.286	0.285	0.286**	27	61	0.272	0.278	0.275**	26	63
10	0.219	0.211	0.215**	20	46	0.219	0.209	0.214**	20	49
20	0.180	0.166	0.173**	16	37	0.171	0.161	0.166**	16	38
40	0.103	0.085	0.094**	9	20	0.114	0.112	0.113**	11	26
60	0.132	0.102	0.117**	11	25	0.059	0.063	0.061**	6	14
90	0.008	0.102	0.100**	9	20	0.081	0.049	0.065**	6	15

*dilution ×100

**dilution ×50

Table 130 Thermal stability at 60 °C, pH 5, of invertase crosslinked with 10 mg/mL DMA at pH 5, 6, 7 and 8

Time (min)	pH 5					pH 6					pH 7					pH 8				
	A_{540}			Act (U/mL)	RA (%)	A_{540}			Act (U/mL)	RA (%)	A_{540}			Act (U/mL)	RA (%)	A_{540}			Act (U/mL)	RA (%)
	1	2	Av			1	2	Av			1	2	Av			1	2	Av		
0	0.295	0.298	0.297*	56	100	0.209	0.210	0.210*	39	100	0.214	0.211	0.213*	40	100	0.221	0.210	0.216*	41	100
5	0.422	0.401	0.412**	39	69	0.278	0.281	0.280**	26	67	0.308	0.304	0.306**	29	72	0.283	0.276	0.280**	26	65
10	0.323	0.351	0.337**	32	57	0.226	0.212	0.219**	21	52	0.233	0.242	0.238**	22	56	0.217	0.223	0.220**	21	51
20	0.262	0.249	0.256**	24	43	0.176	0.167	0.172**	16	41	0.203	0.201	0.202**	19	48	0.162	0.170	0.166**	16	39
40	0.190	0.187	0.189**	18	32	0.109	0.113	0.111**	10	26	0.147	0.131	0.139**	13	33	0.117	0.115	0.116**	11	27
60	0.135	0.152	0.144**	13	24	0.077	0.075	0.076**	7	18	0.104	0.102	0.103**	10	24	0.084	0.082	0.083**	8	19
90	0.128	0.120	0.124**	12	21	0.061	0.056	0.059**	5	14	0.077	0.079	0.078**	7	18	0.055	0.065	0.060**	6	14

RA Relative Activity

*dilution ×100

**dilution ×50

1.3.4 Thermal stabilization by diamines

Table 131 Thermal stability of native invertase at 60 °C, pH 5 (Measurements 1-3)

Time (min)	Measurement 1					Measurement 2					Measurement 3				
	A_{540}			Activity (U/mL)	Relative activity (%)	A_{540}			Activity (U/mL)	Relative activity (%)	A_{540}			Activity (U/mL)	Relative activity (%)
	1	2	Average			1	2	Average			1	2	Average		
0	0.253	0.252	0.253*	47	100	0.279	0.275	0.277*	52	100	0.243	0.235	0.239*	45	100
5	0.365	0.361	0.363**	34	72	0.354	0.366	0.360**	34	65	0.334	0.335	0.335**	32	70
10	0.300	0.309	0.305**	29	60	0.296	0.290	0.293**	28	53	0.272	0.264	0.268**	25	56
20	0.240	0.227	0.234**	22	46	0.233	0.221	0.227**	21	41	0.194	0.180	0.187**	18	39
40	0.179	0.173	0.176**	17	35	0.152	0.146	0.149**	14	27	0.119	0.121	0.120**	11	25
60	0.153	0.152	0.153**	14	30	0.111	0.110	0.111**	10	20	0.096	0.095	0.096**	9	20
90	0.126	0.127	0.127**	12	25	0.087	0.091	0.089**	8	16	0.086	0.074	0.080**	7	15

*dilution ×100

**dilution ×50

Table 132 Thermal stability of native invertase at 60 °C, pH 5 (Measurements 4-5)

Time (min)	Measurement 4					Measurement 5					Relative activity (average,%)	SD
	A_{540}			Activity (U/mL)	Relative activity (%)	A_{540}			Activity (U/mL)	Relative activity (%)		
	1	2	Average			1	2	Average				
0	0.355	0.360	0.358*	67	100	0.241	0.234	0.238*	45	100	100	0
5	0.507	0.528	0.518**	49	72	0.393	0.354	0.374**	35	79	72	4.50
10	0.421	0.423	0.422**	40	59	0.304	0.312	0.308**	29	65	59	4.03
20	0.302	0.324	0.313**	29	44	0.227	0.234	0.231**	22	49	44	3.54
40	0.231	0.223	0.227**	21	32	0.167	0.162	0.165**	15	35	31	4.12
60	0.174	0.175	0.175**	16	24	0.132	0.123	0.128**	12	27	24	3.92
90	0.150	0.160	0.155**	15	22	0.102	0.104	0.103**	10	22	20	3.85

*dilution ×100

**dilution ×50

Table 133 Thermal stability at 60 °C, pH 5, of invertase crosslinked with EDA (0.1-1 mg/mL)

Time (min)	0.1 mg/mL EDA					1 mg/mL EDA				
	A_{540}			Activity (U/mL)	Relative Activity (%)	A_{540}			Activity (U/mL)	Relative Activity (%)
	1	2	Average			1	2	Average		
0	0.264	0.258	0.261*	49	100	0.253	0.249	0.251*	47	100
5	0.385	0.377	0.381**	36	73	0.367	0.351	0.359**	34	72
10	0.302	0.302	0.302**	28	58	0.308	0.294	0.301**	28	60
20	0.235	0.245	0.240**	23	46	0.235	0.221	0.228**	22	46
40	0.158	0.154	0.156**	15	30	0.137	0.136	0.137**	13	28
60	0.091	0.087	0.089**	8	17	0.124	0.108	0.116**	11	23
90	0.056	0.048	0.052**	5	10	0.076	0.066	0.071**	7	14

*dilution ×100

**dilution ×50

Table 134 Thermal stability at 60 °C, pH 5, of invertase crosslinked with EDA (5-10 mg/mL)

Time (min)	5 mg/mL EDA					10 mg/mL EDA				
	A_{540}			Activity (U/mL)	Relative Activity (%)	A_{540}			Activity (U/mL)	Relative Activity (%)
	1	2	Average			1	2	Average		
0	0.249	0.259	0.254*	48	100	0.259	0.269	0.264*	50	100
5	0.353	0.341	0.347**	33	68	0.371	0.371	0.371**	35	70
10	0.279	0.273	0.276**	26	54	0.335	0.319	0.327**	31	62
20	0.192	0.216	0.204**	19	40	0.243	0.255	0.249**	24	47
40	0.127	0.126	0.127**	12	25	0.162	0.148	0.155**	15	29
60	0.092	0.102	0.097**	9	19	0.099	0.117	0.105**	10	20
90	0.049	0.041	0.045**	4	9	0.079	0.081	0.080**	8	15

*dilution ×100

**dilution ×50

Table 135 Thermal stability at 60 °C, pH 5, of invertase crosslinked with DAB (0.1-1 mg/mL)

Time (min)	0.1 mg/mL DAB					1 mg/mL DAB				
	A_{540}			Activity (U/mL)	Relative Activity (%)	A_{540}			Activity (U/mL)	Relative Activity (%)
	1	2	Average			1	2	Average		
0	0.229	0.247	0.238*	45	100	0.242	0.240	0.241*	45	100
5	0.355	0.354	0.355**	33	74	0.355	0.364	0.360**	34	75
10	0.270	0.260	0.265**	25	56	0.297	0.307	0.302**	28	63
20	0.216	0.215	0.216**	20	45	0.240	0.237	0.239**	22	49
40	0.139	0.128	0.134**	13	28	0.158	0.168	0.163**	15	34
60	0.069	0.081	0.075**	7	16	0.119	0.135	0.127**	12	26
90	0.045	0.069	0.057**	5	12	0.100	0.079	0.090**	8	19

*dilution ×100

**dilution ×50

Table 136 Thermal stability at 60 °C, pH 5, of invertase crosslinked with DAB (5-10 mg/mL)

Time (min)	5 mg/mL DAB					10 mg/mL DAB				
	A_{540}			Activity (U/mL)	Relative Activity (%)	A_{540}			Activity (U/mL)	Relative Activity (%)
	1	2	Average			1	2	Average		
0	0.184	0.191	0.188*	35	100	0.170	0.159	0.165*	31	100
5	0.251	0.254	0.253**	24	67	0.273	0.281	0.277**	26	84
10	0.174	0.184	0.179**	17	48	0.235	0.240	0.238**	22	72
20	0.137	0.116	0.127**	12	34	0.159	0.163	0.161**	15	49
40	0.071	0.046	0.059**	5	16	0.104	0.111	0.108**	10	33
60	0.037	0.034	0.036**	3	9	0.068	0.076	0.072**	7	22
90	0.016	0.021	0.019**	2	5	0.060	0.060	0.060**	6	18

*dilution ×100

**dilution ×50

Table 137 Thermal stability at 60 °C, pH 5, of invertase crosslinked with DAH (0.1-1 mg/mL)

Time (min)	0.1 mg/mL DAH					1 mg/mL DAH				
	A_{540}			Activity (U/mL)	Relative Activity (%)	A_{540}			Activity (U/mL)	Relative Activity (%)
	1	2	Average			1	2	Average		
0	0.232	0.234	0.233*	44	100	0.244	0.240	0.242*	45	100
5	0.336	0.318	0.327**	31	70	0.340	0.343	0.342**	32	71
10	0.260	0.271	0.266**	25	57	0.271	0.271	0.271**	25	56
20	0.203	0.186	0.195**	18	42	0.177	0.206	0.192**	18	40
40	0.151	0.150	0.151**	14	32	0.148	0.134	0.141**	13	29
60	0.119	0.125	0.122**	11	26	0.131	0.104	0.118**	11	24
90	0.084	0.096	0.090**	8	19	0.085	0.102	0.094**	9	19

*dilution ×100

**dilution ×50

Table 138 Thermal stability at 60 °C, pH 5, of invertase crosslinked with DAH (5-10 mg/mL)

Time (min)	5 mg/mL DAH					10 mg/mL DAH				
	A_{540}			Activity (U/mL)	Relative Activity (%)	A_{540}			Activity (U/mL)	Relative Activity (%)
	1	2	Average			1	2	Average		
0	0.207	0.219	0.213*	40	100	0.159	0.162	0.161*	30	100
5	0.310	0.305	0.308**	29	72	0.252	0.246	0.249**	23	78
10	0.252	0.224	0.238**	22	56	0.191	0.198	0.195**	18	61
20	0.168	0.179	0.174**	16	41	0.122	0.128	0.125**	12	39
40	0.127	0.126	0.127**	12	30	0.073	0.072	0.073**	7	23
60	0.096	0.098	0.097**	9	23	0.046	0.056	0.051**	5	16
90	0.069	0.047	0.058**	5	14	0.036	0034	0.035**	3	11

*dilution ×100

**dilution ×50

Table 139 Thermal stability at 60 °C, pH 5, of invertase crosslinked with DAO (0.1-1 mg/mL)

Time (min)	0.1 mg/mL DAO					1 mg/mL DAO				
	A_{540}			Activity (U/mL)	Relative Activity (%)	A_{540}			Activity (U/mL)	Relative Activity (%)
	1	2	Average			1	2	Average		
0	0.273	0.251	0.262*	49	100	0.268	0.288	0.278*	52	100
5	0.400	0.390	0.395**	37	75	0.353	0.344	0.349**	33	63
10	0.288	0.296	0.292**	27	56	0.261	0.248	0.255**	24	46
20	0.234	0.213	0.224**	21	43	0.195	0.199	0.197**	19	35
40	0.170	0.185	0.178**	17	34	0.116	0.114	0.115**	11	21
60	0.150	0.131	0.141**	13	27	0.071	0.076	0.074**	7	13
90	0.131	0.098	0.115**	11	22	0.043	0.047	0.045**	4	8

*dilution ×100

**dilution ×50

Table 140 Thermal stability at 60 °C, pH 5, of invertase crosslinked with DAO (5-10 mg/mL)

Time (min)	5 mg/mL DAO					10 mg/mL DAO				
	A_{540}			Activity (U/mL)	Relative Activity (%)	A_{540}			Activity (U/mL)	Relative Activity (%)
	1	2	Average			1	2	Average		
0	0.229	0.230	0.230*	43	100	0.056	0.058	0.057*	11	100
5	0.305	0.295	0.300**	28	65	0.084	0.065	0.075**	7	65
10	0.229	0.250	0.240**	23	52	0.054	0.024	0.039**	4	34
20	0.161	0.178	0.170**	16	37	0.033	0.029	0.031**	3	27
40	0.104	0.104	0.104**	10	23	0.026	0.016	0.021**	2	18
60	0.065	0.068	0.067**	9	14	0.015	0.011	0.013**	1	11
90	0.044	0.032	0.038**	4	8	0.013	0.001	0.007**	0.6	5

*dilution ×100

**dilution ×50

Table 141 Thermal stability at 60 °C, pH 5, of invertase crosslinked with DA10 (0.1-5 mg/mL)

Time (min)	0.1 mg/mL DA10					1 mg/mL DA10					5 mg/mL DA10				
	A_{540}			Activity (U/mL)	Relative activity (%)	A_{540}			Activity (U/mL)	Relative activity (%)	A_{540}			Activity (U/mL)	Relative activity (%)
	1	2	Average			1	2	Average			1	2	Average		
0	0.231	0.212	0.222*	42	100	0.241	0.217	0.229*	43	100	0.209	0.213	0.211*	40	100
5	0.303	0.298	0.301**	28	68	0.305	0.289	0.297**	28	65	0.212	0.216	0.214**	20	50
10	0.224	0.226	0.225**	21	51	0.243	0.241	0.242**	23	53	0.165	0.179	0.172**	16	41
20	0.185	0.180	0.183**	17	41	0.181	0.175	0.178**	17	39	0.108	0.102	0.105**	10	25
40	0.134	0.127	0.131**	12	29	0.114	0.113	0.114**	11	25	0.067	0.077	0.072**	7	17
60	0.098	0.092	0.095**	9	21	0.093	0.089	0.091**	9	20	0.056	0.046	0.051**	5	12
90	0.074	0.066	0.070**	7	16	0.085	0.071	0.078**	7	17	0.030	0.036	0.033**	3	8

*dilution ×100

**dilution ×50

Table 142 Thermal stability at 60 °C, pH 5, of invertase crosslinked with DAD (0.1-5 mg/mL)

Time (min)	0.1 mg/mL DAD					1 mg/mL DAD					5 mg/mL DAD				
	A_{540}			Activity (U/mL)	Relative activity (%)	A_{540}			Activity (U/mL)	Relative activity (%)	A_{540}			Activity (U/mL)	Relative activity (%)
	1	2	Average			1	2	Average			1	2	Average		
0	0.221	0.215	0.218*	41	100	0.223	0.219	0.221*	42	100	0.217	0.208	0.213*	40	100
5	0.334	0.333	0.334**	31	76	0.303	0.305	0.304**	29	69	0.230	0.229	0.230**	22	54
10	0.261	0.261	0.261**	25	60	0.239	0.244	0.242**	23	55	0.143	0.148	0.146**	14	34
20	0.184	0.196	0.190**	18	44	0.160	0.158	0.159**	15	36	0.083	0.082	0.083**	8	19
40	0.095	0.118	0.107**	10	24	0.088	0.091	0.090**	8	20	0.027	0.027	0.027**	3	6
60	0.079	0.075	0.077**	7	18	0.062	0.063	0.063**	6	14	0.013	0.012	0.013**	1	3
90	0.077	0.078	0.078**	7	18	0.041	0.039	0.040**	4	9	0.005	0.006	0.006**	1	1

*dilution ×100

**dilution ×50

Table 143 Thermal stability at 60 °C, pH 5, of α-amylase crosslinked with 1 mg/mL ethyldiamine at pH 5, 6, 7 and 8

Time (min)	pH 5					pH 6					pH 7					pH 8				
	A_{540}			Act (U/mL)	RA (%)	A_{540}			Act (U/mL)	RA (%)	A_{540}			Act (U/mL)	RA (%)	A_{540}			Act (U/mL)	RA (%)
	1	2	Av			1	2	Av			1	2	Av			1	2	Av		
0	0.269	0.265	0.267*	50	100	0.270	0.270	0.270*	51	100	0.231	0.220	0.226*	42	100	0.208	0.219	0.214*	40	100
5	0.407	0.400	0.404**	38	76	0.385	0.388	0.387**	36	72	0.381	0.377	0.379**	36	84	0.317	0.320	0.319**	30	75
10	0.345	0.317	0.331**	31	62	0.330	0.314	0.322**	30	60	0.324	0.285	0.305**	29	68	0.273	0.277	0.275**	26	64
20	0.252	0.234	0.243**	23	46	0.249	0.245	0.247**	23	46	0.226	0.265	0.246**	23	54	0.207	0.199	0.203**	19	48
40	0.180	0.182	0.181**	17	34	0.162	0.142	0.152**	14	28	0.190	0.195	0.193**	18	43	0.147	0.134	0.141**	13	33
60	0.151	0.145	0.148**	14	28	0.122	0.121	0.122**	11	23	0.160	0.159	0.160**	15	35	0.118	0.100	0.109**	10	26
90	0.073	0.111	0.092**	9	17	0.066	0.087	0.077**	7	14	0.140	0.135	0.138**	13	30	0.095	0.094	0.095**	9	22

RA Relative Activity

*dilution ×100

**dilution ×50

2 Crosslinking of invertase

2.1 Size exclusion column

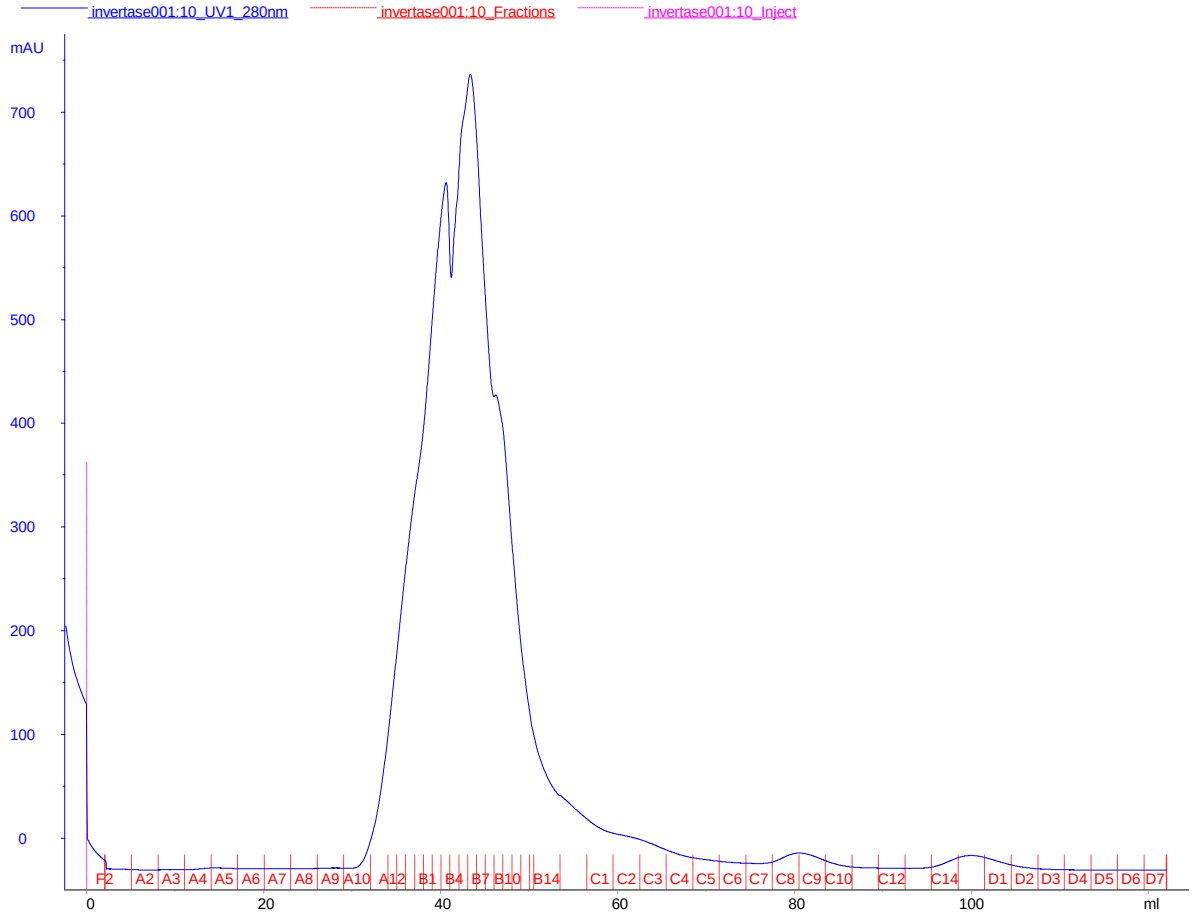

Figure 1 Elution profile of native invertase using SEC on Sephacryl S-300 with flow rate of 0.5 mL/min.

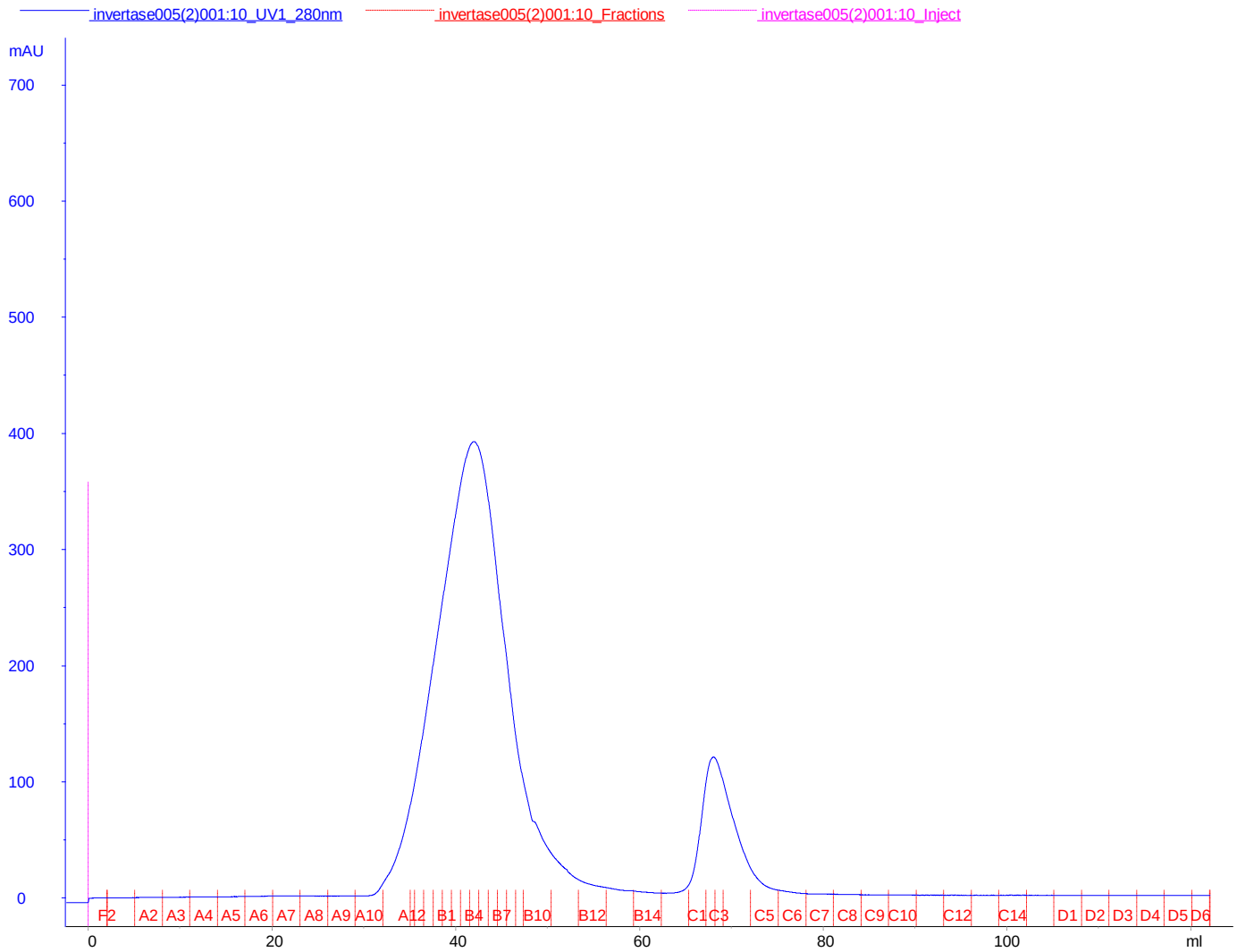

Figure 2 Elution profile of invertase after intramolecular crosslinking using SEC on Sephacryl S-300 with flow rate of 0.5 mL/min.

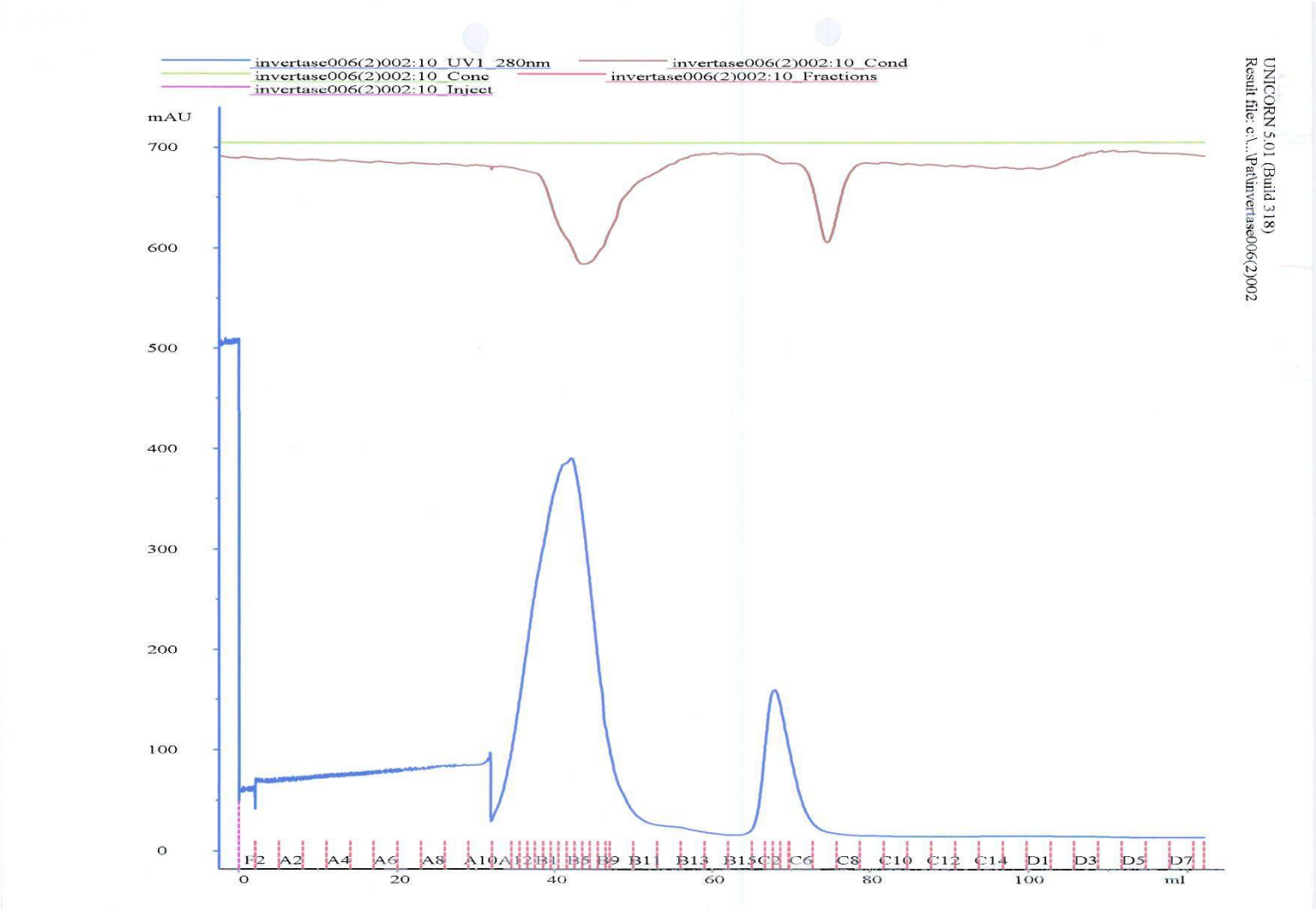

Figure 3 Elution profile of invertase control for intramolecular crosslinking using SEC on Sephacryl S-300 with flow rate of 0.5 mL/min.

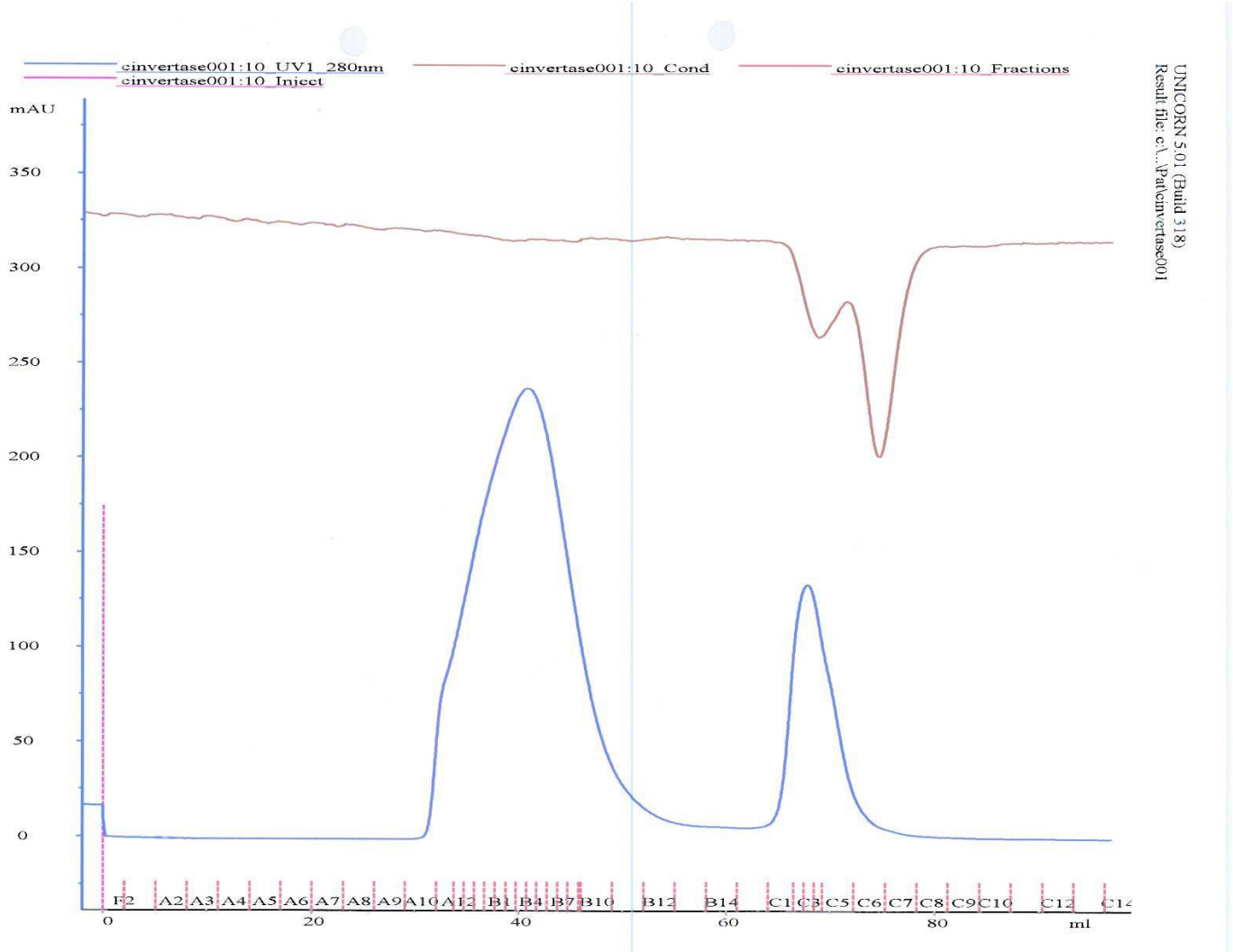

Figure 4 Elution profile of invertase after intermolecular crosslinking using SEC on Sephacryl S-300 with flow rate of 0.5 mL/min.

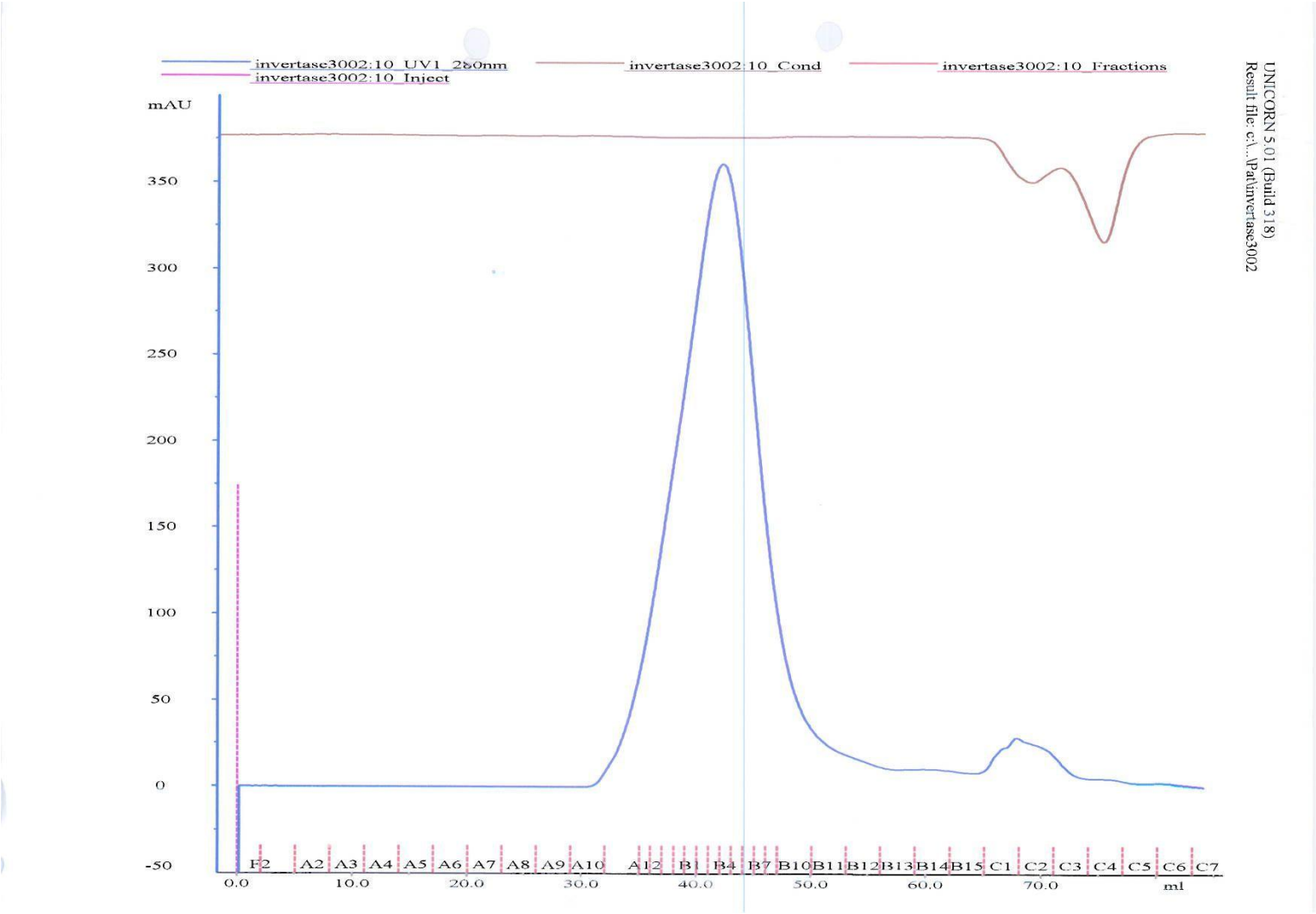

Figure 5 Elution profile of invertase control for intermolecular crosslinking using SEC on Sephacryl S-300 with flow rate of 0.5 mL/min.

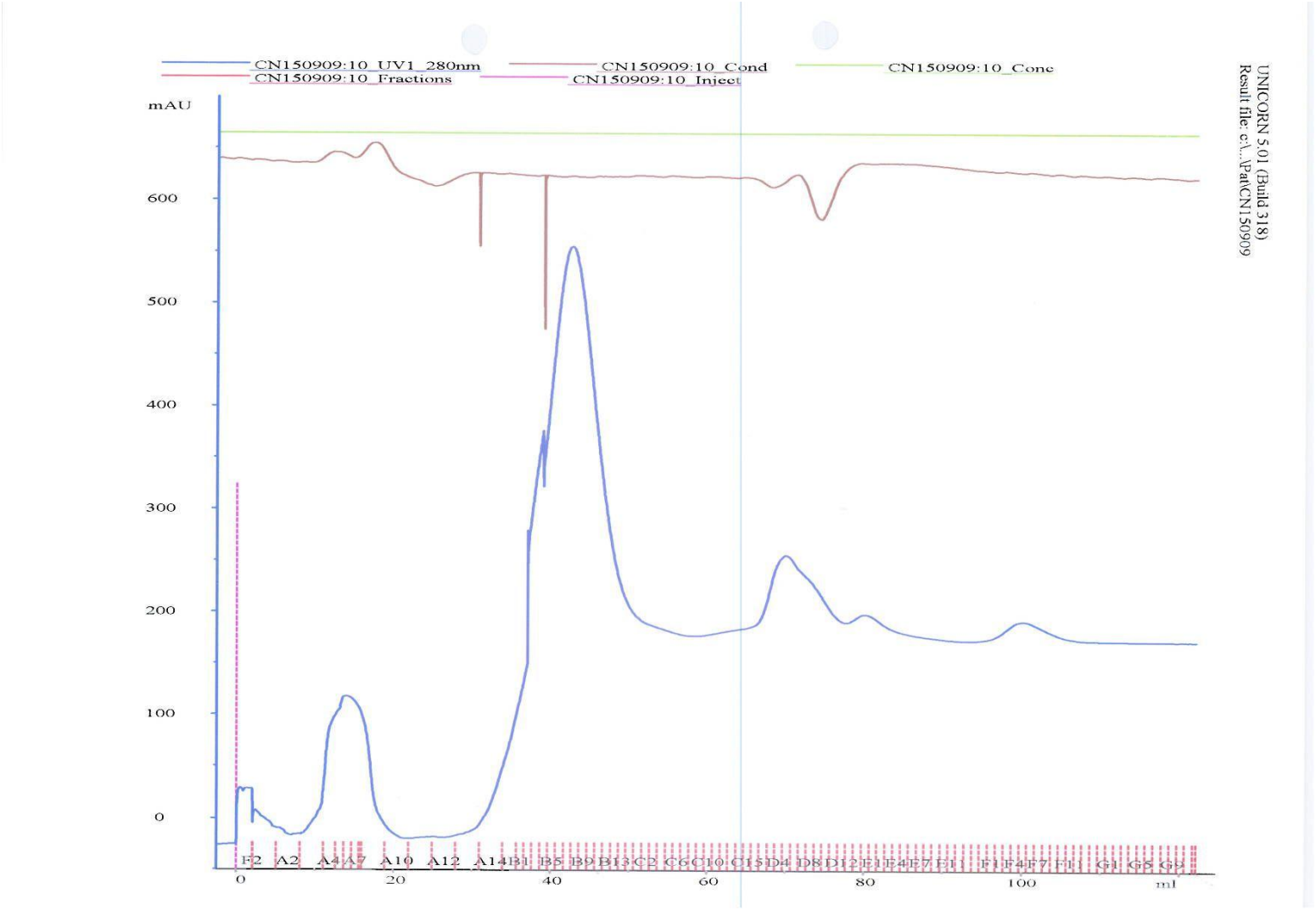

Figure 6 Elution profile of invertase control for deglycosylation using SEC on Sephacryl S-300 with flow rate of 0.5 mL/min.

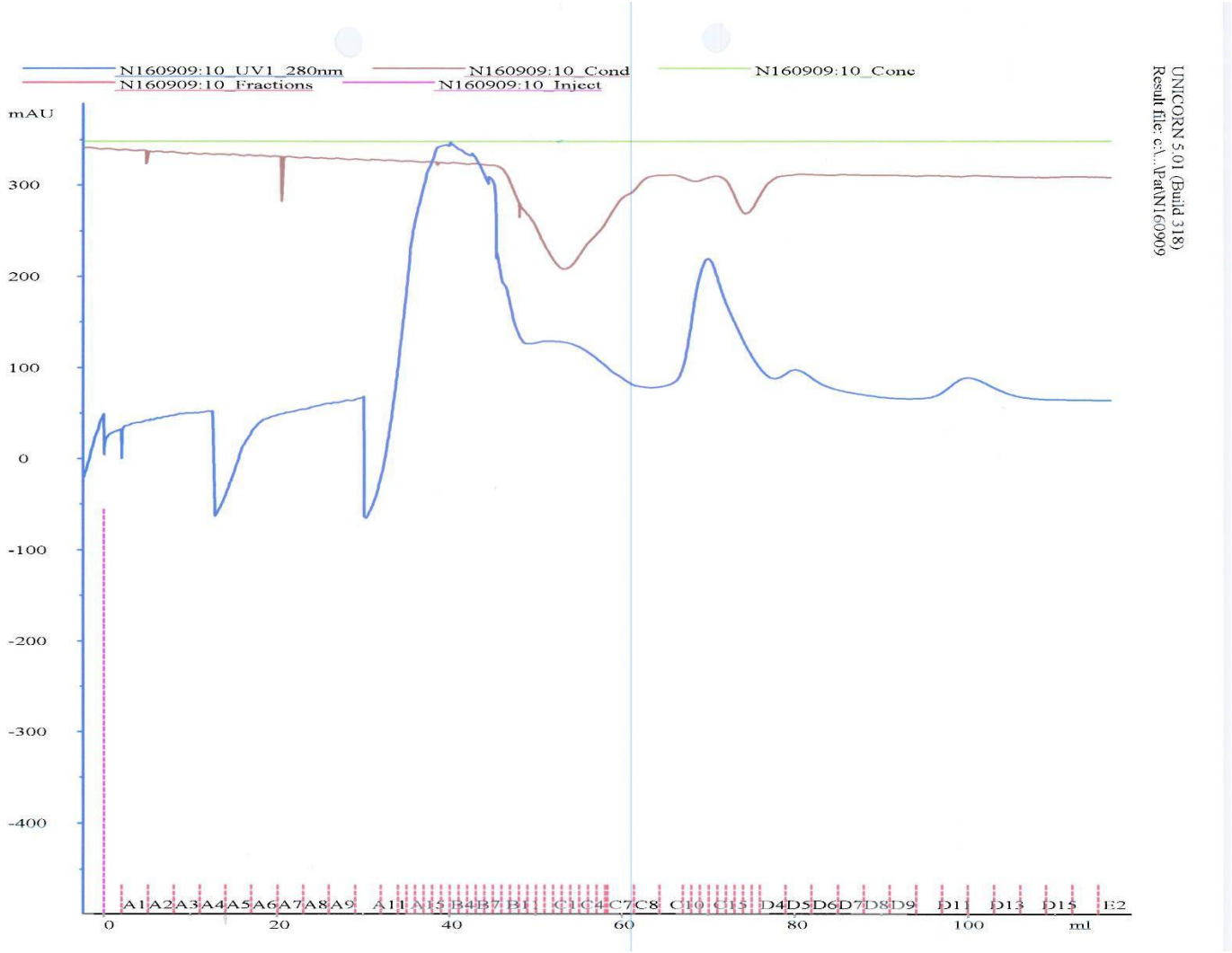

Figure 7 Elution profile of deglycosylated invertase using SEC on Sephacryl S-300 with flow rate of 0.5 mL/min.

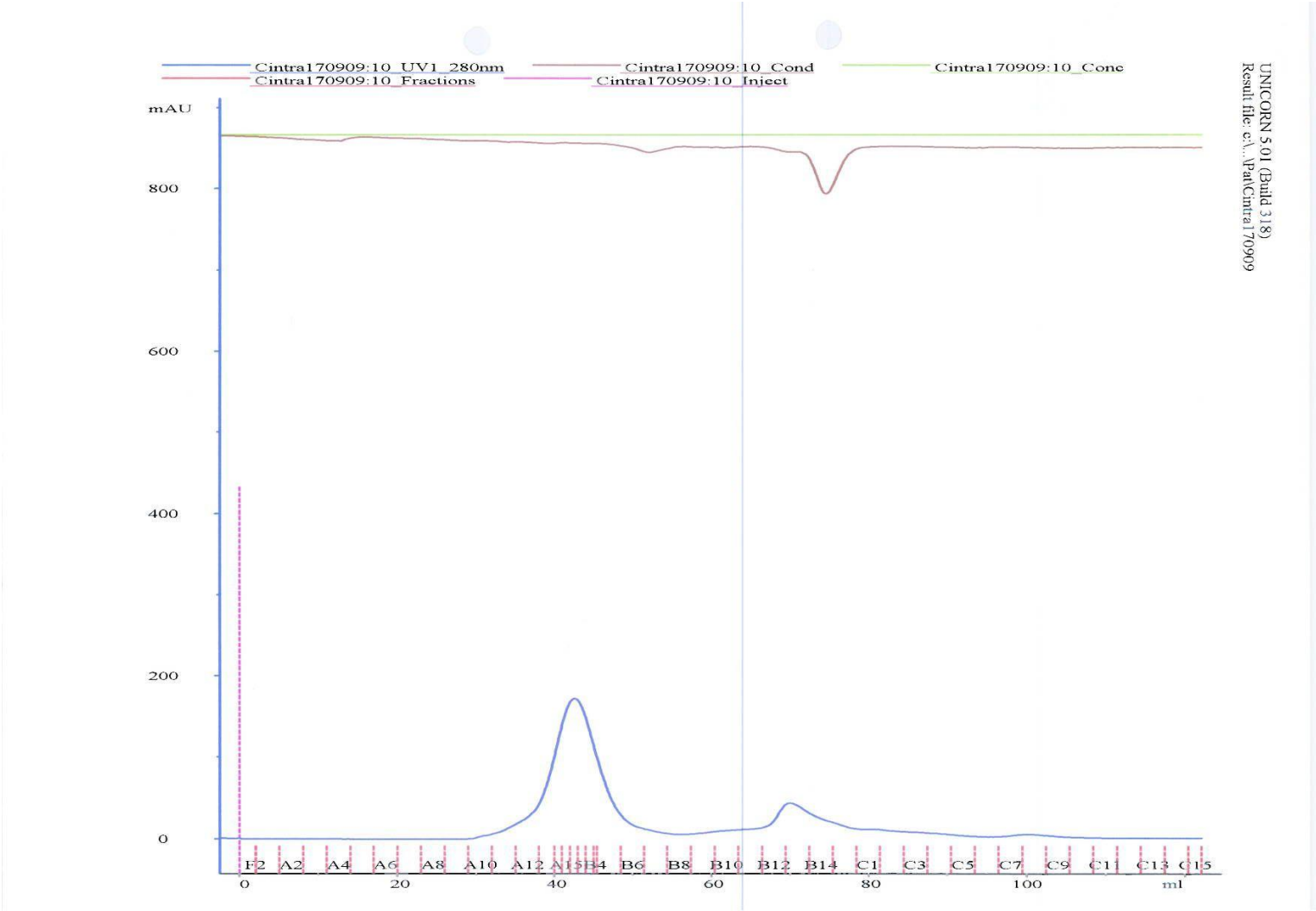

Figure 8 Elution profile of deglycosylated invertase control for intramolecular crosslinking using SEC on Sephacryl S-300 with flow rate of 0.5 mL/min.

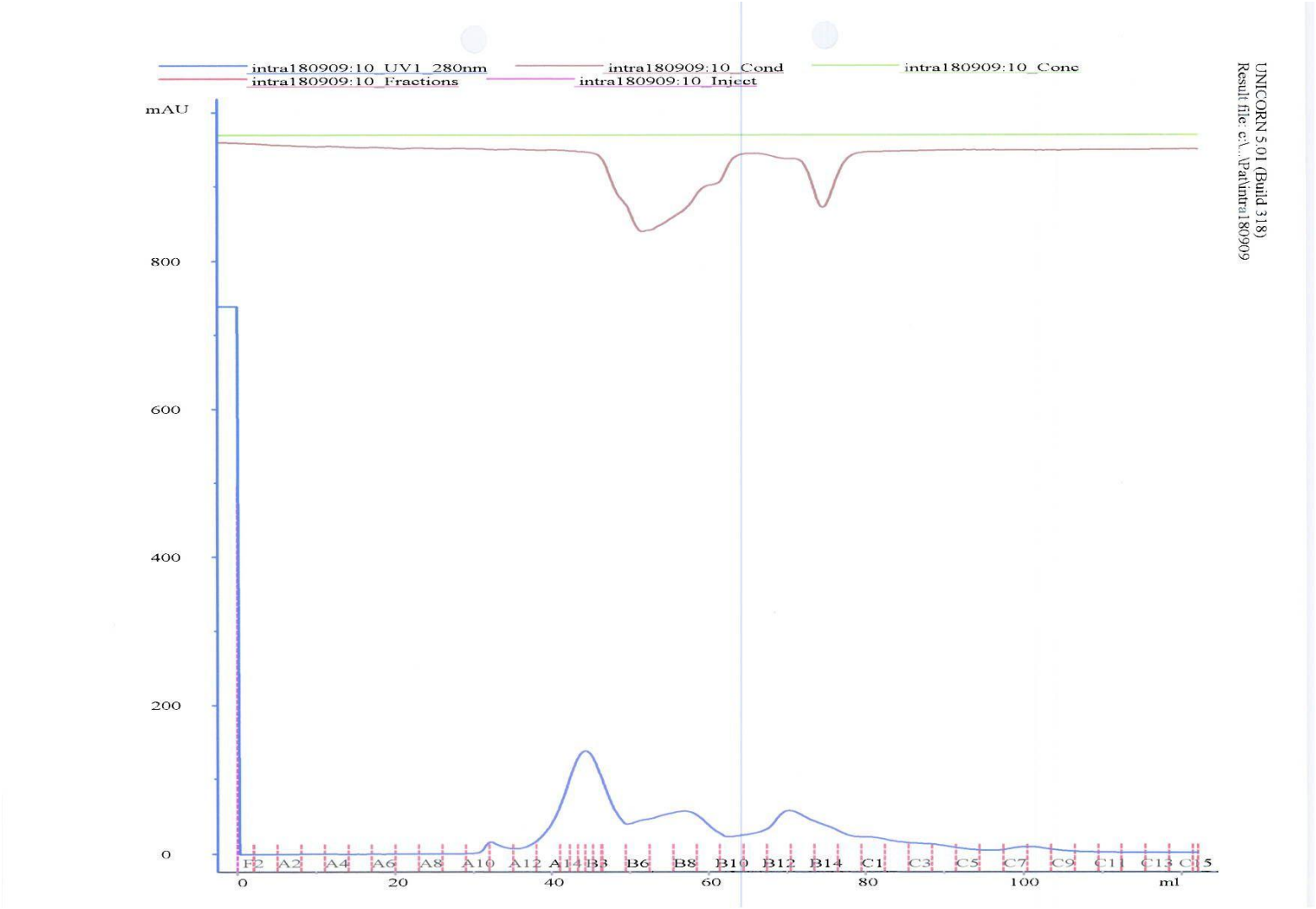

Figure 9 Elution profile of deglycosylated invertase after intramolecular crosslinking using SEC on Sephacryl S-300 with flow rate of 0.5 mL/min.

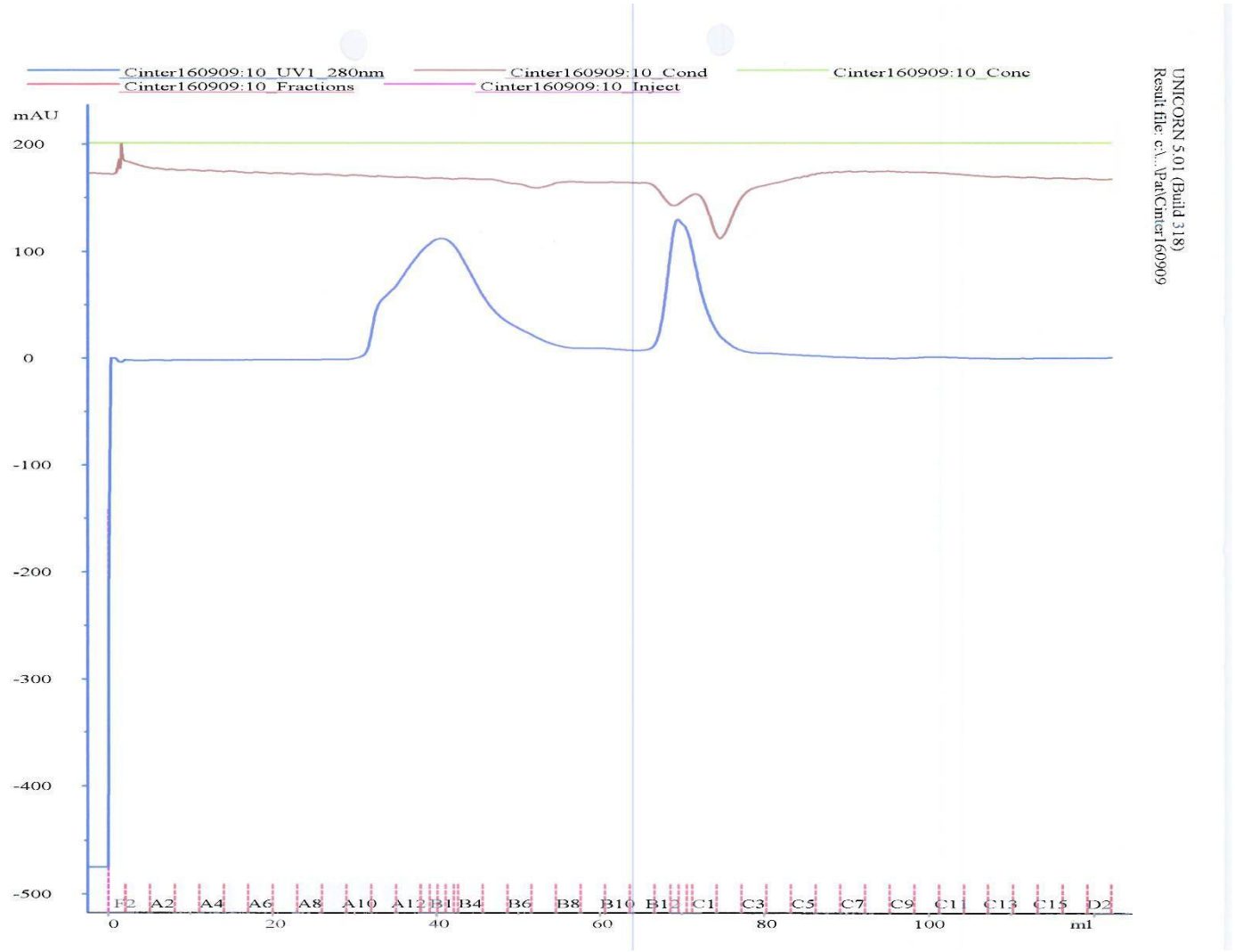

Figure 10 Elution profile of deglycosylated invertase control for intermolecular crosslinking using SEC on Sephacryl S-300 with flow rate of 0.5 mL/min.

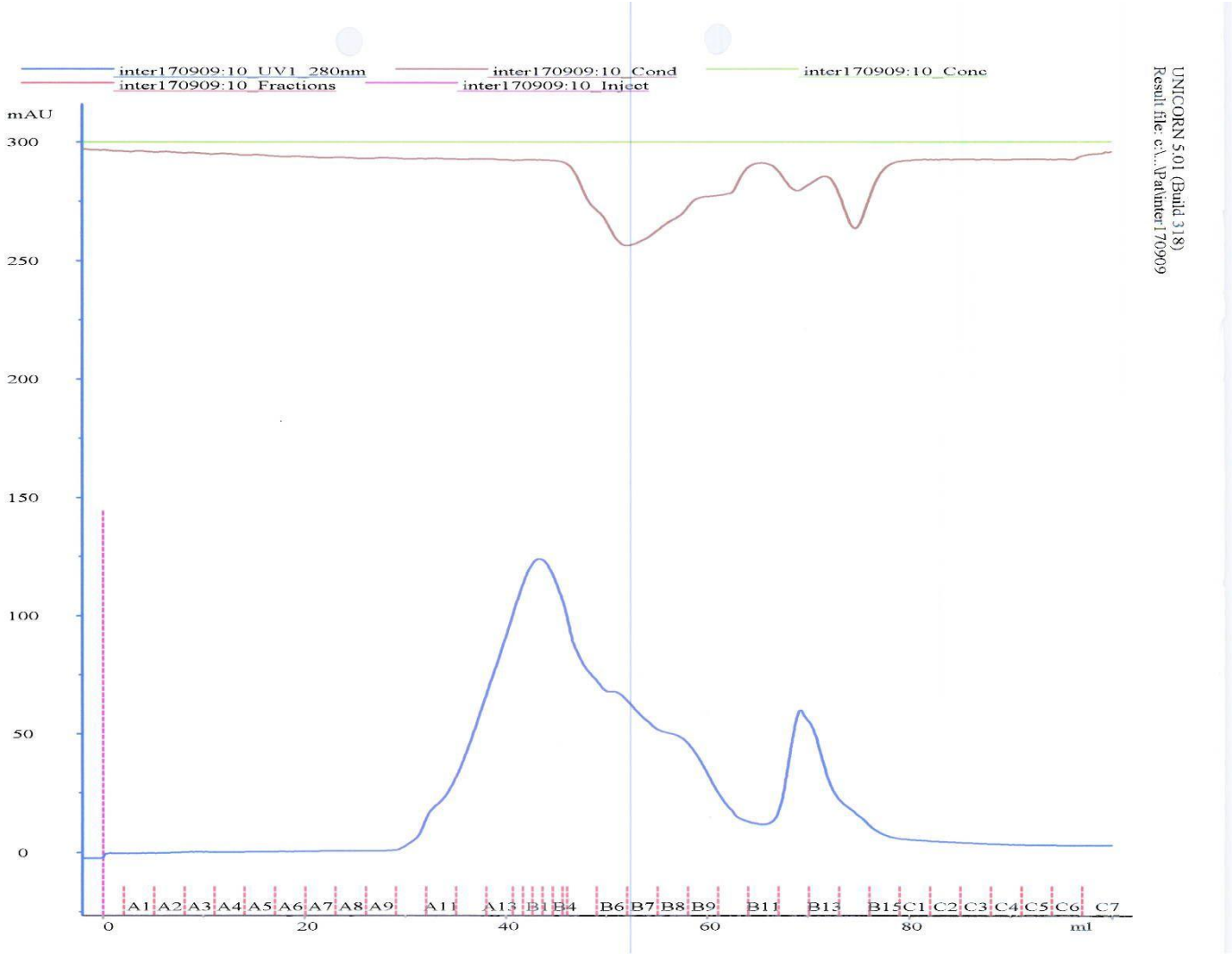

Figure 11 Elution profile of deglycosylated invertase after intermolecular crosslinking using SEC on Sephacryl S-300 with flow rate of 0.5 mL/min.

2.2 Dynamic light scattering

2.2.1 Characterization report of standard ovalbumin using DLS

Protein Characterization Report
v2.0

Malvern

Malvern Instruments Ltd - © Copyright 2008

Sample Details

Sample Name:	O(2)_ 3	**Temperature (°C):**	25.0
File Name:	std20091123.dts	**Solvent:**	Water
Record Number:	18	**Solvent ñ:**	1.330
Meas Date &	Monday, 23 November 2009 ...	**Solvent Vis (cP):**	0.8867

Cumulant Results

Count Rate (kcps):	149.8
Z-Average (d.nm):	556.4
Polydispersity In...	0.609
Polydispersity (d....	434.1
%Polydispersity:	78.0
Estimated MW (k...	1.76e6
Merit (0 to 100):	66.9
Polydispersity:	Polydisperse
Est %Vol Fractio...	.02608

Intensity Distribution Results

	%Int	Mean (n...	Mode (n...	StD (n...	%Pd	MW (kDa)*	Polydispersity
Peak...	48.0	6.548	6.503	1.684	25.7	54.0	Polydisperse
Peak...	35.7	291.5	295.3	44.70	15.3	3.89e5	Monodisperse
Peak...	16.3	50.41	50.75	8.831	17.5	6400	Monodisperse

Mass Distribution Results

	%M...	Mean (n...	Mode (n...	StD (n...	%Pd	MW (kDa)*
Peak ...	99.9	5.459	4.849	1.473	27.0	35.3
Peak...	0.0	299.2	295.3	55.81	18.7	4.13e5
Peak...	0.1	46.48	43.82	9.557	20.6	5290

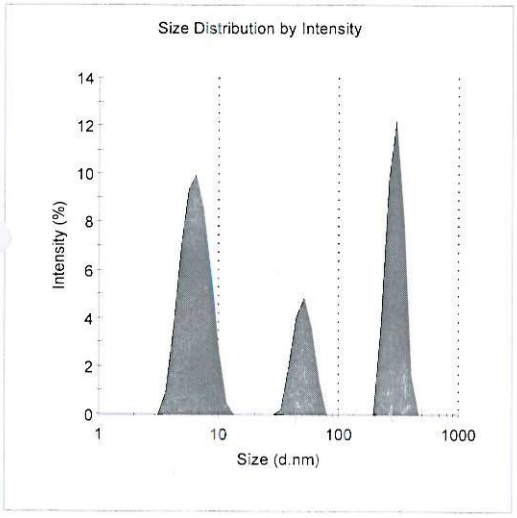

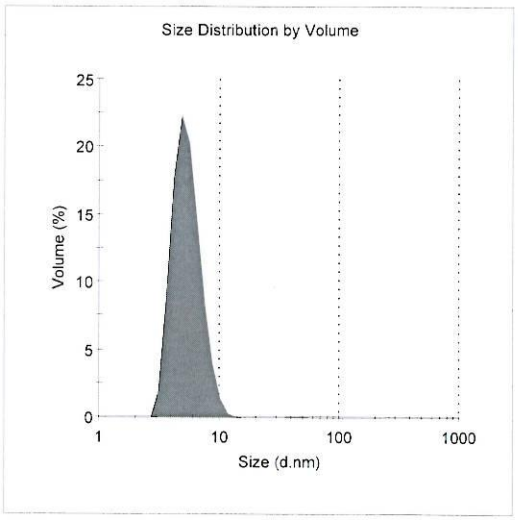

*The molecular weight reported here is only an estimate calculated using an empirical mass vs size calibration curve.

*The estimated concentration is calculated from the size distribution measured by DLS and extrapolated from the total intensity compared to a standard sample of known size concentration and refractive index. If the current sample is non-spherical or the refractive index is incorrect the value of the predicted concentration may be in error.

Malvern Instruments Ltd
www.malvern.com

DTS Ver. 5.10
Serial Number : MAL500836

File name: std20091123.dts
Record Number: 18
23 Nov 2009 12:39:09 p.m.

2.2.2 Characterization report of standard conalbumin using DLS

Protein Characterization Report

v2.0

Malvern

Sample Details

Sample Name: C(2)_ 2
File Name: std20091123.dts
Record Number: 29
Meas Date & Monday, 23 November 2009 ...

Temperature (°C): 25.0
Solvent: Water
Solvent ñ: 1.330
Solvent Vis (cP): 0.8879

Cumulant Results

Count Rate (kcps):	234.7
Z-Average (d.nm):	271.2
Polydispersity In...	0.409
Polydispersity (d....	173.4
%Polydispersity:	64.0
Estimated MW (k...	3.28e5
Merit (0 to 100):	60.1
Polydispersity:	Polydisperse
Est %Vol Fractio...	.04357

Intensity Distribution Results

	%Int	Mean (n...	Mode (n...	StD (n...	%Pd	MW (kDa)*	Polydispersity
Peak...	62.3	8.344	7.531	2.061	24.7	95.2	Polydisperse
Peak...	31.0	244.0	255.0	56.53	23.2	2.56e5	Polydisperse
Peak...	6.7	49.20	50.75	9.997	20.3	6050	Monodisperse

Mass Distribution Results

	%M...	Mean (n...	Mode (n...	StD (n...	%Pd	MW (kDa)*
Peak ...	99.9	7.070	6.503	1.831	25.9	64.6
Peak...	0.0	253.3	255.0	65.36	25.8	2.80e5
Peak...	0.1	44.20	43.82	9.971	22.6	4710

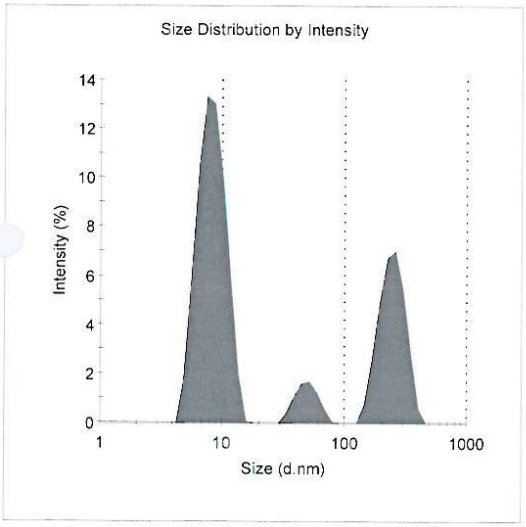

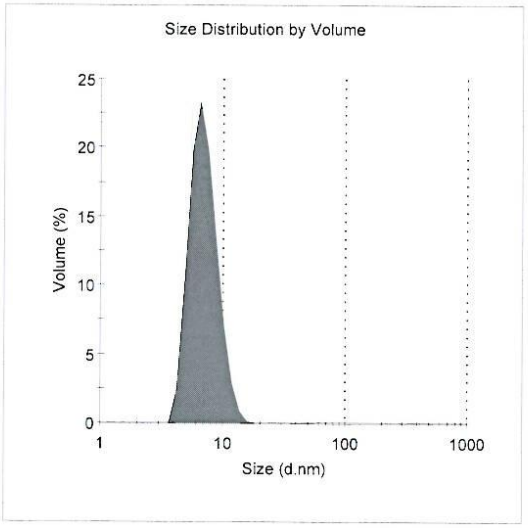

*The molecular weight reported here is only an estimatecalculated using an empirical mass vs size calibration curve

*The estimated concentration is calculated from the size distribution measured by DLS and extrapolated from the total intensity compared to a standard sample of known size concentration, and refractive index. If the current sample is non-spherical or the reftractive index is incorrect the value of the predicted concentration may be in error

2.2.3 Characterization report of standard aldolase using DLS

Protein Characterization Report

v2.0

Malvern

Sample Details

Sample Name: A(2)_ 3
File Name: std20091123.dts
Record Number: 27
Meas Date & Monday, 23 November 2009 ...

Temperature (°C): 25.0
Solvent: Water
Solvent ñ: 1.330
Solvent Vis (cP): 0.8864

Cumulant Results

Count Rate (kcps):	340.1
Z-Average (d.nm):	233.9
Polydispersity In...	0.289
Polydispersity (d....	125.8
%Polydispersity:	53.8
Estimated MW (k...	2.32e5
Merit (0 to 100):	69.8
Polydispersity:	Polydisperse
Est %Vol Fractio...	.02687

Intensity Distribution Results

	%Int	Mean (n...	Mode (n...	StD (n...	%Pd	MW (kDa)*	Polydispersity
Peak...	49.5	10.24	10.10	2.666	26.0	154	Polydisperse
Peak...	37.1	289.6	295.3	94.95	32.8	3.83e5	Polydisperse
Peak...	13.4	78.25	68.06	21.41	27.4	1.79e4	Polydisperse

Mass Distribution Results

	%M...	Mean (n...	Mode (n...	StD (n...	%Pd	MW (kDa)*
Peak ...	99.9	8.533	7.531	2.299	26.9	100
Peak...	0.1	320.5	342.0	104.0	32.4	4.85e5
Peak...	0.1	67.01	58.77	21.59	32.2	1.25e4

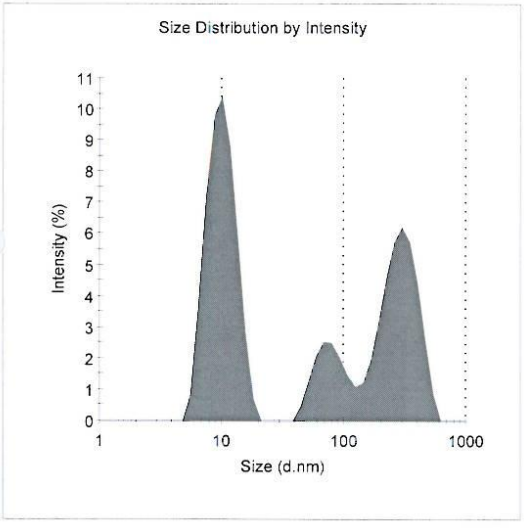

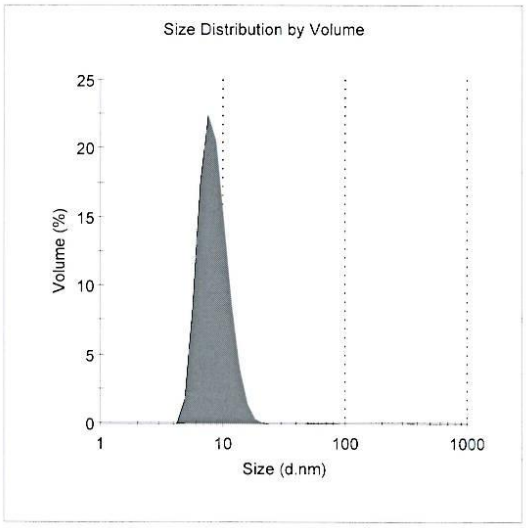

*The molecular weight reported here is only an estimatecalculated using an empirical mass vs size calibration curve

*The estimated concentration is calculated from the size distribution measured by DLS and extrapolated from the total intensity compared to a standard sample of known size concentration, and refractive index. If the current sample is non-spherical or the reftractive index is incorrect the value of the predicted concentration may be in error

2.2.4 Characterization report of standard ferritin using DLS

Protein Characterization Report

v2.0

Malvern

Sample Details

Sample Name: F(2)_ 3
File Name: std20091123.dts
Record Number: 33
Meas Date & Monday, 23 November 2009 ...

Temperature (°C): 25.0
Solvent: Water
Solvent ñ: 1.330
Solvent Vis (cP): 0.8875

Cumulant Results

Count Rate (kcps):	214.3
Z-Average (d.nm):	97.14
Polydispersity In...	1.000
Polydispersity (d....	97.14
%Polydispersity:	100.0
Estimated MW (k...	2.97e4
Merit (0 to 100):	86.7
Polydispersity:	Polydisperse
Est %Vol Fractio...	.02264

Intensity Distribution Results

	%Int	Mean (n...	Mode (n...	StD (n...	%Pd	MW (kDa)*	Polydispersity
Peak...	85.8	511.8	164.2	707.5	138.2	1.45e6	Polydisperse
Peak...	14.2	17.77	18.17	4.665	26.3	558	Polydisperse
Peak...	0.0	0.000	0.000	0.000	0	0.00	

Mass Distribution Results

	%M...	Mean (n...	Mode (n...	StD (n...	%Pd	MW (kDa)*
Peak ...	95.0	14.79	13.54	3.996	27.0	363
Peak...	1.4	131.1	91.28	58.46	44.6	6.00e4
Peak...	3.6	1332	1718	891.4	66.9	1.36e7

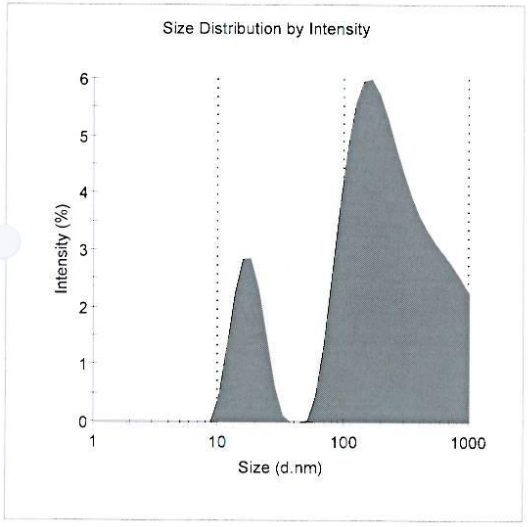

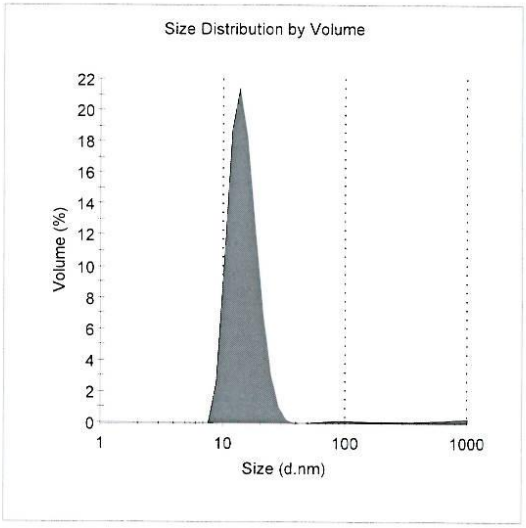

*The molecular weight reported here is only an estimate calculated using an empirical mass vs size calibration curve

*The estimated concentration is calculated from the size distribution measured by DLS and extrapolated from the total intensity compared to a standard sample of known size concentration and refractive index. If the current sample is non-spherical or the refractive index is incorrect the value of the predicted concentration may be in error

2.2.5 Characterization report of standard thyroglobulin using DLS

Protein Characterization Report

v2.0

Malvern

Sample Details

Sample Name: T(2)_ 2
File Name: std20091123.dts
Record Number: 23
Meas Date & Monday, 23 November 2009 ...

Temperature (°C): 25.0
Solvent: Water
Solvent ñ: 1.330
Solvent Vis (cP): 0.8876

Cumulant Results

Count Rate (kcps):	232.0
Z-Average (d.nm):	34.00
Polydispersity In...	0.358
Polydispersity (d....	20.34
%Polydispersity:	59.8
Estimated MW (k...	2550
Merit (0 to 100):	86.8
Polydispersity:	Polydisperse
Est %Vol Fractio...	.02034

Intensity Distribution Results

	%Int	Mean (n...	Mode (n...	StD (n...	%Pd	MW (kDa)*	Polydispersity
Peak...	72.3	19.56	18.17	5.076	26.0	699	Polydisperse
Peak...	22.6	242.0	220.2	78.56	32.5	2.52e5	Polydisperse
Peak...	5.1	5177	5560	487.5	9.4	3.26e8	Monodisperse

Mass Distribution Results

	%M...	Mean (n...	Mode (n...	StD (n...	%Pd	MW (kDa)*
Peak ...	99.8	16.35	15.69	4.370	26.7	460
Peak...	0.1	257.9	255.0	92.37	35.8	2.92e5
Peak...	0.1	5160	5560	743.4	14.4	3.23e8

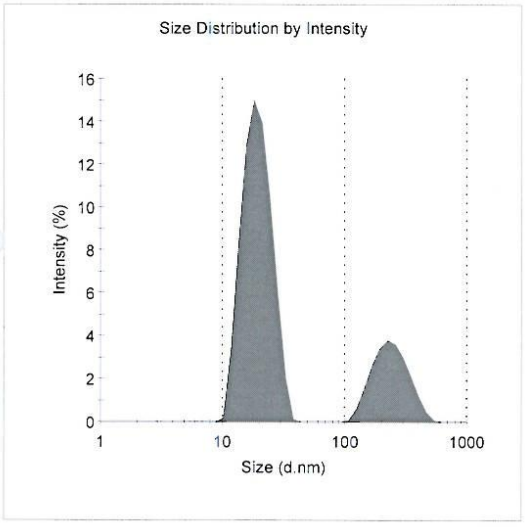

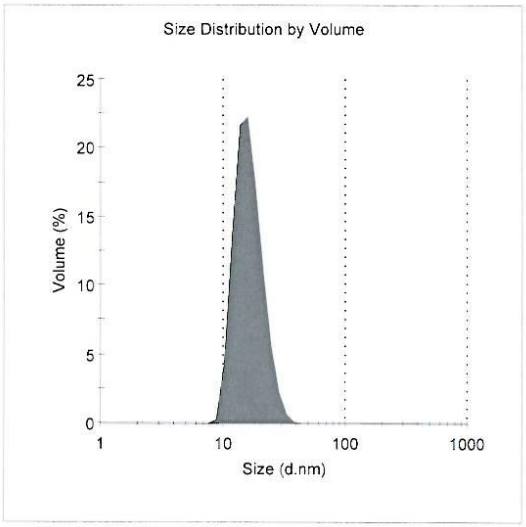

*The molecular weight reported here is only an estimate calculated using an empirical mass vs size calibration curve.

*The estimated concentration is calculated from the size distribution measured by DLS and extrapolated from the total intensity compared to a standard sample of known size concentration, and refractive index. If the current sample is non-spherical or the reftractive index is incorrect the value of the predicted concentration may be in error.

2.2.6 Characterization report of native invertase using DLS

Protein Characterization Report

v2.0

Malvern

Sample Details

Sample Name:
File Name: deglyinvertase20090929.dts
Record Number: 6
Meas Date & Tuesday, 29 September 2009...

Temperature (°C): 25.0
Solvent: Water
Solvent ñ: 1.330
Solvent Vis (cP): 0.8875

Cumulant Results

Count Rate (kcps):	281.4
Z-Average (d.nm):	13.05
Polydispersity In...	0.188
Polydispersity (d....	5.660
%Polydispersity:	43.4
Estimated MW (k...	271
Merit (0 to 100):	66.8
Polydispersity:	Polydisperse
Est %Vol Fractio...	.01594

Intensity Distribution Results

	%Int	Mean (n...	Mode (n...	StD (n...	%Pd	MW (kDa)*	Polydispersity
Peak...	100.0	15.98	13.54	6.218	38.9	436	Polydisperse
Peak...	0.0	0.000	0.000	0.000	0	0.00	
Peak...	0.0	0.000	0.000	0.000	0	0.00	

Mass Distribution Results

	%M...	Mean (n...	Mode (n...	StD (n...	%Pd	MW (kDa)*
Peak ...	100.0	10.86	8.721	4.015	37.0	176
Peak...	0.0	0.000	0.000	0.000	0	0.00
Peak...	0.0	0.000	0.000	0.000	0	0.00

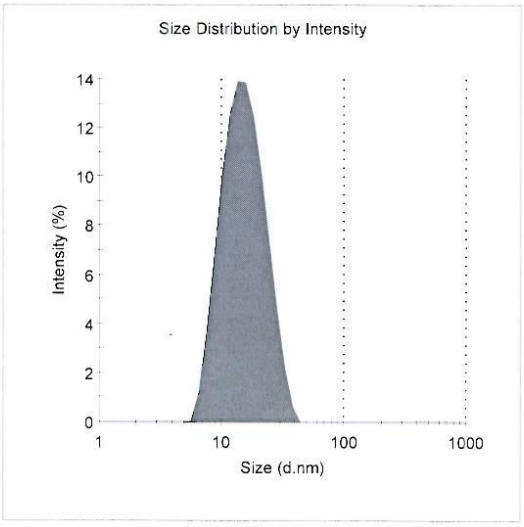

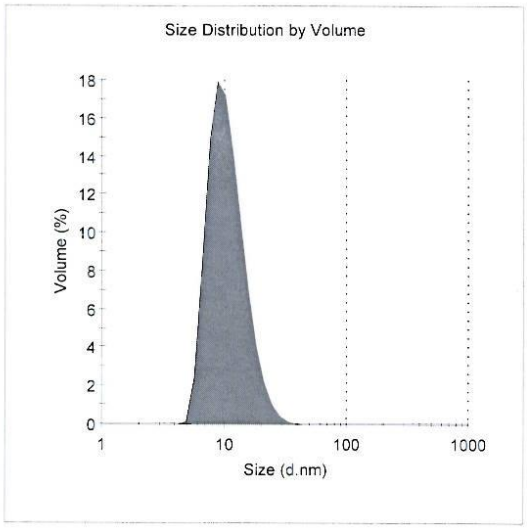

*The molecular weight reported here is only an estimatecalculated using an empirical mass vs size calibration curve

*The estimated concentration is calculated from the size distribution measured by DLS and extrapolated from the total intensity compared to a standard sample of known size concentration, and refractive index. If the current sample is non-spherical or the reftractive index is incorrect the value of the predicted concentration may be in error

2.2.7 Characterization report of invertase after intramolecular crosslinking using DLS

Protein Characterization Report

v2.0

Malvern

Sample Details

Sample Name:
File Name: intrainvertase20090907.dts
Record Number: 51
Meas Date & Monday, 7 September 2009 3...

Temperature (°C): 25.0
Solvent: Water
Solvent ñ: 1.330
Solvent Vis (cP): 0.8873

Cumulant Results

Count Rate (kcps):	218.5
Z-Average (d.nm):	17.30
olydispersity In...	0.319
Polydispersity (d....	9.764
%Polydispersity:	56.5
Estimated MW (k...	524
Merit (0 to 100):	58.0
Polydispersity:	Polydisperse
Est %Vol Fractio...	.00535

Intensity Distribution Results

	%Int	Mean (n...	Mode (n...	StD (n...	%Pd	MW (kDa)*	Polydispersity
Peak...	96.9	22.69	21.04	10.75	47.4	989	Polydisperse
Peak...	3.1	4130	5560	1034	25.0	1.92e8	Polydisperse
Peak...	0.0	0.000	0.000	0.000	0	0.00	

Mass Distribution Results

	%M...	Mean (n...	Mode (n...	StD (n...	%Pd	MW (kDa)*
Peak ...	99.9	13.03	10.10	5.711	43.8	270
Peak...	0.1	3610	3091	1141	31.6	1.40e8
Peak...	0.0	0.000	0.000	0.000	0	0.00

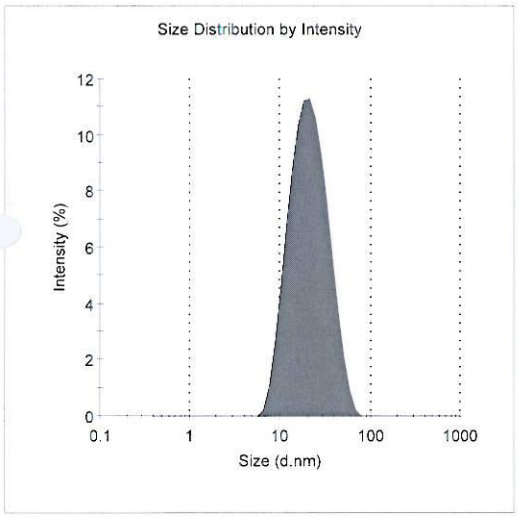

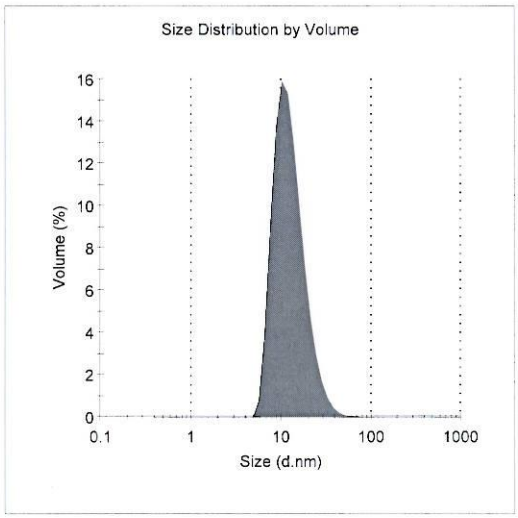

*The molecular weight reported here is only an estimate calculated using an empirical mass vs size calibration curve

*The estimated concentration is calculated from the size distribution measured by DLS and extrapolated from the total intensity compared to a standard sample of known size concentration, and refractive index. If the current sample is non-spherical or the reftractive index is incorrect the value of the predicted concentration may be in error

2.2.8 Characterization report of invertase control for intramolecular crosslinking using DLS

Protein Characterization Report

v2.0

Malvern

Sample Details

Sample Name:		**Temperature (°C):**	25.0
File Name:	intrainvertase20090907.dts	**Solvent:**	Water
Record Number:	18	**Solvent ñ:**	1.330
Meas Date &	Monday, 7 September 2009 1...	**Solvent Vis (cP):**	0.8865

Cumulant Results

Count Rate (kcps):	182.5
Z-Average (d.nm):	13.96
PDI:	0.282
Polydispersity (d....	7.408
%Polydispersity:	53.1
Estimated MW (k...	317
Merit (0 to 100):	57.3
Polydispersity:	Polydisperse
Est %Vol Fractio...	5.23931

Intensity Distribution Results

	%Int	Mean (n...	Mode (n...	StD (n...	%Pd	MW (kDa)*	Polydispersity
Peak...	92.3	17.21	15.69	5.993	34.8	518	Polydisperse
Peak...	6.2	0.7285	0.6213	0.1040	14.3	0.317	Monodisperse
Peak...	1.5	4965	5560	624.1	12.6	2.96e8	Monodisperse

Mass Distribution Results

	%M...	Mean (n...	Mode (n...	StD (n...	%Pd	MW (kDa)*
Peak ...	99.8	0.6950	0.6213	0.1142	16.4	0.284
Peak...	0.2	12.52	10.10	4.269	34.1	246
Peak...	0.0	0.000	0.000	0.000	0	0.00

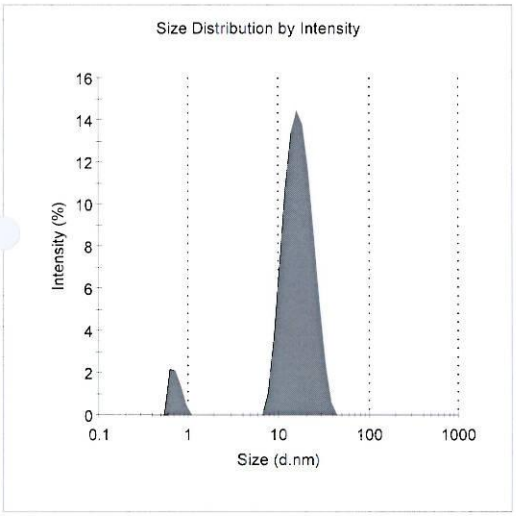

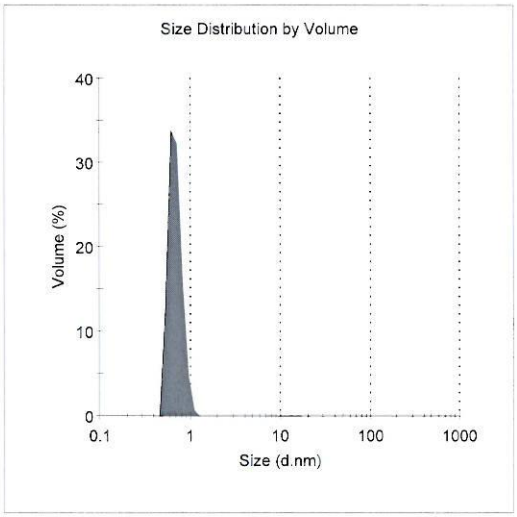

*The molecular weight reported here is only an estimate calculated using an empirical mass vs size calibration curve

*The estimated concentration is calculated from the size distribution measured by DLS and extrapolated from the total intensity compared to a standard sample of known size concentration, and refractive index. If the current sample is non-spherical or the reftractive index is incorrect the value of the predicted concentration may be in error

2.2.9 Characterization report of invertase after intermolecular crosslinking using DLS (selected fraction from the highest of the main peak of SEC)

Protein Characterization Report

v2.0

Malvern

Malvern Instruments Ltd - © Copyright 2008

Sample Details

Sample Name:
File Name: interinvertase.dts
Record Number: 51
Meas Date & Friday, 4 September 2009 4:1...

Temperature (°C): 25.0
Solvent: Water
Solvent ñ: 1.330
Solvent Vis (cP): 0.8873

Cumulant Results

Count Rate (kcps):	154.8
Z-Average (d.nm):	15.50
Polydispersity In...	0.320
Polydispersity (d....	8.770
%Polydispersity:	56.6
Estimated MW (k...	406
Merit (0 to 100):	55.5
Polydispersity:	Polydisperse
Est %Vol Fractio...	.00464

Intensity Distribution Results

	%Int	Mean (n...	Mode (n...	StD (n...	%Pd	MW (kDa)*	Polydispersity
Peak...	97.9	20.53	18.17	8.688	42.3	783	Polydisperse
Peak...	2.1	4209	5560	999.8	23.8	2.01e8	Polydisperse
Peak...	0.0	0.000	0.000	0.000	0	0.00	

Mass Distribution Results

	%M...	Mean (n...	Mode (n...	StD (n...	%Pd	MW (kDa)*
Peak ...	100.0	13.21	11.70	5.171	39.1	279
Peak...	0.0	3730	3580	1126	30.2	1.51e8
Peak...	0.0	0.000	0.000	0.000	0	0.00

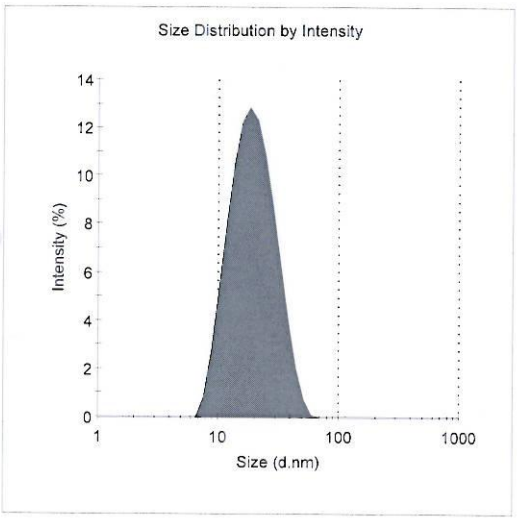

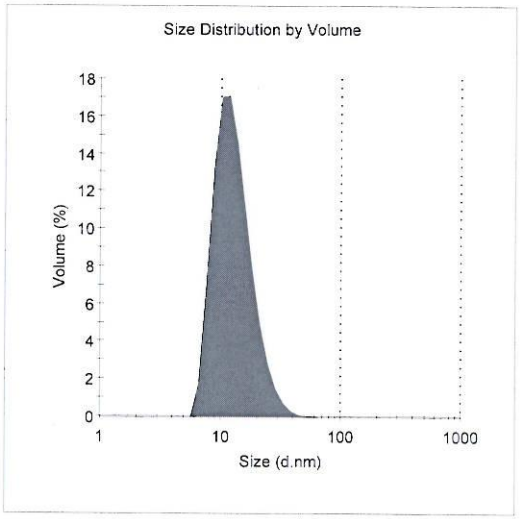

*The molecular weight reported here is only an estimatecalculated using an empirical mass vs size calibration curve

*The estimated concentration is calculated from the size distribution measured by DLS and extrapolated from the total intensity compared to a standard sample of known size concentration, and refractive index. If the current sample is non-spherical or the reftractive index is incorrect the value of the predicted concentration may be in error

Malvern Instruments Ltd
www.malvern.com

DTS Ver. 5.10
Serial Number : MAL500836

File name: interinvertase20090904.dts
Record Number: 51
07 Sep 2009 1:11:04 p.m.

2.2.10 Characterization report of invertase after intermolecular crosslinking using DLS (selected fraction from the shoulder of the main peak of SEC)

Protein Characterization Report

v2.0

Malvern

Sample Details

Sample Name:
File Name: interinvertase.dts
Record Number: 37
Meas Date & Friday, 4 September 2009 3:2...

Temperature (°C): 25.0
Solvent: Water
Solvent ñ: 1.330
Solvent Vis (cP): 0.8865

Cumulant Results

Count Rate (kcps):	215.2
Z-Average (d.nm):	27.74
Polydispersity In...	0.250
Polydispersity (d....	13.88
%Polydispersity:	50.0
Estimated MW (k...	1580
Merit (0 to 100):	68.8
Polydispersity:	Polydisperse
Est %Vol Fractio...	.00138

Intensity Distribution Results

	%Int	Mean (n...	Mode (n...	StD (n...	%Pd	MW (kDa)*	Polydispersity
Peak...	97.1	32.93	28.21	12.72	38.6	2360	Polydisperse
Peak...	2.9	4262	5560	981.4	23.0	2.07e8	Polydisperse
Peak...	0.0	0.000	0.000	0.000	0	0.00	

Mass Distribution Results

	%M...	Mean (n...	Mode (n...	StD (n...	%Pd	MW (kDa)*
Peak ...	99.8	22.79	18.17	8.315	36.5	999
Peak...	0.2	3806	3580	1122	29.5	1.59e8
Peak...	0.0	0.000	0.000	0.000	0	0.00

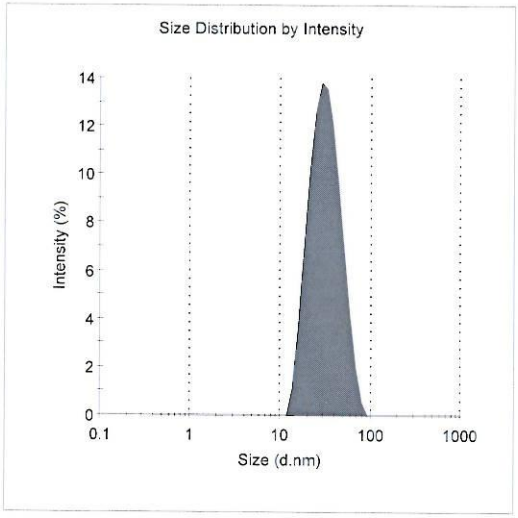

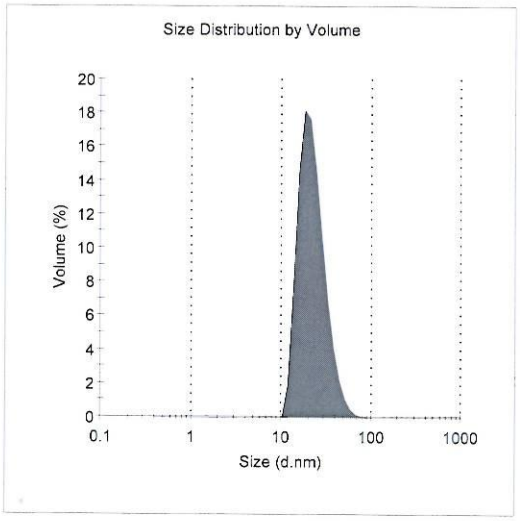

*The molecular weight reported here is only an estimatecalculated using an empirical mass vs size calibration curve

*The estimated concentration is calculated from the size distribution measured by DLS and extrapolated from the total intensity compared to a standard sample of known size concentration, and refractive index. If the current sample is non-spherical or the reftractive index is incorrect the value of the predicted concentration may be in error

2.2.11 Characterization report of invertase control for intermolecular crosslinking using DLS

Protein Characterization Report

v2.0

Malvern

Sample Details

Sample Name:		**Temperature (°C):**	25.0
File Name:	interinvertase.dts	**Solvent:**	Water
Record Number:	18	**Solvent ñ:**	1.330
Meas Date &	Friday, 4 September 2009 12:...	**Solvent Vis (cP):**	0.8878

Cumulant Results

Count Rate (kcps):	122.7
Z-Average (d.nm):	12.60
Polydispersity In...	0.271
Polydispersity (d....	6.558
%Polydispersity:	52.0
Estimated MW (k...	250
Merit (0 to 100):	59.0
Polydispersity:	Polydisperse
Est %Vol Fractio...	2.59544

Intensity Distribution Results

	%Int	Mean (n...	Mode (n...	StD (n...	%Pd	MW (kDa)*	Polydispersity
Peak...	93.5	17.52	15.69	7.558	43.1	540	Polydisperse
Peak...	6.5	0.8160	0.6213	0.2000	24.5	0.413	Polydisperse
Peak...	0.0	0.000	0.000	0.000	0	0.00	

Mass Distribution Results

	%M...	Mean (n...	Mode (n...	StD (n...	%Pd	MW (kDa)*
Peak ...	0.3	10.83	8.721	4.460	41.2	175
Peak...	99.7	0.7220	0.6213	0.1552	21.5	0.310
Peak...	0.0	0.000	0.000	0.000	0	0.00

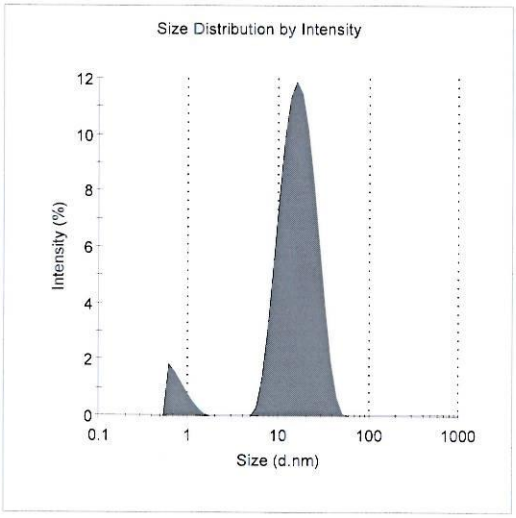

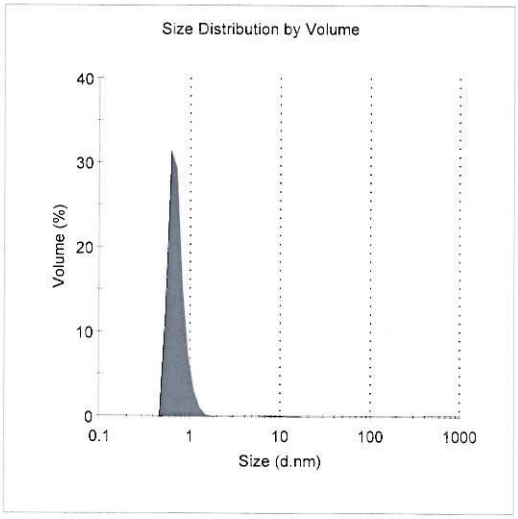

*The molecular weight reported here is only an estimatecalculated using an empirical mass vs size calibration curve

*The estimated concentration is calculated from the size distribution measured by DLS and extrapolated from the total intensity compared to a standard sample of known size concentration, and refractive index. If the current sample is non-spherical or the reftractive index is incorrect the value of the predicted concentration may be in error

2.2.12 Characterization reports of deglycosylated invertase using DLS

Fraction B8 from SEC

Protein Characterization Report

v2.0

Malvern

Sample Details

Sample Name:		**Temperature (°C):**	25.0
File Name:	deglyinvertase20090929.dts	**Solvent:**	Water
Record Number:	40	**Solvent ñ:**	1.330
Meas Date &	Tuesday, 29 September 2009...	**Solvent Vis (cP):**	0.8872

Cumulant Results

Count Rate (kcps):	129.9
Z-Average (d.nm):	12.64
olydispersity In...	0.359
Polydispersity (d....	7.573
%Polydispersity:	59.9
Estimated MW (k...	252
Merit (0 to 100):	53.5
Polydispersity:	Polydisperse
Est %Vol Fractio...	4.4391

Intensity Distribution Results

	%Int	Mean (n...	Mode (n...	StD (n...	%Pd	MW (kDa)*	Polydispersity
Peak...	93.1	20.23	15.69	11.72	57.9	756	Polydisperse
Peak...	6.9	0.7262	0.6213	0.1177	16.2	0.315	Monodisperse
Peak...	0.0	0.000	0.000	0.000	0	0.00	

Mass Distribution Results

	%M...	Mean (n...	Mode (n...	StD (n...	%Pd	MW (kDa)*
Peak ...	0.3	9.344	7.531	4.722	50.5	124
Peak...	99.7	0.6873	0.6213	0.1158	16.8	0.277
Peak...	0.0	0.000	0.000	0.000	0	0.00

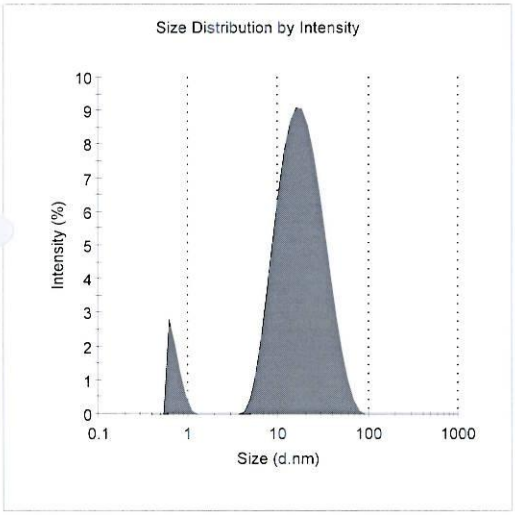

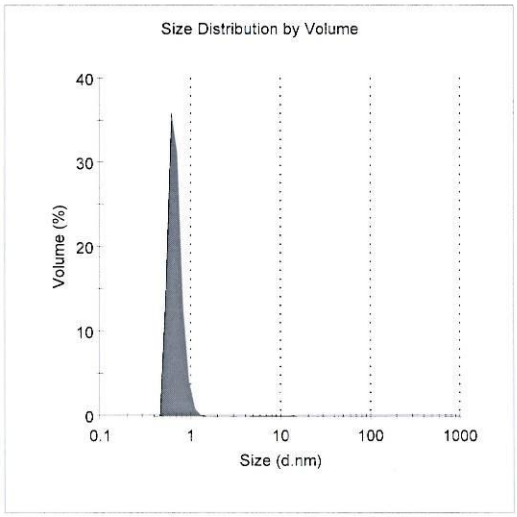

*The molecular weight reported here is only an estimate calculated using an empirical mass vs size calibration curve

*The estimated concentration is calculated from the size distribution measured by DLS and extrapolated from the total intensity compared to a standard sample of known size concentration, and refractive index. If the current sample is non-spherical or the reftractive index is incorrect the value of the predicted concentration may be in error

Fraction B6 from SEC

Protein Characterization Report

v2.0

Malvern

Sample Details

Sample Name:
File Name: intrainvertase20090907.dts
Record Number: 47
Meas Date & Monday, 7 September 2009 3...

Temperature (°C): 25.0
Solvent: Water
Solvent ñ: 1.330
Solvent Vis (cP): 0.8871

Cumulant Results

Count Rate (kcps):	163.1
Z-Average (d.nm):	13.52
olydispersity In...	0.243
Polydispersity (d....	6.661
%Polydispersity:	49.2
Estimated MW (k...	295
Merit (0 to 100):	61.9
Polydispersity:	Polydisperse
Est %Vol Fractio...	.00778

Intensity Distribution Results

	%Int	Mean (n...	Mode (n...	StD (n...	%Pd	MW (kDa)*	Polydispersity
Peak...	100.0	17.57	15.69	6.516	37.1	544	Polydisperse
Peak...	0.0	0.000	0.000	0.000	0	0.00	
Peak...	0.0	0.000	0.000	0.000	0	0.00	

Mass Distribution Results

	%M...	Mean (n...	Mode (n...	StD (n...	%Pd	MW (kDa)*
Peak ...	100.0	12.14	10.10	4.467	36.8	229
Peak...	0.0	0.000	0.000	0.000	0	0.00
Peak...	0.0	0.000	0.000	0.000	0	0.00

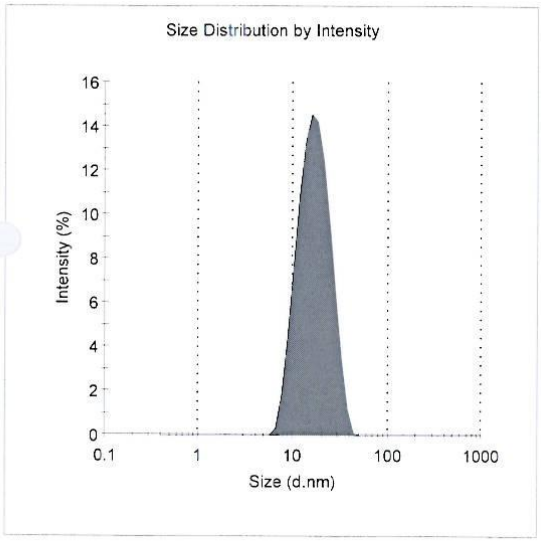

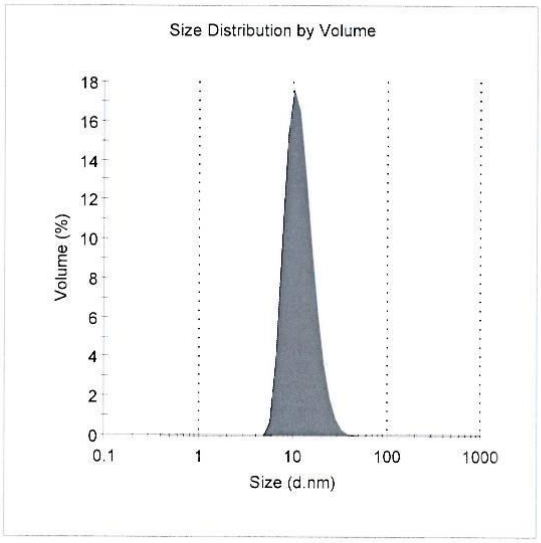

*The molecular weight reported here is only an estimate calculated using an empirical mass vs size calibration curve

*The estimated concentration is calculated from the size distribution measured by DLS and extrapolated from the total intensity compared to a standard sample of known size concentration and refractive index. If the current sample is non-spherical or the refractive index is incorrect the value of the predicted concentration may be in error

2.2.13 Characterization report of deglycosylated invertase after intramolecular crosslinking using DLS

Protein Characterization Report

v2.0

Malvern

Sample Details

Sample Name:
File Name: deglyinvertase20090929.dts
Record Number: 43
Meas Date & Tuesday, 29 September 2009...

Temperature (°C): 25.0
Solvent: Water
Solvent ñ: 1.330
Solvent Vis (cP): 0.8872

Cumulant Results

Count Rate (kcps):	134.4
Z-Average (d.nm):	12.14
`olydispersity In...	0.355
Polydispersity (d....	7.234
%Polydispersity:	59.6
Estimated MW (k...	229
Merit (0 to 100):	45.0
Polydispersity:	Polydisperse
Est %Vol Fractio...	.00512

Intensity Distribution Results

	%Int	Mean (n...	Mode (n...	StD (n...	%Pd	MW (kDa)*	Polydispersity
Peak...	100.0	19.67	18.17	9.982	50.8	708	Polydisperse
Peak...	0.0	0.000	0.000	0.000	0	0.00	
Peak...	0.0	0.000	0.000	0.000	0	0.00	

Mass Distribution Results

	%M...	Mean (n...	Mode (n...	StD (n...	%Pd	MW (kDa)*
Peak ...	100.0	10.33	8.721	4.862	47.1	157
Peak...	0.0	0.000	0.000	0.000	0	0.00
Peak...	0.0	0.000	0.000	0.000	0	0.00

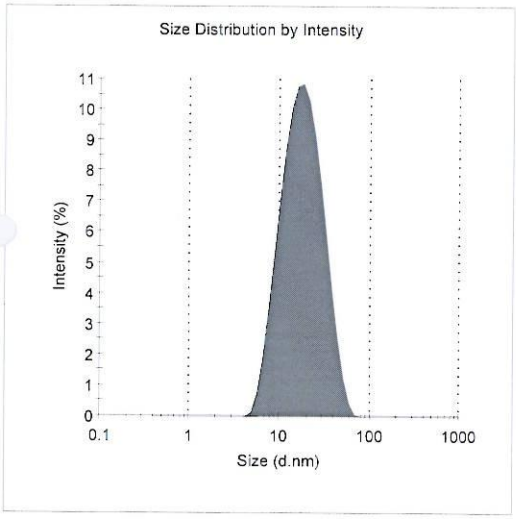

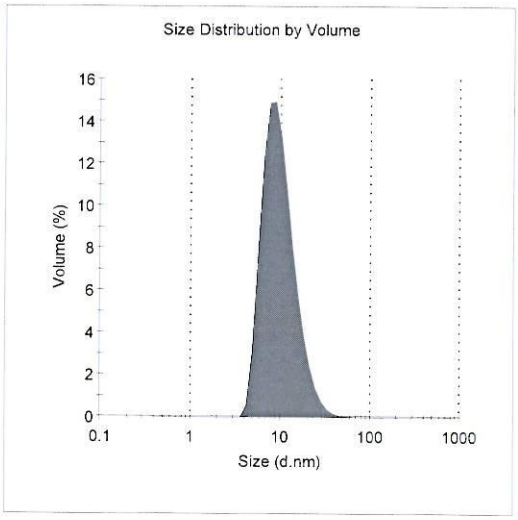

*The molecular weight reported here is only an estimate calculated using an empirical mass vs size calibration curve

*The estimated concentration is calculated from the size distribution measured by DLS and extrapolated from the total intensity compared to a standard sample of known size concentration and refractive index. If the current sample is non-spherical or the reftractive index is incorrect the value of the predicted concentration may be in error

2.2.14 Characterization report of deglycosylated invertase control for intramolecular crosslinking using DLS

Protein Characterization Report

v2.0

Malvern

Sample Details

Sample Name:		**Temperature (°C):**	25.0
File Name:	deglyinvertase20090929.dts	**Solvent:**	Water
Record Number:	36	**Solvent ñ:**	1.330
Meas Date &	Tuesday, 29 September 2009...	**Solvent Vis (cP):**	0.8872

Cumulant Results

Count Rate (kcps):	127.7
Z-Average (d.nm):	11.16
Polydispersity In...	0.302
Polydispersity (d....	6.138
%Polydispersity:	55.0
Estimated MW (k...	188
Merit (0 to 100):	46.6
Polydispersity:	Polydisperse
Est %Vol Fractio...	4.41713

Intensity Distribution Results

	%Int	Mean (n...	Mode (n...	StD (n...	%Pd	MW (kDa)*	Polydispersity
Peak...	91.2	16.36	15.69	6.762	41.3	460	Polydisperse
Peak...	8.8	0.8048	0.6213	0.1772	22.0	0.400	Polydisperse
Peak...	0.0	0.000	0.000	0.000	0	0.00	

Mass Distribution Results

	%M...	Mean (n...	Mode (n...	StD (n...	%Pd	MW (kDa)*
Peak ...	0.2	10.58	8.721	4.147	39.2	166
Peak...	99.8	0.7230	0.6213	0.1508	20.9	0.311
Peak...	0.0	0.000	0.000	0.000	0	0.00

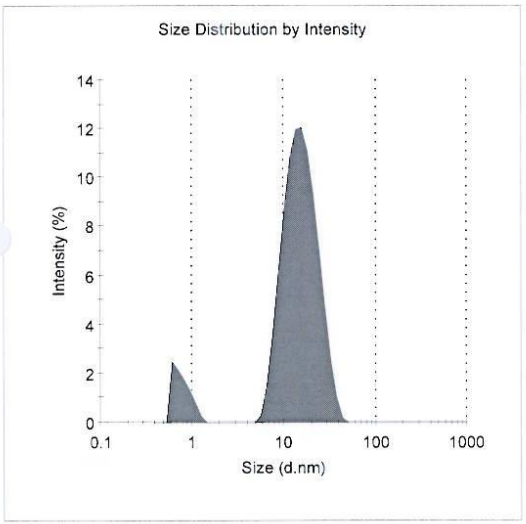

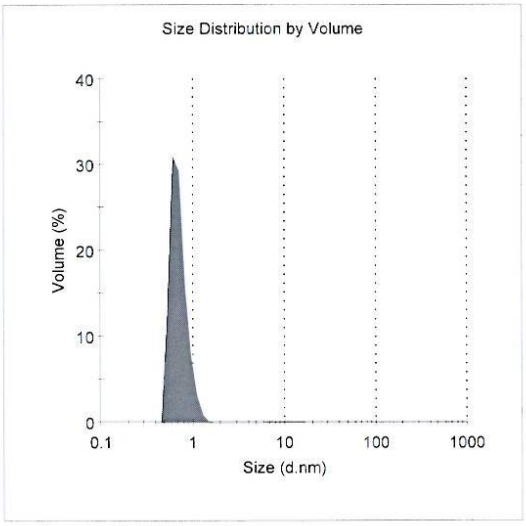

*The molecular weight reported here is only an estimatecalculated using an empirical mass vs size calibration curve

*The estimated concentration is calculated from the size distribution measured by DLS and extrapolated from the total intensity compared to a standard sample of known size concentration, and refractive index. If the current sample is non-spherical or the reftractive index is incorrect the value of the predicted concentration may be in error

2.2.15 Characterization report of deglycosylated invertase after intermolecular crosslinking using DLS (selected fraction from the highest of the main peak of SEC)

Protein Characterization Report

v2.0

Malvern

Sample Details

Sample Name:
File Name: deglyinvertase20090929.dts
Record Number: 88
Meas Date & Thursday, 1 October 2009 2:...

Temperature (°C): 25.0
Solvent: Water
Solvent ñ: 1.330
Solvent Vis (cP): 0.8875

Cumulant Results

Count Rate (kcps):	136.0
Z-Average (d.nm):	14.53
Polydispersity In...	0.407
Polydispersity (d....	9.270
%Polydispersity:	63.8
Estimated MW (k...	349
Merit (0 to 100):	38.6
Polydispersity:	Polydisperse
Est %Vol Fractio...	4.23723

Intensity Distribution Results

	%Int	Mean (n...	Mode (n...	StD (n...	%Pd	MW (kDa)*	Polydispersity
Peak...	89.2	23.62	21.04	10.70	45.3	1090	Polydisperse
Peak...	10.8	0.8209	0.6213	0.1996	24.3	0.419	Polydisperse
Peak...	0.0	0.000	0.000	0.000	0	0.00	

Mass Distribution Results

	%M...	Mean (n...	Mode (n...	StD (n...	%Pd	MW (kDa)*
Peak ...	0.1	14.21	11.70	5.976	42.0	331
Peak...	99.9	0.7254	0.6213	0.1573	21.7	0.314
Peak...	0.0	0.000	0.000	0.000	0	0.00

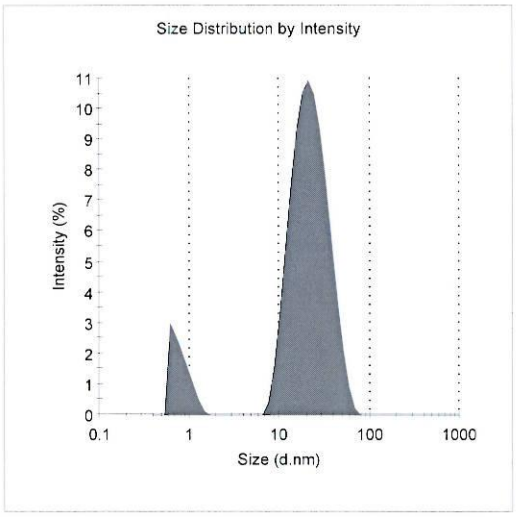

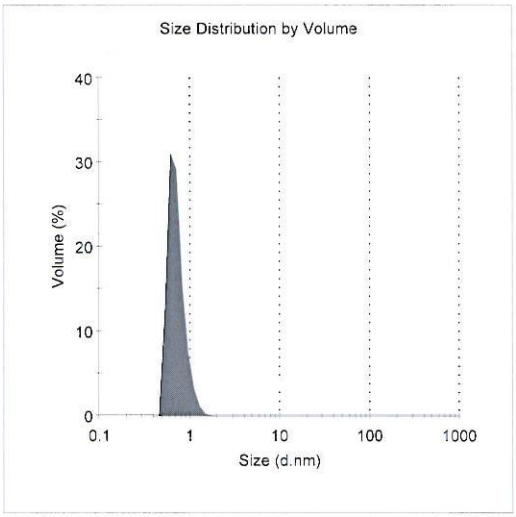

*The molecular weight reported here is only an estimate calculated using an empirical mass vs size calibration curve

*The estimated concentration is calculated from the size distribution measured by DLS and extrapolated from the total intensity compared to a standard sample of known size concentration, and refractive index. If the current sample is non-spherical or the reftractive index is incorrect the value of the predicted concentration may be in error

2.2.16 Characterization report of invertase after intermolecular crosslinking using DLS (selected fraction from the shoulder of the main peak of SEC)

Protein Characterization Report

v2.0

Malvern

Sample Details

Sample Name:		**Temperature (°C):**	25.0
File Name:	deglyinvertase20090929.dts	**Solvent:**	Water
Record Number:	83	**Solvent ñ:**	1.330
Meas Date &	Thursday, 1 October 2009 2:...	**Solvent Vis (cP):**	0.8879

Cumulant Results

Count Rate (kcps):	93.8
Z-Average (d.nm):	18.04
Polydispersity In...	0.577
Polydispersity (d....	13.70
%Polydispersity:	75.9
Estimated MW (k...	578
Merit (0 to 100):	39.5
Polydispersity:	Polydisperse
Est %Vol Fractio...	3.67798

Intensity Distribution Results

	%Int	Mean (n...	Mode (n...	StD (n...	%Pd	MW (kDa)*	Polydispersity
Peak...	85.1	36.13	28.21	20.57	56.9	2940	Polydisperse
Peak...	14.9	0.8141	0.6213	0.1921	23.6	0.411	Polydisperse
Peak...	0.0	0.000	0.000	0.000	0	0.00	

Mass Distribution Results

	%M...	Mean (n...	Mode (n...	StD (n...	%Pd	MW (kDa)*
Peak ...	0.0	17.61	13.54	8.665	49.2	546
Peak...	100.0	0.7245	0.6213	0.1541	21.3	0.313
Peak...	0.0	0.000	0.000	0.000	0	0.00

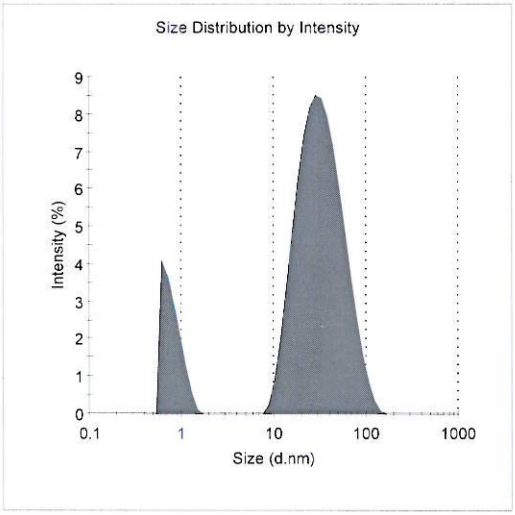

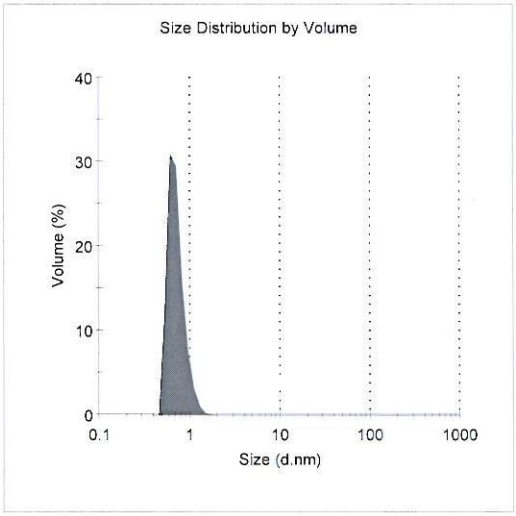

*The molecular weight reported here is only an estimate calculated using an empirical mass vs size calibration curve

*The estimated concentration is calculated from the size distribution measured by DLS and extrapolated from the total intensity compared to a standard sample of known size concentration, and refractive index. If the current sample is non-spherical or the refractive index is incorrect the value of the predicted concentration may be in error

2.2.17 Characterization report of deglycosylated invertase control for intermolecular crosslinking using DLS

Protein Characterization Report

v2.0

Malvern

Sample Details

Sample Name:
File Name: deglyinvertase20090929.dts
Record Number: 70
Meas Date & Thursday, 1 October 2009 11...

Temperature (°C): 25.0
Solvent: Water
Solvent ñ: 1.330
Solvent Vis (cP): 0.8863

Cumulant Results

Count Rate (kcps):	137.5
Z-Average (d.nm):	15.07
Polydispersity In...	0.373
Polydispersity (d....	9.206
%Polydispersity:	61.1
Estimated MW (k...	380
Merit (0 to 100):	43.2
Polydispersity:	Polydisperse
Est %Vol Fractio...	4.87084

Intensity Distribution Results

	%Int	Mean (n...	Mode (n...	StD (n...	%Pd	MW (kDa)*	Polydispersity
Peak...	90.7	23.10	18.17	11.78	51.0	1030	Polydisperse
Peak...	9.3	0.7622	0.7195	0.1317	17.3	0.352	Monodisperse
Peak...	0.0	0.000	0.000	0.000	0	0.00	

Mass Distribution Results

	%M...	Mean (n...	Mode (n...	StD (n...	%Pd	MW (kDa)*
Peak ...	0.1	12.81	10.10	5.660	44.2	260
Peak...	99.9	0.7114	0.6213	0.1299	18.3	0.300
Peak...	0.0	0.000	0.000	0.000	0	0.00

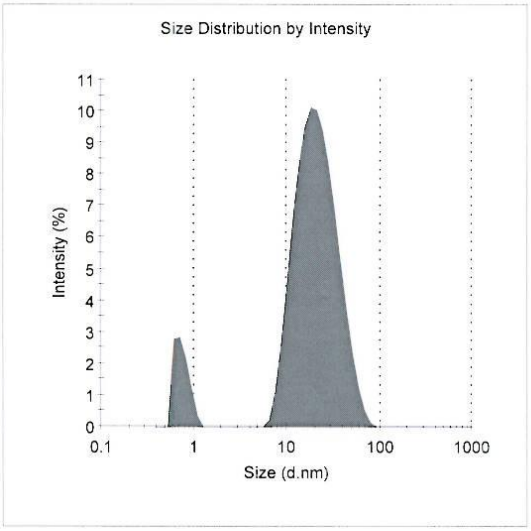

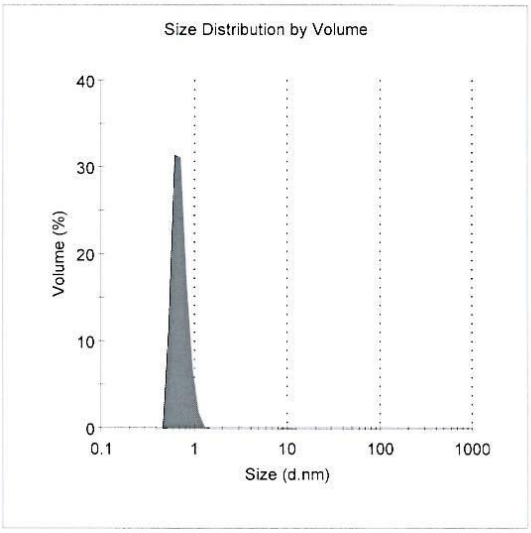

*The molecular weight reported here is only an estimate calculated using an empirical mass vs size calibration curve

*The estimated concentration is calculated from the size distribution measured by DLS and extrapolated from the total intensity compared to a standard sample of known size concentration, and refractive index. If the current sample is non-spherical or the refractive index is incorrect the value of the predicted concentration may be in error

2.3 Multiple angle laser light scattering

2.3.1 Summary report for BSA on Superose 6

ASTRA 4.50 Beta #8 summary Report for BSA001-1

File : C:\DOCUME~1\PTANANCH\DESKTOP\ASTRA\PAT\BSA001-1.ADF
Sample ID : Superose6 Im pH7; 0.4ml/min; BSA 8.mg/ml inject 50ul 08/07/09
Operator: Michelle

COLLECTION INFORMATION

Collection time : Wed Jul 08, 2009 02:30 PM
Instrument type : DAWN DSP
Cell type : K5
Laser wavelength : 632.8 nm
Solvent name : water
Solvent RI : 1.332
Calibration constants
DAWN : 2.7060e-05
» AUX2 : 1.0680e-03
Flow rate : 0.400 mL/min

PROCESSING INFORMATION

Processing time : Thu Jul 30, 2009 10:22 AM
DAWN/AUX2 delay : 0.195 mL
Fit method / model : Debye
Calculation method : dn/dc + AUX Constant
Detectors used : 3 5 6 7 8 9 10 11 12 13 14 15 16 17

PEAK #1

Peak volume : 20.503 - 20.790 mL
Slices in peak : 116
2nd Virial Coefficient : 0.000e+00 mol mL/g²
Detector fit degree : 1
Mass (injected) : 4.3500e-04 g
Mass (calculated) : 1.4706e-05 g
dn/dc : 0.180 mL/g

MOLAR MASS MOMENTS (g/mol)		R.M.S. RADIUS MOMENTS (nm)	
Mn	(1.400 ± 0.013)e+5 (0.9%)	Rn	0.0 ± 0.0 (0%)
Mw	(1.400 ± 0.013)e+5 (0.9%)	Rw	0.0 ± 0.0 (0%)
Mz	(1.400 ± 0.029)e+5 (2.1%)	Rz	0.0 ± 0.0 (0%)

PEAK #2

Peak volume : 22.558 - 22.723 mL
Slices in peak : 67
2nd Virial Coefficient : 0.000e+00 mol mL/g²
Detector fit degree : 1
Mass (injected) : 4.0000e-04 g
Mass (calculated) : 1.0388e-04 g
dn/dc : 0.180 mL/g

MOLAR MASS MOMENTS (g/mol)		R.M.S. RADIUS MOMENTS (nm)	
Mn	(6.778 ± 0.006)e+4 (0.09%)	Rn	3.0 ± 0.8 (25%)
Mw	(6.778 ± 0.006)e+4 (0.09%)	Rw	3.0 ± 0.8 (25%)
Mz	(6.778 ± 0.014)e+4 (0.20%)	Rz	3.0 ± 0.8 (25%)

2.3.2 Summary report for native invertase on Superose 6

ASTRA 4.50 Beta #8 summary Report for INV8B-1

File : C:\DOCUME~1\PTANANCH\DESKTOP\ASTRA\PAT\INV8B-1.ADF
Sample ID : Superose6 Im pH7; 0.4ml/min; ivertase 36mg/ml inject 50ul 25/07/09
Operator: pat

COLLECTION INFORMATION

Collection time : Sat Jul 25, 2009 09:15 PM
Instrument type : DAWN DSP
Cell type : K5
Laser wavelength : 632.8 nm
Solvent name : water
Solvent RI : 1.332
Calibration constants
DAWN : 2.7060e-05
» AUX2 : 1.0680e-03
Flow rate : 0.400 mL/min

PROCESSING INFORMATION

Processing time : Fri Jul 31, 2009 12:55 PM
DAWN/AUX2 delay : 0.195 mL
Fit method / model : Debye
Calculation method : dn/dc + AUX Constant
Detectors used : 3 5 6 7 8 9 10 11 12 13 14 15 16 17

PEAK #1

Peak volume : 7.100 - 7.197 mL
Slices in peak : 30
2nd Virial Coefficient : 0.000e+00 mol mL/g²
Detector fit degree : 1
Mass (injected) : 1.8000e-03 g
Mass (calculated) : 1.9578e-07 g
dn/dc : 0.190 mL/g

MOLAR MASS MOMENTS (g/mol)		R.M.S. RADIUS MOMENTS (nm)	
Mn	(2.750 ± 0.402)e+7 (14%)	Rn	38.0 ± 0.7 (1.9%)
Mw	(3.269 ± 0.737)e+7 (22%)	Rw	38.2 ± 0.7 (1.9%)
Mz	(4.317 ± 2.718)e+7 (62%)	Rz	38.7 ± 0.7 (1.9%)

PEAK #2

Peak volume : 11.490 - 11.610 mL
Slices in peak : 37
2nd Virial Coefficient : 0.000e+00 mol mL/g²
Detector fit degree : 1
Mass (injected) : 1.8000e-03 g
Mass (calculated) : 3.1575e-05 g
dn/dc : 0.190 mL/g

MOLAR MASS MOMENTS (g/mol)		R.M.S. RADIUS MOMENTS (nm)	
Mn	(1.639 ± 0.009)e+5 (0.5%)	Rn	11.0 ± 1.6 (14%)
Mw	(1.639 ± 0.009)e+5 (0.5%)	Rw	11.0 ± 1.6 (14%)
Mz	(1.639 ± 0.020)e+5 (1.2%)	Rz	11.0 ± 1.6 (14%)

PEAK #3

Peak volume : 14.317 - 14.460 mL
Slices in peak : 44
2nd Virial Coefficient : 0.000e+00 mol mL/g²
Detector fit degree : 1
Mass (injected) : 1.8000e-03 g
Mass (calculated) : 6.3669e-05 g
dn/dc : 0.190 mL/g

MOLAR MASS MOMENTS (g/mol)		R.M.S. RADIUS MOMENTS (nm)	
Mn	(1.219 ± 0.006)e+5 (0.5%)	Rn	5.0 ± 3.2 (63%)
Mw	(1.219 ± 0.006)e+5 (0.5%)	Rw	5.0 ± 3.2 (63%)
Mz	(1.219 ± 0.013)e+5 (1.1%)	Rz	5.0 ± 3.2 (63%)

PEAK #4

Peak volume : 16.193 - 16.310 mL
Slices in peak : 36
2nd Virial Coefficient : 0.000e+00 mol mL/g²
Detector fit degree : 1
Mass (injected) : 1.8000e-03 g
Mass (calculated) : 1.0940e-05 g
dn/dc : 0.190 mL/g

MOLAR MASS MOMENTS (g/mol)		R.M.S. RADIUS MOMENTS (nm)	
Mn	(3.611 ± 0.058)e+4 (1.6%)	Rn	10.9 ± 4.8 (43%)
Mw	(3.611 ± 0.058)e+4 (1.6%)	Rw	10.9 ± 4.8 (43%)
Mz	(3.612 ± 0.129)e+4 (3%)	Rz	10.9 ± 4.8 (43%)

PEAK #5

Peak volume : 16.740 - 16.833 mL
Slices in peak : 29
2nd Virial Coefficient : 0.000e+00 mol mL/g²
Detector fit degree : 1
Mass (injected) : 1.8000e-03 g
Mass (calculated) : 5.9241e-06 g
dn/dc : 0.190 mL/g

MOLAR MASS MOMENTS (g/mol)		R.M.S. RADIUS MOMENTS (nm)	
Mn	(3.650 ± 0.085)e+4 (2.3%)	Rn	11.3 ± 6.7 (59%)
Mw	(3.651 ± 0.085)e+4 (2.3%)	Rw	11.3 ± 6.7 (58%)
Mz	(3.653 ± 0.190)e+4 (5%)	Rz	11.4 ± 6.6 (58%)

2.3.3 Summary report for invertase after intramolecular crosslinking on Superose 6

File : C:\DOCUME~1\PTANANCH\DESKTOP\ASTRA\PAT\CIV6-1.ADF
Sample ID : Superose6 Im pH7; 0.4ml/min; c-ivertase 6.8mg/ml inject 50ul 25/07/09
Operator: pat

COLLECTION INFORMATION

Collection time : Sat Jul 25, 2009 12:41 PM
Instrument type : DAWN DSP
Cell type : K5
Laser wavelength : 632.8 nm
Solvent name : water
Solvent RI : 1.332
Calibration constants
DAWN : 2.7060e-05
» AUX2 : 1.0680e-03
Flow rate : 0.400 mL/min

PROCESSING INFORMATION

Processing time : Fri Jul 31, 2009 01:43 PM
DAWN/AUX2 delay : 0.195 mL
Fit method / model : Debye
Calculation method : dn/dc + AUX Constant
Detectors used : 3 5 6 7 8 9 10 11 12 13 14 15 16 17

PEAK #1

Peak volume : 6.923 - 7.123 mL
Slices in peak : 61
2nd Virial Coefficient : 0.000e+00 mol mL/g²
Detector fit degree : 1
Mass (injected) : 3.4000e-04 g
Mass (calculated) : 4.8178e-08 g
dn/dc : 0.190 mL/g

MOLAR MASS MOMENTS (g/mol)		R.M.S. RADIUS MOMENTS (nm)	
Mn	0.000e+00 (0%)	Rn	0.0 ± 0.0 (0%)
Mw	0.000e+00 (0%)	Rw	0.0 ± 0.0 (0%)
Mz	0.000e+00 (0%)	Rz	0.0 ± 0.0 (0%)

PEAK #2

Peak volume : 11.340 - 11.453 mL
Slices in peak : 35
2nd Virial Coefficient : 0.000e+00 mol mL/g²
Detector fit degree : 1
Mass (injected) : 3.4000e-04 g
Mass (calculated) : 4.9315e-06 g
dn/dc : 0.190 mL/g

MOLAR MASS MOMENTS (g/mol)		R.M.S. RADIUS MOMENTS (nm)	
Mn	(1.728 ± 0.016)e+5 (0.9%)	Rn	12.6 ± 1.2 (9%)
Mw	(1.728 ± 0.016)e+5 (0.9%)	Rw	12.6 ± 1.2 (9%)
Mz	(1.729 ± 0.036)e+5 (2.1%)	Rz	12.6 ± 1.2 (9%)

PEAK #3

Peak volume : 14.273 - 14.530 mL
Slices in peak : 78
2nd Virial Coefficient : 0.000e+00 mol mL/g²
Detector fit degree : 1
Mass (injected) : 3.4000e-04 g
Mass (calculated) : 1.0502e-05 g
dn/dc : 0.190 mL/g

MOLAR MASS MOMENTS (g/mol)		R.M.S. RADIUS MOMENTS (nm)	
Mn	(1.304 ± 0.014)e+5 (1.1%)	Rn	12.7 ± 1.6 (12%)
Mw	(1.304 ± 0.014)e+5 (1.1%)	Rw	12.8 ± 1.6 (12%)
Mz	(1.305 ± 0.032)e+5 (2.4%)	Rz	12.8 ± 1.6 (12%)

2.3.4 Summary report for invertase after intermolecular crosslinking on Superose 6

ASTRA 4.50 Beta #8 summary Report for CINV2A-1
File : C:\DOCUME~1\PTANANCH\DESKTOP\ASTRA\PAT\CINV2A-1.ADF
Sample ID : Superose6 Im pH7; 0.4ml/min; c-ivertase 11mg/ml inject 50ul 24/07/09
Operator: pat
COLLECTION INFORMATION
Collection time : Fri Jul 24, 2009 08:31 PM
Instrument type : DAWN DSP
Cell type : K5
Laser wavelength : 632.8 nm
Solvent name : water
Solvent RI : 1.332
Calibration constants
DAWN : 2.7060e-05
» AUX2 : 1.0680e-03
Flow rate : 0.400 mL/min
PROCESSING INFORMATION
Processing time : Fri Jul 31, 2009 11:31 AM
DAWN/AUX2 delay : 0.195 mL
Fit method / model : Debye
Calculation method : dn/dc + AUX Constant
Detectors used : 3 5 6 7 8 9 10 11 12 13 14 15 16 17
PEAK #1
Peak volume : 6.893 - 7.123 mL
Slices in peak : 70
2nd Virial Coefficient : 0.000e+00 mol mL/g²
Detector fit degree : 1
Mass (injected) : 5.5000e-04 g
Mass (calculated) : -1.5911e-07 g
dn/dc : 0.190 mL/g

MOLAR MASS MOMENTS (g/mol)		R.M.S. RADIUS MOMENTS (nm)	
Mn	(1.152 ± 0.483)e+8 (41%)	Rn	45.0 ± 1.0 (2.2%)
Mw	(1.152 ± 0.483)e+8 (41%)	Rw	45.0 ± 1.0 (2.2%)
Mz	(1.152 ± 1.079)e+8 (93%)	Rz	45.0 ± 1.0 (2.2%)

PEAK #2
Peak volume : 11.227 - 11.483 mL
Slices in peak : 78
2nd Virial Coefficient : 0.000e+00 mol mL/g²
Detector fit degree : 1
Mass (injected) : 5.5000e-04 g

Mass (calculated): 2.0887e-05 g
dn/dc : 0.190 mL/g

MOLAR MASS MOMENTS (g/mol)		R.M.S. RADIUS MOMENTS (nm)	
Mn	(1.792 ± 0.014)e+5 (0.8%)	Rn	15.8 ± 1.3 (8%)
Mw	(1.793 ± 0.014)e+5 (0.8%)	Rw	15.8 ± 1.3 (8%)
Mz	(1.793 ± 0.031)e+5 (1.7%)	Rz	15.8 ± 1.3 (8%)

PEAK #3
Peak volume : 14.190 - 14.417 mL
Slices in peak : 69
2nd Virial Coefficient : 0.000e+00 mol mL/g²
Detector fit degree : 1
Mass (injected) : 5.5000e-04 g
Mass (calculated): 2.3935e-05 g
dn/dc : 0.190 mL/g

MOLAR MASS MOMENTS (g/mol)		R.M.S. RADIUS MOMENTS (nm)	
Mn	(1.284 ± 0.009)e+5 (0.7%)	Rn	11.0 ± 1.7 (15%)
Mw	(1.284 ± 0.009)e+5 (0.7%)	Rw	11.0 ± 1.7 (15%)
Mz	(1.284 ± 0.020)e+5 (1.6%)	Rz	11.0 ± 1.7 (15%)

PEAK #4
Peak volume : 16.240 - 16.410 mL
Slices in peak : 52
2nd Virial Coefficient : 0.000e+00 mol mL/g²
Detector fit degree : 1
Mass (injected) : 5.5000e-04 g
Mass (calculated): 4.5111e-06 g
dn/dc : 0.190 mL/g

MOLAR MASS MOMENTS (g/mol)		R.M.S. RADIUS MOMENTS (nm)	
Mn	(6.344 ± 0.268)e+4 (4%)	Rn	22.4 ± 5.6 (24%)
Mw	(6.350 ± 0.268)e+4 (4%)	Rw	22.5 ± 5.6 (24%)
Mz	(6.357 ± 0.601)e+4 (9%)	Rz	22.5 ± 5.6 (24%)

2.3.5 Summary report for native invertase on Sephacryl S-300

ASTRA 4.50 Beta #8 summary Report for INTRA6

File : C:\DOCUME~1\PTANANCH\DESKTOP\ASTRA\PAT2\INTRA6.ADF
Sample ID : Sephacryl S300 60cm column, Citrate Buffer pH6; 0.5ml/min; intra7 1.2 mg/ml inject 1 ml 15/11/09
Operator: Pat

COLLECTION INFORMATION

Collection time : Sat Nov 15, 2008 05:27 PM
Instrument type : DAWN DSP
Cell type : K5
Laser wavelength : 632.8 nm
Solvent name : water
Solvent RI : 1.332
Calibration constants
DAWN : 2.7060e-05
» AUX2 : 1.0680e-03
Flow rate : 0.500 mL/min

PROCESSING INFORMATION

Processing time : Mon Nov 16, 2009 02:27 PM
DAWN/AUX2 delay : 0.442 mL
Fit method / model : Debye
Calculation method : dn/dc + AUX Constant
Detectors used : 7 8 9 10 11 12 13 14 15 16 17

PEAK #1

Peak volume : 67.442 - 68.283 mL
Slices in peak : 102
2nd Virial Coefficient : 0.000e+00 mol mL/g²
Detector fit degree : 1
Mass (injected) : 3.0000e-03 g
Mass (calculated) : 2.1744e-04 g
dn/dc : 0.190 mL/g

MOLAR MASS MOMENTS (g/mol)		R.M.S. RADIUS MOMENTS (nm)	
Mn	(1.146 ± 0.035)e+5 (3%)	Rn	0.0 ± 0.0 (0%)
Mw	**(1.147 ± 0.035)e+5 (3%)**	**Rw**	**0.0 ± 0.0 (0%)**
Mz	(1.149 ± 0.079)e+5 (6%)	Rz	0.0 ± 0.0 (0%)

2.3.6 Summary report for invertase after intramolecular crosslinking on Sephacryl S-300

ASTRA 4.50 Beta #8 summary Report for INTRA5

File : C:\DOCUME~1\PTANANCH\DESKTOP\ASTRA\PAT2\INTRA5.ADF
Sample ID : Sephacryl S300 60cm column, Citrate Buffer pH6; 0.5ml/min; intra5 3 mg/ml inject 1 ml 14/11/09
Operator: Pat

COLLECTION INFORMATION

Collection time : Fri Nov 14, 2008 01:16 PM
Instrument type : DAWN DSP
Cell type : K5
Laser wavelength : 632.8 nm
Solvent name : water
Solvent RI : 1.332
Calibration constants
DAWN : 2.7060e-05
» AUX2 : 1.0680e-03
Flow rate : 0.500 mL/min

PROCESSING INFORMATION

Processing time : Mon Nov 16, 2009 03:07 PM
DAWN/AUX2 delay : 0.233 mL
Fit method / model : Debye
Calculation method : dn/dc + AUX Constant
Detectors used : 7 8 9 10 11 12 13 14 15 16 17

PEAK #1

Peak volume : 67.050 - 67.992 mL
Slices in peak : 114

2nd Virial Coefficient : 0.000e+00 mol mL/g²
Detector fit degree : 1
Mass (injected) : 3.0000e-03 g
Mass (calculated) : 2.7472e-04 g
dn/dc : 0.190 mL/g

MOLAR MASS MOMENTS (g/mol)		R.M.S. RADIUS MOMENTS (nm)	
Mn	(1.254 ± 0.016)e+5 (1.3%)	Rn	0.0 ± 0.0 (0%)
Mw	**(1.255 ± 0.016)e+5 (1.3%)**	**Rw**	**0.0 ± 0.0 (0%)**
Mz	(1.255 ± 0.037)e+5 (2.9%)	Rz	0.0 ± 0.0 (0%)

2.3.7 Summary report for invertase after intermolecular crosslinking on Sephacryl S-300

ASTRA 4.50 Beta #8 summary Report for INTER2B

File : C:\DOCUME~1\PTANANCH\DESKTOP\ASTRA\PAT2\INTER2B.ADF
Sample ID : Sephacryl S300 60cm column, Citrate Buffer pH6; 0.5ml/min; inter5b 3 mg/ml inject 1 ml 14/11/09
Operator: Pat

COLLECTION INFORMATION

Collection time : Fri Nov 14, 2008 08:20 PM
Instrument type : DAWN DSP
Cell type : K5
Laser wavelength : 632.8 nm
Solvent name : water
Solvent RI : 1.332
Calibration constants
DAWN : 2.7060e-05
» AUX2 : 1.0680e-03
Flow rate : 0.500 mL/min

PROCESSING INFORMATION

Processing time : Tue Nov 17, 2009 05:24 PM
DAWN/AUX2 delay : 1.383 mL
Fit method / model : Debye
Calculation method : dn/dc + AUX Constant
Detectors used : 7 8 9 10 11 12 13 14 15 16 17

PEAK #1

Peak volume : 49.858 - 50.267 mL
Slices in peak : 50

2nd Virial Coefficient : 0.000e+00 mol mL/g²
Detector fit degree : 1
Mass (injected) : 3.0000e-03 g
Mass (calculated): 1.4022e-05 g
dn/dc : 0.190 mL/g

MOLAR MASS MOMENTS (g/mol)		R.M.S. RADIUS MOMENTS (nm)	
Mn	(1.740 ± 0.124)e+6 (7%)	Rn	52.3 ± 3.8 (7%)
Mw	**(1.747 ± 0.126)e+6 (7%)**	**Rw**	**52.3 ± 3.8 (7%)**
Mz	(1.755 ± 0.285)e+6 (16%)	Rz	52.3 ± 3.8 (7%)

PEAK #2

Peak volume : 51.950 - 52.475 mL
Slices in peak : 64
2nd Virial Coefficient : 0.000e+00 mol mL/g²
Detector fit degree : 1
Mass (injected) : 3.0000e-03 g
Mass (calculated): 1.2781e-04 g
dn/dc : 0.190 mL/g

MOLAR MASS MOMENTS (g/mol)		R.M.S. RADIUS MOMENTS (nm)	
Mn	(9.799 ± 0.232)e+5 (2.4%)	Rn	37.9 ± 1.7 (4%)
Mw	**(9.833 ± 0.233)e+5 (2.4%)**	**Rw**	**38.0 ± 1.7 (4%)**
Mz	(9.867 ± 0.523)e+5 (5%)	Rz	38.0 ± 1.7 (4%)

PEAK #3

Peak volume : 55.817 - 56.342 mL
Slices in peak : 64
2nd Virial Coefficient : 0.000e+00 mol mL/g²
Detector fit degree : 1
Mass (injected) : 3.0000e-03 g
Mass (calculated): 3.0100e-04 g
dn/dc : 0.190 mL/g

MOLAR MASS MOMENTS (g/mol)		R.M.S. RADIUS MOMENTS (nm)	
Mn	(3.784 ± 0.065)e+5 (1.7%)	Rn	26.3 ± 1.8 (6%)
Mw	**(3.787 ± 0.065)e+5 (1.7%)**	**Rw**	**26.4 ± 1.8 (6%)**
Mz	(3.789 ± 0.146)e+5 (3%)	Rz	26.4 ± 1.8 (6%)

PEAK #4

Peak volume : 64.300 - 66.392 mL
Slices in peak : 252
2nd Virial Coefficient : 0.000e+00 mol mL/g²
Detector fit degree : 1
Mass (injected) : 3.0000e-03 g
Mass (calculated): 1.8913e-03 g
dn/dc : 0.190 mL/g

MOLAR MASS MOMENTS (g/mol)		R.M.S. RADIUS MOMENTS (nm)	
Mn	(1.727 ± 0.021)e+5 (1.2%)	Rn	2.0 ± 17.5 (885%)
Mw	**(1.728 ± 0.021)e+5 (1.2%)**	**Rw**	**2.0 ± 17.1 (845%)**
Mz	(1.729 ± 0.047)e+5 (2.7%)	Rz	2.1 ± 16.7 (809%)

2.4 Circular dichroism

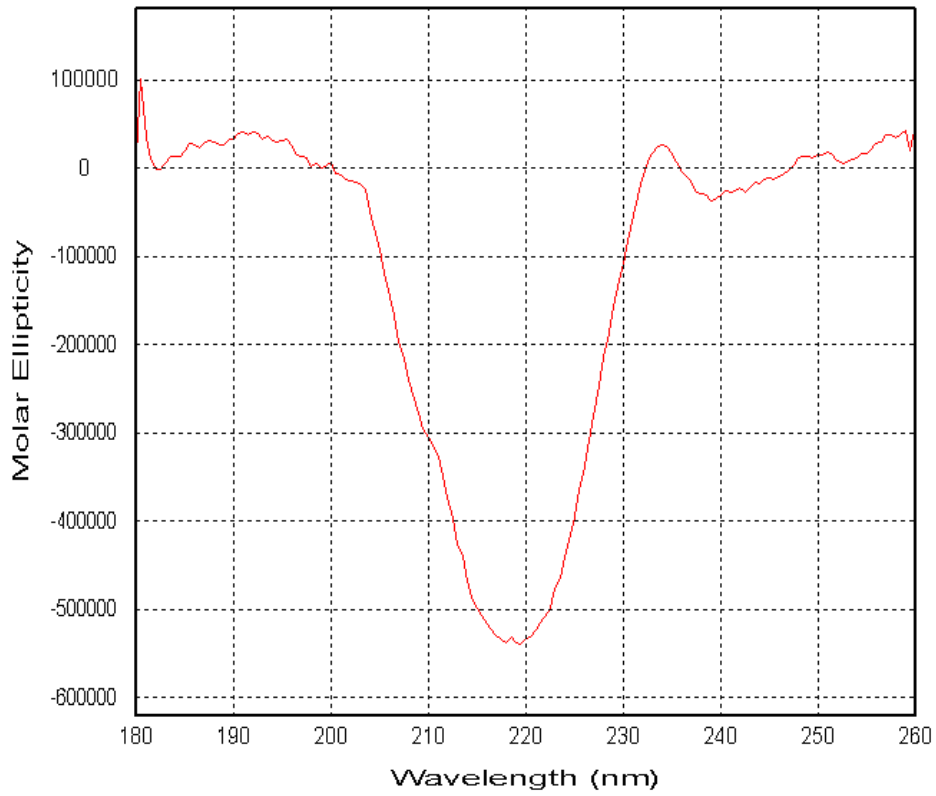

Figure 12 CD spectrum of native invertase.

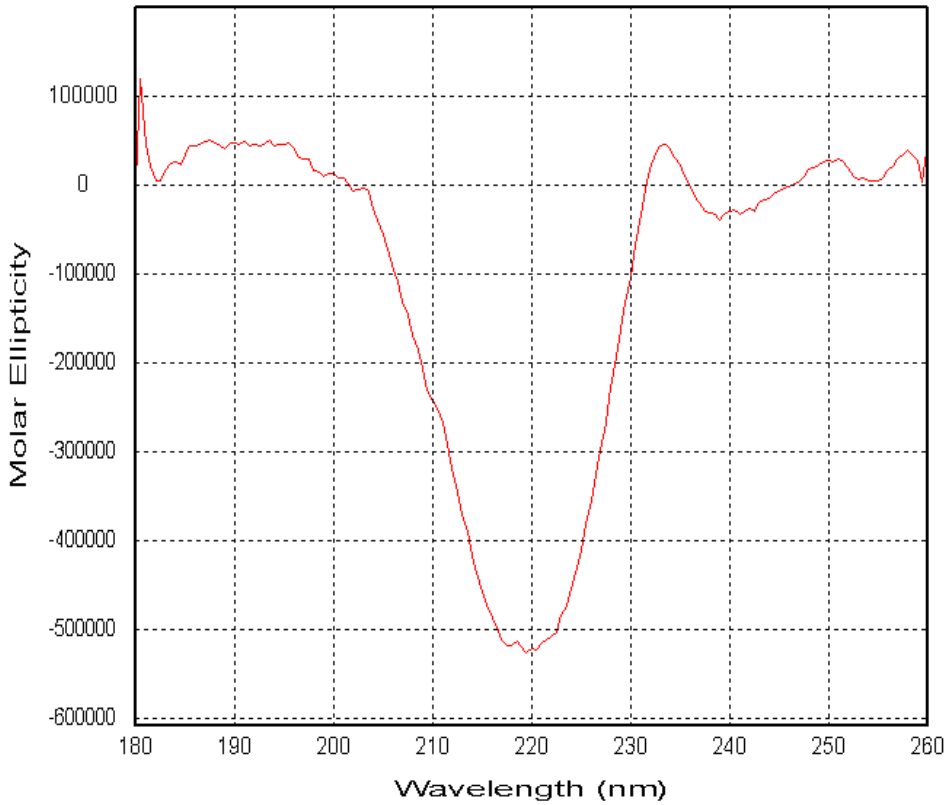

Figure 13 CD spectrum of invertase after intramolecular crosslinking.

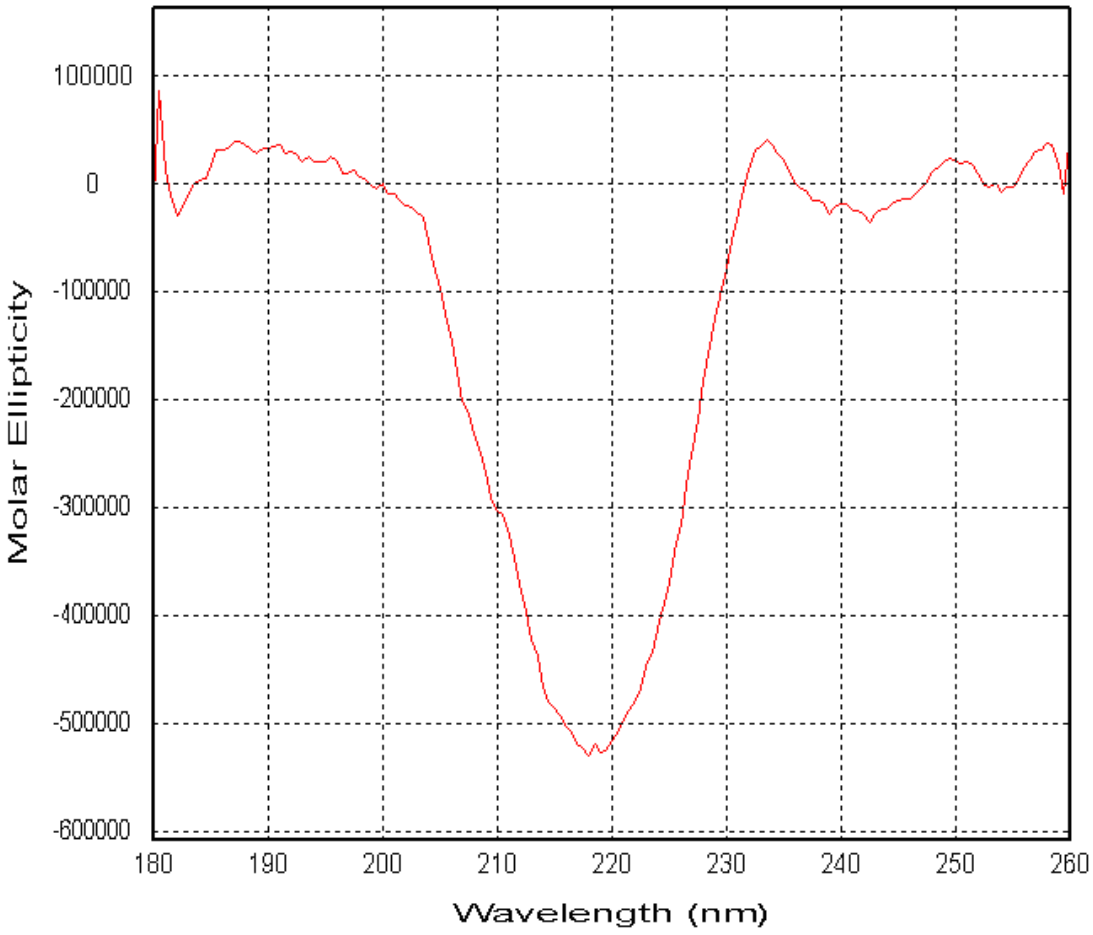

Figure 14 CD spectrum of invertase after intermolecular crosslinking.

3 Investigations into molecular basis of BMDC crosslinking

3.1 Crosslinking of pentapeptide

3.1.1 HPLC analysis of native pentapeptide

	Injection Volume:	**70.0**
RA1	*Channel:*	**UV_VIS_1**
Unknown	*Wavelength:*	**214**
	Bandwidth:	**8**
Default	*Dilution Factor:*	**1.0000**
22/10/2009 13:41	*Sample Weight:*	**1.0000**
55.00	*Sample Amount:*	**1.0000**

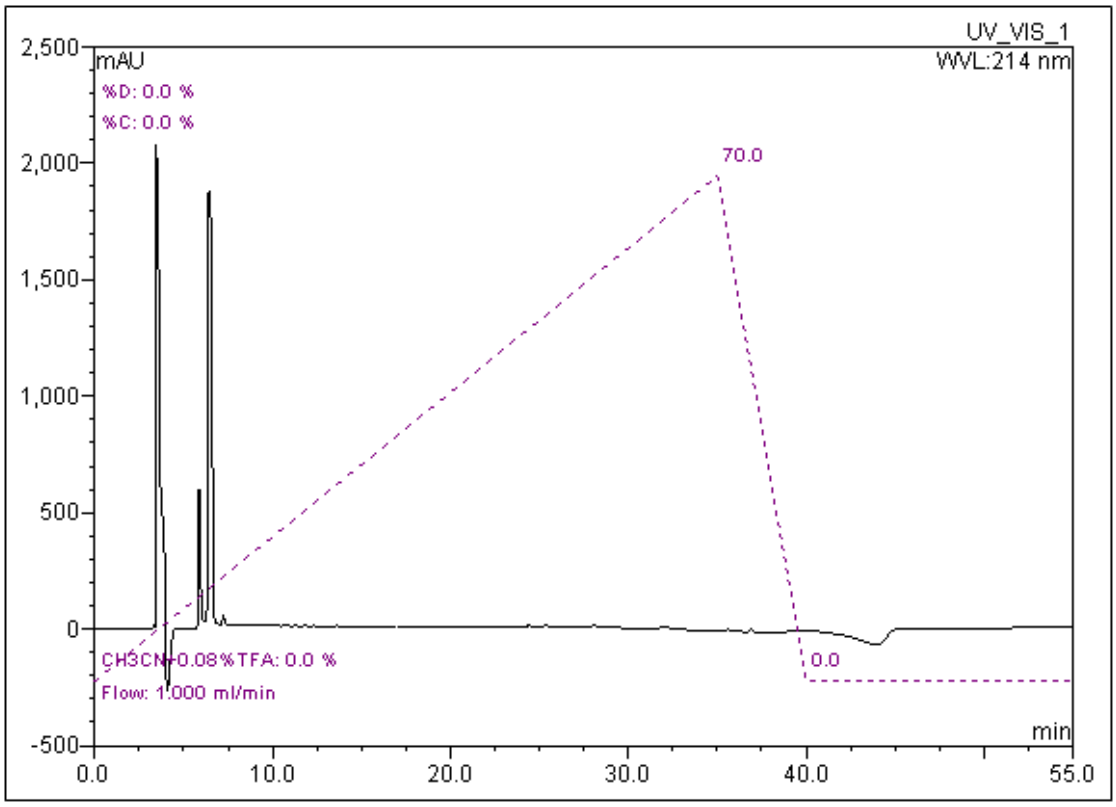

No.	Ret.Time	Peak Name	Height	Area	Rel.Area	Amount	Type
	Min		mAU	mAU*min	%	n.a.	
1	0.04	n.a.	0.029	0.000	0.00	n.a.	BMB
2	1.93	n.a.	0.038	0.003	0.00	n.a.	Ru
3	3.17	n.a.	200.786	300.697	8.15	n.a.	BM
4	3.33	n.a.	16.120	1.141	0.03	n.a.	Ru
5	3.45	n.a.	2302.018	716.810	19.42	n.a.	MB

No.	Ret.Time	Peak Name	Height	Area	Rel.Area	Amount	Type
	Min		mAU	mAU*min	%	n.a.	
6	3.48	n.a.	5.187	0.057	0.00	n.a.	Rd
7	3.50	n.a.	4.740	0.060	0.00	n.a.	Rd
8	5.87	n.a.	833.692	555.813	15.06	n.a.	BM
9	6.18	n.a.	1.100	0.058	0.00	n.a.	Rd
10	6.43	n.a.	2097.358	927.116	25.12	n.a.	M
11	6.92	n.a.	0.703	0.044	0.00	n.a.	Rd
12	7.21	n.a.	42.561	5.307	0.14	n.a.	Rd
13	7.74	n.a.	2.015	0.326	0.01	n.a.	Rd
14	8.30	n.a.	199.329	612.988	16.61	n.a.	M
15	8.82	n.a.	0.698	0.163	0.00	n.a.	Rd
16	9.48	n.a.	1.858	0.782	0.02	n.a.	Rd
17	10.17	n.a.	1.986	0.611	0.02	n.a.	Rd
18	10.82	n.a.	1.595	0.506	0.01	n.a.	Rd
19	11.36	n.a.	1.314	0.411	0.01	n.a.	Rd
20	11.81	n.a.	2.015	0.470	0.01	n.a.	Rd
21	12.06	n.a.	125.501	59.154	1.60	n.a.	M
22	12.75	n.a.	1.205	0.286	0.01	n.a.	Ru
23	13.20	n.a.	1.137	0.216	0.01	n.a.	Ru
24	13.40	n.a.	101.095	358.489	9.71	n.a.	M
25	13.99	n.a.	0.961	0.179	0.00	n.a.	Rd
26	14.37	n.a.	0.810	0.154	0.00	n.a.	Rd
27	14.75	n.a.	0.890	0.224	0.01	n.a.	Rd
28	15.42	n.a.	1.128	0.197	0.01	n.a.	Rd
29	15.74	n.a.	0.788	0.134	0.00	n.a.	Rd
30	16.09	n.a.	0.380	0.051	0.00	n.a.	Rd
31	16.39	n.a.	0.209	0.030	0.00	n.a.	Rd
32	16.80	n.a.	5.262	0.953	0.03	n.a.	Rd
33	17.17	n.a.	0.212	0.030	0.00	n.a.	Rd
34	17.51	n.a.	0.397	0.053	0.00	n.a.	Rd
35	17.79	n.a.	0.450	0.083	0.00	n.a.	Rd
36	18.22	n.a.	7.337	1.531	0.04	n.a.	MB
37	18.66	n.a.	0.095	0.007	0.00	n.a.	bMB
38	18.85	n.a.	0.159	0.013	0.00	n.a.	BMB
39	19.31	n.a.	0.169	0.020	0.00	n.a.	BMB
40	19.70	n.a.	0.445	0.104	0.00	n.a.	BMb
41	20.07	n.a.	0.288	0.038	0.00	n.a.	bMb
42	20.33	n.a.	0.301	0.043	0.00	n.a.	bMB

No.	Ret.Time	Peak Name	Height	Area	Rel.Area	Amount	Type
	Min		mAU	mAU*min	%	n.a.	
43	20.63	n.a.	1.554	0.194	0.01	n.a.	BMB
44	20.99	n.a.	0.208	0.020	0.00	n.a.	BMB
45	21.23	n.a.	0.272	0.020	0.00	n.a.	BM
46	21.36	n.a.	5.187	0.555	0.02	n.a.	MB
47	21.61	n.a.	0.105	0.006	0.00	n.a.	BMB
48	21.75	n.a.	0.209	0.012	0.00	n.a.	BMB
49	22.24	n.a.	0.101	0.008	0.00	n.a.	BMB
50	22.64	n.a.	0.265	0.038	0.00	n.a.	BMB
51	22.93	n.a.	0.356	0.048	0.00	n.a.	BMB
52	23.99	n.a.	0.904	0.140	0.00	n.a.	BM
53	24.06	n.a.	0.852	0.048	0.00	n.a.	M
54	24.39	n.a.	15.265	4.880	0.13	n.a.	M
55	24.60	n.a.	0.819	0.071	0.00	n.a.	Rd
56	25.38	n.a.	17.495	7.005	0.19	n.a.	M
57	25.85	n.a.	0.328	0.032	0.00	n.a.	Rd
58	26.16	n.a.	0.266	0.028	0.00	n.a.	Rd
59	26.46	n.a.	0.475	0.068	0.00	n.a.	Rd
60	26.80	n.a.	0.227	0.018	0.00	n.a.	Ru
61	27.33	n.a.	9.209	7.134	0.19	n.a.	M
62	27.65	n.a.	0.861	0.219	0.01	n.a.	Rd
63	28.03	n.a.	15.531	11.818	0.32	n.a.	MB
64	29.48	n.a.	1.354	0.205	0.01	n.a.	Rd
65	30.57	n.a.	0.120	0.005	0.00	n.a.	BMB
66	30.72	n.a.	0.918	0.112	0.00	n.a.	bMB
67	31.42	n.a.	0.489	0.063	0.00	n.a.	BMB
68	31.96	n.a.	9.958	5.656	0.15	n.a.	BM
69	32.25	n.a.	1.894	0.341	0.01	n.a.	Rd
70	32.70	n.a.	0.781	0.114	0.00	n.a.	MB
71	33.24	n.a.	0.547	0.091	0.00	n.a.	BMB
72	34.26	n.a.	0.423	0.059	0.00	n.a.	BMB
73	34.54	n.a.	1.191	0.072	0.00	n.a.	BM
74	34.56	n.a.	1.246	0.092	0.00	n.a.	M
75	34.69	n.a.	1.264	0.297	0.01	n.a.	MB
76	35.61	n.a.	8.555	2.701	0.07	n.a.	BMB
77	36.31	n.a.	0.789	0.111	0.00	n.a.	BMB
78	36.88	n.a.	11.524	2.870	0.08	n.a.	BMb
79	37.42	n.a.	0.503	0.050	0.00	n.a.	bMB

No.	Ret.Time	Peak Name	Height	Area	Rel.Area	Amount	Type
	Min		mAU	mAU*min	%	n.a.	
80	37.67	n.a.	1.153	0.175	0.00	n.a.	BMB
81	38.11	n.a.	0.988	0.189	0.01	n.a.	BMB
82	40.64	n.a.	27.079	100.466	2.72	n.a.	BMB
Total:			6105.625	3691.382	100.00	0.000	

3.1.2 HPLC analysis of pentapeptide crosslinked at pH 5

	Injection Volume:	**70.0**
RA2	*Channel:*	**UV_VIS_1**
unknown	*Wavelength:*	**214**
	Bandwidth:	**8**
default	*Dilution Factor:*	**1.0000**
22/10/2009 14:36	*Sample Weight:*	**1.0000**
55.00	*Sample Amount:*	**1.0000**

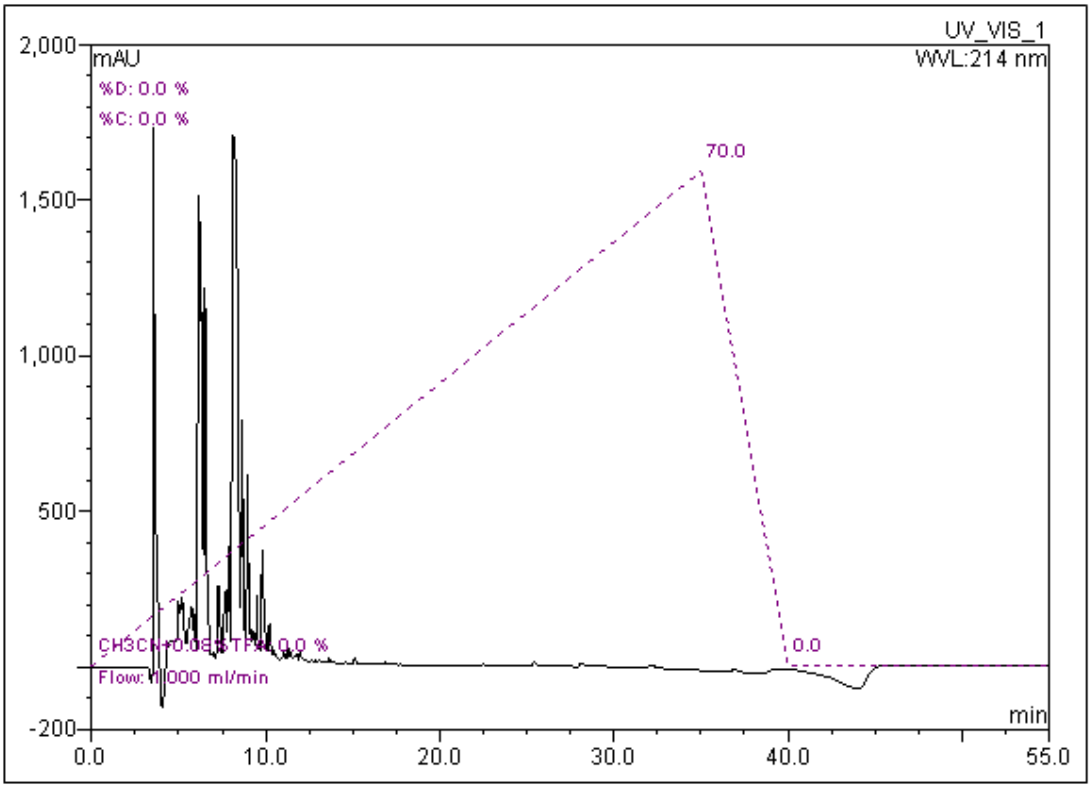

Ret.Time	Peak Name	Height	Area	Rel.Area	Amount	Type
min		mAU	mAU*min	%	n.a.	
0.66	n.a.	0.062	0.004	0.00	n.a.	BMB
1.30	n.a.	0.043	0.003	0.00	n.a.	BMB
1.79	n.a.	0.067	0.002	0.00	n.a.	BMB
3.21	n.a.	43.842	30.556	1.01	n.a.	BMb
3.57	n.a.	1807.256	233.329	7.73	n.a.	bMB
4.38	n.a.	118.810	52.724	1.75	n.a.	Ru
4.97	n.a.	327.463	139.824	4.63	n.a.	BM
5.18	n.a.	336.733	92.855	3.08	n.a.	M
5.74	n.a.	299.902	105.700	3.50	n.a.	M
5.92	n.a.	268.705	33.406	1.11	n.a.	M
6.15	n.a.	1613.014	425.782	14.10	n.a.	M
6.34	n.a.	253.453	16.168	0.54	n.a.	Rd
6.48	n.a.	1316.002	248.202	8.22	n.a.	M
6.87	n.a.	1.512	0.057	0.00	n.a.	Ru
6.99	n.a.	134.216	29.812	0.99	n.a.	M
7.28	n.a.	345.877	84.378	2.79	n.a.	M
7.68	n.a.	320.887	62.445	2.07	n.a.	M
7.85	n.a.	462.518	62.236	2.06	n.a.	M
8.09	n.a.	1780.241	682.337	22.60	n.a.	M
8.63	n.a.	854.688	134.572	4.46	n.a.	M
8.96	n.a.	679.220	109.062	3.61	n.a.	M
9.14	n.a.	25.633	1.424	0.05	n.a.	Rd
9.25	n.a.	6.830	0.258	0.01	n.a.	Ru
9.33	n.a.	168.540	29.670	0.98	n.a.	M
9.48	n.a.	282.674	42.258	1.40	n.a.	M
9.63	n.a.	3.752	0.140	0.00	n.a.	Rd
9.81	n.a.	422.831	92.493	3.06	n.a.	M
9.98	n.a.	15.182	0.747	0.02	n.a.	Rd
10.21	n.a.	180.560	58.737	1.95	n.a.	M
10.47	n.a.	17.077	2.047	0.07	n.a.	Rd
10.90	n.a.	2.476	0.185	0.01	n.a.	Ru
11.05	n.a.	80.209	24.528	0.81	n.a.	M
11.28	n.a.	89.026	24.522	0.81	n.a.	M
11.45	n.a.	14.382	1.026	0.03	n.a.	Rd
11.64	n.a.	7.780	0.704	0.02	n.a.	Ru
11.77	n.a.	58.465	16.845	0.56	n.a.	M
11.96	n.a.	74.351	22.799	0.76	n.a.	M

Ret.Time	Peak Name	Height	Area	Rel.Area	Amount	Type
min		mAU	mAU*min	%	n.a.	
12.12	n.a.	2.407	0.144	0.00	n.a.	Rd
12.33	n.a.	2.052	0.105	0.00	n.a.	Rd
12.45	n.a.	31.294	10.573	0.35	n.a.	M
12.62	n.a.	2.890	0.395	0.01	n.a.	Rd
12.87	n.a.	27.941	4.336	0.14	n.a.	M
13.06	n.a.	23.696	6.489	0.21	n.a.	M
13.26	n.a.	0.587	0.037	0.00	n.a.	Rd
13.46	n.a.	1.187	0.113	0.00	n.a.	Ru
13.64	n.a.	23.932	6.765	0.22	n.a.	Mb
13.89	n.a.	0.759	0.064	0.00	n.a.	Rd
14.29	n.a.	1.402	0.227	0.01	n.a.	bMB
14.59	n.a.	2.446	0.363	0.01	n.a.	BMB
15.12	n.a.	20.855	2.833	0.09	n.a.	BMB
15.62	n.a.	0.151	0.006	0.00	n.a.	Ru
15.76	n.a.	2.116	0.289	0.01	n.a.	BMB
16.01	n.a.	0.409	0.051	0.00	n.a.	BMB
16.28	n.a.	1.016	0.163	0.01	n.a.	BMb
16.69	n.a.	0.603	0.059	0.00	n.a.	bM
16.84	n.a.	5.945	0.847	0.03	n.a.	MB
17.22	n.a.	0.251	0.023	0.00	n.a.	BM
17.25	n.a.	0.308	0.018	0.00	n.a.	MB
17.63	n.a.	0.048	0.002	0.00	n.a.	Ru
17.74	n.a.	0.061	0.002	0.00	n.a.	Ru
17.80	n.a.	0.324	0.107	0.00	n.a.	BMB
18.54	n.a.	0.475	0.064	0.00	n.a.	BM
18.70	n.a.	0.771	0.150	0.00	n.a.	MB
19.33	n.a.	0.339	0.041	0.00	n.a.	BMB
19.54	n.a.	0.320	0.039	0.00	n.a.	BMB
20.03	n.a.	0.254	0.033	0.00	n.a.	BMB
20.22	n.a.	0.250	0.032	0.00	n.a.	BMB
20.67	n.a.	1.303	0.147	0.00	n.a.	BMB
20.84	n.a.	0.030	0.001	0.00	n.a.	BMB
20.89	n.a.	0.153	0.013	0.00	n.a.	bMB
21.16	n.a.	0.205	0.026	0.00	n.a.	BMB
21.27	n.a.	0.031	0.000	0.00	n.a.	BMB
21.38	n.a.	1.687	0.259	0.01	n.a.	BMB
21.79	n.a.	0.160	0.016	0.00	n.a.	BMB

Ret.Time	Peak Name	Height	Area	Rel.Area	Amount	Type
min		mAU	mAU*min	%	n.a.	
21.99	n.a.	0.043	0.002	0.00	n.a.	BMb
22.04	n.a.	0.062	0.002	0.00	n.a.	bMB
22.50	n.a.	6.584	1.023	0.03	n.a.	BMB
22.94	n.a.	1.552	0.258	0.01	n.a.	BMB
23.60	n.a.	0.232	0.030	0.00	n.a.	BMB
23.96	n.a.	0.294	0.034	0.00	n.a.	BMB
24.19	n.a.	0.071	0.002	0.00	n.a.	Ru
24.40	n.a.	2.115	0.500	0.02	n.a.	BMB
25.41	n.a.	12.151	2.596	0.09	n.a.	BMB
26.16	n.a.	0.208	0.016	0.00	n.a.	BMB
26.49	n.a.	0.365	0.065	0.00	n.a.	BMb
26.81	n.a.	0.134	0.011	0.00	n.a.	Ru
27.54	n.a.	2.840	1.261	0.04	n.a.	bMB
28.06	n.a.	8.666	5.525	0.18	n.a.	BMB
28.23	n.a.	0.725	0.078	0.00	n.a.	Rd
29.48	n.a.	0.904	0.137	0.00	n.a.	Rd
30.73	n.a.	0.688	0.086	0.00	n.a.	BMB
31.27	n.a.	0.188	0.014	0.00	n.a.	BM
31.48	n.a.	0.801	0.109	0.00	n.a.	Ru
31.75	n.a.	1.700	0.259	0.01	n.a.	Ru
32.17	n.a.	10.729	5.822	0.19	n.a.	MB
33.23	n.a.	0.534	0.087	0.00	n.a.	BMB
34.31	n.a.	0.359	0.048	0.00	n.a.	BMB
34.55	n.a.	0.931	0.126	0.00	n.a.	BM
34.69	n.a.	1.112	0.171	0.01	n.a.	MB
36.34	n.a.	0.917	0.185	0.01	n.a.	BMB
36.89	n.a.	9.783	2.811	0.09	n.a.	BMB
37.68	n.a.	1.081	0.164	0.01	n.a.	BMB
38.10	n.a.	0.741	0.125	0.00	n.a.	BMB
40.55	n.a.	27.163	101.063	3.35	n.a.	BMB
			3019.282	100.00	0.000	

3.1.3 HPLC analysis of pentapeptide crosslinked at pH 6

	Injection Volume:	**70.0**
RA3	*Channel:*	**UV_VIS_1**
unknown	*Wavelength:*	**214**
	Bandwidth:	**8**
default	*Dilution Factor:*	**1.0000**
22/10/2009 15:32	*Sample Weight:*	**1.0000**
55.00	*Sample Amount:*	**1.0000**

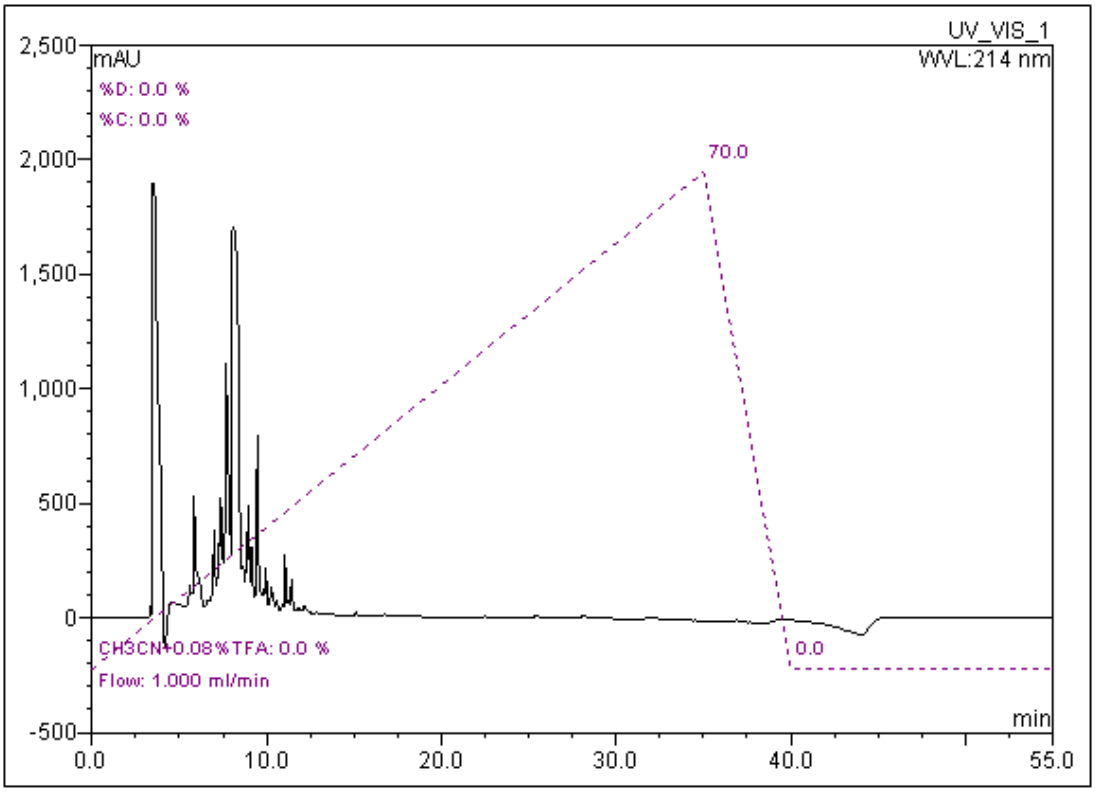

No.	Ret.Time	Peak Name	Height	Area	Rel.Area	Amount	Type
	min		mAU	mAU*min	%	n.a.	
1	0.16	n.a.	0.070	0.005	0.00	n.a.	BMB
2	0.50	n.a.	0.058	0.007	0.00	n.a.	BMB
3	0.91	n.a.	0.040	0.003	0.00	n.a.	BMB
4	1.44	n.a.	0.080	0.005	0.00	n.a.	BMB
5	3.15	n.a.	0.043	0.002	0.00	n.a.	BMB
6	3.33	n.a.	68.209	6.748	0.17	n.a.	BM
7	3.56	n.a.	1947.156	792.285	20.31	n.a.	MB
8	4.55	n.a.	193.974	187.814	4.81	n.a.	BM
9	5.58	n.a.	62.187	6.130	0.16	n.a.	Ru

No.	Ret.Time	Peak Name	Height	Area	Rel.Area	Amount	Type
	min		mAU	mAU*min	%	n.a.	
10	5.83	n.a.	646.215	286.682	7.35	n.a.	M
11	6.63	n.a.	13.107	0.960	0.02	n.a.	Ru
12	6.98	n.a.	493.248	157.847	4.05	n.a.	M
13	7.24	n.a.	72.728	5.116	0.13	n.a.	Ru
14	7.37	n.a.	627.022	173.825	4.46	n.a.	M
15	7.67	n.a.	1210.328	289.686	7.42	n.a.	M
16	7.89	n.a.	91.864	4.156	0.11	n.a.	Rd
17	8.08	n.a.	1802.901	865.135	22.17	n.a.	M
18	8.67	n.a.	43.272	4.346	0.11	n.a.	Rd
19	8.81	n.a.	31.756	1.535	0.04	n.a.	Ru
20	8.93	n.a.	581.026	110.785	2.84	n.a.	M
21	9.12	n.a.	400.605	71.479	1.83	n.a.	M
22	9.46	n.a.	883.234	146.678	3.76	n.a.	M
23	9.83	n.a.	28.029	1.485	0.04	n.a.	Ru
24	9.94	n.a.	297.140	66.702	1.71	n.a.	M
25	10.27	n.a.	213.840	93.457	2.40	n.a.	M
26	10.59	n.a.	34.999	3.856	0.10	n.a.	Rd
27	10.89	n.a.	16.229	1.572	0.04	n.a.	Ru
28	11.04	n.a.	347.567	86.851	2.23	n.a.	M
29	11.21	n.a.	14.867	1.196	0.03	n.a.	Rd
30	11.42	n.a.	236.274	45.037	1.15	n.a.	M
31	11.66	n.a.	4.423	0.207	0.01	n.a.	Ru
32	11.83	n.a.	112.745	41.686	1.07	n.a.	M
33	11.97	n.a.	1.709	0.088	0.00	n.a.	Rd
34	12.15	n.a.	113.191	116.336	2.98	n.a.	M
35	12.48	n.a.	4.026	0.283	0.01	n.a.	Rd
36	12.59	n.a.	1.250	0.057	0.00	n.a.	Rd
37	12.73	n.a.	2.423	0.168	0.00	n.a.	Rd
38	12.87	n.a.	12.565	1.211	0.03	n.a.	Rd
39	13.12	n.a.	1.097	0.067	0.00	n.a.	Rd
40	13.28	n.a.	1.148	0.109	0.00	n.a.	Rd
41	13.66	n.a.	70.727	110.850	2.84	n.a.	M
42	13.86	n.a.	1.103	0.081	0.00	n.a.	Rd
43	14.09	n.a.	0.445	0.079	0.00	n.a.	Rd
44	14.52	n.a.	0.355	0.031	0.00	n.a.	Rd
45	14.69	n.a.	0.240	0.016	0.00	n.a.	Rd
46	15.11	n.a.	13.656	1.953	0.05	n.a.	Rd

No.	Ret.Time	Peak Name	Height	Area	Rel.Area	Amount	Type
	min		mAU	mAU*min	%	n.a.	
47	15.51	n.a.	0.375	0.059	0.00	n.a.	Rd
48	15.61	n.a.	40.905	75.171	1.93	n.a.	M
49	15.99	n.a.	0.622	0.078	0.00	n.a.	Rd
50	16.50	n.a.	0.198	0.019	0.00	n.a.	Rd
51	16.76	n.a.	7.487	1.511	0.04	n.a.	Rd
52	17.13	n.a.	0.258	0.031	0.00	n.a.	Rd
53	17.62	n.a.	0.455	0.071	0.00	n.a.	Rd
54	17.92	n.a.	0.516	0.069	0.00	n.a.	Rd
55	18.18	n.a.	0.242	0.031	0.00	n.a.	Rd
56	18.47	n.a.	0.127	0.012	0.00	n.a.	Ru
57	18.67	n.a.	12.987	10.124	0.26	n.a.	MB
58	19.45	n.a.	0.338	0.104	0.00	n.a.	Rd
59	19.95	n.a.	0.202	0.026	0.00	n.a.	bMB
60	20.09	n.a.	0.032	0.001	0.00	n.a.	BMB
61	20.67	n.a.	0.241	0.030	0.00	n.a.	BMB
62	20.87	n.a.	0.101	0.009	0.00	n.a.	BMB
63	21.06	n.a.	0.029	0.001	0.00	n.a.	BMB
64	21.36	n.a.	1.003	0.173	0.00	n.a.	BMB
65	21.68	n.a.	0.036	0.001	0.00	n.a.	BMB
66	21.93	n.a.	0.049	0.005	0.00	n.a.	BMB
67	22.14	n.a.	0.095	0.005	0.00	n.a.	BMb
68	22.23	n.a.	0.021	0.000	0.00	n.a.	bMB
69	22.50	n.a.	7.974	1.264	0.03	n.a.	BM
70	22.94	n.a.	2.396	0.430	0.01	n.a.	MB
71	23.74	n.a.	0.075	0.005	0.00	n.a.	Ru
72	23.95	n.a.	0.551	0.088	0.00	n.a.	BM
73	24.15	n.a.	0.155	0.014	0.00	n.a.	M
74	24.40	n.a.	0.308	0.045	0.00	n.a.	MB
75	24.44	n.a.	0.056	0.001	0.00	n.a.	Rd
76	24.68	n.a.	0.147	0.018	0.00	n.a.	BMB
77	24.79	n.a.	0.036	0.001	0.00	n.a.	BMB
78	25.41	n.a.	12.049	2.482	0.06	n.a.	BM
79	25.81	n.a.	0.038	0.001	0.00	n.a.	Ru
80	25.87	n.a.	0.691	0.118	0.00	n.a.	Mb
81	26.17	n.a.	0.220	0.023	0.00	n.a.	bMB
82	26.52	n.a.	1.160	0.226	0.01	n.a.	BMB
83	27.16	n.a.	0.255	0.037	0.00	n.a.	Ru

No.	Ret.Time	Peak Name	Height	Area	Rel.Area	Amount	Type
	min		mAU	mAU*min	%	n.a.	
84	27.53	n.a.	2.664	1.075	0.03	n.a.	BMB
85	27.82	n.a.	0.008	0.000	0.00	n.a.	BMB
86	27.85	n.a.	0.010	0.000	0.00	n.a.	BMB
87	27.89	n.a.	0.102	0.003	0.00	n.a.	BM
88	28.06	n.a.	8.848	6.285	0.16	n.a.	Mb
89	28.22	n.a.	1.253	0.146	0.00	n.a.	Rd
90	29.50	n.a.	1.330	0.253	0.01	n.a.	Rd
91	30.07	n.a.	0.048	0.001	0.00	n.a.	bMb
92	30.12	n.a.	0.070	0.002	0.00	n.a.	bMB
93	30.74	n.a.	0.768	0.091	0.00	n.a.	BMb
94	30.89	n.a.	0.076	0.002	0.00	n.a.	bMB
95	30.93	n.a.	0.036	0.002	0.00	n.a.	BMB
96	31.49	n.a.	0.814	0.111	0.00	n.a.	Ru
97	31.74	n.a.	1.673	0.249	0.01	n.a.	Ru
98	32.18	n.a.	10.948	5.998	0.15	n.a.	BMB
99	33.25	n.a.	0.516	0.091	0.00	n.a.	BMB
100	34.29	n.a.	0.275	0.030	0.00	n.a.	BMb
101	34.56	n.a.	0.829	0.102	0.00	n.a.	bM
102	34.70	n.a.	1.071	0.182	0.00	n.a.	MB
103	36.33	n.a.	0.943	0.184	0.00	n.a.	BMB
104	36.89	n.a.	9.870	2.819	0.07	n.a.	BMB
105	37.69	n.a.	1.199	0.190	0.00	n.a.	BMB
106	38.13	n.a.	0.638	0.097	0.00	n.a.	BMB
107	40.63	n.a.	28.330	106.886	2.74	n.a.	BMB
Total:				3901.697	100.00	0.000	

3.1.4 HPLC analysis of pentapeptide crosslinked at pH 7

	Injection Volume:	**70.0**
RA4	*Channel:*	**UV_VIS_1**
unknown	*Wavelength:*	**214**
	Bandwidth:	**8**
default	*Dilution Factor:*	**1.0000**
22/10/2009 16:28	*Sample Weight:*	**1.0000**
42.00	*Sample Amount:*	**1.0000**

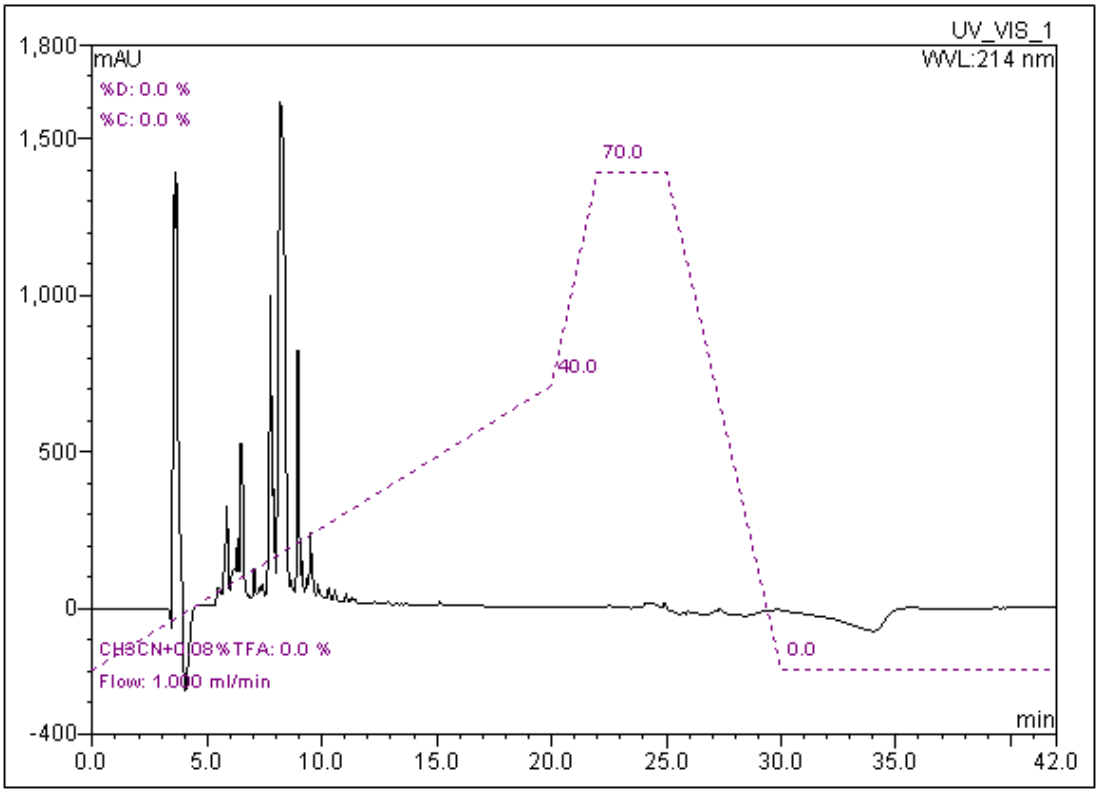

No.	Ret.Time	Peak Name	Height	Area	Rel.Area	Amount	Type
	min		mAU	mAU*min	%	n.a.	
1	0.04	n.a.	0.081	0.009	0.00	n.a.	BMB
2	0.11	n.a.	0.016	0.001	0.00	n.a.	Rd
3	1.49	n.a.	0.063	0.008	0.00	n.a.	BMB
4	2.02	n.a.	0.063	0.004	0.00	n.a.	BMB
5	2.63	n.a.	0.055	0.003	0.00	n.a.	BMB
6	2.81	n.a.	0.043	0.004	0.00	n.a.	BMb
7	3.33	n.a.	41.286	11.494	0.30	n.a.	bMb
8	3.52	n.a.	1280.887	66.264	1.73	n.a.	bM
9	3.59	n.a.	1504.786	124.425	3.25	n.a.	M
10	3.67	n.a.	1496.501	215.756	5.63	n.a.	MB
11	5.46	n.a.	42.692	7.014	0.18	n.a.	Ru
12	5.73	n.a.	24.323	0.969	0.03	n.a.	Ru
13	5.85	n.a.	558.628	504.388	13.17	n.a.	BM
14	6.09	n.a.	36.950	5.831	0.15	n.a.	Ru
15	6.32	n.a.	451.607	135.400	3.54	n.a.	M
16	6.47	n.a.	749.017	217.214	5.67	n.a.	M
17	7.04	n.a.	340.554	76.417	2.00	n.a.	M
18	7.29	n.a.	15.306	1.034	0.03	n.a.	Ru

No.	Ret.Time	Peak Name	Height	Area	Rel.Area	Amount	Type
	min		mAU	mAU*min	%	n.a.	
19	7.40	n.a.	286.805	87.469	2.28	n.a.	M
20	7.75	n.a.	1198.954	258.331	6.75	n.a.	M
21	7.90	n.a.	102.064	6.265	0.16	n.a.	Rd
22	8.06	n.a.	111.238	4.565	0.12	n.a.	Ru
23	8.17	n.a.	1812.875	680.349	17.77	n.a.	M
24	8.65	n.a.	26.636	1.796	0.05	n.a.	Rd
25	8.80	n.a.	2.525	0.090	0.00	n.a.	Rd
26	8.95	n.a.	1008.612	174.738	4.56	n.a.	M
27	9.13	n.a.	65.174	3.934	0.10	n.a.	Rd
28	9.34	n.a.	30.344	3.022	0.08	n.a.	Ru
29	9.49	n.a.	409.774	203.037	5.30	n.a.	M
30	9.83	n.a.	38.332	3.624	0.09	n.a.	Rd
31	10.11	n.a.	0.136	0.004	0.00	n.a.	Ru
32	10.28	n.a.	223.791	138.265	3.61	n.a.	M
33	10.55	n.a.	35.031	3.107	0.08	n.a.	Rd
34	10.89	n.a.	2.052	0.111	0.00	n.a.	Ru
35	11.04	n.a.	192.038	57.792	1.51	n.a.	M
36	11.28	n.a.	174.382	137.112	3.58	n.a.	M
37	11.44	n.a.	8.344	0.731	0.02	n.a.	Rd
38	11.60	n.a.	1.446	0.078	0.00	n.a.	Rd
39	11.85	n.a.	4.081	0.633	0.02	n.a.	Rd
40	12.25	n.a.	144.040	71.151	1.86	n.a.	M
41	12.48	n.a.	1.174	0.074	0.00	n.a.	Rd
42	12.62	n.a.	0.338	0.044	0.00	n.a.	Ru
43	12.87	n.a.	132.136	64.754	1.69	n.a.	M
44	13.06	n.a.	121.617	37.203	0.97	n.a.	M
45	13.14	n.a.	0.553	0.038	0.00	n.a.	Rd
46	13.37	n.a.	116.546	51.648	1.35	n.a.	M
47	13.44	n.a.	1.232	0.094	0.00	n.a.	Rd
48	13.83	n.a.	107.885	111.129	2.90	n.a.	M
49	14.12	n.a.	0.210	0.020	0.00	n.a.	Rd
50	14.32	n.a.	1.509	0.273	0.01	n.a.	Rd
51	14.76	n.a.	0.989	0.209	0.01	n.a.	Rd
52	15.11	n.a.	95.591	112.898	2.95	n.a.	M
53	15.44	n.a.	0.983	0.117	0.00	n.a.	Rd
54	15.76	n.a.	1.420	0.227	0.01	n.a.	Rd
55	16.08	n.a.	0.604	0.132	0.00	n.a.	Rd

No.	Ret.Time	Peak Name	Height	Area	Rel.Area	Amount	Type
	min		mAU	mAU*min	%	n.a.	
56	16.55	n.a.	0.032	0.001	0.00	n.a.	Ru
57	16.74	n.a.	58.405	93.670	2.45	n.a.	MB
58	17.25	n.a.	0.124	0.008	0.00	n.a.	Rd
59	17.79	n.a.	0.027	0.001	0.00	n.a.	Rd
60	18.07	n.a.	0.308	0.033	0.00	n.a.	Rd
61	18.34	n.a.	0.103	0.010	0.00	n.a.	Rd
62	18.68	n.a.	0.929	0.119	0.00	n.a.	Rd
63	18.87	n.a.	0.272	0.022	0.00	n.a.	Rd
64	19.15	n.a.	0.428	0.057	0.00	n.a.	Rd
65	19.44	n.a.	0.234	0.038	0.00	n.a.	Rd
66	19.86	n.a.	0.265	0.031	0.00	n.a.	bMB
67	20.08	n.a.	0.089	0.003	0.00	n.a.	BMB
68	20.34	n.a.	0.165	0.018	0.00	n.a.	BMB
69	20.92	n.a.	0.036	0.001	0.00	n.a.	BMB
70	21.38	n.a.	0.525	0.090	0.00	n.a.	BMB
71	21.67	n.a.	0.140	0.012	0.00	n.a.	BMB
72	22.28	n.a.	0.057	0.002	0.00	n.a.	BMB
73	22.50	n.a.	8.068	1.208	0.03	n.a.	BMB
74	22.93	n.a.	2.243	0.384	0.01	n.a.	BMB
75	23.71	n.a.	3.952	0.837	0.02	n.a.	BM
76	24.30	n.a.	24.088	19.836	0.52	n.a.	M
77	24.93	n.a.	32.201	7.360	0.19	n.a.	MB
78	25.74	n.a.	7.744	0.660	0.02	n.a.	BMB
79	25.96	n.a.	8.274	1.338	0.03	n.a.	BM
80	26.14	n.a.	7.593	2.562	0.07	n.a.	M
81	27.08	n.a.	3.157	0.340	0.01	n.a.	Ru
82	27.34	n.a.	19.955	7.925	0.21	n.a.	MB
83	28.05	n.a.	1.654	0.267	0.01	n.a.	BMB
84	29.85	n.a.	32.601	111.121	2.90	n.a.	BMB
Total:				3829.251	100.00	0.000	

3.1.5 HPLC analysis of pentapeptide crosslinked at pH 8

	Injection Volume:	**70.0**
RA5	*Channel:*	**UV_VIS_1**
unknown	*Wavelength:*	**214**
	Bandwidth:	**8**
default	*Dilution Factor:*	**1.0000**
22/10/2009 17:11	*Sample Weight:*	**1.0000**
42.00	*Sample Amount:*	**1.0000**

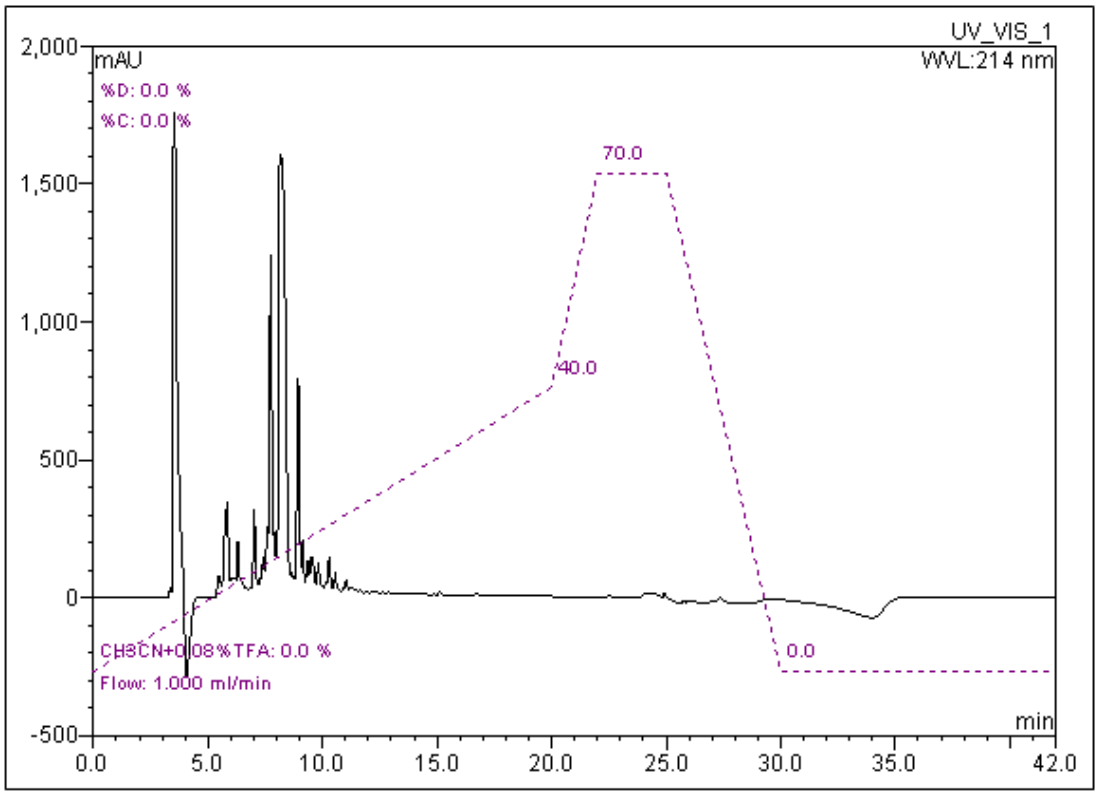

No.	Ret.Time	Peak Name	Height	Area	Rel.Area	Amount	Type
	min		mAU	mAU*min	%	n.a.	
1	0.57	n.a.	0.038	0.003	0.00	n.a.	BM
2	0.71	n.a.	0.045	0.003	0.00	n.a.	MB
3	1.41	n.a.	0.086	0.008	0.00	n.a.	BMB
4	3.35	n.a.	19.928	1.574	0.02	n.a.	Ru
5	3.52	n.a.	1989.612	722.446	9.90	n.a.	BMB
6	5.48	n.a.	54.246	7.454	0.10	n.a.	Ru
7	5.83	n.a.	630.484	574.659	7.87	n.a.	BM
8	6.01	n.a.	4.085	0.188	0.00	n.a.	Ru
9	6.14	n.a.	348.412	91.505	1.25	n.a.	M
10	6.30	n.a.	484.449	178.761	2.45	n.a.	M

No.	Ret.Time	Peak Name	Height	Area	Rel.Area	Amount	Type
	min		mAU	mAU*min	%	n.a.	
11	6.82	n.a.	5.749	0.347	0.00	n.a.	Ru
12	7.01	n.a.	282.576	28.996	0.40	n.a.	Ru
13	7.29	n.a.	12.066	0.604	0.01	n.a.	Ru
14	7.40	n.a.	63.480	4.153	0.06	n.a.	Ru
15	7.61	n.a.	63.048	5.803	0.08	n.a.	Ru
16	7.73	n.a.	1513.864	558.545	7.65	n.a.	M
17	7.89	n.a.	29.980	1.540	0.02	n.a.	Rd
18	8.17	n.a.	1871.460	730.693	10.01	n.a.	M
19	8.64	n.a.	16.720	0.907	0.01	n.a.	Rd
20	8.77	n.a.	8.460	0.416	0.01	n.a.	Ru
21	8.94	n.a.	1056.555	260.730	3.57	n.a.	M
22	9.12	n.a.	118.863	8.410	0.12	n.a.	Rd
23	9.35	n.a.	63.580	6.442	0.09	n.a.	Ru
24	9.50	n.a.	401.473	167.325	2.29	n.a.	M
25	9.53	n.a.	3.019	0.217	0.00	n.a.	Rd
26	9.81	n.a.	379.146	105.540	1.45	n.a.	M
27	10.16	n.a.	11.720	0.710	0.01	n.a.	Ru
28	10.29	n.a.	396.825	225.395	3.09	n.a.	M
29	10.55	n.a.	61.991	5.696	0.08	n.a.	Rd
30	10.89	n.a.	3.030	0.172	0.00	n.a.	Ru
31	11.04	n.a.	309.992	262.714	3.60	n.a.	M
32	11.27	n.a.	12.638	1.227	0.02	n.a.	Rd
33	11.45	n.a.	6.094	0.482	0.01	n.a.	Rd
34	11.60	n.a.	6.999	0.631	0.01	n.a.	Rd
35	11.85	n.a.	1.057	0.059	0.00	n.a.	Ru
36	11.93	n.a.	258.672	70.273	0.96	n.a.	M
37	12.13	n.a.	0.866	0.065	0.00	n.a.	Ru
38	12.25	n.a.	254.046	281.906	3.86	n.a.	M
39	12.33	n.a.	1.283	0.086	0.00	n.a.	Rd
40	12.48	n.a.	0.896	0.051	0.00	n.a.	Rd
41	12.61	n.a.	3.500	0.294	0.00	n.a.	Rd
42	12.89	n.a.	5.192	0.757	0.01	n.a.	Rd
43	13.29	n.a.	1.057	0.084	0.00	n.a.	Ru
44	13.44	n.a.	241.396	731.066	10.02	n.a.	M
45	13.67	n.a.	3.989	0.618	0.01	n.a.	Rd
46	14.12	n.a.	0.323	0.037	0.00	n.a.	Rd
47	14.29	n.a.	1.439	0.121	0.00	n.a.	Rd

No.	Ret.Time	Peak Name	Height	Area	Rel.Area	Amount	Type
	min		mAU	mAU*min	%	n.a.	
48	14.48	n.a.	0.751	0.095	0.00	n.a.	Rd
49	14.87	n.a.	1.191	0.166	0.00	n.a.	Rd
50	15.11	n.a.	10.503	1.368	0.02	n.a.	Rd
51	15.44	n.a.	0.403	0.055	0.00	n.a.	Rd
52	15.77	n.a.	0.870	0.119	0.00	n.a.	Rd
53	16.24	n.a.	0.421	0.054	0.00	n.a.	Rd
54	16.50	n.a.	0.138	0.010	0.00	n.a.	Ru
55	16.74	n.a.	212.987	392.166	5.37	n.a.	M
56	17.10	n.a.	0.067	0.003	0.00	n.a.	Rd
57	17.29	n.a.	0.116	0.022	0.00	n.a.	Rd
58	17.65	n.a.	0.335	0.050	0.00	n.a.	Rd
59	17.92	n.a.	0.228	0.030	0.00	n.a.	Rd
60	18.06	n.a.	0.083	0.004	0.00	n.a.	Rd
61	18.48	n.a.	0.154	0.016	0.00	n.a.	Ru
62	18.69	n.a.	192.747	922.214	12.64	n.a.	M
63	19.14	n.a.	0.252	0.048	0.00	n.a.	Rd
64	19.49	n.a.	0.071	0.004	0.00	n.a.	Rd
65	19.67	n.a.	0.159	0.016	0.00	n.a.	Rd
66	19.96	n.a.	0.223	0.029	0.00	n.a.	Rd
67	20.93	n.a.	0.188	0.029	0.00	n.a.	Rd
68	21.36	n.a.	0.550	0.123	0.00	n.a.	Rd
69	21.75	n.a.	0.154	0.013	0.00	n.a.	Rd
70	21.87	n.a.	0.115	0.024	0.00	n.a.	Rd
71	22.13	n.a.	0.203	0.018	0.00	n.a.	Rd
72	22.51	n.a.	3.864	0.580	0.01	n.a.	Rd
73	22.94	n.a.	2.236	0.400	0.01	n.a.	Rd
74	23.59	n.a.	0.149	0.019	0.00	n.a.	Rd
75	24.22	n.a.	161.965	274.508	3.76	n.a.	M
76	24.93	n.a.	16.619	2.061	0.03	n.a.	Rd
77	25.75	n.a.	8.155	0.668	0.01	n.a.	Ru
78	25.94	n.a.	122.530	53.072	0.73	n.a.	M
79	26.14	n.a.	118.514	67.338	0.92	n.a.	M
80	27.10	n.a.	3.563	0.444	0.01	n.a.	Ru
81	27.34	n.a.	120.247	130.333	1.79	n.a.	M
82	28.00	n.a.	97.226	55.445	0.76	n.a.	M
83	29.82	n.a.	99.393	357.577	4.90	n.a.	MB
Total:				7298.830	100.00	0.000	

3.2 Crosslinking of heptapeptide

3.2.1 HPLC analysis of native pentapeptide

Sample Name:		*Injection Volume:*	**100.0**
Vial Number:	**BA1**	*Channel:*	**UV_VIS_1**
Sample Type:	**unknown**	*Wavelength:*	**214**
Control Program:		*Bandwidth:*	**8**
Quantif. Method:	**Default**	*Dilution Factor:*	**1.0000**
Recording Time:	**16/12/2009 14:09**	*Sample Weight:*	**1.0000**
Run Time (min):	**45.00**	*Sample Amount:*	**1.0000**

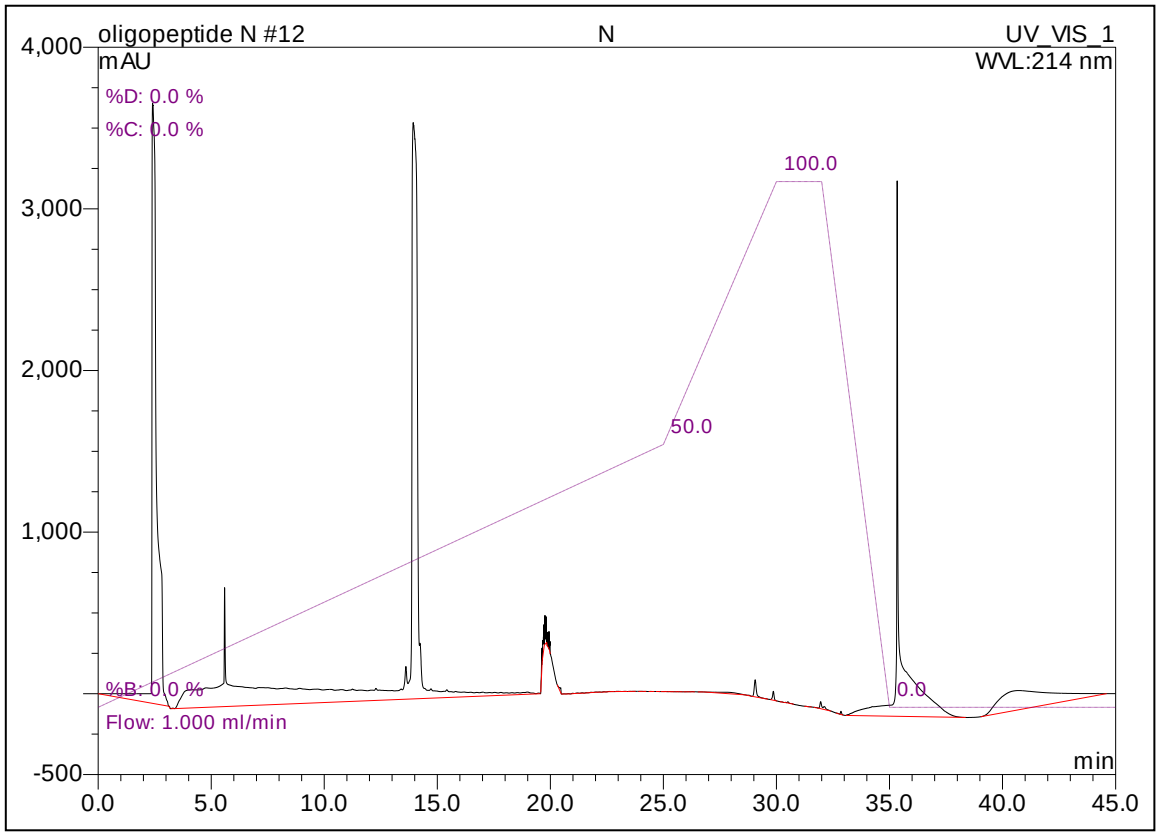

No.	Ret.Time	Peak Name	Height	Area	Rel.Area	Amount	Type
	min		mAU	mAU*min	%		
1	2.41	n.a.	3714.642	956.996	23.81	n.a.	BMb
2	3.15	n.a.	5.414	0.211	0.01	n.a.	bMB
3	3.31	n.a.	2.951	0.291	0.01	n.a.	BMB
4	5.59	n.a.	735.903	416.478	10.36	n.a.	BM
5	7.13	n.a.	108.663	352.887	8.78	n.a.	M
6	7.30	n.a.	0.489	0.042	0.00	n.a.	Rd
7	7.50	n.a.	1.689	0.257	0.01	n.a.	Rd

No.	Ret.Time	Peak Name	Height	Area	Rel.Area	Amount	Type
	min		mAU	mAU*min	%		
8	8.29	n.a.	6.416	2.236	0.06	n.a.	Rd
9	8.91	n.a.	6.083	1.637	0.04	n.a.	Rd
10	9.71	n.a.	4.311	1.459	0.04	n.a.	Rd
11	10.29	n.a.	4.850	1.445	0.04	n.a.	Rd
12	10.74	n.a.	5.004	1.314	0.03	n.a.	Rd
13	11.25	n.a.	75.737	62.100	1.55	n.a.	M
14	11.62	n.a.	2.582	0.644	0.02	n.a.	Rd
15	12.09	n.a.	2.020	0.336	0.01	n.a.	Ru
16	12.29	n.a.	74.419	73.399	1.83	n.a.	M
17	12.45	n.a.	1.297	0.092	0.00	n.a.	Rd
18	12.58	n.a.	0.468	0.036	0.00	n.a.	Rd
19	12.71	n.a.	0.427	0.024	0.00	n.a.	Rd
20	12.99	n.a.	1.650	0.139	0.00	n.a.	Rd
21	13.40	n.a.	63.873	20.081	0.50	n.a.	M
22	13.61	n.a.	202.356	28.190	0.70	n.a.	M
23	13.94	n.a.	3566.014	907.978	22.59	n.a.	M
24	14.23	n.a.	342.970	71.495	1.78	n.a.	M
25	14.72	n.a.	11.123	0.794	0.02	n.a.	Rd
26	14.87	n.a.	0.621	0.040	0.00	n.a.	Rd
27	15.29	n.a.	0.839	0.073	0.00	n.a.	Ru
28	15.42	n.a.	47.938	46.308	1.15	n.a.	M
29	15.60	n.a.	1.134	0.116	0.00	n.a.	Rd
30	15.81	n.a.	4.230	0.515	0.01	n.a.	Rd
31	16.18	n.a.	1.927	0.275	0.01	n.a.	Rd
32	16.48	n.a.	2.081	0.283	0.01	n.a.	Rd
33	16.74	n.a.	2.031	0.245	0.01	n.a.	Ru
34	17.01	n.a.	23.717	11.871	0.30	n.a.	M
35	17.32	n.a.	1.623	0.211	0.01	n.a.	Ru
36	17.54	n.a.	19.457	15.761	0.39	n.a.	M
37	17.81	n.a.	3.331	0.408	0.01	n.a.	Rd
38	18.06	n.a.	1.691	0.207	0.01	n.a.	Rd
39	18.30	n.a.	2.085	0.247	0.01	n.a.	Ru
40	18.55	n.a.	2.246	0.269	0.01	n.a.	Ru
41	18.81	n.a.	0.953	0.122	0.00	n.a.	Ru
42	18.99	n.a.	13.231	11.329	0.28	n.a.	M
43	19.21	n.a.	0.875	0.115	0.00	n.a.	Rd
44	19.48	n.a.	4.362	0.572	0.01	n.a.	MB

No.	Ret.Time	Peak Name	Height	Area	Rel.Area	Amount	Type
	min		mAU	mAU*min	%		
45	19.63	n.a.	107.324	3.578	0.09	n.a.	BMb
46	19.71	n.a.	152.211	6.744	0.17	n.a.	bMb
47	19.76	n.a.	178.166	3.243	0.08	n.a.	bM
48	19.80	n.a.	123.494	1.804	0.04	n.a.	M
49	19.82	n.a.	162.023	2.336	0.06	n.a.	Mb
50	19.86	n.a.	78.519	1.172	0.03	n.a.	bMb
51	19.88	n.a.	86.483	3.275	0.08	n.a.	bMb
52	19.94	n.a.	107.184	1.250	0.03	n.a.	bMB
53	19.97	n.a.	59.748	1.415	0.04	n.a.	BMB
54	20.31	n.a.	0.101	1.881	0.05	n.a.	BMB
55	20.61	n.a.	1.003	0.104	0.00	n.a.	BMB
56	20.81	n.a.	1.828	0.183	0.00	n.a.	bMB
57	20.99	n.a.	2.549	0.241	0.01	n.a.	BMB
58	21.20	n.a.	2.429	0.276	0.01	n.a.	bMB
59	21.41	n.a.	2.566	0.261	0.01	n.a.	bMB
60	21.59	n.a.	1.531	0.145	0.00	n.a.	BMB
61	21.81	n.a.	2.229	0.238	0.01	n.a.	bMB
62	22.01	n.a.	1.576	0.173	0.00	n.a.	bMB
63	22.18	n.a.	1.095	0.085	0.00	n.a.	bMB
64	22.37	n.a.	2.093	0.217	0.01	n.a.	BMB
65	22.60	n.a.	1.819	0.212	0.01	n.a.	bMB
66	22.76	n.a.	0.352	0.029	0.00	n.a.	bMB
67	22.98	n.a.	1.940	0.301	0.01	n.a.	BMB
68	23.30	n.a.	1.236	0.137	0.00	n.a.	bMB
69	23.54	n.a.	0.517	0.048	0.00	n.a.	BMB
70	23.67	n.a.	0.242	0.023	0.00	n.a.	bMB
71	24.02	n.a.	0.391	0.038	0.00	n.a.	BMB
72	24.15	n.a.	0.138	0.010	0.00	n.a.	BMB
73	24.43	n.a.	0.444	0.046	0.00	n.a.	BMB
74	24.75	n.a.	0.332	0.032	0.00	n.a.	BMB
75	25.09	n.a.	0.702	0.095	0.00	n.a.	BMB
76	25.27	n.a.	0.444	0.074	0.00	n.a.	BMB
77	25.61	n.a.	0.315	0.030	0.00	n.a.	BMB
78	25.78	n.a.	0.216	0.018	0.00	n.a.	BMB
79	25.96	n.a.	0.173	0.012	0.00	n.a.	BMB
80	26.10	n.a.	0.143	0.012	0.00	n.a.	BMB
81	26.28	n.a.	0.990	0.096	0.00	n.a.	BMB

No.	Ret.Time	Peak Name	Height	Area	Rel.Area	Amount	Type
	min		mAU	mAU*min	%		
82	26.68	n.a.	0.602	0.087	0.00	n.a.	BMB
83	26.79	n.a.	0.027	8.251	0.21	n.a.	BMb
84	28.61	n.a.	0.044	0.353	0.01	n.a.	bMB
85	29.06	n.a.	106.009	11.395	0.28	n.a.	BMB
86	29.49	n.a.	0.010	0.075	0.00	n.a.	BMB
87	29.86	n.a.	55.336	4.340	0.11	n.a.	BMB
88	30.15	n.a.	0.001	0.085	0.00	n.a.	BMB
89	30.41	n.a.	2.092	0.100	0.00	n.a.	BMB
90	30.50	n.a.	7.659	0.476	0.01	n.a.	BMB
91	30.67	n.a.	1.759	0.141	0.00	n.a.	BMB
92	31.23	n.a.	0.001	0.079	0.00	n.a.	BMB
93	31.50	n.a.	0.881	0.038	0.00	n.a.	BMB
94	31.65	n.a.	0.006	0.027	0.00	n.a.	BMB
95	31.77	n.a.	1.406	0.073	0.00	n.a.	BMB
96	31.96	n.a.	43.481	3.691	0.09	n.a.	BM
97	32.11	n.a.	18.036	2.458	0.06	n.a.	MB
98	32.63	n.a.	0.009	0.063	0.00	n.a.	BMB
99	32.75	n.a.	2.525	0.104	0.00	n.a.	BMB
100	32.85	n.a.	20.258	1.143	0.03	n.a.	BMB
101	35.34	n.a.	3313.224	628.632	15.64	n.a.	BMB
102	40.71	n.a.	119.330	326.515	8.12	n.a.	BM
103	44.59	n.a.	0.335	11.288	0.28	n.a.	MB
Total:				4018.772	100.00	0.000	

3.2.2 HPLC analysis of BMDC

Sample Name:		*Injection Volume:*	**100.0**
Vial Number:	**BA1**	*Channel:*	**UV_VIS_1**
Sample Type:	**unknown**	*Wavelength:*	**214**
Control Program:		*Bandwidth:*	**8**
Quantif. Method:	**Default**	*Dilution Factor:*	**1.0000**
Recording Time:	**18/12/2009 10:21**	*Sample Weight:*	**1.0000**
Run Time (min):	**45.00**	*Sample Amount:*	**1.0000**

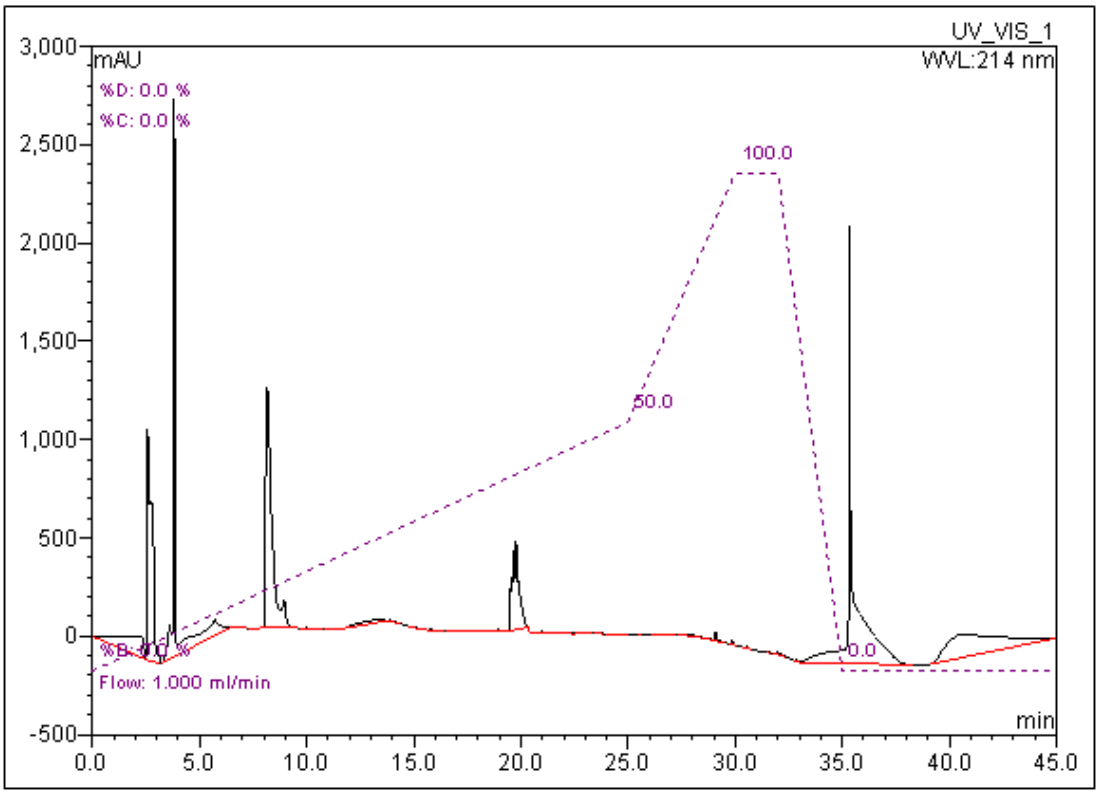

No.	Ret.Time	Peak Name	Height	Area	Rel.Area	Amount	Type
	min		mAU	mAU*min	%		
1	0.42	n.a.	20.294	135.923	5.94	n.a.	BMB
2	2.52	n.a.	498.046	15.490	0.68	n.a.	BM
3	2.58	n.a.	1179.124	229.860	10.05	n.a.	M
4	2.74	n.a.	209.946	50.471	2.21	n.a.	Rd
5	3.11	n.a.	47.167	1.901	0.08	n.a.	MB
6	3.60	n.a.	168.091	30.286	1.32	n.a.	BM
7	3.81	n.a.	2833.636	163.103	7.13	n.a.	M
8	5.74	n.a.	81.692	116.560	5.10	n.a.	MB
9	6.60	n.a.	4.149	0.864	0.04	n.a.	bMB
10	6.96	n.a.	3.483	0.517	0.02	n.a.	BMB
11	7.16	n.a.	0.951	0.053	0.00	n.a.	BMB
12	7.33	n.a.	0.001	0.037	0.00	n.a.	BMB
13	7.63	n.a.	2.875	0.337	0.01	n.a.	BMB
14	7.88	n.a.	1.643	0.230	0.01	n.a.	bMB
15	8.15	n.a.	1222.185	401.038	17.54	n.a.	bMb
16	8.94	n.a.	84.092	11.459	0.50	n.a.	Rd
17	9.54	n.a.	5.375	0.408	0.02	n.a.	bMB
18	9.95	n.a.	6.587	1.716	0.08	n.a.	BMB

No.	Ret.Time	Peak Name	Height	Area	Rel.Area	Amount	Type
	min		mAU	mAU*min	%		
19	10.56	n.a.	4.742	1.209	0.05	n.a.	BMB
20	10.98	n.a.	0.497	0.052	0.00	n.a.	BMb
21	11.09	n.a.	2.618	0.264	0.01	n.a.	bMB
22	11.49	n.a.	3.783	0.754	0.03	n.a.	BMB
23	12.46	n.a.	14.871	6.567	0.29	n.a.	BM
24	12.85	n.a.	19.474	6.694	0.29	n.a.	M
25	13.22	n.a.	18.183	6.084	0.27	n.a.	M
26	13.50	n.a.	15.225	3.729	0.16	n.a.	Mb
27	13.88	n.a.	6.226	0.890	0.04	n.a.	bMB
28	14.16	n.a.	3.814	0.685	0.03	n.a.	BMB
29	14.71	n.a.	0.001	0.431	0.02	n.a.	BMB
30	15.11	n.a.	2.154	0.320	0.01	n.a.	BMB
31	15.34	n.a.	4.704	0.996	0.04	n.a.	BMB
32	15.78	n.a.	3.340	0.447	0.02	n.a.	BMB
33	16.05	n.a.	1.247	0.156	0.01	n.a.	BMB
34	16.29	n.a.	1.758	0.245	0.01	n.a.	BMB
35	16.65	n.a.	3.372	0.486	0.02	n.a.	BMB
36	16.89	n.a.	1.399	0.160	0.01	n.a.	BMB
37	17.17	n.a.	4.595	0.667	0.03	n.a.	BMB
38	17.47	n.a.	2.641	0.385	0.02	n.a.	BMB
39	17.70	n.a.	2.879	0.325	0.01	n.a.	BMB
40	17.93	n.a.	1.700	0.203	0.01	n.a.	BMB
41	18.17	n.a.	2.802	0.329	0.01	n.a.	BMB
42	18.38	n.a.	0.425	0.038	0.00	n.a.	Ru
43	18.69	n.a.	3.847	0.856	0.04	n.a.	BM
44	18.94	n.a.	3.969	0.602	0.03	n.a.	Mb
45	19.12	n.a.	0.390	0.144	0.01	n.a.	bMB
46	19.39	n.a.	1.767	0.169	0.01	n.a.	BMb
47	19.55	n.a.	62.365	1.307	0.06	n.a.	Ru
48	19.66	n.a.	399.752	49.452	2.16	n.a.	bM
49	19.70	n.a.	452.634	23.829	1.04	n.a.	M
50	19.76	n.a.	375.419	11.713	0.51	n.a.	M
51	19.79	n.a.	433.231	64.179	2.81	n.a.	Mb
52	19.82	n.a.	66.525	0.646	0.03	n.a.	Rd
53	19.85	n.a.	56.370	1.800	0.08	n.a.	Rd
54	20.30	n.a.	4.292	0.166	0.01	n.a.	bMb
55	20.37	n.a.	9.714	0.190	0.01	n.a.	bMB

No.	Ret.Time	Peak Name	Height	Area	Rel.Area	Amount	Type
	min		mAU	mAU*min	%		
56	20.52	n.a.	1.758	0.171	0.01	n.a.	BMB
57	20.71	n.a.	1.791	0.142	0.01	n.a.	BMb
58	20.98	n.a.	10.292	1.704	0.07	n.a.	bMB
59	21.31	n.a.	1.806	0.152	0.01	n.a.	BMb
60	21.42	n.a.	1.435	0.137	0.01	n.a.	bMB
61	21.69	n.a.	2.062	0.260	0.01	n.a.	BMb
62	21.89	n.a.	1.589	0.213	0.01	n.a.	bMB
63	22.11	n.a.	0.567	0.046	0.00	n.a.	BMb
64	22.30	n.a.	4.024	0.582	0.03	n.a.	bMB
65	22.64	n.a.	1.321	0.296	0.01	n.a.	BMb
66	22.84	n.a.	2.107	0.390	0.02	n.a.	bMB
67	23.17	n.a.	0.200	0.012	0.00	n.a.	BMB
68	23.30	n.a.	0.130	0.010	0.00	n.a.	BMB
69	23.41	n.a.	0.126	0.008	0.00	n.a.	BMB
70	23.60	n.a.	0.501	0.068	0.00	n.a.	BMB
71	23.79	n.a.	0.295	0.022	0.00	n.a.	BMB
72	24.07	n.a.	0.625	0.086	0.00	n.a.	BMB
73	24.37	n.a.	0.296	0.023	0.00	n.a.	BMb
74	24.47	n.a.	0.163	0.011	0.00	n.a.	bMB
75	24.69	n.a.	0.360	0.028	0.00	n.a.	BMB
76	24.82	n.a.	0.188	0.013	0.00	n.a.	BMB
77	24.98	n.a.	0.250	0.021	0.00	n.a.	BMB
78	25.55	n.a.	0.109	0.011	0.00	n.a.	BMB
79	26.30	n.a.	0.491	0.082	0.00	n.a.	BMB
80	26.58	n.a.	4.661	0.532	0.02	n.a.	BMB
81	26.90	n.a.	0.538	0.066	0.00	n.a.	BMb
82	27.08	n.a.	2.409	0.271	0.01	n.a.	bMB
83	27.47	n.a.	0.342	0.041	0.00	n.a.	BMB
84	27.81	n.a.	3.617	3.753	0.16	n.a.	BMB
85	28.86	n.a.	5.391	0.484	0.02	n.a.	BMB
86	29.08	n.a.	42.232	4.920	0.22	n.a.	BMB
87	29.87	n.a.	21.957	1.847	0.08	n.a.	BMB
88	30.40	n.a.	2.793	0.133	0.01	n.a.	BMB
89	30.53	n.a.	7.107	0.518	0.02	n.a.	BMB
90	30.64	n.a.	0.047	0.077	0.00	n.a.	BMB
91	31.54	n.a.	5.643	0.289	0.01	n.a.	BMB
92	31.97	n.a.	11.719	1.305	0.06	n.a.	BM

No.	Ret.Time	Peak Name	Height	Area	Rel.Area	Amount	Type
	min		mAU	mAU*min	%		
93	32.11	n.a.	9.108	1.432	0.06	n.a.	MB
94	32.86	n.a.	6.318	0.378	0.02	n.a.	BMB
95	35.34	n.a.	2227.040	577.341	25.25	n.a.	BMB
96	40.74	n.a.	113.874	341.178	14.92	n.a.	BMB
Total:				2286.473	100.00	0.000	

3.2.3 HPLC analysis of heptapeptide crosslinked at pH 5

Sample Name:		*Injection Volume:*	**100.0**
Vial Number:	**BA3**	*Channel:*	**UV_VIS_1**
Sample Type:	**unknown**	*Wavelength:*	**214**
Control Program:		*Bandwidth:*	**8**
Quantif. Method:	**Default**	*Dilution Factor:*	**1.0000**
Recording Time:	**16/12/2009 15:55**	*Sample Weight:*	**1.0000**
Run Time (min):	**45.00**	*Sample Amount:*	**1.0000**

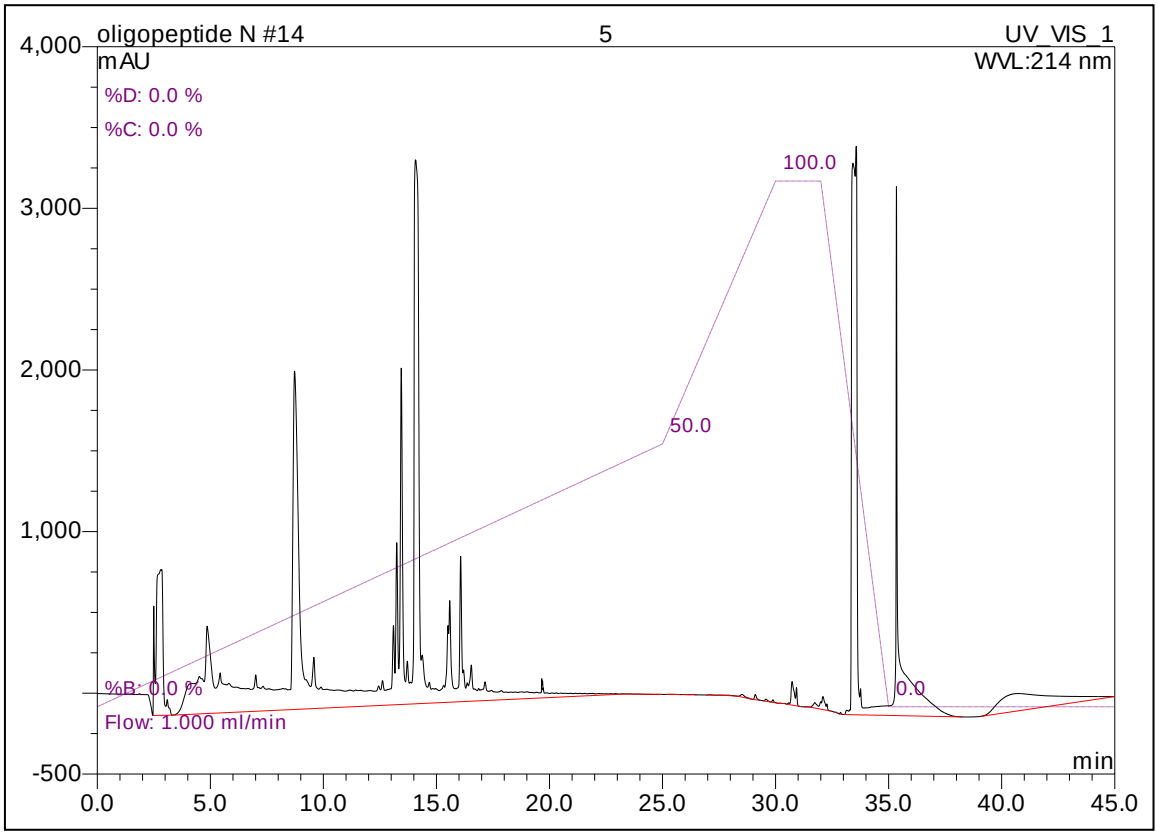

No.	Ret.Time	Peak Name	Height	Area	Rel.Area	Amount	Type
	min		mAU	mAU*min	%		
1	2.50	n.a.	675.843	35.614	0.61	n.a.	BM
2	2.85	n.a.	901.296	285.661	4.89	n.a.	MB
3	3.10	n.a.	55.729	5.669	0.10	n.a.	Rd
4	4.52	n.a.	231.214	181.796	3.11	n.a.	BM
5	4.63	n.a.	4.147	0.397	0.01	n.a.	Rd
6	4.86	n.a.	540.010	160.262	2.74	n.a.	M
7	5.44	n.a.	247.225	252.590	4.33	n.a.	M
8	5.82	n.a.	13.112	1.500	0.03	n.a.	Rd
9	6.17	n.a.	3.789	0.599	0.01	n.a.	Rd
10	6.44	n.a.	0.603	0.059	0.00	n.a.	Rd
11	6.68	n.a.	3.858	0.433	0.01	n.a.	Rd
12	7.01	n.a.	225.119	144.495	2.47	n.a.	M
13	7.13	n.a.	2.118	0.113	0.00	n.a.	Rd
14	7.33	n.a.	14.874	1.387	0.02	n.a.	Rd
15	7.59	n.a.	4.892	0.656	0.01	n.a.	Rd
16	8.22	n.a.	132.830	81.086	1.39	n.a.	M
17	8.33	n.a.	2.686	0.178	0.00	n.a.	Rd
18	8.52	n.a.	124.223	11.952	0.20	n.a.	M
19	8.73	n.a.	2092.658	594.294	10.18	n.a.	M
20	9.24	n.a.	180.903	36.760	0.63	n.a.	M
21	9.58	n.a.	317.326	191.256	3.28	n.a.	M
22	9.89	n.a.	13.597	1.147	0.02	n.a.	Rd
23	10.15	n.a.	2.777	0.402	0.01	n.a.	Rd
24	10.65	n.a.	4.034	1.122	0.02	n.a.	Rd
25	11.18	n.a.	6.642	1.170	0.02	n.a.	Ru
26	11.43	n.a.	102.496	82.354	1.41	n.a.	M
27	11.66	n.a.	3.631	0.490	0.01	n.a.	Rd
28	11.86	n.a.	0.171	0.008	0.00	n.a.	Ru
29	12.03	n.a.	95.424	40.668	0.70	n.a.	M
30	12.44	n.a.	26.904	2.135	0.04	n.a.	Ru
31	12.62	n.a.	153.086	49.071	0.84	n.a.	M
32	12.86	n.a.	97.471	16.434	0.28	n.a.	M
33	12.97	n.a.	100.418	9.230	0.16	n.a.	M
34	13.10	n.a.	490.331	48.424	0.83	n.a.	M
35	13.24	n.a.	1002.071	98.139	1.68	n.a.	M
36	13.45	n.a.	2081.032	257.626	4.41	n.a.	M
37	13.71	n.a.	131.877	9.378	0.16	n.a.	Rd

No.	Ret.Time	Peak Name	Height	Area	Rel.Area	Amount	Type
	min		mAU	mAU*min	%		
38	13.85	n.a.	135.250	13.226	0.23	n.a.	M
39	14.07	n.a.	3365.998	759.402	13.01	n.a.	M
40	14.37	n.a.	298.990	68.585	1.17	n.a.	M
41	14.68	n.a.	35.832	2.566	0.04	n.a.	Rd
42	14.82	n.a.	3.827	0.339	0.01	n.a.	Ru
43	14.97	n.a.	88.770	28.229	0.48	n.a.	M
44	15.32	n.a.	17.571	1.062	0.02	n.a.	Ru
45	15.51	n.a.	474.629	68.051	1.17	n.a.	M
46	15.59	n.a.	628.453	75.449	1.29	n.a.	M
47	16.07	n.a.	898.595	108.919	1.87	n.a.	M
48	16.20	n.a.	45.345	2.651	0.05	n.a.	Rd
49	16.36	n.a.	24.944	1.470	0.03	n.a.	Ru
50	16.54	n.a.	223.831	52.915	0.91	n.a.	M
51	16.68	n.a.	4.073	0.415	0.01	n.a.	Rd
52	16.87	n.a.	12.285	0.729	0.01	n.a.	Ru
53	16.98	n.a.	2.167	0.089	0.00	n.a.	Ru
54	17.05	n.a.	1.254	0.045	0.00	n.a.	Ru
55	17.15	n.a.	115.557	78.643	1.35	n.a.	M
56	17.44	n.a.	8.179	0.775	0.01	n.a.	Rd
57	17.87	n.a.	10.453	1.133	0.02	n.a.	Rd
58	18.07	n.a.	1.461	0.132	0.00	n.a.	Rd
59	18.30	n.a.	1.684	0.207	0.00	n.a.	Ru
60	18.48	n.a.	43.834	18.286	0.31	n.a.	M
61	18.76	n.a.	2.781	0.425	0.01	n.a.	Ru
62	19.00	n.a.	42.103	35.894	0.61	n.a.	M
63	19.43	n.a.	3.591	0.385	0.01	n.a.	Rd
64	19.66	n.a.	119.537	6.029	0.10	n.a.	M
65	19.69	n.a.	104.286	11.813	0.20	n.a.	M
66	19.73	n.a.	17.595	0.349	0.01	n.a.	Rd
67	19.88	n.a.	2.570	0.285	0.00	n.a.	Rd
68	20.11	n.a.	2.879	0.307	0.01	n.a.	Ru
69	20.30	n.a.	26.754	9.650	0.17	n.a.	M
70	20.51	n.a.	24.129	4.923	0.08	n.a.	M
71	20.68	n.a.	21.829	2.316	0.04	n.a.	M
72	20.74	n.a.	21.364	2.405	0.04	n.a.	M
73	20.95	n.a.	20.299	4.264	0.07	n.a.	M
74	21.14	n.a.	19.297	3.241	0.06	n.a.	M

No.	Ret.Time	Peak Name	Height	Area	Rel.Area	Amount	Type
	min		mAU	mAU*min	%		
75	21.35	n.a.	17.266	3.505	0.06	n.a.	M
76	21.56	n.a.	15.547	3.354	0.06	n.a.	M
77	21.78	n.a.	1.484	0.132	0.00	n.a.	Ru
78	21.92	n.a.	13.339	4.404	0.08	n.a.	M
79	22.15	n.a.	10.831	2.258	0.04	n.a.	M
80	22.31	n.a.	8.973	1.324	0.02	n.a.	M
81	22.52	n.a.	7.543	1.349	0.02	n.a.	M
82	22.70	n.a.	6.365	1.080	0.02	n.a.	M
83	22.92	n.a.	5.215	1.119	0.02	n.a.	M
84	23.24	n.a.	2.266	0.476	0.01	n.a.	Mb
85	23.58	n.a.	1.266	0.187	0.00	n.a.	bMB
86	23.92	n.a.	0.988	0.180	0.00	n.a.	BMB
87	24.14	n.a.	0.208	0.028	0.00	n.a.	BMB
88	24.45	n.a.	0.558	0.080	0.00	n.a.	BMB
89	24.61	n.a.	0.104	0.007	0.00	n.a.	BMB
90	24.75	n.a.	0.387	0.028	0.00	n.a.	BMB
91	24.89	n.a.	0.242	0.018	0.00	n.a.	BMB
92	25.39	n.a.	1.059	0.394	0.01	n.a.	BMB
93	25.98	n.a.	0.194	0.028	0.00	n.a.	BMB
94	26.33	n.a.	1.015	0.197	0.00	n.a.	BMB
95	27.10	n.a.	1.978	0.299	0.01	n.a.	BMB
96	27.49	n.a.	0.281	0.041	0.00	n.a.	BMB
97	27.80	n.a.	1.699	1.073	0.02	n.a.	BMB
98	28.51	n.a.	17.161	4.026	0.07	n.a.	BMB
99	29.10	n.a.	32.324	3.337	0.06	n.a.	BMB
100	29.57	n.a.	13.232	1.682	0.03	n.a.	BMB
101	29.88	n.a.	16.034	1.361	0.02	n.a.	BMB
102	30.18	n.a.	1.103	0.144	0.00	n.a.	BMB
103	30.35	n.a.	0.694	0.029	0.00	n.a.	BMB
104	30.42	n.a.	1.985	0.086	0.00	n.a.	BMB
105	30.59	n.a.	11.556	1.041	0.02	n.a.	BM
106	30.73	n.a.	146.065	21.170	0.36	n.a.	M
107	30.93	n.a.	113.268	6.866	0.12	n.a.	MB
108	31.33	n.a.	0.964	0.096	0.00	n.a.	BM
109	31.44	n.a.	0.957	0.052	0.00	n.a.	MB
110	31.74	n.a.	33.471	6.753	0.12	n.a.	BM
111	31.99	n.a.	13.574	0.631	0.01	n.a.	Ru

No.	Ret.Time	Peak Name	Height	Area	Rel.Area	Amount	Type
	min		mAU	mAU*min	%		
112	32.10	n.a.	80.187	14.448	0.25	n.a.	M
113	32.27	n.a.	39.254	2.380	0.04	n.a.	MB
114	32.59	n.a.	0.005	0.180	0.00	n.a.	BMB
115	32.87	n.a.	10.315	0.570	0.01	n.a.	BMB
116	33.14	n.a.	26.338	3.481	0.06	n.a.	BM
117	33.28	n.a.	29.531	1.650	0.03	n.a.	M
118	33.42	n.a.	3412.628	565.194	9.68	n.a.	M
119	33.57	n.a.	3517.250	332.564	5.70	n.a.	M
120	33.76	n.a.	161.496	15.764	0.27	n.a.	M
121	33.97	n.a.	44.347	5.086	0.09	n.a.	M
122	34.25	n.a.	50.615	12.725	0.22	n.a.	M
123	35.35	n.a.	3273.111	532.317	9.12	n.a.	MB
124	40.73	n.a.	107.473	313.841	5.37	n.a.	BMB
Total:				5839.194	100.00	0.000	

3.2.4 HPLC analysis of heptapeptide crosslinked at pH 6

Sample Name:		*Injection Volume:*	**100.0**
Vial Number:	**BA4**	*Channel:*	**UV_VIS_1**
Sample Type:	**unknown**	*Wavelength:*	**214**
Control Program:		*Bandwidth:*	**8**
Quantif. Method:	**Default**	*Dilution Factor:*	**1.0000**
Recording Time:	**16/12/2009 16:41**	*Sample Weight:*	**1.0000**
Run Time (min):	**45.00**	*Sample Amount:*	**1.0000**

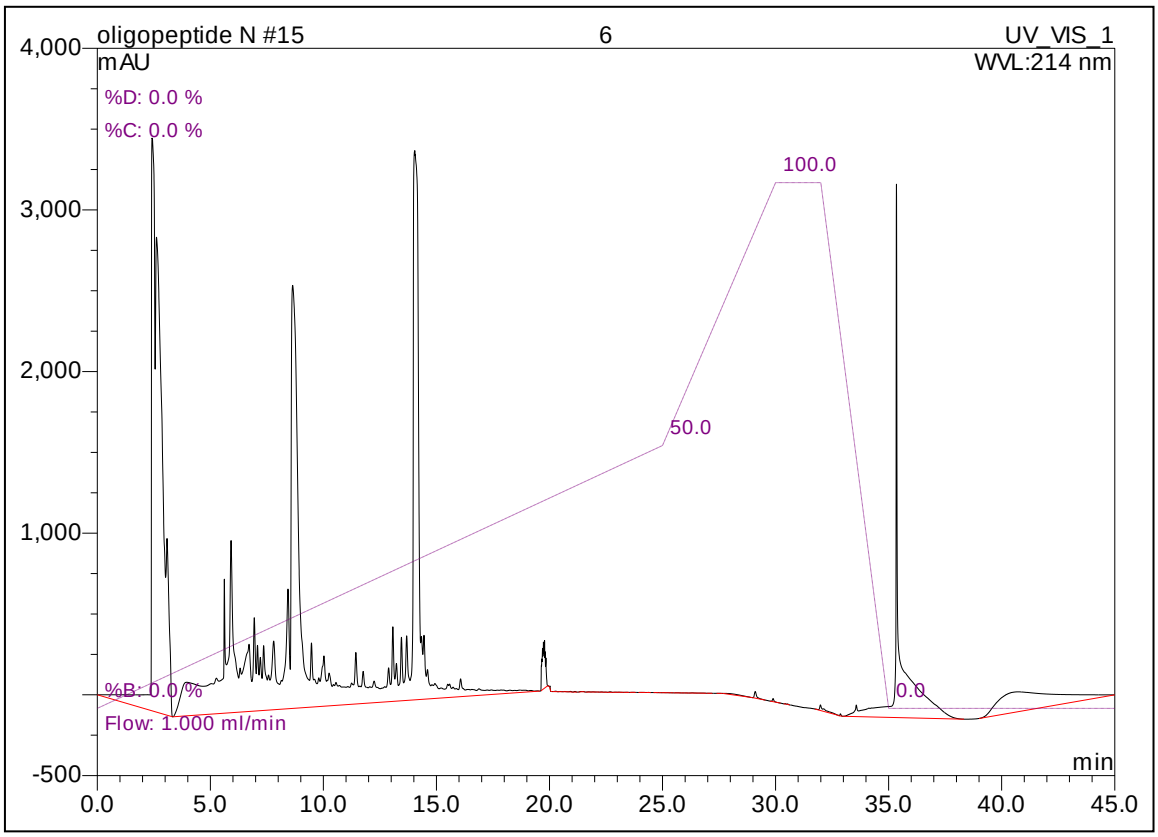

No.	Ret.Time	Peak Name	Height	Area	Rel.Area	Amount	Type
	min		mAU	mAU*min	%		
1	2.42	n.a.	3543.911	653.697	9.51	n.a.	BM
2	2.62	n.a.	2938.215	1062.409	15.46	n.a.	MB
3	3.08	n.a.	432.753	63.580	0.93	n.a.	Rd
4	3.96	n.a.	127.913	89.556	1.30	n.a.	Ru
5	5.05	n.a.	5.508	0.900	0.01	n.a.	Ru
6	5.27	n.a.	27.135	2.870	0.04	n.a.	Ru
7	5.62	n.a.	829.549	342.781	4.99	n.a.	BM
8	5.91	n.a.	1065.060	241.288	3.51	n.a.	M
9	6.32	n.a.	50.688	2.853	0.04	n.a.	Ru
10	6.71	n.a.	415.911	167.358	2.44	n.a.	M
11	6.94	n.a.	577.770	66.644	0.97	n.a.	M
12	7.09	n.a.	405.336	36.979	0.54	n.a.	M
13	7.21	n.a.	329.605	36.980	0.54	n.a.	M
14	7.36	n.a.	401.053	82.223	1.20	n.a.	M
15	7.57	n.a.	32.007	1.737	0.03	n.a.	Rd
16	7.80	n.a.	425.381	104.247	1.52	n.a.	M
17	8.14	n.a.	177.929	19.039	0.28	n.a.	M
18	8.44	n.a.	517.587	60.678	0.88	n.a.	Ru

No.	Ret.Time	Peak Name	Height	Area	Rel.Area	Amount	Type
	min		mAU	mAU*min	%		
19	8.64	n.a.	2617.563	963.463	14.02	n.a.	M
20	9.47	n.a.	396.826	69.040	1.00	n.a.	M
21	9.61	n.a.	11.292	0.726	0.01	n.a.	Rd
22	9.80	n.a.	28.447	1.661	0.02	n.a.	Ru
23	10.03	n.a.	311.211	82.289	1.20	n.a.	M
24	10.18	n.a.	3.171	0.098	0.00	n.a.	Ru
25	10.25	n.a.	202.266	40.776	0.59	n.a.	M
26	10.45	n.a.	8.795	0.466	0.01	n.a.	Ru
27	10.56	n.a.	141.816	52.126	0.76	n.a.	M
28	10.71	n.a.	6.397	0.441	0.01	n.a.	Rd
29	10.86	n.a.	110.717	36.845	0.54	n.a.	M
30	10.93	n.a.	0.566	0.031	0.00	n.a.	Rd
31	11.08	n.a.	4.160	0.310	0.00	n.a.	Rd
32	11.25	n.a.	19.480	1.454	0.02	n.a.	Ru
33	11.44	n.a.	318.368	72.753	1.06	n.a.	M
34	11.61	n.a.	3.715	0.179	0.00	n.a.	Rd
35	11.76	n.a.	198.690	39.451	0.57	n.a.	M
36	11.93	n.a.	0.950	0.042	0.00	n.a.	Rd
37	12.05	n.a.	5.009	0.341	0.00	n.a.	Ru
38	12.24	n.a.	133.782	53.419	0.78	n.a.	M
39	12.39	n.a.	1.552	0.109	0.00	n.a.	Rd
40	12.71	n.a.	5.934	0.376	0.01	n.a.	Ru
41	12.89	n.a.	209.494	49.445	0.72	n.a.	M
42	13.07	n.a.	461.486	45.554	0.66	n.a.	M
43	13.23	n.a.	232.812	26.804	0.39	n.a.	M
44	13.45	n.a.	289.130	20.883	0.30	n.a.	Ru
45	13.69	n.a.	284.581	24.263	0.35	n.a.	Ru
46	14.04	n.a.	3398.876	965.025	14.04	n.a.	M
47	14.34	n.a.	66.789	3.407	0.05	n.a.	Rd
48	14.45	n.a.	168.454	10.518	0.15	n.a.	Rd
49	14.61	n.a.	181.781	24.618	0.36	n.a.	M
50	14.80	n.a.	5.717	0.306	0.00	n.a.	Ru
51	14.93	n.a.	92.607	40.869	0.59	n.a.	M
52	15.20	n.a.	5.770	0.644	0.01	n.a.	Rd
53	15.50	n.a.	15.042	0.859	0.01	n.a.	Ru
54	15.58	n.a.	82.494	36.182	0.53	n.a.	M
55	15.74	n.a.	9.697	0.623	0.01	n.a.	Rd

No.	Ret.Time	Peak Name	Height	Area	Rel.Area	Amount	Type
	min		mAU	mAU*min	%		
56	15.88	n.a.	3.939	0.281	0.00	n.a.	Rd
57	16.07	n.a.	110.005	18.781	0.27	n.a.	M
58	16.37	n.a.	41.532	9.202	0.13	n.a.	M
59	16.43	n.a.	0.846	0.049	0.00	n.a.	Rd
60	16.57	n.a.	39.881	9.743	0.14	n.a.	M
61	16.65	n.a.	0.404	0.068	0.00	n.a.	Rd
62	16.88	n.a.	40.218	12.260	0.18	n.a.	M
63	17.25	n.a.	2.141	0.192	0.00	n.a.	Ru
64	17.43	n.a.	28.257	12.311	0.18	n.a.	M
65	17.70	n.a.	1.235	0.118	0.00	n.a.	Ru
66	17.86	n.a.	23.715	10.648	0.15	n.a.	M
67	17.96	n.a.	1.375	0.143	0.00	n.a.	Rd
68	18.25	n.a.	18.452	4.519	0.07	n.a.	M
69	18.46	n.a.	1.465	0.130	0.00	n.a.	Ru
70	18.69	n.a.	14.710	5.877	0.09	n.a.	M
71	18.86	n.a.	12.397	2.877	0.04	n.a.	M
72	18.93	n.a.	0.464	0.085	0.00	n.a.	Rd
73	19.17	n.a.	7.978	1.904	0.03	n.a.	MB
74	19.47	n.a.	1.518	0.197	0.00	n.a.	Rd
75	19.69	n.a.	255.172	13.574	0.20	n.a.	BM
76	19.73	n.a.	290.087	9.714	0.14	n.a.	M
77	19.75	n.a.	284.107	7.472	0.11	n.a.	M
78	19.78	n.a.	295.217	9.846	0.14	n.a.	M
79	19.81	n.a.	57.096	0.794	0.01	n.a.	Rd
80	19.84	n.a.	180.488	7.095	0.10	n.a.	Mb
81	19.94	n.a.	2.187	0.075	0.00	n.a.	bMB
82	20.02	n.a.	16.129	0.382	0.01	n.a.	BMB
83	20.07	n.a.	0.166	0.009	0.00	n.a.	BMB
84	20.28	n.a.	2.771	0.294	0.00	n.a.	BMB
85	20.47	n.a.	1.385	0.160	0.00	n.a.	BMB
86	20.68	n.a.	1.509	0.164	0.00	n.a.	BMB
87	20.93	n.a.	3.209	0.312	0.00	n.a.	BMB
88	21.12	n.a.	3.926	0.360	0.01	n.a.	BMB
89	21.39	n.a.	1.623	0.159	0.00	n.a.	BMb
90	21.50	n.a.	1.331	0.111	0.00	n.a.	bMB
91	21.73	n.a.	1.358	0.155	0.00	n.a.	BMB
92	21.92	n.a.	1.132	0.124	0.00	n.a.	BMB

No.	Ret.Time	Peak Name	Height	Area	Rel.Area	Amount	Type
	min		mAU	mAU*min	%		
93	22.12	n.a.	0.315	0.022	0.00	n.a.	BMB
94	22.30	n.a.	1.084	0.105	0.00	n.a.	BMB
95	22.48	n.a.	0.729	0.069	0.00	n.a.	BMB
96	22.69	n.a.	3.130	0.337	0.00	n.a.	BMB
97	22.91	n.a.	0.923	0.100	0.00	n.a.	BMb
98	23.08	n.a.	0.669	0.082	0.00	n.a.	bMB
99	23.42	n.a.	0.981	0.120	0.00	n.a.	BMB
100	23.64	n.a.	0.429	0.032	0.00	n.a.	BMb
101	23.72	n.a.	0.112	0.012	0.00	n.a.	bMB
102	24.01	n.a.	0.152	0.012	0.00	n.a.	BMb
103	24.15	n.a.	0.336	0.036	0.00	n.a.	bMB
104	24.38	n.a.	0.537	0.053	0.00	n.a.	BMB
105	24.70	n.a.	0.276	0.029	0.00	n.a.	BMB
106	24.89	n.a.	0.346	0.026	0.00	n.a.	BMB
107	25.05	n.a.	0.263	0.034	0.00	n.a.	BMB
108	25.23	n.a.	0.077	0.009	0.00	n.a.	BMB
109	25.39	n.a.	0.250	0.022	0.00	n.a.	BMB
110	25.62	n.a.	0.679	0.136	0.00	n.a.	BMB
111	25.88	n.a.	0.109	0.007	0.00	n.a.	BMB
112	26.02	n.a.	0.170	0.017	0.00	n.a.	BMB
113	26.32	n.a.	1.131	0.192	0.00	n.a.	BMB
114	26.74	n.a.	0.616	0.124	0.00	n.a.	BMB
115	27.10	n.a.	0.251	0.031	0.00	n.a.	BMB
116	27.50	n.a.	0.520	0.066	0.00	n.a.	BMB
117	27.78	n.a.	2.520	4.622	0.07	n.a.	BMB
118	29.10	n.a.	41.547	4.800	0.07	n.a.	BMB
119	29.89	n.a.	19.478	1.637	0.02	n.a.	BMB
120	30.43	n.a.	2.673	0.126	0.00	n.a.	BMB
121	30.53	n.a.	2.801	0.190	0.00	n.a.	BMB
122	31.98	n.a.	34.674	3.399	0.05	n.a.	BM
123	32.12	n.a.	15.270	4.381	0.06	n.a.	MB
124	32.75	n.a.	1.226	0.061	0.00	n.a.	BMB
125	32.87	n.a.	12.700	0.698	0.01	n.a.	BMB
126	33.57	n.a.	71.681	14.582	0.21	n.a.	BM
127	34.13	n.a.	53.432	22.747	0.33	n.a.	M
128	34.25	n.a.	55.217	5.795	0.08	n.a.	M
129	35.35	n.a.	3299.963	593.040	8.63	n.a.	MB

No.	Ret.Time	Peak Name	Height	Area	Rel.Area	Amount	Type
	min		mAU	mAU*min	%		
130	40.73	n.a.	122.949	372.027	5.41	n.a.	BMB
Total:				6872.177	100.00	0.000	

3.2.5 HPLC analysis of heptapeptide crosslinked at pH 7

Sample Name:		*Injection Volume:*	**100.0**
Vial Number:	**BA5**	*Channel:*	**UV_VIS_1**
Sample Type:	**unknown**	*Wavelength:*	**214**
Control Program:		*Bandwidth:*	**8**
Quantif. Method:	**Default**	*Dilution Factor:*	**1.0000**
Recording Time:	**16/12/2009 17:27**	*Sample Weight:*	**1.0000**
Run Time (min):	**45.00**	*Sample Amount:*	**1.0000**

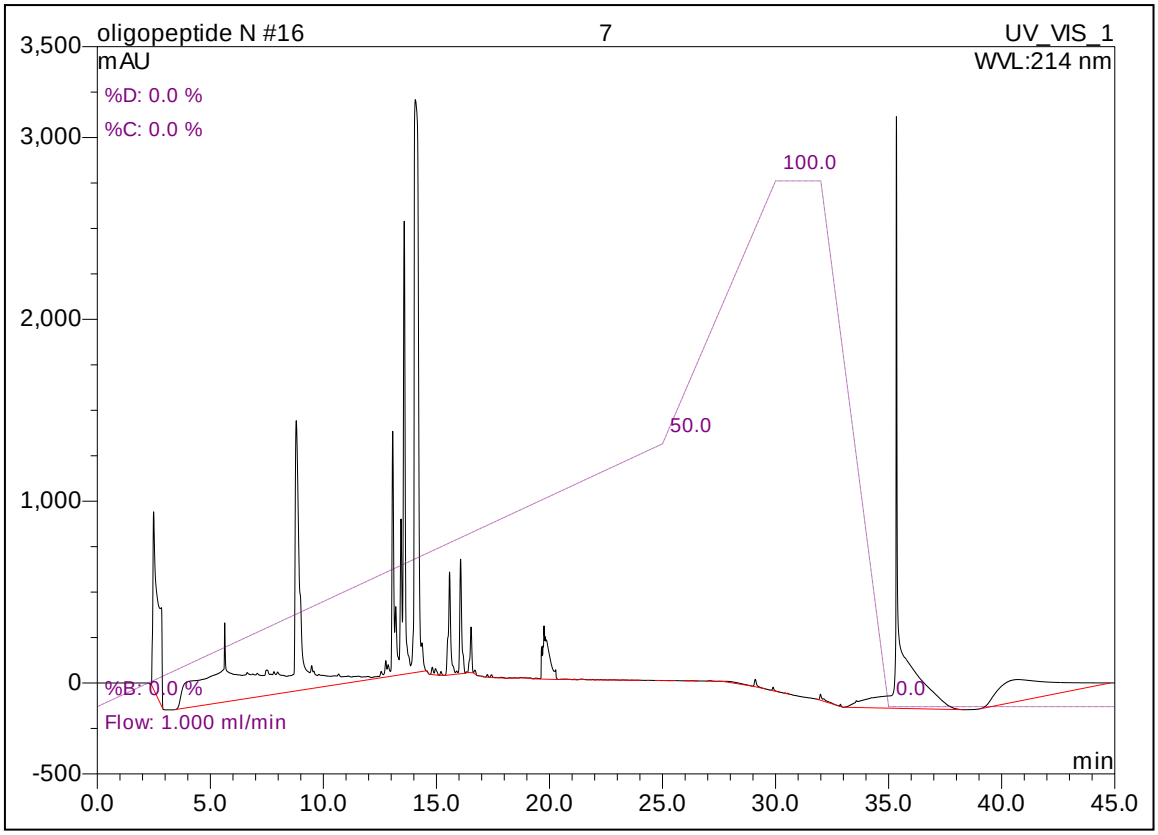

No.	Ret.Time	Peak Name	Height	Area	Rel.Area	Amount	Type
	min		mAU	mAU*min	%		
1	2.37	n.a.	6.544	0.261	0.01	n.a.	BMb
2	2.49	n.a.	976.519	220.071	5.79	n.a.	bM
3	2.84	n.a.	540.531	44.980	1.18	n.a.	MB
4	5.64	n.a.	435.182	414.112	10.89	n.a.	BM

No.	Ret.Time	Peak Name	Height	Area	Rel.Area	Amount	Type
	min		mAU	mAU*min	%		
5	6.09	n.a.	0.281	0.039	0.00	n.a.	Rd
6	6.47	n.a.	0.407	0.018	0.00	n.a.	Ru
7	6.63	n.a.	142.701	111.969	2.94	n.a.	M
8	6.88	n.a.	4.274	0.255	0.01	n.a.	Rd
9	7.08	n.a.	9.378	0.789	0.02	n.a.	Rd
10	7.48	n.a.	140.311	53.282	1.40	n.a.	M
11	7.52	n.a.	4.470	0.287	0.01	n.a.	Rd
12	7.67	n.a.	2.068	0.116	0.00	n.a.	Rd
13	7.81	n.a.	124.919	65.557	1.72	n.a.	M
14	7.98	n.a.	14.588	1.224	0.03	n.a.	Rd
15	8.23	n.a.	1.352	0.132	0.00	n.a.	Rd
16	8.80	n.a.	1486.653	353.948	9.31	n.a.	M
17	9.48	n.a.	126.135	29.362	0.77	n.a.	M
18	9.58	n.a.	9.737	0.506	0.01	n.a.	Rd
19	9.80	n.a.	71.778	35.289	0.93	n.a.	M
20	9.93	n.a.	0.861	0.204	0.01	n.a.	Rd
21	10.15	n.a.	0.945	0.046	0.00	n.a.	Rd
22	10.26	n.a.	0.885	0.045	0.00	n.a.	Rd
23	10.51	n.a.	1.774	0.256	0.01	n.a.	Ru
24	10.68	n.a.	56.843	38.633	1.02	n.a.	M
25	11.11	n.a.	5.089	0.939	0.02	n.a.	Rd
26	11.34	n.a.	1.612	0.090	0.00	n.a.	Ru
27	11.45	n.a.	0.555	0.033	0.00	n.a.	Ru
28	11.56	n.a.	27.771	11.894	0.31	n.a.	M
29	11.77	n.a.	0.477	0.031	0.00	n.a.	Ru
30	11.97	n.a.	18.440	7.531	0.20	n.a.	M
31	12.31	n.a.	1.045	0.168	0.00	n.a.	Ru
32	12.41	n.a.	1.843	0.101	0.00	n.a.	Ru
33	12.56	n.a.	35.014	7.064	0.19	n.a.	M
34	12.76	n.a.	90.711	8.144	0.21	n.a.	M
35	12.86	n.a.	66.256	6.796	0.18	n.a.	M
36	13.07	n.a.	1346.437	137.463	3.61	n.a.	M
37	13.20	n.a.	186.663	11.646	0.31	n.a.	Rd
38	13.44	n.a.	856.587	71.214	1.87	n.a.	M
39	13.58	n.a.	2491.518	229.806	6.04	n.a.	M
40	14.06	n.a.	3151.803	663.783	17.45	n.a.	M
41	14.36	n.a.	157.470	15.808	0.42	n.a.	Mb

No.	Ret.Time	Peak Name	Height	Area	Rel.Area	Amount	Type
	min		mAU	mAU*min	%		
42	14.57	n.a.	2.161	0.247	0.01	n.a.	bMB
43	14.82	n.a.	40.435	3.339	0.09	n.a.	BM
44	14.96	n.a.	34.864	3.708	0.10	n.a.	MB
45	15.20	n.a.	21.699	1.666	0.04	n.a.	BMB
46	15.58	n.a.	566.272	68.489	1.80	n.a.	BM
47	15.89	n.a.	17.122	1.489	0.04	n.a.	M
48	16.07	n.a.	630.041	61.618	1.62	n.a.	MB
49	16.33	n.a.	5.828	0.310	0.01	n.a.	BMb
50	16.53	n.a.	250.963	22.615	0.59	n.a.	bMb
51	16.71	n.a.	21.530	1.728	0.05	n.a.	bMB
52	16.85	n.a.	0.763	0.035	0.00	n.a.	BMB
53	17.03	n.a.	2.791	0.153	0.00	n.a.	BMB
54	17.25	n.a.	14.677	1.077	0.03	n.a.	BMb
55	17.44	n.a.	15.125	1.264	0.03	n.a.	bMB
56	17.68	n.a.	0.978	0.085	0.00	n.a.	BMb
57	17.86	n.a.	3.995	0.644	0.02	n.a.	bMB
58	18.27	n.a.	2.184	0.376	0.01	n.a.	BM
59	18.47	n.a.	1.609	0.216	0.01	n.a.	MB
60	18.75	n.a.	2.532	0.278	0.01	n.a.	BMb
61	18.93	n.a.	1.205	0.127	0.00	n.a.	bMb
62	19.13	n.a.	2.844	0.358	0.01	n.a.	bMB
63	19.40	n.a.	4.326	0.768	0.02	n.a.	BM
64	19.66	n.a.	177.772	6.775	0.18	n.a.	M
65	19.68	n.a.	36.487	0.451	0.01	n.a.	Ru
66	19.76	n.a.	292.644	30.080	0.79	n.a.	M
67	19.80	n.a.	22.716	0.498	0.01	n.a.	Rd
68	19.84	n.a.	215.914	50.219	1.32	n.a.	MB
69	19.86	n.a.	13.872	1.856	0.05	n.a.	Rd
70	20.20	n.a.	1.595	0.033	0.00	n.a.	Rd
71	20.27	n.a.	26.538	0.785	0.02	n.a.	Rd
72	20.56	n.a.	0.332	0.082	0.00	n.a.	BMb
73	20.74	n.a.	1.018	0.145	0.00	n.a.	bMb
74	20.89	n.a.	0.873	0.066	0.00	n.a.	bMB
75	21.10	n.a.	2.612	0.296	0.01	n.a.	BMB
76	21.38	n.a.	1.573	0.129	0.00	n.a.	BMb
77	21.47	n.a.	0.466	0.044	0.00	n.a.	bMB
78	21.77	n.a.	1.079	0.078	0.00	n.a.	BMb

No.	Ret.Time	Peak Name	Height	Area	Rel.Area	Amount	Type
	min		mAU	mAU*min	%		
79	21.93	n.a.	2.160	0.191	0.01	n.a.	bMB
80	22.11	n.a.	1.575	0.151	0.00	n.a.	BMb
81	22.28	n.a.	1.197	0.101	0.00	n.a.	bMb
82	22.45	n.a.	0.815	0.088	0.00	n.a.	bMB
83	22.69	n.a.	0.939	0.096	0.00	n.a.	BMb
84	22.86	n.a.	0.958	0.091	0.00	n.a.	bMB
85	23.03	n.a.	0.477	0.043	0.00	n.a.	BMB
86	23.25	n.a.	1.184	0.143	0.00	n.a.	BMb
87	23.43	n.a.	0.290	0.030	0.00	n.a.	bMB
88	23.64	n.a.	0.539	0.062	0.00	n.a.	BMb
89	23.90	n.a.	0.519	0.072	0.00	n.a.	bMB
90	24.35	n.a.	0.147	0.009	0.00	n.a.	BMB
91	24.75	n.a.	0.258	0.073	0.00	n.a.	BMB
92	25.04	n.a.	0.461	0.086	0.00	n.a.	BMB
93	25.41	n.a.	0.378	0.045	0.00	n.a.	BMB
94	26.03	n.a.	0.370	0.041	0.00	n.a.	BMB
95	26.32	n.a.	1.229	0.166	0.00	n.a.	BMB
96	27.11	n.a.	3.016	0.440	0.01	n.a.	BMB
97	27.50	n.a.	0.302	0.035	0.00	n.a.	BMb
98	27.79	n.a.	3.022	4.804	0.13	n.a.	bMb
99	29.10	n.a.	41.531	4.823	0.13	n.a.	bMB
100	29.89	n.a.	19.404	1.644	0.04	n.a.	BMB
101	30.43	n.a.	2.436	0.116	0.00	n.a.	BMb
102	30.53	n.a.	2.995	0.220	0.01	n.a.	bMB
103	31.99	n.a.	33.364	2.993	0.08	n.a.	BM
104	32.12	n.a.	13.222	2.979	0.08	n.a.	MB
105	32.72	n.a.	0.002	0.075	0.00	n.a.	BMB
106	32.87	n.a.	12.182	0.690	0.02	n.a.	BMB
107	33.58	n.a.	37.872	9.628	0.25	n.a.	BM
108	35.34	n.a.	3253.859	616.610	16.21	n.a.	MB
109	40.73	n.a.	119.417	343.861	9.04	n.a.	BM
110	44.81	n.a.	0.000	6.541	0.17	n.a.	MB
Total:				3802.968	100.00	0.000	

3.2.6 HPLC analysis of heptapeptide crosslinked at pH 8

Sample Name:		*Injection Volume:*	**100.0**
Vial Number:	**BA6**	*Channel:*	**UV_VIS_1**
Sample Type:	**unknown**	*Wavelength:*	**214**
Control Program:		*Bandwidth:*	**8**
Quantif. Method:	**Default**	*Dilution Factor:*	**1.0000**
Recording Time:	**16/12/2009 18:12**	*Sample Weight:*	**1.0000**
Run Time (min):	**45.00**	*Sample Amount:*	**1.0000**

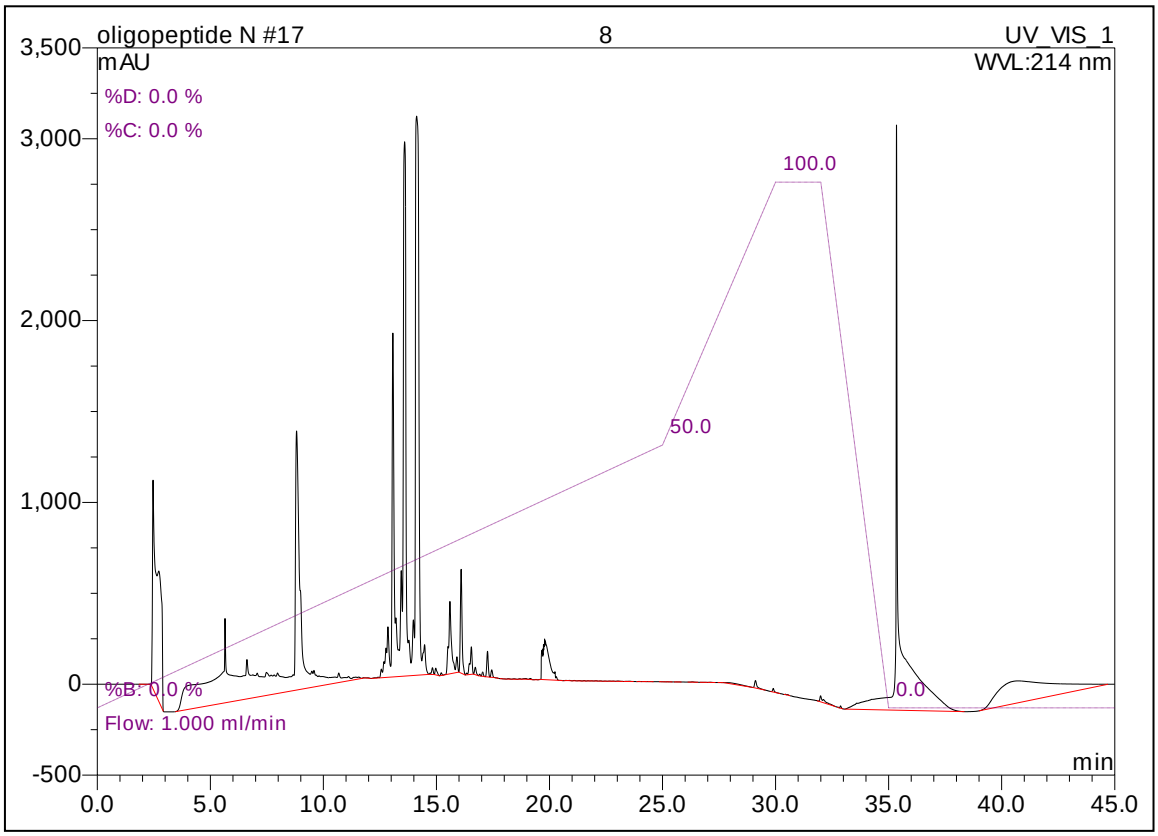

No.	Ret.Time	Peak Name	Height	Area	Rel.Area	Amount	Type
	min		mAU	mAU*min	%		
1	2.26	n.a.	0.427	0.096	0.00	n.a.	BMB
2	2.36	n.a.	5.146	0.257	0.01	n.a.	BMb
3	2.46	n.a.	1146.632	169.462	4.39	n.a.	bM
4	2.72	n.a.	716.987	162.750	4.21	n.a.	MB
5	5.65	n.a.	463.754	369.145	9.56	n.a.	BM
6	6.62	n.a.	216.905	137.658	3.56	n.a.	M
7	6.88	n.a.	3.499	0.209	0.01	n.a.	Rd
8	7.07	n.a.	15.915	1.024	0.03	n.a.	Rd
9	7.24	n.a.	0.628	0.060	0.00	n.a.	Rd

No.	Ret.Time	Peak Name	Height	Area	Rel.Area	Amount	Type
	min		mAU	mAU*min	%		
10	7.48	n.a.	126.556	26.229	0.68	n.a.	M
11	7.69	n.a.	4.919	0.302	0.01	n.a.	Ru
12	7.82	n.a.	105.211	65.722	1.70	n.a.	M
13	7.97	n.a.	18.378	1.721	0.04	n.a.	Rd
14	8.51	n.a.	80.152	17.205	0.45	n.a.	M
15	8.66	n.a.	87.572	12.652	0.33	n.a.	M
16	8.81	n.a.	1425.376	306.186	7.93	n.a.	M
17	9.49	n.a.	15.001	0.778	0.02	n.a.	Ru
18	9.58	n.a.	91.299	45.030	1.17	n.a.	M
19	9.68	n.a.	2.609	0.134	0.00	n.a.	Rd
20	9.81	n.a.	4.043	0.221	0.01	n.a.	Rd
21	9.94	n.a.	1.883	0.305	0.01	n.a.	Rd
22	10.27	n.a.	0.982	0.050	0.00	n.a.	Ru
23	10.51	n.a.	2.322	0.337	0.01	n.a.	Ru
24	10.68	n.a.	52.202	19.827	0.51	n.a.	M
25	10.95	n.a.	0.969	0.150	0.00	n.a.	Ru
26	11.11	n.a.	23.612	8.405	0.22	n.a.	M
27	11.35	n.a.	1.853	0.122	0.00	n.a.	Ru
28	11.43	n.a.	13.122	3.129	0.08	n.a.	M
29	11.56	n.a.	10.318	1.357	0.04	n.a.	M
30	11.78	n.a.	2.333	0.181	0.00	n.a.	Mb
31	11.96	n.a.	2.022	0.275	0.01	n.a.	bMB
32	12.32	n.a.	2.242	0.386	0.01	n.a.	BM
33	12.42	n.a.	4.405	0.369	0.01	n.a.	M
34	12.56	n.a.	29.975	1.816	0.05	n.a.	Ru
35	12.68	n.a.	26.865	1.273	0.03	n.a.	Ru
36	12.77	n.a.	47.877	2.180	0.06	n.a.	Ru
37	12.86	n.a.	277.759	43.993	1.14	n.a.	M
38	13.07	n.a.	1891.607	196.358	5.08	n.a.	M
39	13.21	n.a.	69.221	3.775	0.10	n.a.	Rd
40	13.33	n.a.	147.087	7.287	0.19	n.a.	M
41	13.45	n.a.	308.064	18.545	0.48	n.a.	Ru
42	13.59	n.a.	2939.168	402.499	10.42	n.a.	M
43	13.78	n.a.	196.349	19.315	0.50	n.a.	M
44	13.98	n.a.	306.094	29.768	0.77	n.a.	M
45	14.13	n.a.	3075.446	517.220	13.39	n.a.	M
46	14.48	n.a.	165.444	23.680	0.61	n.a.	MB

No.	Ret.Time	Peak Name	Height	Area	Rel.Area	Amount	Type
	min		mAU	mAU*min	%		
47	14.72	n.a.	3.818	0.174	0.00	n.a.	Ru
48	14.82	n.a.	37.168	3.041	0.08	n.a.	BMb
49	14.97	n.a.	37.182	3.480	0.09	n.a.	bMB
50	15.21	n.a.	14.647	0.930	0.02	n.a.	BMB
51	15.51	n.a.	38.449	2.021	0.05	n.a.	Ru
52	15.60	n.a.	398.284	55.722	1.44	n.a.	bMb
53	15.91	n.a.	77.139	5.597	0.14	n.a.	Rd
54	16.09	n.a.	571.183	48.639	1.26	n.a.	bMB
55	16.33	n.a.	9.547	0.577	0.01	n.a.	BM
56	16.46	n.a.	18.454	0.914	0.02	n.a.	Ru
57	16.54	n.a.	150.938	14.578	0.38	n.a.	Mb
58	16.72	n.a.	40.774	3.350	0.09	n.a.	bMB
59	16.91	n.a.	9.467	0.556	0.01	n.a.	BMB
60	17.04	n.a.	23.401	1.618	0.04	n.a.	BMB
61	17.26	n.a.	140.830	10.813	0.28	n.a.	BMb
62	17.45	n.a.	41.305	3.183	0.08	n.a.	bMB
63	17.57	n.a.	0.454	0.022	0.00	n.a.	BMB
64	17.66	n.a.	0.888	0.079	0.00	n.a.	BMB
65	17.81	n.a.	0.001	0.046	0.00	n.a.	BMB
66	18.02	n.a.	0.416	0.024	0.00	n.a.	BMB
67	18.18	n.a.	2.568	0.285	0.01	n.a.	BMB
68	18.43	n.a.	2.432	0.318	0.01	n.a.	BMB
69	18.68	n.a.	2.577	0.244	0.01	n.a.	BMb
70	18.95	n.a.	3.788	0.636	0.02	n.a.	bMB
71	19.15	n.a.	5.565	0.557	0.01	n.a.	BMB
72	19.40	n.a.	1.834	0.186	0.00	n.a.	BMB
73	19.58	n.a.	0.928	0.061	0.00	n.a.	BMb
74	19.67	n.a.	159.710	9.982	0.26	n.a.	bM
75	19.69	n.a.	30.903	0.400	0.01	n.a.	Rd
76	19.74	n.a.	40.768	0.460	0.01	n.a.	Ru
77	19.78	n.a.	224.058	60.579	1.57	n.a.	M
78	19.82	n.a.	20.537	3.108	0.08	n.a.	Rd
79	20.18	n.a.	1.316	0.032	0.00	n.a.	Rd
80	20.24	n.a.	19.735	0.453	0.01	n.a.	Rd
81	20.30	n.a.	19.642	1.330	0.03	n.a.	MB
82	20.49	n.a.	0.471	0.059	0.00	n.a.	BMB
83	20.73	n.a.	0.968	0.112	0.00	n.a.	BMb

No.	Ret.Time	Peak Name	Height	Area	Rel.Area	Amount	Type
	min		mAU	mAU*min	%		
84	20.89	n.a.	1.398	0.131	0.00	n.a.	bMB
85	21.10	n.a.	2.233	0.241	0.01	n.a.	BMB
86	21.31	n.a.	1.612	0.216	0.01	n.a.	BMB
87	21.54	n.a.	2.166	0.196	0.01	n.a.	BMB
88	21.70	n.a.	1.404	0.113	0.00	n.a.	BMB
89	21.86	n.a.	0.743	0.061	0.00	n.a.	BMB
90	22.06	n.a.	1.530	0.157	0.00	n.a.	BMB
91	22.25	n.a.	1.448	0.143	0.00	n.a.	BMB
92	22.45	n.a.	1.049	0.099	0.00	n.a.	BMB
93	22.67	n.a.	0.750	0.080	0.00	n.a.	BMb
94	22.82	n.a.	0.836	0.069	0.00	n.a.	bMB
95	23.02	n.a.	1.676	0.297	0.01	n.a.	BMB
96	23.55	n.a.	1.321	0.306	0.01	n.a.	BMB
97	23.97	n.a.	0.792	0.094	0.00	n.a.	BMB
98	24.15	n.a.	0.355	0.061	0.00	n.a.	BMB
99	24.40	n.a.	0.136	0.007	0.00	n.a.	BMB
100	24.52	n.a.	0.291	0.024	0.00	n.a.	BMB
101	24.92	n.a.	0.141	0.010	0.00	n.a.	BMB
102	25.05	n.a.	0.192	0.015	0.00	n.a.	BMB
103	25.21	n.a.	0.297	0.024	0.00	n.a.	BMB
104	25.34	n.a.	0.265	0.024	0.00	n.a.	BMB
105	25.65	n.a.	0.349	0.063	0.00	n.a.	BMB
106	26.32	n.a.	1.878	0.291	0.01	n.a.	BMB
107	26.74	n.a.	0.226	0.029	0.00	n.a.	BM
108	26.85	n.a.	0.318	0.032	0.00	n.a.	MB
109	27.12	n.a.	1.010	0.138	0.00	n.a.	BMB
110	27.51	n.a.	0.182	0.025	0.00	n.a.	BMB
111	27.80	n.a.	2.346	4.408	0.11	n.a.	BMB
112	29.11	n.a.	41.530	4.865	0.13	n.a.	BMB
113	29.90	n.a.	19.817	1.664	0.04	n.a.	BMB
114	30.43	n.a.	2.407	0.112	0.00	n.a.	BMB
115	30.53	n.a.	2.725	0.176	0.00	n.a.	BMB
116	31.99	n.a.	33.382	2.857	0.07	n.a.	BM
117	32.12	n.a.	18.005	3.502	0.09	n.a.	MB
118	32.73	n.a.	0.012	0.075	0.00	n.a.	BMB
119	32.87	n.a.	13.001	0.755	0.02	n.a.	BMB
120	33.59	n.a.	34.067	8.928	0.23	n.a.	BM

No.	Ret.Time	Peak Name	Height	Area	Rel.Area	Amount	Type
	min		mAU	mAU*min	%		
121	35.35	n.a.	3218.730	628.175	16.27	n.a.	MB
122	40.74	n.a.	120.221	330.899	8.57	n.a.	BM
123	44.64	n.a.	1.693	18.708	0.48	n.a.	MB
Total:				3861.676	100.00	0.000	

3.3 Crosslinking of lysozyme

3.3.1 Size exclusion column

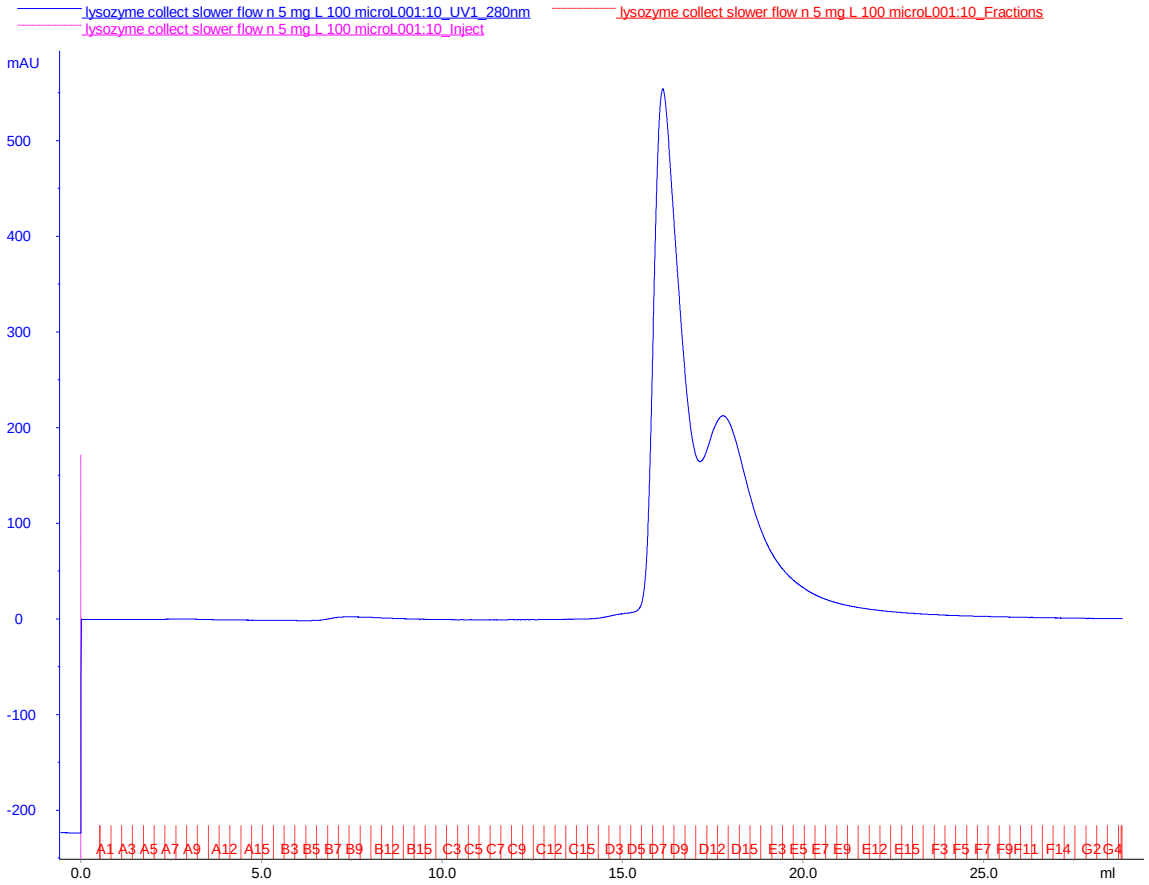

Figure 15 Elution profile of native lysozyme using SEC on Superdex G-75 with flow rate of 0.3 mL/min.

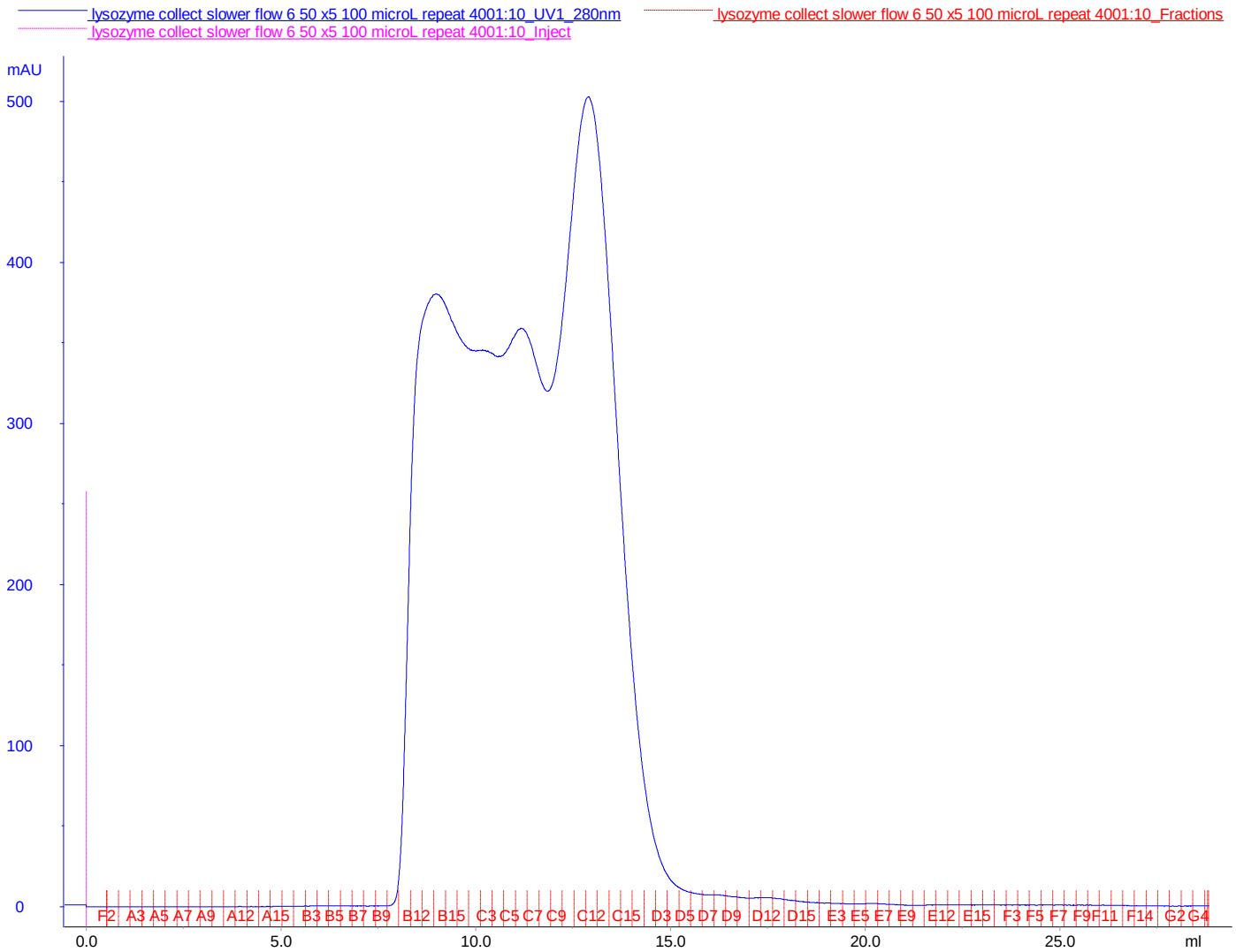

Figure 16 Elution profile of lysozyme after intermolecular crosslinking using SEC on Superdex G-75 with flow rate of 0.3 mL/min.

3.3.2 HPLC

3.3.2.1 HPLC analysis of lysozyme control for tryptic digestion

monitered at 280 nm.

Sample Name:		*Injection Volume:*	**100.0**
Vial Number:	**RA3**	*Channel:*	**UV_VIS_2**
Sample Type:	**unknown**	*Wavelength:*	**280**
Control Program:		*Bandwidth:*	**8**
Quantif. Method:	**default**	*Dilution Factor:*	**1.0000**
Recording Time:	**7/04/2010 12:44**	*Sample Weight:*	**1.0000**
Run Time (min):	**42.00**	*Sample Amount:*	**1.0000**

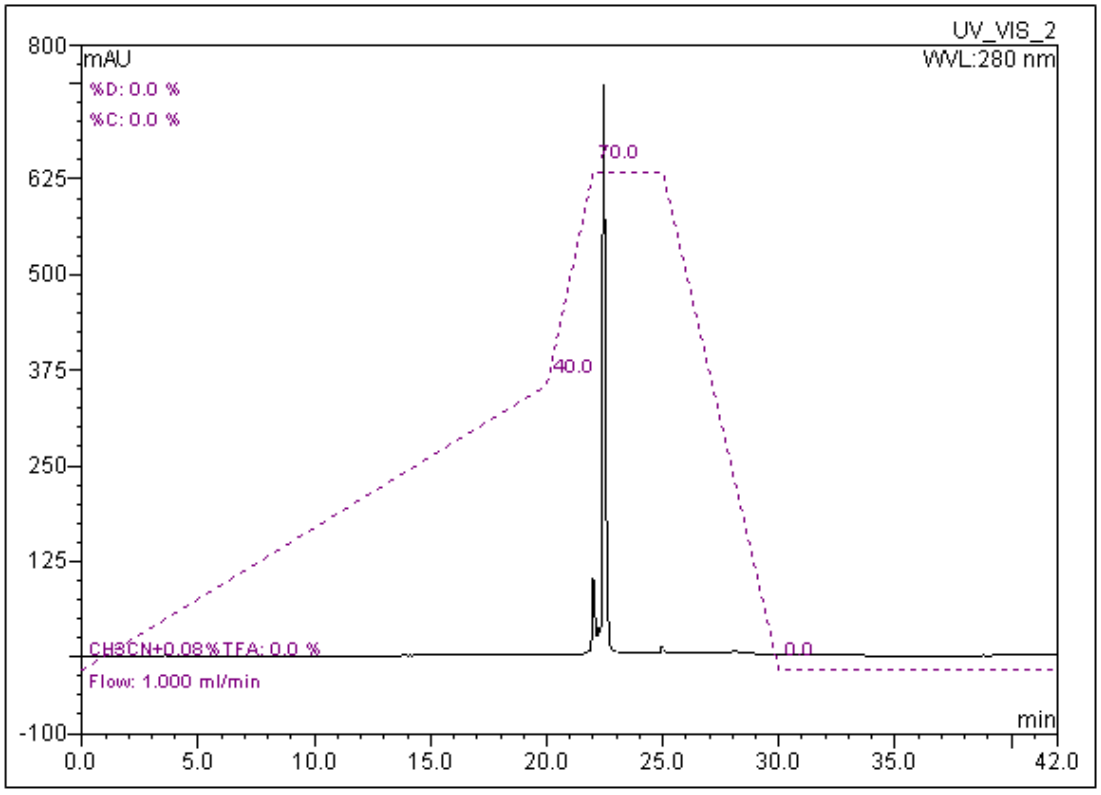

No.	Ret.Time	Peak Name	Height	Area	Rel.Area	Amount	Type
	min		mAU	mAU*min	%	n.a.	
1	1.24	n.a.	0.013	0.000	0.00	n.a.	BMB
2	1.98	n.a.	0.032	0.003	0.00	n.a.	BMB
3	2.74	n.a.	0.023	0.004	0.00	n.a.	BMB
4	3.43	n.a.	0.746	0.073	0.05	n.a.	Ru
5	3.56	n.a.	3.786	0.313	0.23	n.a.	BMB
6	4.59	n.a.	0.046	0.005	0.00	n.a.	BMB
7	5.71	n.a.	0.204	0.026	0.02	n.a.	BMB

No.	Ret.Time	Peak Name	Height	Area	Rel.Area	Amount	Type
	min		mAU	mAU*min	%	n.a.	
8	6.78	n.a.	0.115	0.019	0.01	n.a.	BMB
9	7.83	n.a.	0.053	0.002	0.00	n.a.	BMB
10	9.17	n.a.	0.140	0.023	0.02	n.a.	BM
11	9.45	n.a.	0.055	0.012	0.01	n.a.	MB
12	10.29	n.a.	0.026	0.002	0.00	n.a.	BMB
13	12.26	n.a.	0.075	0.006	0.00	n.a.	BMB
14	12.66	n.a.	0.020	0.001	0.00	n.a.	BMB
15	13.87	n.a.	0.075	0.010	0.01	n.a.	BMB
16	14.25	n.a.	0.077	0.011	0.01	n.a.	BMB
17	15.96	n.a.	0.079	0.006	0.00	n.a.	BMB
18	16.81	n.a.	0.154	0.059	0.04	n.a.	BM
19	17.35	n.a.	0.094	0.031	0.02	n.a.	M
20	17.77	n.a.	0.071	0.028	0.02	n.a.	MB
21	20.96	n.a.	0.110	0.016	0.01	n.a.	BMB
22	21.14	n.a.	0.108	0.009	0.01	n.a.	BM
23	21.51	n.a.	0.279	0.055	0.04	n.a.	M
24	22.00	n.a.	100.734	15.457	11.18	n.a.	M
25	22.24	n.a.	35.789	4.369	3.16	n.a.	M
26	22.45	n.a.	743.889	110.967	80.28	n.a.	M
27	23.32	n.a.	1.434	0.467	0.34	n.a.	M
28	24.06	n.a.	1.164	0.819	0.59	n.a.	M
29	24.96	n.a.	10.050	3.145	2.28	n.a.	M
30	25.39	n.a.	0.193	0.021	0.02	n.a.	Rd
31	25.58	n.a.	0.244	0.019	0.01	n.a.	Rd
32	25.73	n.a.	1.403	0.201	0.15	n.a.	Rd
33	26.12	n.a.	0.876	0.391	0.28	n.a.	M
34	26.97	n.a.	0.059	0.003	0.00	n.a.	Ru
35	27.07	n.a.	0.297	0.075	0.05	n.a.	MB
36	27.30	n.a.	0.037	0.001	0.00	n.a.	Rd
37	27.44	n.a.	1.151	0.193	0.14	n.a.	BMB
38	28.05	n.a.	4.705	1.295	0.94	n.a.	bMB
39	28.83	n.a.	0.140	0.024	0.02	n.a.	BMB
40	29.11	n.a.	0.096	0.013	0.01	n.a.	BMB
41	34.29	n.a.	0.061	0.005	0.00	n.a.	BM
42	34.41	n.a.	0.042	0.003	0.00	n.a.	M
43	34.53	n.a.	0.037	0.002	0.00	n.a.	Mb
44	34.68	n.a.	0.050	0.002	0.00	n.a.	bMb

No.	Ret.Time	Peak Name	Height	Area	Rel.Area	Amount	Type
	min		mAU	mAU*min	%	n.a.	
45	34.74	n.a.	0.033	0.002	0.00	n.a.	bMB
46	35.08	n.a.	0.066	0.005	0.00	n.a.	BMB
47	35.39	n.a.	0.036	0.003	0.00	n.a.	BMB
48	35.75	n.a.	0.044	0.001	0.00	n.a.	BMb
49	35.88	n.a.	0.035	0.003	0.00	n.a.	bMB
50	36.17	n.a.	0.027	0.001	0.00	n.a.	BMB
51	36.72	n.a.	0.027	0.002	0.00	n.a.	BMB
52	37.02	n.a.	0.036	0.001	0.00	n.a.	BMB
53	37.59	n.a.	0.021	0.002	0.00	n.a.	BMB
54	39.93	n.a.	0.040	0.002	0.00	n.a.	BMB
55	40.10	n.a.	0.026	0.002	0.00	n.a.	BM
56	40.23	n.a.	0.039	0.002	0.00	n.a.	M
57	40.35	n.a.	0.022	0.002	0.00	n.a.	MB
58	40.83	n.a.	0.042	0.005	0.00	n.a.	BMB
59	41.64	n.a.	0.051	0.004	0.00	n.a.	BMB
60	41.94	n.a.	0.017	0.001	0.00	n.a.	BMB
Total:			909.394	138.223	100.00	0.000	

monitored at 214 nm.

Sample Name:		*Injection Volume:*	**100.0**
Vial Number:	**RA3**	*Channel:*	**UV_VIS_1**
Sample Type:	**unknown**	*Wavelength:*	**214**
Control Program:		*Bandwidth:*	**8**
Quantif. Method:	**default**	*Dilution Factor:*	**1.0000**
Recording Time:	**7/04/2010 12:44**	*Sample Weight:*	**1.0000**
Run Time (min):	**42.00**	*Sample Amount:*	**1.0000**

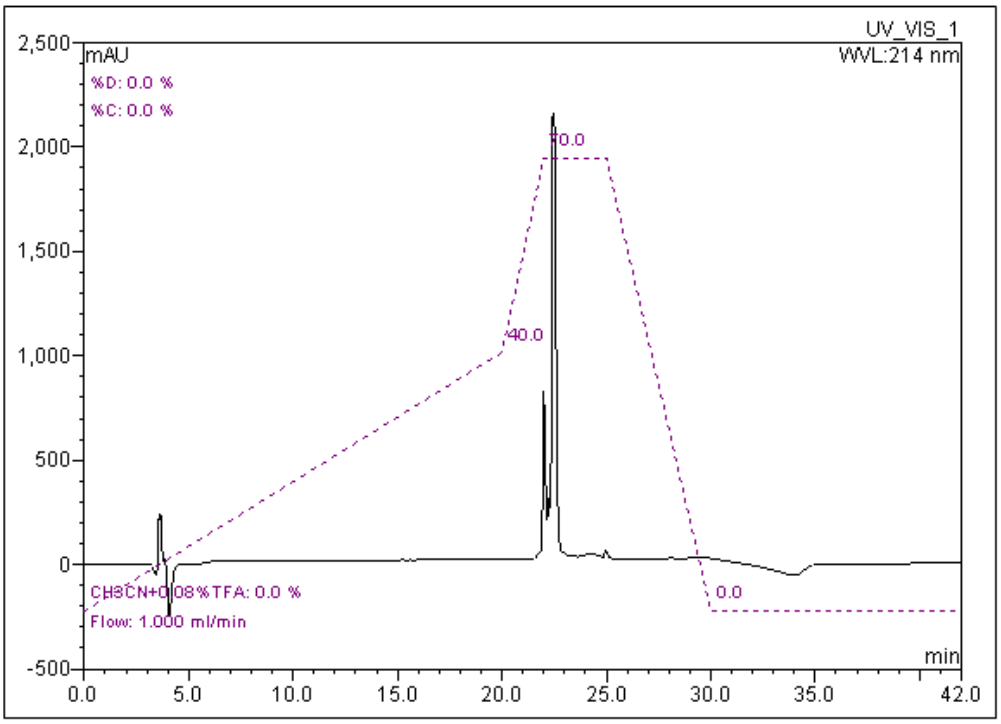

No.	Ret.Time	Peak Name	Height	Area	Rel.Area	Amount	Type
	min		mAU	mAU*min	%	n.a.	
1	0.21	n.a.	0.034	0.001	0.00	n.a.	BMB
2	2.72	n.a.	0.095	0.024	0.00	n.a.	Ru
3	3.06	n.a.	0.040	0.002	0.00	n.a.	Ru
4	3.16	n.a.	46.515	72.543	1.26	n.a.	BMB
5	3.65	n.a.	356.879	100.017	1.74	n.a.	BMB
6	3.90	n.a.	80.323	12.940	0.23	n.a.	Rd
7	22.00	n.a.	957.593	3742.187	65.10	n.a.	BM
8	22.24	n.a.	77.027	5.442	0.09	n.a.	Ru
9	22.46	n.a.	2289.209	711.481	12.38	n.a.	M
10	23.30	n.a.	159.882	394.115	6.86	n.a.	M
11	24.21	n.a.	11.562	8.172	0.14	n.a.	Rd
12	24.97	n.a.	30.442	4.738	0.08	n.a.	Rd
13	25.57	n.a.	2.214	0.185	0.00	n.a.	Rd
14	25.72	n.a.	4.973	0.522	0.01	n.a.	Rd
15	25.98	n.a.	124.184	602.807	10.49	n.a.	MB
16	26.26	n.a.	4.749	0.838	0.01	n.a.	Rd
17	26.96	n.a.	1.620	0.434	0.01	n.a.	Rd
18	28.08	n.a.	9.509	2.323	0.04	n.a.	Rd
19	29.87	n.a.	25.506	89.830	1.56	n.a.	Rd
Total:			4182.359	5748.600	100.00	0.000	

3.3.2.2 HPLC analysis of lysozyme after tryptic digestion

monitored at 280 nm.

Sample Name:		*Injection Volume:*	**100.0**
Vial Number:	**RA4**	*Channel:*	**UV_VIS_2**
Sample Type:	**unknown**	*Wavelength:*	**280**
Control Program:		*Bandwidth:*	**8**
Quantif. Method:	**default**	*Dilution Factor:*	**1.0000**
Recording Time:	**7/04/2010 13:27**	*Sample Weight:*	**1.0000**
Run Time (min):	**42.00**	*Sample Amount:*	**1.0000**

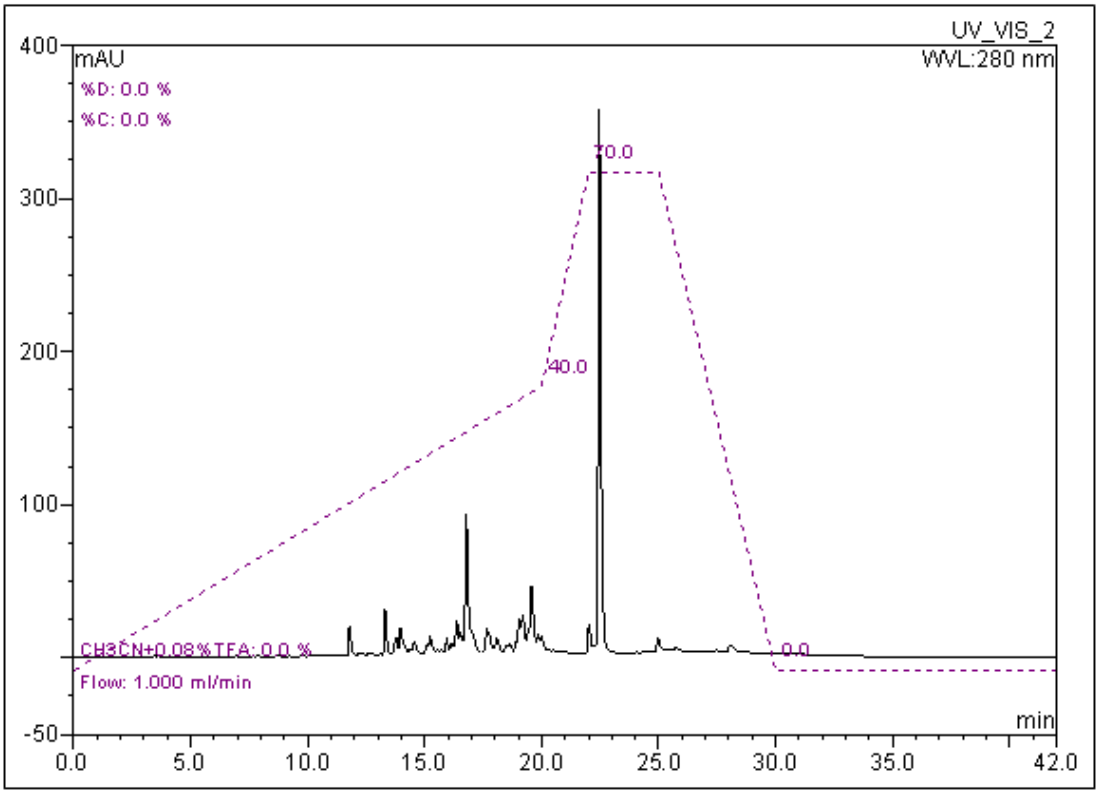

No.	Ret.Time	Peak Name	Height	Area	Rel.Area	Amount	Type
	min		mAU	mAU*min	%	n.a.	
1	0.34	n.a.	0.047	0.005	0.00	n.a.	BMb
2	0.52	n.a.	0.030	0.002	0.00	n.a.	bMB
3	0.77	n.a.	0.030	0.003	0.00	n.a.	BMB
4	3.44	n.a.	1.172	0.144	0.12	n.a.	BM
5	3.55	n.a.	2.356	0.259	0.22	n.a.	MB
6	3.61	n.a.	0.332	0.011	0.01	n.a.	Rd
7	3.85	n.a.	0.054	0.002	0.00	n.a.	Rd
8	4.49	n.a.	0.074	0.016	0.01	n.a.	BM
9	4.78	n.a.	0.084	0.027	0.02	n.a.	MB

No.	Ret.Time	Peak Name	Height	Area	Rel.Area	Amount	Type
	min		mAU	mAU*min	%	n.a.	
10	5.27	n.a.	0.012	0.000	0.00	n.a.	BMB
11	5.88	n.a.	0.275	0.073	0.06	n.a.	BM
12	6.10	n.a.	0.046	0.002	0.00	n.a.	Mb
13	6.20	n.a.	0.228	0.032	0.03	n.a.	bMB
14	6.74	n.a.	0.098	0.012	0.01	n.a.	BM
15	6.85	n.a.	0.029	0.000	0.00	n.a.	Ru
16	6.96	n.a.	0.425	0.062	0.05	n.a.	MB
17	7.36	n.a.	0.091	0.007	0.01	n.a.	BMB
18	7.69	n.a.	0.314	0.028	0.02	n.a.	BM
19	7.87	n.a.	0.774	0.078	0.07	n.a.	MB
20	8.20	n.a.	0.152	0.013	0.01	n.a.	BMB
21	8.68	n.a.	0.365	0.084	0.07	n.a.	BMB
22	9.19	n.a.	0.091	0.007	0.01	n.a.	BMB
23	9.74	n.a.	0.028	0.002	0.00	n.a.	BM
24	9.87	n.a.	0.055	0.004	0.00	n.a.	MB
25	10.32	n.a.	0.071	0.011	0.01	n.a.	BMB
26	10.80	n.a.	1.448	0.152	0.13	n.a.	BMB
27	11.42	n.a.	0.863	0.095	0.08	n.a.	BM
28	11.56	n.a.	0.607	0.063	0.05	n.a.	M
29	11.67	n.a.	0.043	0.001	0.00	n.a.	MB
30	11.79	n.a.	19.372	2.102	1.78	n.a.	BMb
31	12.04	n.a.	0.192	0.008	0.01	n.a.	bMB
32	12.16	n.a.	0.381	0.016	0.01	n.a.	Ru
33	12.26	n.a.	1.662	0.217	0.18	n.a.	BM
34	12.38	n.a.	1.074	0.105	0.09	n.a.	MB
35	12.60	n.a.	1.474	0.124	0.10	n.a.	BM
36	12.72	n.a.	1.808	0.259	0.22	n.a.	MB
37	13.10	n.a.	0.579	0.054	0.05	n.a.	BMB
38	13.31	n.a.	29.370	3.273	2.77	n.a.	BM
39	13.80	n.a.	10.844	1.701	1.44	n.a.	M
40	13.97	n.a.	16.981	2.855	2.42	n.a.	M
41	14.39	n.a.	3.271	0.295	0.25	n.a.	M
42	14.58	n.a.	7.241	1.390	1.18	n.a.	MB
43	14.77	n.a.	0.337	0.016	0.01	n.a.	Rd
44	14.89	n.a.	0.441	0.031	0.03	n.a.	BM
45	15.11	n.a.	6.025	0.658	0.56	n.a.	M
46	15.24	n.a.	11.173	1.996	1.69	n.a.	M

No.	Ret.Time	Peak Name	Height	Area	Rel.Area	Amount	Type
	min		mAU	mAU*min	%	n.a.	
47	15.56	n.a.	1.077	0.099	0.08	n.a.	Rd
48	15.74	n.a.	1.004	0.097	0.08	n.a.	Rd
49	15.94	n.a.	9.363	0.967	0.82	n.a.	M
50	16.12	n.a.	5.379	0.893	0.76	n.a.	M
51	16.20	n.a.	0.814	0.040	0.03	n.a.	Rd
52	16.37	n.a.	20.589	2.747	2.33	n.a.	M
53	16.53	n.a.	12.981	1.888	1.60	n.a.	M
54	16.78	n.a.	89.922	15.192	12.87	n.a.	MB
55	17.11	n.a.	2.645	0.266	0.23	n.a.	Rd
56	17.44	n.a.	0.425	0.025	0.02	n.a.	BM
57	17.66	n.a.	15.273	3.055	2.59	n.a.	M
58	17.76	n.a.	2.659	0.197	0.17	n.a.	Rd
59	18.08	n.a.	9.577	1.555	1.32	n.a.	MB
60	18.51	n.a.	3.778	0.509	0.43	n.a.	BM
61	18.64	n.a.	4.714	0.618	0.52	n.a.	MB
62	18.89	n.a.	2.021	0.120	0.10	n.a.	Ru
63	19.03	n.a.	20.321	2.578	2.18	n.a.	BM
64	19.19	n.a.	23.121	3.984	3.37	n.a.	M
65	19.40	n.a.	1.929	0.104	0.09	n.a.	Ru
66	19.56	n.a.	42.482	8.205	6.95	n.a.	M
67	19.83	n.a.	10.637	1.329	1.13	n.a.	M
68	19.99	n.a.	9.508	1.520	1.29	n.a.	Mb
69	20.27	n.a.	0.335	0.025	0.02	n.a.	Rd
70	20.50	n.a.	0.536	0.078	0.07	n.a.	bMB
71	20.91	n.a.	0.342	0.051	0.04	n.a.	BMb
72	21.10	n.a.	0.056	0.001	0.00	n.a.	bMB
73	21.55	n.a.	0.143	0.011	0.01	n.a.	BMB
74	21.70	n.a.	0.203	0.022	0.02	n.a.	BMB
75	21.82	n.a.	0.030	0.002	0.00	n.a.	Rd
76	22.02	n.a.	18.948	2.632	2.23	n.a.	BM
77	22.26	n.a.	4.883	0.469	0.40	n.a.	M
78	22.46	n.a.	355.085	48.451	41.04	n.a.	Mb
79	23.28	n.a.	0.033	0.001	0.00	n.a.	bMB
80	23.99	n.a.	0.157	0.048	0.04	n.a.	BMB
81	24.39	n.a.	0.042	0.002	0.00	n.a.	BMB
82	24.97	n.a.	9.546	1.708	1.45	n.a.	BM
83	25.39	n.a.	0.203	0.023	0.02	n.a.	Ru

No.	Ret.Time	Peak Name	Height	Area	Rel.Area	Amount	Type
	min		mAU	mAU*min	%	n.a.	
84	25.58	n.a.	1.087	0.357	0.30	n.a.	M
85	25.74	n.a.	2.606	0.450	0.38	n.a.	MB
86	27.01	n.a.	0.305	0.026	0.02	n.a.	BM
87	27.08	n.a.	0.310	0.037	0.03	n.a.	MB
88	27.46	n.a.	1.112	0.181	0.15	n.a.	BMB
89	28.07	n.a.	4.576	1.158	0.98	n.a.	BMB
90	28.82	n.a.	0.083	0.004	0.00	n.a.	BMB
91	28.97	n.a.	0.054	0.003	0.00	n.a.	BMb
92	29.03	n.a.	0.051	0.001	0.00	n.a.	bMB
93	29.20	n.a.	0.043	0.002	0.00	n.a.	BMB
94	33.84	n.a.	0.077	0.007	0.01	n.a.	BMB
95	34.01	n.a.	0.045	0.001	0.00	n.a.	BMB
96	35.70	n.a.	0.029	0.002	0.00	n.a.	BMB
97	36.92	n.a.	0.024	0.001	0.00	n.a.	BMb
98	37.07	n.a.	0.036	0.002	0.00	n.a.	bMB
99	37.58	n.a.	0.021	0.001	0.00	n.a.	BMB
100	39.50	n.a.	0.018	0.002	0.00	n.a.	BMB
101	40.18	n.a.	0.016	0.001	0.00	n.a.	BMB
102	40.43	n.a.	0.015	0.002	0.00	n.a.	BMB
103	40.82	n.a.	0.021	0.001	0.00	n.a.	BMB
104	41.23	n.a.	0.054	0.005	0.00	n.a.	BMB
105	41.53	n.a.	0.036	0.001	0.00	n.a.	BMB
106	41.88	n.a.	0.049	0.004	0.00	n.a.	BMB
Total:			813.849	118.061	100.00	0.000	

monitored at 214 nm.

Sample Name:		*Injection Volume:*	**100.0**
Vial Number:	**RA4**	*Channel:*	**UV_VIS_1**
Sample Type:	**unknown**	*Wavelength:*	**214**
Control Program:		*Bandwidth:*	**8**
Quantif. Method:	**Default**	*Dilution Factor:*	**1.0000**
Recording Time:	**7/04/2010 13:27**	*Sample Weight:*	**1.0000**
Run Time (min):	**42.00**	*Sample Amount:*	**1.0000**

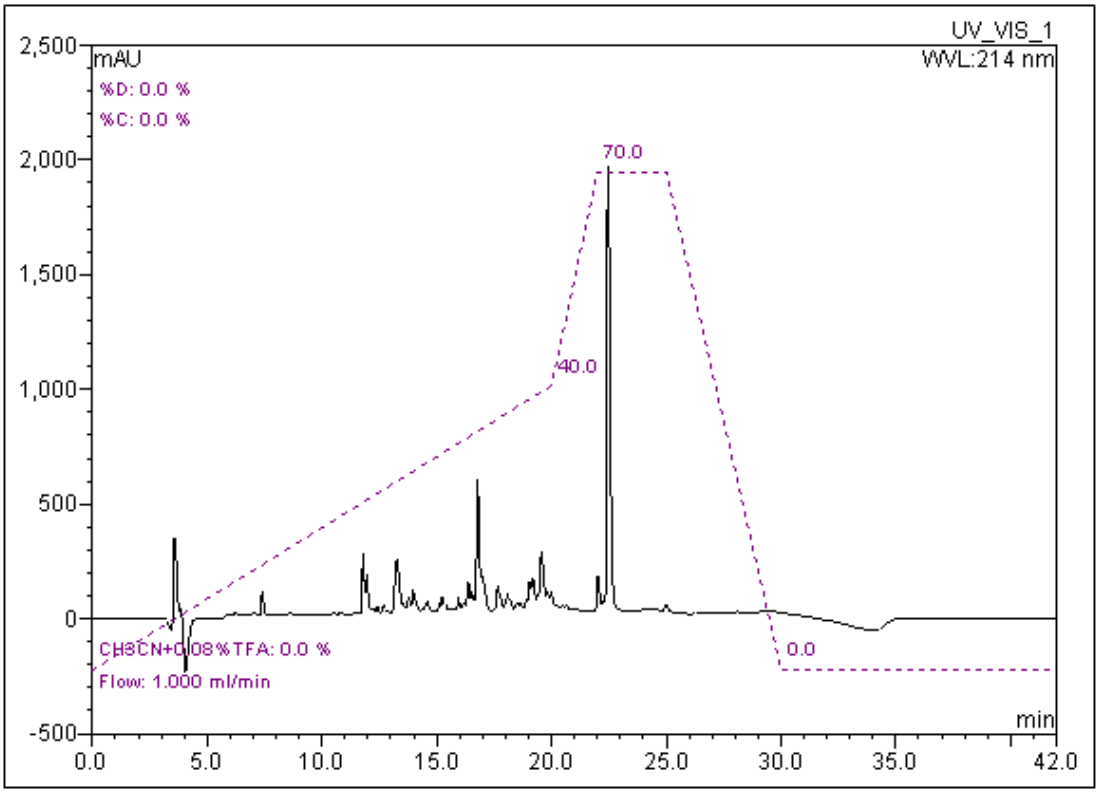

No.	Ret.Time	Peak Name	Height	Area	Rel.Area	Amount	Type
	min		mAU	mAU*min	%	n.a.	
1	0.16	n.a.	0.036	0.003	0.00	n.a.	BMb
2	0.71	n.a.	7.338	1.745	0.10	n.a.	bM
3	1.41	n.a.	0.060	0.011	0.00	n.a.	Ru
4	2.27	n.a.	0.077	0.015	0.00	n.a.	Ru
5	3.16	n.a.	45.454	71.819	4.31	n.a.	MB
6	3.58	n.a.	447.551	108.170	6.50	n.a.	BMB
7	3.89	n.a.	99.251	15.236	0.92	n.a.	Rd
8	4.43	n.a.	205.252	371.060	22.29	n.a.	BM
9	6.51	n.a.	102.311	33.856	2.03	n.a.	M
10	6.59	n.a.	0.829	0.056	0.00	n.a.	Rd
11	7.04	n.a.	9.058	1.705	0.10	n.a.	Ru
12	7.39	n.a.	157.069	66.032	3.97	n.a.	M
13	7.67	n.a.	1.310	0.096	0.01	n.a.	Rd
14	7.86	n.a.	6.168	0.540	0.03	n.a.	Rd
15	7.99	n.a.	15.047	1.776	0.11	n.a.	M
16	8.14	n.a.	7.989	0.683	0.04	n.a.	Mb
17	8.58	n.a.	7.880	1.561	0.09	n.a.	bMB
18	9.21	n.a.	3.755	0.769	0.05	n.a.	BMB
19	9.59	n.a.	0.563	0.090	0.01	n.a.	Rd

No.	Ret.Time	Peak Name	Height	Area	Rel.Area	Amount	Type
	min		mAU	mAU*min	%	n.a.	
20	9.90	n.a.	2.933	0.466	0.03	n.a.	BM
21	10.06	n.a.	3.872	0.573	0.03	n.a.	MB
22	10.31	n.a.	0.200	0.011	0.00	n.a.	BMB
23	10.49	n.a.	8.775	0.889	0.05	n.a.	BMb
24	10.79	n.a.	9.899	1.033	0.06	n.a.	bMB
25	11.08	n.a.	0.510	0.031	0.00	n.a.	BM
26	11.17	n.a.	0.610	0.057	0.00	n.a.	M
27	11.31	n.a.	0.199	0.013	0.00	n.a.	M
28	11.43	n.a.	6.174	0.702	0.04	n.a.	M
29	11.56	n.a.	5.054	0.639	0.04	n.a.	M
30	11.79	n.a.	261.140	26.985	1.62	n.a.	M
31	11.95	n.a.	171.842	21.903	1.32	n.a.	M
32	12.17	n.a.	22.628	1.772	0.11	n.a.	M
33	12.25	n.a.	20.855	1.942	0.12	n.a.	M
34	12.41	n.a.	35.087	4.015	0.24	n.a.	M
35	12.69	n.a.	37.127	6.547	0.39	n.a.	M
36	13.21	n.a.	226.567	20.013	1.20	n.a.	M
37	13.30	n.a.	231.834	37.309	2.24	n.a.	M
38	13.80	n.a.	65.221	10.624	0.64	n.a.	M
39	13.97	n.a.	100.569	17.522	1.05	n.a.	M
40	14.38	n.a.	8.930	0.526	0.03	n.a.	Ru
41	14.59	n.a.	49.675	11.283	0.68	n.a.	M
42	14.89	n.a.	6.217	0.563	0.03	n.a.	M
43	15.11	n.a.	37.745	4.474	0.27	n.a.	M
44	15.24	n.a.	69.036	13.902	0.83	n.a.	M
45	15.39	n.a.	8.595	0.489	0.03	n.a.	Rd
46	15.57	n.a.	3.964	0.326	0.02	n.a.	Rd
47	15.73	n.a.	4.954	0.440	0.03	n.a.	Ru
48	15.94	n.a.	59.839	8.224	0.49	n.a.	M
49	16.12	n.a.	35.083	5.954	0.36	n.a.	M
50	16.20	n.a.	4.801	0.232	0.01	n.a.	Rd
51	16.37	n.a.	127.861	17.228	1.03	n.a.	M
52	16.53	n.a.	84.826	11.904	0.71	n.a.	M
53	16.78	n.a.	578.522	108.207	6.50	n.a.	M
54	17.04	n.a.	28.616	4.529	0.27	n.a.	Rd
55	17.44	n.a.	6.737	0.623	0.04	n.a.	M
56	17.66	n.a.	114.587	22.479	1.35	n.a.	M

No.	Ret.Time	Peak Name	Height	Area	Rel.Area	Amount	Type
	min		mAU	mAU*min	%	n.a.	
57	18.08	n.a.	75.314	17.265	1.04	n.a.	M
58	18.20	n.a.	8.229	0.532	0.03	n.a.	Rd
59	18.50	n.a.	33.595	5.124	0.31	n.a.	M
60	18.63	n.a.	36.467	5.672	0.34	n.a.	M
61	18.89	n.a.	13.473	0.902	0.05	n.a.	Ru
62	19.03	n.a.	127.001	18.851	1.13	n.a.	M
63	19.19	n.a.	139.428	24.717	1.48	n.a.	M
64	19.40	n.a.	11.443	0.621	0.04	n.a.	Ru
65	19.56	n.a.	260.727	74.175	4.45	n.a.	M
66	19.83	n.a.	22.886	1.513	0.09	n.a.	Rd
67	20.00	n.a.	33.779	3.292	0.20	n.a.	Rd
68	20.27	n.a.	20.609	3.653	0.22	n.a.	M
69	20.50	n.a.	23.209	2.765	0.17	n.a.	M
70	20.64	n.a.	19.634	2.953	0.18	n.a.	M
71	20.90	n.a.	7.920	1.477	0.09	n.a.	Mb
72	21.22	n.a.	0.682	0.074	0.00	n.a.	bMB
73	21.55	n.a.	2.145	0.204	0.01	n.a.	BM
74	21.70	n.a.	2.014	0.171	0.01	n.a.	M
75	21.81	n.a.	1.549	0.161	0.01	n.a.	M
76	22.02	n.a.	154.707	21.607	1.30	n.a.	M
77	22.26	n.a.	40.781	4.060	0.24	n.a.	M
78	22.46	n.a.	1935.747	326.039	19.58	n.a.	MB
79	23.45	n.a.	0.509	0.095	0.01	n.a.	BMB
80	24.33	n.a.	11.854	8.103	0.49	n.a.	BMb
81	24.97	n.a.	30.621	4.834	0.29	n.a.	bMB
82	25.57	n.a.	2.353	0.199	0.01	n.a.	BMB
83	25.73	n.a.	7.592	0.864	0.05	n.a.	BMB
84	26.27	n.a.	6.456	1.417	0.09	n.a.	BM
85	26.71	n.a.	0.265	0.017	0.00	n.a.	Ru
86	27.06	n.a.	3.956	1.845	0.11	n.a.	M
87	27.45	n.a.	5.830	1.647	0.10	n.a.	M
88	28.09	n.a.	10.348	2.851	0.17	n.a.	Mb
89	29.90	n.a.	25.274	87.679	5.27	n.a.	bMB
Total:			6634.474	1665.032	100.00	0.000	

3.3.2.3 HPLC analysis of intramolecularly crosslinked lysozyme control for tryptic digestion

monitored at 280 nm.

Sample Name:		*Injection Volume:*	**100.0**
Vial Number:	**RA2**	*Channel:*	**UV_VIS_2**
Sample Type:	**unknown**	*Wavelength:*	**280**
Control Program:		*Bandwidth:*	**8**
Quantif. Method:	**default**	*Dilution Factor:*	**1.0000**
Recording Time:	**8/04/2010 11:26**	*Sample Weight:*	**1.0000**
Run Time (min):	**42.00**	*Sample Amount:*	**1.0000**

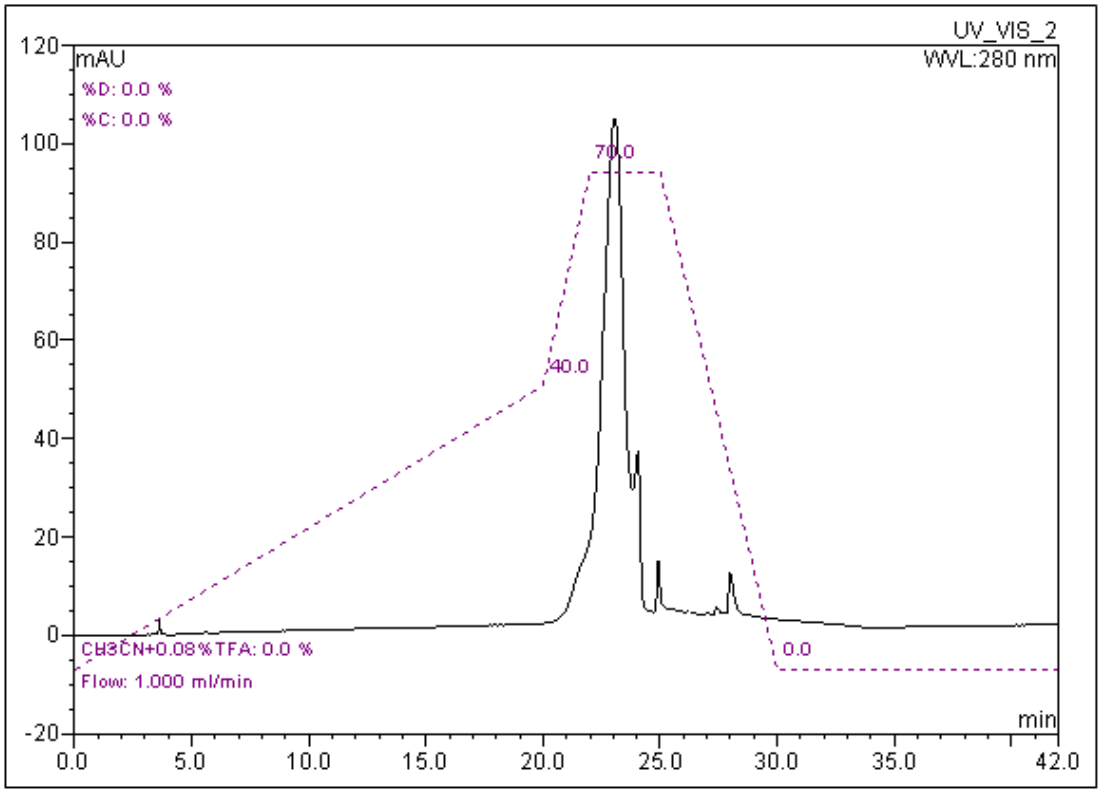

No.	Ret.Time	Peak Name	Height	Area	Rel.Area	Amount	Type
	min		mAU	mAU*min	%	n.a.	
1	0.09	n.a.	0.027	0.001	0.00	n.a.	BMb
2	0.25	n.a.	0.036	0.003	0.00	n.a.	bMB
3	0.40	n.a.	0.053	0.005	0.00	n.a.	bMB
4	0.57	n.a.	0.032	0.003	0.00	n.a.	bMB
5	0.93	n.a.	0.058	0.005	0.00	n.a.	BMB
6	1.62	n.a.	0.091	0.008	0.01	n.a.	BMB
7	3.48	n.a.	0.184	0.029	0.02	n.a.	BM

No.	Ret.Time	Peak Name	Height	Area	Rel.Area	Amount	Type
	Min		mAU	mAU*min	%	n.a.	
8	3.53	n.a.	0.146	0.006	0.00	n.a.	M
9	3.61	n.a.	2.701	0.163	0.12	n.a.	MB
10	3.84	n.a.	0.096	0.008	0.01	n.a.	BMB
11	4.50	n.a.	0.130	0.037	0.03	n.a.	BM
12	4.70	n.a.	0.106	0.026	0.02	n.a.	M
13	5.03	n.a.	0.083	0.005	0.00	n.a.	MB
14	6.95	n.a.	0.050	0.002	0.00	n.a.	BMB
15	7.67	n.a.	0.025	0.002	0.00	n.a.	BMB
16	8.26	n.a.	0.031	0.003	0.00	n.a.	BMB
17	9.62	n.a.	0.030	0.004	0.00	n.a.	BMB
18	9.87	n.a.	0.051	0.002	0.00	n.a.	BMB
19	10.41	n.a.	0.083	0.012	0.01	n.a.	BMB
20	11.27	n.a.	0.035	0.002	0.00	n.a.	BM
21	11.83	n.a.	0.063	0.024	0.02	n.a.	M
22	11.96	n.a.	0.076	0.021	0.02	n.a.	M
23	12.38	n.a.	0.094	0.010	0.01	n.a.	M
24	12.61	n.a.	0.060	0.008	0.01	n.a.	M
25	12.79	n.a.	0.031	0.002	0.00	n.a.	Mb
26	12.97	n.a.	0.105	0.014	0.01	n.a.	bMB
27	13.58	n.a.	0.047	0.003	0.00	n.a.	BMB
28	14.07	n.a.	0.094	0.008	0.01	n.a.	BMB
29	14.20	n.a.	0.018	0.000	0.00	n.a.	BMB
30	15.86	n.a.	0.030	0.003	0.00	n.a.	BMB
31	17.60	n.a.	0.058	0.012	0.01	n.a.	BM
32	17.96	n.a.	0.051	0.005	0.00	n.a.	MB
33	23.05	n.a.	102.045	123.818	92.13	n.a.	BM
34	24.07	n.a.	20.053	4.133	3.08	n.a.	Rd
35	24.91	n.a.	11.504	2.392	1.78	n.a.	M
36	25.40	n.a.	0.109	0.005	0.00	n.a.	Ru
37	25.54	n.a.	1.606	1.190	0.89	n.a.	MB
38	25.92	n.a.	0.132	0.007	0.01	n.a.	Rd
39	26.19	n.a.	0.183	0.029	0.02	n.a.	Rd
40	26.51	n.a.	0.049	0.003	0.00	n.a.	Rd
41	27.03	n.a.	0.286	0.047	0.03	n.a.	Rd
42	27.39	n.a.	1.568	0.228	0.17	n.a.	BMB
43	27.99	n.a.	8.295	2.057	1.53	n.a.	BMB
44	28.80	n.a.	0.088	0.011	0.01	n.a.	BMB

No.	Ret.Time	Peak Name	Height	Area	Rel.Area	Amount	Type
	min		mAU	mAU*min	%	n.a.	
45	30.45	n.a.	0.021	0.001	0.00	n.a.	BMB
46	33.12	n.a.	0.042	0.002	0.00	n.a.	BMB
47	35.49	n.a.	0.025	0.002	0.00	n.a.	BMB
48	36.39	n.a.	0.027	0.001	0.00	n.a.	BMB
49	37.05	n.a.	0.060	0.006	0.00	n.a.	BM
50	37.15	n.a.	0.055	0.003	0.00	n.a.	MB
51	37.40	n.a.	0.069	0.004	0.00	n.a.	BM
52	37.50	n.a.	0.046	0.003	0.00	n.a.	MB
53	37.75	n.a.	0.031	0.001	0.00	n.a.	BMB
54	38.28	n.a.	0.051	0.004	0.00	n.a.	BMB
55	39.76	n.a.	0.005	0.000	0.00	n.a.	BMB
56	41.25	n.a.	0.060	0.005	0.00	n.a.	BMB
57	41.97	n.a.	0.046	0.002	0.00	n.a.	BMB
Total:			151.231	134.391	100.00	0.000	

monitored at 214 nm.

Sample Name:		*Injection Volume:*	**100.0**
Vial Number:	**RA2**	*Channel:*	**UV_VIS_1**
Sample Type:	**unknown**	*Wavelength:*	**214**
Control Program:		*Bandwidth:*	**8**
Quantif. Method:	**default**	*Dilution Factor:*	**1.0000**
Recording Time:	**8/04/2010 11:26**	*Sample Weight:*	**1.0000**
Run Time (min):	**42.00**	*Sample Amount:*	**1.0000**

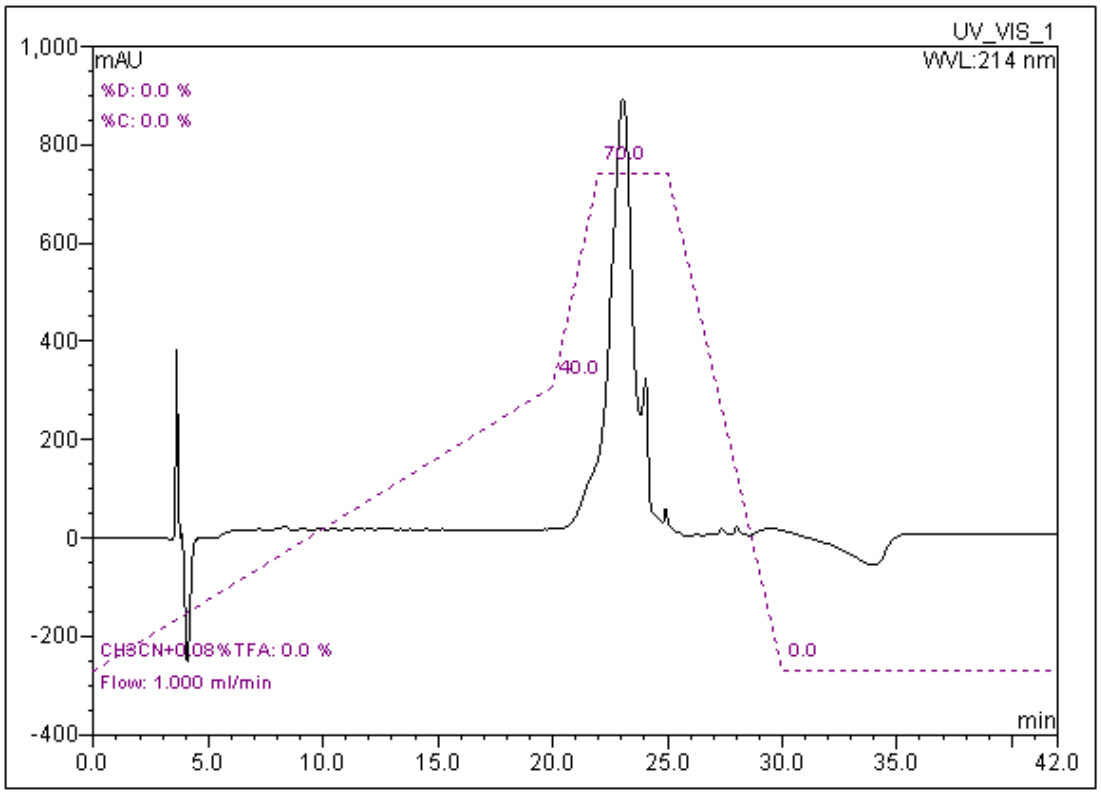

No.	Ret.Time	Peak Name	Height	Area	Rel.Area	Amount	Type
	min		mAU	mAU*min	%	n.a.	
1	0.33	n.a.	0.067	0.008	0.00	n.a.	BMB
2	0.48	n.a.	0.065	0.005	0.00	n.a.	bMB
3	0.80	n.a.	0.053	0.004	0.00	n.a.	BMB
4	1.25	n.a.	0.061	0.004	0.00	n.a.	BMB
5	1.89	n.a.	0.049	0.003	0.00	n.a.	BMb
6	3.06	n.a.	4.748	3.694	0.08	n.a.	bMb
7	3.60	n.a.	470.523	91.229	2.05	n.a.	bMB
8	3.84	n.a.	62.123	12.423	0.28	n.a.	Rd
9	8.38	n.a.	226.316	1054.606	23.73	n.a.	BM
10	9.15	n.a.	213.145	295.766	6.66	n.a.	M
11	9.91	n.a.	2.094	0.693	0.02	n.a.	Rd
12	10.56	n.a.	1.748	0.668	0.02	n.a.	Ru
13	11.03	n.a.	1.666	0.414	0.01	n.a.	Ru
14	11.59	n.a.	185.905	413.003	9.29	n.a.	M
15	11.98	n.a.	1.129	0.300	0.01	n.a.	Rd
16	12.47	n.a.	175.136	279.373	6.29	n.a.	M
17	12.67	n.a.	0.089	0.010	0.00	n.a.	Rd
18	12.98	n.a.	0.769	0.146	0.00	n.a.	Rd
19	13.34	n.a.	0.548	0.121	0.00	n.a.	Rd

No.	Ret.Time	Peak Name	Height	Area	Rel.Area	Amount	Type
	min		mAU	mAU*min	%	n.a.	
20	13.78	n.a.	0.991	0.190	0.00	n.a.	Rd
21	14.16	n.a.	0.624	0.100	0.00	n.a.	Ru
22	14.48	n.a.	151.517	106.090	2.39	n.a.	M
23	14.86	n.a.	0.556	0.087	0.00	n.a.	Ru
24	15.19	n.a.	143.017	225.082	5.07	n.a.	M
25	15.53	n.a.	0.328	0.044	0.00	n.a.	Rd
26	15.84	n.a.	0.686	0.098	0.00	n.a.	Rd
27	16.14	n.a.	0.466	0.069	0.00	n.a.	Rd
28	16.45	n.a.	0.498	0.091	0.00	n.a.	Ru
29	16.78	n.a.	0.397	0.066	0.00	n.a.	Ru
30	17.08	n.a.	120.782	147.917	3.33	n.a.	M
31	17.31	n.a.	0.080	0.010	0.00	n.a.	Rd
32	17.67	n.a.	0.297	0.041	0.00	n.a.	Ru
33	17.91	n.a.	111.304	87.084	1.96	n.a.	M
34	18.47	n.a.	0.212	0.030	0.00	n.a.	Ru
35	18.74	n.a.	0.064	0.004	0.00	n.a.	Ru
36	18.98	n.a.	0.291	0.049	0.00	n.a.	Ru
37	19.45	n.a.	0.275	0.033	0.00	n.a.	Ru
38	19.66	n.a.	91.724	145.615	3.28	n.a.	M
39	19.92	n.a.	89.080	22.671	0.51	n.a.	M
40	23.05	n.a.	927.646	1382.389	31.11	n.a.	M
41	24.05	n.a.	168.924	35.511	0.80	n.a.	Rd
42	24.91	n.a.	74.315	30.569	0.69	n.a.	M
43	25.52	n.a.	1.258	0.137	0.00	n.a.	Rd
44	26.24	n.a.	5.774	3.582	0.08	n.a.	M
45	26.60	n.a.	0.496	0.196	0.00	n.a.	MB
46	27.02	n.a.	1.356	0.308	0.01	n.a.	Ru
47	27.37	n.a.	13.385	4.590	0.10	n.a.	bM
48	28.02	n.a.	17.237	4.522	0.10	n.a.	MB
49	29.70	n.a.	25.912	93.994	2.12	n.a.	BMB
Total:			3295.727	4443.638	100.00	0.000	

3.3.2.4 HPLC analysis of intramolecularly crosslinked lysozyme after tryptic digestion

monitored at 280 nm.

Sample Name:		*Injection Volume:*	**100.0**
Vial Number:	**RA5**	*Channel:*	**UV_VIS_2**
Sample Type:	**unknown**	*Wavelength:*	**280**
Control Program:		*Bandwidth:*	**8**
Quantif. Method:	**default**	*Dilution Factor:*	**1.0000**
Recording Time:	**7/04/2010 14:10**	*Sample Weight:*	**1.0000**
Run Time (min):	**42.00**	*Sample Amount:*	**1.0000**

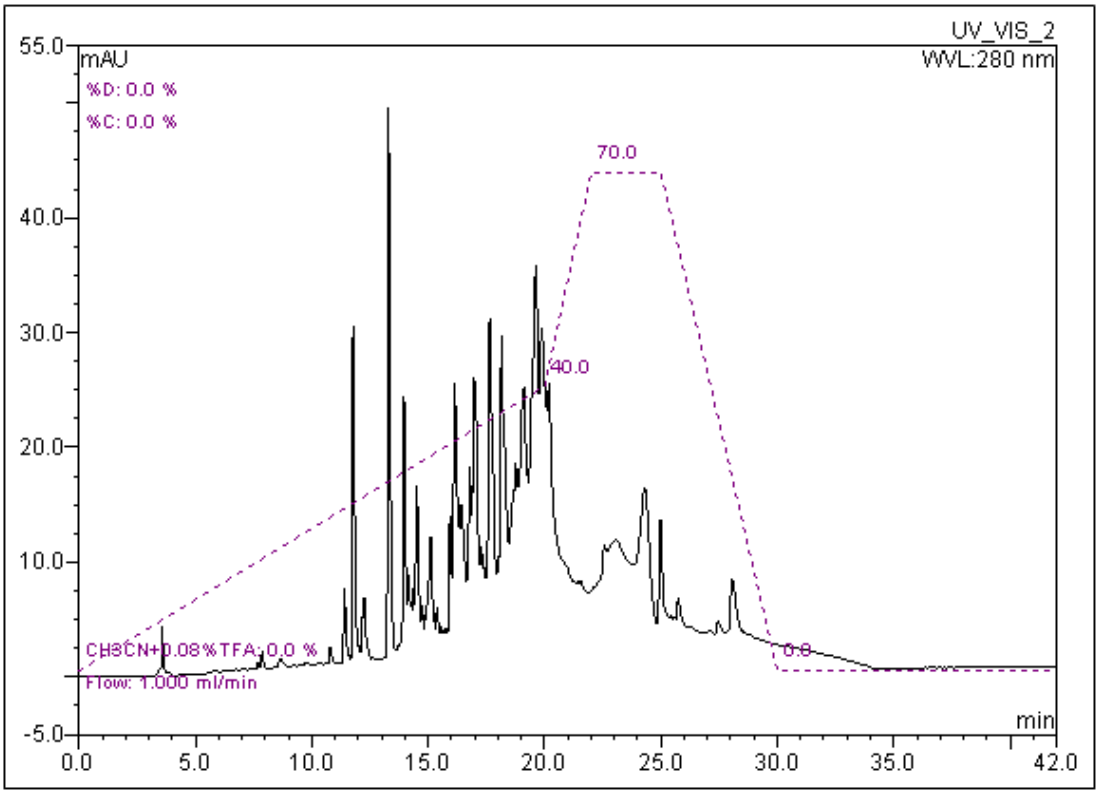

No.	Ret.Time	Peak Name	Height	Area	Rel.Area	Amount	Type
	min		mAU	mAU*min	%	n.a.	
1	0.04	n.a.	0.044	0.001	0.00	n.a.	BMB
2	0.34	n.a.	0.053	0.006	0.00	n.a.	BMB
3	1.04	n.a.	0.039	0.002	0.00	n.a.	BMb
4	1.19	n.a.	0.041	0.005	0.00	n.a.	bMB
5	1.61	n.a.	0.042	0.003	0.00	n.a.	BMb
6	1.73	n.a.	0.044	0.003	0.00	n.a.	bMB
7	3.56	n.a.	4.365	0.467	0.35	n.a.	BM
8	3.63	n.a.	0.891	0.026	0.02	n.a.	Rd

No.	Ret.Time	Peak Name	Height	Area	Rel.Area	Amount	Type
	min		mAU	mAU*min	%	n.a.	
9	3.83	n.a.	0.395	0.074	0.06	n.a.	Mb
10	4.07	n.a.	0.030	0.001	0.00	n.a.	bMB
11	4.38	n.a.	0.091	0.018	0.01	n.a.	BM
12	4.60	n.a.	0.092	0.007	0.01	n.a.	MB
13	5.31	n.a.	0.063	0.004	0.00	n.a.	BMB
14	5.86	n.a.	0.044	0.002	0.00	n.a.	BMB
15	6.78	n.a.	0.070	0.004	0.00	n.a.	BMB
16	7.04	n.a.	0.117	0.012	0.01	n.a.	BMB
17	7.37	n.a.	0.051	0.005	0.00	n.a.	BMB
18	7.67	n.a.	0.630	0.061	0.05	n.a.	BM
19	7.86	n.a.	1.489	0.152	0.12	n.a.	MB
20	8.67	n.a.	0.748	0.172	0.13	n.a.	BMB
21	9.32	n.a.	0.047	0.003	0.00	n.a.	BMB
22	9.77	n.a.	0.235	0.036	0.03	n.a.	BM
23	10.03	n.a.	0.107	0.010	0.01	n.a.	M
24	10.29	n.a.	0.229	0.034	0.03	n.a.	M
25	10.58	n.a.	0.135	0.016	0.01	n.a.	MB
26	10.80	n.a.	1.556	0.171	0.13	n.a.	BMB
27	11.15	n.a.	0.050	0.002	0.00	n.a.	BMB
28	11.40	n.a.	6.362	0.755	0.57	n.a.	BMB
29	11.77	n.a.	29.017	3.322	2.53	n.a.	BM
30	12.02	n.a.	1.205	0.098	0.07	n.a.	M
31	12.24	n.a.	5.378	0.985	0.75	n.a.	MB
32	12.63	n.a.	0.123	0.014	0.01	n.a.	BMB
33	13.15	n.a.	0.117	0.009	0.01	n.a.	BM
34	13.30	n.a.	48.059	5.608	4.26	n.a.	M
35	13.61	n.a.	0.841	0.078	0.06	n.a.	M
36	13.73	n.a.	1.095	0.084	0.06	n.a.	M
37	13.96	n.a.	22.759	3.741	2.84	n.a.	M
38	14.16	n.a.	2.572	0.169	0.13	n.a.	Rd
39	14.27	n.a.	0.312	0.012	0.01	n.a.	Rd
40	14.36	n.a.	1.669	0.092	0.07	n.a.	Ru
41	14.51	n.a.	14.930	3.155	2.40	n.a.	M
42	14.76	n.a.	1.580	0.098	0.07	n.a.	Rd
43	14.91	n.a.	0.693	0.048	0.04	n.a.	Ru
44	15.10	n.a.	10.304	2.487	1.89	n.a.	M
45	15.38	n.a.	4.149	0.577	0.44	n.a.	M

No.	Ret.Time	Peak Name	Height	Area	Rel.Area	Amount	Type
	min		mAU	mAU*min	%	n.a.	
46	15.56	n.a.	2.348	0.308	0.23	n.a.	M
47	15.76	n.a.	2.348	0.392	0.30	n.a.	M
48	15.94	n.a.	12.048	1.393	1.06	n.a.	M
49	16.14	n.a.	23.570	7.339	5.58	n.a.	M
50	16.44	n.a.	3.614	0.539	0.41	n.a.	Rd
51	16.79	n.a.	16.183	2.645	2.01	n.a.	M
52	16.97	n.a.	23.959	7.504	5.70	n.a.	M
53	17.29	n.a.	1.715	0.116	0.09	n.a.	Rd
54	17.39	n.a.	0.292	0.012	0.01	n.a.	Rd
55	17.65	n.a.	29.024	6.885	5.23	n.a.	M
56	17.76	n.a.	2.327	0.147	0.11	n.a.	Rd
57	18.01	n.a.	0.585	0.028	0.02	n.a.	Ru
58	18.15	n.a.	27.341	7.591	5.77	n.a.	M
59	18.64	n.a.	1.100	0.065	0.05	n.a.	Ru
60	18.76	n.a.	2.372	0.193	0.15	n.a.	Ru
61	19.12	n.a.	22.794	12.944	9.84	n.a.	M
62	19.62	n.a.	33.165	32.877	24.99	n.a.	M
63	19.88	n.a.	6.247	0.994	0.76	n.a.	Rd
64	20.20	n.a.	5.197	0.598	0.45	n.a.	Rd
65	21.42	n.a.	0.103	0.005	0.00	n.a.	Rd
66	21.56	n.a.	0.382	0.039	0.03	n.a.	Rd
67	22.56	n.a.	1.650	0.184	0.14	n.a.	Ru
68	23.05	n.a.	8.801	13.252	10.07	n.a.	M
69	24.30	n.a.	13.125	7.608	5.78	n.a.	M
70	24.97	n.a.	10.318	3.091	2.35	n.a.	M
71	25.42	n.a.	0.162	0.014	0.01	n.a.	Rd
72	25.58	n.a.	0.214	0.016	0.01	n.a.	Rd
73	25.74	n.a.	1.995	0.281	0.21	n.a.	Rd
74	26.19	n.a.	0.839	0.331	0.25	n.a.	M
75	27.08	n.a.	0.245	0.071	0.05	n.a.	MB
76	27.45	n.a.	1.092	0.169	0.13	n.a.	BMB
77	28.06	n.a.	4.589	1.254	0.95	n.a.	BMB
78	30.64	n.a.	0.044	0.003	0.00	n.a.	BMB
79	34.19	n.a.	0.096	0.008	0.01	n.a.	BMB
80	34.37	n.a.	0.014	0.001	0.00	n.a.	BMb
81	34.52	n.a.	0.022	0.001	0.00	n.a.	bMB
82	36.20	n.a.	0.020	0.003	0.00	n.a.	BMb

No.	Ret.Time	Peak Name	Height	Area	Rel.Area	Amount	Type
	min		mAU	mAU*min	%	n.a.	
83	36.37	n.a.	0.069	0.005	0.00	n.a.	bMB
84	36.68	n.a.	0.043	0.002	0.00	n.a.	BMB
85	37.04	n.a.	0.039	0.004	0.00	n.a.	BMB
86	38.69	n.a.	0.019	0.001	0.00	n.a.	BMB
87	38.99	n.a.	0.069	0.008	0.01	n.a.	BMB
Total:			423.041	131.552	100.00	0.000	

monitored at 214 nm.

Sample Name:		*Injection Volume:*	**100.0**
Vial Number:	**RA5**	*Channel:*	**UV_VIS_1**
Sample Type:	**unknown**	*Wavelength:*	**214**
Control Program:		*Bandwidth:*	**8**
Quantif. Method:	**Default**	*Dilution Factor:*	**1.0000**
Recording Time:	**7/04/2010 14:10**	*Sample Weight:*	**1.0000**
Run Time (min):	**42.00**	*Sample Amount:*	**1.0000**

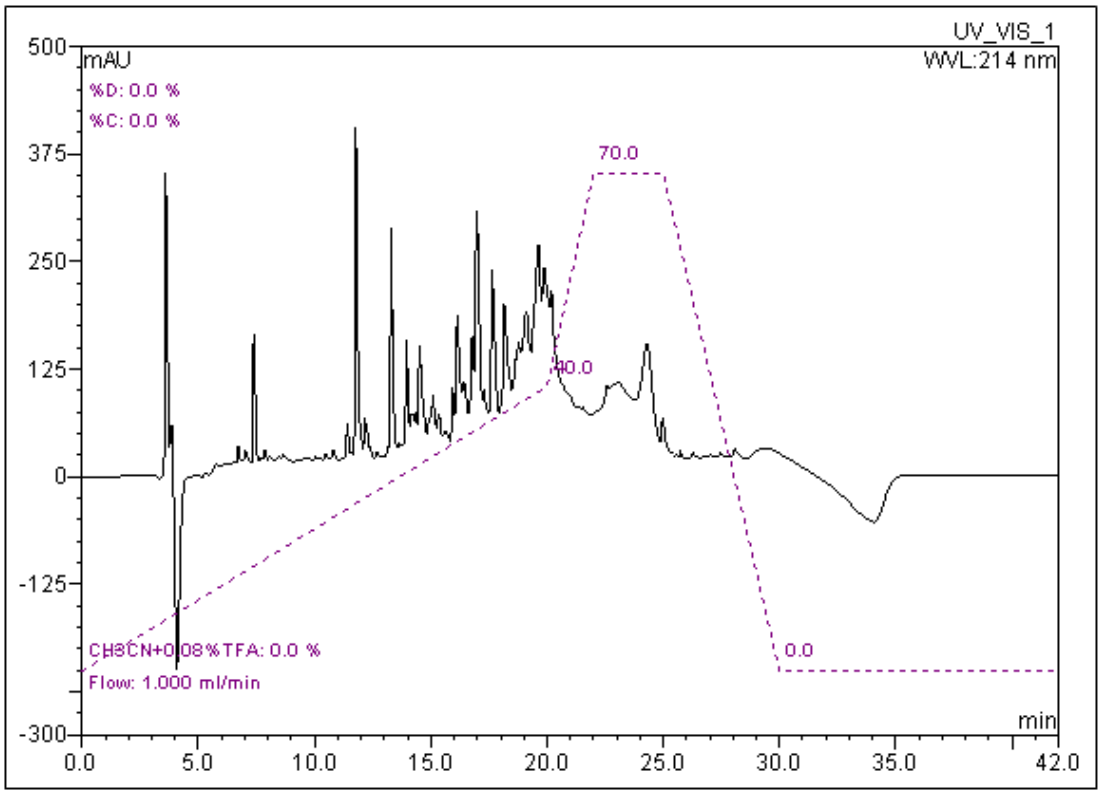

No.	Ret.Time	Peak Name	Height	Area	Rel.Area	Amount	Type
	min		mAU	mAU*min	%	n.a.	
1	0.34	n.a.	0.041	0.003	0.00	n.a.	BMb
2	0.46	n.a.	0.066	0.004	0.00	n.a.	bMB
3	0.97	n.a.	0.037	0.003	0.00	n.a.	BMb
4	1.19	n.a.	0.061	0.006	0.00	n.a.	bMB
5	2.12	n.a.	0.043	0.003	0.00	n.a.	Ru
6	2.29	n.a.	0.085	0.020	0.00	n.a.	Ru
7	2.78	n.a.	1.986	1.215	0.02	n.a.	BM
8	3.12	n.a.	2.463	1.024	0.02	n.a.	MB
9	3.58	n.a.	425.940	72.585	1.23	n.a.	BM
10	3.86	n.a.	217.718	44.312	0.75	n.a.	MB
11	6.72	n.a.	244.729	684.801	11.63	n.a.	BM
12	7.03	n.a.	13.074	1.841	0.03	n.a.	Rd
13	7.39	n.a.	371.853	89.692	1.52	n.a.	M
14	7.66	n.a.	2.956	0.261	0.00	n.a.	Ru
15	7.86	n.a.	233.645	144.877	2.46	n.a.	M
16	8.05	n.a.	4.352	0.501	0.01	n.a.	Rd
17	8.44	n.a.	1.920	0.170	0.00	n.a.	Ru
18	8.66	n.a.	223.878	189.500	3.22	n.a.	M
19	9.20	n.a.	2.312	0.275	0.00	n.a.	Ru
20	9.73	n.a.	2.543	0.763	0.01	n.a.	Ru
21	10.03	n.a.	215.128	270.142	4.59	n.a.	M
22	10.28	n.a.	1.365	0.151	0.00	n.a.	Rd
23	10.49	n.a.	6.289	0.640	0.01	n.a.	Ru
24	10.79	n.a.	217.784	138.977	2.36	n.a.	M
25	11.41	n.a.	244.348	133.001	2.26	n.a.	M
26	11.60	n.a.	2.374	0.149	0.00	n.a.	Rd
27	11.77	n.a.	586.887	132.358	2.25	n.a.	M
28	12.16	n.a.	247.359	102.260	1.74	n.a.	M
29	12.25	n.a.	7.244	0.400	0.01	n.a.	Rd
30	12.38	n.a.	2.359	0.132	0.00	n.a.	Rd
31	12.68	n.a.	7.618	0.869	0.01	n.a.	Ru
32	13.14	n.a.	5.087	0.273	0.00	n.a.	Ru
33	13.30	n.a.	459.723	230.515	3.92	n.a.	M
34	13.63	n.a.	5.710	0.461	0.01	n.a.	Ru
35	13.96	n.a.	327.054	121.493	2.06	n.a.	M
36	14.15	n.a.	5.791	0.275	0.00	n.a.	Ru
37	14.23	n.a.	239.771	75.617	1.28	n.a.	M

No.	Ret.Time	Peak Name	Height	Area	Rel.Area	Amount	Type
	min		mAU	mAU*min	%	n.a.	
38	14.36	n.a.	10.357	0.579	0.01	n.a.	Rd
39	14.52	n.a.	316.397	106.005	1.80	n.a.	M
40	14.91	n.a.	7.121	0.482	0.01	n.a.	Ru
41	15.10	n.a.	254.829	218.448	3.71	n.a.	M
42	15.35	n.a.	19.492	2.170	0.04	n.a.	Rd
43	15.64	n.a.	9.003	1.503	0.03	n.a.	Rd
44	15.93	n.a.	48.011	3.802	0.06	n.a.	Ru
45	16.14	n.a.	343.898	197.390	3.35	n.a.	M
46	16.44	n.a.	20.261	2.867	0.05	n.a.	Rd
47	16.78	n.a.	60.920	6.163	0.10	n.a.	Ru
48	16.97	n.a.	458.621	244.938	4.16	n.a.	M
49	17.29	n.a.	15.504	1.363	0.02	n.a.	Rd
50	17.65	n.a.	386.965	125.016	2.12	n.a.	M
51	18.01	n.a.	3.384	0.159	0.00	n.a.	Ru
52	18.15	n.a.	344.630	144.749	2.46	n.a.	M
53	18.64	n.a.	8.301	0.516	0.01	n.a.	Ru
54	18.77	n.a.	15.851	1.520	0.03	n.a.	Ru
55	19.12	n.a.	47.619	9.306	0.16	n.a.	Ru
56	19.63	n.a.	405.622	930.074	15.80	n.a.	M
57	19.89	n.a.	40.888	6.754	0.11	n.a.	Rd
58	20.20	n.a.	37.770	4.032	0.07	n.a.	Rd
59	21.55	n.a.	3.114	0.422	0.01	n.a.	Rd
60	22.55	n.a.	13.761	1.544	0.03	n.a.	Ru
61	23.04	n.a.	225.234	387.821	6.59	n.a.	M
62	24.29	n.a.	264.348	374.303	6.36	n.a.	M
63	24.97	n.a.	29.206	4.371	0.07	n.a.	Rd
64	25.58	n.a.	2.369	0.200	0.00	n.a.	Rd
65	25.74	n.a.	7.743	0.879	0.01	n.a.	Rd
66	26.27	n.a.	124.717	77.156	1.31	n.a.	M
67	27.00	n.a.	1.957	0.504	0.01	n.a.	Ru
68	27.44	n.a.	117.683	500.841	8.51	n.a.	MB
69	28.09	n.a.	9.330	2.272	0.04	n.a.	Rd
70	29.89	n.a.	25.875	89.452	1.52	n.a.	Rd
Total:			8012.370	5887.168	100.00	0.000	

3.3.2.5 HPLC analysis of lysozyme treated with BIC control for tryptic digestion

monitored at 280 nm.

Sample Name:		*Injection Volume:*	**100.0**
Vial Number:	**RA5**	*Channel:*	**UV_VIS_2**
Sample Type:	**unknown**	*Wavelength:*	**280**
Control Program:		*Bandwidth:*	**8**
Quantif. Method:	**default**	*Dilution Factor:*	**1.0000**
Recording Time:	**14/04/2010 14:11**	*Sample Weight:*	**1.0000**
Run Time (min):	**42.00**	*Sample Amount:*	**1.0000**

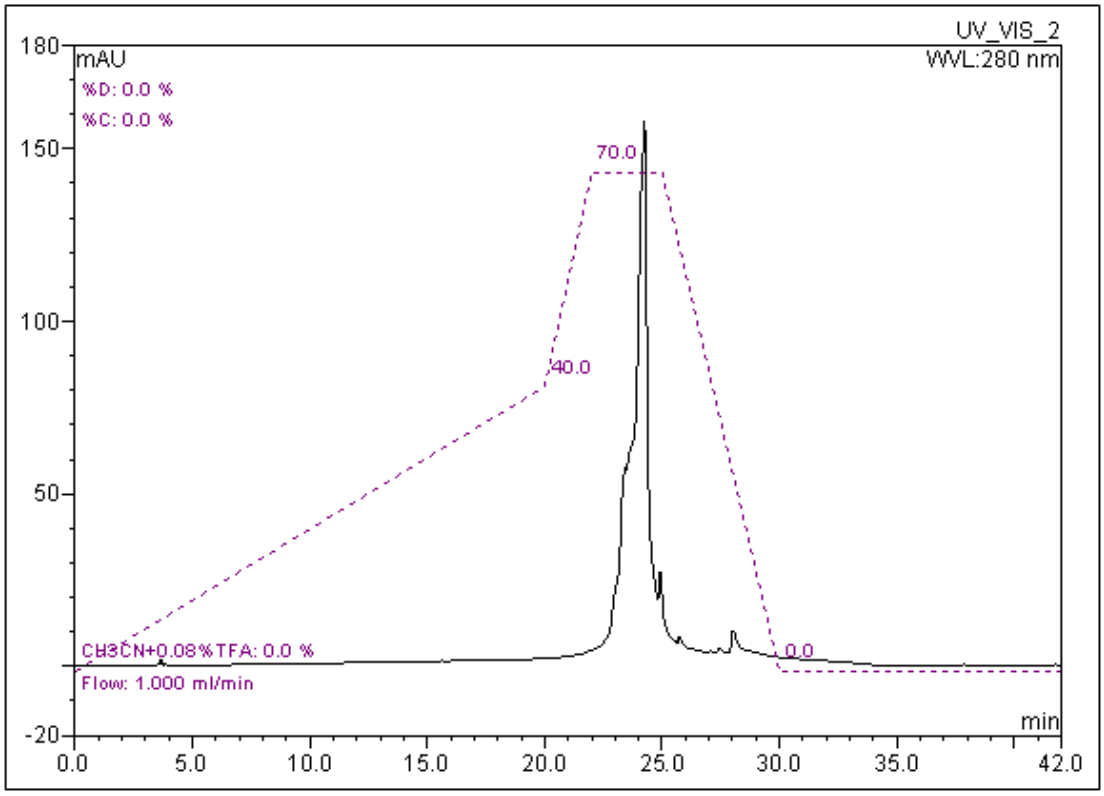

No.	Ret.Time	Peak Name	Height	Area	Rel.Area	Amount	Type
	min		mAU	mAU*min	%	n.a.	
1	0.06	n.a.	0.035	0.001	0.00	n.a.	BMB
2	0.29	n.a.	0.028	0.002	0.00	n.a.	BMB
3	1.73	n.a.	0.038	0.003	0.00	n.a.	BMB
4	2.34	n.a.	0.060	0.005	0.00	n.a.	BM
5	2.47	n.a.	0.078	0.007	0.01	n.a.	MB
6	3.16	n.a.	0.069	0.005	0.00	n.a.	BM
7	3.60	n.a.	0.100	0.002	0.00	n.a.	Ru
8	3.66	n.a.	2.044	0.281	0.23	n.a.	M
9	3.82	n.a.	1.101	0.109	0.09	n.a.	MB

No.	Ret.Time	Peak Name	Height	Area	Rel.Area	Amount	Type
	min		mAU	mAU*min	%	n.a.	
10	4.36	n.a.	0.154	0.058	0.05	n.a.	BM
11	4.72	n.a.	0.093	0.015	0.01	n.a.	M
12	4.84	n.a.	0.051	0.006	0.00	n.a.	MB
13	5.75	n.a.	0.192	0.044	0.03	n.a.	BM
14	6.00	n.a.	0.055	0.008	0.01	n.a.	MB
15	7.06	n.a.	0.035	0.001	0.00	n.a.	BMB
16	7.55	n.a.	0.026	0.002	0.00	n.a.	BMB
17	8.13	n.a.	0.038	0.001	0.00	n.a.	BMB
18	8.70	n.a.	0.097	0.010	0.01	n.a.	BM
19	8.87	n.a.	0.045	0.002	0.00	n.a.	Ru
20	8.95	n.a.	0.029	0.002	0.00	n.a.	Ru
21	9.13	n.a.	0.256	0.049	0.04	n.a.	M
22	9.40	n.a.	0.107	0.021	0.02	n.a.	M
23	9.69	n.a.	0.054	0.004	0.00	n.a.	M
24	9.99	n.a.	0.096	0.014	0.01	n.a.	MB
25	10.53	n.a.	0.050	0.004	0.00	n.a.	BMB
26	10.82	n.a.	0.063	0.005	0.00	n.a.	BMB
27	11.83	n.a.	0.071	0.004	0.00	n.a.	BMB
28	12.53	n.a.	0.097	0.009	0.01	n.a.	BMB
29	12.73	n.a.	0.058	0.005	0.00	n.a.	bMb
30	12.98	n.a.	0.133	0.021	0.02	n.a.	bMB
31	13.50	n.a.	0.064	0.004	0.00	n.a.	BMB
32	13.76	n.a.	0.103	0.015	0.01	n.a.	bMB
33	14.22	n.a.	0.287	0.065	0.05	n.a.	BMB
34	15.61	n.a.	0.185	0.016	0.01	n.a.	BMB
35	16.17	n.a.	0.021	0.001	0.00	n.a.	BM
36	16.30	n.a.	0.298	0.038	0.03	n.a.	MB
37	16.66	n.a.	0.073	0.006	0.00	n.a.	BMB
38	17.94	n.a.	0.059	0.005	0.00	n.a.	BMB
39	18.32	n.a.	0.075	0.005	0.00	n.a.	BMB
40	19.18	n.a.	0.056	0.002	0.00	n.a.	BMB
41	20.25	n.a.	0.046	0.003	0.00	n.a.	BMB
42	20.75	n.a.	0.173	0.020	0.02	n.a.	BMB
43	24.25	n.a.	152.730	120.060	96.22	n.a.	BMB
44	24.92	n.a.	10.154	1.326	1.06	n.a.	Rd
45	25.73	n.a.	2.047	0.284	0.23	n.a.	BMB
46	27.06	n.a.	0.267	0.040	0.03	n.a.	BMB

No.	Ret.Time	Peak Name	Height	Area	Rel.Area	Amount	Type
	min		mAU	mAU*min	%	n.a.	
47	27.42	n.a.	1.479	0.231	0.19	n.a.	BMB
48	28.01	n.a.	6.148	1.873	1.50	n.a.	BMB
49	35.94	n.a.	0.107	0.020	0.02	n.a.	BMB
50	36.13	n.a.	0.114	0.013	0.01	n.a.	BM
51	36.38	n.a.	0.028	0.004	0.00	n.a.	MB
52	36.84	n.a.	0.053	0.003	0.00	n.a.	BMB
53	37.12	n.a.	0.030	0.003	0.00	n.a.	BMB
54	37.87	n.a.	0.093	0.006	0.00	n.a.	BMB
55	38.45	n.a.	0.023	0.001	0.00	n.a.	BMB
56	38.96	n.a.	0.050	0.004	0.00	n.a.	BMB
57	39.68	n.a.	0.041	0.003	0.00	n.a.	BMb
58	39.81	n.a.	0.039	0.003	0.00	n.a.	bM
59	40.32	n.a.	0.070	0.013	0.01	n.a.	MB
60	41.31	n.a.	0.049	0.001	0.00	n.a.	BMB
61	41.75	n.a.	0.044	0.003	0.00	n.a.	BMB
Total:			180.356	124.772	100.00	0.000	

monitored at 214 nm.

Sample Name:		*Injection Volume:*	**100.0**
Vial Number:	**RA5**	*Channel:*	**UV_VIS_1**
Sample Type:	**unknown**	*Wavelength:*	**214**
Control Program:		*Bandwidth:*	**8**
Quantif. Method:	**default**	*Dilution Factor:*	**1.0000**
Recording Time:	**14/04/2010 14:11**	*Sample Weight:*	**1.0000**
Run Time (min):	**42.00**	*Sample Amount:*	**1.0000**

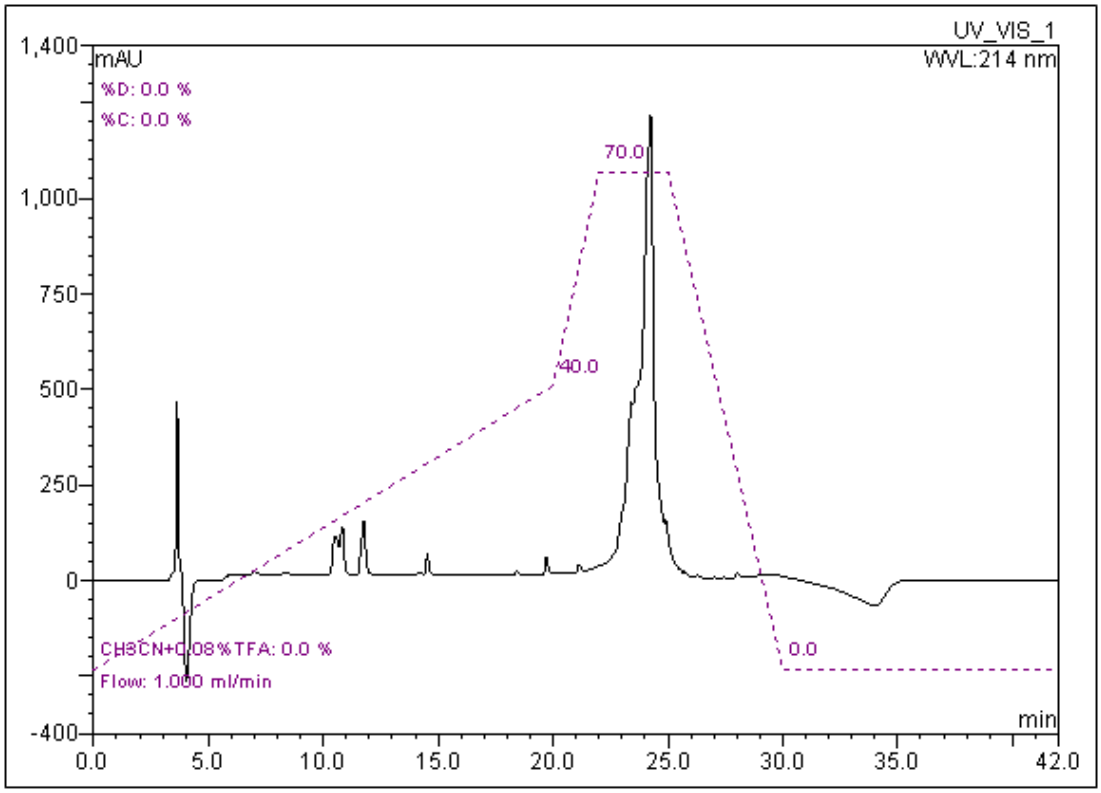

No.	Ret.Time	Peak Name	Height	Area	Rel.Area	Amount	Type
	min		mAU	mAU*min	%	n.a.	
1	0.04	n.a.	0.012	0.000	0.00	n.a.	BMB
2	0.13	n.a.	0.021	0.001	0.00	n.a.	bMB
3	0.35	n.a.	0.065	0.003	0.00	n.a.	BM
4	0.43	n.a.	0.091	0.005	0.00	n.a.	MB
5	0.68	n.a.	0.029	0.001	0.00	n.a.	BMB
6	1.09	n.a.	0.042	0.002	0.00	n.a.	BMB
7	3.63	n.a.	692.624	383.007	11.51	n.a.	BMB
8	3.88	n.a.	60.742	7.830	0.24	n.a.	Rd
9	4.51	n.a.	249.894	997.577	29.98	n.a.	BM
10	7.64	n.a.	0.749	0.108	0.00	n.a.	Rd
11	8.40	n.a.	4.867	2.116	0.06	n.a.	Rd
12	8.82	n.a.	167.161	113.286	3.40	n.a.	M
13	9.53	n.a.	151.271	101.286	3.04	n.a.	M
14	9.65	n.a.	0.726	0.078	0.00	n.a.	Rd
15	10.52	n.a.	231.604	89.867	2.70	n.a.	M
16	10.82	n.a.	249.424	98.400	2.96	n.a.	M
17	11.75	n.a.	242.655	170.927	5.14	n.a.	M
18	12.54	n.a.	1.216	0.306	0.01	n.a.	Rd
19	12.95	n.a.	1.333	0.222	0.01	n.a.	Ru

No.	Ret.Time	Peak Name	Height	Area	Rel.Area	Amount	Type
	min		mAU	mAU*min	%	n.a.	
20	13.40	n.a.	1.314	0.248	0.01	n.a.	Ru
21	13.81	n.a.	0.672	0.097	0.00	n.a.	Ru
22	14.20	n.a.	3.269	0.783	0.02	n.a.	Ru
23	14.52	n.a.	92.128	132.150	3.97	n.a.	M
24	14.94	n.a.	0.415	0.051	0.00	n.a.	Rd
25	15.25	n.a.	1.871	0.401	0.01	n.a.	Rd
26	15.45	n.a.	15.707	4.056	0.12	n.a.	M
27	15.76	n.a.	9.021	1.910	0.06	n.a.	MB
28	16.32	n.a.	1.989	0.303	0.01	n.a.	bMB
29	16.69	n.a.	0.705	0.091	0.00	n.a.	BM
30	16.82	n.a.	0.623	0.075	0.00	n.a.	Mb
31	17.15	n.a.	0.461	0.074	0.00	n.a.	bMB
32	17.53	n.a.	0.893	0.307	0.01	n.a.	BMb
33	18.01	n.a.	0.530	0.044	0.00	n.a.	bM
34	18.17	n.a.	0.673	0.101	0.00	n.a.	MB
35	18.43	n.a.	11.442	1.499	0.05	n.a.	BMb
36	18.74	n.a.	0.353	0.032	0.00	n.a.	bMB
37	19.01	n.a.	0.172	0.016	0.00	n.a.	BM
38	19.26	n.a.	1.100	0.258	0.01	n.a.	M
39	19.70	n.a.	46.342	7.062	0.21	n.a.	M
40	20.07	n.a.	4.337	0.797	0.02	n.a.	M
41	20.40	n.a.	4.801	1.824	0.05	n.a.	M
42	20.94	n.a.	8.332	2.827	0.08	n.a.	M
43	21.13	n.a.	27.627	6.909	0.21	n.a.	M
44	24.25	n.a.	1206.993	1061.826	31.91	n.a.	M
45	24.92	n.a.	28.252	3.421	0.10	n.a.	Rd
46	25.53	n.a.	19.324	2.597	0.08	n.a.	M
47	25.72	n.a.	14.959	2.281	0.07	n.a.	Mb
48	26.19	n.a.	0.257	0.005	0.00	n.a.	bM
49	26.28	n.a.	5.171	0.696	0.02	n.a.	MB
50	26.70	n.a.	0.370	0.030	0.00	n.a.	BM
51	27.03	n.a.	1.704	0.419	0.01	n.a.	MB
52	27.41	n.a.	4.572	0.735	0.02	n.a.	BMB
53	28.05	n.a.	17.576	7.361	0.22	n.a.	BM
54	28.39	n.a.	0.081	0.003	0.00	n.a.	Rd
55	29.78	n.a.	31.955	120.977	3.64	n.a.	MB
Total:			3620.517	3327.287	100.00	0.000	

3.3.2.6 HPLC analysis of lysozyme treated with BIC after tryptic digestion

monitored at 280 nm.

Sample Name:		*Injection Volume:*	**100.0**
Vial Number:	**RA6**	*Channel:*	**UV_VIS_2**
Sample Type:	**unknown**	*Wavelength:*	**280**
Control Program:		*Bandwidth:*	**8**
Quantif. Method:	**default**	*Dilution Factor:*	**1.0000**
Recording Time:	**14/04/2010 14:54**	*Sample Weight:*	**1.0000**
Run Time (min):	**42.00**	*Sample Amount:*	**1.0000**

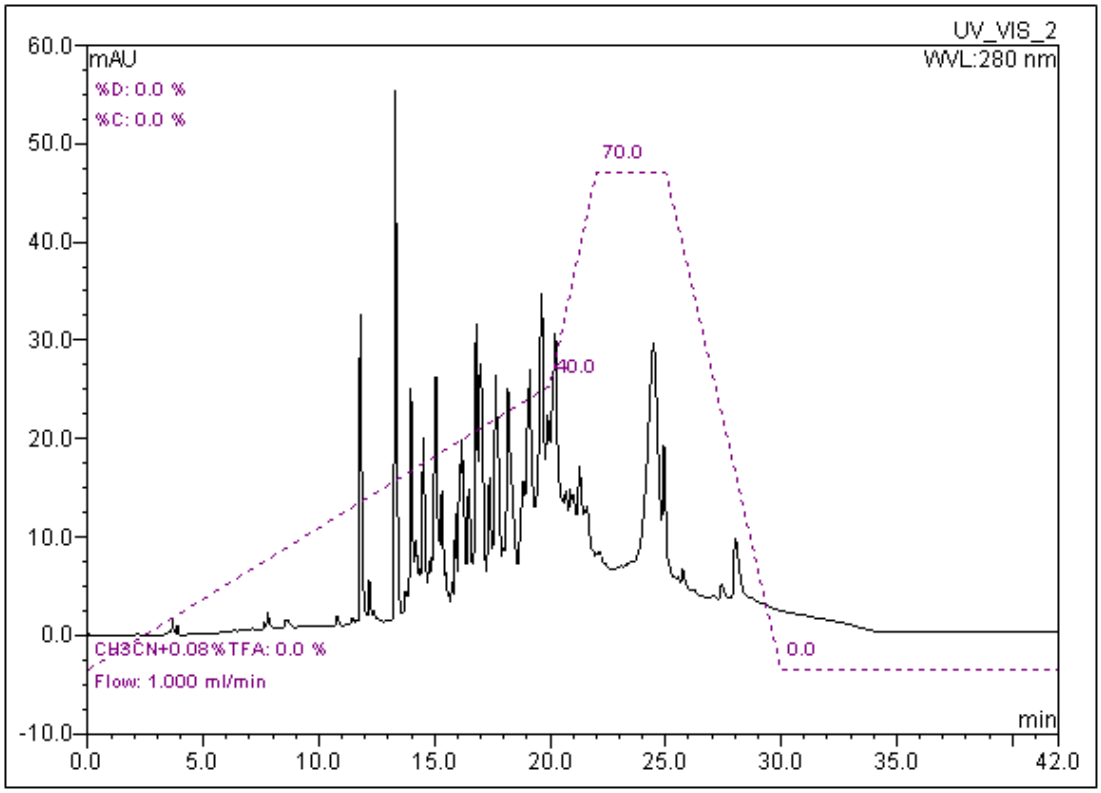

No.	Ret.Time	Peak Name	Height	Area	Rel.Area	Amount	Type
	min		mAU	mAU*min	%	n.a.	
1	0.05	n.a.	0.068	0.002	0.00	n.a.	BMB
2	0.37	n.a.	0.055	0.006	0.01	n.a.	BMB
3	1.15	n.a.	0.052	0.003	0.00	n.a.	BMB
4	2.11	n.a.	0.085	0.014	0.01	n.a.	BMB
5	3.61	n.a.	0.178	0.005	0.00	n.a.	Ru
6	3.67	n.a.	1.673	0.237	0.23	n.a.	BM
7	3.88	n.a.	1.139	0.094	0.09	n.a.	MB
8	4.34	n.a.	0.043	0.014	0.01	n.a.	BMB
9	5.06	n.a.	0.075	0.007	0.01	n.a.	BMB

No.	Ret.Time	Peak Name	Height	Area	Rel.Area	Amount	Type
	min		mAU	mAU*min	%	n.a.	
10	5.42	n.a.	0.029	0.003	0.00	n.a.	BMB
11	6.18	n.a.	0.059	0.004	0.00	n.a.	BM
12	6.28	n.a.	0.075	0.006	0.01	n.a.	MB
13	7.13	n.a.	0.149	0.019	0.02	n.a.	BMB
14	7.25	n.a.	0.023	0.001	0.00	n.a.	bMb
15	7.40	n.a.	0.054	0.003	0.00	n.a.	bMB
16	7.65	n.a.	0.737	0.066	0.06	n.a.	BM
17	7.79	n.a.	1.681	0.194	0.19	n.a.	MB
18	8.58	n.a.	0.877	0.210	0.20	n.a.	BMB
19	9.16	n.a.	0.046	0.002	0.00	n.a.	BMB
20	10.22	n.a.	0.053	0.004	0.00	n.a.	BMB
21	10.53	n.a.	0.084	0.009	0.01	n.a.	BMB
22	10.79	n.a.	1.038	0.101	0.10	n.a.	BMB
23	11.46	n.a.	0.708	0.076	0.07	n.a.	BM
24	11.63	n.a.	0.499	0.055	0.05	n.a.	M
25	11.79	n.a.	31.495	3.694	3.53	n.a.	M
26	12.17	n.a.	4.375	0.610	0.58	n.a.	M
27	12.36	n.a.	0.632	0.050	0.05	n.a.	Rd
28	12.75	n.a.	0.056	0.004	0.00	n.a.	Mb
29	12.86	n.a.	0.101	0.007	0.01	n.a.	bM
30	12.99	n.a.	0.162	0.015	0.01	n.a.	MB
31	13.30	n.a.	53.724	6.044	5.78	n.a.	BMB
32	13.63	n.a.	0.046	0.002	0.00	n.a.	BMB
33	13.75	n.a.	1.612	0.119	0.11	n.a.	BM
34	13.82	n.a.	0.425	0.019	0.02	n.a.	MB
35	13.98	n.a.	20.961	2.248	2.15	n.a.	BM
36	14.18	n.a.	5.105	0.772	0.74	n.a.	M
37	14.28	n.a.	0.735	0.033	0.03	n.a.	Rd
38	14.38	n.a.	0.510	0.022	0.02	n.a.	Ru
39	14.52	n.a.	15.091	1.914	1.83	n.a.	MB
40	14.76	n.a.	1.570	0.085	0.08	n.a.	Ru
41	14.87	n.a.	0.811	0.040	0.04	n.a.	Ru
42	15.06	n.a.	21.527	3.756	3.59	n.a.	BM
43	15.32	n.a.	10.226	1.387	1.33	n.a.	MB
44	15.49	n.a.	0.844	0.048	0.05	n.a.	Rd
45	15.75	n.a.	1.588	0.111	0.11	n.a.	Ru
46	15.91	n.a.	8.692	0.865	0.83	n.a.	BM

No.	Ret.Time	Peak Name	Height	Area	Rel.Area	Amount	Type
	min		mAU	mAU*min	%	n.a.	
47	16.08	n.a.	13.665	1.177	1.13	n.a.	M
48	16.18	n.a.	16.137	2.674	2.56	n.a.	M
49	16.49	n.a.	11.046	1.901	1.82	n.a.	M
50	16.80	n.a.	27.595	3.361	3.22	n.a.	M
51	16.97	n.a.	23.572	4.982	4.77	n.a.	M
52	17.38	n.a.	11.833	1.816	1.74	n.a.	M
53	17.65	n.a.	21.923	4.855	4.65	n.a.	M
54	17.97	n.a.	0.628	0.035	0.03	n.a.	Ru
55	18.17	n.a.	20.534	5.909	5.65	n.a.	M
56	18.81	n.a.	3.547	0.518	0.50	n.a.	Ru
57	19.12	n.a.	21.955	7.829	7.49	n.a.	M
58	19.64	n.a.	29.581	7.574	7.25	n.a.	M
59	19.89	n.a.	3.655	0.372	0.36	n.a.	Ru
60	20.22	n.a.	25.282	13.170	12.60	n.a.	M
61	20.69	n.a.	1.634	0.155	0.15	n.a.	Rd
62	20.87	n.a.	9.109	2.784	2.66	n.a.	M
63	21.02	n.a.	1.004	0.101	0.10	n.a.	Rd
64	21.28	n.a.	11.273	4.363	4.18	n.a.	M
65	21.61	n.a.	2.174	0.358	0.34	n.a.	Rd
66	21.88	n.a.	0.273	0.015	0.01	n.a.	Rd
67	22.01	n.a.	0.125	0.006	0.01	n.a.	Ru
68	22.11	n.a.	2.272	0.834	0.80	n.a.	MB
69	22.43	n.a.	0.151	0.010	0.01	n.a.	Rd
70	22.73	n.a.	0.159	0.015	0.01	n.a.	Rd
71	22.95	n.a.	0.136	0.017	0.02	n.a.	BMB
72	24.47	n.a.	23.085	12.236	11.71	n.a.	BM
73	24.92	n.a.	13.073	2.229	2.13	n.a.	MB
74	25.57	n.a.	0.327	0.028	0.03	n.a.	BMB
75	25.73	n.a.	1.521	0.215	0.21	n.a.	BMB
76	27.02	n.a.	0.332	0.056	0.05	n.a.	BMB
77	27.42	n.a.	1.499	0.241	0.23	n.a.	BMB
78	27.82	n.a.	0.055	0.002	0.00	n.a.	BM
79	28.01	n.a.	6.044	1.593	1.52	n.a.	MB
80	28.78	n.a.	0.137	0.015	0.01	n.a.	BMB
81	33.18	n.a.	0.061	0.003	0.00	n.a.	BMB
82	34.39	n.a.	0.044	0.004	0.00	n.a.	BM
83	34.55	n.a.	0.049	0.007	0.01	n.a.	Mb

No.	Ret.Time	Peak Name	Height	Area	Rel.Area	Amount	Type
	min		mAU	mAU*min	%	n.a.	
84	34.84	n.a.	0.031	0.003	0.00	n.a.	bMB
85	36.74	n.a.	0.077	0.005	0.00	n.a.	BM
86	36.84	n.a.	0.040	0.010	0.01	n.a.	MB
87	37.78	n.a.	0.045	0.002	0.00	n.a.	BMB
88	37.89	n.a.	0.026	0.002	0.00	n.a.	BMb
89	38.08	n.a.	0.042	0.002	0.00	n.a.	bMB
90	38.98	n.a.	0.052	0.004	0.00	n.a.	BM
91	39.09	n.a.	0.039	0.003	0.00	n.a.	M
92	39.22	n.a.	0.031	0.003	0.00	n.a.	MB
93	39.85	n.a.	0.070	0.008	0.01	n.a.	BMb
94	39.99	n.a.	0.038	0.002	0.00	n.a.	bMB
95	40.85	n.a.	0.047	0.003	0.00	n.a.	BMb
96	40.99	n.a.	0.082	0.004	0.00	n.a.	bMB
97	41.10	n.a.	0.034	0.003	0.00	n.a.	bMB
98	41.82	n.a.	0.039	0.002	0.00	n.a.	BMB
99	41.96	n.a.	0.037	0.001	0.00	n.a.	BMB
Total:			495.987	104.495	100.00	0.000	

monitored at 214 nm.

Sample Name:		*Injection Volume:*	**100.0**
Vial Number:	**RA6**	*Channel:*	**UV_VIS_1**
Sample Type:	**unknown**	*Wavelength:*	**214**
Control Program:		*Bandwidth:*	**8**
Quantif. Method:	**default**	*Dilution Factor:*	**1.0000**
Recording Time:	**14/04/2010 14:54**	*Sample Weight:*	**1.0000**
Run Time (min):	**42.00**	*Sample Amount:*	**1.0000**

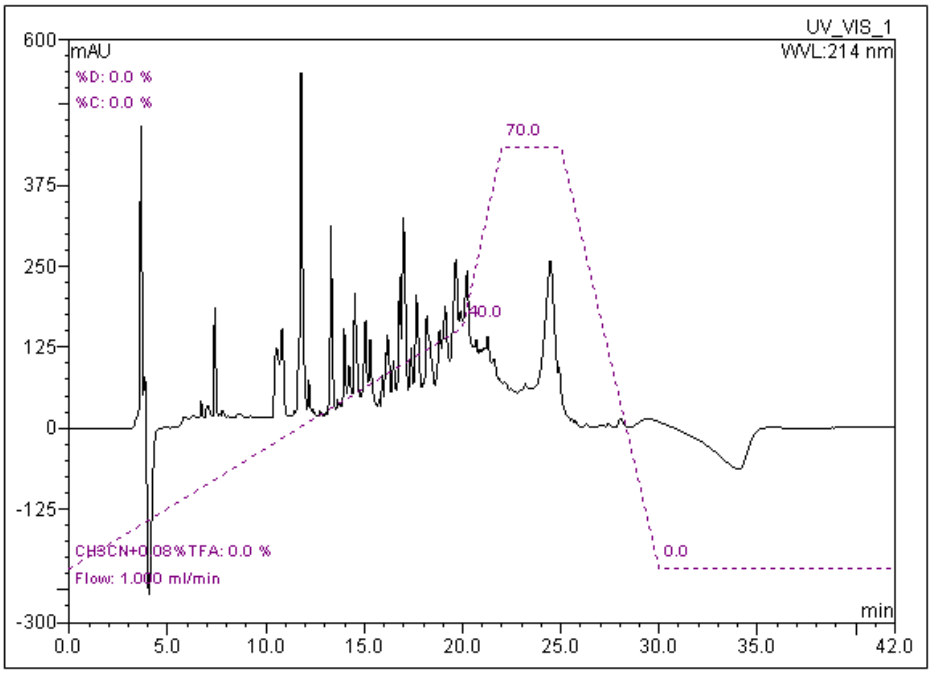

No.	Ret.Time	Peak Name	Height	Area	Rel.Area	Amount	Type
	min		mAU	mAU*min	%	n.a.	
1	0.23	n.a.	0.039	0.005	0.00	n.a.	BMB
2	0.58	n.a.	0.038	0.002	0.00	n.a.	BMB
3	0.78	n.a.	0.053	0.002	0.00	n.a.	BMB
4	1.38	n.a.	0.068	0.006	0.00	n.a.	BMB
5	2.31	n.a.	0.033	0.002	0.00	n.a.	BMB
6	3.08	n.a.	0.064	0.003	0.00	n.a.	BMB
7	3.63	n.a.	603.967	134.093	2.07	n.a.	BMB
8	3.83	n.a.	116.734	18.997	0.29	n.a.	Rd
9	6.70	n.a.	282.022	683.682	10.56	n.a.	BM
10	6.99	n.a.	5.229	0.481	0.01	n.a.	Ru
11	7.07	n.a.	271.733	110.479	1.71	n.a.	M
12	7.39	n.a.	422.525	91.832	1.42	n.a.	M
13	7.65	n.a.	2.821	0.183	0.00	n.a.	Ru
14	7.79	n.a.	261.150	163.519	2.53	n.a.	M
15	8.07	n.a.	3.316	0.281	0.00	n.a.	Rd
16	8.42	n.a.	0.156	0.010	0.00	n.a.	Ru
17	8.62	n.a.	250.822	188.126	2.91	n.a.	M
18	9.21	n.a.	243.171	187.245	2.89	n.a.	M
19	9.56	n.a.	1.176	0.133	0.00	n.a.	Rd
20	9.98	n.a.	236.462	125.311	1.94	n.a.	M
21	10.17	n.a.	0.411	0.065	0.00	n.a.	Rd
22	10.53	n.a.	64.449	12.710	0.20	n.a.	Ru

No.	Ret.Time	Peak Name	Height	Area	Rel.Area	Amount	Type
	min		mAU	mAU*min	%	n.a.	
23	10.82	n.a.	366.958	227.969	3.52	n.a.	M
24	11.22	n.a.	1.786	0.201	0.00	n.a.	Ru
25	11.45	n.a.	5.662	0.397	0.01	n.a.	Ru
26	11.79	n.a.	757.604	488.028	7.54	n.a.	M
27	12.17	n.a.	46.975	4.065	0.06	n.a.	Rd
28	12.35	n.a.	4.111	0.233	0.00	n.a.	Rd
29	12.75	n.a.	7.336	0.672	0.01	n.a.	Rd
30	12.98	n.a.	0.659	0.037	0.00	n.a.	Ru
31	13.07	n.a.	2.177	0.127	0.00	n.a.	Ru
32	13.30	n.a.	510.528	178.322	2.75	n.a.	M
33	13.64	n.a.	238.901	57.015	0.88	n.a.	M
34	13.74	n.a.	3.932	0.194	0.00	n.a.	Rd
35	13.98	n.a.	346.118	156.033	2.41	n.a.	M
36	14.23	n.a.	43.566	5.271	0.08	n.a.	Rd
37	14.52	n.a.	398.849	120.180	1.86	n.a.	M
38	14.75	n.a.	3.918	0.204	0.00	n.a.	Rd
39	14.89	n.a.	2.026	0.133	0.00	n.a.	Ru
40	15.06	n.a.	351.974	102.203	1.58	n.a.	M
41	15.31	n.a.	321.244	156.671	2.42	n.a.	M
42	15.75	n.a.	9.082	0.656	0.01	n.a.	Rd
43	15.91	n.a.	41.195	3.214	0.05	n.a.	Ru
44	16.09	n.a.	21.613	1.474	0.02	n.a.	Ru
45	16.18	n.a.	323.095	141.184	2.18	n.a.	M
46	16.49	n.a.	46.316	5.740	0.09	n.a.	Ru
47	16.80	n.a.	407.462	139.323	2.15	n.a.	M
48	16.98	n.a.	498.308	132.496	2.05	n.a.	M
49	17.38	n.a.	58.343	6.516	0.10	n.a.	Ru
50	17.65	n.a.	375.113	179.852	2.78	n.a.	M
51	17.98	n.a.	3.275	0.183	0.00	n.a.	Ru
52	18.18	n.a.	340.859	187.707	2.90	n.a.	M
53	18.83	n.a.	47.362	6.541	0.10	n.a.	Ru
54	19.12	n.a.	348.525	209.256	3.23	n.a.	M
55	19.66	n.a.	418.198	220.849	3.41	n.a.	M
56	19.89	n.a.	15.488	1.288	0.02	n.a.	Rd
57	20.23	n.a.	395.605	245.255	3.79	n.a.	M
58	20.55	n.a.	1.589	0.079	0.00	n.a.	Rd
59	20.70	n.a.	17.240	1.537	0.02	n.a.	Rd

No.	Ret.Time	Peak Name	Height	Area	Rel.Area	Amount	Type
	min		mAU	mAU*min	%	n.a.	
60	20.87	n.a.	7.095	0.429	0.01	n.a.	Ru
61	21.00	n.a.	2.277	0.149	0.00	n.a.	Ru
62	21.12	n.a.	4.570	0.291	0.00	n.a.	Ru
63	21.27	n.a.	288.360	460.620	7.12	n.a.	M
64	21.60	n.a.	15.748	2.571	0.04	n.a.	Rd
65	21.87	n.a.	3.258	0.222	0.00	n.a.	Rd
66	22.00	n.a.	0.706	0.031	0.00	n.a.	Rd
67	22.11	n.a.	3.987	0.943	0.01	n.a.	Rd
68	22.42	n.a.	1.989	0.230	0.00	n.a.	Rd
69	23.19	n.a.	10.459	2.164	0.03	n.a.	Ru
70	24.47	n.a.	383.786	723.614	11.18	n.a.	M
71	24.91	n.a.	20.181	2.424	0.04	n.a.	Rd
72	25.55	n.a.	3.845	0.381	0.01	n.a.	Rd
73	25.73	n.a.	5.155	0.493	0.01	n.a.	Rd
74	26.28	n.a.	4.964	0.771	0.01	n.a.	Rd
75	26.73	n.a.	0.209	0.015	0.00	n.a.	Ru
76	27.03	n.a.	1.831	0.429	0.01	n.a.	Ru
77	27.42	n.a.	113.429	126.073	1.95	n.a.	M
78	28.04	n.a.	117.480	356.717	5.51	n.a.	MB
79	29.37	n.a.	22.759	96.212	1.49	n.a.	Rd
Total:				6473.052	100.00	0.000	